UNIVERSITY OF CALIFORNIA, SAN DIEGO
3 1822 02331 4578

MULTIPART ITEM - Consists of:

TEXT VOLUME AND 25 PLATES
IN BACK POCKET.

7
U59

UNIVERSITY OF CALIFORNIA, SAN DIEGO
3 1822 02331 4578

MULTIPART ITEM - Consists of:

TEXT VOLUME AND 25 PLATES
IN BACK POCKET.

University of California, San Diego
Please Note: This item is subject to recall.
Date Due

JUN 25 1997

CI 39a (4/91) *UCSD Lib.*

Mode of Flow of Saskatchewan Glacier Alberta, Canada

By MARK F. MEIER

GEOLOGICAL SURVEY PROFESSIONAL PAPER 351

Measurement and analysis of ice movement, deformation, and structural features of a typical valley glacier

U.S. DEPARTMENT OF THE INTERIOR
March 3, 1849

UNITED STATES GOVERNMENT PRINTING OFFICE, WASHINGTON: 1960

UNITED STATES DEPARTMENT OF THE INTERIOR

FRED A. SEATON, *Secretary*

GEOLOGICAL SURVEY

Thomas B. Nolan, *Director*

The U.S. Geological Survey Library has catalogued this publication as follows:

Meier, Mark Frederick, 1925–
Mode of flow of Saskatchewan Glacier, Alberta, Canada. Washington, U.S. Govt. Print. Off., 1959.
ix, 70 p. illus. (1 col.) maps, diagrs., profiles, tables. 30 cm. (U.S. Geological Survey. Professional paper 351)
Part of illustrative matter folded in pocket.
Measurement and analysis of ice movement, deformation, and structural features of a typical valley glacier.
Bibliography: p. 67-68.
1. Glaciers — Alberta. 2. Saskatchewan Glacier, Canada. I. Title. (Series)

For sale by the Superintendent of Documents, U. S. Government Printing Office
Washington 25, D. C.

PREFACE

This report deals with principles of glacier flow that are applicable to the many glaciers in Alaska and other parts of the United States. Permission to work in Canada was extended by the Canadian Department for External Affairs, and access to the National Park was arranged by Mr. J. R. B. Coleman, then supervisor of Banff National Park. Saskatchewan Glacier was chosen for study because it is readily accessible and affords an unusually good opportunity to obtain data and develop principles that have a direct bearing on studies being made in the United States. The work started in the summer of 1952 and was supported by a grant from an Arctic Institute of North America project of the Office of Naval Research. Equipment was supplied by the California Institute of Technology under a contract with the Office of Naval Research. The work in 1953–54 was supported solely by the Office of Naval Research. The final phases of computation and manuscript preparation were supported by the U.S. Geological Survey. The author's work in the Geological Survey was under the general supervision of C. C. McDonald, chief, Branch of General Hydrology.

The success of this project in its conception, field program and preparation of this final report is due in large measure to the direction and the assistance given by Robert P. Sharp, B. Gunnar Bergmann, James E. Conel, Donald O. Emerson, Jean A. Hoerni, Benjamin F. Jones, William B. Lindley, Lee R. Magnolia, Jack Rocchio, Gordon Seele, Jack B. Shepard and George Wallerstein assisted in the field without compensation, and this assistance was of greatest value. Clarence R. Allen sacrificed his own research time to conduct seismic studies on the glacier which provided essential data on the thickness of ice and configuration of the bedrock channel. Kermit Jacobson, purchasing agent of the California Institute of Technology, took time from his regular duties to expedite the shipment of material and equipment to Canada. William Black, formerly warden of the Saskatchewan District, Banff National Park, and Peter Withers of Jasper National Park assisted the project in many ways beyond their official duties. Permission to use the Saskatchewan Hut was kindly extended by the Alpine Club of Canada, R. C. Hind, hut chairman. A Parsons Drill Hole Inclinometer was generously loaned by the Parsons Survey Co., South Gate, Calif. Thanks are also due to the Defence Research Board of Canada for the loan of magnesium sleds, and the California Institute of Technology for the acquisition and loan of special surveying equipment. The critical comments of C. R. Allen, W. B. Ray and W. D. Simons have been most helpful in the preparation of the manuscript.

GLOSSARY

Ablation. Wastage of ice and snow by melting, evaporation, erosion, calving, and other minor processes. On Saskatchewan Glacier wastage occurs mostly as surface melting.

Accumulation. Deposition of snow, hail, hoarfrost, rime and ice on a glacier. Most of this deposition takes place as snowfall on the glacier surface on Saskatchewan Glacier.

Accumulation area. That part of the glacier surface where accumulation exceeds ablation for a 1-year period.

Compressing flow. Flow in which the velocity decreases in the downglacier direction.

Extending flow. Flow in which the velocity increases in the downglacier direction.

Firn. Material in transition from snow to glacier ice. It consists of coarse granules, is compact but permeable, and ranges in density from about 0.4 to about 0.84 gram per cubic centimeter.

Firn limit. Line separating the accumulation area from the ablation area.

Flow centerline. An imaginary line on the surface of the glacier that is everywhere parallel to the projection on the surface of the velocity vectors and which passes as closely as possible through points of maximum surface velocity in transverse profiles.

Flow law. Steady-state creep rate as a function of the applied stress for a given material.

Foliation. A compact, layered structure or planar anisotropy caused by flow, as defined in this report. It is expressed mainly by differences in grain size or bubble content of the ice.

Octahedral shear stress (or strain rate). A value expressing the intensity of shearing stress (or strain rate) in a body equal to the stress (or strain rate) acting on planes of an octahedron oriented with its corners on the axes of principal stress (or strain rate).

Plastic flow. Flow in which the strain rate is not linearly proportional to the applied shear stress.

Principal axes of stress (or strain rate). In a general state of stress (or strain rate) there are three mutually perpendicular planes on which the shear stresses (shear strain rates) vanish. The three principal axes are normal to these three planes.

Principal stresses (or strain rates). The normal (strain rates) in the direction of the principal axes of stress (strain rate).

Strain rate. Velocity of deformation, usually restricted to the velocity of shearing deformation in this report.

Temporary snowline. Line delineating the snow-covered area at any instant.

Viscous flow. Flow in which the strain rate is linearly proportional to the applied shear stress.

SYMBOLS

A	area of a cross section
C	$=\frac{R}{d}\gamma \sin \alpha$
d	depth
$f(\ )$	a function of ( )
i,j,k	$=x, y,$ or z
k,k_1,k_2	arbitrary, empirical constants
n	empirical constant
p	iced perimeter, analogous to the wetted perimeter as used in hydraulics, except that p is measured in a cross section perpendicular to the glacier surface
R	$=\frac{A}{p}$, the hydraulic radius (measured in a plane perpendicular to the surface of the glacier)

s	standard deviation
$\mathsf{S}, \delta\mathsf{S}, \delta S$	surfaces (defined on p. 25)
u	displacement
$\mathbf{V}$	the velocity vector
V	the absolute magnitude of $\mathbf{V}$
V_s	the surfaceward flow (defined on p. 20)
V_i, V_j	velocity component parallel to a coordinate axis i or j ($i,j = x, y,$ or z)
V_x, V_y, V_z	velocity components parallel to the x, y, z-axes
V_x', V_y'	velocity components parallel to the x', y'-axes
w	width
x, y, z	rectangular coordinate axes (defined on p. 10)
$x'y'$	curvilinear "natural" coordinate axes (defined on p. 11)
x_i, x_j	coordinate axes ($i, j = x, y,$ or z)
α	surface slope, measured from the horizontal in the direction of the x'-axis
β	bed slope, measured from the horizontal in the direction of the x'-axis
γ	specific weight of ice (generally assumed to be 56.1 pounds per cubic foot)
δ_{ij}	Kronicker delta or idem factor ($\delta = 0$ when $i = j, = 1$ when $i \neq j$)
$\dot{\epsilon}_{ij}$	strain rate
$\dot{\epsilon}_{xx}$	normal strain rate in the direction of the x-axis, extending strain rates are considered positive
$\dot{\epsilon}_{xy}$	shearing strain rate on a plane perpendicular to the x axis, in the direction of the y axis
$\dot{\epsilon}_1$	greatest (most extending) principal strain rate
$\dot{\epsilon}_2$	least (most compressing) principal strain rate
$\dot{\epsilon}'_{ij}$	deviator of strain rate (defined on p. 38)
$\dot{\epsilon}_0, \dot{\epsilon}_0'$	octahedral strain rate (defined on p. 38, 41)
θ	horizontal angle between x' axis and ϵ_1 (table 4)
ξ	inclination of streamline from the horizontal
ρ	density of ice
σ_{ij}	stress
σ	hydrostatic (mean) stress
σ_{xx}	normal stress in the direction of the x axis, tensile stresses are considered positive
σ_{xy}	shearing stress on a plane perpendicular to the x axis, in the direction of the y axis
$\sigma_1, \sigma_2, \sigma_3$	principal stresses
σ_{ij}'	deviator of stress (defined on p. 38)
σ_0, σ_0'	octahedral shear stress (defined on p. 38, 41)
ϕ	horizontal angle between x' axis and $\mathbf{V}$ (fig. 17)
$\dot{\omega}$	rotation rate (table 4)

CONTENTS

Page
- Abstract 1
- Introduction 1
  - Physical setting of Saskatchewan Glacier 2
  - General characteristics of the glacier 5
  - Surface configuration 6
  - Recent changes in surface level 6
  - Channel configuration 6
  - Ablation 8
- Surface velocity observations 10
  - Method of measurement 10
  - Time-variation of velocity 11
    - Yearly changes 14
    - Seasonal variations 14
    - Short-interval variations 16
    - Summary of time dispersion of velocity 18
  - Configuration of the surface velocity field 19
    - Horizontal downglacier component 21
    - Horizontal sideways component 21
    - Absolute vertical component 22
    - Component of surface rise due to ice motion 24
    - Direction of the velocity vector 27
    - Velocity pattern at the medial moraine 27
- Englacial velocity measurements 28
  - Sites 28
  - Method 28
  - Boreholes 30
  - Results 31
- Some interpretations of the velocity data 32
  - Surface strain-rate field 32
    - Fundamental relations 32
    - Deformation of the surface 37
    - Deformation in three dimensions 37
  - Flow law of ice 37
    - Fundamental relations 38

Page

Some interpretations of the velocity data—Continued

Flow law of ice—Continued

- Vertical profile 38
- Transverse profile 41
- Discussion of the flow-law results 42
- Discharge relations 45
  - Velocity at depth 45
    - Method of computation 45
    - Results 46
  - Mass budget 46
    - Flow into Castleguard sector 46
    - Surfaceward flow 46
  - Streamlines 46
    - Method of determining 46
    - Checks on accuracy 48
    - Conclusions from these results 49
- Longitudinal profile 49
  - Significance of the profile 49
  - Constant basal shearing-stress calculations 49
  - Hypothesis for the longitudinal profile 50
- Structural features 50
  - Stratification 50
  - Foliation 52
  - Cracks 54
  - Faults 57
  - Fold axes 57
  - Structures of Castleguard sector 57
  - Origin of tectonic features 59
    - Foliation 59
    - Main crack system (crevasses) 60
- Significant findings 62
- Accuracy of the velocity data 64
- References cited 67
- Index 69

ILLUSTRATIONS

[Plates 1-5 are in pocket]

Page

PLATE 1. Longitudinal and transverse profiles.
2. Structural features of Saskatchewan Glacier.
3. Structural features of the terminus of Saskatchewan Glacier.
4. Saskatchewan Glacier in 1954.
5. Velocity vectors and calculated vertical velocity profiles and streamlines in a longitudinal section.
6. Saskatchewan Glacier viewed west from Parker Ridge, July 11, 1952 Facing 2
7. Stratification exposed below the firn limit in Castle guard sector Facing 50
8. Stratification and strong foliation below the firn limit Facing 52
9. Contorted foliation, stratification(?) offset by foliation, and in echelon crevasse belts Facing 54

Page

FIGURE 1. Map of the eastern part of the Columbia Icefield, Alberta-British Columbia, Canada 4
2. Area-altitude graph of Saskatchewan Glacier and firn 5
3. Castleguard sector in 1952–54 7
4. Average surface lowering, 1948–54, in feet per year 8
5. Bedrock topography 9
6. Cross sections in Castleguard sector 10
7. Daily ablation rate, positions of the temporary snowline, and average yearly ablation expressed as a function of elevation along the central part of Saskatchewan Glacier 11
8. Total ablation and positions of temporary snowlines 12
9. Nomenclature of velocity stakes, transit points, and coordinate systems 13
10. Dates of survey of velocity stakes 14
11. Relative difference between summer and yearly velocity as a funtion of longitudinal position 16
12. Velocity variations in 1952 16
13. Short-interval velocity variations in 1953 17
14. Velocity deviations and meteorological observations, 1953 18
15. Relation of deviation of velocity to temperature 19
16. Velocity dispersion spectrum at stake 6–4 19
17. Definition sketch of velocity components 20
18. Distribution of V_z' and V_s on Saskatchewan Glacier 20
19. Distribution of V_x, and horizontal projection of velocity vectors in Castleguard sector 21
20. Distribution of V_y' in Castleguard sector 23
21. Distribution of V_z in Castleguard sector 23
22. Distribution of V_s in Castleguard sector 24
23. Downglacier, surfaceward, and vertical velocities and surface slope along the flow centerline 25
24. Downglacier velocity along four transverse profiles in Castleguard sector 26
25. Ratio of downglacier velocity (V_x) to centerline downglacier velocity ($V_{x,c}$) as a function of relative distance from the centerline for four transverse profiles 26
26. Ablation velocity (V_a) compared with difference between surface lowering velocity (V_e) and surfaceward flow velocity (V_s) 26
27. Velocity vectors projected onto a transverse plane perpendicular to the glacier surface at $x' = 10{,}000$, viewed upglacier 27
28. Simplified sketch of hotpoint 29
29. Configurations of borehole number 1 in 1952 and 1954 30
30. Deformation of vertical borehole parallel to the centerline of flow. Circles indicate measurement points, short horizontal lines indicate approximate limits of measurement error 31
31. Measured velocity gradients in Castleguard sector 32
32. Mohr's circle constructions showing changes in strain rate along a transverse profile at $x' = 10{,}000$ 33
33. Orientations and magnitudes of principal strain rates in Castleguard sector 33
34. Principal strain-rate trajectories in Castleguard sector 34
35. Trajectories of greatest shear-strain rate in Castleguard sector 34
36. Normal strain rates parallel to the x'- and y'-axes in Castleguard sector 36
37. Definition sketch for analysis of stress and deformation in a vertical profile 39
38. Vertical gradient of horizontal velocity along vertical borehole. Circles indicate measurement points, short horizontal lines indicate approximate limits of measurement error 39
39. Strain rate as a function of shear stress in Saskatchewan Glacier 40
40. Strain rate as a function of shear stress, data from many sources 43
41. Difference between velocity at the surface and velocity at depth as a function of depth 47
42. Distribution of velocity in transverse section at $x' = 5{,}000$ 48
43. Diagrammatic longitudinal section of a glacier showing sedimentary layering 52
44. Crevasses in Castleguard sector 56
45. Orientation of structural features in Castleguard sector 58
46. Crevasse and open-crack orientations as a function of transverse location 61
47. Phantom view of part of Saskatchewan Glacier showing possible fracture planes leading to formation of en echelon crevasses at the surface 63
48. Error distribution for 50 measurements of a fixed angle 65

TABLES

Page
TABLE 1. Measured summer and annual velocity components, in feet per year 15
2. Standard deviation of velocity 16
3. Velocity components, slope, ablation, and surface lowering at velocity stakes 22
4. Strain-rate components 35
5. Stress and strain-rate data from vertical borehole 41
6. Stress and strain-rate data from transverse surface profile 42
7. Mass-budget data for the south half of the tongue of Saskatchewan Glacier 46
8. Criteria for distinguishing foliation from stratification 54
9. Characteristics of orientation maxima 59
10. Coordinates of velocity stakes 66
11. Inclination data for boreholes 67

MODE OF FLOW OF SASKATCHEWAN GLACIER, ALBERTA, CANADA

By Mark F. Meier

ABSTRACT

Research in 1952–54 on Saskatchewan Glacier was directed toward the measurement of velocity on the surface and at depth, the surface and bedrock topography, ablation, and structures produced by flow. These field data are used to test current theories of flow and to derive new conclusions about the flow of a valley glacier.

Positions in space of 51 velocity stations fixed in the ice were computed from triangulation surveys. Summer velocities are generally greater than yearly velocities. Short-interval (½–1 day) observations recorded great velocity fluctuations and intermittent backward movements. Some of these fluctuations represent domains not more than 100 feet in extent. Dispersion values indicate that jerkey motion is probably due to irregular shearing and is not predominantly perpendicular to crevasses. Dispersion of velocity decreases with increasing time intervals of measurement. Maximum surface velocity of 383 fpy (feet per year) occurs at the firn limit; velocity decreases unevenly along the midglacier line to 12 fpy at the terminus. Velocity vectors plunge below the surface along the centerline from above the firn limit to 1.3 miles below. Further downglacier the vectors rise out from the surface and the angular divergence increases both downglacier and toward the margins. The flow of ice toward the surface is constant at 10 fpy in the lower 3 miles. Rates of surface lowering computed from these data and ablation data agree approximately with independently measured thinning.

Velocity gradients in an area of detailed study are analyzed to determine the surface strain-rate field. Deformation is largely caused by the transverse gradient of the longitudinal velocity. Longitudinal and transverse extensions and compressions were measured. One principal strain-rate trajectory lies along the flow centerline; a trajectory of maximum shearing strain rate parallels the valley wall at the margin.

Velocity to a depth of 140 feet decreases exponentially. The flow law of ice is determined by an analysis of this short vertical profile and a transverse velocity profile on the surface. The two sets of data give consistent results which agree with results from other glaciers, and suggest that the flow law is unaffected by either hydrostatic pressure or extending or compressing flow. The strain rate cannot be expressed as a simple power function of the stress. A viscouslike flow seems to predominate at low stresses. Above a shear stress of 0.7 bar the flow velocity changes much more rapidly with slight changes in stress.

The derived flow law is used to compute velocity as a function of depth and the mass-budget. These results show that the ice currently being supplied to the surface is not as great as the surface ablation but is just sufficient to keep the glacier thinning at an unchanged rate in time. Computed streamlines parallel the bedrock channel closely.

Three main classes of features in the ice are distinguished: (1) primary sedimentary layering, (2) secondary flow foliation and (3) secondary cracks and crevasses. Primary stratification is flatlying in general but wrinkled longitudinally in detail. Foliation generally dips steeply, strikes longitudinally, and shears other structures. However, some foliation attitudes do not relate to measured directions of maximum shearing strain rate at the point of observation or at any conceivable point of origin. The orientation of the most prominent set of cracks agrees approximately with measured trajectories of principal compressing strain rate. Other minor sets of cracks are related to trajectories of maximum shearing strain rate.

INTRODUCTION

> "One of the difficulties in the past has been that theories of glacier flow have often had to start from arbitrary assumptions about the mechanical properties of ice, which had never been adequately investigated, and to proceed to predictions about velocity distributions in glaciers which could not be verified by experiment." (Gerrard, Perutz, and Roch, 1952, p. 547)

The flow of glaciers has long been a subject of controversy, and many completely different theories of flow have been propounded. Rigorous checking by field measurement, however, has lagged far behind the development of theoretical concepts. The complete velocity field on the surface or at depth of a glacier has never been satisfactorily measured. This information is basic to the framing and testing of theories of flow.

The objective of the study on Saskatchewan Glacier was to gather these basic data, together with essential supplementary information such as the variation of the velocity field with time, the shape of the glacier and its bed, and the structures produced by flow. An ultimate goal was to relate these field data to known mechanical properties of ice and modern theories of glacier flow. Saskatchewan Glacier is favorably situated for this study because it is easily accessible, facilitating fieldwork, and is of simple geometrical shape, simplifying the mathematical treatment. The detailed mechanism of flow (the process by which individual crystals yield to stress) is not a matter of principal concern here, and the glacier is assumed to be a continuous, homogenous body. Some work has been done on the mechanism of flow of Saskatchewan Glacier by G. P. Rigsby.[1]

The organization of this report is as follows: Data bearing on the general characteristics of the glacier, its physical setting, surface topography, channel configuration and surface ablation are presented first. This basic information is the background material for analysis of the flow.

Results of measurement of the surface velocity field are then described. Velocity at fixed points varied from day to day and from season to season, but changed little from year to year. Short-interval (12-hr) fluctuations in velocity are greater and offer some insight into the mechanism of flow. These fluctuations limit the accuracy with which the time-averaged velocity field can be measured. After the time variations in velocity are described, attention is given to the time-averaged configuration of the surface velocity field. This is a vector field and the vectors do not parallel the surface, so it is necessary to measure three components of velocity in space. Values of the horizontal component directed downglacier, the horizontal transverse component, and the vertical component relative to a fixed coordinate system are discussed. A vertical component measured relative to the instantaneous ice surface, which represents the surfaceward flow, is then presented. Finally, results of measurement of velocity at depth are given.

The mentioned sections which present basic data are followed by interpretive discussions. The surface strain rate field is computed from measured velocity gradients, providing information on the deformation of ice at the surface. An analysis of the geometry of flow is made involving: (1) The total discharge of the glacier as compared with the surfaceward flow and ablation on the surface; (2) a computation of the streamlines of flow at depth; and (3) some statements about the equilibrium and quasiequilibrium longitudinal profiles of this glacier. The data from Saskatchewan Glacier offer some insight into the flow law (strain rate as a function of stress) of ice, and these results are presented and analyzed.

Structural features in the ice offer additional insight into the mode of flow and are discussed in the final section. A prominent flow foliation is apparently a shear phenomenon but cannot be related precisely to measured planes of greatest shearing distortion. Cracks form in close correspondence to the principal elongations and are used as indicators of strain rate and stress conditions on parts of the glacier where the flow was not measured.

Fieldwork on Saskatchewan Glacier was done from June 23 to September 2, 1952; June 19 to September 8, 1953; and from July 8 to August 13, 1954. Camps were maintained at the Alpine Club of Canada's Saskatchewan Hut (1.7 miles below the glacier terminus) and outside the south lateral moraine near Castleguard Pass (fig. 1). A road extends to within 2,000 feet of the present terminus of the ice, making the glacier easily accessible. Most of the movement of equipment and supplies on the glacier was by backpack, but some material was hauled upglacier by truck and packhorses. Uncertain weather, unpredictable operation of specially designed equipment, necessity for precautions against the hazards of glacier travel, as well as time spent on logistical matters, severely restricted the amount of scientific work that could be done in a field season, even on this easily accessible glacier.

PHYSICAL SETTING OF SASKATCHEWAN GLACIER

Saskatchewan Glacier, at the head of North Saskatchewan River in Banff National Park, is the largest of the six principal outlet tongues[2] of the Columbia Icefield (fig. 1). This icefield lies astride the Alberta-British Columbia line in the Canadian Rockies (lat 52°08′, long 117°12′). The part of the firn region of the Columbia Icefield that feeds Saskatchewan Glacier is entirely in Alberta and covers an area of about 9 square miles and ranges in altitudes from 8,000 to 11,300 feet. Almost half of this area lies between altitudes 8,500 and 9,000 feet (fig. 2). About 2 square miles of firn is split off the main part of the icefield by a high mountain ridge, and the only medial moraine on Saskatchewan Glacier is formed where this ice joins the flow from the main icefield. Two former tributaries approach the trunk glacier on each side about 2 miles above the terminus, but do not join at present. The usual firn limit lies almost at the juncture between icefield and tongue and ranges in altitude from 8,000 to slightly more than 8,300 feet. The tongue is 5.5 miles long and descends to an altitude of 5,900 feet (pl. 6). It is about 1 mile wide in the upper 2.5 miles

---

[1] Rigsby, G. P., 1953, Studies of crystal fabrics and structures in glaciers, Ph.D. thesis, California Inst. Technology, 51 p. *See also* Meier, Rigsby and Sharp (1954, p. 21-24).

[2] In this report, the term "Saskatchewan Glacier" refers to the tongue only and does not include the firn area within the Columbia Icefield. The glacier according to this definition lies entirely below the firn limit.

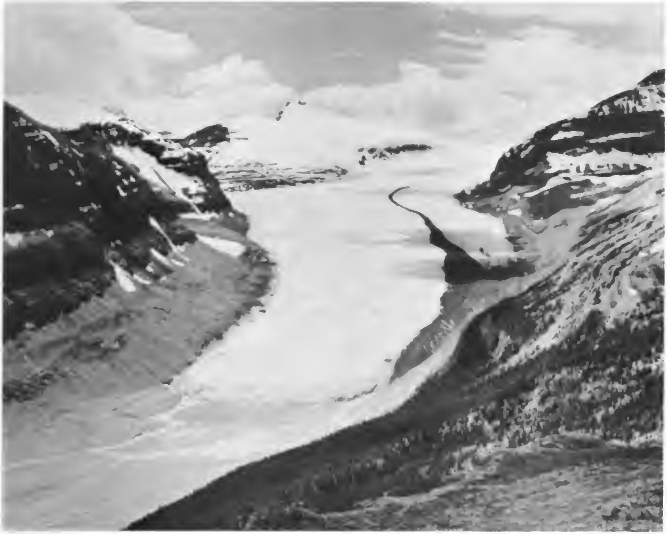

SASKATCHEWAN GLACIER VIEWED FROM PARKER RIDGE, JULY 11, 1952

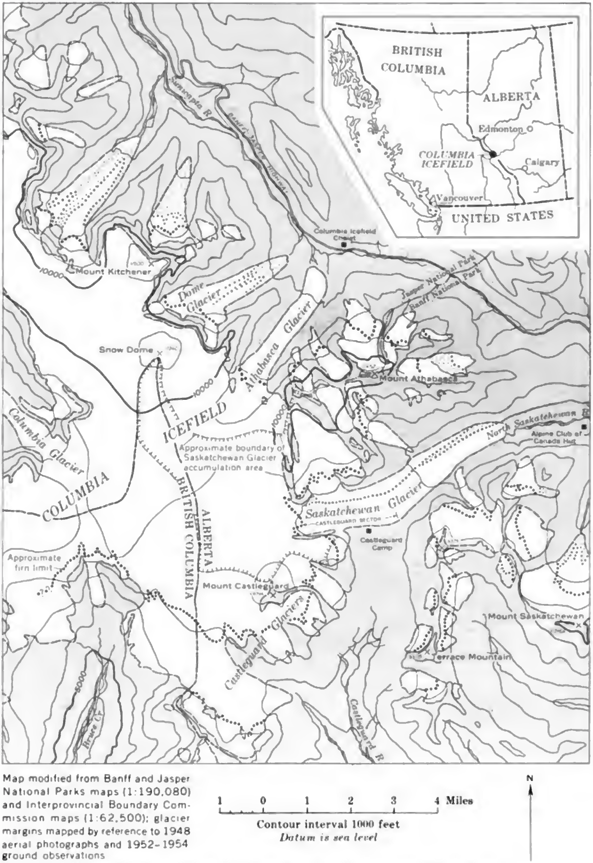

Map modified from Banff and Jasper National Parks maps (1:190,080) and Interprovincial Boundary Commission maps (1:62,500); glacier margins mapped by reference to 1948 aerial photographs and 1952–1954 ground observations

FIGURE 1.—Map of the eastern part of the Columbia Icefield, Alberta–British Columbia, Canada.

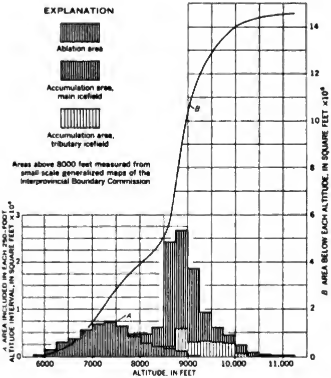

FIGURE 2.—Area-altitude graph of Saskatchewan Glacier and firn.

(the "Castleguard sector," see fig. 1) and tapers to a width of 2,000 feet near the terminus. It has only one gentle curve of about 30° 3.5 miles above the terminus.

The total area of Saskatchewan Glacier and its firn field is 14.5 square miles of which the accumulation area embraces 68 percent. The average net accumulation over this area can be computed because the amount of ice discharged into the Saskatchewan Glacier tongue is known for 1953–54. An average annual accumulation of 3.2 feet of water over the area of the firn basin would have supplied this known discharge.

GENERAL CHARACTERISTICS OF THE GLACIER

Glaciers can be classified and compared in three ways according to Ahlmann (1948, p. 59–67): by shape (morphological), by activity (dynamic), and by thermal characteristics (geophysical). The shape of this glacier, as indicated by the area-altitude graph (fig. 2), is that of a valley glacier of the alpine type (Ahlmann, 1948, p. 62, type II). It may be termed an "outlet" glacier but not an "outflow" glacier in the sense used by Finsterwalder (1951, p. 557).

The activity—or the metabolism—of a glacier can be expressed quantitatively as the gradient of net accumulation (total yearly accumulation minus total yearly ablation) with increasing altitude at the firn limit. This parameter has been termed the "energy of glacierization" by Shumskii (1947) and it expresses the "degree of activity" as discussed by Ahlmann (1948, p. 63). The gradient on Saskatchewan Glacier is 0.013 (13 mm per meter) just below the firn limit. This indicates a high degree of activity, comparable to that of glaciers of the Alps—Rhone Glacier, 12.4 mm per meter and Hintereisferner, 15.8 mm per meter according to Shumskii (1947) and suggests some maritime quality in the local climate.

No investigations were made of the thermal regimen of Saskatchewan Glacier, but it is assumed to be thermally temperate because it lies at a relatively low latitude, and copious meltwater is produced in the summer. However, unexpected freezing conditions were found in drilling operations (p. 31). This suggests that subfreezing temperatures can exist in the crustal ice even in late summer, although the bulk of the glacier probably exists at the pressure-melting temperature.

It seems reasonable to treat Saskatchewan Glacier in its larger aspects as a homogeneous and isotropic body in spite of many small-scale inhomogeneities. Exposed ice in the ablation area shows irregular patterns of differences in grain size. Average grain sizes over areas of several feet range from about 1 millimeter to nearly 10 centimeters. Grains are largest along the margins, smallest along the centerline, and show an uneven but noticeable increase downglacier. Complex intergrowths of crystals were observed in coarse-grained ice. Except for local zones of young, partly icified firn in midglacier, all of the exposed ice seems to be of about the same compactness and hardness. The density is assumed to range between 0.85 and 0.91. Except for a foliated structure that is pronounced near the margins no consistent patterns of differences in bubble content were observed, and no crystal-shape orientation patterns were discovered. Crystal-fabric studies by Rigsby[3] and Meier, Rigsby and Sharp (1954, p. 21–24) revealed very weak crystal axes orientations except along the extreme margins and at the terminus. To a reasonable approximation, therefore, the bulk of the glacier can be described as constant in density, homogenous, and isotropic in physical characteristics. This approximation is probably not valid near the valley walls.

Saskatchewan Glacier apparently began to with-draw from its greatest recent extent in 1854 (Field and Heusser, 1954, p. 135), and the terminus has retreated subsequently about 4,000 feet. High abandoned lateral moraines indicate a concurrent thinning of more than 100 feet over most of the tongue. Recession and thinning were continuing at the time of these field studies.

---

[3] Rigsby, G. P., op. cit.

SURFACE CONFIGURATION

Quantitative study of stress and flow in a glacier requires an accurate topographic map of the surface. In 1952–53, a triangulation net of 14 bench marks was established along both sides of the glacier. Nine of these bench marks were used as control for the construction of a topographic map from Royal Canadian Air Force stereoscopic aerial photographs taken in 1948. In addition, a map of the terminus (1953), 3 transverse profiles (1952) and a 5-mile longitudinal profile (1954) were compiled from stadia surveys. These data, plus 46 accurate spot elevations on the glacier surface, were used to construct maps of the glacier surface as it existed in 1954 (pl. 4, fig. 3). Longitudinal and transverse profiles are shown in plate 1.

These data show that Saskatchewan Glacier has a very uniform longitudinal slope which averages 3°23′, exceeding this markedly only at the extreme terminus (maximum of 11°9′) and near the firn limit (reaching 8°40′). The transverse profiles are flat to slightly concave near the firn limit and flat to slightly convex (sometimes with a slight concavity along the centerline) over the rest of the tongue. Marginal troughs are prominent in the Castleguard sector.

RECENT CHANGES IN SURFACE LEVEL

Comparison of a longitudinal profile drawn from the map constructed from 1948 aerial photographs with the 1954 stadia profile suggests pronounced thinning over the whole tongue (pl. 1). The elevation difference between those profiles is probably accurate to within 10 or 15 feet in the vicinity of 13 accurately surveyed velocity markers and 25 feet elsewhere. The possibility of cumulative error is discounted because both the stereoscopic model and the elevations of velocity markers were controlled by the same points on bedrock. Thinning data for the whole glacier, computed in this manner, are shown in figure 4. In figure 4 and plate 1 the five firn limit points were computed as of 1953 (they were buried under snow in the 1954 field season) and the glacier surface was assumed not to have changed in elevation at these points from 1953 to 1954.

The thinning data show that the tongue is not in equilibrium, but is wasting downward at a rate of 4 to 13 feet per year (fpy). Thinning rates oscillate between 11 fpy at the firn limit, 5 fpy 2 miles below the firn limit, 16 fpy 3.5 miles below the firn limit, 5 fpy at 5 miles below, and a maximum of 15 fpy at the extreme terminus. Thinning is more conservative along the south margin; few data are available for the north margin. Whether this apparent periodicity along the centerline represents a wavelike flow response or periodic climatic changes, or just coincidence, is not clear. However, the data are too crude for firm conclusions.

Recent abandoned lateral moraines which can be traced for more than 4 miles upglacier indicate that thinning has been going on for some time. The elevations above the ice of the two most prominent moraines are plotted in plate 1, and show that thinning has not been uniform in the past.

CHANNEL CONFIGURATION

Seismic explorations in 1952 by C. R. Allen provide information on the shape of the glacier's bedrock channel. Reliable reflections were obtained at 9 locations comprising 1 longitudinal and 2 transverse profiles, using equipment and techniques described elsewhere (Allen and Smith, 1953, p. 756). These data[4] (C. R. Allen, written communication) are plotted on figure 5 together with the approximate bedrock topography and 7 transverse cross sections. The channel shape at the firn limit is unknown, but the approximate area has been computed from flow data (p. 46) and a half-elliptical shape has been assumed.

These data show a broad, U-shaped, evenly inclined channel section. The shape of the whole glacier in its channel approximates a circular cylinder having a diameter of 5,250 feet, inclined east at an agle of 0°46′, curved slightly in a horizontal direction, and cut by a plane inclined 3°23′, in the same direction.

In Castleguard sector the southern parts of the cross sections are nearly elliptical (fig. 6). Because the sections are not quite symmetrical, most of the analytical work was concentrated on the southern part. The term "plane of symmetry" is defined by the vertical projection of the flow centerline. This flow centerline was determined from surface ve-

---

[4] The data from the shot point nearest the terminus are open to several interpretations; the first identifiable reflection (565 feet) may be from a contact between bedrock and moraine or outwash materials, because the plunge of surface velocity vectors in the glacier (p. 27) and geologic evidence beyond the terminus suggests that the ice is no more than 240 feet thick here. A reflection from less than 300 feet would probably have been obscured by noise from the initial explosion.

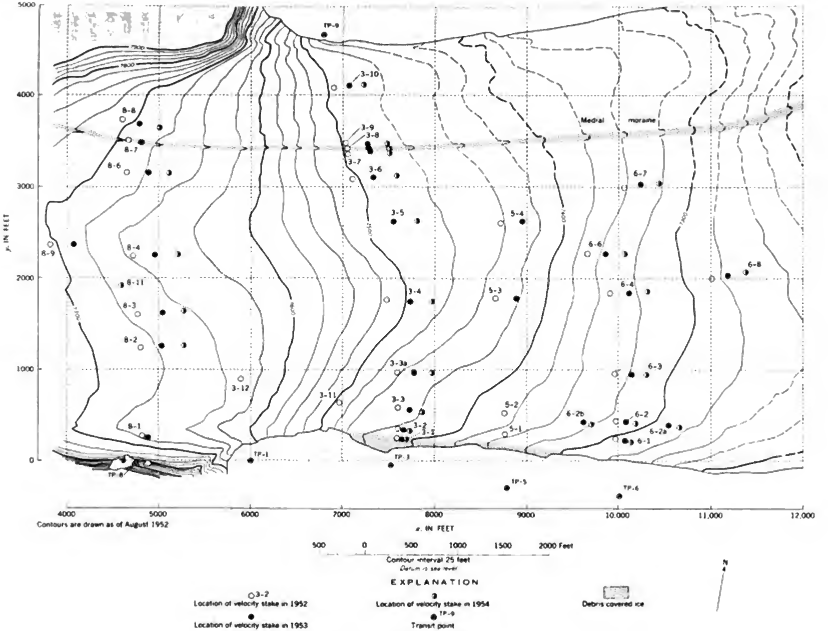

FIGURE 3.—Castleguard sector in 1952-54.

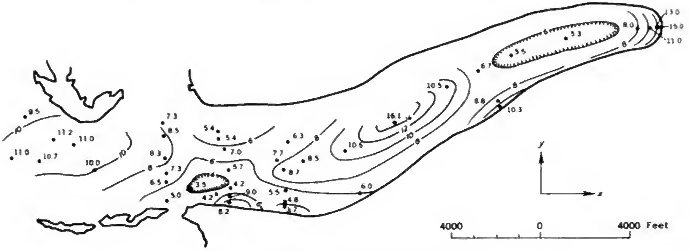

FIGURE 4.—Average surface lowering, 1948–54, in feet per year.

locity measurement (p. 10), but it conforms closely with the geometric symmetry plane of the cross sections. Data on the width, depth, area, ice perimeter and hydraulic radius[5] are given for the Castleguard sector cross sections in figure 6.

ABLATION

The regimen of Saskatchewan Glacier was not measured directly, but ablation measurements were made for comparison with surfaceward flow data. Records were kept of the lowering by melting of the ice surface at each velocity marker at irregular intervals during the 1952 field season and only as markers were reset after that. Values of ablation are reported in feet of ice melted per year. No density measurements were made. Probably the density of ice in the tongue ranges from 0.85 to 0.91, and the error due to this variance is less than the probable error of measurement.

Measured ablation rates are shown as a function of altitude in figure 7*a*. The rates reported here are average values for a period of observation of not less than a month, taken at the height of the ablation season. Points near the lateral margins are not included. These data show that ablation rate decreases slightly, but very irregularly, with increasing altitude. The noticeable scatter is presumably due to differences in ice density, roughness, exposure, and albedo at different points. The scatter is greatest in the higher altitudes where local differences in ice density and character are greatest; farther downglacier these local differences are largely eliminated by recrystallization and the scatter in ablation rates is less. Apparently ablation rates in 1953 were generally less than in 1952 and 1954.

The total ablation of ice decreases markedly from a high value at the terminus to zero at the firn limit, but the measured daily rates decrease only slightly. Therefore the total ablation at a given point must be determined largely by the length of the ice ablation season. Lengths of the actual ice ablation seasons can be estimated from data on positions of the temporary snowline; these data are shown in figures 7 and 8. The data in figure 7*b* show the progress of ablation during the seasons of 1952, 1953, and 1954. The time of the first permanent snowfall in autumn (marking the end of ablation of ice) is not known but is assumed to be about the end of September. In 1954 the season began at the lower altitudes not less than 6 weeks later than in 1952 or 1953, but the temporary snowline progressed rapidly upglacier and was about 1 month behind 1953 in the Castleguard sector (7,300 to 7,700 feet). On the basis of the measurements in 1952–54 and photographs and verbal reports from previous years, 1953 probably had the most "normal" ablation conditions of the years studied.

Velocity stakes were reset at irregular intervals during the summers so it was necessary to interpolate or extrapolate the observed ablation data to obtain equivalent values of total ablation during 1953. This required consideration of the different rates and lengths of ablation seasons in the three summers. The final 1953 equivalent ablation values may be incorrect by as much as a foot in some instances. Average yearly ablation values are presented as a function of altitude in figure 7*c* (marginal points excepted), and the variation of ablation over the

---

[5] The term "hydraulic radius" as commonly used in the hydraulics of rivers (area divided by wetted perimeter) is measured in a vertical plane. In this report hydraulic radius is defined similarly but is measured in a plane perpendicular to the surface.

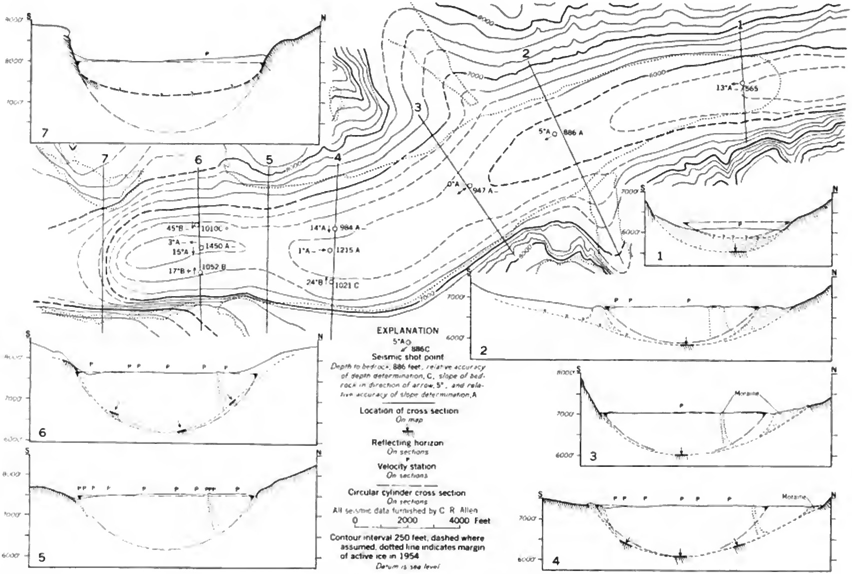
EXPLANATION
5°A
886C
Seismic shot point
Depth to bedrock, 886 feet, relative accuracy of depth determination, C, slope of bedrock in direction of arrow, 5°, and relative accuracy of slope determination, A
Location of cross section
On map
Reflecting horizon
On sections
P
Velocity station
On sections
Circular cylinder cross section
On sections
All seismic data furnished by C. R. Allen
0
2000
4000 Feet
Contour interval 250 feet, dashed where assumed, dotted line indicates margin of active ice in 1954
Datum is sea level
1
2
3
4
5
6
7
13°A
565
5°A
886 A
0°A
947 A
14°A
984 A
1°A
1215 A
24°B
1021 C
45°B
1010C
3°A
15°A
1450 A
17°B
1052 B
8000
7000
6000
S
N
Moraine

Figure 5.—Bedrock topography.

Coordinate distance x, feet	5000	10,000
Half width, feet	2040	2070
Maximum depth d, feet	1450	1240
Half area $A/2$, square feet	2.20×10^6	2.02×10^6
Half iced perimeter $P/2$, feet	2750	2630
Hydraulic radius $R (= A/p)$, feet	800	768
Shape factor R/d	0.552	0.620

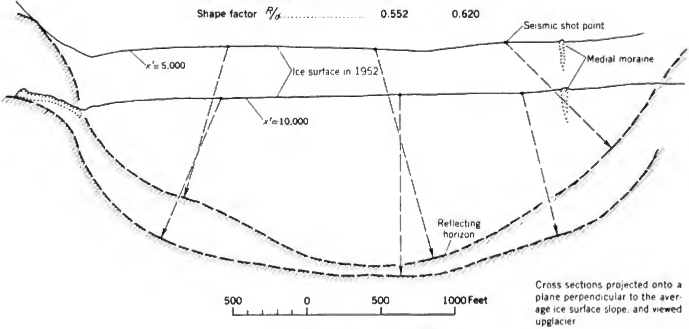

FIGURE 6.—Cross sections in Castleguard sector.

surface is mapped in figure 8. Rates of ablation and yearly ablation at each velocity stake are also given in page 22. These data show that seasonal ablation decreases smoothly, almost linearly, from terminus to firn limit. Ablation is greater along the south margin than in midglacier, especially in the Castleguard sector. This is undoubtedly due to the warmer climatic environment and the dirtier marginal ice; the effect may be especially pronounced in the Castleguard sector because of a lack of protecting cliffs. Total ablation is markedly less than normal on both sides of the medial moraine because of a persistent drift of snow that delays the ablation season. The average ablation, obtained by measuring areas within the ablation contours of figure 8, was 3.2 fpy in the highest part of Castleguard sector, 8.7 fpy in Castleguard sector as a whole, and 13.2 fpy for the remainder of the tongue below Castleguard sector.

SURFACE VELOCITY OBSERVATIONS

METHOD OF MEASUREMENT

The surface movement was measured by transit or theodolite surveys of velocity stations on the ice from fixed points on bedrock or stable deposits. Positions of the 15 transit points were determined by a triangulation survey using as its base line the distance between Mount Castleguard and "point 86" (9,376-foot peak), 2 survey points of the Alberta-British Columbia Interprovincial Boundary Survey. The base line length may be slightly in error; this would introduce a constant scale-factor error of negligible magnitude (probably less than 0.1 percent) in all measured velocities. Transit points were surveyed to an internal precision of about 1 foot for horizontal locations, and vertical locations are probably more precise. Nomenclature and locations of the transit stations and the form of the triangulation net are shown in figure 9.

All transit-point and velocity-station locations are referred to an arbitrary rectangular coordinate system defined as follows: $x = 6{,}000$, $y = 0$, and $z = 7{,}741.6$ feet at TP–1, the x- and y-axes are horizontal and the z-axis is directed upwards, and the bearing of TP–9 as seen from TP–1 is assumed to be 9°30′0″ to the right of the positive y-direction. The

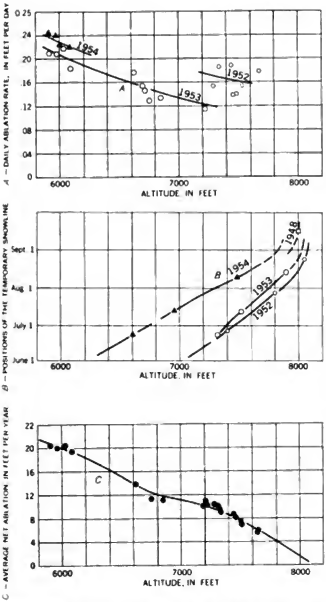

FIGURE 7.—Daily ablation rate, positions of the temporary snowline, and average yearly ablation expressed as a function of altitude along the central part of Saskatchewan Glacier.

y-axis is therefore directed approximately to 8°55′ west of true north. In addition, a 2-dimensional curvilinear coordinate system is defined as follows: $x' = y' = 0$ at $x = 0$, $y = +2{,}250$ feet; the positive x'-axis is directed along the horizontal projection of the "flow centerline"[6] in the direction of movement; the y'-axis is horizontal, perpendicular to x', and considered positive to the left when viewed downglacier. In the Castleguard sector the x, y and x', y' coordinate systems approximately coincide except for a translation of 2,250 feet in the y-direction. The x' coordinate measures the distance below the approximate firn limit, and the y' coordinate measures the distance away from the flow centerline. These coordinate systems are shown on figure 9.

Velocity stations on the glacier surface generally consisted of 1-inch wooden dowel stakes set snugly in holes bored 8 to 9 feet into the ice. Holes were drilled with a modified "Ahlmann spoon" (Allen and Smith, 1953, p. 757). Stakes were reset periodically as ablation demanded. About a cubic foot of sand was packed around each stake on top of the ice to retard enlargement of the hole by melting; this technique was only partly successful. Sighting was done to the center of the top of each stake, which generally remained tight until more than 8 feet had been exposed by ablation; only 3 times were stakes found to be loose in the holes a day or so after setting.

Originally 53 stakes were set and surveyed but only 47 were retained for velocity determinations. In addition, 4 stations of other types (aluminum pipestem, log structures) were surveyed, but 3 of these stations provided no information on vertical motion independent of ablation. The nomenclature and mean location of each of the 51 velocity stations is shown on figure 9, and the locations of the 34 stations in Castleguard sector during each field season are shown on figure 3. These stations form a longitudinal profile from terminus to above the firn limit and 8 partial or complete transverse profiles. The main ice stream south of the medial moraine in Castleguard sector was covered in greatest detail.

Angles were measured from bench marks to the velocity stations using either a precise transit or theodolite. Coordinate locations and velocity components were computed from the triangulation information. An essential part of this project was to measure the experimental error so that the reality of many apparent fluctuations in glacier velocity can be established. The precision of the measuring procedure is discussed on page 64. In general, the probable error of measurement of yearly velocities is about 0.7 fpy for horizontal components and 1.3 fpy for vertical components. Velocities measured over an interval of less than a year are generally not as accurate.

TIME-VARIATION OF VELOCITY

Most velocity stations were surveyed twice during each of two summers and once during the third summer so that the two average summer velocities could be compared with average velocities measured over 1 or 2 years. In addition, a few stations were sur-

---

[6] An imaginary line on the surface of the glacier that is everywhere parallel to the projection on the surface of the velocity vectors and which passes as closely through points of maximum surface velocity in transverse profiles.

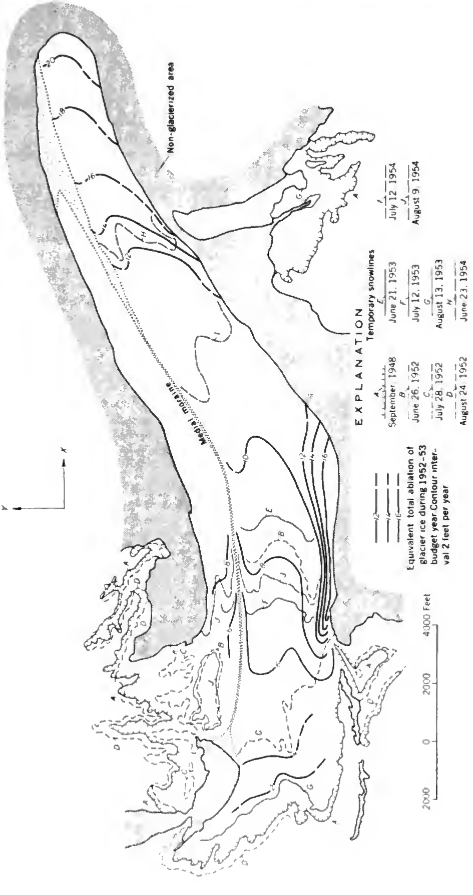

FIGURE 8.—Total ablation and positions of temporary snowlines.

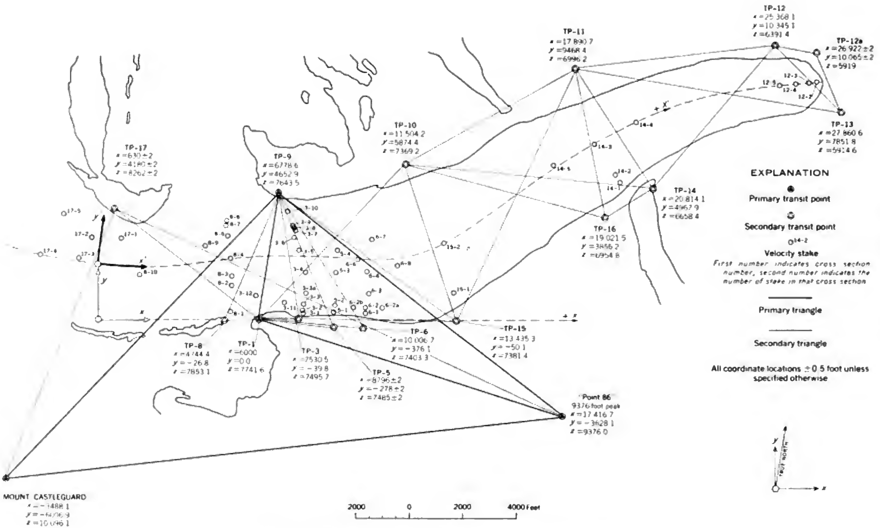

FIGURE 9.—Nomenclature of velocity stakes, transit points, and coordinate systems.

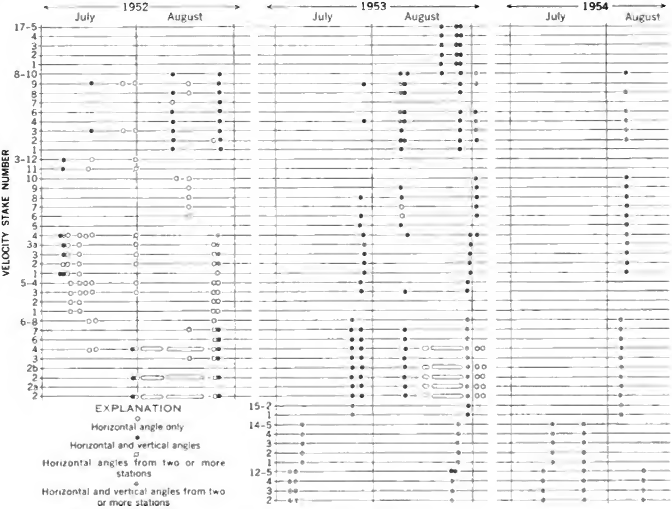

FIGURE 10.—Dates of survey of velocity stakes.

veyed at more frequent intervals to obtain detailed knowledge of the behavior of the velocity field as a function of time. The dates of survey of each stake are shown in figure 10. Measured summer and annual velocity components are reported in table 1, and coordinate locations of the stations at different times are given in table 10. All velocities are reported in feet per year; 1 fpy equals approximately 10^{-6} cm per second.

YEARLY CHANGES

Table 1 suggests a general deceleration from 1953 to 1954. Much of this apparent deceleration, however, was due to the movement of stations into locations of less velocity and does not indicate a general change in the field. However, there seems to be a slight residual deceleration (about 0.7 percent in the Castleguard sector) which is real. This could be due to the slight inequilibrium thinning because velocity of flow depends on a high power of ice thickness, but the effect is less than expected.[7]

SEASONAL VARIATIONS

In general, summer velocities are markedly greater than yearly average velocities. The percentage difference in the two velocities is apparently a function of position in the tongue (fig. 11) but the data do not show a consistent trend. The large variation in the data is probably due to short-interval jerkiness in the motion. Apparently summer and yearly velocities are nearly equal at the west end of Castleguard sector ($x' = 4,000$). The difference between yearly and summer velocity is greatest in the eastern part of Castleguard sector ($x' = 10,000$). Seasonal peaks

---

[7] Assuming Glen's experimental formula for creep (Glen, 1955, p. 528) and Nye's integrations for a glacier in a semicircular or very wide channel (Nye, 1952a, p. 84-85), the difference in velocity between surface and base should be approximately proportional to the 4th power of ice thickness. For the average observed thinning in Castleguard sector (6 years) this would suggest a 2 percent drop in differential velocity per year. The unknown effect of thinning on basal sliding must also be considered, however.

TABLE 1.—*Measured summer and annual velocity components, in feet per year*

[The location of each stake is shown on figure 9]
V_x = velocity component parallel to the x axis
V_y = velocity component parallel to the y axis
V_z = velocity component parallel to the z axis

Stake	1952 summer		1953 summer		1952-53 year[*]			1953-54 year[*]		
	V_x	V_z	V_x	V_z	V_x	V_y	V_z	V_x	V_y	V_z
17-5			[1,2] 209	[2] −28						
4			[1,2] 323	[2] −68						
3			[1,2] 378	[2] −45						
2			[1,2] 331	[2] −17						
1			[1,2] 305	[2] 3						
8-10			[1] 324							
9	285		244		253	17				
8	179	0	206	−17.4	182	−49	−13.4	215	−42	−15.3
7	[1] 185									
6	230		232	−11.2	232		[3] 9.1	238	−2.4	−9.1
4	266		255	−8.1	247		−8.1	246	12.7	−7.6
3	254	−12.5	[4] 252		[4] 241	[3] 14	−9.1	239	13.7	−7.9
2	239		[4] 235		231		[4] 6.2	230	19.7	−9.5
1	[1] 38	8.4			[1] 37		5.5			
3-12	[1] 212									
-11	[5] 194									
10	170				[1,2] 164			168		10.6
9					[1] 231			234		−3.4
8			[4] 204		230			235	18.5	−3.3
7					[1] 233			[1] 235		−2.7
6					[1] 243			[1] 244		−3.9
3-5								[1,4] 249		[3] −9.1
4	[6] 262	−21.5	253	−13.6	[4] 243	[4] −9.6	[3] −11.4	242	−6.0	−13.0
3a	222	−15.8	221	−9.8	[4] 204		[3] −12.0	206	−17.7	−10.2
3	[1] 156	−1.0	[1] 153	4.6	[1,4] 126		[3] 1.0	[1] 133		3.6
2	[1] 93				[1,4] 71			[1] 72		6.6
1	[1] 51		[1,4] 49		[1,4] 38		[3] 2.2	[1] 35		6.4
5-4	[1] 217	−10.1	[1] 241	−13.5						
3	[1] 213	−14.0	[1] 235	−13.4						
2	[1] 120	6.4								
1	[1] 67									
6-8			232	−4.3				183	40.3	−2.4
7			237	−13.9	[4] 186	[4] 19.3	[3] −5.3	194	23.2	−4.8
6			233	−12.9	214	1.6	−9.1	214		−11.5
4	237		225	−8.6	208	2.8	−10.4	[4] 209	[4] 18.6	−4.1
3			200	16.0	[4] 175			157.8	−6.8	3.3
2b			121	2.4				99.5	−17.5	7.8
2	129		119	10.5	[4] 99	[4] −22		98.3	−18.4	6.6
2a			109	10.3				86.4	−13.5	8.6
1	92	7.8	91	15.7	[4] 85	[4] −14.7		64.2	−17.4	7.8
15-2			[4] 141					143.2	73.1	1.9
1			[4] 44					38.5	20.7	6.2
14-5	122							120.3	54.1	2.3
4	104							94.9	40.6	1.6
3	118		[2] 137					107.5	45.8	1.8
2	118		[2] 125	[2] 17				98.6	37.0	1.6
1	98		[2] 65	[2] 6				85.4	33.5	9.0
5	53		25	1				38.4	5.3	−.8
4	45		26	−3				31.6	6.1	.6
3	22		19	−1				23.4	6.7	
2	20		11	−1				11.7	.5	3.8

[1] Horizontal flow direction assumed.
[2] Time interval 10 days or less.
[3] Uncertainty due to resetting ±1 fpy.
[4] Uncertainty due to resetting, ±3 fpy.
[5] $V_y = -71$.
[6] $V_y = 1.6$.
[*] The 1952-53 year and 1953-54 year values represent average velocities from late July or early August of the first year to a similar date in the second year.

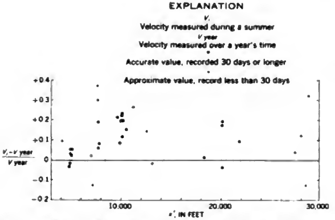

FIGURE 11.—Relative difference between summer and yearly velocity as a function of longitudinal position.

in velocity may progress from the firn, in winter, to the extreme terminus in fall in some valley glaciers (Hess, 1933, p. 73). It is possible that similar "waves" passed through the lower part of Castleguard sector during the July and August measuring periods.

SHORT-INTERVAL VARIATIONS

Glacier motion is known to be jerky with respect to measurements made on an hourly or daily schedule (Klebelsberg, 1948, p. 86–88), but the detailed form of the variations and their cause is not known. The velocity of stakes 6–1, 6–2, and 6–4 was measured once a day for 22 days in 1952 to obtain data on these short-interval fluctuations. A marked variation in flow rates was found (fig. 12).

In 1953 the measurements were continued at 12-hour intervals for 18 days (fig. 13) using 5 stakes arranged in a cross, one arm transverse and the other parallel to the direction of flow. Angles to the stakes were turned from a reference mark painted on the cliff near TP–9. Experimental error was greatly reduced by using a theodolite housed in a tent, and the precision of the measuring procedure was tested (see p. 64). Probable errors of measurement and the limits within which there is 95 percent confidence that the measurement was correct are shown with the velocity data in figure 13. Percent deviations from the mean velocity for each stake and the average deviation for each time interval of observation are shown in figure 14. Concurrently with the 1953 velocity measurements, atmospheric pressure at camp was recorded with a barograph, air temperature 4.5 feet above the ice at stake 6–2 was measured with a thermograph calibrated with a mercury thermometer, and synoptic observations of precipitation, cloud cover and wind were made at the time of each observation. These meteorological data are shown in figure 14. The standard deviation of velocity for each stake, expressed in feet per year and in percentage of the mean velocity, and the standard deviation of the velocity of each stake from the 5-stake average velocity during each time interval (s_{v-v_a}) is given in table 2.

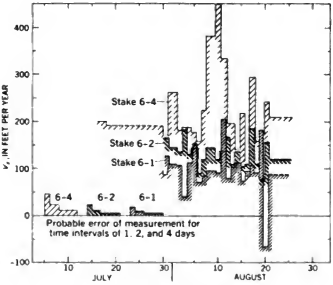

FIGURE 12.—Velocity variations in 1952.

TABLE 2.—*Standard deviation of velocity*

Stake	s_v (fpy)	s_v (percent)	s_{v-v_a} (percent)
6–1	0.127	51	18
2a	.210	77	42
2	.146	53	20
2b	.121	45	19
4	.309	57	40

These velocity data show profound fluctuations. Sudden increases in velocity up to 170 percent and decreases as large as 230 percent (resulting in backward motion) were recorded. As shown in table 2 the dispersion of velocity is greatest for the stake with the highest velocity (6–4). Percentagewise, however, a very slight increase in dispersion from margin (6–1) to midglacier (6–4) is shown. A profile downglacier, from 6–2b through 6–2 to 6–2a, shows a marked increase in dispersion. This effect could have been caused by a jerkiness predominantly in a direction more perpendicular to the line of sight of 6–2a than of 6–2b, or it might have been due to differences in the local structural environment. Stakes 6–2a and 6–4 moved independently, while stakes 6–1, 6–2 and 6–2b moved somewhat as a solid

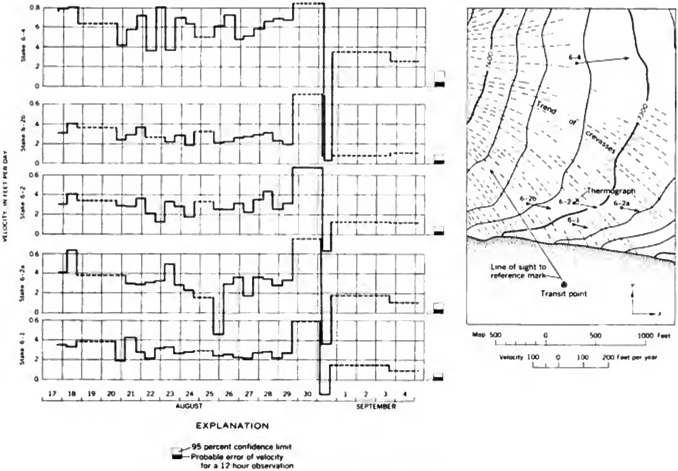

FIGURE 13.—Short-interval velocity variations in 1953.

unit (their dispersion from the 5-stake average motion averages only 19 percent).

Most of the erratic 12-hour fluctuations were not synchronous from one stake to another. However, fluctuations of 1.5 days or longer were often indicated simultaneously by all stakes. No evidence was found from the 1953 data that short-period "waves" of increased velocity traveled down or across the glacier, but there is a suggestion in the 1952 data that some major fluctuations in midglacier velocity were felt by the marginal stakes after a delay of 2 to 3 days.

A slight relation between air temperature and velocity is apparent. The air temperature was measured at a point 4.5 feet above the ice near stake 6-2, and is representative of the air temperature at this height at all 5 velocity stakes, but is not representative of the temperature at the measuring instrument location. Average velocity deviation is plotted as a function of temperature in figure 15. The correlation coefficient of these data to a linear relationship (fitted by the method of least-squares) is 0.307. By a standard statistical analysis (Hoel, 1947, p. 89) it was determined that this correlation was not significant and that there is about 1 chance in 6 that as good an apparent relation as this could be obtained from a random sampling of unrelated variables.

Precipitation seems to have some effect on velocity. Perhaps it is significant that the great increase in velocity shown by all stakes August 29 to 31 coincided with the heaviest rainfall. However, these rainfall data are not quantitative and no firm conclusions can be drawn. Barometric pressure, wind, and cloudiness show little or no relation to velocity. Incoming radiation from sky and sun is a function of the degree of cloud cover; so it seems that the velocity and radiation data are not related—contrary to many statements in the literature (Drygalski and Machatschek, 1942, p. 111–112; Klebelsberg, 1948, p. 86).

The jerky motion cannot be explained satisfactorily. The sharpest variations are not synchronous from stake to stake, therefore, they cannot be due to any general or regional effects such as weather

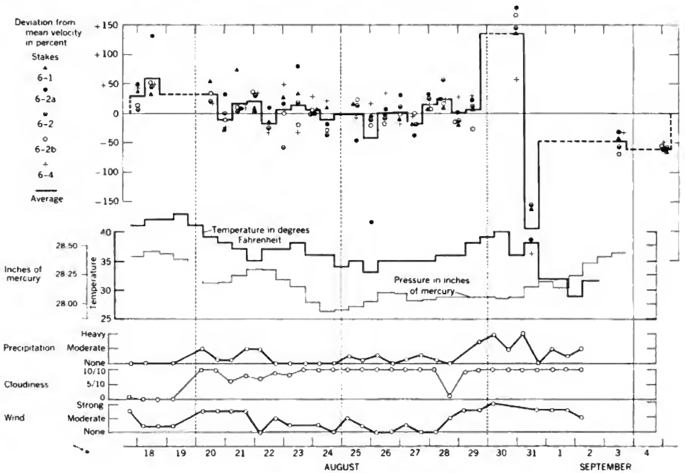

FIGURE 14.—Velocity deviations and meteorological observations, 1953.

changes. Longer variations might be caused, or aided, by lubrication of shear surfaces or the bedrock channel during warm or wet periods. The jerkiness involves domains of limited size (not more than a few hundreds of feet in horizontal dimension) because these domains cannot be larger than the distance between stakes. Therefore, irregular differential movements which may be due to irregular tilting or fracturing of blocks between crevasses, must take place within the ice. However the observation that dispersion increases from stake 6–2b to 6–2a suggests that the main direction of jerkiness (if there is one) is not perpendicular to the crevasses. If there was a preferred direction of jerkiness perpendicular to the crevasses, the dispersion would have appeared larger at stake 6–2b than at 6–2a because of the method of observation (fig. 13). Irregular rotations of the intercrevasse blocks may contribute to the jerkiness. Local domains of plastic shearing probably become active sporadically because ice shows negligible strain hardening. Behavior of this type has been observed along shear planes in an ice cliff in Greenland (White, 1956, p. 40–46) and in the Alps (Chamberlin, 1928, p. 16–19), and on a microscopic scale in laboratory experiments (Ivanov and Lavrov, 1950). This effect could have caused the observed velocity fluctuations.

SUMMARY OF TIME-DISPERSION OF VELOCITY

The velocity at a given point on the glacier surface shows a complete time spectrum of variations. Observations for months or years indicate variations that may be due to changes in melt water lubrication or changes in ice thickness and are generally synchronous between nearby points. Fluctuations having wavelengths sufficiently short to be detected in daily or twice-daily observations reflect irregular differential movements of small domains of ice and may be due to local sporadic shearing. The amount of the fluctuations decreases with increasing wavelength (period of observation) as shown in figure 16. This suggests two conclusions of great importance: (1) The accuracy of a single velocity observation, as a measure of "average" velocity, depends on the length

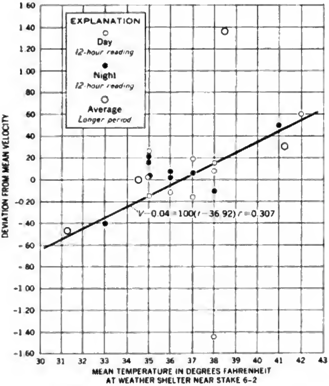

FIGURE 15.—Relation of deviation of velocity to temperature.

of the observation period even with perfect experimental procedure. (2) The flow appears to be comprised of a large number of individual short wavelength "pulses" or fluctuations. The relation between dispersion and wavelength might suggest the magnitude of individual fluctuations that make up the flow, but the dispersion values for long periods of observation are too crude for firm conclusions.

CONFIGURATION OF THE SURFACE VELOCITY FIELD

Accumulation or ablation represents a flux of ice through the surface of a glacier; therefore streamlines of ice flow are generally not parallel to the surface. The rates of accumulation or ablation and flow vary across a glacier; therefore streamlines of flow are generally not parallel to the valley walls. Thus measurement of three components of velocity of the ice at each point is necessary to define the velocity field. Components of velocity parallel to the x, y, and z coordinate axes were measured by triangulation and other components of the vector ($V_{x'}$, $V_{y'}$, V_z) resolved from these.

The following components are measured in a vertical direction. Upwards movement is considered positive. All components are referred to a coordinate system fixed in space unless otherwise specified.

V_p The velocity of a particle of ice.

V_a The velocity of accumulation or ablation (a positive value denotes accumulation, a negative value ablation), relative to a coordinate fixed in the ice very close to the surface.

V_d The velocity of rise of the glacier surface, due to ice motion, which would occur if there were no accumulation or ablation. This velocity component relates the moving coordinate system of V_a to the fixed coordinate system.

V_s The actual velocity of rise of the glacier surface, due to the action of both V_a and V_d. $V_s = V_a + V_d$.

These components are illustrated in figure 17. Measured and assumed values for the different components of the average velocity at each stake are reported, along with x' and y' coordinate locations and surface slope (tan α), in table 3. The observed variation of $V_{x'}$ and V_d over the whole of the tongue

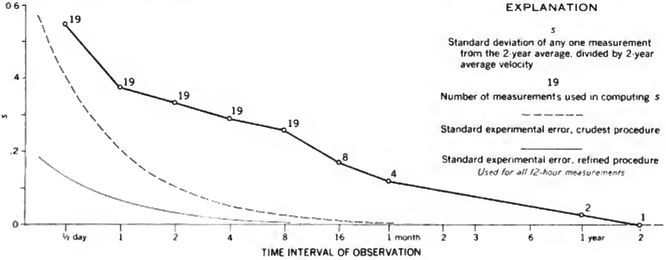

FIGURE 16.—Velocity dispersion spectrum at stake 6-4.

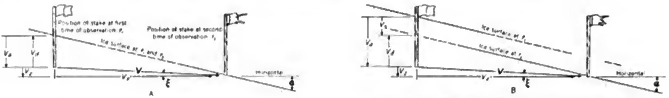
Position of stake at first time of observation t_1
Position of stake at second time of observation t_2
Ice surface at t_1 and t_2
V_a
V_d
V_z
V
$V_{x'}$
ξ
Horizontal
α
A
V_s
Ice surface at t_1
Ice surface at t_2
B

A Special case of a point on the centerline of the flow of an equilibrium glacier. The diagram is referred to an observer fixed in space. These quantities are defined:

- **V** Velocity of a particle of ice; in general this refers to a particle of ice adjacent to the base of a velocity stake. The scalar magnitude of **V** is given by V. Both **V** and V are always considered positive.
- **α** Slope of the surface, measured from the horizontal in the direction of **V**. This angle is considered negative if the surface slopes down in the direction of glacier movement.
- **ξ** Slope of **V** measured from the horizontal in the direction of **V** and considered positive if **V** points upwards in the direction of movement. $\tan \xi = \frac{V_z}{V_{x'}}$
- $V_{x'}$ Component of **V** in the direction of the x' axis, taken positive in the direction of the $+x'$ axis. $V_{x'} = V \cos \xi$ (See below)
- V_z Component of **V** in the vertical direction, taken positive upwards. $V_z = V \sin \xi$
- V_a Component in a vertical direction of the velocity of surface accumulation (positive) or ablation (negative). This is measured by the change in position of the ice surface on a stake fixed in the ice. This velocity is relative to a coordinate system moving through space with the ice.
- V_d Component in a vertical direction of velocity of rise (positive) or fall (negative) of the ice surface, due solely to ice motion, which would occur if there were no surface ablation or accumulation. $V_d = V_z - V_{x'} \tan \alpha = V (\sin \xi - \tan \alpha \cos \xi)$
- t_1, t_2 Two different times of observation, $t_2 > t_1$

B Special case of a point on the centerline of the flow, but for a nonequilibrium glacier. In addition to the quantities given above, an additional quantity is defined:

- V_s Component in a vertical direction of the net velocity of rise (positive) or fall (negative) of the glacier surface, due to the action of both V_a and V_d. $V_s = V_a + V_d$

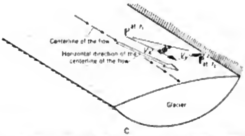

C General case for a point off the flow centerline for a nonequilibrium glacier. The following additional components are defined and the formula for $V_{x'}$ is modified as follows:

- **ϕ** Angle between **V** and the x' axis, measured in a horizontal plane, considered positive on the $+y'$ side of the x' axis.
- $V_{y'}$ Component of **V** in the direction of the y' axis. $V_{y'} = V \sin \phi$
- $V_{x'} = V \cos \xi \cos \phi$

Figure 17.—Definition sketch of velocity components.

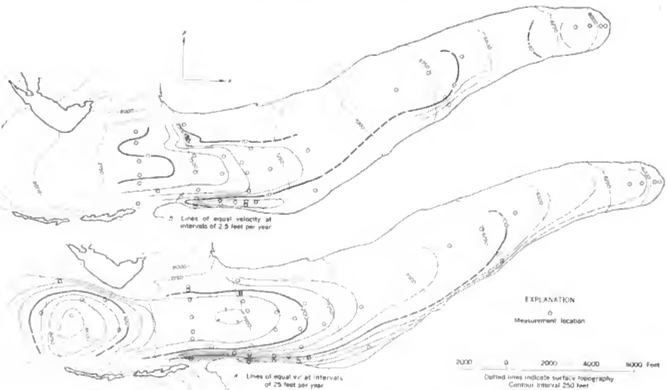
5000
Lines of equal velocity at intervals of 2.5 feet per year
Lines of equal $V_{x'}$ at intervals of 25 feet per year
EXPLANATION
o
Measurement location
2000
0
2000
4000
6000 Feet
Dotted lines indicate surface topography
Contour interval 250 feet
Datum is sea level

Figure 18.—Distribution of $V_{x'}$ and V_a on Saskatchewan Glacier. A, refers to $V_{x'}$; B, refers to V_a.

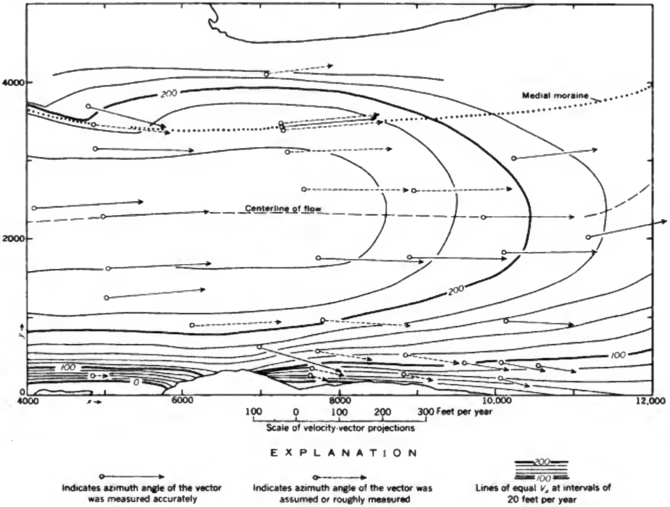
4000
2000
0
y
4000
x
6000
8000
10,000
12,000
200
100
0
Medial moraine
Centerline of flow
100 0 100 200 300 Feet per year
Scale of velocity-vector projections
EXPLANATION
Indicates azimuth angle of the vector was measured accurately
Indicates azimuth angle of the vector was assumed or roughly measured
200
100
Lines of equal V_x at intervals of 20 feet per year

FIGURE 19.—Distribution of $V_{x'}$ and horizontal projection of velocity vectors in Castleguard sector.

is shown in figure 18. For the Castleguard sector the variation of $V_{x'}$ is shown in figure 19, $V_{y'}$ in figure 20, V_z in figure 21 and V_d in figure 22. Profiles of $V_{x'}$, V_z, V_d and surface slope along the centerline are shown in figure 23. Transverse profiles of $V_{x'}$ in Castleguard sector are presented in figures 24 and 25.

HORIZONTAL DOWNGLACIER COMPONENT

This component ($V_{x'}$) ranges from 383 fpy at the firn limit to 12 fpy at the extreme terminus. The data show variations similar to that commonly observed on valley glaciers—gradual decrease from firn limit to terminus because of the decreasing quantity of ice transported, and a decrease from centerline toward margin because of the drag of the valley walls. The decrease along the centerline is uneven because of changes of surface slope (fig. 23). In Castleguard sector the velocity is constant within 10 percent across the central half of the glacier but falls off rapidly in the outer quarters of the width to a very small amount at the margins (fig. 24). Extrapolation of the transverse profiles shows that margin slip along the south border of the glacier in Castleguard sector is less than 5 percent of the centerline velocity (fig. 25) except where a resistant bedrock bulge constricts the flow between $x' = 6{,}000$ and $x' = 7{,}000$. In this area the valley wall is vertical, strongly polished and striated, and the marginal ice is highly crevassed and contorted; whereas elsewhere moraine-covered stagnant ice borders the flowing glacier, crevasses die out toward the margin, and the transition from flowing to stagnant ice occurs over a zone several feet wide.

HORIZONTAL SIDEWAYS COMPONENT

A transverse component of flow ($V_{y'}$) in the ablation zone of a valley glacier results from decreased marginal velocity in relation to average of the cross section (Nielsen, 1955, p. 11–21). This effect is clearly shown in the transverse profiles of

TABLE 3.—*Velocity components, slope, ablation, and surface lowering at velocity stakes*

Stake	Quantities computed directly from the raw triangulation and topographic map data							Quantities computed from the data in the left-hand columns using formulas given in figure 17						Quantities which were directly observed		
(fig. 9)	x' (feet)	y' (feet)	z (feet)	α	V_x (fpy)	V_y (fpy)	V_z (fpy)	ϵ	ϕ	V (fpy)	$V_{x'}$ (fpy)	$V_{y'}$ (fpy)	V_a (fpy)	V_e summer (fpd)	V_e year (fpy)	V_s (fpy)
17–5	−1,630	+1,700	8,237	−4°44′	209	−111	−28	−6°44′	...	239	...	...	−9	...	...	−9
4	−2,200	0	8,263	−4°14′	323	−25	−66	−11°52′	[1]0	330	324	[1]0	−50	...	...	−11.0
3	−770	+150	8,125	−6°44′	378	−53	−45	−6°42′	[1]0	385	383	[1]0	+3	...	...	−10.7
1	−790	+1,050	8,070	−8°52′	305	−59	+3	+0°34′	...	311	...	...	+48	...	...	−11.0
8–10	+1,580	−230	7,800	[2]−2°50′	324	...	...	...	...	...	...	...	...	...	...	...
9	+4,080	+131	...	[2]−2°00′	253	+17	...	...	...	...	...	...	...	...	...	...
8	+4,788	+1,432	7,697	−3°15′	196	−46	+14.3	+3°59′	−15°41′	204	196	−56.2	−3.0	...	[2]−6	−7.3
7	+4,800	+1,130	...	...	202	[2]−19	...	...	...	...	...	[2]−28.6	...	...	...	...
6	+4,888	+903	7,667	−2°36′	235	−2.4	−9.1	−2°13′	−3°41′	236	235	15 −.1	+1.8	...	[2]−6	−8.5
4	−4,977	0	7,636	−1°43′	246.5	+12.7	−7.9	−1°50′	[1]0	247	247	[1]0	−.5	...	[2]−7	−8.3
3	+5,089	−627	7,650	−1°58′	240	+13.7	−8.4	−2°00′	+0°14′	241	241	+1.0	−.2	−0.177	−5.6	−7.3
2	+5,043	−993	7,692	−2°02′	230.5	+19.7	−7.8	−1°57′	+1°58′	231	231	+7.9	+.8	...	[2]−6	−6.5
1	+4,875	−1,985	[2]7,680	[2]−0°00′	37	[2]0	+5.5	+7°51′	[2]+22°00′	37	34	[2]+15	+5.5	...	[2]−10	−5.0
3–12	+6,323	−1,390	[2]7,630	−4°05′	212	[2]+12	...	...	...	...	...	...	...	...	...	...
11	+7,090	−1,700	[2]7,490	−0°10′	172	−57	...	...	...	...	...	...	...	...	...	...
10	+7,066	+1,790	[2]7,507	−3°35′	168	[2]+20	+10.6	+3°37′	...	166	...	...	[2]+21.1	...	−7.6	...
9	+7,254	+1,168	...	−2°24′	232.5	[2]+19.5	−3.4	−0°50′	+5°32′	233	232	+22.5	+6.3	...	−3.9	...
8	+7,273	+1,119	7,518	−2°23′	232.5	+18.5	−3.3	−0°49′	+5°18′	233	232	+21.5	+6.4	...	−6.1	−5.4
7	+7,287	+1,076	...	−2°24′	234	[2]+17.5	−2.7	−0°40′	+5°00′	235	234	+20.5	+7.0	...	−4.4	...
3–6	+7,338	+794	[2]7,480	[2]−2°50′	243.5	[2]+9	−3.9	−0°55′	+2°49′	244	244	+12	[2]+8.3	...	−6.9	−5.4
5	+7,551	+313	7,507	[2]−2°24′	249	[2]0	−9.1	−2°06′	+0°41′	249	249	+3	[2]+1.4	...	−5.2[2]	−7.0
4	+7,735	−550	7,500	−4°20′	242.5	−6.0	−12.2	−2°53′	−0°43′	243	243	−3	+6.2	−0.129	−7.4	−5.7
3a	+7,787	−1,320	7,450	−4°02′	205	[2]−10	−11.1	−3°06′	−2°31′	206	205	−9	+3.4	...	−8.6	−4.2
3	+7,730	−1,720	7,428	−2°42′	138	[2]−20	+2.3	+0°57′	−7°26′	139	138	−18	+8.8	...	−9.5	−7.0
2	+7,669	−1,954	7,420	−2°55′	71.5	[2]−13.7	+6.6	+5°11′	−10°14′	73	72	−13	+10.3	...	−12.5	−8.2
1	+7,624	−2,045	7,408	−2°42′	36.5	[2]−8.2	+6.4	+9°51′	12°32′	38	36	−8	+8.1	...	[2]−16	...
5–4	+8,840	+320	[2]7,468	−3°40′	228	[2]+5	−11.8	−2°58′	+1°15′	228	228	+5	+2.8	...	...	...
3	+8,860	−300	[2]7,454	−3°35′	223	[2]−1.5	−13.4	−3°27′	−0°23′	223	223	−1.5	+.6	...	[2]−8	−6.0
2	+8,880	−1,755	[2]7,393	−3°11′	125	[2]−17.4	+6.4	−2°54′	−7°56′	127	125	−17.4	+13.3	...	−9.2	...
1	+8,830	−2,005	[2]7,360	...	70	[2]−14.6	...	...	−11°47′	...	70	−14.6	...	...	[2]−11	...
6–8	+11,200	−320	7,281	−2°45′	183	+40.5	−2.4	−0°44′	...	188	...	...	+6.6	−.104	[2]−10.5	−8.9
7	+10,245	+746	7,340	−3°40′	193	+23.2	−4.8	−1°25′	+6°27′	194	193	+21.8	+7.6	...	[2]−9	−6.3
6	+9,870	0	7,354	−4°24′	214	+1.6	−10.3	−2°46′	[1]0	214	214	[1]0	+6.2	...	...	...
4	+10,100	−427	7,329	−3°24′	209	+2.8	−7.3	−2°00′	+0°20′	209	209	+1.2	+5.1	−.184	[2]−9.7	−8.7
3	+10,129	−1,312	7,322	−3°01′	168	−6.8	+3.3	+1°12′	−2°54′	158	158	−8.0	+5.0	...	[2]−10	−5.5
2b	+9,614	−1,840	7,323	−3°24′	99.5	−17.0	+7.8	+4°24′	−10°03′	101	100	−17.7	+13.8	−.147	−14.8	−4.8
2	+10,068	−1,833	7,305	−3°24′	98.3	−18.4	+6.6	+3°47′	−11°02′	100	98	−19.1	+12.4	−.147	−15.0	−4.8
2a	+10,543	−1,874	7,287	−3°46′	86.4	−13.5	+8.6	+5°40′	−9°18′	88	86	−14.1	+14.3	−.167	−15.9	−4.6
1	+10,068	−2,035	7,290	−3°11′	64.2	−17.4	+7.8	+6°42′	−15°37′	67	64	−17.9	+11.4	...	−17	−3.7
15–2	+13,080	0	7,194	−2°35′	143.2	+73.1	+1.9	+0°41′	[1]0	161	161	[1]0	+9.2	...	[2]−10	−10.5
1	+12,570	−1,670	7,212	...	38.5	−20.7	+6.2	+8°05′	−0°57′	44	43.7	−1.1	...	...	[2]−11	...
14–5	+18,300	+170	6,848	−3°20′	120.3	+54.1	+2.3	+1°00′	[1]0	132	132	0	+9.9	−0.133	−11.2	−10.5
4	+21,800	0	6,622	−4°15′	94.9	+40.6	+2.7	+1°30′	[1]0	103	103	[1]0	+10.2	−.175	−13.8	−5.8
3	+20,120	0	6,753	−3°15′	107.5	+45.8	−1.8	+0°53′	[1]0	117	117	[1]0	+8.4	−.129	−11.2	−6.7
2	+20,150	+1,400	6,720	−4°25′	98.6	+37.0	+1.6	+0°52′	−2°43′	105	105	−5.0	+10.0	−.146	−12.3	−8.8
1	+20,150	+1,780	6,712	−4°35′	85.4	+33.5	+9.0	+5°38′	−1°49′	92	92	−2.9	+16	−.154	−14.2	−10.3
12–5	+27,493	0	6,098	−7°10′	38.4	+5.3	+1	+1°28′	[1]0	39	39	[1]0	+5.9	−.202	−19.3	−8.0
4	+27,990	0	6,040	−7°55′	31.6	+6.1	+1	+1°47′	+3°03′	32	32	+1.7	+5.5	−.220	−20.3	−11.0
3	+28,431	0	5,966	−10°45′	23.4	+6.7	[3]+2	+4°44′	+8°18′	24	24	+3.5	+6.5	−.224	−20.1	−13.0
2	+28,691	0	5,920	−10°50′	11.7	+.5	+3.8	+17°30′	−5°14′	12	12	−1.1	+6.1	−.227	−20.3	−15.0

[1] These points determine the flow centerline.
[2] Approximate value.
[3] Assumed value.

the 3, 6, 15, and 14-series (table 3). In the lowest of the profiles (the 14 series, $x' = 20{,}000$) the marginal flow diverges from the centerline by 4.0 fpy, but the angle the right margin makes with the centerline of the glacier is such that the horizontal velocity component normal to the margin is about 34 fpy. Opposite Castleguard camp ($x' = 10{,}000$) the transverse velocity along the south margin is about 18 fpy relative to the centerline (fig. 20) and 9 fpy relative to the margin. On the other hand, the lateral flow in the 8-series profile ($x' = 5{,}000$) is strongly convergent. This is undoubtedly due to the supply of ice from both margins at and upglacier from this profile, and the bedrock bulge at $x' = 6{,}500$ may have an influence. The transition from convergent to divergent flow occurs at $x' = 6{,}500$ and shows as a "saddle" in the map of $V_{y'}$ (fig. 20).

ABSOLUTE VERTICAL COMPONENT

This component (V_z) was measured in relation to a coordinate system fixed in space and thus records the absolute rate of change in elevation of a particle of ice. Along the centerline, the vertical velocity is negative (downwards) from the firn limit through Castleguard sector but slightly positive (about 2 fpy) and relatively constant over the lower half of the tongue (fig. 23). In transverse profiles the vertical velocity is invariably upwards along the margins, giving a pronounced transverse gradient in the upper parts of the glacier. In Castleguard sector a large

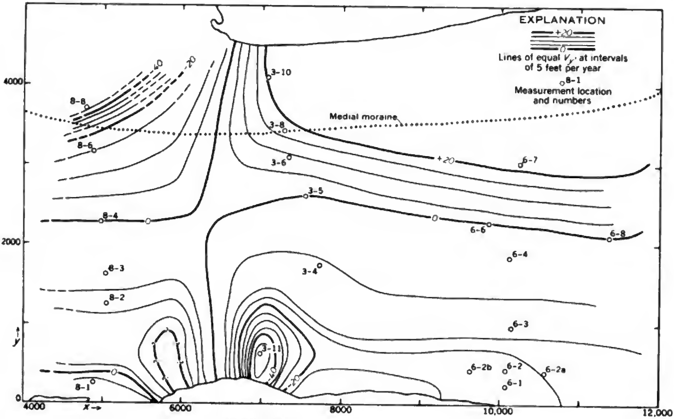

FIGURE 20.—Distribution of V_y, in Castleguard sector.

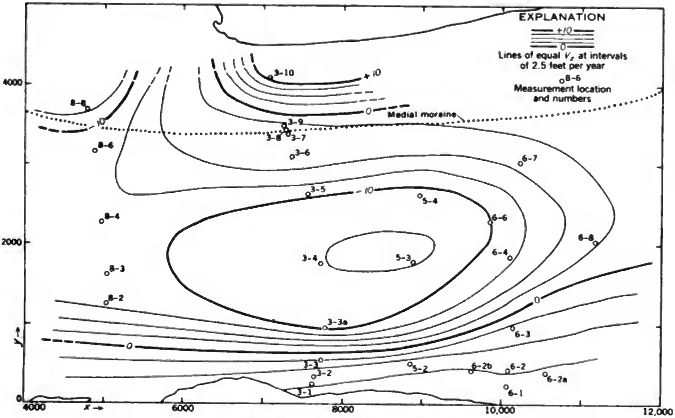

FIGURE 21.—Distribution of V_z in Castleguard sector.

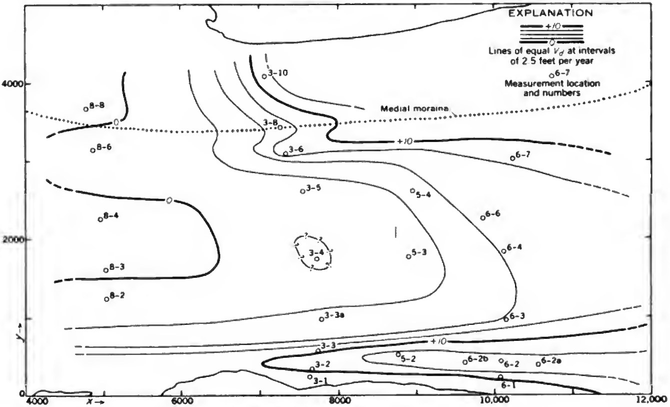

FIGURE 22.—Distribution of V_d in Castleguard sector.

oval-shaped area in midglacier shows negative vertical motion of more than 10 fpy (fig. 21).

COMPONENT OF SURFACE RISE DUE TO ICE MOTION

This component (V_d) is the velocity of rise or fall of the ice surface which would take place, due to ice motion, if there were no accumulation or ablation on the surface. With respect to a coordinate system fixed in space, it represents a flow of ice towards or away from the ice surface. Therefore it is not necessarily equal in magnitude to the flux of ice through the surface (the accumulation or ablation, V_a) because the surface is generally sweeping upwards or downwards in space. This component should not be confused with V_z (the absolute change in elevation of a particle of ice) which depends on the angle between the velocity vector and the horizontal. The component V_d depends on the angle between the velocity vector and the ice surface: If the velocity vector is inclined downwards more steeply than the surface slopes, V_d will show a flow of ice down and away from the surface (negative). If the velocity vector parallels the surface, V_d is zero. If the velocity vector plunges less steeply than the surface, or is horizontal, or is inclined upwards, V_d will show a flow of ice toward the surface (positive).

If the elevation of the ice surface is stationary in space for a long period (an equilibrium glacier), V_d and V_a (the accumulation velocity) are equal in magnitude but opposite in sign. Thus the component V_d in an equilibrium glacier compensates for accumulation or ablation at the ice surface. This relation has been pointed out by Reid (1896, p. 917–918; 1901, p. 750).

If the elevation of the ice surface is not stationary in space for a long period, the glacier is in a nonequilibrium condition. V_d over- or under-compensates the accumulation or ablation, resulting in a velocity of surface thickening or thinning (V_s) according to the relation

$$V_s = V_a + V_d$$

This relation follows directly from the vector diagram (fig. 17).

The quantity V_d can be postulated as the sum of a laminar-flow component and a component due to horizontal divergence of velocity. The laminar-flow component represents motion parallel to the bed and results in a surface change if the bed and surface are not parallel.

A glacier with negligible internal or basal ablation and composed of ice which does not change in density

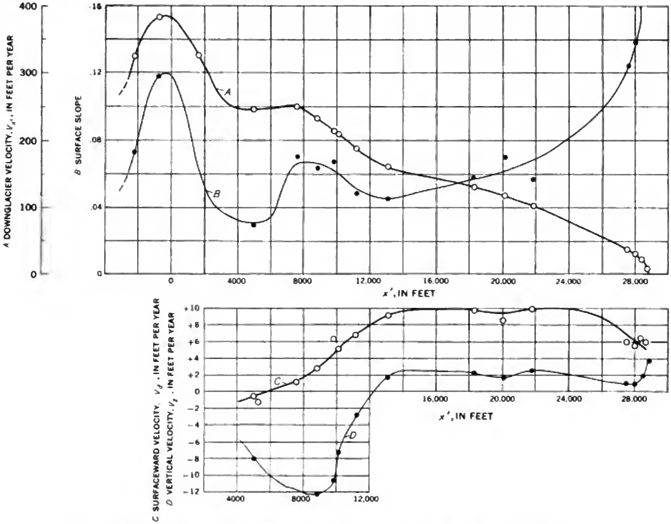

FIGURE 23.—Downglacier, surfaceward, and vertical velocities and surface slope along the flow centerline.

with time, measurements of V_d on the surface can be used to determine the ice flow into or out of specific parts of the glacier. This can be seen as follows: In the ensuing discussions of flow, attention will be directed on points or regions fixed in space, and the flow of material through these regions will be studied (the so-called Eulerian method of hydrodynamics). Consider a surface $\mathbf{S}$ parallel and in the same general vicinity as the glacier surface, but fixed in space and time. If the velocity of the ice is given by $\mathbf{V}$, the velocity of flow through a small element of that surface $\delta\mathbf{S}$ is $\mathbf{V}\cdot\delta\mathbf{S}$. If $\mathbf{V}$ and $\delta\mathbf{S}$ intersect a horizontal plane at angles of ξ and α respectively, the velocity of flow through $\delta\mathbf{S}$ is given by $\mathbf{V}\cdot\delta\mathbf{S} = V \sin(\xi - \alpha)\,\delta S$ wherein V and δS represent the scalar magnitudes of $\mathbf{V}$ and $\delta\mathbf{S}$. The projection of $\delta\mathbf{S}$ onto a horizontal plane (a map) has the area $\delta S \cos \alpha$. From figure 17, $V_d = -V(\tan \alpha \cos \xi - \sin \xi)$. Therefore $V_d \cdot \delta S \cos \alpha = \mathbf{V}\cdot\delta\mathbf{S}$. Thus, the total flow velocity through $\mathbf{S}$, that is the integral of $\mathbf{V}\cdot\delta\mathbf{S}$ evaluated over the irregular surface $\mathbf{S}$, can be determined by the simple operation of summing products of V_d and map area. Unless there is appreciable density change or internal ablation, this sum measures the net flow of ice into the volume underlain by $\mathbf{S}$ because of the restriction of continuity. Therefore measurements of V_d can yield valuable information on ice discharge and velocity at depth.

Along the centerline, V_d is negative from the firn limit to $x' = 6{,}000$, but in Castleguard sector it increases downglacier to a value of +10 fpy at $x' = 14{,}000$, and is constant at this value for the lower half of the tongue except for a slight decrease at the terminus (figs. 18, 23). In transverse profiles V_d increases away from the centerline reaching a maximum near, but not at, the margin (fig. 22).

Actual lowering of the surface of Saskatchewan Glacier was measured during the interval 1948–54, showing that this glacier was in a nonequilibrium condition. Values of V_d can be compared with surface lowering and ablation (fig. 26). These three quantities were measured independently: V_d was measured by triangulation surveys of the movement of a stake in space, V_a by the depression of the ice surface down the length of the stake, and V_s by topographic surveys of the glacier at two different times. The poor correlation between the two sets of data is attributed to the relative inaccuracy of the lowering and ablation values. The surface-lowering velocity was measured from 1948 to 1954 whereas the other velocities were measured from 1952 to 1954. Probably the rate of surface lowering or the ablation has changed with time; these possibilities would also cause scatter in figure 26.

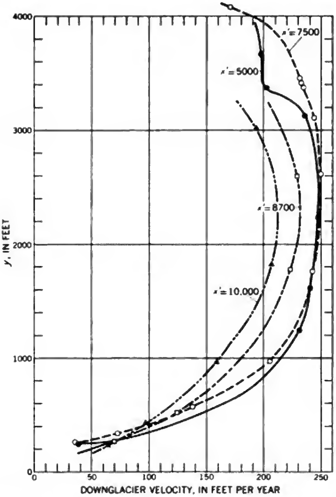

FIGURE 24.—Downglacier velocity along four transverse profiles in Castleguard sector.

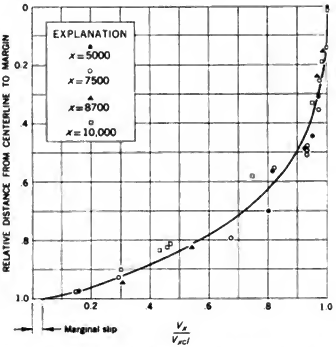

FIGURE 25.—Ratio of downglacier velocity (V_x) to centerline downglacier velocity (V_{xcl}) as a function of relative distance from the centerline for four transverse profiles.

The average value of V_d obtained by measuring areas within contours of V_d on figure 18 was 4.1 fpy in Castleguard sector and 9.9 fpy for the tongue below Castleguard sector. The average ablation for these two areas was 8.7 fpy and 13.2 fpy, respectively. The differences between these values 4.6 fpy and 3.3 fpy, reaffirm the previous conclusion that

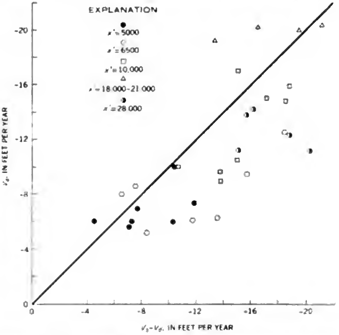

FIGURE 26.—Ablation velocity (V_a) compared with difference between surface lowering velocity (V_s) and surfaceward flow velocity (V_d).

thinning was actually slightly greater in Castleguard sector than in the lower part of the tongue.

DIRECTION OF THE VELOCITY VECTOR

The plunge of the velocity vector of a particle of ice shows a gradual change along the flow centerline from a slight negative angle in the Castleguard sector to a positive angle at the terminus (pl. 5). The plunge is slightly greater than the surface slope in the upper part of Castleguard sector. The angle between the ice surface and velocity vector increases steadily downglacier reflecting increase or constancy in V_4 and decrease in $V_{r'}$ in this direction.

Velocity vectors in a map view converge in the upper part of Castleguard sector and diverge in the lower part, and the angular spreading increases slightly but steadily downglacier (fig. 19).

In a transverse profile perpendicular to the ice surface the velocity vectors spread away from the centerline (fig. 27). It is especially interesting to note that at the margin the vectors in this plane did not parallel the margin. This angular relationship is necessary so that ablated ice at the margin can be continually replenished.

VELOCITY PATTERN AT THE MEDIAL MORAINE

A medial moraine represents the contact between two separate streams of ice. Currents of ice in a single stream moving side by side at different velocities have been observed (Battle, 1951, p. 560), and it has been suggested that the ice streams on the two sides of a medial moraine might flow independently. This would cause severe shearing along the moraine. Foliation, a structure in the ice apparently caused by shear, is intense along and in the medial moraine of Saskatchewan Glacier. It is instructive to examine the velocity pattern there.

A sharp change in velocity at the moraine occurs at the highest transverse profile, $x' = 5{,}000$ (fig. 24). The trunk glacier flows 235 fpy at a point 200 feet from the medial moraine, only 11 fpy less than the centerline velocity. The velocity at the center of the moraine is only 202 fpy, and 300 feet farther north (well into the tributary ice stream) the velocity is 198 fpy. This indicates a strong transverse gradient in velocity along the trunk-glacier side of the medial moraine.

On the other hand, the transverse gradient in velocity at $x' = 7{,}500$ shows no great change at the medial moraine (fig. 24). Three stakes were placed in a 92-foot transverse profile across the moraine to measure shearing but the difference in horizontal velocity recorded between the end stakes is only 1.5 fpy, which is close to the experimental error. The difference in vertical velocity is only 0.7 fpy. This measuring location is not conveniently located for accurate triangulation so horizontal converging or spreading of velocity vectors across the moraine could not be measured.

These results show that the flow of the tributary glacier, which initially has no component parallel to the main glacier, is gradually picked up by the trunk glacier for a distance of less than 4,000 feet. Most of this eastward flow is imparted in the first 2,200 feet. Beyond the 4,000-foot interval the trunk and tributary glaciers flow together as a unit and the medial moraine ceases to mark a discontinuity in velocity.

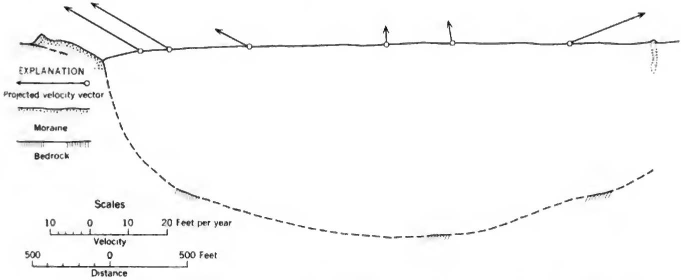

FIGURE 27.—Velocity vectors projected onto a transverse plane perpendicular to the glacier surface at $x' = 10{,}000$, viewed upglacier.

ENGLACIAL VELOCITY MEASUREMENTS

The velocity distribution within a flowing glacier has long been a matter of theoretical speculation but few actual measurements have been made. Gerrard, Perutz, and Roch (1952) measured the velocity distribution from surface to supposed bedrock in a firn basin near the Jungfraujoch in Switzerland. Sharp (1953) measured the velocity change with depth along a vertical line reaching halfway to bedrock in Malaspina Glacier, Alaska. McCall (1952) measured three-dimensional components of velocity in a horizontal tunnel to bedrock in a small cirque glacier. Some observations of various components of velocity have been made in tunnels within a small firn cap (Haefeli and Brentani, 1955–56) and in several icefalls (Haefeli, 1951; Glen, 1956). Apparently the velocity distribution at depth in a valley glacier flowing in a channel of simple configuration has never been measured. Such data would be of first-order importance for the framing and testing of theories of flow, because the approximate stress distribution at depths can be calculated. Therefore, a project to determine englacial velocity at depth in Saskatchewan Glacier was given highest priority.

SITES

Attempts to measure englacial velocities were made along the flow centerline in Castleguard sector, because the surface velocity and deformation fields and the bedrock configuration were known in greatest detail. The first location selected ($x = 9{,}660$, $y = 2{,}268$, $z = 7.370$ in 1952) is approximately opposite Castleguard camp. This point is designated as 6–6 (fig. 3). The following velocity and strain rate ($\dot{\epsilon}$, p. 32) components and slope were measured on the surface at this site:

$V_x' = 214$ fpy $\dot{\epsilon}_{xx} = -0.014\ \text{yr}^{-1}$
$V_y' = 0$ $\dot{\epsilon}_{yy} = +0.005\ \text{yr}^{-1}$
$V_z = -10.8$ fpy $\dot{\epsilon}_{xy} = 0$
$V_d = +6.2$ fpy
$V_s = -9.5$ fpy $\alpha = 4.41°$

This location is in a region of relatively steep surface slope and markedly nonlaminar "compressing flow" (p. 37). The cross section of the channel here is nearly elliptical and the depth is about 1,215 feet.

Attempts to measure englacial velocity were made in 1953 and 1954 at a site farthur upglacier ($x = 4{,}590$, $y = 1{,}920$, $z = 7{,}670$ in 1954) designated as stake 8–11 in 1954 (fig. 3). Velocity at this point was not measured directly, but components of velocity and strain rate have been interpolated from nearby stations 8–3 and 8–4 as follows:

$V_x' = 243$ fpy $\dot{\epsilon}_{xx} = +0.001\ \text{yr}^{-1}$
$V_y' = +0.5$ fpy $\dot{\epsilon}_{yy} = -0.001\ \text{yr}^{-1}$
$V_z = -8.2$ fpy $\dot{\epsilon}_{xy} = +0.003\ \text{yr}^{-1}$
$V_d = -0.8$ fpy
$V_s = -6.5$ fpy $\alpha = 1.84°$

This location, ideally suited for mathematical analysis, is in an area where the flow is neither extending nor compressing and the velocity vector is nearly parallel to the surface. The cross section is almost semicircular.

METHOD

The plan called for sinking a pipe vertically to the floor of the glacier and determining the subsequent deformation of the pipe by means of repeated inclinometer surveys, a procedure already used in other areas (Gerrard, Perutz, and Roch, 1952; Sharp. 1953). Aluminum pipe of inner diameter 1.38 inches and outer diameter 1.65 inches, in 10- or 12-foot sections joined by aluminum couplings, served as drill stem. The threads of the couplings were coated with calking compound, and little water leaked into the pipe. Aluminum was used instead of steel because it permitted use of a small-diameter inclinometer in which the bearings of inclination readings could be determined magnetically. Boring in the ice was made by electric hotpoints of 2.0 inches outside diameter (fig. 28). The source of power was a portable, 2,500-watt 220-volt a-c generator driven by a small gasoline engine. The pipe served as one conductor and the other was an insulated No. 8 stranded-wire cable strung inside the pipe with a pullout plug at the bottom. Normally the hotpoints were operated at 8.0 to 9.5 amperes, dissipating 1,020 to 1,450 watts at the bottom of the hole. Drilling speeds of 14.3 feet to a maximum of 16.6 feet per hour were generally obtained. A hole diameter of 2.7 inches for normal operation was computed on the assumption of no heat loss up the drill stem. A hole diameter of 2.85 inches actually formed at the surface, using a somewhat lower velocity of boring. Heat losses, therefore, were not important but some efficiency was lost in melting the sides of the hole by warm water.

After completion of boring and withdrawal of the cable, the orientation of the drill pipe was determined at 25-foot intervals with a small single-shot inclinometer generously loaned by the Parsons Survey Co.

The inclinometer measured the inclination of the pipe from a vertical direction. In this section, the term inclination or inclination angle refers to an angle measured from the vertical direction.

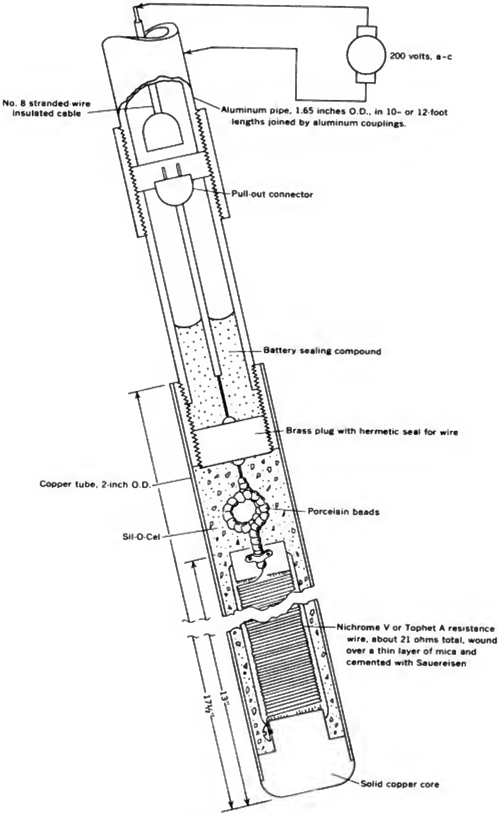
200 volts, a-c
No. 8 stranded-wire insulated cable
Aluminum pipe, 1.65 inches O.D., in 10- or 12-foot lengths joined by aluminum couplings.
Pull-out connector
Battery sealing compound
Brass plug with hermetic seal for wire
Copper tube, 2-inch O.D.
Porcelain beads
Sil-O-Cel
Nichrome V or Tophet A resistance wire, about 21 ohms total, wound over a thin layer of mica and cemented with Sauereisen
13"
17½"
Solid copper core

FIGURE 28.—Simplified sketch of hotpoint.

Relative displacements of points along the pipe were computed from the inclinometer data as follows: The inclination angles were first resolved into a plane parallel to the flow centerline by multiplying each inclination angle by the cosine of the horizontal angle between the direction of inclination and the direction of the flow centerline. The resolved configuration of the pipe was then computed to a first approximation by assuming that the resolved inclinations were constant from one point midway between two reading points to the next midpoint. The horizontal displacement of each midpoint differs from that of the next midpoint by the product of the distance along the pipe by the sine of the resolved inclination angle. This first-approximation configuration was then plotted on graph paper. A smooth curve, representing a better approximation to the true configuration, was drawn tangent to the known resolved inclination at each reading point (fig. 29). The relative displacements are given by the horizontal distances between two such curves taken at different times. The relative strain rates (the vertical gradients in V_r) are given by the relative displacements divided by the vertical distances and the time interval of measurement. The bottom of the pipe is considered as the fixed point, because pieces of pipe had to be removed from the top as ablation progressed.

In normal operation the inclinometer readings were reproducible to 0°05′ in inclination and 2° in azimuth. Other possible errors (such as the effect of ice streaming past the pipe, sagging of the pipe due to its own weight, and resistance of the couplings to flow along the pipe) are discussed by Gerrard, Perutz, and Roch (1952, p. 555–556). These errors are negligible for the Saskatchewan pipe owing to the extremely slight deformation.

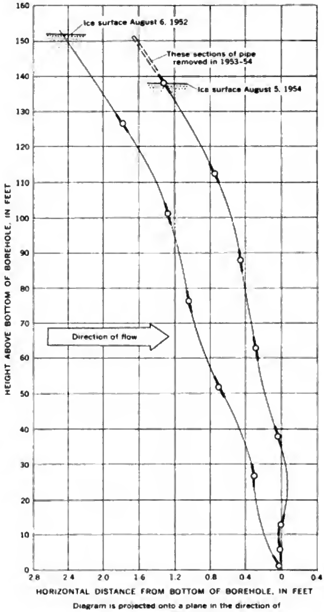

Diagram is projected onto a plane in the direction of the centerline of flow

FIGURE 29.—Configuration of borehole 1 in 1952 and 1954.

BOREHOLES

The first borehole drilling in 1952, stopped at a depth of 85 feet owing to a burned-out hotpoint. A second borehole reached a depth of 155 feet, where penetration gradually slowed and eventually stopped, but electrical evidence indicated that the hotpoint was functioning properly. By the next morning the pipe was bound tightly in the hole; 2 hours work with full power applied to the hotpoint and 3 men pulling on the pipestem failed to free the unit. This unit was used in this condition for measurements. A third attempt at drilling was started 1,100 feet farther downglacier. After a few unsuccessful attempts caused by faulty hotpoint connections, normal drilling speeds were obtained. Penetration ceased with only 38 feet of pipe in the ice; again the hotpoint was apparently functioning correctly. After several hours work the pipe was forced past the obstruction, and drilling speeds of 7.51 and 10.9 feet per hour were reached. At a depth of 113 feet progress again ceased, and after 3 hours of operation failed to gain an additional inch. During this period the pipe was becoming increasingly tight in the hole. The pipe was extracted with great difficulty and had a noticeable kink 20 feet above the bottom. This hole was abandoned.

In 1953 a more favorable site was found farther upglacier, where surface features suggested less active deformation. This operation also ended in failure when the deepest hole, 395 feet, was lost in the process of replacing a shorted-out hotpoint. Improper functioning of five electrical hotpoints was the principal cause of failure in 1953; but a gradual seizing near the surface, drifting into the side of the hole, and dropping a pipe wrench into a borehole contributed to the lack of success.

The 1954 field season was largely devoted to a final attempt at boring a deep hole at the 1953 site using improved, water-tight hotpoints. However, when boring was started on July 31, nearly 6 feet of snow and slush covered the ice, which is normally bare by early or middle July. The electrical equipment functioned satisfactorily and high drilling speeds were obtained. However, progress in the first hole stopped at a depth of 238 feet and a second hole reached only 290 feet. Failure was due to gradual seizing of the pipe in the hole, apparently at a shallow depth. This was probably due to a cold zone—perhaps a remnant of the previous winter's cold that was not ameliorated because of insulation by the heavy blanket of snow.

Three summers' work drilling with hotpoints resulted in the successful emplacement of one 150-foot pipe opposite Castleguard Pass (1952, 6–6) and the two pipes less than 300 feet long farther upglacier (1954, 8–11). (See fig. 3.) One of these latter pipes became useless when a connection was loosened allowing water to enter and freeze inside the pipe.

RESULTS

In the 2-year interval the 150-foot pipe was slightly tilted and bent; the top moved 0.71 foot farther downglacier than the base (fig. 29). The base moved 428 feet in these 2 years. The velocity decrease from top to base formed a smooth curve (fig. 30) similar to the curve found in the Jungfraufirn (Gerrard, Perutz, and Roch, 1952, p. 553).

This curve is significant in that it is entirely within the so-called "brittle crust" of the glacier. Matthes (1900, p. 190) and Demorest (1938, p. 724), among others, have suggested that a critical thickness of more than 100 feet of ice is necessary to start glacier flow. Matthes, (1942, p. 174), however, noticed that the gradual tilting of boring rods left in place in the Hintereisferner indicated some differential flow at shallower depths. The Saskatchewan data show evidence of shearing even in the upper 20 feet although the differential flow at such shallow depth is very slight. It is perhaps more significant that there is no evidence of a marked change in flow at any crit-

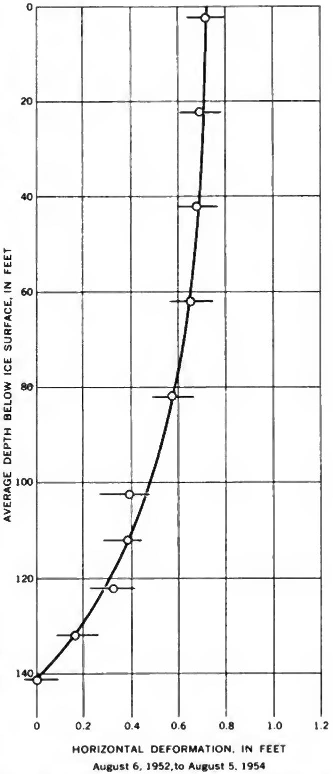

FIGURE 30.—Deformation of vertical borehole parallel to the centerline of flow. Circles indicate measurement points, short horizontal lines indicate approximate limits of measurement error.

ical depth. There is no possible suggestion of extrusion flow (Demorest, 1942, p. 31–38) in these results.

The inclinometer measurement data of the configuration of the 150-foot pipe in 1952, 1953, and 1954 and of the 238-foot pipe in 1954 are presented in table 11.

SOME INTERPRETATIONS OF THE VELOCITY DATA

SURFACE STRAIN-RATE FIELD

FUNDAMENTAL RELATIONS

The gradients of velocity on the surface of Saskatchewan Glacier furnish information on the deformation of the surface ice. Components ($\dot{\epsilon}_{ij}$) of the strain-rate tensor in terms of velocity components V_i relative to Cartesian coordinates x_i $(i=1, 2, 3)$ fixed in space are given by the relations (Nye, 1957, p. 115)

$$\dot{\epsilon}_{ij}=\frac{1}{2}\left(\frac{\partial V_i}{\partial x_j}+\frac{\partial V_j}{\partial x_i}\right) \qquad (1)$$

DEFORMATION OF THE SURFACE

Strain-rate components on the surface can be readily found if the surface velocity gradients are known. For this case relations (1) may be written

$$\dot{\epsilon}_{xx}=\frac{\partial V_x}{\partial x} \qquad (2a)$$

$$\dot{\epsilon}_{yy}=\frac{\partial V_y}{\partial y} \qquad (2b)$$

$$\dot{\epsilon}_{xy}=\frac{1}{2}\left(\frac{\partial V_x}{\partial y}+\frac{\partial V_y}{\partial x}\right) \qquad (2c)$$

where the coordinates (x, y) are as defined on page 10. Values of V_x and V_y were plotted on 4 transverse and 8 longitudinal profiles in the Castleguard sector, smooth curves were drawn through the points, and values of the 4 velocity gradients were determined at the 32 places where the profiles intersect (fig. 31). From these data the strain rates $\dot{\epsilon}_{xx}$, $\dot{\epsilon}_{yy}$, and $\dot{\epsilon}_{xy}$ were determined using relations (2). Values of the greatest principal elongation rate ($\dot{\epsilon}_1$) the least (most compressing) principal elongation rate ($\dot{\epsilon}_2$) and the maximum shearing deformation rate $\frac{1}{2}(\dot{\epsilon}_1-\dot{\epsilon}_2)$ were determined by Mohr's circle constructions (fig. 32). These data are summarized in table 4 and are portrayed in terms of the orientations and magnitudes of the principal elongation rates in figure 33, trajectories of principal strain rate in figure 34, trajectories of maximum shearing strain

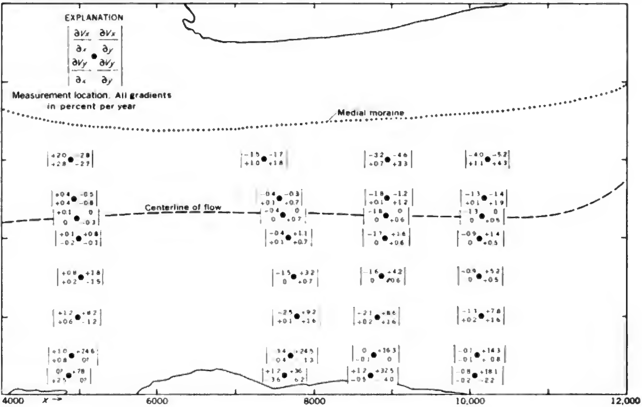
EXPLANATION
$\frac{\partial V_x}{\partial x}$ $\frac{\partial V_x}{\partial y}$ $\frac{\partial V_y}{\partial x}$ $\frac{\partial V_y}{\partial y}$
Measurement location. All gradients in percent per year
Medial moraine
Centerline of flow
4000
2000
0
y
4000
x →
6000
8000
10,000
12,000

FIGURE 31.—Measured velocity gradients in Castleguard sector.

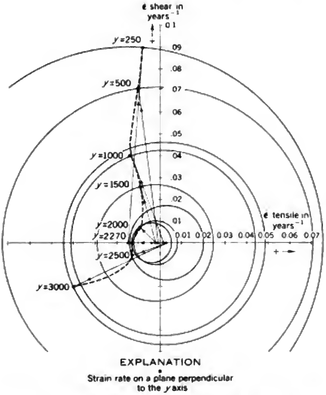

FIGURE 32.—Mohr's circle constructions showing changes in strain rate along a transverse profile at $x' = 10{,}000$.

rate in figure 35, and magnitudes of the normal strain rates parallel to the x- and y-axes in figure 36.

Many assumptions and approximations are involved in these computations. The more significant of these are:

Approximation of plane strain.—By this it is assumed that the vertical component of velocity is approximately constant independent of position. This assumption is necessary in order to compute the orientations of the principal strain rates. The following line of reasoning suggests that the deformation must be predominantly in the form of plane strain: The stress tensor must have a principal axis perpendicular to the surface because air can sustain no shear stress. The ice in Castleguard sector is approximately isotropic in mechanical properties except along the extreme margins and at the terminus (p. 5). For an isotropic material, it is generally assumed that the principal axes of stress and strain increment (or strain rate) coincide at all times (Hill, 1950, p. 38). Thus the strain-rate tensor probably has a principal axis perpendicular to the surface. Inspection of the velocity gradient data (fig. 31) shows that the sum $\epsilon_{xx} + \epsilon_{yy}$ does not equal zero at most points, and inspection of the map of V_z (fig. 21) shows that a slight horizontal gradient of

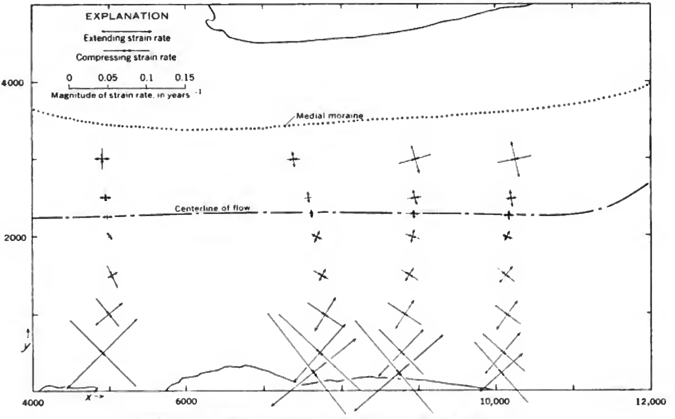

FIGURE 33.—Orientations and magnitudes of principal strain rates in Castleguard sector.

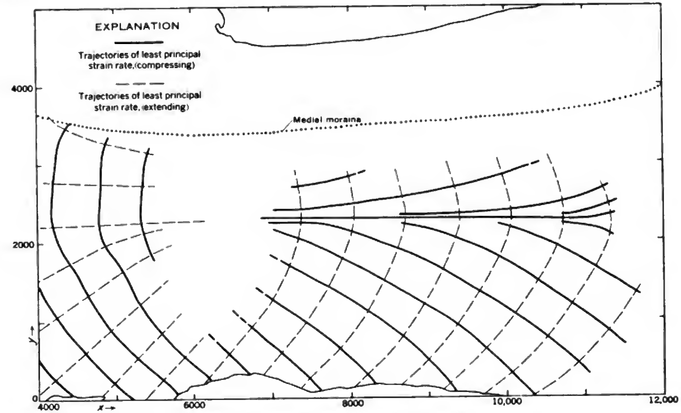
EXPLANATION
Trajectories of least principal strain rate (compressing)
Trajectories of least principal strain rate (extending)
Medial moraine
4000
2000
0
y →
4000
x →
6000
8000
10,000
12,000

FIGURE 34.—Principal strain-rate trajectories in Castleguard sector.

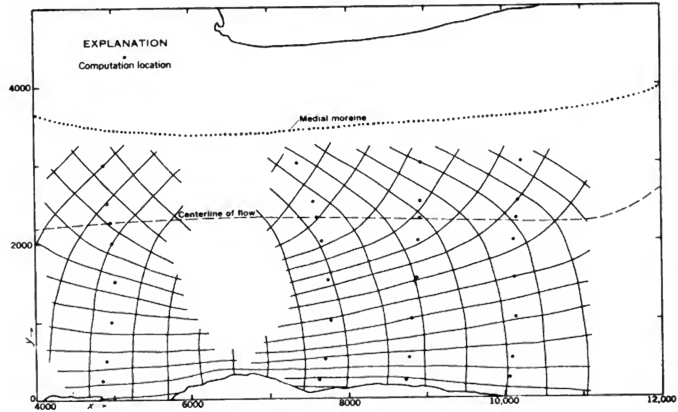

FIGURE 35.—Trajectories of greatest shear-strain rate in Castleguard sector.

TABLE 4.—*Strain-rate components*

[Columns 4–8, 10, and 12. Symbols for strain-rate and rotation-rate components are given on page 32. all values of strain-rate and rotation-rate components are given in percent per year. Column 9. Angle between ϵ_1 and the x axis, in degrees. Column 12. ω_{xy}, the rotation rate, is given by $\omega_{xy} = \frac{1}{2} \frac{\partial V_x}{\partial y} + \frac{\partial V_y}{\partial x} \Big]$

Point (1)	x (feet) (2)	y (feet) (3)	$\dot{\epsilon}_{xx}$ (4)	$\dot{\epsilon}_{yy}$ (5)	$\dot{\epsilon}_{xy}$ (6)	$\dot{\epsilon}_1$ (7)	$\dot{\epsilon}_2$ (8)	θ (9)	$\frac{1}{2}(\dot{\epsilon}_1 + \dot{\epsilon}_2)$ (10)	$\frac{1}{2}(\dot{\epsilon}_1 - \dot{\epsilon}_2)$ (11)	$\dot{\omega}_{xy}$ (12)
8-h	5,000	3,000	2.0	−2.7	0	2.0	−2.7	0	−0.4	2.4	−2.8
g	5,000	2,500	.4	−.8	0	.4	−.8	0	−.2	.6	−.4
f	5,000	2,260	.1	−.3	0	.1	−.3	0	−.1	.2	0
e	5,000	2,000	.1	−.1	0.3	.3	−.3	35.8	0	.3	.5
5	5,000	1,500	.8	−1.5	1.0	1.2	−2.7	24.5	−.4	1.5	.6
e	5,000	1,000	1.2	−1.2	4.4	4.6	−4.6	37.4	0	4.6	3.8
6	5,000	500	1.0	0.	12.7	13.2	−12.2	42.8	.5	12.7	11.9
a	5,000	250	0?	0?	High	High	High	45.0	0	High	High
3-h	7,700	3,000	−1.5	1.8	−.4	1.8	−1.6	−83.2	.2	1.7	−2.0
g	7,700	2,500	−.4	.7	−.1	.7	−.4	−84.9	.2	.6	−.7
f	7,700	2,300	−.4	.7	0	.7	−.4	90	.2	.6	0
e	7,700	2,000	−.4	.7	.6	1.0	−.7	66.3	.2	.8	.7
d	7,700	1,500	−1.5	.7	1.6	1.5	−2.3	62.3	−.4	1.9	2.6
c	7,700	1,000	−2.5	1.6	4.6	5.2	−5.5	56.9	−.4	5.1	3.8
b	7,700	500	−3.4	−1.3	12.0	9.7	−14.4	47.6	−2.4	12.1	7.2
a	7,700	250	1.2	−6.2	16.2	14.1	−19.2	38.6	−2.5	16.6	9.2
5-h	8,850	3,000	−3.2	3.3	−2.0	3.9	−3.8	−74.2	0	3.8	−2.6
g	8,850	2,500	−1.8	1.2	−.6	1.3	−1.9	−79.1	−.3	1.6	−.6
f	8,850	2,280	−1.8	.6	0	.6	−1.8	90	−.6	1.2	0
e	8,850	2,000	−1.7	.6	.8	.9	−1.8	72.6	−.6	1.4	.8
d	8,850	1,500	−1.6	.6	2.1	1.9	−2.9	58.8	−.5	2.4	2.1
c	8,850	1,000	−2.1	1.6	4.4	4.5	−5.0	56.4	−.2	4.8	4.2
b	8,850	500	0	0	8.2	8.2	−8.2	45.0	0	8.2	8.4
a	8,850	250	1.2	−4.0	16.0	14.9	−17.7	40.4	−1.4	16.2	16.5
6-h	10,000	3,000	−4.0	4.3	−2.0	4.8	−4.5	−77.1	.1	4.6	−3.2
g	10,000	2,500	−1.3	1.9	−.6	2.0	−1.4	−79.7	.3	1.7	−.8
f	10,000	2,270	−1.3	.5	0	.5	−1.3	90	−.4	.9	0
e	10,000	2,000	−.9	.5	.7	.8	−1.2	67.2	−.2	1.0	.7
d	10,000	1,500	−.9	.5	2.6	2.5	−2.9	52.5	−.2	2.7	2.6
c	10,000	1,000	−1.3	1.6	4.0	4.4	−4.1	54.9	.1	4.3	3.8
b	10,000	500	−1.0	.8	7.1	7.1	−7.3	48.6	−.1	7.2	7.2
a	10,000	250	−.8	−2.2	9.0	7.5	−10.5	42.0	−1.5	9.0	9.2

V_z exists, so the measured strain rates do not indicate a perfect plane-strain condition. This is only partly due to the fact that V_z was not measured perpendicular to the surface.

Substitution of average for instantaneous velocities.—This occurs when finite displacements are divided by intervals of time in order to determine velocity. Actual strains up to 20 percent were measured in a year's time, and if velocity varies with time in these regions of high strain rate the resulting average velocity field will be inaccurate. However, the resulting strain-rate configuration probably is valid because (1) high rates of strain occur only very near the margin and (2) near the margin the deformation is nearly pure shear. In pure shear, gradients of velocity are small in the direction of the velocity vector, and the average velocity for an extended time interval is a good approximation of the instantaneous velocities.

Method of measuring velocity gradients.—Drawing a smooth curve through widely separated points is a subjective procedure, and gradients determined in this manner are certainly of questionable validity. Different curves through the same points determined values of strain-rate components differing as much as a strain rate of 0.3 percent per year of strain rate. In the vicinity of the flow centerline this is an appreciable fraction of the measured strain-rate components. Thus the strain-rate components in the central strip of the glacier are not precise but the general configuration must hold.

Assumption of a horizontal ice surface.—Velocity components parallel to the surface must be used if this computation is to be exact. Horizontal components were used instead. This is equivalent to assuming that the ice surface is horizontal. The surface slopes 3°23′ in the $+x'$ direction with a pronounced lateral slope only near the margins. Therefore the horizontal velocity components must not differ by more than 1 percent from the corresponding

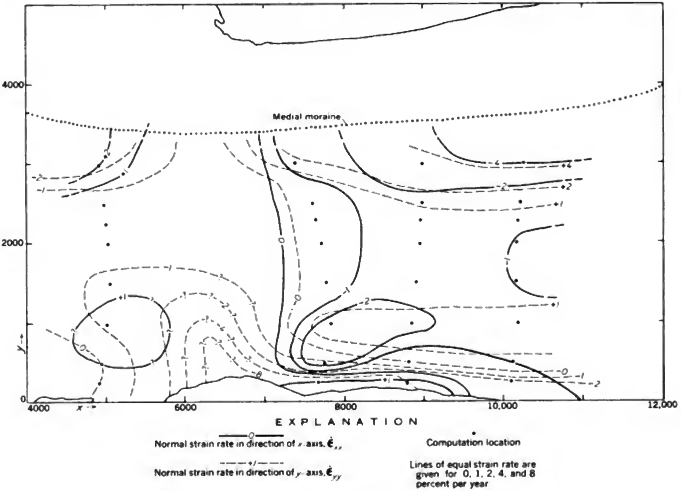
4000
2000
0
y'→
4000
x'→
6000
8000
10,000
12,000
Medial moraine
EXPLANATION
Normal strain rate in direction of x'-axis, $\dot{\epsilon}_{x'x'}$
Normal strain rate in direction of y'-axis, $\dot{\epsilon}_{y'y'}$
Computation location
Lines of equal strain rate are given for 0, 1, 2, 4, and 8 percent per year

FIGURE 36.—Normal strain rates parallel to the x'- and y'-axes in Castleguard sector.

components parallel to the surface. Longitudinal distances along the surface, however, are incorrect by as much as 6 percent. Furthermore, the two principal strains on the surface are not exactly perpendicular when projected onto a horizontal plane. The combined error of all of these approximations cannot be greater than 10 percent for most points and general configuration should be valid.

The results show that most of the surface deformation is caused by the transverse gradient of longitudinal velocity and that all other velocity gradients are relatively small. The principal axes of deformation are, therefore, longitudinal and transverse to the flow along the centerline and intersect the margins at approximately 45° (figs. 33, 34). The influence on the orientation and magnitudes of the principal strain rates of this increase in $\epsilon_{x'y'}$ toward the margin is shown in the progressive changes in the Mohr's circle constructions along transverse profiles (fig. 32). Trajectories of maximum shearing-strain rate (analogous to slip lines) are almost parallel or perpendicular to the margin except near the flow centerline where they swing, abruptly, into a 45° relation to the flow (fig. 35).

In addition to this shearing deformation due to the drag of the valley walls, there are finite values of longitudinal ($\epsilon_{x'x'}$) and transverse ($\epsilon_{y'y'}$) normal elongations caused by other factors (fig. 36). In the upper part of Castleguard sector there is a very slight longitudinal extension along the centerline amounting to about 0.1 percent per year. This is "extending flow" in the terminology of Nye (1952a, p. 87), who has postulated that extending flow may develop in a very wide, plastic-rigid glacier if there is accumulation on the surface or a bedrock channel convex upwards in longitudinal profile (Nye, 1951, p. 561). This area is below the firn limit; therefore according to the postulate it must be assumed that the bedrock is markedly convex in longitudinal profile. The measured surface and bedrock profiles (pl. 1) show this.

At about $x' = 7{,}000$ the longitudinal normal strain rate is zero and below this point it is negative ("compressing flow") reaching a maximum value of −1.8 percent at $x' = 9{,}000$ along the centerline. This is apparently due to ablation (Nye, 1951, p. 561).

The transverse normal strain rates change from compressive in the upper part of Castleguard sector to extending the lower part. This is due to a pinching of the channel at $x' = 6{,}500$ and the change from marginal accumulation above $x' = 5{,}000$ to pronounced marginal ablation below $x' = 7{,}000$.

The transition from longitudinal extension and transverse compression to longitudinal compression and transverse extension causes a strong warp in the strain-rate field with a branch point along the south margin at about $x' = 6{,}500$. This area sustains a complex fracture pattern: two sets of crevasses intersect with the formation of curving bands of contorted en echelon fractures (p. 56, 57).

The strain-rate data at most points show a net compression ($\dot{\epsilon}_{ii}$ is negative). The average value of $\dot{\epsilon}_{xx} + \dot{\epsilon}_{yy}$ for the 3 lower profiles is −0.23 percent per year. One can safely assume that there is no volumetric plastic compression of the ice because the density does not change appreciably. The compressing velocity in the x-y plane must be relieved by a vertical extending velocity in order to preserve incompressibility. If it is assumed that the horizontal compressing rate does not change with depth, and if the base and the surface slopes are the same, then the vertical extension rate for a vertical prism may be computed as

$$-(\dot{\epsilon}_{xx} + \dot{\epsilon}_{yy})d = \dot{\epsilon}_{zz}d = V_d \qquad (3)$$

where d is the thickness of the glacier (length of the prism). This vertical velocity is identical with the component V_d mentioned previously (p. 24). All quantities in equation (3) except d can be measured on the surface so this equation could be used to determine ice thickness. The Saskatchewan strain-rate data are too crude to use for quantitative depth measurements. For the south half of the Castleguard sector, the average value of V_d was measured as +4.1 fpy. The computed average depth is 1,740 feet. This is of the proper order of magnitude, but differs from the measured depth by nearly a factor of 2.

DEFORMATION IN THREE DIMENSIONS

Computation of all nine components of the strain-rate tensor on the surface requires knowledge of the vertical gradients of both horizontal velocity components. These data are not readily obtainable, and therefore little is known about the orientation and magnitudes of all axes of the rate of deformation tensor as a function of position.

The complete strain-rate tensor is known at the vertical borehole site on the centerline (stake 6–6). The following components were computed in percent per year:

$$\begin{array}{lll}
\dot{\epsilon}_{xx} = -1.8 & \dot{\epsilon}_{yx} = 0 & \dot{\epsilon}_{zx} = +0.1 \\
\dot{\epsilon}_{xy} = 0 & \dot{\epsilon}_{yy} = +0.5 & \dot{\epsilon}_{zy} = 0 \\
\dot{\epsilon}_{xz} = +0.1 & \dot{\epsilon}_{yz} = 0 & \dot{\epsilon}_{zz} = +0.8
\end{array}$$

Within the limits of error, the principal axes of strain rate are oriented parallel and perpendicular to the surface at this point, and two principal axes are in the plane of the centerline. The greatest principal elongation is vertical, the greatest principal compression horizontal and longitudinal. Probably the deformation state is similar to this all along the centerline up to $x' = 7{,}700$. Farther upglacier, the relative values, but not the orientations, of the principal axes are different.

The principal axes are probably nearly perpendicular and parallel to the surface over most of the glacier surface. However, definite transverse gradients in vertical velocity were measured. A slight inclination of the principal axes is required to allow for this vertical shearing. The amount of inclination cannot be approximated because the vertical gradient in transverse velocity is not known and is probably appreciable.

FLOW LAW OF ICE

A flow law—"the quasi-viscous creep rate as a function of stress" (Nye, 1953, p. 477)—is the starting point for calculating the flow of glaciers. No flow law derived from theory for polycrystalline ice has been generally accepted, so recourse to experiments is necessary. A nonlinear empirical relation between shear stress and strain rate has been discovered for artificial polycrystalline ice in the laboratory (Glen, 1955) and for glacier ice in place (Gerrard, Perutz, and Roch, 1952, p. 554). However, the exact form of this relation and the values of the empirical coefficients have not been clearly established because different types of experiments have given inconsistent results. Furthermore, the possibility that strain rate may be a function of the mean stress ("hydrostatic pressure") in glaciers has not been investigated thoroughly.

Observations on Saskatchewan Glacier contribute to the understanding of the flow law for glacier ice. A flow law can be derived, with several broad assumptions, from a transverse velocity profile (where the mean stress is only atmospheric pressure), and from a short vertical profile of velocity (where mean stress increases with depth). These data can be compared with each other and with data from two other vertical velocity profiles in glaciers, numerous tunnel closing-rate experiments and experimental deformation of ice.

FUNDAMENTAL RELATIONS

In order to compare these various experiments the stress and strain-rate data must be reduced to a uniform basis. Stress and strain rate can be related for a slowly flowing material if the material is isotropic and incompressible, because in this case the stress and strain-rate principal axes remain parallel during plastic flow (Hill, 1950, p. 34, 38). The yield criterion for metals and presumably most other polycrystalline substances is not affected by hydrostatic pressure (Hill, 1950, p. 16). In order to determine if this statement is valid for ice the assumption is made that it is, and then results from experiments involving different amounts of hydrostatic pressure are compared.

Nye's assumption (1953, p. 479), that the stress is not a function of the total plastic strain and that no strain hardening occurs is also adopted. It is then assumed that the strain rate is a function of the deviator of stress:

$$\dot{\epsilon}_{ij} = f(\sigma_{ij'})$$

where

$$\sigma_{ij}' = \sigma_{ij} - \frac{1}{3}\,\delta_{ij}\,\sigma_{kk} \qquad (4)$$

The magnitude of the deviator of stress is measured here by the octahedral shear stress σ_0 defined as

$$\sigma_0 = \frac{1}{3}\sqrt{(\sigma_1-\sigma_2)^2+(\sigma_2-\sigma_3)^2+(\sigma_3-\sigma_1)^2} \qquad (5)$$

where σ_1, σ_2, and σ_3 are the three principal stresses (Nadai, 1950, p. 103).

An octahedral shearing strain rate $\dot{\epsilon}_0$ is similarly defined as

$$\dot{\epsilon}_0 = \frac{1}{3}\sqrt{(\dot{\epsilon}_1-\dot{\epsilon}_2)^2+(\dot{\epsilon}_2-\dot{\epsilon}_3)^2+(\dot{\epsilon}_3-\dot{\epsilon}_1)^2} \qquad (6)$$

where $\dot{\epsilon}_1$, $\dot{\epsilon}_2$, and $\dot{\epsilon}_3$ are the 3 principal strain rates. The flow law relation to be measured and tested can then be written as

$$\dot{\epsilon}_0 = f'(\sigma_0) \qquad (7)$$

Strain rates are obtained directly from measured velocity gradients according to the relations (1). Stresses, on the other hand, must be computed and these computations require additional assumptions for each special case. It is important to note that the methods of Somigliana and Lagally (Lagally, 1929, p. 285–293) for computing stresses in a glacier cannot be used because they derive stress from predicted strains.

The more important assumptions made in this approach are summarized as follows:

1. Hydrostatic pressure has no effect on the flow.
2. The flow is determined only by the stress deviator.
3. Total plastic strain has no effect on the flow (neither strain hardening nor strain softening occurs).
4. The effects of transient creep are negligible.
5. The flow is slow and steady so that inertial forces are negligible.
6. Elastic strains are negligible compared with the plastic strains accumulated during the period of observation.
7. The ice is isotropic, homogeneous, and incompressible.

VERTICAL PROFILE

STRESS AND DEFORMATION IN LAMINAR FLOW

The simplest assumption that can be made about the state of deformation which produced the known velocity gradient is that the deformation occurred as simple shear in a direction parallel to the surface, and the only shear-stress components are those which produced the simple shear flow. This is equivalent to saying that the flow was laminar. The velocity vector did not quite parallel either the surface or the horizontal at the vertical profile measuring site and a longitudinal compression was measured, but this state of simple shear is a reasonable starting assumption. It is necessary to assume also that the simple shear planes were parallel at all depths.

Stress

The stress on a plane parallel to the surface for a unit width of ice (fig. 37)[*] can be computed as follows:

The shear stress σ_{zx} is approximately the tangential component of the pressure due to the weight of the column

$$\sigma_{zx} = \gamma z \sin\alpha$$

where γ is the specific weight of ice and α is the surface slope.

This formula is valid only if the glacier is infinitely wide. For a glacier flowing in a channel formed by half of a circular cylinder the flow has axial symmetry. In this case the increase of σ_{zx} with increasing depth is only half as great as for an infinitely wide

---

[*] Note that the x'- and z-axes are defined as parallel and perpendicular, respectively, to the surface. This is a difference definition than the one used in all other parts of this report, and applies only to this section on the vertical profile.

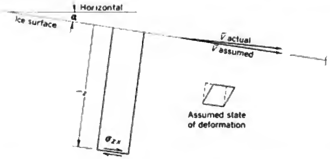

FIGURE 37.—Definition sketch for analysis of stress and deformation in a vertical profile.

glacier but is still linear (Nye, 1952a, p. 85). On a vertical plane through the axis of a semicircular channel

$$\sigma_{zx}=\frac{1}{2}\gamma z \sin \alpha$$

It seems logical to follow the *a priori* argument of Nye (1952a, p. 85–86) that these two cases can be expressed as special cases of a more general relation. A simple general relation is that the increase of stress along the centerline is always linear and that the rate of increase depends on a "shape factor" given by the ratio of hydraulic radius *R* to total depth *d*. This shape factor reduces to 1 for an infinitely wide glacier and to one-half for a semicircular cross section. In general it will be between these two limits for most valley glaciers. Thus we assume that

$$\sigma_{zx}=\frac{R}{d}\gamma z \sin \alpha$$

The principal stresses are $(\sigma_{zx}+\sigma, -\sigma_{zx}+\sigma, \sigma)$ where σ is the hydrostatic pressure. The octahedral shear stress is

$$\sigma_0=\sqrt{\frac{2}{3}}\frac{R}{d}\gamma z \sin \alpha \qquad (8)$$

Strain Rate

The shearing strain rate from equations (1) is

$$\dot{\epsilon}_{zx}=\frac{1}{2}\frac{\partial V_x}{\partial_z}$$

The principal strain rates are approximately $(\dot{\epsilon}_{zx}, -\dot{\epsilon}_{zx}, 0)$, and the equivalent octahedral shearing strain rate is

$$\dot{\epsilon}_0=\sqrt{\frac{2}{3}}\dot{\epsilon}_{zx}=\sqrt{\frac{1}{6}}\frac{\partial V_x}{\partial z} \qquad (6)$$

Assumptions Used

In addition to the assumptions listed under "Fundamental relations," two major approximations have been added:

1. The increase of stress with depth is assumed to be linear and the gradient of stress increase was assumed to be proportional to a shape factor.
2. The deformation in the x, z-plane is assumed to be correctly shown in figure 37, V at all depths is parallel to V at the surface, and V does not increase or decrease in the x-direction.

RESULTS

Values of $\frac{\partial V_x}{\partial z}$ were computed from borehole displacements (fig. 30) and are shown in figure 38.

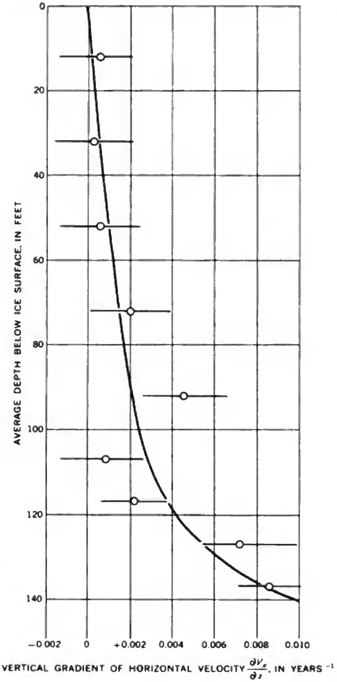

FIGURE 38.—Vertical gradient of horizontal velocity along vertical borehole. Circles indicate measurement points, short horizontal lines indicate approximate limits of measurement error.

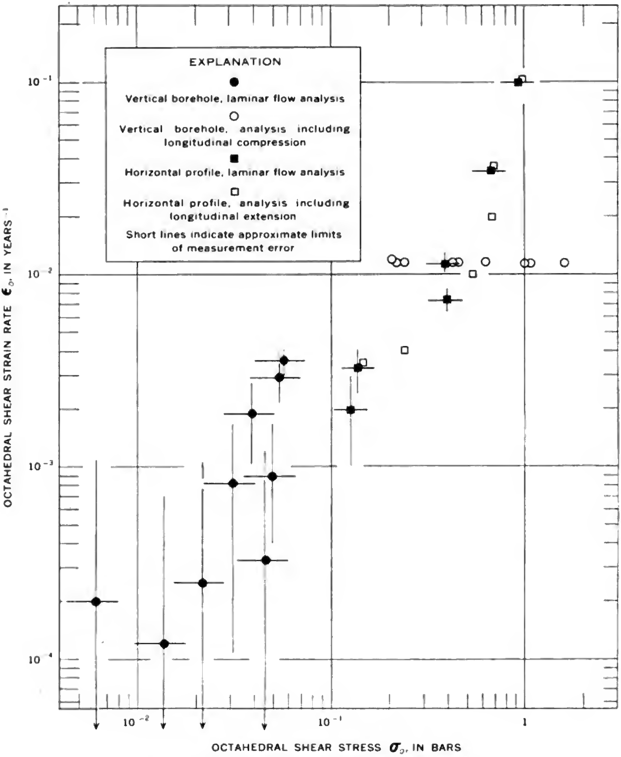

FIGURE 39.—Strain rate as a function of shear stress in Saskatchewan Glacier.

Values of σ_0 computed from equation (8) and $\dot{\epsilon}_0$ computed from equation (9) are presented in table 5 and in figure 39. It can be seen that the relation between these quantities is not linear.

No evidence of a yield stress appears in these data. The shearing rates at the lowest stresses (apparently the lowest which have yet been measured for ice) are somewhat faster than what one would predict from the behavior at higher stresses.

EFFECT OF LONGITUDINAL EXTENSION

When this borehole was emplaced and the results first analyzed, it was not possible to account for shearing stresses or strain rates due to horizontal extension or compression. In an analysis published subsequently, Nye has included horizontal longitudinal extension or compression within the framework of a general theory of stress and velocity in glaciers. He has also analyzed the Jungfraufirn borehole results (Gerrard, Perutz, and Roch, 1952) within this framework by using a trial assumption of a flow law. Some of his results can be applied to the Saskatchewan data.

TABLE 5.—*Stress and strain-rate data from vertical borehole*

[Formulas and definitions of symbols are given on p. 32, 42]

z (feet)	σ_0 (bars)*	σ_0' (bars)*	$\frac{\partial V_x}{\partial z}$ (years^{-1})	$\dot{\epsilon}_0$ (years^{-1})	$\dot{\epsilon}_0'$ (years^{-1})
15	0.006	0.43	0.0005	0.0002	0.0114
35	.014	1.01	.0003	.0001	.0114
55	.022	1.08	.0006	.0002	.0114
75	.031	.44	.0020	.0008	.0115
95	.039	.24	.0046	.0019	.0116
110	.046	1.60	.0008	.0003	.0114
120	.050	.63	.0022	.0009	.0115
130	.054	.21	.0072	.0030	.0118
139	.057	.21	.0086	.0035	.0120

* 1 bar = 10^6 dynes per square centimeter = 14.5 pounds per square inch.

According to Nye's analysis (1957, p. 126), stress and strain-rate values can be deduced from a borehole experiment using the expressions

$$\sigma_0' = \sigma_0 \frac{\dot{\epsilon}_0'}{\dot{\epsilon}_0} = \sqrt{\frac{2}{3}}\,\frac{R}{d}\,\gamma\, z \sin\alpha\, \frac{\dot{\epsilon}_0'}{\dot{\epsilon}_0} \quad (8)$$

$$\dot{\epsilon}_0'^2 = \dot{\epsilon}_0^2 + \frac{2}{3}\,\dot{\epsilon}_{xx}^2 = \frac{1}{6}\left(\frac{\partial V_x}{\partial z}\right)^2 + \frac{2}{3}\left(\frac{\partial V_x}{\partial x}\right)^2$$

in which σ_0' and ϵ_0' are octahedral shear stress and octahedral shear rate modified to account for a longitudinal compressive strain rate $\dot{\epsilon}_{xx}$.[9] In addition to the assumptions given previously Nye assumes that no stresses or strains are active in the y-direction and that σ_{xx} and σ_0 are functions of x only and not of y. Transverse and vertical extending strain rates are known at the borehole site. These additional components of deformation could be considered by an extension of Nye's theory. However, in view of the lack of information on these components at depth, the inaccuracies in measurement, and the certain paucity of useful information in the final results, further refinement is not justified.

The effect of this modification of σ_0 and $\dot{\epsilon}_0$ is to seriously impair the usefulness of the Saskatchewan borehole data for deducing a flow law (table 5 and fig. 39). This is because the constant shear due to longitudinal compression overpowers the variable shears due to laminar flow, confining the spread of strain-rate values on a graph to an extremely small region. The lack of correspondence between relative values of σ_0 and σ_0' is noteworthy (table 5).

Nye has shown that if the flow law is of the form

$$\dot{\epsilon}_0 = k\sigma_0^n \quad (10)$$

where k and n are empirical coefficients, the effect of longitudinal extension on the Jungfraufirn results is to lower the apparent power-law coefficient n as calculated in a simple laminar-flow analysis. By assuming equation (10) one can show that the Saskatchewan data behave somewhat similarly. The average shearing-strain rate measured by the deformation of the borehole was only a tiny fraction of the prevailing shearing-strain rate due to longitudinal compression, and even at the bottom of the borehole the borehole deformation shear was only one-fourth of the compressional shear. This would suggest that if equation (10) were correct for ice, the simple analysis of the Saskatchewan data (p. 38–39) should have yielded an apparent flow law of the Newtonian viscous type. The fact that it did not do this (fig. 39) indicates that either equation (10) is not correct or that Nye's analysis does not apply perfectly. However, the basic approach we wish to use here is to first present the data and then see which type of flow-law relation best describes them.

TRANSVERSE PROFILE

STRESS AND DEFORMATION IN LAMINAR FLOW

The cross section of Saskatchewan Glacier at $x' = 5{,}000$ approximates a semicircle (fig. 6). This is the only cross-section shape for a valley glacier that is amenable to mathematical analysis at the present time. In this case surfaces of maximum shearing stress and strain rate form cylinders concentric about the flow centerline. We begin by assuming laminar flow. The complication of longitudinal extension or compression is not pronounced at this location.

---

[9] These relations when combined with equations (8) and (9) and modified to use the symbols of this report are identical with Nye's equations except for a factor of $\sqrt{2/3}$. Nye reports his flow law data in terms of an effective shear stress and strain rate which are $\sqrt{3/2}$ times the octahedral shear stress and strain rate.

Stress

The shear stress on these cylindrical surfaces as given by Nye (1952a, p. 85) is

$$\sigma_{rx} = \frac{1}{2} r \gamma \sin \alpha \qquad (11)$$

where r is the distance from the centerline and α is the surface slope. The actual cross section is slightly elliptical. The eccentricity is slight, so it may be valid to allow for it by extending r slightly in the horizontal direction and compressing it slightly in the vertical direction as was done in equation (8). On the surface, equation (11) may be written as

$$\sigma_{yx} = \frac{R}{w} \gamma y' \sin \alpha$$

where w is the width of the glacier. The octahedral shear stress σ_0 is

$$\sigma_0 = \sqrt{\frac{2}{3}} \sigma_{yx} = \sqrt{\frac{2}{3}} \frac{R}{w} \gamma y' \sin \alpha \qquad (12)$$

Strain Rate

The shearing strain rate corresponding to equation (11) is given by relations (1) as

$$\dot{\epsilon}_{yx} = \frac{1}{2} \frac{\partial V_x}{\partial y}$$

and the octahedral shearing strain rate is

$$\dot{\epsilon}_0 = \sqrt{\frac{2}{3}} \dot{\epsilon}_{yx} = \sqrt{\frac{1}{6}} \frac{\partial V_x}{\partial y} \qquad (13)$$

Assumptions Used

1. It is assumed that the transverse gradient in shear stress is linear and is proportional to the gradient for a semicircular cross section.
2. It is also assumed that V is parallel to the surface and that the surface is level in a cross-glacier direction, and that there is no longitudinal or transverse extension or compression.

RESULTS

Values of stress computed from equation (12) and strain rate computed from equation (13) are shown in table 6 and in figure 39. These data follow the same flow-law trend found from the vertical profile, but they cover a range of higher stresses. Insufficient measuring points were available in the center of the glacier to define the strain gradient at low stresses so the ranges of stress do not overlap.

EFFECT OF LONGITUDINAL EXTENSION

The slight longitudinal extension which was measured along this profile can be considered similarly to the compression of the vertical borehole. In this case, equations (12) and (13) must be modified by use of equations (8′) and (9′) so that

TABLE 6.—*Stress and strain-rate data from transverse surface profile*

[Formulas and definitions of symbols are given on p. 32, 42]

y' (feet)	σ_0 (bars)	σ_0' (bars)	$\frac{\partial V_x}{\partial y}$ (years)	$\frac{\partial V_x}{\partial x}$ (years^{-1})	$\dot{\epsilon}_0$ (years^{-1})	$\dot{\epsilon}_0'$ (years^{-1})
−260	0.137	0.141	0.008	0.001	0.003	0.003
−760	.400	.540	.018	.008	.007	.010
−1260	.663	.690	.082	.012	.034	.036
−1760	.926	.926	.246	.010	.100	.100
+240	.126	.240	.005	.004	.002	.004
+740	.390	.680	.028	.020	.011	.020

$$\sigma_0' = \sqrt{\frac{2}{3}} \frac{R}{w} \gamma y' \sin \alpha \frac{\dot{\epsilon}_0'}{\dot{\epsilon}_0} \qquad (12')$$

$$\dot{\epsilon}_0'^2 = \frac{1}{6} \left(\frac{\partial V_x}{\partial y} \right)^2 + \frac{2}{3} \left(\frac{\partial V_x}{\partial x} \right)^2 \qquad (13')$$

The longitudinal extension rate $\frac{\partial V_x}{\partial x}$ varied along the profile, and these values are tabulated in table 6 along with values of σ_0' and $\dot{\epsilon}_0'$ calculated according to equations (12′) and (13′). Transverse and vertical normal strain rates are also known along this profile, but the further refinement necessary to incorporate them is not justified for reasons similar to those given in the case of the vertical borehole.

The result of this modification of a laminar-flow analysis is to move several points toward slightly higher values of stress and strain rate (fig. 39). This does not appreciably change the indicated flow-law relation.

DISCUSSION OF THE FLOW-LAW RESULTS

The relation between shear stress and shear-strain rate computed from vertical and transverse velocity profiles in Saskatchewan Glacier is shown on figure 40. Also shown on this graph are results from the Malaspina borehole (kindly supplied in advance of publication by R. P. Sharp), the Jungfraufirn borehole, McCall's Skauthöe, Glen's Austerdalsbre, and Haefeli's Z'Mutt and Arolla tunnel contraction data (as computed by Nye), and Glen's laboratory experiments at temperatures near the melting point. All of these data have been converted to octahedral shear stress and octahedral shear-strain rate.

Some uncertainty exists about the correct placement of Nye's and Glen's data on this diagram. Nye's stress data are reported in terms of an "effective shear stress" which is also called the "octahedral shear stress" and is defined as

$$2 \sigma_0^2 = \sigma_{ij}' \sigma_{ij}'$$

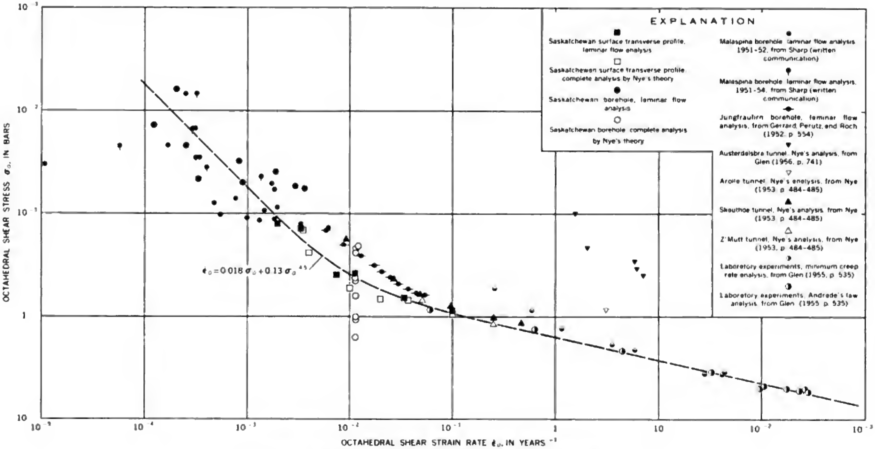

FIGURE 40.—Strain rate as a function of shear stress, data from numerous sources

where σ_{ij}' is the deviator of stress (1953, p. 478). Glen (1955, p. 536) analyzes his results "in the way described by Nye," and reports his data in terms of "octahedral shear stress." Strain rates are reported similarly by these investigators. However, these values of "octahedral shear stress" appear to be different by a factor of $\sqrt{2/3}$ from the shear stress on the octahedral planes as given by Nadai (1950, p. 103). The discrepancy is not too important because of the large scatter of the flow law data.

The tunnel data could not be placed directly on the diagram because a power-law relation must be assumed to convert from mean stress away from the tunnel to octahedral shear stress along the tunnel walls in Nye's method of computation. The Skauthöe and Z'Mutt mean stress and contraction rate data fit a power-law relation reasonably well (Nye, 1953, fig. 1). The tunnel data have been converted point by point assuming this relation.

Stress and strain-rate values were obtained independently in all other experiments.

In spite of the scatter of points and the many gross assumptions involved in the calculations, the data point toward several distinct conclusions:

1. Hydrostatic pressure has little effect on the flow rate, at least at shallow depths. This is indicated by the close similarity of the vertical and transverse profile data from Saskatchewan Glacier, and the similarity between the data from the Saskatchewan, Malaspina, and Jungfraufirn boreholes. These boreholes were drilled in glaciers of markedly different slope and therefore reached the same shear stress at markedly differing pressures. This conclusion agrees with recent laboratory results on the velocity of shear deformation of single ice crystals when the temperature difference between ice sample and melting point is kept constant (Rigsby, 1957).

2. Extending and compressing flow have minor effect on the flow-law relation except at low stresses. The Jungfraufirn borehole was in the center of an accumulation basin, in an area where the flow was markedly extended (0.14 years^{-1}). The Malaspina borehole was in an area of strong compressing flow, the Saskatchewan borehole was in an area of slight compressing flow (0.014 years^{-1}), and the Saskatchewan transverse profile was in an area of very slight extension (0.001 to 0.012 years^{-1}). These differences in environment do not cause a major displacement of the flow-law curves computed on a laminar-flow assumption.

3. All of the data give similar flow-law results except for those data from the Austerdalsbre and Arolla tunnels. This suggests that Nye's analysis of tunnel contraction breaks down when the general stress environment is not hydrostatic. In addition, the data suggest that Glen's analysis of creep curves using Andrade's law (Glen, 1955, p. 529) leads to results consistent with field relations. It is interesting to note that the actual measured points for the Skauthöe and Z'Mutt tunnels fit the general trend of results better than the power-law relation assumed by Nye (1953, p. 486).

4. There is no evidence for a yield stress of ice, even at stresses less than 0.01 bar. Movement along a glide plane in a single crystal probably occurs only when a critical shearing stress is reached on that plane (Turner, 1948, p. 229), and in the case of the ice crystal this stress may be about 5 bars (Bjerrum, 1952, p. 390). Therefore, intracrystalline deformation in ice must take place through the movement of dislocations—small imperfections in the crystal lattice.

5. The flow is more 'viscous" at low stresses and more "plastic" at high stresses, and the flow law seems to be more complex than a simple power-law relation.

Several analytical equations have been suggested by recent theoretical work on the flow of ice or metals. It is instructive to note how closely these equations fit the data. The theoretical equations of greatest interest have these forms:

$$\dot{\epsilon}_0 = \sigma_0^n \tag{10}$$

$$\left.\begin{array}{l} \dot{\epsilon}_0 = \sigma_0^n \\ \text{where} \\ k = k_1 \text{ and } n = n_1 \text{ at } \sigma_0 \leqq \sigma_0 \text{ critical} \\ \text{and} \\ k = k_2 \text{ and } n = n_2 \text{ at } \sigma_0 > \sigma_0 \text{ critical} \end{array}\right\} \tag{10a}$$

$$\epsilon_0 = k_1 \sinh\ (k_2\sigma_0) \tag{10b}$$

Equation (10) was suggested as a good fit to laboratory results on the deformation of polycrystalline ice by Glen (1955, p. 528) and for single crystals by Steinemann (1954, p. 404). Subsequently, Weertman (1957) published a dislocation climb model for steady-state creep. This model does not require the formation of immobile dislocations and can therefore be applied to hexagonal crystals such as ice.[10] This theory (Weertman, 1957, p. 363) suggests equation (10) for low stresses in which the exponent n

---

[10] Considerable care must be used in interpreting the deformation of polycrystalline ice in terms of the behavior of single crystals. As far as is known, ice can glide only on its basal plane. Uniform plastic strain requires the simultaneous operation of five independent sets of planes if it is to be produced by slip alone (Hill, 1950, p. 8). Therefore contact between grains cannot be maintained by slip along basal planes alone, and effects at the grain boundaries must have an important influence on the flow.

has the value of 4.5. Figure 40 suggests that a simple power-law dependence (equation 10) is not quite correct. The Saskatchewan transverse profile and the laboratory results (Andrade's law analysis) of Glen both indicate that a real discrepancy at low stresses exists in spite of the effect of longitudinal extension or compression. Landauer (1957, p. 6) also suggests that a simple power-law relation is an over simplification.

Equation (10a) describes the flow law of aluminum at elevated temperatures (Servi and Grant, 1951, p. 911). This discontinuous behavior is attributed by these authors to an abrupt transition from grain boundary to intragranular creep. Many mechanisms have been suggested for the creep of ice (Sharp, 1954, p. 826–828) and the activation energy of creeping snow suggests that several mechanisms may act simultaneously (Landauer, 1955, p. 6). However, it is difficult to understand why any two possible creep mechanisms in ice should operate in this discontinuous manner. It would seem more logical for the two mechanisms to appear as separate terms in a flow-law equation. It must be noted that the strain softening observed by Steinemann (1954, p. 408), Griggs and Coles (1954, p. 10–20) and Glen (1955, p. 525) cannot be related to equation (10*a*) or to a break in slope on the stress-strain rate graph because the onset of strain softening is a function of the total strain, not the strain rate.

Equation (10*b*) states that the velocity of shear is proportional to the hyperbolic sine of the applied stress. This relation has been suggested on theoretical grounds by Eyring (Eyring, Glasstone, and Laidler, 1941, p. 483) for the laminar flow of a generalized fluid considered as a chemical-rate process. This theory has been applied to the flow of solid metals (Dushman, Dunbar, and Huthsteiner, 1944). Equation (10*b*) does not apply to the field data at the higher stresses, but affords a good fit at the lower stresses. A similar equation has been given for the creep of a single hexagonal crystal (Weertman, 1957, p. 363), but does not follow the data at higher stresses.

The flow data which have been assembled in figure 40 seem to indicate that two mechanisms of flow operate simultaneously. The relation

$$\dot{\epsilon}_0 = k_1\,\sigma_0 + k_2\,\sigma_0^{\,n} \qquad (10c)$$

seems to approximate the data quite well. This relation would be probable if steady-state creep in ice was due to two theoretically plausible mechanisms operating simultaneously: first, a Newtonian viscous flow due to grain-boundary creep (Jellinek and Brill, 1956, p. 1207; Cottrell, 1953, p. 210–211) and second, a power-law steady-state flow due to intracrystalline gliding produced by dislocation climb (Weertman, 1957). This suggested flow-law relation cannot be rigorously tested by the observed data, but it is not inconsistent with them. The following empirical coefficients are suggested:

$$k_1 = 0.018,\ k_2 = 0.13,\ n = 4.5$$

DISCHARGE RELATIONS

VELOCITY AT DEPTH

METHOD OF COMPUTATION

Velocity at depth can be calculated along the centerline of a valley glacier flowing in a simple channel if some assumptions about the stress are made, and information about the relation between stress and strain rates is available. Velocity distributions at depth have been calculated for other glaciers, but the situation for Saskatchewan Glacier is unique in that the calculation involves very few assumptions that have not been previously tested, and the results can be checked by several independent means.

The shearing stress that produces the shearing flow must first be determined. For simplicity, the stress on planes parallel to the surface will be computed. As can be seen on plate 5, the shear stress resolved on planes parallel to the surface is not very different from the stress resolved on planes parallel to the velocity vector or the streamlines. Consequently, equation (8) is applicable; this equation has been approximately verified by giving consistent flow law results (fig. 40). The cross section, surface slope and specific weight of ice are constant at any one vertical profile in Saskatchewan Glacier, so equation (8) can be written simply as

$$\sigma_0 = Cz \qquad (8')$$

where $C = \frac{R}{d}\,\gamma \sin \alpha$ and is expressed in pounds per cubic foot. The flow law relation is

$$\dot{\epsilon}_0 = f'\,(\sigma_0) \qquad (7)$$

and

$$\dot{\epsilon}_0 = \sqrt{\frac{2}{3}}\,\frac{\partial V_x}{\partial z}. \qquad (9)$$

Therefore,

$$\frac{\partial V_x}{\partial z} = \sqrt{\frac{3}{2}}\,f'\,(C_z)$$

$$V_{x_0} - V_{x_z} = \sqrt{\frac{3}{2}}\int_0^{-z} f'\,(Cz)\,dz \qquad (14)$$

where $V_{s_0} = V_s$ at the surface and $V_{s_z} = V_s$ at depth $-z$.

RESULTS

Vertical velocity profiles at eight places along the longitudinal centerline profile of Saskatchewan Glacier are presented in plate 5. The curve for the highest profile (*h*) is a crude approximation because the cross-sectional characteristics could only be estimated. These results show that, in spite of the great differences in depth, slope and surface velocity, the curves all demonstrate a very low velocity at the bed. This bed velocity ranges from −11 fpy (probably due to a depth value that is slightly too large) to +50 fpy in absolute amount, or from −10 to +58 percent of the surface velocity. For the 7 best known cross sections the bed velocity averages 19.8 percent of the surface velocity.

The average velocity (area of the velocity-depth profile divided by the depth) ranges from 94 percent of the surface velocity at the terminus to 55 percent of the surface velocity in Castleguard sector (profiles *f* and *g*). There seems to be little justification for the frequently made assumption that the average velocity is approximately equal to the surface velocity (Nielson, 1955, p. 7–8). This seems to be true only where the ice is very thin such as at the terminus of Saskatchewan Glacier or under a thin cirque glacier (McCall, 1952, p. 126).

MASS BUDGET

FLOW INTO CASTLEGUARD SECTOR

The surface velocity and cross section at the upper part of Castleguard sector ($x' = 5{,}000$) are known with reasonable accuracy. Furthermore, the cross section here is amenable to stress calculation with few drastic assumptions, and the flow is nearly parallel to the surface. The discharge through this cross section can be computed with a reasonable assurance of accuracy.

Lines of equal velocity were drawn on a diagram of this cross section using as control the known distribution of velocity at the surface and the computed velocity (using fig. 41) at depth along the centerline (fig. 42). The total discharge through this cross section was computed by multiplying the area between each pair of equal-velocity lines by the average of the two velocity values and summing the results. This computation was done for the south half only, because of the complicated geometry and discharge relations along the north margin. The resulting discharge for the south half is 356×10^6 cfy, or 11.3 cfs.

SURFACEWARD FLOW

The discharge through a given cross section must be equal to the flux of ice toward the surface over the whole area of the glacier below that cross section. Thus the discharge and the depth of a glacier can be computed from measurements of the component V_d. (See p. 25.)

The total supply of ice to the south half of the glacier surface below $x' = 5{,}000$ was computed by graphically integrating the values of V_d given on figure 18. The result is 367×10^6 cfy. This agrees very well with the computed discharge through the cross section at $x' = 5{,}000$. The error of 3 percent is less than expected considering the crudeness of the V_d data along the sides of the glacier below Castleguard sector. The agreement in these values also indicates that the glacier is in a state of "constant unbalance": the ice that is being discharged into the tongue is just sufficient to maintain the present rate of thinning.

These and additional mass budget data are summarized in table 7.

STREAMLINES

METHOD OF DETERMINING

A streamline is a curve drawn so that its direction

TABLE 7.—*Mass-budget data for the south half of the tongue of Saskatchewan Glacier*

	Discharge (cfy × 10⁶)	Method of computation
At the firn limit....	360	Integral of V_d over tongue.
	553	Integral of ablation over tongue.
At $x = 5{,}000$......	356	Double integral of measured velocity at surface and computed velocity at depth.
	367	Integral of V_d over area below this section.
	523	Integral of ablation over area below this section.
At $x^1 = 10{,}000$.....	317	Integral of V_d over area below this section.
	438	Integral of ablation over area below this section.
Deficit for the whole half-tongue.	186	Integral of ablation minus integral of V_d over the whole half-tongue.
Average contribution to streamflow by ice melt during ablation season.	[1] 70.3	Integral of ablation expressed as cubic feet per second during a 3-month ablation season, assuming no losses.

[1] In cubic feet per second.

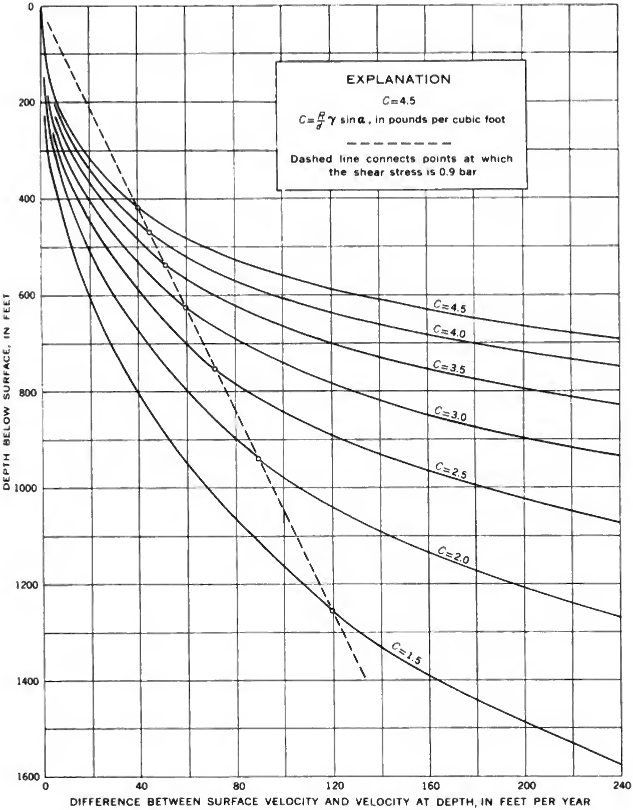

FIGURE 41.—Difference between velocity at the surface and velocity at depth as a function of depth.

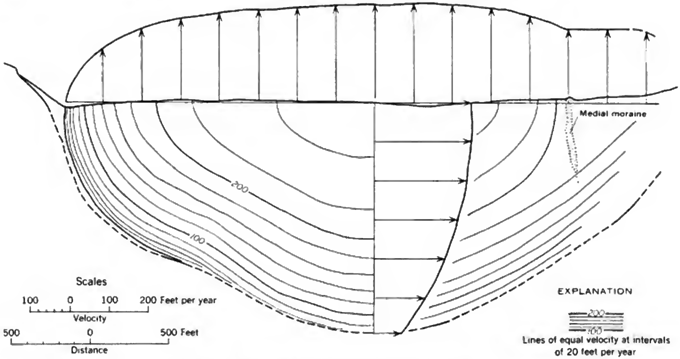
Medial moraine
200
100
Scales
100 0 100 200 Feet per year
Velocity
500 0 500 Feet
Distance
EXPLANATION
200
100
Lines of equal velocity at intervals of 20 feet per year

FIGURE 42.—Distribution of velocity in transverse section at $x' = 5{,}000$.

at every point coincides with the direction of the velocity vector. In steady flow (flow that does not vary in the course of time) the streamlines also coincide with the paths taken by separate particles (Prandtl and Tietjens, 1934, p. 73). The streamlines that pass through a closed curve collectively form a stream tube, and in steady flow no material can pass through the boundary of a stream tube. Thus the mass discharge through any stream tube must be constant. The flow of Saskatchewan Glacier is virtually steady, the ice is relatively constant in density, and very little internal ablation occurs, so the volume discharge through any stream tube must also be constant. Positions and shapes of streamlines along the centerline plane can be computed using this constancy of discharge relation. For simplicity of calculation, a unit width (in the y' direction) of flowing material is assumed throughout the calculations. This is not completely realistic because transverse extensions or compressions ($\dot{\epsilon}_{yy}$) do occur. However, these effects along the flow centerline of Saskatchewan Glacier are small compared to the shears ($\dot{\epsilon}_{xz}$) involved, and the simple analysis seems to offer a close approximation to the actual behavior.

The calculation proceeded as follows: The area under a graph of the vertical component of flow toward the surface (V_d) as a function of distance along the centerline (x', fig. 23c) was divided into 10 equal parts from the terminus back to $x' = 5{,}000$ feet. These equal parts represent equal discharges to the surface (see p. 24) of about 17.5×10^3 cubic feet per year per foot of width. Vertical profiles of the horizontal component of velocity were computed at or near 7 points marking multiples of these equal surfaceward discharges (pl. 5). The area of each of these profiles was divided into the same number of parts as the number of surfaceward discharge parts emerging downglacier from the profile. Lines were drawn dividing these equal parts of the discharge at depth so as to intersect the surface at points separating the equal surfaceward discharges. These lines represent streamlines of flow, and the volumes between adjacent pairs of lines and the unit width represent stream tubes handling constant discharges. These results are shown on plate 5.

CHECKS ON ACCURACY

The accuracy of these constructions can be checked several ways: First, the actual streamlines should crop out at the surface exactly parallel to the velocity vectors. The constructed streamlines with reasonable accuracy, as shown on plate 5. The streamlines and velocity profile at profile C are not very accurate because the cross section is not known exactly and there is some divergence between the velocity vectors and the streamlines in this area.

A second check on the entire construction (including the vertical velocity profiles) is that the discharges represented by each of the vertical profiles should be equal to the discharge to the surface downglacier from that profile. The discharges through a vertical section are determined by $V_{s'}$ on the surface, the depth, slope and cross section at that point. The discharges to the surface are determined by the integral of V_d times the area, and these values are computed from the surface profile, $V_{s'}$ and V_s. Thus these two quantities are almost independent and can be compared. The increments of discharge to the surface were 17.5×10^3 cfy per foot of width. As shown in the tabulated data on plate 5, the incremental discharges at depth were similar to this value for most vertical profiles. The agreement is close considering the many approximations and assumptions involved in this calculation. Therefore we can assume that plate 5 gives a virtually correct interpretation of the distribution of streamlines at depth under the flow centerline.

CONCLUSIONS FROM THESE RESULTS

The two most striking features of the streamline distribution are (1) the close spacing near the surface and (2) the parallelism of streamlines to the bed profile.

The close spacing of streamlines near the surface is necessary because the velocity is greatest near the surface. However, in the several diagrammatic profiles showing hypothetical streamlines which have been published, close spacing has not always been considered. This spacing indicates that the ice which crops out 1½ miles upglacier from the terminus was never buried more deeply than one-half the total depth of the glacier. Thus the presence of slightly recrystallized ice still showing a primary stratification in the lower part of the tongue need not be considered unusual.

A more significant feature of the streamline distribution is the close parallelism between streamlines and bedrock. This parallelism is modified very slightly in the upper layers where the curvature of the streamlines is somewhat reduced. In general it seems that the shape of the streamlines is virtually independent of the thickness or speed of the glacier and is determined mainly by the long profile of the bedrock. The significance of this fact will be discussed in the next section.

LONGITUDINAL PROFILE

SIGNIFICANCE OF THE PROFILE

The length, thickness, and slope of a glacier are expressed in its longitudinal profile. Advances, recessions, and waves of thickening can be expressed quantitatively as transient changes in the profile. The shape of an equilibrium profile is ultimately determined only by the bedrock configuration and by the prevailing gradients of potential accumulation and ablation. Past climates might be quantitatively reconstructed from studies of old moraines if knowledge of bedrock topography and meteorological conditions could be used in predicting the longitudinal profile of a glacier which was in equilibrium with this environment. And likewise present-day climatic trends might be determined from present-day profiles. Glacial geology, paleoclimatology, and hydrology would benefit inestimably.

This prediction cannot be made at the present state of glaciological knowledge. The first task is to determine which geometrical factors are most important in shaping a longitudinal profile for a given discharge. The method which has been used most often in the past and the research that could be pursued in the future will be discussed in the following paragraphs.

CONSTANT BASAL SHEARING-STRESS CALCULATION

The profile of a large ice sheet resting on a horizontal floor has been calculated by Orowan (1949), Hill (see Nye, 1951, p. 571), and Nye (1951, p. 570–571; 1952a, p. 91–93) by assuming that the shear stress on the bed was everywhere constant. In a further calculation Nye (1952c) allowed the bed slope to change gradually along a line of flow. A similar analysis was applied to a valley glacier similar to Saskatchewan Glacier (Nye, 1952b).

These calculations gave good results along one profile in Greenland (Nye, 1952c, p. 531), but predicted a great depression of the bedrock over the northern half of Greenland which has not been confirmed by subsequent seismic and gravity measurements (Bruce and Bull, 1955). The valley-glacier profile, when adjusted by changing the "average shear stress on the bed" to the best fit for the glacier as a whole, did not give good results at the terminus and did not predict the proper length of the glacier.

The shear stress on the bed of a glacier is not constant, as has been shown for an icecap (Orvig, 1953) and for the Saskatchewan Glacier (pl. 5). This variability is a very significant objection to this theory because of the high sensitivity of flow rates to slight changes in shearing stress (fig. 40).

The most significant objection to this method of computing the profile of a glacier is the change in lengths and thicknesses of a glacier in response to changing climate. The constant basal shear stress theory cannot account for any changes in profile with time. Even if this method could be modified to produce consistent results when applied to present-day glaciers, it would disclose nothing about the relation of glaciers to their climatic environment. Therefore further pursuant of this method of calculation seems fruitless.

HYPOTHESIS FOR THE LONGITUDINAL PROFILE

A few comments on how a long profile might be calculated are offered. The Saskatchewan data reveal two significant facts that provide a starting point for this calculation: (1) the streamline shapes are determined only by the bed and (2) the velocity at the bed is a minimum.

Visualize a field of streamlines fixed in space above a certain longitudinal bedrock profile. As a first approximation, the plunge of the streamlines ξ is equal to the slope of the bed β. At any one vertical section the surface slope α must cut these streamlines at the proper angle $\alpha - \xi$ so that $\frac{V \sin(\alpha - \xi)}{\cos \alpha} = -V_d$. For an equilibrium condition, $V_d = -V_a$. However, V is determined by α, z, and the cross-section shape, and V_a is also a function of z. The mathematical difficulties treating all of these interrelationships analytically preclude a simple solution to the problem at this time. Furthermore, the form of the flow-law relation (equations 10*a*, *b*, *c* or *d*) must be clarified. When these interrelationships can be stated in a usable analytic form so that actual glacier profiles can be constructed, it will be possible to relate glaciers to their climatic environment in a quantitative manner.

STRUCTURAL FEATURES

Glacier ice first accumulates as a sedimentary deposit. It is then metamorphosed by flowage and other agents, causing secondary flow structures to be impressed on the primary sedimentary features. Structural features form continually in this deforming material, and are of great interest because they illustrate the formation of many structures which occur in deformed rocks. The following discussion is included for a different reason: A study of the features produced by flow lends insight into the flow process. Furthermore, if the relation of structures to flow geometry can be demonstrated in certain areas, the structures can be used to predict the flow geometry in other areas where no flow measurements have been made. Structural studies, therefore, are a useful adjunct to a thorough investigation of glacier movement.

As in some thoroughly metamorphosed schists, it is often difficult to differentiate primary from secondary structures in glacier ice. After 3 years of observation on Saskatchewan Glacier and several years of study on other glaciers, the author could distinguish between primary and secondary structures with confidence only about 50 percent of the time. Structural studies and interpretations were handicapped by this uncertainty. Differentiation was obtained by classifying features solely on the basis of orientation groupings.

Structures were mapped in a reconnaissance over the entire tongue of Saskatchewan Glacier (pl. 2*A*). A detailed map of structures at the terminus was constructed by planetable means (pl. 3). Structures were studied most intensively in the lower part of Castleguard sector because the geometry was relatively simple and the flow was best known, but even here the minute complexity of features on the surface of this large area (nearly a square mile) made it necessary to sample, not map, them. In order to eliminate appreciable bias, the attitude and general appearance of structures at many sampling points were recorded. Attitudes were measured by Brunton compass. In some areas of low relief, dips were difficult to measure, and an inaccuracy of less than ±5° could not be obtained.

With few exceptions, all of the structures observed can be placed in these five main classifications:

Stratification.—A primary sedimentary layering inherited from the firn.

Foliation.—A secondary compact layered structure produced by deformation.

Cracks.—Secondary planes of weakness distinguished by noticeable separation of the two walls.

Faults.—Secondary planes of weakness distinguished by appreciable shearing movement parallel to the walls and little separation of the walls.

Fold axes.—A preferred orientation of fold axes was the only lineation observed.

STRATIFICATION

APPEARANCE

Primary layering in this glacier is most easily recognized close to the firn limit. Here it appears as gently dipping layers of loose, granular, partly reconstituted firn alternating with ice layers and lenses formed by freezing of percolating melt water (pl. 7*A*, *B*). The granular layers are much too thick (as much as 6 feet) and variable to be a product of shearing. Sedimentary layers can be identified with certainty as far as 3 miles below the firn limit and with less certainty within 3,000 feet of the terminus. The layering is most easily recognized from a high

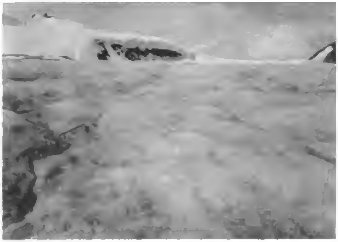

A, STRATIFICATION EXPOSED AT THE SURFACE 3.0 MILES BELOW FIRN LIMIT

A prominent stratum runs from lower left-hand corner to center horizon, dipping in direction of ice axe. The photograph shows vertical foliation that extends diagonally from upper left to lower right intersecting the stratification

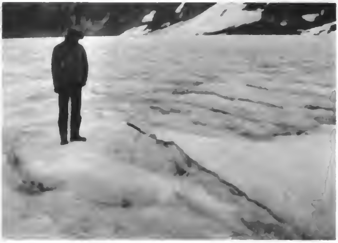

B, PROMINENT STRATUM EXPOSED SOUTH OF CENTERLINE IN MID-GLACIER, 2.1 MILES BELOW FIRN LIMIT

Outcrop trace appears as short-line segments; individual parts of the stratum dip in direction of ice axe (toward the south margin and slightly downglacier)

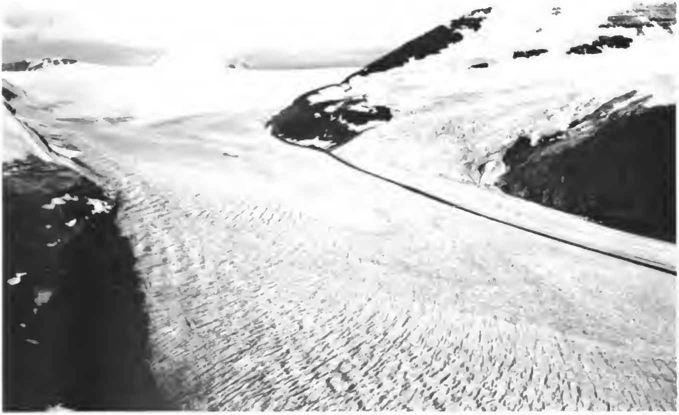

C, OUTCROP PATTERN OF STRATIFICATION IN CASTLEGUARD SECTOR

View upglacier from cliff on south margin below Castleguard Pass. Splaying and en echelon crevasses are also visible distant vantage point (pl. 7*C*), where it appears as zones or alternating bands of grayish and white ice. In some areas this broad tone banding can be traced over the glacier surface by an observer on foot and is seen to coincide with the layering of coarse- and fine-grained ice mentioned above. In many places the outcrop of granular layers appears distinct because fine mineral debris collects in the fine-grained intergranular depressions whereas it is washed off the smooth surface of coarse-grained ice layers. In fresh exposures made by digging, the fine-grained granular layers do not seem to contain any more dirt than the adjacent layers of coarse ice. It seems likely, though not certain, that the dirty appearance of the granular layers is due to a surficial deposit of silt, secondarily acquired from wind or melt water. Very fine grained granular layers are less common toward the terminus and contrasts between the appearance of adjacent layers are also less marked downglacier. This is evidently due to recrystallization. Little evidence of a rhythmic or cyclic repetition of bands was found, and annual layers of deposition could not be recognized.

OUTCROP PATTERN

The outcrop pattern of this stratification resembles that of truncated beds in a plunging fold (pls. 2*A*, 7*C*). The bands are most conspicuous in Castleguard sector and gradually become indistinguishable downglacier and toward the margins. None has been recognized in the area between the firn limit and $x' = 3{,}000$, but evidence indicates that they may have been hidden by unconformable overlying layers.

The main apex of the "fold" lies in the middle of the glacier and points downglacier. Spacing and width of the bands are not uniform and the sharpness of curvature and axial length of the curves increases downglacier because of faster movement in the center.

Many of the measured attitudes in Castleguard sector imply that the sedimantary layering has the shape of an anticline plunging downglacier (pl. 7*B*, *C*) with respect to the glacier surface. Older ice, which underlies younger ice, crops out farther downglacier; therefore an upglacier dip with respect to the glacier surface is expectable (fig. 43). A possible explanation of this puzzling outcrop pattern is exceptional thinning in Castleguard sector that has truncated nearly horizontal beds causing a local downglacier dip of stratification in relation to the present surface. An alternative and equally plausible explanation is that the apparent anticline is due to a biased sampling of attitudes and is not real. Stratification here is nearly flat lying in broad aspect but highly wrinkled in detail and it is virtually impossible to measure the gross orientation from observations at a few points.

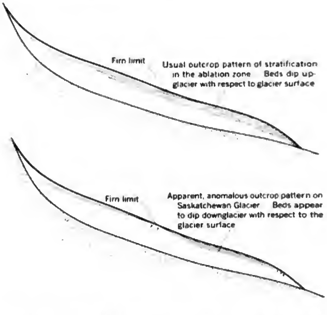
Firn limit
Usual outcrop pattern of stratification in the ablation zone Beds dip upglacier with respect to glacier surface
Firn limit
Apparent, anomalous outcrop pattern on Saskatchewan Glacier Beds appear to dip downglacier with respect to the glacier surface

FIGURE 43.—Diagrammatic longitudinal sections of a glacier showing sedimentary layering.

Although individual layers must crop out in broad zones that cross the glacier, stratification as seen on the glacier surface appears as discontinuous longitudinal lines (pl. 7*B*). This is apparently due to wrinkling parallel to longitudinal foliation. This change in outcrop pattern from transverse bands to longitudinal lines has been observed elsewhere (Kalesnik, 1939, p. 80). On Saskatchewan Glacier this wrinkling was probably formed when the broad sheets of firn from the Columbia Icefield were drawn through the narrow throat and into the valley occupied by the tongue.

FOLIATION

Much of the recrystallized surface ice of Saskatchewan Glacier shows a pronounced layered structure seemingly related to deformation. The name foliation is appropriate for this structure (Chamberlin and Salisbury, 1909, p. 247), and in this report the term will be restricted to compact secondary planar features caused by flow. In this sense, foliation may be identified with the "Feinbänderung" of Schwarzacher and Untersteiner (1953, p. 114–115), but prudence should be used in comparing it directly with banded structures in other glaciers described under diverse names such as "blue bands," longitudinal bands," "tectonic blue bands," "Bänderung,"

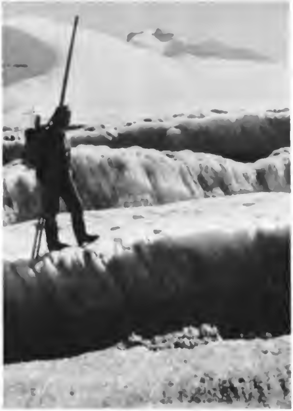

A, STRONG FOLIATION NEAR SOUTH MARGIN, 2.6 MILES BELOW FIRN LIMIT

Viewed upglacier. Foliation attitude is apparently conformable with valley wall to the left

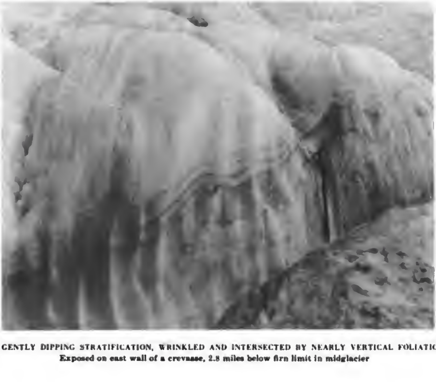

B, GENTLY DIPPING STRATIFICATION, WRINKLED AND INTERSECTED BY NEARLY VERTICAL FOLIATION

Exposed on east wall of a crevasse, 2.8 miles below firn limit in midglacier

"Blätterung," "Pflugfurcheneis," "Druckschichtung," and "Scherflächen."

APPEARANCE

Foliation on Saskatchewan Glacier generally appears as alternating laminae of white bubbly ice and bluish clearer ice. Intercalated with these laminae are some thin layers of very fine grained, apparently brecciated ice. Locally, foliation is expressed by minor but abrupt differences in grain size. In some areas the foliated structure is obvious on either fresh or weathered surfaces (pl. 8*A*) and in such areas the thickness of individual folia is less than 1 inch. Over most of the glacier, however, foliation cannot be detected on a fresh ice surface and is only visible as a faint grain on the surface of weathered ice.

Many exposures show this layered structure as transecting (pl. 7*A*), wrinkling (pl. 8*B*), or offsetting (pl. 9*A*) other structures including primary stratification. In a few localities, however, the foliation appears to be truncated by sedimentary layering but these anomalous relations can be explained by differences in mechanical properties of adjacent ice layers. Shear strain in a mass of ice may form foliation in one layer by recrystallization and be taken up by undetectable intragranular movements in a less compact layer.

Criteria for differentiating foliation from primary stratification are presented in table 8.

OUTCROP PATTERN AND INTENSITY OF DEVELOPMENT

Foliation on Saskatchewan Glacier has a steeply dipping, longitudinal orientation (pl. 2*A*) except at the extreme terminus (pl. 3). Foliation parallels the valley wall at the margin, but dips are steeper in midglacier and nearly vertical dips predominate in the central third of the glacier. In Castleguard sector foliation dips about 75° toward the south margin in a strip 900 feet in from that margin. Folia are somewhat planar in the first 4 miles below the firn limit. Below that point the faint folia in midglacier are increasingly contorted (pl. 9*B*). Within 1,000 feet of the terminus the foliation forms a spoon-shaped structure dipping upglacier at a slight angle (pl. 3).

Foliation varies greatly in intensity of development, as expressed by closeness of spacing of folia, contrast in grain size, and contrast in bubble content across adjacent folia. Several degrees of foliation intensity are mapped in plate 2*B*. Foliation is most intense near the margins and along the medial moraine. Belts or zones of abnormally strong marginal foliation occur next to valley-wall bulges. These do not persist more than 1 mile below their apparent point of origin. Strongest foliation along the lower part of the medial moraine is in the tributary ice adjacent to but not under the moraine. In the upper part of Castleguard sector, however, foliation intensity is greatest under the center of the medial moraine. No difference in average foliation intensity across the glacier was detected from the upper part of Castleguard sector ($x' = 5{,}000$) to the terminus.

TABLE 8.—*Criteria for distinguishing foliation from stratification*

Stratification	Foliation
1. Subtle, best seen from a high, distant vantage point. May not be visible in a close view.	1. Indistinct when viewed from a distance, usually obvious in a close view.
2. Contorted or obscured by shearing, and is therefore best observed in the middle of the glacier.	2. Definitely related to zones of great shearing and therefore strongest near margins and in medial moraines.
3. Layers generally not thin, but some ice layers 1 to 2 mm thick may be separated by much thicker layers of unrecrystallized firn.	3. Folia may be very close together (separated by less than a millimeter.
4. Layers may be obviously irregular or lenticular and less perfectly parallel.	4. Folia are generally planar and parallel except where secondarily contorted.
5. May include obvious structures inherited from the firn (ice lenses, glands).	5. Never includes ice lenses, glands, or other structures of the firn.
6. Usually recognizable on close inspection by contrasts in grain size, or by dirt content when viewed from a distance. Layers of fine-grained, loose grains (beds of only partially recrystallized firn) may be many feet thick.	6. Usually recognizable by contrasts in bubbliness of ice in adjacent folia. May also be grain size differences. Fine-grained, granulated ice only in very thin zones. Usually no conformable dirt.
7. Seldom causes other structures to be offset.	7. Often recognizable as a secondary structure by offsetting or transgressing other features.
8. Dips usually gentle except where severely contorted.	8. Attitude tends to parallel valley walls in strike and dip, hence steep.

CRACKS

APPEARANCE

These planar structures are sharp discontinuities in the ice and they often have an air- or water-filled space between the walls. Some cracks are filled with ice crystals that have grown from the freezing of water that filled the crack after it had opened. These secondary "candle-ice" crystals are elongated perpendicular to the crack and are unlike ordinary glacier ice. It was easy to distinguish these features from foliation or stratification. Many cracks show shearing displacements. The strain on most of the surface of this glacier is strongly rotational (table 4), therefore all old cracks will show some shearing deformation. No effort was made to measure shear on open cracks or to classify them in this regard. Young closed fractures with appreciable shearing displacement are classed as faults and are discussed in the next section.

The cracks range in width from tiny, sharp fractures with openings of a millimeter or less

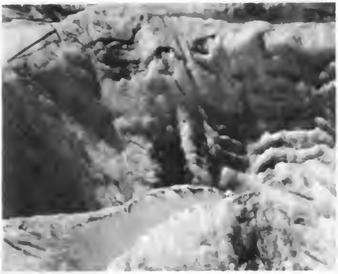

A. STRATFICATION(?) OFFSET BY FOLIATION

Viewed upglacier from a point 30 feet in from south margin, 2.5 miles below firn limit

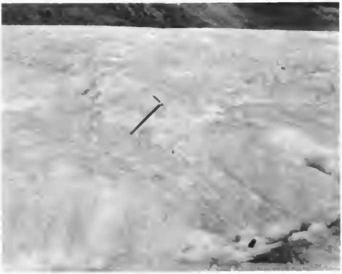

B. FAINT CONTORTED FOLIATION, 0.8 MILE ABOVE TERMINUS, SLIGHTLY SOUTH OF CENTERLINE

Viewed downglacier. Foliation is nearly vertical and longitudinal in attitude. It appears as faintly wrinkled grain on the ice surface and trends directly away from the observer in the center of the field of view. Primary stratum crosses the field of view, dipping in the direction of the ice axe

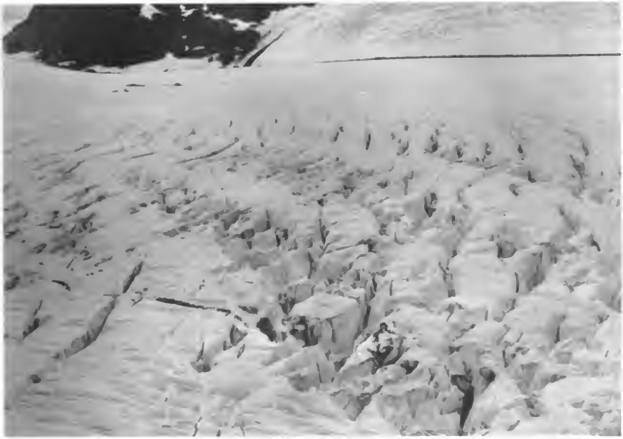

C. EN ECHELON CREVASSE BELTS NEAR SOUTH MARGIN, 1.6 MILES BELOW FIRN LIMIT VIEWED NORTHWEST

("Haarrisse") to crevasses many yards wide. A distinction was made in the field between crevasses (more than 1 foot in width) and other cracks, but this distinction has no genetic or mechanical significance. The longest cracks extend for 1,000 feet; none less than about 20 feet was measured. Cracks are generally planar, although in the center of the glacier a few fractures of irregular shape were seen. The dip of cracks is almost invariably normal to the glacier surface. Crack depths were not measured.

PATTERN

The largest cracks (crevasses) form regular patterns on the glacier surface (fig. 44). Four different patterns are distinguished:

Splaying crevasses.—Crevasses having a longitudinal orientation in midglacier splay out toward the margin intersecting it at an angle slightly greater than 45° (fig. 44*A*). The apex of the acute angle at the margin always points downglacier. These crevasses are best displayed in Castleguard sector (pl. 7*C*). "Longitudinal crevasses," often mentioned in the literature, are merely splaying crevasses as observed in midglacier; true logitudinal crevasses cannot exist except along the centerline in a valley glacier.

Transverse crevasses.—These crevasses are convex upglacier and are normal to the flow direction in midglacier but curve to strike the margin at the same angle as splaying crevasses (fig. 44*B*). Where transverse and splaying crevasses occur together on a valley glacier they can be differentiated only in the central half. Transverse crevasses dominate a weaker pattern of splaying crevasses on and above the ice fall of the only tributary to Saskatchewan Glacier.

Chevron crevasses.—Straight crevasses (fig. 53*C*) extend from the margin toward the center of the glacier at a constant angle equal to the marginal acute angle mentioned under types (*A*) and (*B*). These do not extend to the centerline, and chevron crevasses from the two sides do not intersect. These crevasses are well formed just below Castleguard sector on Saskatchewan Glacier.

En echelon crevasses.—Short, wide crevasses ar-

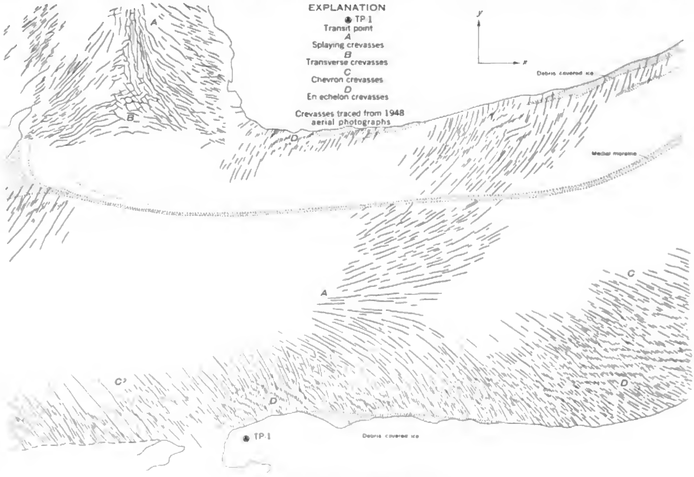

FIGURE 44.—Crevasses in Castleguard sector.

ranged in subequally spaced narrow belts (pls. 7*C*, 9*C*, fig. 44) are oriented en echelon. They are generally parallel in trend to one of the larger patterns. On Saskatchewan Glacier en echelon crevasses are best seen in three areas in Castleguard sector, where the narrow belts intersect the margin at acute angles of 20° to 35°.

In addition to the crevasses which form these different patterns, many minor cracks with apparently random orientation are seen on the surface of Saskatchewan Glacier. These define specific patterns, but a statistical approach must be used, and description of these features is postponed to the discussion of an area of detailed study.

FAULTS

Faults are fractures or discontinuities having noticeable shearing displacement and little or no normal separation of the two bounding blocks. They may be associated with the "Scherrisse" of the Alpine literature (Klebelsberg, 1948, p. 62–69). Left-hand strike-slip faults are common along the south margin just below Castleguard sector, where the glacier is shoved to the left by a curving valley wall. Most of the faults show horizontal displacements of a foot or less, and many of them also show slight dip-slip displacements (downglacier block had moved down). These are nearly vertical in dip and curve in strike from nearly parallel to the valley wall at the edge (the sharp acute angle pointed upglacier) to a nearly transverse orientation a few hundred feet in on the glacier. None could be traced farther. Other faults occur in Castleguard sector (pl. 3c).

FOLD AXES

Several types of linear structures, such as elongated grains and bubbles, have been observed in glacier ice (Schwarzacher and Untersteiner, 1953, p. 115). None of these is obvious on Saskatchewan Glacier, and the only lineation recorded is that formed by the axes of folds in contorted stratification. The plunge of these axes could not be measured except in fortuitous situations; consequently the nine measurements are too few to be statistically significant.

All measured fold axes plunge against the direction of flow, generally at angles much steeper (as much as 56°) than the velocity vector. Clearly, this lineation is not parallel to the direction of transport of the ice. Indirect evidence (the stratification outcrop pattern) suggests that the majority of fold axes near the flow centerline are nearly parallel to the glacier surface, but few measurements could be made. The lineation apparently lies in or near the plane of the associated foliation.

STRUCTURES OF CASTLEGUARD SECTOR

In order to study the myriads of small cracks and folia in an area where the surface deformation and flow conditions were known, structural information was obtained by a sampling technique in Castleguard sector. A total of 78 points were spaced at equal intervals (about 100 feet) on 3 transverse profiles extending from the south margin to within 800 feet of the medial moraine. All structures visible within about 20 feet of each point were measured. The total area covered was divided into three longitudinal strips (pl. 2*A*), one along the margin, one spanning the flow centerline and one covering the intermediate area. All measured structural attitudes from within each strip were collated onto an equal-area projection diagram (pl. 2*C*). No consistent differences in attitude could be detected by comparing data from the highest to the lowest transverse profile. Thus each of the three resulting diagrams shows the attitudes of structures within an area of reasonably uniform flow conditions. A similar plotting technique has been used by Untersteiner (1955, p. 504–505).

All observed structures were tentatively classified in the field as "crevasses," "cracks," "folia," "dirt layers," or "fold axes," and these field identifications have been indicated on plate 2*C*. However, with this method of plotting the distribution of orientation maxima can be studied without recourse to subjective identifications.

The density of points on each of these diagrams is contoured in order to bring out the various maxima more clearly (fig. 45). Orientation of the average velocity vector, surface strain-rate tensor and surface slope for each strip are also presented in figure 45.

These data show several clear maxima indicating preferred orientations of structural features. These preferred orientations can be followed with changing strain-rate tensor orientations from the margin to the centerline. The characteristics of each maximum are summarized in table 9.

The attitude diagram for the flow centerline shows orthorhombic, almost tetragonal, symmetry reflecting a symmetry of flow about the centerline. The diagram for the marginal strip is triclinic, almost monoclinic.

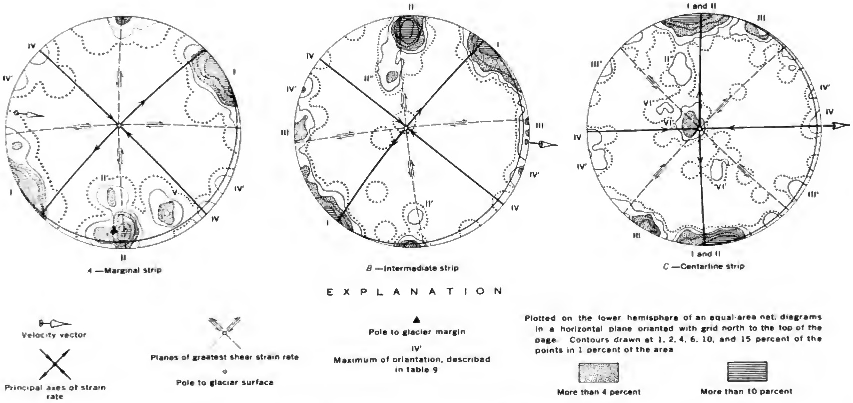

Plotted on the lower hemisphere of an equal-area net; diagrams in a horizontal plane oriented with grid north to the top of the page. Contours drawn at 1, 2, 4, 6, 10, and 15 percent of the points in 1 percent of the area

FIGURE 45.—Orientation of structural features in Castleguard sector.

ORIGIN OF TECTONIC FEATURES

FOLIATION

The origin of foliation has been a subject of considerable speculation. Recent studies have been made of the relation of crystal axes orientations to foliation (Bader, 1951; Rigsby, 1951; Schwarzacher and Untersteiner, 1953), but the results have been perplexing, and the mechanism of the origin of both this structure and the crystal orientations is still in doubt. On Saskatchewan Glacier additional important data (known strain geometry) was brought to bear on the problem, but only a few additional conclusions were forthcoming, as follows:

Foliation is related to shearing deformation.—This is evident from the warping or wrinkling of sedimentary layers (pls. 8*B*, 9*A*). Plunging fold axes that lay in the foliation plane (fig. 45*A*, *B*) also suggest a relation to shearing.

Foliation does not always form parallel to planes of greatest shearing strain.—The planes of maximum shearing strain rate intersect the principal strain rate axes at 45°. From symmetry considerations it is apparent that at the flow centerline one principal strain rate must always be directed along the centerline, both at the surface and at depth. Foliation which crops out on the surface at the plane of symmetry must have originated somewhere on that same plane of symmetry. Therefore the conclusion necessarily follows that foliation which stands parallel to a principal strain-rate plane where observed along the flow centerline could not have formed parallel to a maximum shearing strain-rate plane *either at its point of observation or at any logical place of origin.* Furthermore, there is no rotation so that planes of maximum shearing *strain* should not be different in orientation from the planes of maximum shearing *strain rate* along the flow centerline.

Further evidence suggests that foliation and maximum shearing strain-rate planes do not correspond. In the intermediate strip south of the centerline (fig. 45*B*) foliation dips to the south. The nearest plane of maximum shear stands approximately vertical at the surface, and at depth it must dip north in order to swing into approximate parallelism with the bedrock channel. Thus a discrepancy in attitude of the two planes is apparent.[11]

Feinbänderung on the Pasterze Glacier, which is apparently the same as foliation on Saskatchewan Glacier, seems to originate nearly perpendicular to the compressing principal strain-rate plane in midglacier (Untersteiner, 1954, table 1, profile 10, p. 238). Glen (1956, p. 740–742) observed a banded structure at the foot of an icefall in Norway that was within 5° of perpendicular to the compressing principal strain rate. Possibly the foliation in midglacier in Castleguard sector could have originated in this manner farther upglacier where a transverse compression occurred. However, this explanation does not apply to marginal foliation. It also seems unlikely that marginal foliation and midglacier foliation had different causes, because there was no evidence of any discontinuity in appearance or attitude.

Although it is not possible to state what actually

---

[11] This discrepancy may, however, be explained in another way: An icefall supplies ice to the south margin of the glacier below the normal firn limit. This ice is first superimposed (Sharp, 1948, p. 182) on the trunk glacier and its nearly horizontal stratification, but quickly sinks into the surrounding ice and becomes inset. Probably the preexisting stratification is bent down in the process to a steep south dip. Farther downglacier this relic stratification might be mistaken for foliation, or anisotropy due to the stratification might control the orientation of a later foliation. One argument against this is that the supply of ice from this icefall seems insufficient to account for such a large inset tributary.

TABLE 9.—*Characteristics of orientation maxima*

Designation	Strength	Orientation	Field identification	Comments on origin
I	Strong	Perpendicular to $\dot{\epsilon}_1$,* but smeared clockwise	Cracks and crevasses.	Chiefly tensile fractures. (This is the main crevasse system.)
II	do.	Very steep dip, parallel to V in strike, attitude essentially independent of strain rate tensor axes.	Folia and few dirt layers.	Not related to strain or stress tensor at point of observation. (This is the main foliation.)
II′	Moderate	Dip 45°–60°, parallel to V in strike, separated from II by 31°–40° rotation.	Folia	Apparently independent of strain tensor and related to II.
II″	do.	Dip 45°–50°, parallel to V in strike, separated from II by 36°–49° rotation in opposite sense from II′.	Folia, some dirt layers.	Do.
III	do.	Vertical, 45° to $\dot{\epsilon}_1$, missing in marginal strip	Cracks	Failure on planes of maximum shear almost perpendicular to the margin and foliation. Not developed in marginal strip because of restricting conditions at margin.
III′	Weak	Vertical, 45° to $\dot{\epsilon}_1$* (90° to III)	do.	Failure on other set of planes of maximum shear. Noticed only where not obscured by foliation.
IV	do.	Vertical, perpendicular to $\dot{\epsilon}_2$	do.	Plattungsebene? Or, cold weather construction cracks?
IV′	do.	Vertical, 15°–18° counterclockwise from IV	do.	Origin unknown, probably related to IV.
V	Strong	Strike N. 62° E.,** dip 67° N., appears only in marginal strip.	Folia and dirt layers.	Distorted primary stratification or a relic foliation? Origin unknown.
VI	Moderate	Almost parallel to surface, slight dip downglacier. Apparent only in central strip.	Dirt layers	Primary stratification.
VI′	Weak	Strike about N. 45° E.,** dip 20°–350° either north or south.	do.	Perhaps just a smearing out of VI by wrinkles with flat-lying axes.

* $\dot{\epsilon}_1$ = greatest (most extending) principal strain rate.
$\dot{\epsilon}_2$ = least (most compressing) principal strain rate.

V = velocity vector.
** Strike referred to grid north (y-axis).

determines the orientation of foliation, recognition of the fact that foliation does not necessarily indicate plans of maximum shearing stress or strain rate may be an important step in the understanding of the mechanics of crystal axis orientation.

Foliation appears to form—or be preserved—only at shallow depths.—Maps of foliation attitude and intensity suggest that foliation forms only at shallow depths (pl. 2*A*, *B*). Had foliation been formed by shearing drag of the bed it would crop out as spoon-shaped surfaces crossing the flow centerline. No such folia were observed anywhere along the centerline except within 2,000 feet of the terminus where the ice is thin. Intense transverse compression probably would subsequently crumple the spoon-shaped surfaces to unrecognizable isoclinal folds, but it is difficult to find either a mechanism for this below the firn limit or evidence of such compression in the strain rate data or in crevasse arrangements. Additional evidence that foliation is not formed—or preserved—at great depth is offered by the belts of abnormally strong foliation which apparently disappear less than a mile below their point of origin.

This conclusion is in direct contradiction with the observation of Untersteiner that the Pasterze Glacier foliation (Feinbänderung), once formed, rode passively down the whole length of the tongue and could be identified even in the oldest ice of the terminus (Untersteiner, 1954, p. 239). Merrill (1956, p. 61), however, suggests that foliation in the northern Greenland icecap is easily obliterated by recrystallization and does not generally persist. Some of the petrofabric data from Pasterze Glacier suggest recrystallization at the surface (Schwarzacher and Untersteiner, 1953, p. 116), but presumably this has not been sufficient to obliterate the Feinbänderung.

If foliation forms or is preserved only at shallow depths, some change in the mechanical properties of ice with increasing hydrostatic pressure must be assumed. Such a change has been suggested repeatedly in the literature (Demorest, 1942, p. 36–37; Haefeli, 1948, p. 197), but it has also been challenged (Hess, 1937, p. 3–5; Nye, 1953, p. 489). The flow-law data from Saskatchewan Glacier show no effects that could be related to hydrostatic pressure (p. 44), and apparently no laboratory experiments have detected any influence of hydrostatic pressure on strain rates. Observations at points of local concentration of pressure and shearing strain beneath glaciers (Carol, 1947; Meier, 1951a, p. 112 and 1951b, p. 130–134) have shown that under these conditions ice can become so soft and "spongy" that a small mass curls and settles under its own weight. Laboratory experiments (Steinemann, 1954, p. 408) show that after a shearing strain of 10 to 20 percent a single ice crystal abruptly softens and remains soft, even after removal of stress, until recrystallized. This strain-softening behavior suggests a pronounced instability in the flow of ice and indicates the great effect of recrystallization on the flow.

A speculative mechanism for the origin of foliation is offered. Under an applied stress, ice begins to yield by plastic flow (grain boundary creep and intracrystalline gliding, see p. 45). Some local areas will strain more rapidly than others because of slight differences in grain shapes and orientations. When the critical strain necessary for crystal softening is reached in any small region, that region becomes locally a weak zone which tends to propagate by capturing more strain. These soft zones may grow most rapidly in a specific planar direction, so that layers of soft ice alternate with layers of hard ice, producing a foliated structure. The larger plastic strain in the soft ice may drive air bubbles into the neighboring ice, alter the grain sizes and shapes, and produce a preferred crystal axes orientation pattern. The soft layers need not be oriented parallel to the direction of maximum shearing strain and their orientation may be controlled by a minor prevailing anisotropy in the ice. The relative amounts of hard and soft ice which will exist at any one time in any one place will depend on (a) the total plastic strain, (b) the strain rate, and (c) the rate of recrystallization.

If the rate of recrystallization is a function of depth or hydrostatic pressure, a mechanism is produced for the observed distribution of foliation. If the rate of recrystallization increases with depth, at a critical depth it will be great enough to prevent the propagation of soft zones and the resulting ice will be homogeneous and unfoliated. If the rate of recrystallization decreases with depth, the zones of soft ice may increase to the point of eliminating all of the hard ice and the resulting ice will again be homogeneous and unfoliated. What determines recrystallization in glacier ice is not fully understood and it may be presumptuous to assume that recrystallization rates vary with depth, but this seems to be the most reasonable explanation for the conclusion that foliation forms only at shallow depths.

MAIN CRACK SYSTEM (CREVASSES)

It is generally assumed that crevasses break at right angles to the greatest principal elongation or stress (Lagally, 1929, p. 293; Nye, 1952a, p. 90–91;

Untersteiner, 1955, p. 505). On the other hand, the fracture condition for metals (Nadai, 1950, p. 207–228), dry sand (Hubbert, 1951, p. 360–362), wind-packed snow (Haefeli, 1948, p. 681), and granitic rocks (Robertson, 1955, p. 1295–1304) involves both normal and shearing stresses. Data from northern Greenland (Meier, 1956) suggest that crevasses in firn form at an angle to the greatest principal elongation rate in an environment where the other principal strain rate is compressing.

As shown on figures 45 and 46, the cracks and crevasses on Saskatchewan Glacier approach but do not exactly coincide in attitude with the principal axes of strain rate. However, four effects mitigate against a direct comparison: (a) after a crevasse forms it is rotated passively in the deforming ice until it has melted out and disappears;[12] (b) the ice is somewhat anisotropic owing to foliation near the margins; (c) minor differences in stress or strength environments cause some variation in fracture orientations; and (d) the measured principal strain rate orientations in midglacier are not precise (see p. 35).

The results from this study of cracks and crevasses in a limited area can be extended qualitatively to all crevasse patterns. The following method of analysis is similar to that used by Hopkins (1862) and Nye (1952a, p. 89–91). In order to explain a crevasse pattern, the stress distribution on the surface must be described.

The splaying crevasses in Castleguard sector indicate transverse tension at the flow centerline. This is probably caused by transverse expansion of the glacier after passing a constriction in the channel at $x' = 6{,}000$. The margin of a glacier must be identified with a plane of greatest shearing stress so that the principal stresses must swing to a nearly 45° orientation at the margin. Crevasses may be of any orientation in midglacier but toward the margin a shear stress parallel to the valley wall must be dominant and crevasses will intersect the margins diagonally. In Castleguard sector this changing orientation of principal stress and strain-rate axes can be followed from the centerline to the margin both in the Mohr's circle constructions (fig. 32) and the map of principal strain rate trajectories (fig. 34).

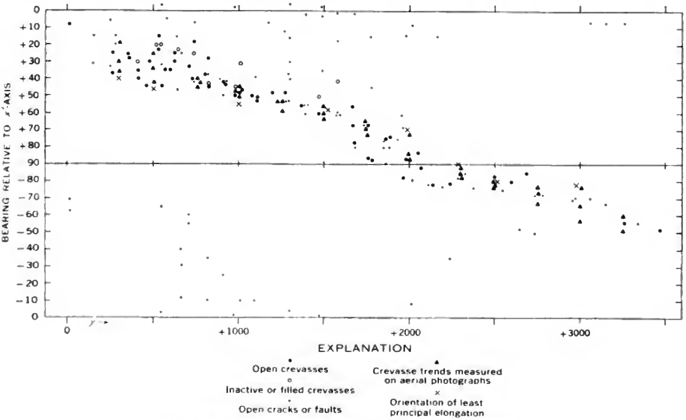

FIGURE 46.—Crevasse and open-crack orientations as a function of transverse location.

---

[12] The effect of rotation can be estimated by the following sample computation at $y = 1{,}000$, $x = 7{,}000$. The greatest elongating strain rate here is 0.052 per year. This would cause crevasses to form to a depth of 31 feet according to a formula suggested by Nye for temperate ice (Nye, p. 513) and approximately cofirmed by field measurements in polar ice (Meier, 1956). After removal of stress these crevasses would have a life of 3.3 years under the measured rate of ablation. The rotation rate measured here was 0.039 radians per year. Therefore, if a crevasse formed instantly and was not widened further, it would be rotated through about 7.3° before disappearing.

The transverse tension which causes splaying crevasses on the icefall of the only tributary glacier (fig. 44) must be due to a different mechanism because here the glacier's boundaries do not diverge. The upper reach of this ice stream is confined in a broad valley but the lower half flows in an unconfined course down the steep wall of the trunk valley; in effect it becomes a "wall-sided glacier" (Ahlman, 1940, p. 192). This probably causes a transverse spreading of the surface on the lower half, forming splaying crevasses.

Transverse crevasses on the icefall of this tributary glacier (fig. 44) indicate a longitudinal principal tension at the centerline. This is caused by the convex longitudinal bed profile. These transverse crevasses intersect the margin at the same angle as playing crevasses, and for the same reasons as given above.

Both transverse and splaying crevasses occur in midglacier on this tributary icefall, so both principal stresses must be tensile there. This condition can generally exist only in midglacier: the pure shear component introduced by marginal shear will cancel one of the principal tensions along the sides of the glacier. Intersecting crevasses, then, must be rare along glacier margins except where the stress field is greatly warped. The longitudinal tension is apparently stronger than the transverse tension on the centerline of the tributary icefall, because the transverse crevasses are dominant and continuous and the splaying crevasses die out near the margin.

The third major crevasse type—chevron crevasses—are related to pure shear caused by the drag of the valley walls. These crevasses indicate that the principal stresses are either zero or exactly equal. This stress field is probably rare.

The last, and most unusual, type of crevasse pattern which must be explained are en echelon crevasses. These indicate the intersection of two crevasse patterns or trends, but the crevasses do not intersect for the reasons given above. In echelon crevasses the stress field at depth must be strongly warped so that continuous surfaces cannot be formed that are everywhere perpendicular to the axis of principal tension. This is a general property of stress fields in three dimensions (Lagally, 1929, p. 294–295), and it must be assumed that long, even crevasses (such as the splaying crevasses in Castleguard sector) indicate little change in stress with depth except for the addition of hydrostatic pressure.

En echelon fractures have been commonly assumed in the geological literature to indicate a major shear at depth. The crevasse bands on Saskatchewan Glacier, however, are not parallel to a direction of great shearing strain but are more nearly parallel to a direction of principal elongation.

The en echelon crevasse pattern along the south margin at $x = 6{,}000$ (pl. 9*C*, fig. 44) suggests that the stress field at depth is oriented so as to produce splaying crevasses at the surface. The stress field at the surface is different and suggests chevron crevasses generated at the margin which intersect it at a steeper angle. These chevron crevasses are evidently related to the nearly vertical bulge in the valley wall. Irregular surfaces perpendicular to the suggested principal tension axes (fig. 47) would outcrop on the surface with a pattern similar to that of the en echelon crevasses. The crevasses seem to be twisted at depth in the manner shown in figure 47.

SIGNIFICANT FINDINGS

The flow of Saskatchewan Glacier was studied from several viewpoints. The velocity of the ice at points on the surface was measured both in regard to spatial configuration and to variation in time; some information was obtained on the change of velocity with depth along a shallow borehole; and studies were made of the structures produced by flow. In addition, the bedrock and ice and surface topography was measured and ablation data were obtained. Although measurement of these items over the entire glacier surface was not possible, the sampling of data was adequate to define the velocity and deformation fields and the structural patterns on the surface. Consequently Saskatchewan Glacier is the first glacier in the Western Hemisphere for which sufficient data were collected to provide a valid basis for conclusions on flow law, discharge at depth, and geometry of flow. The following conclusions are of the greatest significance:

1. Saskatchewan Glacier in the years 1952–54 showed a type of behavior which might be described as "constant unbalance." It was not in equilibrium because the surface was lowering, but the lowering proceeded at a nearly constant rate in time and space. The rate of lowering from terminus to firn limit was remarkably uniform (parallel downwasting). Furthermore, the discharge of ice through a high cross section was the exact amount to keep the rest of the tongue thinning at the prevailing rate. Thus there was no suggestion of any forthcoming change in the glacier's behavior.

2. Velocity measured at any one point depends on the time interval of observation. Very little time

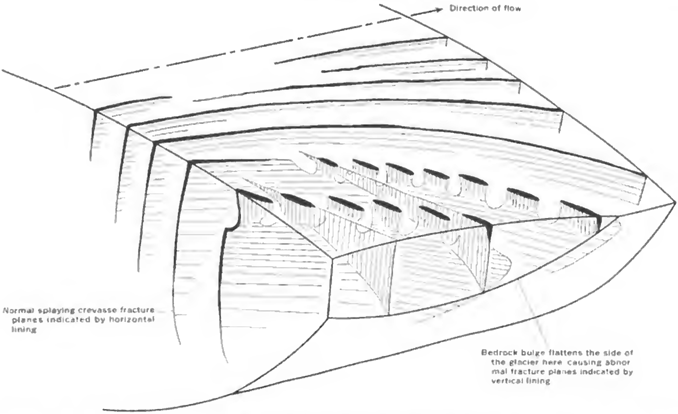
Direction of flow
Normal splaying crevasse fracture planes indicated by horizontal lining
Bedrock bulge flattens the side of the glacier here causing abnormal fracture planes indicated by vertical lining

FIGURE 47.—Phantom view of part of Saskatchewan Glacier showing possible fracture planes leading to formation of en echelon crevasses at the surface.

variation can be detected in the velocity field over a long period except for a slight deceleration due to thinning. However, erratic fluctuations are noticed when velocity readings are made at shorter and shorter intervals. Fluctuations of more than 100 percent of the average velocity are not uncommon in measurements made over 12-hour intervals. The size of the fluctuations is inversely proportional to the logarithm of the time interval of measurement. It is suggested that the total flow is built up from many minor jumps or jerks along shearing planes; it is probable that the jerkiness is not due to the erratic opening or closing of crevasses.

3. The absolute value of velocity decreases down-glacier along the centerline and toward the margins. This causes a prevailing compressing strain rate in a longitudinal direction along the centerline which near the edge is outweighed by a shearing strain rate parallel to the margin. Thus, one principal axis of strain rate parallels the centerline at the centerline, and both principal strain-rate axes intersect the margin at 45°. Generally there is a component of velocity toward the margins. This prevailing deformation pattern is locally modified in the upper part of Castleguard sector: a flux of ice in from the margins and a slight constriction in the channel makes the velocity vectors converge in map view, causing a transverse compression and a longitudinal extension in spite of reverse slope in the bedrock channel and very low surface slope. Thus the amount of extending or compressing flow along the centerline is sensitive to changes in width. The orientations of the principal axes of strain rate are computed from known velocity gradients, and the results are checked against the orientations of crevasses.

4. A component of velocity (V_d) is defined which represents the rise or fall of the ice surface which would take place if there were no accumulation or ablation. This tendency for the elevation of the surface to change is due solely to translational and deformational motions of the ice. If the glacier is in equilibrium, V_d is equal in magnitude but opposite in direction to the surface accumulation or ablation V_a averaged over a year's time. The response, or state of health, of a glacier at any instant is given by the difference between V_a, which is a function only of the current climate, and V_d, which is a function only of the glacier's current dimensions.[13] Thus V_d is a

---

[13] In the case of polar and subpolar glaciers this statement is not true because the prevailing climate has an important effect on the thermodynamics of the flow process, and therefore on V_d. This effect probably is not important in the case of temperate glaciers such as the Saskatchewan because the temperature distribution within the bulk of the glacier is virtually unchanging with time.

factor of greatest significance in any study of the response or adjustment of a glacier to its climatic environment. The component V_d was also shown to be useful for computing discharge and velocity distribution at depth.

5. The flow law (shear strain rate as a function of stress) of ice was investigated using data compiled from Saskatchewan Glacier and other sources. The results show that:

(*a*) Hydrostatic pressure has no appreciable effect on the flow law relation.

(*b*) There is a transition in behavior from a nearly viscous flow at low stresses to a plastic flow at high stresses; the transition occurs at a stress of about 0.7 bar. Glen's formula for creep does not apply at low stresses.

(*c*) Probably two mechanisms of flow operate simultaneously. At low stresses the flow may take place largely by grain-boundary creep; at high stresses intracrystalline gliding may predominate.

6. Streamlines of flow on a plane along the centerline generally parallel the bedrock. This suggests that the longitudinal profile of a glacier tends to adjust itself so that V_d (determined by the depth, surface slope and streamline slope) just balances the ablation at each altitude. This hypothesis has not yet been stated in usable form. Considerable research effort along these lines is justified because determination of the longitudinal profile is the important link to an understanding of glaciers as climatic indicators, and because existing schemes of calculation (such as the constant basal shearing stress theory) lead to wrong or unusable results.

7. Several different types of structures can be distinguished in the ice of Saskatchewan Glacier. The following three structures are of greatest interest to this study of flow:

(*a*) Primary stratification, a planar structure inherited from the firn, rides passively down the tongue until obliterated by deformation or recrystallization.

(*b*) Secondary foliation, a planar tectonic structure formed by shearing, is sometimes difficult to distinguish from primary stratification because both structures are manifest by differences in grain size or ice texture. Foliation seems to form, or to be preserved, only near the surface and could not always be related to planes of maximum shearing strain. Foliation may be due to local zones of intense plastic flow separated by zones that are only slightly strained because ice exhibits strain-softening behavior. Recrystallization probably has an important influence on its formation, and the fact that recrystallization rates may be a function of depth might explain the lack of foliation in basal ice. The origin of foliation is still an unsolved problem, and much remains to be done. This problem is closely related to the problem of defining and explaining the flow-law relation.

(*c*) Cracks of several types were recognized. The major crevasse systems are related in orientation to the greatest principal strain rate although there is some suggestion of slight differences in angle. Several minor crack systems are related to planes of greatest shearing strain rate, and in one surprising case to the axis of least (most compressing) strain rate. Cracks can be of great value in determining stress and strain-rate axes orientations.

ACCURACY OF THE VELOCITY DATA

Two important questions should be asked about this, or any other, method of glacier velocity measurements: First, how exact are the final velocity data as indicators of the actual ice motion at the time? Secondly, how exact are the true average velocities measured for a certain time interval as indicators of the average ice motion for a different time interval? In order to answer the first question a series of tests was made on the reproducibility of the instrumental and computational methods; in answer to the second question, observations were made on the variation of the velocity field with time. (See table 10.)

In 1952 the velocity stations were surveyed using a 20-second engineers transit; horizontal angles were generally repeated four times and vertical angles read in both erect and inverted positions of the telescope. In 1953 and 1954 a T2 1-second optical theodolite was used; horizontal and vertical angles were generally read twice by two operators.

The survey data were analyzed three different ways:

(1) For all stations with reliable triangulation information, coordinate locations were determined once or twice each summer using 8-place trigonometric tables (or rarely, 6-place logarithms). From these data and the resetting data, velocity components parallel to the coordinate axes were readily obtained.

(2) For these same stations, velocity components at shorter intervals (½ day to 1 month) were obtained by computations of slide-rule accu-

racy, using increments of arc and assuming that the stake moved along the path found by the precise calculation.

(3) Insufficient data were available from some stakes to define accurately the direction of travel. For these, a direction was assumed by reference to nearby stakes, and calculation was done to slide-rule accuracy. Transverse velocity profiles were generally arranged directly opposite transit points, so that lack of information on the direction of ice motion would have minimum effect on computed longitudinal and vertical components of velocity.

Precision of measurement is determined by the accuracy of setup, pointing, reading and the inherent precision of the instrument; stability of instrument, transit point and sighting point; varying atmospheric refraction; resetting measurement precision; computational precision and accuracy; and human errors.

In order to determine the precision of the horizontal measuring procedure, a fixed angle between two bedrock points on the north side of the glacier was measured from a transit point on the south side. One line of sight barely grazed the flat surface of the glacier so that atmospheric effects would have a large influence on the results. The instrument (T2) was enclosed in a tent for protection against wind and direct sunlight, in the same manner as was used for a series of short-interval measurements in 1953. The fixed angle was measured 50 times by different operators under what was believed to be a representative sampling of different weather conditions and with several setups. The results, therefore, reflect the combined effects of instrumental error, precision in setup, sighting and reading, and atmospheric refraction. The data when plotted on arithmetic probability paper (fig. 48) show a normal error distribution with a standard deviation of angle of 3.0 seconds. This value is of the same order of magnitude as the reproducibility of pointing and reading the instrument, suggesting that other errors have negligible influence. From these data and tests of the reproducibility of readings with other setups, it is assumed that the probable angular error (0.67 times the standard deviation) of measurement ranges from about 6 seconds for the unshielded engineer's transit to 2 seconds for refined measurement with the T2. The probable error in locating the instrument horizontally over a point is negligible for the T2 (0.005 to 0.01 foot) but reaches a maximum of 0.05 foot (or more in a very high wind) for the transit.

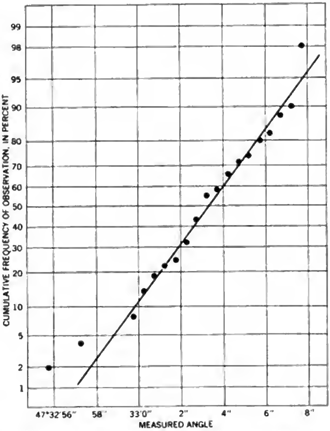

FIGURE 48.—Error distribution for 50 measurements of a fixed angle.

On this basis the probable error in longitudinal horizontal location for stations in midglacier ranges from about 0.05 to 0.7 foot, depending on the instrument used and the refiement of measuring procedure. For these same stakes the probable error in transverse location is estimated to range from 0.2 to 1.2 foot. Longitudinal locations are much more precise and transverse locations slightly more precise for stakes near the margin.

Vertical locations are less accurate. Changing atmospheric refraction and poor reproducibility of measuring vertical angles with the transit causes great variability of results; errors from all other causes are relatively negligible. Comparison between stake locations, measured simultaneously from two transit stations and elevations determined on successive days from the same station, suggested that the probable error in vertical location may have been as great as 1 foot for many stations. This was an appreciable fraction of the yearly vertical movement for some stations.

Other sources of error in location or velocity are difficult to evaluate. Some transit points on old moraines may have moved, but no suggestions of such movement appears in the data, and a precise experiment to measure movement of TP–6 in 1952 gave completely negative results. Some stakes, after considerable ablation, were visibly vibrating in the wind at the time of observation, but it is not likely that an error greater than 0.1 foot was caused by this. Measurements made of the new positions as stakes were reset were generally as accurate as the surveyed locations. However, in 1953 the field party failed to record this information, completely or in part, for several stakes in the 8, 3 and 6 series. In a few places the missing information was obtained by surveys just before and just after resetting; in other places the data had to be estimated causing an error of up to 3 feet in location. Those data were discarded in which lack of resetting measurements caused an uncertainty in the velocity values of more than a few percent, and all other data with appreciable uncertainty are so specified. Computational precision was kept within the limits of instrumental inaccuracy, and the possibility of undiscovered human error in the triangulation computations was eliminated by a double calculation scheme.

In general, it is assumed that the yearly velocities reported here are correctly measured to within 1 fpy for the horizontal component and 2 fpy for the vertical component, unless otherwise specified. Summer and short-interval velocities were not as accurate. Actually, the inaccuracy of measurement of horizontal velocity over a summer's or year's time is only a negligible fraction of the probable error introduced by assuming that that measurement is representative of the mean velocity over a longer period of time.

Table 10.—*Coordinates of velocity stakes*

Stake	Date	*x*	*y*	*z*
17-5	Aug. 29, 1953	1,300 ±5	3,898 ±5	8,237 ±2
4	do	2,160 ±5	2,305 ±5	8,263 ±2
3	do	727 ±5	2,219 ±5	8,125 ±2
2	do	221 ±5	2,991 ±5	8,097 ±2
1	do	856 ±5	2,908 ±5	8,070 ±2
8-10	do	1,570 ±10	1,584 ±5	7,860 ±2
9	Sept. 3, 1953	4,080.0	2,371.4	
9	Sept. 3, 1953	4,080.0	2,371.4	......
8	Aug. 12, 1952	4,603.0	3,723.0	7,709.0
	Aug. 10, 1953	4,788 ±1	3,672 ±1	7,697 ±1
	Aug. 7, 1954	4,999.9	3,629.9	7,683.2
7	Aug. 12, 1952	4,615 ±5	3,370 ±10	......
6	do	4,650 ±5	3,148 ±3	7,680 ±5
	Aug. 29, 1953	4,887.7	3,143.0	7,667.2
	Aug. 7, 1954	5,112.0	3,140.7	7,658.6
4	Aug. 12, 1952	4,720 ±5	2,229 ±5	7,647 ±5
	Aug. 29, 1953	4,976.6	2,240.3	7,636.1
	Aug. 7, 1954	5,208.2	2,252.2	7,629.0
3	Aug. 12, 1952	4,774.2	1,593.0	7,673.5
	Aug. 29, 1953	5,039.2	1,613.0	7,649.6
	Aug. 7, 1951	5,264.2	1,625.9	7,642.2
2	Aug. 12, 1952	4,801 ±1	1,238 ±1	7,682 ±5
	Aug. 29, 1953	5,042.6	1,247.3	7,662.1
	Aug. 7, 1954	5,260.8	1,265.8	7,653.2
1	Aug. 12, 1952	4,837 ±2	256 ±5	7,684 ±2
3-12	July 8, 1952	6,102 ±2	899 ±2	7,639 ±2
11	do	6,968 ±2	637 ±2	7,499 ±2
	July 7, 1952	6,981 ±2	636 ±2	......
10	Aug. 17, 1952	6,898 ±2	4,070 ±5	7,497 ±2
9	do	7,024 ±5	3,448 ±5	......
8	do	7,043 ±2	3,401 ±5	7,501 ±2
	Aug. 10, 1953	7,272.9	3,419.3	7,515.4
7	Aug. 17, 1952	7,054 ±5	3,356 ±5	......
6	do	7,100 ±5	3,078 ±5	7,506 ±2
	Aug. 10, 1953	7,338.2	3,093.7	......
5	do	7,551.0	2,612.7	7,506.7
4	July 8, 1952	7,474.3	1,759.7	7,526.4
	July 31, 1952	7,491.5	1,759.8	......
	July 29, 1953	7,731.2	1,749.5	7,500.3
	Aug. 7, 1954	7,979.3	1,743.3	7,487.0
3a	Aug. 26, 1953	7,602 ±10	980 ±5	7,456 ±2
	July 29, 1953	7,782.6	980.1	7,449.9
	Aug. 7, 1954	7,993.8	961.9	7,439.4
3	Aug. 8, 1952	7,600 ±5	583 ±5	7,432 ±2
2	do	7,597 ±5	356 ±10	7,423 ±2
1	do	7,589 ±5	262 ±15	7,409 ±2
5-4	do	8,640 ±20	2,600 ±10	7,473 ±5
3	do	8,660 ±20	1,780 ±10	7,459 ±5
2	do	8,760 ±10	530 ±10	7,396 ±2
1	do	8,770 ±10	280 ±10	7,360 ±2
6-8	July 25, 1953	11,189.8	2,035.0	7,281.6
	Aug. 31, 1953	11,211.4	2,039.6	7,281.2
	Mar. 5, 1954	11,381.6	2,070.0	7,279.0
6-7	Aug. 26, 1952	10,064.0	2,996.1	7,354.0
	July 28, 1953	10,235.0	3,013.9	7,341.1
	Aug. 31, 1953	10,257.1	3,017.8	7,339.8
	Aug. 5, 1954	10,437.1	3,039.4	7,335.3
6	Aug. 26, 1952	9,661.8	2,268.5	7,372.8
	July 28, 1953	9,858.8	2,272.0	7,354.4
	Aug. 5, 1954	10,076.5	......	7,342.6
4	Aug. 26, 1952	9,903.8	1,841.7	7,339.0
	July 28, 1953	10,088.9	1,844.3	7,329.5
	Aug. 31, 1953	10,109.9	1,845.1	7,328.6
	Aug. 5, 1954	10,304.3	1,862.4	7,324.8
3	Aug. 26, 1952	9,958.7	966.5	7,331.8
	July 28, 1953	10,119.6	974.6	7,321.4
	Aug. 31, 1953	10,137.9	960.2	7,322.9
	Aug. 5, 1954	10,284.5	953.9	7,326.0
2b	July 5, 1953	9,612.9	434.5	7,327.3
	Aug. 31, 1953	9,615.8	431.9	7,320.6
	Aug. 5, 1954	9,708.1	416.1	7,327.8
2	Aug. 26, 1952	9,968.0	458.8	7,320.8
	July 28, 1953	10,059.3	438.6	7,308.0
	Aug. 31, 1953	10,077.0	440.1	7,303.4
	Aug. 5, 1954	10,167.7	423.0	7,309.5
2a	July 7, 1953	10,535.0	398.5	7,289.8
	Aug. 31, 1953	10,551.9	397.0	7,284.0
	Aug. 5, 1954	10,632.0	384.5	7,290.6
1	Aug. 26, 1952	9,983.4	253.1	7,304.0
	July 28, 1953	10,061.8	239.6	7,291.5
	July 28, 1953	10,074.4	231.3	7,288.5
	Aug. 5, 1954	10,134.1	215.1	7,295.9
15-2	July 25, 1953	12,881.1	2,787.0	7,194.2
	Aug. 5, 1954	13,028.5	2,862.3	7,190.2
1	July 25, 1953	13,247.4	1,065.2	7,211.8
	Aug. 5, 1954	13,314.1	1,076.5	7,210.5
14-5	July 9, 1953	17,085.7	5,853.6	6,847.6
	July 14, 1954	17,204.2	5,900.3	6,835.8
4	July 9, 1953	20,187.8	7,463.0	6,626.0
	Aug. 28, 1955	20,192.9	7,456.0	6,617.3
	July 14, 1954	20,274.5	7,494.8	6,613.5
	July 24, 1954	20,276.2	7,514.4	6,613.4
3	July 9, 1953	18,711.3	6,686.6	6,753.0
	July 14, 1954	18,819.2	6,726.4	6,741.0
2	July 9, 1953	19,453.1	5,452.0	......
	July 14, 1954	19,544.2	5,488.2	6,710.0
1	July 9, 1953	19,619.8	5,151.4	6,711.8
	July 14, 1954	19,697.7	5,183.2	6,694.1
12-5	July 5, 1953	25,591.4	8,838.8	6,104.6
	Aug. 26, 1953	25,595.6	8,839.9	6,094.6
	July 24, 1954	25,627.0	8,847.8	6,085.0
	Aug. 12, 1954	25,631.6	8,848.2	6,084.2
4	July 5, 1953	26,089.3	8,925.7	6,044.6
	Aug. 26, 1953	26,090.7	8,927.9	6,037.7
	July 11, 1954	26,113.2	8,937.4	6,024.7
	July 24, 1954	26,114.4	8,937.5	6,024.8
	Aug. 12, 1954	26,119.0	8,939.6	6,023.8
3	July 5, 1953	26,530.8	8,983.9	5,972.3
	Aug. 26, 1953	26,530.8	8,984.4	5,960.9
	July 11, 1954	26,545.3	8,990.8	......
	July 24, 1954	26,545.3	8,991.0	5,952.9
	Aug. 12, 1954	26,551.6	8,989.7	5,951.6
2	July 5, 1953	26,792.8	9,032.8	5,925.7
	Aug. 26, 1953	26,790.2	9,025.9	5,912.7
	July 11, 1954	26,786.0	9,031.0	5,908.2
	July 24, 1954	26,786.6	9,031.2	5,908.2
	Aug. 12, 1954	26,789.5	9,031.1	5,907.8

The data obtained from inclonometer surveys of the boreholes are presented in table 11.

TABLE 11.—*Inclination data for boreholes*

Borehole	Date of survey	Depth below top of pipe (feet)	Inclination from vertical	Direction
1	Aug. 6, 1952	25	1°55′	S. 86° E.
		50	0°50′	S. 85° E.
		75	0°30′	S. 90° E.
		100	1°45′	N. 14° E.
		125	1°20′	N. 17° W.
		151	1°05′	N. 15° E.
		[1] 151.8		
1	Aug. 5, 1954	0	2°05′	S. 76° E.
		25	1°20′	S. 90° E.
		50	0°50′	S. 60° E.
		75	0°45′	N. 05° E.
		100	1°40′	N. 10° W.
		125	[2] 1°35′	[3] N. 50° W.
		132	0°35′	N. 25° W.
		138	(4)	
2	Aug. 4, 1954	5	0°05′	N. 60° W.
		50	0°45′	S. 75° E.
		100	0°30′	S. 75° E.
	Aug. 5, 1954	150	0°20′	S. 90° E.
		200	0°30′	N. 70° E.
		238	0°10′	S. 65° E.
		[1] 238.5		

[1] Bottom of hole.

[2] ±10′

[3] ±10°

[4] The change of length of borehole 1 was due to the removal of sections from the top as ablation progressed.

REFERENCES CITED

Ahlmann, H. W., 1940, The relative influence of precipitation and temperature on glacier regime: Geog. Annaler, v. 22, p. 188–205.

——— 1948, Glaciological research on the North Atlantic coasts: Royal Geog. Soc., Res. ser. 1, 83 p.

Allen, C. R., and Smith, G. I., 1953, Seismic and gravity investigations on the Malaspina Glacier, Alaska: Amer. Geophys. Union Trans., v. 34, p. 755–760.

Bader, Henri, 1951, Introduction to ice petrofabrics: Jour. Geology, v. 59, p. 519–536.

Battle, W. R. B., 1951, Glacier movement in northeast Greenland: Jour. Glaciology, v. 1, p. 559–563.

Bjerrum, Niels, 1952, Structure and properties of ice: Science, v. 115, p. 385–390.

Bruce, R. J. M., and Bull, Colin, 1955, Geophysical work in north Greenland: Nature, v. 175, p. 892–893.

Carol, Hans, 1947, The formation of roches moutonnées: Jour. Glaciology, v. 1, p. 57–59.

Chamberlin, R. T., 1928, Instrumental work on the nature of glacier motion: Jour. Geology, v. 36, p. 1–30.

Chamberlin, T. C., and Salisbury, R. D., 1909, Geology: v. 1, New York, Henry Holt and Co., 684 p.

Cottrell, A. H., 1953, Dislocations and plastic flow in crystals, Oxford, Oxford Univ. Pres, 223 p.

Demorest, Max, 1938, Ice flowage as revealed by glacial striae: Jour. Geology, v. 46, p. 700–725.

Demorest, Max, 1942, Glacier regimens and ice movement within glaciers: Am. Jour. Sci., v. 240, p. 31–66.

——— 1953, Processes of ice deformation within glaciers: Jour. Glaciology, v. 2, p. 201–203.

Drygalski, E. V., and Machatschek, Fritz, 1942, Gletscherkunde (Glaciology): Enzyklopädie der Erdkunde, Vienna, Franz Deuticke, 261 p.

Dushman, Saul, Dunbar, L. W., and Huthsteiner, H., 1944, Creep of metals: Jour. Applied Physics, v. 15, p. 108–124.

Eyring, Henry, Glasstone, Samuel, and Laidler, K. J., 1941, The theory of rate processes, New York, McGraw-Hill Book Co., 611 p.

Field, W. O., and Heusser, C. J., 1954, Glacier and botanical studies in the Canadian Rockies, 1953: Canadian Alpine Jour., v. 37, p. 128–140.

Finsterwalder, Richard, 1951, The glaciers of Jostedalsbreen: Jour. Glaciology, v. 1, p. 557–558.

Gerrard, J. A. F., Perutz, M. F., and Roch, André, 1952, Measurement of the velocity distribution along a vertical line through a glacier: Royal Soc. London Proc., ser. A, v. 213, p. 546–558.

Glen, J. W., 1955, The creep of polycrystalline ice: Royal Soc. London Proc., ser. A., v. 228, p. 519–538.

——— 1956, Measurement of the deformation of ice in a tunnel at the foot of an ice fall: Jour. Glaciology, v. 2, p. 735–745.

Goranson, R. W., 1940, Flow in stressed solids, an interpretation: Geol. Soc. America Bull., v. 51, p. 1023–1034.

Griggs, D. T., and Coles, N. E., 1954, Creep of single crystals of ice: U.S. Army, Corps of Engineers, Snow, Ice and Permafrost Research Establishment, Rept. 11, 24 p.

Haefeli, R., 1948, Schnee, Lawinen, Firn und Gletscher (Snow, avalanches, firn and glaciers) *in* Bendel, L., Ingenieur-Geologie, Vienna, Springer-Verlag, Band 2, p. 663–735.

——— 1951, Some observations on glacier flow: Jour. Glaciology, v. 1, p. 496–500.

Haefeli, R., and Brentani, F., 1955–56, Observations in a cold ice cap: Jour. Glaciology, v. 2, p. 571–581, 623–630.

Hess, Hans, 1904, Die Gletscher (Glaciers): Braunschweig, F. Vieweg, 426 p.

——— 1933, Das Eis der Erde (The ice of the earth): Handbuch der Geophysik, Band 7, Abt. 1, p. 1–121.

——— 1937, Über den Zustand des Eises im Gletscher (On the state of the ice in glaciers): Zeitschr. f. Gletscherk., Band 25, p. 1–16.

Hill, R., 1950, The mathematical theory of plasticity, Oxford, Clarendon Press, 350 p.

Hoel, P. G., 1947, Introduction to mathematical statistics, New York, John Wiley and Sons, 258 p.

Hopkins, W., 1862, On the theory of the motion of glaciers: Philos. Trans., v. 152, part 2, p. 677–745.

Hubbert, M. K., 1951, Mechanical basis for certain familiar geologic structures: Geol. Soc. America Bull., v. 62, p. 355–372.

Ivanov, K. E., and Lavrov, V. V., 1950, Ob odnoi osobennocti mekhanizma plasticheskoi deformatsli l'da (A peculiarity of the mechanism of plastic deformation of ice): Zhurnal Tecknichol Fizikl, v. 20, p. 230–331 (*see also* U.S. Army, Corps of Engineers, Snow, Ice and Permafrost Research Establishment Trans. 10).

Jellinek, H. H. G., and Brill, R., 1956, Viscoelastic properties of ice: Jour. App. Physics, v. 27, p. 1198–1209.

Kalesnik, S. V., 1939, Obshchaia Gliatsciologiia izdatel'stvo (General glaciology), Leningrad, Gos. Utsch.-Pedag. Isd., 327 p.

Klebelsberg, R. V., 1948, Handbuch der Gletscherkunde und Glazialgeologie (Handbook of glaciology and glacial geology), Vienna, Springer-Verlag, Band 1, 403 p.

Lagally, M., 1929, Versuch einer Theorie der Spaltenbildung in Gletschern (A trial theory of crevasse formation in glaciers): Zeitschr. f. Gletscherk., Band 17, p. 285–301.

Landauer, J. K., 1955, Stress-strain relations in snow under uniaxial compression: U.S. Army, Corps of Engineers, Snow, Ice and Permafrost Research Establishment Rept. 12, 9 p.

——— 1957, Some preliminary observations on the plasticity of Greenland glaciers: U.S. Army, Corps of Engineers, Snow, Ice and Permafrost Research Establishment Rept. 33, 6 p.

Matthes, F. E., 1900, Glacial sculpture of the Bighorn Mountains, Wyo.: U.S. Geol. Survey, 21st Ann. Rept., part 2, p. 167–190.

——— 1942, Glaciers: Chap. V, p. 149–219, in Meinzer, O. E. (ed.), Hydrology, New York, McGraw Hill Book Co., 712 p.

McCall, J. G., 1952, The internal structure of a cirque glacier: Jour. Glaciology, v. 2, p. 122–131.

Meier, M. F., 1951a, Glaciers of the Gannett-Fremont Peak area, Wyo.: Am. Alpine Jour., v. 8, p. 109–113.

———1956, Preliminary study of crevasse formation: U.S. Army, Corps of Engineers, Snow, Ice and Permafrost Research Establishment Rept. 38, 61 p.

Meier, M. F., Rigsby, G. P., and Sharp, R. P., 1954, Preliminary data from Saskatchewan Glacier, Alberta, Canada: Arctic, v. 7, p. 3–26.

Merrill, W. M., 1956, Structure of the ice cliff, in Goldthwait, R. P., Study of ice cliff in Nunatarssuaq Greenland: U.S. Army, Corps of Engineers, Snow, Ice and Permafrost Research Establishment Rept. 39, 150 p.

Nadai, A., 1950, Theory of flow and fracture of solids, New York, McGraw-Hill Book Co., V. 1, 572 p.

Nielsen, L. E., 1955, Regimen and flow in equilibrium glaciers: Geol. Soc. America Bull., v. 66, p. 1–8.

Nye, J. F., 1951, The flow of glaciers and ice-sheets as a problem in plasticity: Roy. Soc. London Proc., ser. A, v. 207, p. 554–572.

——— 1952a, The mechanics of glacier flow: Jour. Glaciology, v. 2, p. 82–93.

——— 1952b, A comparison between the theoretical and the measured long profile of the Unteraar Glacier: Jour. Glaciology, v. 2, p. 103–107.

——— 1952c, A method of calculating the thicknesses of the ice-sheets: Nature, v. 169, p. 529–553.

——— 1953, The flow law of ice from measurements in glacier tunnels, laboratory experiments and the Jungfraufirn borehole experiment: Roy. Soc. London Proc. ser. A, v. 219, p. 477–489.

——— 1955, Comments on Dr. Loewe's letter and notes on crevasses: Jour. Glaciology, v. 2, p. 512–514.

——— 1957, The distribution of stress and velocity in glaciers and ice-sheets: Royal Soc. London Proc., ser. A, v. 39, p. 113–133.

Orowan, E., 1949, The flow of ice and other solids: Jour. Glaciology, v. 1, p. 231–236.

Orvig, S., 1953, On the variation of shear stress on the bed of an ice cap: Jour. Glaciology, v. 2, p. 242–247.

Perutz, M. F., 1954, Glaciers: Royal Inst. Great Britain, v. 35, p. 571–582.

Perutz, M. F., and Seligman, Gerald, 1939, A crystallographic investigation of glacier structure and the mechanism of glacier flow: Royal Soc. London Proc., ser. A, v. 172, p. 335–360.

Prandtl, L., and Tietjens, O. G., 1934, Fundamentals of hydro- and aero-mechanics, New York, McGraw-Hill Book Co., 265 p.

Reid, H. F., 1896, The mechanics of glaciers: Jour. Geology, v. 4, p. 912–928.

——— 1901, De la progression des glaciers, leur stratification et leur veines bleues: 8th Inter. Geol. Cong., Compt Rendu, pt. 2, p. 749–755.

Rigsby, G. P., 1951, Crystal fabric studies on Emmons Glacier, Mount Rainier, Wash.: Jour. Geology, v. 59, p. 590–598.

——— 1957, Effect of hydrostatic pressure on velocity of shear deformation of single crystals of ice: U.S. Army, Corps of Engineers, Snow, Ice and Permafrost Research Establishment Report 32, 7 p.

Robertson, E. C., 1955, Experimental study of the strength of rocks: Geol. Soc. America Bull., v. 66, p. 1275–1314.

Schwarzacher, W., and Untersteiner, Norbert, 1953, Zum problem der Bänderung des Gletschereises (On the problem of the banding of glacier ice): Sitz. d. Osterr. Akad. Wiss., Wien, Math.-naturwiss., Abt. IIa, Band 162, p. 111–145.

Servi, I. S., and Grant, N. J., 1951, Creep and stress rupture behavior of aluminum as a function of purity: Jour. Metals, v. 3, p. 909–916.

Sharp, R. P., 1948, The constitution of valley glaciers: Jour. Glaciology, v. 1, p. 182–189.

——— 1953, Deformation of borehole in Malaspina Glacier, Alaska: Geol. Soc. America Bull., v. 64, p. 97–100.

——— 1954, Glacier flow, a review: Geol. Soc. America Bull., v. 65, p. 821–838.

Shumskii, P. A., 1947, Energiia oledeneniia i zhizn lednikov (Energy of glacierization and the life of glaciers): Moscow, Geografgiz, Translated by William Mandel, The Stefansson Library, New York, 1950, 60 p.

Steinemann, Samuel, 1954, Results of preliminary experiments on the plasticity of ice crystals: Jour. Glaciology, v. 2, p. 404–413.

Turner, F. J., 1948, Mineralogical and structural evolution of the metamorphic rocks: Geol. Soc. America Memoir 30, 342 p.

Untersteiner, Norbert, 1954, Über die Feinbänderung und Bewegung des Gletschereises (On the fine-banding and movement of glacier ice): Archiv für Met., Geophysik u. Bioklima., ser. A, Band 7, p. 231–242.

——— 1955, Some observations on the banding of glacier ice: Jour. Glaciology, v. 2, p. 502–506.

Weertman, J., 1957, Steady-state creep through dislocation climb: Jour. App. Physics, v. 28, p. 362–364.

White, S. E., 1956, Motion in the ice cliff, in Goldthwait, R. P., Study of ice cliff in Nunatarssuaq Greenland: U.S. Army, Corps of Engineers, Snow, Ice and Permafrost Research Establishment Rept. 39, 150 p.

INDEX

Page

A

- Ablation, definition iv
  - measurements 8
  - rate 8, 10, 19, 26, 62
  - surface 2
  - total 10
  - velocity 26
  - yearly values 8, 10, 11
- Absolute vertical component 22, 23
- Accumulation 5
  - velocity 24
- Accuracy, attitudes of structural features 50
  - englacial velocity measurements 20
  - of streamline constructions 48
  - strain-rate measurements 33, 35, 36
  - velocity measurements 64–66
- Activity of glacier 5
- Altitude of area 2, 16
- Andrade's law 44, 45
- Approximation of plane strain 33
- Arolla tunnel 42, 44
- Austerdalsbre tunnel 42, 44

B

- Banded structure 52, 59
- Blätterung 54
- Blue bands 52
- Boreholes, configuration 30
  - inclination data 66, 67
  - sites 30, 31
  - stress and strain-rate data 41
- Brittle crust 31

C

- Cartesian coordinates 32
- Castleguard sector, ablation in 10
  - altitude 8
  - crevasses in 56
  - cross sections 10, 21, 46
  - definition of 4, 5
  - distribution of velocity components 22, 23
  - flow into 46
    - structures 50
  - location 4, 5
  - mechanical properties of ice 33
  - structural features 50, 57, 58
  - surfaceward flow 24
  - velocity components 20, 21, 26
- Classification of glaciers 5
- Columbia Icefield 2, 4, 52
- Component of, absolute vertical 22, 23
  - laminar flow 24
  - strain rate 32
  - surface rise 24
  - velocity 2, 19, 20, 21, 32, 33, 64
- Configuration of, bedrock 28
  - borehole 30
  - channel 2
  - surface 6, 19
- Coordinate systems 2, 11, 13, 19, 22, 24, 32
- Cracks 4, 50, 54, 57, 60, 61, 64

Page

- Crevasses, chevron 56
  - en echelon 56, 62
  - longitudinal 56
  - splaying 56, 61, 62
  - transverse 56, 62
- Criteria for distinguishing foliation from stratification 54
- Crystal-fabric studies 5

D

- Density of ice 5
- Deviator of stress 38
- Drilling with hotpoints, results 31
- Druckschichtung 54

E

- Energy of glacierization 5
- Eulerian method of hydrodynamics 25
- Extending flow iv, 36

F

- Faults 50, 57
- Feinbänderung 52, 59, 60
- Firn limit iv, 2, 5, 6, 8, 21, 22, 25, 36, 50, 52, 62
- Flow centerline iv, 6, 11, 27, 28, 35, 36, 41, 45, 48, 49, 59
- Flow law ix, 2, 37, 41, 44, 45, 50, 64
- Fold axes 50, 57
- Foliation iv, 27, 50, 52, 59, 60

G

- Gerrard, quoted 1
- Glen's flow law for ice 14, 41, 44, 64
- Grain-boundary creep 60, 64
- Greenland icecap 60

H

- Haarisse 54, 56
- Hintereisferner 5
- Horizontal downglacier component of velocity 2, 21
  - ice surface, assumption 35
  - transverse component of velocity 2, 21

I

- Instantaneous ice surface 2
  - velocities, substitution of average 35

J

- Jungfraufirn 28, 41, 42, 44

L

- Laminar flow, analysis 41, 42
  - component 24
  - deformation in 38, 40, 41
- Lateral moraines 6
- Longitudinal bands 52
  - extension 41, 42
  - orientation of foliation 54; pl. 2A
  - profile 2, 49, 50, 64
    - hypothesis 50
    - significance 49

Page

M

Malaspina Glacier 28, 42, 44
Mass-budget data 46
Medial moraine 2, 10
    velocity pattern 27
Meteorological observations 18
Mohr's circle constructions 32, 33, 36, 61

N

Nye, equations quoted 39, 41, 42

O

Objective of study 1
Octahedral shear stress iv, 38, 42, 44
    strain rate iv, 38, 42, 44
Orientation maximum, characteristics 59
Outcrop pattern 51, 52, 54, 57
Outlet glacier 5

P

Parallelism between streamlines and bedrock 49
Pasterze Glacier 59, 60
Pattern of crevasses 54
    stratification pl. 7
Pflugfurchenein 54
Physical setting of glacier 2
Plane of symmetry 6
Principal strain rates iv, 38
    stresses iv, 38

R

Ratio of downglacier velocity to centerline velocity 26
Relation between air temperature and velocity 17
    deviation of velocity and temperature 19
    dispersion and wavelength of velocity variations 19
Rhone Glacier 5
Roads, accessibility 2
Rotation rate 25

S

Scherflächen 54
Secondary flow structures 50
Sedimentary layers 50, 52
Seismic explorations 6
Shape of glacier 1, 2, 5, 6
Shear stress on bed 49
Skauthöe tunnel 42, 44

Page

Sources of error in measurements of velocity 65
Strain rate 28, 32-45
    basic equations 32, 38, 39, 41, 42
    components 28, 32, 33, 35, 37, 41, 42
    function of shear stress. *See* Flow law.
    relation to structures 57, 58, 59
    tensor 32, 33, 37, 57
    trajectories 32, 34, 36, 61
Stratification 50, 52, 57, 64
Streamline distribution 46, 48, 49, 64
    parallelism with bed 49, 64
Structural features 2, 50-62
Surface deformation 32-37
    lowering, rate 26
Surfaceward flow 2, 24-26, 46

T

Tectonic blue bands 52
Tectonic features, origin 59, 60, 61, 64
Temporary snowline 8, 12
Thermal characteristics 5
Thinning data 6, 8
Topography, bedrock 6, 8
Transit stations, locations 10, 13
    nomenclature 10, 12, 13
Transition from convergent to divergent flow 22, 23
Transverse component of flow 21
    profile 25, 41, 42, 45

V

Velocity, at bed 46, 50
    at depth 2, 45, 46
    components. *See* Components, velocity.
    data, accuracy 64-66
    deviation of 16, 17
    dispersion of 16, 17
    distribution 19-28, 31, 45, 48
    englacial 28, 31, 32
    instantaneous 25
    stakes 8, 10, 11, 13, 66
        coordinates of 66
        dates of survey 14
    standard deviation of 16
    stations 8, 10, 11, 13, 65
    time-dispersion of 16-18
    time variation 11, 12, 16, 17
    variations, short-interval 16, 17, 18
    vector, direction 27
    yearly changes 14, 16, 66
Vertical profiles 31, 37, 38, 45, 46

U.S. GOVERNMENT PRINTING OFFICE : 1966 O - 509755

Recent Sedimentation and Erosional History of Fivemile Creek Fremont County, Wyoming

By RICHARD F. HADLEY

EROSION AND SEDIMENTATION IN A SEMIARID ENVIRONMENT

GEOLOGICAL SURVEY PROFESSIONAL PAPER 352-A

Prepared as part of a program of the
Department of the Interior for development
of the Missouri River basin and part of
the soil and moisture program

March 3, 1849

UNITED STATES GOVERNMENT PRINTING OFFICE, WASHINGTON : 1960

UNITED STATES DEPARTMENT OF THE INTERIOR

FRED A. SEATON, *Secretary*

GEOLOGICAL SURVEY

Thomas B. Nolan, *Director*

For sale by the Superintendent of Documents, U.S. Government Printing Office
Washington 25, D.C.

CONTENTS

Page
Abstract 131
Introduction 132
Acknowledgments 133
Physical Setting 133
  Geography 133
    Location and topography 133
    Drainage 133
    Alluvial fans 134
    Vegetation 134
    Climate 135
      Precipitation 135
      Temperature 137
      Winds 137
  Summary of Geology 137
    Aspects of Pleistocene Geology 140
Basic Data 141
  Clastic sediments 145
  Largest particles 145
  The pebble fraction 145
  The granule-to-clay fraction 149
    Granules 149
    Silt and clay 154
    Parameters of the size distribution 156
      Mean size 156
      Standard deviation 158
Basic Data—Continued
  The granule-to-clay fraction—Continued
    Parameters of the size distribution—Continued
      Skewness 158
      Kurtosis 160
      Summary of size-distribution parameters 162
    Clay mineralogy 162
Sediment Transport 165
  Competence considerations 165
  Distribution of estimated tractive force 167
  Directions of sediment transport 167
Channels on alluvial fans 170
Cause of trenching 174
  Tectonic explanation 175
  Tractive-force explanation 175
Contrast between the modern and former processes 176
  Mudflows 176
  The former process 177
  Frequency of precipitation 179
Process rates 180
Formation of the alluvial fans 182
  The evolutionary hypothesis 182
  The equilibrium hypothesis 182
  The climatic hypothesis 183
References 190

ILLUSTRATIONS

PLATE 8. Generalized geologic map of Deep Springs Valley, Calif. In pocket
9. Map and profile of the active channel on the Antelope Springs fan In pocket
FIGURE 85-89. Aerial photographs: Page
85. Antelope Springs fan 135
86. Southeastern part of Deep Springs Valley 136
87. Wyman-Crooked Creeks fan 137
88. Paiute Chute 138
89. Crystal Peak reentrant 139
90. Map showing sampling stations in the north end of Deep Springs Valley 142
91. Map showing sampling stations on the Antelope Springs fan 143
92. Graph showing the relation of maximum particle size to slope at stations in the north end of Deep Springs Valley 146
93. Graph showing the relation of maximum particle size to slope at stations on the Antelope Springs fan 147
94. Map showing mean pebble size in the north end of Deep Springs Valley 148
95. View of a shallow wash in the Crystal Peak area 149
96. Map showing mean pebble roundness in the north end of Deep Springs Valley 150
97. Map showing pebble lithology in the north end of Deep Springs Valley 151
98. View of the basalt mass and small fan at the base of Piper Mountain 152
99. Map showing the distribution of granules in the north end of Deep Springs Valley 153
100. Map showing silt:clay ratios and the inferred wind track in the north end of Deep Springs Valley 155
101. Map showing the mean size of the granule-to-clay fraction in the north end of Deep Springs Valley 157
102. Graph showing the relation of the mean size of the granule-to-clay fraction to distance from the fan apex in the Antelope Springs channel 158

EROSION AND SEDIMENTATION IN A SEMIARID ENVIRONMENT

THE EFFECT OF SEDIMENT CHARACTERISTICS ON EROSION AND DEPOSITION IN EPHEMERAL STREAM CHANNELS

By S. A. Schumm

ABSTRACT

This study of five semiarid valleys emphasizes the importance of physical properties of sediment in determining stream-channel shape and differences in the mechanics of erosion and deposition between areas. Prerequisites for selection of the five areas were a progressive decrease in the percent silt-clay in stream channels and banks, active aggradation or erosion within a reach of the stream channel, and nearly uniform lithology within each drainage basin.

A comparison of the data obtained from each area demonstrates that in a drainage channel composed of fine-grained, highly cohesive sediment, deposition occurs on the sides of the channel as well as on the channel floor. The result is a reduction in the channel width-depth ratio across an aggrading reach. Vegetation seems to aid deposition by its rapid growth on recently deposited fine alluvium, but it is not the initial cause of aggradation. Bank caving yields only small amounts of sediment and, caved blocks are often nuclei for deposition along channel sides because of their resistance to disintegration. Degradation in the finer sediments is generally by upstream headcut migration.

In contrast, those channels containing only small amounts of silt-clay are aggraded from bottom to top. No plastering of fine sediments on the banks occurs. Less vegetation grows on these poorly cohesive, highly mobile sediments. Headcutting occurs only where the coarser sediments are capped by a layer of fine material. In general, a break in the longitudinal profile of this type channel is quickly removed by channel degradation. Bank caving seems to supply more sediment to the stream load, for the blocks of poorly cohesive alluvium disintegrate upon impact.

Deposition causes marked changes in the ephemeral-stream channels. As the reach of maximum aggradation is approached channel gradient decreases, and depending on the amount of silt-clay in channel and banks, the width-depth ratio may increase or even decrease. In all channels studied percent silt-clay increases and median grain size decreases with aggradation. At the lower end of an aggrading reach, the gradient steepens, but sediment is still fine and vegetation generally covers the entire valley floor. The reach of maximum deposition may migrate upstream with time, but renewed degradation on the downstream reach of steep gradient may cause a trench to cut through the valley plug, renewing through transport of sediment and runoff.

The aggradation in the study areas is apparently a result of high sediment yields in the headwater parts of the drainage basins. Deposition in the channel occurs; however, where the rate of increase of drainage area per mile of channel length is low. In these reaches of small tributary contribution, water loss into the alluvium and the subsequent increase in sediment concentration causes deposition.

The shape of stable cross sections, expressed as a width-depth ratio, is dependent on the weighted mean percent silt-clay in banks and channels such that width-depth ratio increases with decreased silt-clay in the alluvium. Gradient also shows an inverse relation to weighted mean percent silt-clay for these small streams of low annual discharge.

It is suggested that the relation between channel shape and silt-clay can be used as a criterion of channel stability, for aggrading channels generally plot well above the width-depth, silt-clay regression line; whereas, degrading channels plot below the line.

The study suggests that preventive conservation may be the most practical solution to some erosion problems, such as arroyo cutting. Deposition, if it is desired to fill a trenched channel, should be induced in reaches where conditions are most favorable for natural aggradation. Conservation measures should be modified depending on the character of the valley and its alluvium. Only certain critical reaches of a channel need be controlled to prevent erosion over larger areas.

INTRODUCTION

Recently there has been an increase in studies of stream morphology. Leopold and Maddock (1953) have discussed downstream changes in width and depth of a stream channel with increased discharge. Additional studies by Wolman (1955), Leopold and Miller (1956), and Wolman and Leopold (1957) have tended to confirm Leopold and Maddock's conclusions under diverse conditions and have revealed much about stream-channel development. The writer in another investigation introduced a parameter for sediment type and stressed the importance of the effect of sediment type on channel shape (Schumm, 1960b). All the above investigations were restricted to stable channels, or at least channels that were not rapidly aggrading or degrading. The present study concerns some small ephemeral-stream channels that are being actively aggraded or eroded.

A knowledge of the mechanics of deposition and erosion in semiarid valleys would not only be academically valuable, but could also provide the basis for conservation measures aimed at restoring gullied valleys to their prior condition. Much has been written on the need for careful use of the semiarid valley floor, for it may be the only productive land within a drainage basin. For example, Peterson (1950), as a result of interviews with several early settlers, states that at the time of white settlement in the valley of San Simon Creek, Ariz., the valley floor was flat and unbroken. Large areas were covered with grass, luxuriant enough to be harvested for hay. The creek itself was perennial throughout most of its length and lined with trees. During the 1880's, 50,000 head of cattle are said to have grazed the valley. At present the valley floor is trenched from its confluence with the Gila River for nearly 70 miles upstream, although a reach of about 2 miles is uncut about 40 miles above the mouth. The stream is now ephemeral, and barren flats and miniature badlands border the gully. Other valleys in the West have a similar history.

Much thought has been devoted to the development of conservation measures; nevertheless, until the mechanics of sediment deposition and removal are better understood, truly effective conservation measures will not be realized. This report is a contribution toward the development of that necessary understanding of semiarid erosional and depositional processes.

Many students of stream activity have recognized that the type of sediment transported by a stream greatly influences the characteristics of that stream. Therefore, in order to form general conclusions, areas of diverse sediment types must be studied.

A study of the relation between sediment type and stream-channel shape (Schumm, 1960a) has shown that for stable stream channels containing less than 40 percent gravel and cobbles, the channel shape expressed as a width-depth ratio (F) bears the following relation to a weighted mean value for the percent silt-clay in bank and channel samples (M): $F=255\ M^{-1.08}$. Silt-clay is defined as the sediment passing through the 200-mesh sieve, smaller than 0.074 mm.

Areas which had a wide range in the percent silt-clay in channel and banks were selected for study because it was believed that such differences might be fundamental with regard to the mechanics of sediment deposition and erosion.

This report is composed of two main parts. The first contains a geographic description of each study area as well as a discussion of the changes in sediment and channel characteristics along each channel. In the second part the data collected in the five study areas are combined to show the relations between sediment type and channel character, and the causes of, and the differences in, erosional and deposition processes in the study areas. In addition, conclusions and their practical application are discussed.

ACKNOWLEDGMENTS

During the summer of 1957 the following assisted the writer in the field: William Krummel, C. T. Sumsion, and R. H. Taylor. Irene Lapke performed the hydrometer analysis of the finer sediment samples. The writer wishes to acknowledge the constructive criticism offered by J. H. Mackin, M. G. Wolman, and J. T. Hack.

John Rutter, superintendent, Badlands National Monument, and Philip Ward, ranger, Great Sand Dunes National Monument, aided the fieldwork, and their courtesy and assistance are greatly appreciated.

METHODS OF INVESTIGATION

Five drainage basins were selected for study. Both a range in alluvial characteristics from area to area and active deposition or erosion within the channel were basic prerequisites. To eliminate as many variables as possible, areas were selected in which differences in lithology within a drainage basin did not affect the stream in any recognizable manner. This necessitated the selection of small drainage basins; the largest basin chosen had a drainage area of about 90 square miles.

The reaches of each channel in which deposition was important generally could be readily identified, perhaps most easily by the recognition of recently deposited alluvium by its fresh appearance and lack of vegetative cover. Downstream changes in channel shape and gradient and sediment character, also confirmed the location of aggrading reaches. These deposition criteria will be discussed in more detail under "Deposition in ephemeral streams." Unfortunately discharge data were not available for each channel studied.

The five areas selected, although scattered from southern South Dakota to northern New Mexico (fig. 17), fulfilled all the basic requirements and were similar in annual precipitation and land use. Similar observations were made in each area. Where topographic maps of good quality, large scale, and small contour interval were available, the fieldwork was limited to the collection of data at many locations along the channel. Cross sections were chosen primarily to illustrate the changes occurring in the channel and on the flood plain as deposition or erosion became increasingly important in the downstream direction. Photo-

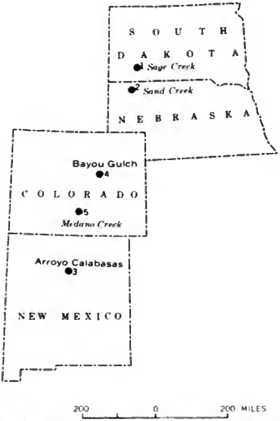

FIGURE 17.—Index map showing location of five study areas.

graphs and sediment samples of channel, bank, and overbank deposits were taken, and the gradient of the stream was measured at each section. The locations of the sections were marked on maps or aerial photographs. The longitudinal profile of the stream was surveyed along the aggrading reach when topographic maps were not available. In brief, the downstream changes in channel character accompanying deposition were documented by many surveyed cross sections of the channels, spaced closely enough to reveal the manner of channel filling. In addition, observations were made on the influence of vegetation on deposition.

The width and depth of the drainage channels were especially difficult to determine: (a) where recent incision formed a steep-sided trench, in which all the runoff was contained; or (b) where a filled channel held only the smaller flows. In the first type, depth of water during the recent floods was estimated from observations of the height of scour or deposition on the banks. In the second type, depth was measured to the lowest elevation on the profile from the edge of the first permanent surface or bank above the channel floor. On figures 19, 24, 29, 33, and 37 the dashed line on each cross section shows the width measured at that section. Width was measured from one edge of a bank to the opposite, at a distance above the channel floor determined by channel depth.

Samples of sediment were taken from the stream channel, its banks, and the flood plain. Samples of the surface inch of channel sediment were taken from 10 to 15 points along the cross sections, depending on channel width. These samples were combined to give a composite sample of the channel alluvium.

In the laboratory, a size analysis of each sediment sample was made. Since the author had found previously (Schumm, 1960), that the median grain size of the sample alone is not the most important characteristic of the sediment, the cumulative grain-size curve was used to select other parameters of possible value, such as those used to determine the engineering properties of granular materials. Burmister (1952) has prepared tables which allow estimation of permeability, cohesion, and frost-heaving characteristics of a soil from the grain size below which 10 percent of the sample is finer (Hazen's effective size, D_{10}). Burmister's tables were used to describe in general terms the physical properties of each sample.

The percent silt-clay in the sample, taken as that part of each sample passing the 200-mesh sieve, was also selected for comparison between areas. Burmister gives physical reasons for selecting the 200-mesh sieve or 0.074 mm as the boundary between silt-clay and sand, for the soil becomes less well drained and capillarity increases as the percentage of material passing the 200-mesh sieve increases; in addition, the 200-mesh sieve is the practical lower limit of sieving. In a recent paper Dunn (1959) demonstrates that the resistance of alluvium to tractive force is, related directly to the silt-clay content of the sediment. Dunn, however, defines silt-clay as sediment finer than 0.06 mm.

AREAS OF STUDY

For each of the five study areas a geographic description will be presented. This will be followed by a general description and a quantitative description of sediment and channel variations downstream. Comparisons of the five areas will be made in a later section.

SAGE CREEK, SOUTH DAKOTA

DESCRIPTION

Location.—Sage Creek, a tributary to the White River, (figs. 17, 18) drains an area of about 92 square miles in the southeastern corner of Pennington County, S. Dak. The northern drainage divide is about 11 miles south of the town of Wall, and the eastern divide is about 7 miles west of the town of Interior. The headwaters lie within the boundary of Badlands National Monument. That part of Sage Creek studied in detail

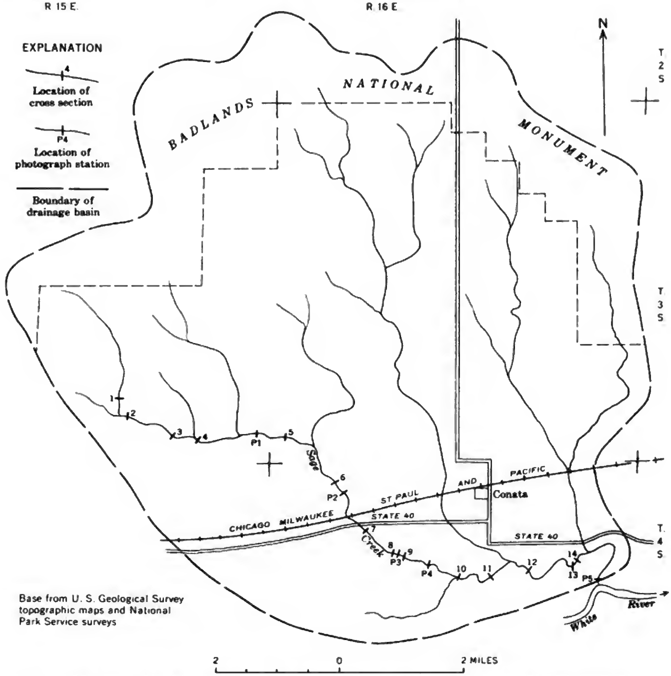
R 15 E.
R 16 E
N
T 2 S
T 3 S
T. 4 S
EXPLANATION
Location of cross section
P4
Location of photograph station
Boundary of drainage basin
BADLANDS NATIONAL MONUMENT
Sage Creek
CHICAGO MILWAUKEE ST PAUL AND PACIFIC
STATE 40
Conata
White River
P1
P2
P3
P4
P5
1
2
3
4
5
6
7
8
9
10
11
12
13
14
2
0
2 MILES

Base from U. S. Geological Survey topographic maps and National Park Service surveys

Figure 18.—Index map of Sage Creek, S. Dak., drainage basin showing location of cross sections and photograph stations.

is shown on two Geological Survey topographic maps, the Conata and Bouquet Table quadrangles.

Annual precipitation.—The mean annual precipitation at Interior, based on a 10-year record, is 16.53 inches (table 1). The greatest part of this mean annual precipitation, 13.97 inches, occurred during the period April through October. According to Thornthwaite's climate classification (1941), the Sage Creek area is semiarid.

Vegetation and land use.—Most of the drainage basin is used as grazing land, although some alfalfa is grown on that part of the basin that lies on the flood plain of the White River. Vegetation is of the short grass prairie type, although in the badlands vegetation is generally absent.

Physiography and geology.—The headwaters of Sage Creek drain the precipitous badland escarpment known locally as the Wall. This escarpment, composed of

TABLE 1.—*Precipitation at stations near the study areas*

[U.S. Weather Bureau data]

Station	Length of record (years)	Mean precipitation (inches)												
		Annual	January	February	March	April	May	June	July	August	September	October	November	December
Interior, S. Dak	10	16.53	0.45	0.34	0.78	1.75	2.97	2.64	2.62	1.74	1.05	1.20	0.52	0.47
Fort Robinson, Nebr	40	17.19	.47	.63	1.00	2.19	2.79	2.49	2.07	1.64	1.51	1.29	.48	.63
Santa Fe, N. Mex	40	14.19	.66	.74	.81	1.07	1.46	1.19	2.28	1.90	1.68	1.11	.71	.58
Santa Fe (AP), N. Mex	15	10.80	.32	.42	.54	.67	.71	.93	1.80	2.42	1.29	.99	.23	.48
Parker (9E), Colo	23	13.42	.34	.36	.69	1.91	2.21	1.60	1.83	1.83	1.05	.75	.56	.29
Blanca, Colo	11	9.20	.10	.25	.17	1.09	.87	.56	2.20	2.05	.73	.82	.19	.17
La Veta Pass, Colo	30	20.98	1.13	1.73	2.54	2.39	1.78	1.09	2.19	2.13	1.27	1.44	1.69	1.60

TABLE 2.—*Channel and sediment characteristics, Sage Creek, S. Dak.*

[Class: A=aggrading; D=degrading; S=stable; U=unclassified]

Cross section	Class	Drainage area (square miles)	Distance between cross sections (miles)	Median grain size D_{50} (mm)	Hazen's effective size D_{10} (mm)	Trask sorting index	Silt-clay (percent)	Gradient	Channel width (feet)	Channel depth (feet)	Width-depth ratio (F)	Weighted mean silt-clay, M (percent)
						Channel sediment						
1	U	1.65	--------	0.04	0.00055	3.63	74	0.0055	33	3.0	11.0	--------
2	S	1.71	0.076	.06	.00036	11.20	55	.0055	16	7.0	2.3	73
3	S	3.42	1.36	.06	.001	1.42	68	.0045	20	7.0	2.9	79
4	S	9.48	.94	.12	.009	4.61	40	.0045	31	5.0	6.2	54
5	U	13.08	2.12	3.00	.005	11.80	29	.0007	34	6.5	5.4	44
6	A	14.33	1.21	.10	.007	5.96	45	.002	32	6.2	4.9	53
7	A	14.59	1.06	.09	.0001	13.80	47	.002	12	4.0	3.0	61
8	U	18.11	1.32	.034	.0001	4.45	86	.002	22	8.0	2.8	87
9	D	18.12	.30	--------	--------	--------	--------	.0022	18	10.0	1.8	--------
10	A	45.12	1.36	.067	.0012	2.14	60	.002	21	3.0	7.0	67
11	A	45.40	.91	.032	.0002	1.63	92	.002	15	3.0	5.0	91
12	A	80.25	1.44	.047	.016	1.29	78	.0022	22	4.0	5.5	78
13	U	80.65	.99	--------	--------	--------	--------	--------	12	2.5	4.8	--------
14	U	82.84	.38	.044	.004	1.54	93	.0017	32	6.5	4.9	89
Mean	--------	--------	--------	0.31	0.0037	5.29	64	--------	--------	--------	--------	--------
						Bank sediment						
2	--------	--------	--------	0.028	0.0005	2.20	93	--------	--------	--------	--------	--------
3	--------	--------	--------	.030	.0003	2.24	93	--------	--------	--------	--------	--------
4	--------	--------	--------	.028	.0005	2.00	96	--------	--------	--------	--------	--------
5	--------	--------	--------	.035	.001	1.83	90	--------	--------	--------	--------	--------
6	--------	--------	--------	.032	.00032	1.68	84	--------	--------	--------	--------	--------
7	--------	--------	--------	.038	.0013	2.00	83	--------	--------	--------	--------	--------
8	--------	--------	--------	.031	.0007	2.68	88	--------	--------	--------	--------	--------
10	--------	--------	--------	.033	.0006	1.91	90	--------	--------	--------	--------	--------
11	--------	--------	--------	.027	.0013	2.13	89	--------	--------	--------	--------	--------
12	--------	--------	--------	.015	.0045	2.00	79	--------	--------	--------	--------	--------
13	--------	--------	--------	.007	.0002	5.10	97	--------	--------	--------	--------	--------
14	--------	--------	--------	.060	.015	1.19	81	--------	--------	--------	--------	--------
Mean	--------	--------	--------	0.030	0.0022	2.25	89	--------	--------	--------	--------	--------
						Overbank sediment						
1	--------	--------	--------	0.040	0.0006	3.63	74	--------	--------	--------	--------	--------
7	--------	--------	--------	.035	.0002	1.89	90	--------	--------	--------	--------	--------
13	--------	--------	--------	.007	.0002	5.10	97	--------	--------	--------	--------	--------
14	--------	--------	--------	.044	.0007	1.78	85	--------	--------	--------	--------	--------
Mean	--------	--------	--------	0.032	0.0004	3.10	87	--------	--------	--------	--------	--------

the sandstones, siltstones, and claystones of the White River group of Oligocene age, is being eroded rapidly. On many of the slopes a depth of 0.5 inch of material is eroded during 1 year (Schumm, 1956). Sediment eroded from the scarp must be transported at least 10 miles across a gently sloping surface formed by the northward retreat of the badland scarp, to reach the White River. In spite of the gentle slope of this surface, about 20 feet to the mile, it is trenched by ephemeral streams. A few residuals or outliers of the main badland mass rise above it.

Over almost the entire drainage area the White River group is exposed at the surface, although a geologic map of the area (Ward, 1922), which unfortunately fails to cover the entire drainage basin, suggests that the Pierre shale of Cretaceous age crops out in the lower part of the Sage Creek valley. However, since the creek flows on an alluvial fill derived predominantly from the White River group, no change in valley character was recognized due to change of rock type.

Alluvium.—The sediment derived from the erosion of the White River Badlands is fine grained (table 2). Median grain size of channel sediment for all sections is 0.31 mm, Trask's sorting coefficient is 5.29, and Hazen's effective size is 0.0037 mm. Using Burmister's tables (1952), it is found that a soil having D_{10} of 0.0037 mm is nearly impermeable. Potential capillarity of the soil is high, and it is very susceptible to frost heaving. This indicates that the alluvium in general is highly cohesive, and much energy is required to detach a particle from the mass of alluvium. The mean percent silt-clay in the channel samples is 64, confirming the highly cohesive nature of this material.

Samples taken of overbank deposits and deposits on the sides of the channel contain an even greater percent silt-clay and smaller value for D_{10} (table 2), indicating even higher cohesion.

Samples were taken from the recently trenched valley sides. These contained 89 percent silt-clay and D_{10} was 0.0022 mm, indicating that the fill is impermeable. The potential capillarity is high, and the banks are susceptible to frost heaving.

GENERAL CHANNEL VARIATIONS

Considering the nature of the alluvium, a general discussion will now be presented of the changes in channel characteristics at the 14 sections surveyed.

On figure 18 the location of the 14 surveyed sections and 5 photograph stations are shown. Photographs of some sections, shown on figures 20 and 21, pertain to the following discussion. Cross sections are shown at their respective positions on the longitudinal profile in figure 19 which is based on topographic maps.

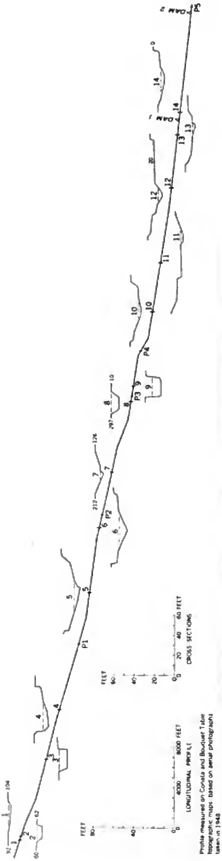

Profile measured on Conata and Bouquet Table topographic maps based on aerial photographs taken in 1948

FIGURE 19.—Longitudinal profile in 1948 and cross sections measured in 1957 on Sage Creek, S. Dak. Numbers at ends of some cross sections give distance in feet to edge of flood plain.

The uppermost section (No. 1) has only a poorly defined channel. Past deposition has smoothed the valley floor until now flood waters cover a width of about 240 feet (fig. 20*A*). A short distance below section 1 is a headcut below which the valley floor is trenched. The headcut is not shown on figure 19, for its height is much less than the contour interval of the topographic maps on which figure 19 is based.

Bank caving has widened the newly incised channel between sections 2 and 3 (figs. 19, 20*B*), but the cohesiveness of the bank material prevents rapid disintegration of the slump blocks. Some of the larger fragments on which vegetation still grows are nuclei for deposition in the channel (fig. 20*C*).

At section 3 this process has become more pronounced, and locally what seem to be incipient point bars are forming about slump blocks. The channel widens and deepens rapidly downstream as tributaries join the main channel. At section 4 an inner channel has formed; that is, deposition has built terraces along both banks (fig. 20*D*). The characteristic mode of deposition in this area seems to be a plastering of sediment along the sides of the channel. The recently deposited, fine-grained highly cohesive sediment aids plant growth, and all recent sediment deposits are covered with grass and weeds, which in turn further increase deposition.

Midway between photograph station 1 and section 5 there is a noticeable decrease in stream gradient (fig. 19), suggesting that deposition probably increases below section 5. Downstream the inner terraces encroach on the channel proper and mount higher on the original banks of the channel until at section 6 only about 3 feet of these banks are exposed, and a short distance downstream only 1 foot (fig. 20*E*), and finally at section 7 (fig. 20*F*), the banks are completely covered. Owing to this deposition along the sides of the channel, bank caving has stopped. Overbank deposition is important at section 7, and the vegetation on the surface adjacent to the channel is partly buried. Downstream from section 7 the channel becomes shallower and narrower, approaching complete filling by building from the sides as well as from the bottom of the original channel. Thus in about 5 miles the channel of Sage Creek has been transformed from a raw trench to one almost completely aggraded. The complete filling of the channel, however, is interrupted by renewed trenching below section 8. At section 8 the channel is deeper and wider than at section 7; however, at section 8 much recently deposited alluvium is found in the channel, suggesting that aggradation may be occurring or has occurred after channel erosion.

Figure 21*A* shows a reach of intense erosion accompanied by channel widening below section 8. At section 9 the channel is at maximum depth but about 1 mile downstream at photograph station 4 (fig. 21*B*) deposition has begun again, especially along the sides of the channel and on slump blocks in the bottom. A short distance below this point a remnant of the old channel floor is preserved on the west wall of the new trench. It lies 6 feet below the prairie surface, suggesting that complete filling had not occurred before the renewed trenching. This may explain the absence of a headcut above section 8. Between photograph station 4 and section 10 (fig. 21*C*), more than 1 mile downstream, channel deposition becomes increasingly important, until at section 10 the cross section most nearly resembles that of section 7 (fig. 19).

Deposition at section 10 (fig. 21*C*) was heavy during the floods before the survey, and at this section the manner of deposition is most clearly illustrated. Just above section 10 the stream bends sharply to the north. With rapid deposition, the point bar deposit on the inside of the bend is expected, but of greater interest is the deposition on the outside of the bend where bank cutting should logically occur. Figure 21*D* is a view of the deposit on the outside bank. The fieldbook is at the contact between what may be deposition by floods in the spring of 1957 and earlier floods. The sediment is laid in against the bank, effectively narrowing the channel at this section with little or no decrease in channel depth.

A trench dug across the deposit reveals that stratification is not horizontal; rather it curves downward from the bank toward the channel. Therefore, these lateral deposits are built upward as well as outward from the bank. The deposit shown on figure 21*D* has been scoured by recent floods, but on the inside of the bend (figs. 21*C*, *E*) the building of the deposit outward into the channel has not been hindered by erosion. Complete filling of the channel by a union of the lateral deposits and deposition on the channel floor will result in a channel-fill deposit containing concave-up stratification (Schumm, 1960a). This type of lateral deposition could only occur in areas of fine-grained cohesive sediments containing a high percentage of silt-clay. Figure 21*E* shows the growth of weeds on the recent deposits. The cohesiveness, ability to hold water, and the fertility of the fine sediment aids rapid and luxurious vegetative growth.

Proceeding downstream from section 10, the water table apparently approaches the surface, for willow and cottonwood saplings appear which further promote deposition. At section 12 the growth of willows is dense and at section 13 (fig. 21*F*) the channel is almost completely filled. A dam built in the fall of 1956 may be the cause of ponded water in the channel

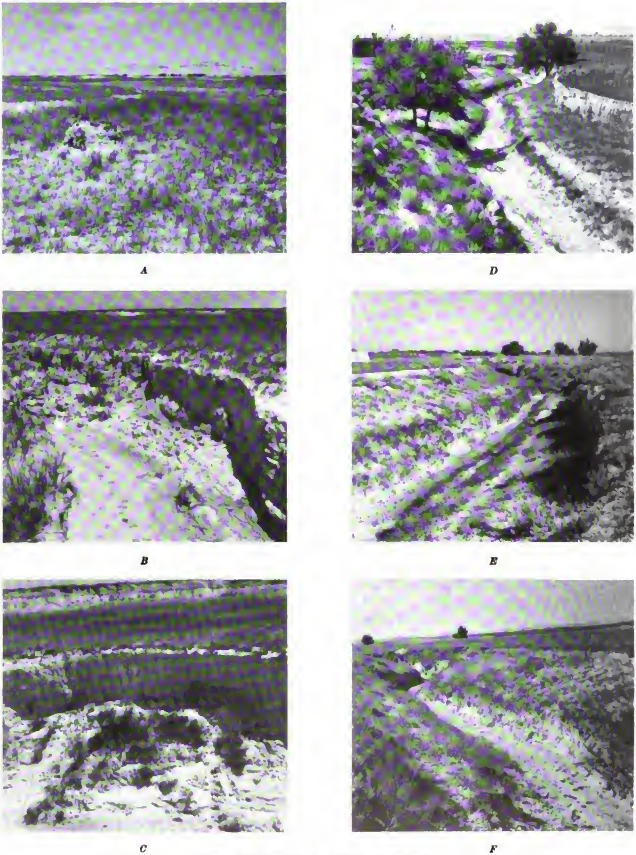

A D B E C F

FIGURE 20.—Sage Creek, S. Dak., above section 8.

at section 13, but the heavy deposition alone might have caused it. The 8 months since construction of the dam probably has been insufficient for that structure to cause accumulation of any measurable alluvial deposit at section 13. At section 14 just below the new dam, overbank deposition ranges in depth from 1 to 1½ feet. A second dam was constructed at the mouth of Sage Creek in the fall of 1956.

Probably little runoff enters the White River from the mouth of Sage Creek. The upper dam diverts much of the flow across the flood plain and into the river upstream. The remaining runoff is held by the lower dam. As a result high flows in the White River enter the lower end of Sage Creek and deposit sediment in that channel, thus plugging the mouth of the creek. This type of deposit has been termed a "reverse delta" by Leighly (1934).

QUANTITATIVE CHANNEL VARIATIONS

As shown in the general discussion of variations, there are marked changes in channel character along Sage Creek. A comparison now will be made of the channel and sediment characteristics at each cross section. The parameters of most importance to this discussion are channel gradient, the shape of the channel expressed as a width-depth ratio, median-grain size, sorting index of sediment, and the percent silt-clay in each channel sample. As noted above, the percent silt-clay is taken as that part of the sample smaller than the 200-mesh sieve or 0.074 mm.

To illustrate graphically the changes, the value for each of the above indices is plotted against section number on figure 22.

On figure 22 the width-depth ratio is much lower at section 2 than at section 1. This change occurs abruptly as one passes the headcut between sections 1 and 2 because channel degradation commonly causes a narrow and deep channel. Where the trench at sections 3 and 4 has been widened by bank caving, the width-depth ratio is higher. Gradient is less at sections 3 and 4 than at sections 1 and 2, and it shows a large decrease between sections 4 and 5. Percent silt-clay also decreases to a minimum for the sections at section 5; however, the largest median grain size was found at section 5 (3 mm). To keep within the limits of the diagram, median grain size for section 5 is not plotted on figure 22.

A question arises at this point as to the reason for increased median grain size at section 5. Perhaps the low graident at section 5 (fig. 19) causes deposition of the coarser fraction of the sediment in the channel; whereas, the finer fraction continues downstream and is deposited where the channel becomes smaller because of aggradation (section 7). Deposition becomes important below section 5, and this is accompanied by a decrease in width-depth ratio and sediment size and an increase in percent silt-clay and gradient.

To understand the above changes in channel and sediment character as measured at the cross sections, the manner of channel filling by aggradation should be summarized. In general, the beginning of aggradation decreases channel gradient and relatively coarse sediment is deposited in this reach of the channel. The finer sediments continue to move down the channel across the reach of reduced gradient. At some point down stream, however, aggradation has almost completely filled the channel, and it is here that overbank flooding and deposition become important. With each flow of water much fine sediment is deposited in the remaining vestiges of the channel and on the flood plain. Continued deposition on the flood plain causes steepening of the gradient of the valley. The finer fraction of the alluvium is therefore found on the steeper reaches of the channel and valley floor. The above is discussed in more detail later in the report.

To return to a discussion of the cross sections on Sage Creek, the renewed degradation beginning below section 8 and continuing below section 9 causes a decrease in the width-depth ratio at section 9. Percent silt-clay decreases and median grain size increases at section 10,

---

EXPLANATION OF FIGURE 20

- *A*, Cross section 1, view upstream. Channel has been filled by aggradation and is now grass covered. Badlands are visible in background.
- *B*, Cross section 2, view upstream. Remnants of blocks of alluvium in channel are the result of bank caving, and indicate active widening of channel.
- *C*, Recent deposition around blocks of bank material which have caved into the channel near cross section 3. The block has not rotated, and flood-plain vegetation is flourishing on the surface of the block several feet below its original position.
- *D*, Station 1, view upstream. The inner terrace formed by lateral deposition along both banks is best displayed in this reach, between sections 4 and 5.
- *E*, View upstream from station 2 a short distance downstream from section 6. Lateral deposition of fine sediment has almost covered banks of gully.
- *F*, Cross section 7, view downstream. Banks are completely covered by recent deposits. The small raw channel at the bottom of the gully may be the result of renewed degradation.

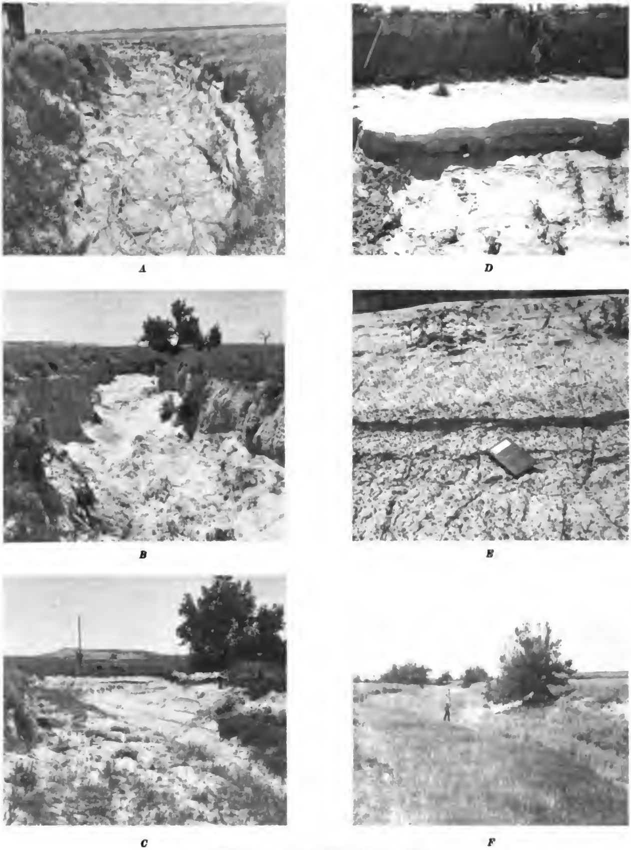

FIGURE 21.—Sage Creek, S. Dak., below section 8.

but the general trend of the channel sediment is toward increasing fineness below section 7. Gradient also decreases slightly as does width-depth ratio below section 10. The plot of sorting index indicates little except that the sediment is less well sorted on the aggrading reach between sections 5 to 7.

The percent silt-clay in samples of the inner terrace (table 2) changes little in a downstream direction, suggesting that sediments with more than 70 percent silt-clay are very susceptible to the type of deposition in the Sage Creek channel.

SUMMARY OF SAGE CREEK AREA

In a drainage channel carrying large sediment loads of fine-grained highly cohesive sediment, deposition occurs on the sides of the channel and deposition can occur on the outside of bends as well as on the streambed itself. The result is a reduction in the width-depth ratio across the aggrading reach. Median grain size increases and percent silt-clay and gradient decreases as deposition begins. This is followed by a decrease in median grain size and an increase in silt-clay and gradient as deposition increases. The final result will be a broad convex stream profile, the downstream part covered by the finer sediment.

Rapid growth of vegetation on recently deposited alluvium seems to aid deposition. Bank caving yields only minor amounts of sediment except in the recently cut reach, and caved blocks become nuclei for deposition along the sides of the channel.

SAND CREEK, NEBRASKA

DESCRIPTION

Location.—Sand Creek (fig. 17) drains an area of about 26 square miles in western Dawes County and northeastern Sioux County. The southern drainage divide is 6 miles north of the town of Crawford, Nebr., and the headwaters drain a part of the Pine Ridge escarpment, which here forms the major drainage divide between the White and Cheyenne River basins. Sand Creek flows to the east from the escarpment and enters the White River northeast of Crawford (fig. 23). No topographic maps were available for this area.

Annual precipitation.—Mean annual precipitation is 17.19 inches (table 1) based on a 40-year record at Fort Robinson, 3 miles southwest of Crawford. Most of this precipitation occurred during the months of April through October. According to Thornthwaite's (1941) climate classification, the Sand Creek area lies near the east limit of semiaridity.

Vegetation and land use.—The short grass prairie vegetation, covering all the drainage basin except the badland areas near the western divide, affords good grazing land. Only a small part of the basin shows evidence of former attempts at agriculture; however, farming is important to the south and along the White River. A large part of the headwater area of the drainage basin is badlands.

Physiography and geology.—The upper reaches of Sand Creek are supplied with large amounts of sediment derived from erosion along the western drainage divide. A photograph taken near the divide (fig. 25*A*) shows the removal of the protective grass cover from slopes by gullying and the formation of badlands. Badland development is characteristic of the White River group of Oligocene age.

The westward migration of the White River drainage divide leaves a pediment at the base of the Pine Ridge escarpment. The area near the scarp resembles that near Sage Creek, S. Dak., but farther to the east this surface has been dissected to form an area of gently

---

EXPLANATION OF FIGURE 21

A. View downstream from station 3. Recent trenching has exposed cottonwood tree roots on floor of channel. View typical of conditions at section 9 except for exposed roots.

B. View upstream, station 4. This reach is about 1 mile downstream from section 9. Deposition of sediment has begun here on floor of channel and along banks. Depth of gully is 16 feet.

C. Cross section 10, view upstream. Progressive deposition in the channel between station 4 and this section has almost filled the channel. The maximum depth of the gully was probably only 10 feet in contrast to the upstream sections.

D. Lateral bank deposit on outside of bend at cross section 10. Fieldbook is at contact of what is assumed to be the deposits from the 1956 and 1957 floods. A trench dug into these deposits reveals stratification planes curving downward (convex) toward the channel floor.

E. Weeds growing on recently deposited alluvium at cross section 10. Older plants (cockleburrs) are partly buried. Establishment of vegetation is rapid on the fine alluvium.

F. Cross section 13, view downstream. A more advanced stage of aggradation and vegetative growth is shown at this section about 3.3 miles downstream from cross section 10.

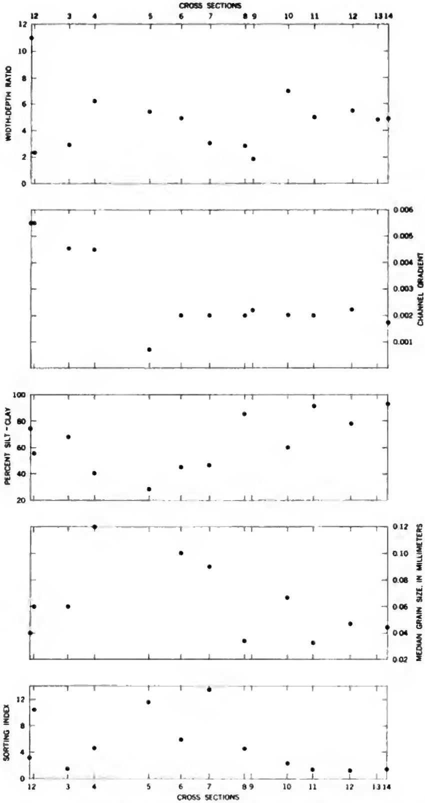

FIGURE 22.--Variations in channel and sediment characteristics, Sage Creek, S. Dak. The spacing of the cross sections along the abscissa is proportional to the distances between sections in the field.

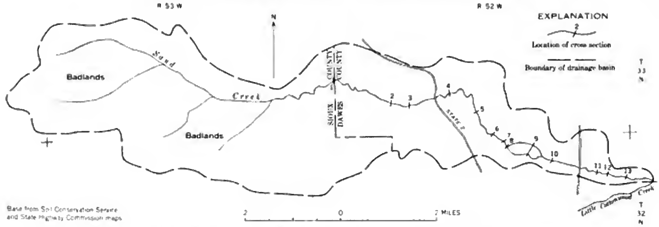

Base from Soil Conservation Service and State Highway Commission maps

FIGURE 23.—Index map of Sand Creek basin showing locations of cross sections.

rolling hills that contributes relatively little sediment to the channel.

Again, as in the South Dakota area, almost the entire drainage basin of Sand Creek is underlain by formations of the White River group. A negligible part, as regards influence on the stream, is underlain by the Pierre shale of Cretaceous age.

Alluvium.—Although derived from erosion of rocks of the White River group, the alluvium sampled in the Sand Creek valley is somewhat different from that derived from the South Dakota badlands (table 3). As suggested by the name of the creek, it is coarser. Median grain size for all channel samples is 0.37 mm; Trask's sorting index is 2.81 and Hazen's effective size 0.040 mm. Burmister's tables indicate that a soil with D_{10} of 0.040 is not impermeable, but it is drained with difficulty and is near the approximate lower limit of effective use of well points for lowering ground water (0.02 mm). The mean values for all sections show that potential capillarity is high and that the soil is very susceptible to frost heaving.

The above data suggest that the sediment would be cohesive and difficult to detach from adjacent particles, but the individual samples differ from the South Dakota area in that the channel samples taken above the aggrading reach are proportionally more sandy (compare figs. 22 and 27), having as little as 10 percent silt-clay at section 6.

Samples of the bank material contain 69 percent silt-clay, and D_{10} is 0.0044. Effective size (D_{10}) is larger than that for the Sage Creek sediment, but it still indicates a nondrainable system with high capillarity and high susceptibility to frost heaving.

GENERAL CHANNEL VARIATIONS

The high sediment yields from badlands in the headwaters of Sand Creek cause deposition in the downstream reaches of the channel. No topographic maps were available so the profile was surveyed from above section 6 to the mouth of Little Cottonwood Creek (fig. 23). At sections 4 and 5 the altitude of the channel floor was obtained by altimeter. Above State Highway 2 the gradient was measured at each section. On figure 24 are shown the longitudinal profile of the stream, the cross sections across the aggrading reach, and the profile of the flood plain above the channel.

Starting upstream in the area of badlands (fig. 25*A*), a continuous channel exists to the area of major aggradation at section 9. The channel is relatively deep at sections 1 and 2, but it becomes shallower and wider until at sections 3 and 4 (fig. 25*B*) it is a fairly wide sandy channel. The gradient at section 4 is about one-half of that of section 1, and as the aggrading reach is approached, the gradient decreases and the channel becomes shallower. Bank caving occurs in many places. At section 6 (fig. 25*C*) a recent slump has occurred. The large block, although cohesive (D_{10} is 0.005), has broken into many smaller fragments. The lack of other blocks in reaches of bank cutting strongly suggests that, unlike the Sage Creek area (D_{10} is 0.00035) slump blocks will not remain in the channel and form nuclei for channel deposition but will be swept away.

TABLE 3.—*Channel and sediment data, Sand Creek, Nebr.*

[Class: A=aggrading; D=degrading; S=stable; U=unclassified]

Cross section	Class	Drainage area (square miles)	Distance between cross sections (miles)	Median grain size D_{50} (mm)	Hazen's effective size D_{10} (mm)	Trask sorting index	Silt-clay (percent)	Gradient	Channel width (feet)	Channel depth (feet)	Width-depth ratio (F)	Weighted mean silt-clay, M (percent)
Channel sediment												
1	U	10. 6		0. 30	0. 045	2. 95	46	0. 003	20	4	5	
2	U	16. 1	2. 0	. 70	. 074	2. 17	7	. 0018	16	6	2. 7	42
3	S	16. 5	. 6	. 30	. 020	2. 28	17	. 0035	36	3	12	23
4	S	17. 9	1. 25	. 72	. 0013	2. 77	14	. 0015	75	7	10. 7	23
5	S	22. 2	1. 00	. 73	. 030	2. 93	15	. 003	65	7	9. 3	22
6	S	22. 5	. 75	. 35	. 075	1. 82	10	. 001	36	4	9	20
7	A	22. 7	. 30	. 024	. 0013	2. 62	87	. 0015	44	4	11	87
8	A	23. 1	. 15	. 020	. 0013	2. 25	91	. 0005	40	1. 5	26. 6	89
9	A	23. 9	. 60	. 019	. 0013	2. 48	100	. 003				
10	D	24. 2	. 50	. 027	. 0010	2. 39	85	. 0065	15	10	1. 5	90
11	D		1. 20	1. 10	. 14	1. 98	5	. 0017	21	10	2. 1	27
12	U		. 30	. 49	. 13	1. 53	5	. 0017	16	7	2. 3	21
13	U	25. 7	. 45	. 055	. 0013	8. 35	56	. 001	6	4	1. 5	
Mean				0. 37	0. 040	2. 81	39					
Bank sediment												
2				0. 040	0. 011	1. 47	90					
3				. 049	. 0014	1. 30	70					
4				. 053	. 0016	1. 29	70					
5				. 050	. 002	1. 64	60					
6				. 045	. 006	2. 74	65					
7				. 030	. 002	2. 17	88					
8				. 043	. 0013	3. 27	63					
10				. 014	. 00065	3. 59	93					
11				. 080	. 008	2. 12	48					
12				. 095	. 010	1. 82	39					
Mean				0. 050	0. 0044	2. 14	69					
Overbank sediment												
2				0. 040	0. 011	1. 47	90					
9				. 019	. 0002	4. 06	92					
12				. 026	. 001	2. 32	100					
13				. 017	. 0011	2. 93	93					
Mean				0. 026	0. 0033	2. 69	94					

Point bars and sandbanks are forming on the major bends of the channel, and in many places coarse gravel is introduced into the channel at the cut banks. Below section 6, pronounced changes occur, which are due to deposition. Between sections 6 and 7 the gradient decreases. There is a change in the nature of channel sediment and some tendency for deposition along the banks (fig. 25*D*). Changes in channel depth are much greater than those in channel width. Vegetation grows on both sides of the channel, and it in turn aids further deposition. Deposition increases downstream until at section 8 (fig. 25*E*) the channel is almost completely filled and can be recognized only by its bare appearance. Vegetation, however, is encroaching on this bare channel from both sides. Flood waters at section 8 cover a width of 190 feet of the valley floor. A short distance below section 8 the vegetation has covered the entire channel, and the gradient of the valley floor increases sharply in this area of maximum deposition. The deposition, no longer confined to filling the channel, has built up the center of the valley until it has a convex cross section at sections 9 and 10 (fig. 24). There is ponded water on the south side of the valley between sections 8 and 9 where deposition in the valley center has exceeded that near the south margin forming an undrained depression or natural lake.

The aerial photographs (fig. 26 *A*, *B*,) show the area of greatest deposition along Sand Creek. The light color of the recently deposited alluvium delimits the aggrading areas. Downstream from the area of major deposition vegetation becomes dense on the flood plain and trees are more abundant.

At section 9 there is a channel at the south side of the valley. Cross section 9 (fig. 24) reveals that the edge of this channel is higher than the rest of the valley floor. Field investigation shows that this channel carries only minor amounts of water. It has not been aggraded completely because the flood waters are diverted to the low north side of the valley, where renewed trenching has occurred at section 10. The headcut and longitudinal profile of the floor of the recent trench are shown on figure 24. Thus, although the locus of points of maximum deposition is migrating up channel, following it is a trench, which unless controlled will probably unite with the upper channel to form a continuous channel throughout Sand Creek valley. Figure 25*F* shows the new channel dissecting the valley fill. Much bank caving is in progress, widening the channel. Downstream at the confluence of Sand and Little Cottonwood Creeks the channel has filled again and overbank deposition is important.

QUANTITATIVE CHANNEL VARIATIONS

It has been suggested under the general discussion that marked changes occur in channel and sediment characteristics as the aggrading area is approached and crossed and that these changes differ somewhat from the changes in the Sage Creek area. The values for sediment and channel characteristics are plotted for each cross section on figure 27.

Above section 6 width-depth ratio is a maximum at section 3 but shows a general increase from section 1 to section 6. Gradient decreases at downstream sections in the manner to be expected. Percent silt-clay remains nearly constant. Median grain size varies but not in relation to any known control. Thus above section 6 the parameters vary in a downstream direction, probably much as they would in any channel. Between sections 6 and 7 deposition becomes noticeable, and at section 7 a pronounced change in channel and sediment character occurs. Width-depth ratio increases, suggesting a widening and shallowing of the channel or a greater decrease in depth than in width. This increase continues to section 8 beyond which the channel is completely filled. Accompanying the increase in width-depth ratio is a slight decrease in gradient, a great increase in percent silt-clay, and a decrease in median grain size.

Continuing downstream toward the headcut, at section 10, little change occurs except for an increase in gradient and a sharp decrease in width-depth ratio. Stream gradient is initially decreased by deposition and then steepened as deposition becomes excessive. With renewed trenching gradient decreases, but it still is steeper than above the aggrading reach. Percent silt-

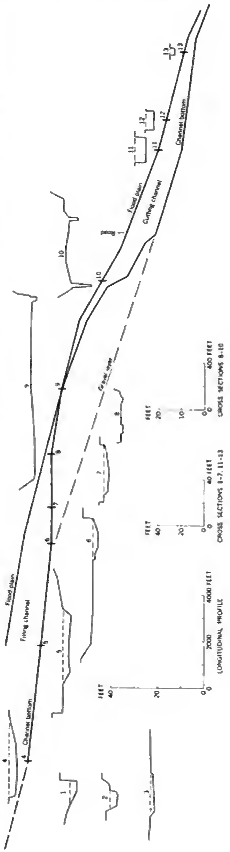

FIGURE 24.—Longitudinal profile and cross sections surveyed between section 4 and the mouth of Sand Creek, Nebr. Note that the scale of cross sections 8, 9 and 10 is smaller than for the remaining cross sections.

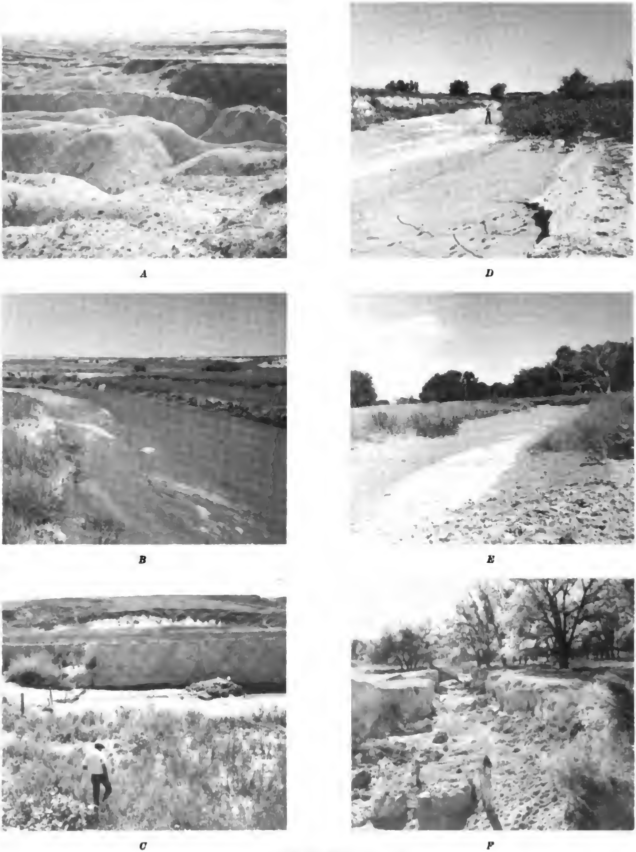

Figure 25.—Sand Creek, Nebr.

clay decreases and median grain size increases. Downstream from section 11 recent cutting probably has not occurred, and the channel and sediment characteristics vary accordingly.

Between sections 8 and 13 the samples of overbank material show a slight increase in the percent of silt-clay (table 3). The sorting index does not change greatly between sections 1 and 12.

HISTORIC CHANGES

Conversations with local ranchers reveal that the zone of maximum deposition, now located above and below section 9 (fig. 24), was about a mile downstream, near the county road, in 1917, 40 years ago. The filling of the valley has been a type of backfilling, that is, a migration upstream of the zone of maximum deposition rather than a general raising of the lower part of the valley.

A fence at section 9 has been replaced 5 times in 40 years as each installation was partly buried by alluvium. Total deposition at section 9 was estimated by the owner to be about 15 feet.

The headcut, now near section 10, started about 1950 between ½ to 1 mile below the county road. It has then advanced at least 1 mile in 7 years. This information suggests that incision did not begin at the confluence of Sand and Little Cottonwood Creeks but on the section of steepest gradient below the road. This indicates further that the shallowing of the channel below the road may not be due predominantly to deposition but may result from lack of recent trenching in lower reaches of the valley. Segments of the old shallow channel are preserved near the new trench below the road. The old channel was about 5 feet deep and 13 feet wide; whereas, the new channel is now 13 feet deep and 20 feet wide.

The two aerial photographs in figure 26 show the changes that have occurred at and near the reach of maximum deposition between 1939 and 1954, a period of 15 years. Upon comparing the photographs, the channel between sections 7 and 8 seems to have filled. Above section 7 the photographs suggest no more than minor channel changes. Overbank deposition is present farther to the west (upstream) in 1954 as indicated by the upstream and lateral expansion of the light-colored areas of recent deposition, and the cutoff channel has been filled. The lake between sections 8 and 9 was formed by 1954, and the darker patches of flood plain to the north of the lake are gray probably due to flooding and recent deposition on these surfaces. Also, the aggradation in the center of the valley has forced the channel to the south side of the valley in 1954. Another noticeable difference between the two photographs is the growth of vegetation on the light-colored surfaces of recent deposition, shown on the 1939 photograph near the county road, giving them a darker appearance on the 1954 photograph.

In addition, a trenched channel exists below the county road in the 1954 photograph in contrast to the smaller 1939 channel. Perhaps the darker color of the valley below the road in the 1954 photograph is the result of this trenching, for the channel now carries all the flood water, preventing overbank deposition. Marked changes have occurred, suggesting progressive aggradation in the upper area and trenching downstream. The upper limit of both deposition and new vegetation seem to have moved up channel.

SUMMARY OF SAND CREEK AREA

In a drainage channel in which the sediment is composed of silt-clay and sand in the proportion 2 to 3, deposition occurs on the channel floor. Plastering of fine sediments on the channel banks occurs only in those aggrading reaches in which sand has become a minor part of the sediment. The width-depth ratio therefore increases along the aggrading reach until the channel has been completely filled.

Vegetation is of little importance except in the reaches of channel where fine sediments cover the banks and channel floor. Sediment from bank caving is moved downstream almost immediately and rarely aids in the beginning of channel deposition. A noticeable contrast with Sage Creek is the short distance in which deposition appears and channel-filling is completed, between sections 6 and 9 (6,000 feet).

EXPLANATION OF FIGURE 25

A, Badlands in headwaters of Sand Creek. Removal of the protective sod cover allows development of badlands in soft rocks of the White River group.

B, Cross section 3, view downstream. Relatively wide sandy channel typical of Sand Creek above aggrading reaches.

C, Cross section 6. Note recent slump block at base of bank. Fence to left shows signs of recent partial burial.

D, Cross section 7, view downstream. Note development of berms along sides of channel. Vegetative growth is promoted by deposition of fine sediments.

E, Cross section 8, view downstream. Channel is almost completely filled by recent deposition. Vegetation is encroaching on the parts of the channel that are bare.

F, Recently formed gully at county road between cross sections 10 and 11.

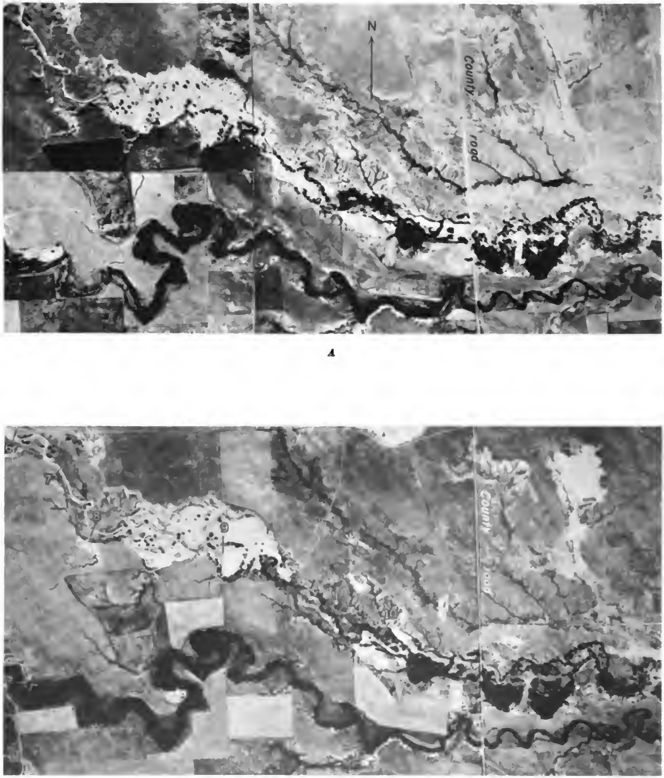

FIGURE 26.—Aerial photographs of part of the Sand Creek drainage basin, Nebr. *A*, taken in 1939; *B*, taken in 1954. Light-colored area at upper left of both photographs is area of maximum deposition. Locations of cross sections 6 to 10 are given on photograph *B*.

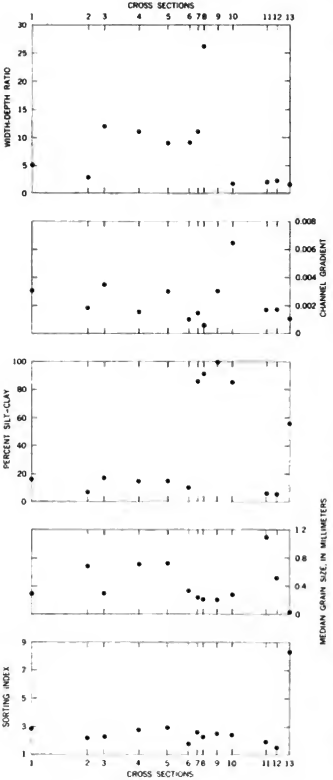

FIGURE 27.—Variations in channel and sediment characteristics, Sand Creek, Nebr. (The spacing of the cross sections along the abscissa is proportional to the distances between cross sections in the field.

In summary, the Sand Creek channel had few similarities in the manner of aggradation with Sage Creek. These differences are attributed mainly to the smaller percentage of silt-clay in the alluvium of Sand Creek.

ARROYO CALABASAS, NEW MEXICO

DESCRIPTION

Location.—Arroyo Calabasas (fig. 17) drains an area of about 48 square miles in central Santa Fe County, N. Mex. The drainage basin lies parallel to and about 1 mile northwest of U.S. Highway 85 between Santa Fe and the Santa Fe Airport (fig. 28), and a part of its headwaters lies within the Santa Fe city limits. Arroyo Calabasas is a tributary to the Santa Fe River. The Arroyo Calabasas drainage basin is shown on the following Geological Survey topographic maps: Santa Fe, Agua Fria, Turquoise Hill, Tetilla Peak, and Montoso Peak.

Annual precipitation.—A 40-year record of precipitation for Santa Fe (table 1) gives a mean annual precipitation of 14.19 inches. Of this total, 10.69 inches fell during the months of April through October. At the Santa Fe Airport a 15-year record gives a mean annual precipitation of only 10.80 inches. A comparison of the same 11 years of record from the 2 stations shows an average of 3.1 inches less rainfall at the airport. The Sangre de Cristo Mountains to the east probably produce a sufficient orographic effect to cause this difference in rainfall between mouth and headwaters of Arroyo Calabasas. The drainage basin apparently lies within a narrow zone of semiarid climate between the more humid mountains and the arid zone to the west.

Vegetation and land use.—Vegetational cover is poor except on the untrenched valley bottoms. Piñon and juniper grow on the hills. Grass is nearly absent except in the valleys, but slopes have a scant cover of Russian-thistle. Cattle and horses graze the undissected valley bottoms. The few dwellings within the drainage basin apparently are owned by people who work in the city of Santa Fe. No land cultivation has been attempted within the drainage basin.

Physiography and geology.—Unlike the two areas described previously, no prominent escarpment forms the drainage divide and no pediment development has taken place. Instead, a dendritic drainage pattern has developed, dissecting the poorly consolidated sediments into a network of valleys and divides. Hilltops are convex, bordered by valley-side slopes of varying steepness depending on the activity of the adjacent ephemeral stream.

The Arroyo de los Frijoles is a major tributary to Arroyo Calabasas. Their drainage areas are about

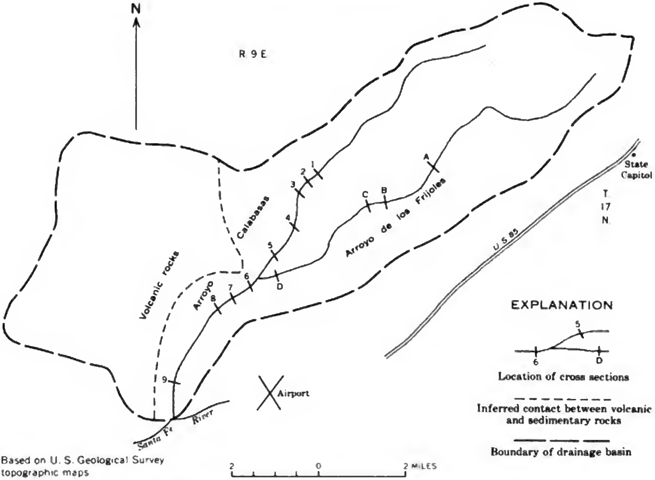
N
R 9 E
State Capitol
T 17 N
U S 85
Arroyo Calabasas
Arroyo de los Frijoles
Volcanic rocks
1
2
3
4
5
6
7
8
9
4
C
B
D
Airport
Santa Fe River
EXPLANATION
5
6
D
Location of cross sections
Inferred contact between volcanic and sedimentary rocks
Boundary of drainage basin
Based on U. S. Geological Survey topographic maps
2
0
2 MILES

FIGURE 28.—Index map of Arroyo Calabasas, N. Mex., drainage basin showing location of cross sections.

equal at the junction of the two (fig. 28). In the field, Arroyo de los Frijoles seems to be the main stream, for at the junction it is a well-defined trench; whereas, the Arroyo Calabasas channel is completely aggraded and grassed a short distance above the junction.

The drainage basins are underlain by the unconsolidated or partly consolidated silts and sands (marls) of the Santa Fe group of middle (?) Miocene to Pleistocene (?) age. The irregular shape of the drainage basin is due to volcanic rocks in the western part of the basin. The extent of the volcanic rocks, as inferred from the topographic maps, is indicated on figure 28. The streams draining this area enter Arroyo Calabasas near its mouth, but the resistance and permeability of the volcanic rocks result in little sediment and runoff from this part of the basin.

Alluvium.—The stream channels transporting sediment eroded from the Santa Fe formation seem to be filled entirely with sand, and the percent silt-clay in the channel of Arroyo Calabasas is only 17 (table 4). Median grain size is 0.59 mm; Trask's sorting index is 2.01, and Hazen's effective size, 0.17 mm. Burmister's tables suggest that soil with D_{10} of 0.17 mm is permeable with free flow. Potential capillarity is slight and frost heaving is negligible. The above factors suggests that none of the particles in the channels are bound together but act independently. The bank material, however, where sampled, has a mean of 20 percent silt-clay and D_{10} of 0.040 mm. Thus, although the material in the channel bottoms is not cohesive the material in the banks is, forming stable sides to the channel.

The samples taken in the channel are not truly representative, for in some sections gravel, cobbles, and even a boulder in some places cover about 5 percent of the streambed. However, this small fraction of larger grain sizes did not seem to influence the general channel and sediment character in any noticeable manner, and for convenience only the finer material was sampled.

TABLE 4.—*Channel and sediment data, Arroyo Calabasas and Arroyo de los Frijoles, N. Mex.*

[Class: A=aggrading; S=stable; U=unclassified]

Cross section	Class	Drainage area (square miles)	Distance between cross sections (miles)	Median grain size D_{50} (mm)	Hazen's effective size D_{10} (mm)	Trask sorting index	Silt-clay (percent)	Gradient	Channel width (feet)	Channel depth (feet)	Width-depth ratio (F)	Weighted mean silt-clay, M (percent)
Channel sediment												
A	S	3.83		0.84	0.28	1.68	3.	0.013	79	3.	26	4.1
B	A	4.68	1.17	.58	.18	1.91	4	.013	257	2	129	4.1
C	U	4.81	.27					.013	88	2.5	35	
D	S	12.85	2.90	1.00	.20	2.10	5	.014	67	4.5	15	8.5
1	S	8.47		.85	.16	2.34	6	.010	84	5	17	9.0
2	S	8.91	.30	.90	.26	2.33	2.	.010	63	1	63	2.4
3	A	9.30	.43	.51	.24	1.53	.5	.013				
4	A	9.85	.61	.56	.27	1.52	2	.014				
5	A		.76	.035	.0012	3.37	80	.018				
6	S	24.2	.64	.50	.18	1.47	3	.009	92	4	23	4.8
7	S	25.8	.49	.75	.16	2.01	5	.011	100	4	25	5.8
8	A	26.4	.34	.48	.14	1.92	5	.009	90	1.5	60	5.1
9	A	42.3	1.89	.031	.0015	1.94	89					
Mean				0.59	0.17	2.01	17					
Bank sediment												
A				0.28	0.034	2.00	18					
B				.30	.060	1.83	12					
D				.13	.001	3.16	35					
1				.15	.005	4.13	34					
2				.20	.045	2.14	14					
6				.16	.040	2.30	26					
7				.30	.035	2.00	16					
8				.32	.090	1.42	8					
Mean				0.23	0.040	2.37	20					
Overbank sediment												
3				0.034	0.0049	2.16	80					
4				.33	.044	2.07	16					
9				.033	.0015	1.94	89					
Mean				0.13	0.003	2.39	62					

GENERAL CHANNEL VARIATIONS

Five cross sections were surveyed on Arroyo Calabasas above the confluence with Arroyo de los Frijoles; 3 were surveyed on Arroyo de los Frijoles, and 4 below the junction of both streams.

Above the junction, Arroyo Calabasas has a broadly convex longitudinal profile (fig. 29). At section 1 the stream channel is 8 feet deep and seems recently cut (fig. 29). Downstream the channel is progressively filled with sand until at section 3 recent floods have covered the entire valley floor (fig. 30*A*). The valley floor in turn becomes better covered with vegetation until at section 5 there is no indication that a channel exists upstream (fig. 30*B*). This part of the valley is used for grazing.

A short distance below section 5 is the junction of Arroyo Calabasas and Arroyo de los Frijoles. Section 6, located just below the junction, was surveyed across the deep channel, which is continuous in the Frijoles drainage basin (fig. 30*C*). A headcut has started to migrate up the Arroyo Calabasas valley, but the valley floor is hanging 8 feet above the trenched channel near the junction.

The longitudinal profile of Arroyo de los Frijoles is flatter than that of Arroyo Calabasas near their junction (fig. 29), but 3 miles upstream it steepens and at section *B* the channel is 30 feet higher than the corresponding point in the Calabasas channel. At section *A* the channel is shallow and sandy (fig. 29). Downstream at section *B* (fig. 29) the channel has widened considerably and aggraded. The photograph of the channel below section *B* (fig. 30*D*) shows that sand has been deposited out of the channel and among the trees near the channel. Several channels have formed; these cut around the partly buried brush and trees forming islands and a braided channel. No headcut is present, but the channel

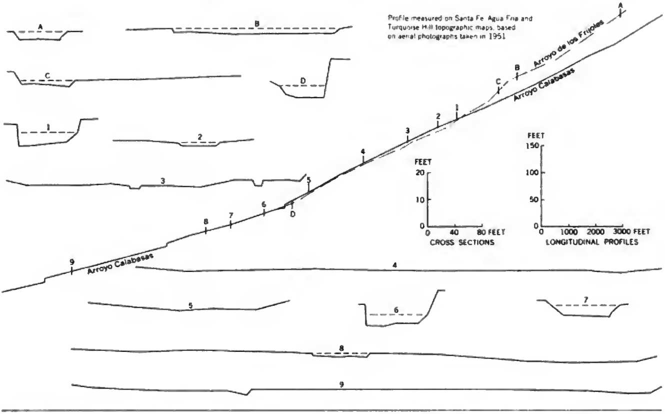

FIGURE 29.—Longitudinal profile and cross sections surveyed along Arroyo Calabasas and Arroyo de los Frijoles, N. Mex. Cross sections on Arroyo de los Frijoles are given a letter designation.

is nevertheless being lowered downstream from the aggraded cross section *B*, as indicated by plant roots that are exposed in the banks and by the rough appearance of the channel floor (fig. 30*E*) as contrasted with the smooth, flat floor characteristic of reaches of deposition. At section *C* the channel is narrower and bordered by well-defined banks. Continuing downstream the channel becomes deeper until at section *D* it is 5 feet deep. This, then, is the first example of channel rejuvenation in which headcutting is not important. A definite nick in the longitudinal profile is noted (fig. 29), but the noncohesive material in the channel prevents the development of a headcut, so typical of rejuvenation in the finer, more cohesive alluvium (Sage Creek between sections 1 and 2; Sand Creek near section 10). Below the junction of the two streams the channel, perhaps due to the decrease in gradient (fig. 29), is filled within a short distance.

At section 7 the channel is only 4 feet deep and at section 8 it is only 1.5 feet deep (fig. 30*F*). The width changes little, for the lack of large amounts of silt-clay prevent any deposition along the sides. Even at section 8 the remnants of the once high banks seem unchanged. Channels are filled solely from the bottom up. Deposition is complete below section 8 and vegetation covers the fill. A small discontinuous gully has formed between sections 8 and 9, but as its headcut moves upstream the lower end of the channel is filled. Here a headcut has formed. Samples of the alluvium taken across the valley show that, where the channel has been filled, the alluvium contains 66 percent silt-clay, which forms a tough, cohesive layer over the underlying predominantly sandy channel fill. This cohesive layer plus the vegetation cover is a protective cap, and headcut erosion again is the means of gully lengthening.

At section 9 the channel is completely filled, and the valley floor resembles that of section 5 (fig. 30*B*). The grass cover is good and cattle graze the valley floor. Below section 9 is another headcut that has worked headward from the junction of Arroyo Calabasas with the Santa Fe River (fig. 29).

Vegetation apparently does not aid the filling of channels here. The sandy nature of the alluvium prevents deposition along the banks, and no vegetation was noted in the channel bottom. The lack of vegetation in the channel is attributed to the lack of cohesion of the channel sediment. Any plant that takes root in the channel bottom would be washed out during the first flood as the sandy sediment is set in motion. The growth of weeds in a sandy channel downstream from a stock-water reservoir demonstrates that the channel sediments will support vegetation if undisturbed. The reservoir has retained all flow, and the seeds and plants were not washed out of the sediment by floods.

Blocks of bank-caved material were not common in the channel, probably because the low cohesion of the bank material allows crumbling and removal of fallen material by the next flood.

QUANTITATIVE CHANNEL VARIATIONS

To simplify this discussion the data obtained at the cross sections on Arroyo de los Frijoles have been plotted as if they were sections measured upstream from section 1 on Arroyo Calabasas (sections *A–D*, fig 31).

Moving downstream from section *A* (fig. 31), three areas of deposition are crossed at sections *B*; 3, 4, 5; and 8, 9. These sections are characterized by a high width-depth ratio. Deposition causes filling of the channels from bottom to top without changing the width, thereby greatly increasing this ratio. Even in the trenched areas, this ratio is nearly 20, which greatly exceeds that in the areas of finer grained sediment.

Gradient is steep between sections *B* and *C* owing to recent incision. It is steep also at section 5 and where measured below section 9 near the Santa Fe River (*X* on fig. 29). These last two increases in gradient are due to the steepening of the valley floor by deposition. Each of the steeper reaches of deposition is associated with sediments of smaller grain size, although percent silt-clay is high only at sections 5 and 9. Perhaps this is because aggradation at section *B* is not so far advanced as at sections 5 and 9. This relation seems anomolous—finer sediment on the steepest parts of the longitudinal profile—but it is simply the result of channel and flood-plain deposition as discussed previously.

The samples at sections 3, 4, and 8 are not so fine as those at sections 5 and 9 even though in areas of heavy aggradation, because they were taken in the last vestiges of the channels, which were generally little more than sand-filled swales. However, the valley floor as a whole is characterized by finer sediments. For example, sediments adjacent to these inadequate channels contained up to 80 percent silt-clay (table 4). As mentioned above, D_{50} and percent silt-clay show the greatest changes on the aggraded reaches. If the samples taken at sections 5 and 9 were not plotted on figure 31, percent silt-clay would show hardly any change; whereas, D_{50} would decrease, but only slightly in a downstream direction.

The sorting index is highest at section 5 in the aggraded Arroyo Calabasas valley above the junction with Arroyo de los Frijoles.

SUMMARY OF ARROYO CALABASAS AREA

In a drainage area in which silt-clay occurs in small amounts the channels are filled from bottom to top. No plastering of fine sediments on the banks occurs, and vegetation is not an important cause of deposition. Vegetation, however, becomes important in stabilizing the deposit when flooding occurs over the entire valley floor.

Headcutting occurs only where channel-filling has been completed, and the coarser sediments are capped by a layer of fine material which supports a heavy grass cover. The suggestion here is that a channel in coarse sediment, when filled, may acquire the characteristics of an area of finer sediment.

The gradient of the valley increases on the reaches of deposition due to piling up of sediment on the valley floor. These steep gradient sections are covered with the finest sediments.

BAYOU GULCH, COLORADO

DESCRIPTION

Location.—Bayou Gulch (figs. 17, 32) drains an area of about 23 square miles in northeastern Douglas and northwestern Elbert Counties, Colo. It is a tributary of Cherry Creek, entering that stream at a point about 3 miles north of Franktown and about 5.5 miles south of Parker. State Highway 83 crosses Bayou Gulch about 0.4 mile above the mouth. The drainage basin is shown on the Castle Rock and Elizabeth quadrangles.

Annual precipitation.—Based on a 23-year record of precipitation at Parker (9E) (table 1) the mean annual precipitation is 13.42 inches. Of the total, 11.81 inches fell during the months of April through October. According to Thornthwaite's climate classification (1941) the area is semiarid.

Vegetation and land use.—Vegetational cover is heavy. Pine trees grow on the divides and cottonwood trees are plentiful along the upper reaches of the creek. Alfalfa is raised on a terrace above the present flood plain. The rest of the drainage basin is used for grazing except for a few fields of wheat and corn on the divide.

Physiography and geology.—This drainage basin, except for the heavier vegetational cover and a general appearance of coarser sediment, resembles that of the Santa Fe area. A dendritic drainage pattern has incised the poorly consolidated sediments into a network

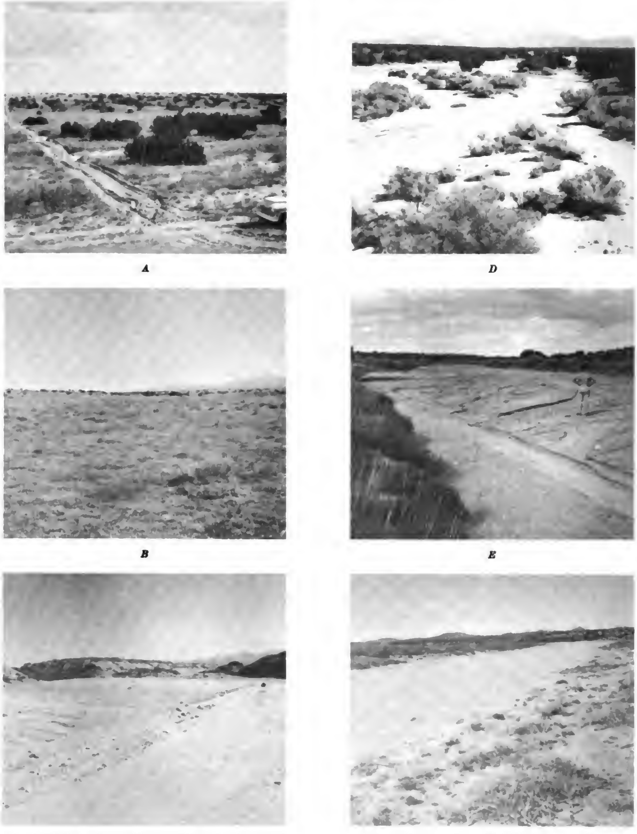

A *D*

B *E*

C *F*

Figure 30.—Arroyo Calabasas, N. Mex.

of valleys and rounded divides in marked contrast to the South Dakota area.

The entire drainage basin is underlain by poorly consolidated sandstones and shales of the Denver formation of Late Cretaceous and Paleocene age.

Alluvium.—The channel sediment contains 5 percent silt-clay (table 5). The median grain size is 0.57 mm, Trask's sorting index is 1.84, and Hazen's effective size is 0.17 mm. The characteristics of the channel sediment here and its behavior are little different than that in the Santa Fe area (table 4) for effective size is the same for both areas; however, the mechanics of aggradation seem to be somewhat different, and, indeed, the width-depth ratios are greater in this area. The bank material in Bayou Gulch differs from that in the Santa Fe area, for silt-clay is only 8 percent where sampled. Median size is 0.49 mm and D_{10} is 0.12, indicating that cohesion is low and that the banks would not have any great resistance to erosion in contrast to the more cohesive banks of the Santa Fe area.

GENERAL CHANNEL VARIATIONS

Above section 1 (figs. 32, 33) the channel narrows as the divide is approached. In the reaches of permanent flow above section 1, vegetation is encroaching on the channel but with difficulty because of the mobility of the channel material.

Below section 1 (fig. 34*A*) a wide sandy channel is characteristic of Bayou Gulch to its mouth. At sections 4 and 5 (fig. 34*B*) channel deposition may be occurring, for sand has been deposited over the flood plain, and the channel has been filled and widened. The observer has difficulty in determining what process is operative in each section of this channel. Where deposition is assumed to occur, widening of the sand-covered areas

TABLE 5.—*Channel and sediment data, Bayou Gulch, Colorado*

[Class: A=aggrading; S=stable; U=unclassified]

Cross section	Class	Drainage area (square miles)	Distance between cross sections (miles)	Median grain size D_{50} (mm)	Hazen's effective size D_{10} (mm)	Trask sorting index	Silt-clay (percent)	Gradient	Channel width (feet)	Channel depth (feet)	Width-depth ratio (F)	Weighted mean silt-clay, M (percent)
Channel sediment												
1	S	13.00	....	0.74	0.27	1.63	2	0.013	207	2.5	83	....
2	S	18.95	0.43	.50	.13	1.85	6	.009	122	2	61	5.9
3	S	19.66	.24	.58	.17	1.69	4	.010	130	3	43	4.4
4	A	21.95	.47	.55	.17	1.84	2	.011	330	2	165	2.0
5	A	22.44	.16	.47	.06	2.50	12	.010	250	1.5	167	12.2
6	U	22.90	.95	.55	.21	1.51	4	.016	128	1.5	85	4.1
Mean	....	....	....	0.57	0.17	1.84	5	....	....	....	....	....
Bank sediment												
2	....	....	....	0.82	0.26	....	2	....	....	....	....	....
3	....	....	....	.40	.055	....	13	....	....	....	....	....
4	....	....	....	.48	.075	2.13	10	....	....	....	....	....
5	....	....	....	.27	.070	....	11	....	....	....	....	....
6	....	....	....	.46	.15	1.60	6	....	....	....	....	....
Mean	....	....	....	0.49	0.12	....	8.4	....	....	....	....	....

EXPLANATION OF FIGURE 30

A. Cross section 2. Channel has been filled and flood waters cover area between truck and hill in background. Three small sandy swales convey low flows through this reach.

B. Cross section 5, view upstream. The valley floor is grass covered and is utilized for grazing. No channel is present at this cross section.

C. Near cross section 6, view upstream toward confluence of Arroyo de los Frijoles on right. Headcut on Arroyo Calabasas is less than 200 feet upstream from confluence.

D. Channel of Arroyo de los Frijoles near cross section *B*. Several channels appear to be degrading between sagebrush and juniper trees, thereby forming a braided channel.

E. Irregular channel surface suggests incipient degradation in Arroyo de los Frijoles downstream from cross section *C*.

F. Near cross section 8, view downstream. Channel is being progressively filled. Compare with photograph of section 6 (fig. 30 *C*).

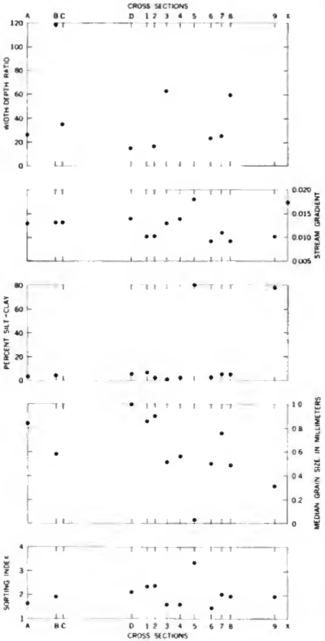

Figure 31.—Variations in channel and sediment characteristics, Arroyo Calabasas and Arroyo de los Frijoles, N. Mex. The spacing of the cross sections along the abscissa is proportional to the distances between cross sections in the field.

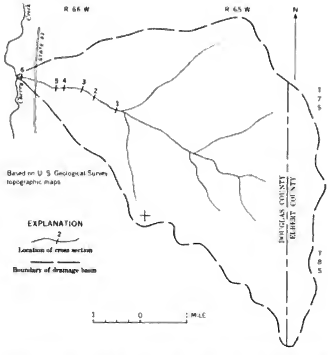
R 66 W
R 65 W
N
Cherry Creek
State 83
T 7 S
T 8 S
DOUGLAS COUNTY
ELBERT COUNTY
Based on U S Geological Survey topographic maps
EXPLANATION
Location of cross section
Boundary of drainage basin
1 0 1 MILE

Figure 32.—Index map of Bayou Gulch, Colo., drainage basin showing location of cross sections.

can be noted, but in contrast to the other areas investigated, there is no veneer of fine sediments over the coarser material and no encroachment of vegetation into the channel.

Below section 5, in order to confine the channel and thereby to prevent deposition of sand on the adjacent field and possible cutting around the bridge abutments, a dike has been built. The dike is sand piled in a ridge along the channel, and although it looks unstable it seems to be effective at least for the low floodflows.

At the bridge over Bayou Creek, the gradient steepens in response to erosion (fig. 33). In contrast, the 1939 stream profile, obtained from the topographic maps, shows no such steepening. This steepening and the narrowing of the channel at section 6 (fig. 34*C*) suggest strongly that erosion is occurring or has occurred in the past in the lower reaches of Bayou Gulch. Owing to the lack of cohesion in the sediment, no headcut is present, and as will be shown later, the only indication that erosion is occurring other than the profile change is the increase in gradient at section 6 and a decrease in the width-depth ratio. Above section 6, 2 feet of sand has been deposited on the surface adjacent to the channel, indicating recent deposition before incision.

Very little vegetation grows on what are assumed to be reaches of major deposition, sections 4 and 5. Although bank caving has contributed to channel widening, the caved material is removed by the next flood.

QUANTITATIVE CHANNEL VARIATIONS

The downstream changes are summarized in figure 35. The major change in channel width-depth ratio is at the aggrading reach where the channel becomes very wide and shallow, sections 4 and 5. Gradient varies little but it increases at section 6 where the steepening is attributed to incision of the channel. The percent

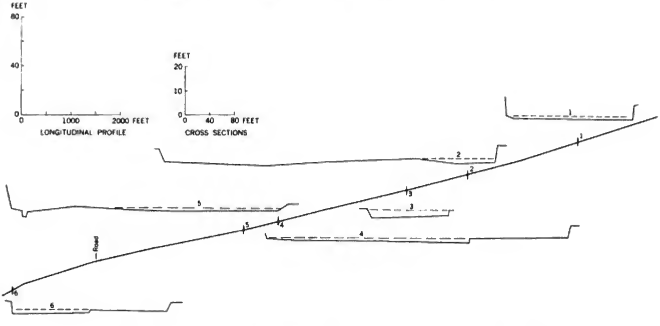

Figure 33.—Longitudinal profile and cross sections surveyed along Bayou Gulch, Colo.

of silt-clay in the samples is a maximum at section 5 where deposition is most noticeable.

Median grain size decreases downstream but increases slightly at section 6 due perhaps to channel incision. Sorting index varies slightly but increases at section 5, suggesting that sorting is poorer on reaches of deposition.

SUMMARY OF BAYOU GULCH AREA

The conclusions reached are little different from those of the Santa Fe area. The sediment is deposited on the channel floor, resulting in an increase in width-depth ratio. Vegetation apparently does not aid initial deposition.

In spite of the similarity of the Santa Fe and Bayou Gulch areas the width-depth ratio is much greater in Bayou Gulch. This is probably due to the decreased silt-clay content of bank material (see tables 4, 5).

MEDANO CREEK, COLORADO

DESCRIPTION

To complete the series of silt-clay to sand sediment types, Medano Creek was selected because both channel and bank material are composed almost entirely of sand.

Location.—Medano Creek (figs. 17 and 36) drains an area of about 29 square miles along the west flank of the Sangre de Cristo Mountains in the southeastern part of Saguache County and the northeast corner of Alamosa County. The part of the stream investigated lies within the boundary of the Great Sand Dunes National Monument in San Luis Valley. The drainage basin is shown on the Huerfano Park and Great Sand Dunes National Monument quadrangles.

Annual precipitation.—Precipitation records at the Great Sand Dunes National Monument headquarters are of short duration, but an 11-year record at Blanca, about 20 miles to the south, shows the mean annual precipitation to be 9.20 inches (table 1). However, rainfall in the mountains is much higher than in the San Luis Valley. A 30-year record at La Veta Pass about 16 miles to the east shows mean annual precipitation to be 20.98 inches. Thus the climate ranges from subhumid to arid from divide to the lower parts of the valley.

Vegetation and land use.—Vegetation ranges from typical alpine types in the high mountains to none on the sand dunes adjacent to the part of the creek studied. The basin is not used for agriculture.

Physiography and geology.—The mountains are composed of Permian sedimentary rocks and Precambrian metamorphic and igneous rocks. Sediments derived from erosion in the mountains are not found in large amounts in the channel sediment a short distance below the mountain front, for as the stream flows between the mountains and the main sand dune mass to the west (fig. 34*D*), windblown sand becomes the predominant sediment found in the channel. What might be a perennial flow from the mountains is, within a few miles, completely absorbed by the sand. In 1957 the channel

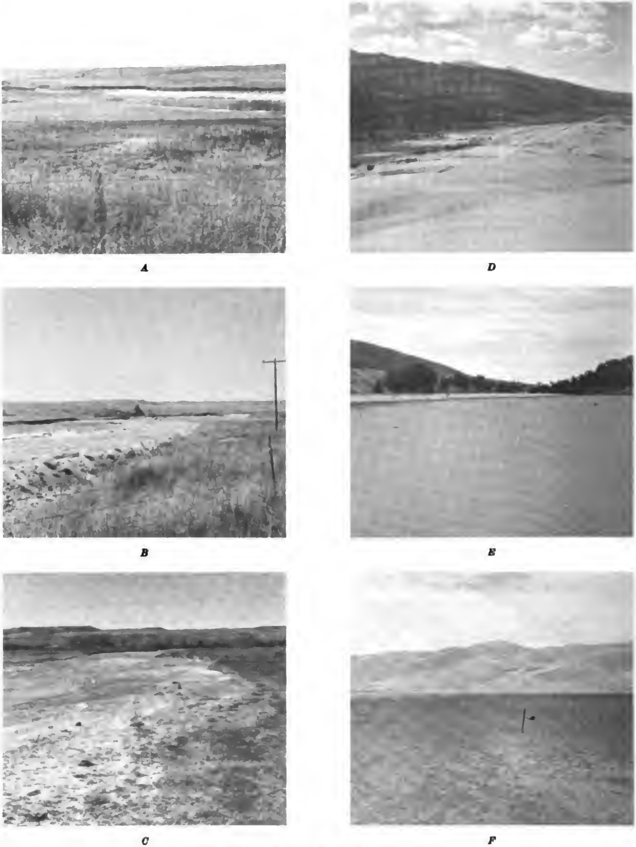

FIGURE 34.—Bayou Gulch and Medano Creek, Colo.

TABLE 6.—*Channel and sediment data*

[Class 8=stable]

Cross section	Class	Drainage area (square miles)	Distance between cross sections (miles)	Median grain size D_{50} (mm)	Hazen's effective size D_{10} (mm)	Trask sorting index	Silt-clay (percent)	Gradient	Channel width (feet)	Channel depth (feet)	Width-depth ratio (F)	Weighted mean silt-clay, M (percent)
Channel sediment												
1	8	25. 85		0. 24	0. 15	1. 23	1	0. 017	340	2	170	1
2	8	26. 10	0. 36	. 24	. 15	1. 23	1	. 019	800	3	267	1
3	8	28. 84	. 65	. 24	. 15	1. 23	. 5	. 016	820	2. 5	328	. 5
Mean				. 24	. 15	1. 23	. 8					
Bank sediment												
1				0. 24	0. 014	1. 23	0. 5					
3				. 31	. 019	1. 19	. 5					
Mean				. 28	. 017	1. 21	. 5					

contained migrating sand dunes 2 miles below the campgrounds of the national monument.

The eolian sand aparently accumulates here due to a re-entrant in the mountain front. Sand blown along the mountain front is trapped in this pocket, and over the years has accumulated into a tremendous mass of sand in places more than 500 feet high (fig. 34*F*).

Alluvium.—Both the banks and channel of Medano Creek, in the reaches studied, are composed of sand derived from the main dune mass to the west (table 6). In the channel at the 3 cross sections surveyed, median grain size is identical, 0.24 mm, as is D_{10}, 0.15 mm. Mean percent silt-clay is 0.8. Sorting index is 1.23. The bank material has even less silt-clay, 0.5 percent, but median size is 0.28 mm and D_{10} is 0.17 mm.

The almost complete absence of silt-clay indicates (Burmister, 1952) that the material in banks and channel is freely drained and has no cohesion. The banks, in fact, are at the angle of repose of dune sand, about 26°.

Although by inspection this area would seem to have the coarsest sediment, the average median size for all cross sections is finer than for any of the other areas. This is due to the excellent sorting of the windblown sand; no appreciable sediment larger than 0.5 mm or smaller than 0.15 mm was found in the samples.

QUANTITATIVE CHANNEL VARIATIONS

Neglecting changes in channel character near and in the mountains, the several miles of channel readily accessible showed only slight changes. At section 1 the channel is confined between the dunes to the west and sand piled against the mountain front (fig. 34*E*). Downstream, however, the channel widens and width-depth ratio increases (fig. 37; table 6). Gradient decreases but the character of the alluvium remains almost constant.

Water was flowing in the channel during the study, and discharge was estimated as 10 cubic feet per second. A remarkable feature is that the water was flowing on a part of the channel well above the lowest point on the cross section. The water covered only a small part of the total channel width, about 80 to 100 feet, and ranged in depth from a thin film to 0.3 foot. During a flood, however, water would cover 800 feet of channel at the campground (fig. 34*F*).

EXPLANATION OF FIGURE 34

A. Bayou Gulch, view upstream between cross sections 2 and 3. Channel is relatively wide and sandy. Bank cutting is common in this reach.

B. Bayou Gulch, view downstream toward cross section 5. Small levee on right side of channel prevents flooding of field to right of photograph.

C. Bayou Gulch, view downstream from highway bridge toward cross section 6. Tree line indicates location of Cherry Creek.

D. View from crest of sand dunes in Great Sand Dunes National Monument across Medano Creek toward the Sangre de Cristo Mountains.

E. Medano Creek, cross section 1, view upstream. Note that water is flowing on only a small part of the cross section. The cross section plotted on figure 37 shows that the water is not flowing on the lowest part of the channel floor.

F. Medano Creek, cross section 3, view to west toward main sand-dune mass. Point in channel from which photograph was taken is about 2 feet lower than part of channel on which water is flowing.

Possibly between floods the water shifts laterally across the channel, building up by deposition that part of the channel on which it flows. This would and does result in the peculiar situation of water flowing at an altitude higher than much of the channel bottom. The channel surface on which water flows is braided. Possibly, this is because there are no banks confining the small flows and also because water loss into the sand is high.

Although only a shallow layer of water was moving downstream, large amounts of sand were in movement. Sand grains and even a few half-submerged pebbles were being rolled along the channel bottom. The water was clear, owing to the low percent silt-clay, and this enabled the author to see antidunes form on the channel bottom and move upstream. The upstream movement of the antidune itself could be observed rather than just its effect on the water surface.

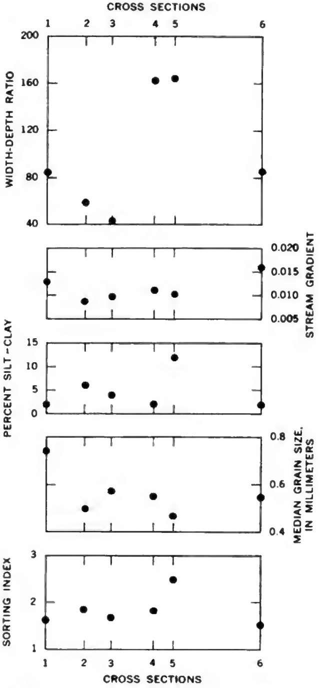

FIGURE 35.—Variations in channel and sediment characteristics, Bayou Gulch, Colo. The spacing of the cross sections along the abscissa is proportional to the distances between cross sections in field.

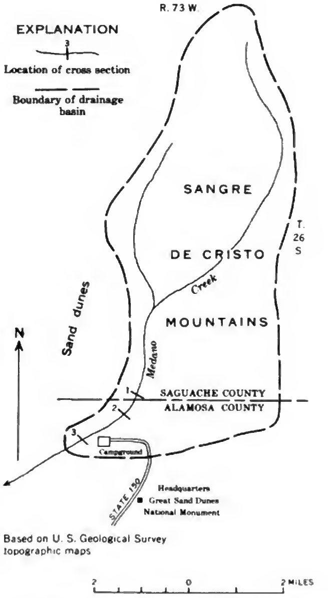

Based on U. S. Geological Survey topographic maps

FIGURE 36.—Index map of Medano Creek, Colo., showing location of cross sections.

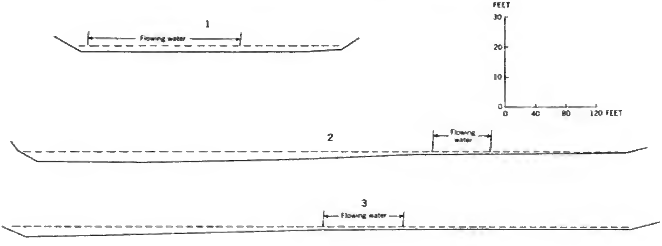

FIGURE 37.—Cross sections surveyed along Medano Creek, Colo.

Water flowing at and above the campground was completely absorbed by the sandy channel within one-half mile downstream. It was not possible to study the aggrading reach below the campground because sand dunes had migrated into that part of the channel. In addition, a veneer of windblown sand covered the channel making the distinction between aeolian and fluvial deposition difficult.

SUMMARY OF MEDANO CREEK AREA

This channel, composed of dune sand with banks of the same material, is the widest and shallowest of the channels studied. The channel and sediment character changes little downstream. Even though average median sediment size is the smallest sampled, this channel is typical of those carrying the less cohesive sediments.

COMPARISON OF SEDIMENT AND CHANNEL CHARACTERISTICS BETWEEN AREAS

In the preceding section the changes in sediment type and channel character along a stream are discussed for five areas differing in alluvial characteristics. In this part of the report, the differences and comparisons among the five areas will be reviewed, additional data will be presented, and practical applications of the conclusions will be discussed.

During this investigation, which was aimed mainly at revealing the mechanics of erosion and deposition in small ephemeral-stream channels, data were collected at some cross sections that were ultimately determined to be stable rather than aggrading or degrading. This was unavoidable, for during the early stages of the study, the stable cross sections could not be readily identified. However, the availability of the stable cross section data allows comparison of the stable channel characteristics among the five study areas. In addition, if the stable sections are discussed first, then the characteristics and variability of the unstable sections can be compared with the characteristics of stable cross sections.

RELATION BETWEEN SEDIMENT AND CHANNEL CHARACTERISTICS

The stable channel cross sections were selected from all those studied. The separation was made partly for comparative purposes, for it is assumed that those sections approaching or having reached stability will afford a better basis for comparison of channel and sediment characteristics among the five areas than a mean value for all sections studied in each area.

The mean values for channel and sediment characteristics for the stable cross sections as well as similar data for those sections which are being actively aggraded are shown in table 7. It was more difficult to determine if a particular section was being actively degraded although three cross sections are so classed (tables 2, 3). Those sections not listed in table 7 were either doubtfully stable or not being aggraded and are the unclassified channels of tables 2–5. All cross sections classed as aggrading, however, are not listed on table 7, for at many such sections the channel was completely filled.

The study areas are listed on this table in the order in which they were discussed in the preceding sections, namely, in the order of apparent coarsening of the channel alluvium and increasing width-depth ratio.

TABLE 7.—*Mean values of channel and sediment data*

Study area	Type of cross section	Cross section	Median grain size D_{50} (mm)	Hazen's effective size D_{10} (mm)	Trask sorting index	Silt-clay (percent)	Gradient	Channel width (feet)	Channel depth (feet)	Width-depth ratio (F)	Weighted mean silt-clay, M (percent)
Sage Creek	Stable	2, 3, 4	0.080	0.0035	5.74	54	0.0048	22	6.3	3.8	69
	Aggrading	6, 7, 10, 11 12.	.067	.0049	4.96	65	.002	20	4.0	5.1	70
Do	Stable	3, 4, 5, 6	.53	.032	2.45	14	.0023	53	5.3	10.3	22
	Aggrading	7, 8	.022	.0013	2.43	89	.001	42	2.7	18.8	88
Arroyo Calabasas	Stable	A, D, 1, 2, 6, 7.	.81	.21	1.99	4	.011	81	3.6	28.1	5.7
	Aggrading	B, 3, 8	.52	.19	1.79	3.2	.012	[1] 173	[1] 1.8	[1] 94.5	[1] 4.6
Bayou Gulch	Stable	1, 2, 3	.61	.19	1.72	4	.011	153	2.5	62	5.1
	Aggrading	4, 5	.51	.12	2.17	7	.010	290	1.8	166	7.1
Medano Creek	Stable	1, 2, 3	.24	.15	1.23	0.8	.017	653	2.5	255	.8
	Aggrading										

[1] Based on sections B and 8 only.

A glance at table 7, however, immediately suggests the order to be incorrect, for there is no progressive increase in median grain size (D_{50}) or D_{10} from area 1 to 5 in spite of appearances in the field. The percent silt-clay in the channel samples, however, progressively decreases from a high value for the Sage Creek area to a negligible amount for the Medano Creek area, although the values for Arroyo Calabasas and Bayou Gulch are the same.

The character of the sediment forming the perimeter of the channel can be expressed as a weighted mean percent silt-clay, designated M (Schumm, 1960b). M is calculated as follows

$$M=\frac{Sc\times W+Sb\times 2D}{W+2D}$$

in which Sc=percent silt-clay in channel alluvium,
Sb=percent silt-clay in bank alluvium,
D=channel depth,
W=channel width.

The weighted mean percent silt-clay, hereafter referred to as M in the text, is given for all cross sections at which bank and channel samples were collected (see tables 2–6), and the mean values for stable and aggrading sections are presented in table 7. M for the stable cross sections decreases in a manner similar to that for channel silt-clay.

It is interesting to note that the mean sorting index decreases progressively from area 1 to 5; the samples become better sorted as the percent silt-clay decreases. This may be explained by the fact that none of the streams contained appreciable amounts of gravel, so as the finer components of the sediment were eliminated the sorting naturally improved.

The mean width and depth of the channels bear an inverse relation to each other, but both show a progressive change as percent silt-clay decreases. The mean width-depth ratio shows a progressive increase as channel percent silt-clay and M decreases. In figure 38 the values of width-depth ratio for 18 stable cross sections are plotted against weighted mean percent silt-clay (M) of the channel and bank samples taken at each of the cross sections.

The relation is such that a narrow and deep channel is associated with sediments high in silt-clay; whereas, those channels containing little silt-clay are wide and shallow. The regression line for figure 38, although not the best fit for the data shown, is based on data for 69 cross sections including those plotted on figure 38 (Schumm, 1960b).

The gradients of the streams show a general steepening with decreasing silt-clay, but this is not progressive, for the Sand Creek area has a somewhat gentler gradient than Sage Creek. A plot of M against gradient (fig. 39) reveals that stream gradient increases as M decreases. Thus for those small ephemeral streams where the annual rainfall is in the range 10 to 20 inches both channel shape and gradient are related to M. It is probable that a different relation exists between gradient and M for larger streams and those in more humid regions. The relation between M and width-depth ratio is valid for a large range of streams in different climatic regions (Schumm, 1960b).

SUMMARY OF COMPARISONS

Differences in sediment type among the study areas are related to variations in channel characteristics. As progressively wider and shallower sections of the stable channels were considered an accompanying decrease in the percent silt-clay composing the perimeter of the channel was noted. In addition, a decrease in channel gradient occurred as M increased.

It is assumed that these relations may be only the most obvious. Further work may reveal that other aspects of fluvial hydraulics and morphology are related to a parameter, such as M, expressive of the physical properties of the alluvium forming stream channels.

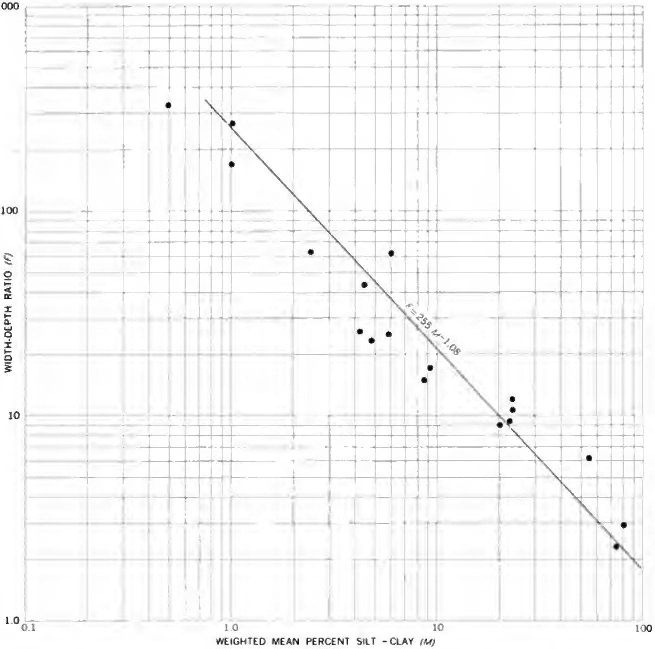

FIGURE 38.—Relation between width-depth ratio (F) and weighted mean percent silt-clay (M) in bank and channel sediments for stable cross sections.

DEPOSITION IN EPHEMERAL STREAMS

CROSS SECTIONS

During the discussion of the study areas, some comparisons between the manner of aggradation in each area were made. The changes in width-depth ratio as an aggrading reach was approached and crossed indicates that as deposition increased the channels containing highly cohesive sediments with a high percent silt-clay became progressively narrower; whereas, channels containing low-cohesion sediments became shallower with little change in width. The modification of the shape of a stream channel by aggradation seems to be determined by the mechanics of sediment deposition in the channel.

Blench (1957, p. 13) describes lateral deposition of silt along the sides of Indian regime canals and explains how this phenomenon is used in the repair of breached canals and in design. According to Blench, the typical Indian canal has a sand bed and berms of silty-clay

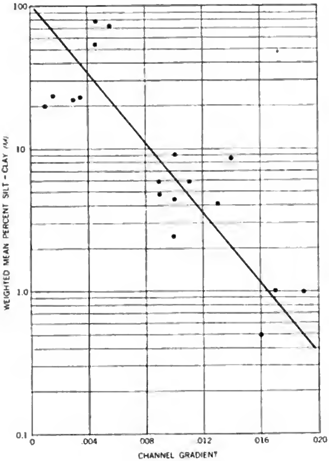

FIGURE 39.—Relation between stream gradient and weighted mean percent silt-clay (*M*) for stable cross sections.

loam. The berms are deposited from suspended load. Two study areas of this investigation, Sage Creek and even Sand Creek at section 7, show berm development. The channels with low percent silt-clay in banks and channel, Bayou Gulch, Arroyo Calabasas, and Medano Creek, show only deposition on the channel bottom.

Lateral deposition is due both to the cohesiveness of the finer sediment and to its high concentration throughout the mass of flowing water. Hjulstrom's (1935, p. 274) calculations demonstrate that a mixture of silt and clay with an average grain size of 0.001 mm will have a concentration 5 meters above the channel floor only slightly less than that measured just above the channel floor; whereas, the concentration of sediment with an average size of 0.10 mm rapidly decreases to 10 percent of that just above the channel at a height of only 25 cm. Thus, under similar conditions of turbulence the finest sediment is available for deposition along the banks; whereas, the coarse material will only be deposited on the channel floor.

It has been suggested that the correlation between width-depth ratio and *M* might be used as a criterion of aggradation or degradation (Schumm, 1960b). That is, since stable channels fall about the line described by the equation $F=255\ M^{-1.08}$, then points that plot well above this line might be assumed to be aggrading; whereas, those plotting below the line would be degrading. To test this hypothesis the data for stable degrading, and aggrading cross sections were plotted on figure 40 about this regression line.

The 11 aggrading sections plotted all fall above the regression line; however, only 7 would be recognized as aggrading from their position on the graph. The unstable condition of the remainder would be obscured by the natural scatter about the regression line. However, since the Sage Creek cross sections have a decrease in width-depth ratio with aggradation, these points would not be expected to fall above the regression line. In any event, it seems that those cross sections which plot well above the regression line may be considered aggrading.

Of 3 cross sections originally classed as degrading, there are adequate data for plotting of 2 (Sand Creek sections 10 and 11; table 3). These two sections plot below the regression line of figure 40. Perhaps on the basis of the location on figure 40 of sections known to be aggrading or degrading, it may be possible to classify the remaining cross sections, that is, those listed as unclassified on tables 2 through 6.

Twelve of the 49 cross sections studied are unclassified. Insufficient data are available to allow computation of width-depth ratio or *M* for six of these. The remaining 6 cross sections (Sand Creek 2 and 12; Sage Creek 5, 8, and 14; Bayou Gulch 6) are plotted on figure 40. Four of these are located close to the regression line (Sage Creek 2 and 8, Sand Creek 5, Bayou Gulch 6), and these sections may be stable.

If the field information on the nature of these cross sections is considered, each is located on a reach of channel either affected in the past by channel changes or to be affected by channel changes in the future. For example, the channels of Sage Creek at section 2 and Bayou Gulch at section 6 have been degraded in the past but have apparently reverted to a stable form. Sand Creek section 5, on the other hand, has not yet been affected by the aggradation occurring downstream at section 6. Sage Creek section 8, although believed to have been eroded and then subjected to recent deposition, also has a form characteristic of a stable channel. The erosion occurring a short distance downstream, however, will undoubtedly cause marked changes at this section in the near future.

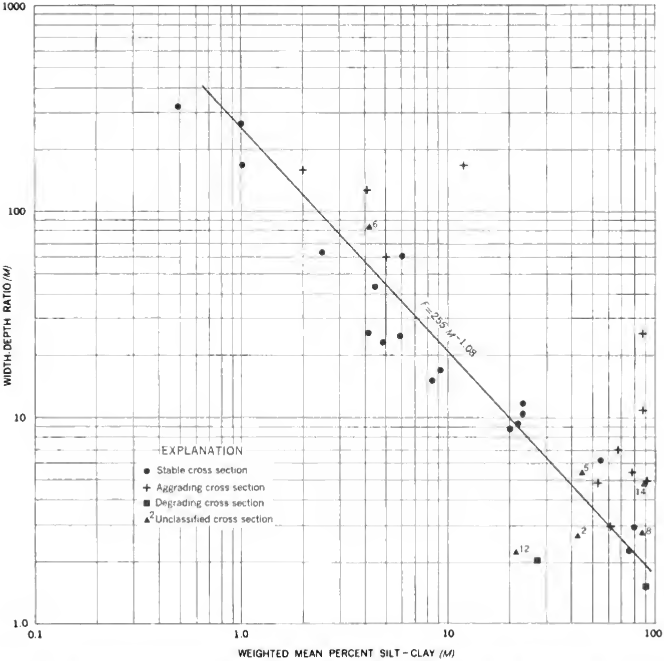

FIGURE 40.—Relation between width-depth ratio and weighted mean percent silt-clay for stable and unstable cross sections. Numbers refer to cross sections, tables 2, 3, and 5.

The remaining two sections plot far from the regression line. Sage Creek section 14 plots well above the line, and it was noted in the field that water diverted onto the flood plain by a small dam enters the channel and causes deposition at this section. Sand Creek section 12 plots well below the line indicating channel erosion. Section 12 is located only 0.3 mile below section 11 which was previously classified as degrading. Either degradation is still occurring at section 12 or the section has not been able to adjust its form as yet to stable conditions. The above suggests that the location of the unclassified sections with regard to the regression line of figure 40 makes it possible to classify the sections as to their stability or lack of it.

SLOPE

In addition to changes in channel shape accompanying aggradation, there are concomitant changes in the longitudinal profile of the stream. As is well known and was noted in each of the study areas, stream gradient is decreased on the upstream part of the aggrading reach. The slopes measured at the cross sections in the field do not show this in all cases (figs. 22, 27, 31, 35) but the longitudinal profiles do (figs. 19, 24, 29, 33).

All the graphs and longitudinal profiles show an increase in gradient downstream on the aggarding reach. In all aggrading channels this steepening enables the stream to increase its capacity for sediment load. Generally, incision occurs on the steepened reach (Schumm and Hadley, 1957). Where the channel is completely filled by deposition on the steeper reach, the anomalous situation arises that the finer alluvium is found on the steeper aggrading reaches. See section 10 on figure 27 and sections *B*, 5, and *X* on figure 31.

The data collected at cross sections located on the aggrading reaches of the study areas give a fairly complete picture of what might occur at one cross section during the complete filling of the channel. During the discussion of the historic changes on Sand Creek it was concluded that the upstream limit of aggradation shifted upchannel as aggradation progressed. Channel aggradation, therefore, may be somewhat analagous to backfilling of the channel, rather than to a general filling of the channel simultaneously over a long distance.

Assuming that aggradation begins at one particular point in the channel and then progresses upstream, it is possible to outline the steps in the complete cycle of aggradation and retrenching of that channel. Gradient is decreased by the initial channel deposit, and if it is not swept away by the next flood, this alluvial deposit induces further deposition in the channel. As the channel fills, the zone where major deposition of the coarser fraction of the alluvium occurs, migrates upchannel, and progressively finer sediment is deposited over the originally coarser grained sediment at the site of initial aggradation.

In several reaches of the Sand Creek and Arroyo Calabasas channels the sediments in the banks, where exposed by trenching, show a progressive coarsening of the alluvium from top to bottom of the deposit. Thus, at any one point in an aggrading channel, sediment size generally decreases as deposition progresses, and accompanying this is a decrease in channel size. When the channel is almost filled overbank deposition becomes very important. Continued overbank deposition of fine sediment causes a steepening of the valley floor. In a short time the channel is completely filled, and floodwaters cover almost the entire valley floor. Nevertheless, a short distance upstream the channel still exists, but it is being filled. The progressive shallowing of the channel downstream is best shown between cross sections 6 and 9 on figure 24 as is the decrease in gradient as deposition in the channel begins (fig. 24, sections 6–8). The steepening of the gradient after complete filling of the channel (fig. 24, sections 9, 10) is also clearly shown (see also Schumm and Hadley, 1957, figs. 3*B*, 6*A*). Accompanying the change in gradient, percent silt-clay increases from section 6 to a maximum for all sections at 9, and median grain size decreases from cross section 6 to 9.

In the trench above the aggrading reach on Sand Creek the sediments exposed in the bank between sections 5 and 6 from bottom to top are: 2 feet coarse gravel and cobbles; 6 feet coarse-to-fine sand and silt; 6 feet of silt and clay with some fine sand. In the trench below the aggrading reach the same type of sequence occurs. From auger holes bored in the recent sediments, the gravel layer was found at the level of the channel floor between sections 5 and 6, at a depth of 2.5 feet at section 6; at 4.0 feet at section 7; and at 9.3 feet at section 8. The gravel reappears in the channel floor just above the country road, and its inferred relation to the longitudinal profile is shown by the dashed line below the profile on figure 24. This gravel layer may be the level of the channel floor before aggradation. If this is so, the convexity on the longitudinal profile shown between sections 6 and 10 above the gravel layer (fig. 24) is probably the recent channel and valley fill. Renewed trenching has occurred on the lower end of the deposit between sections 10 and 11. This cycle of channel filling, aggradation and steepening of the valley floor, and retrenching of the alluvium has been previously discussed as the common pattern in semiarid valleys (Schumm and Hadley, 1957).

To summarize, the decrease in grain size and increase in silt-clay across an aggrading reach, as shown on figures 22, 27, 31, and 35, indicates that as one moves downstream along an aggrading ephemeral stream relatively coarse sediment will be found upstream and the finer sediments will be found on the downstream edge of the deposit. In addition, there should also be an upward decrease in grain size from bottom to top of the deposit at any one location. The change in gradient is from a decrease in the filling channel to an increase where the channel has been filled and flood-plain deposition is dominant.

In the studying of aggrading channels, it is important to recognize and to anticipate marked variations in channel character and sediment type downstream due to aggradation. In other words, the orderly relation shown in many streams will be disrupted by aggradation, and anomalies are to be expected. This is especially true of channels which do not have permanent flow between floods. The generally assumed ability of a stream to adjust to changed conditions does not apply to ephemeral streams in channels that are being rapidly aggraded. The ephemeral streams, when attempts to adjust fail, follow a pattern of alternate deposition and erosion (Schumm and Hadley, 1957).

VEGETATION

Observations have shown that the influence of vegetation differed between the silty and sandy study areas. In silty sediments, typified by the Sage Creek area, growth of vegetation was rapid on the modern sediments. The photographs of the Sage Creek channel (figs. 20 *C–F*; 21*C*, *E*, *F*) show vegetation on the banks, berm, and channel bottom. Figure 21*E* shows that vegetation quickly establishes itself after the spring floods. In a channel the vegetation grows only on areas where deposition has occurred since channel incision. Vegetation, therefore, may aid deposition once it has begun, but fresh alluvium in the channel seems necessary for growth of vegetation.

The establishment of vegetation on the noncohesive, highly mobile sediments is much more difficult. These channels were remarkably free of vegetation even when aggrading (figs. 25*B*, *C*; 30*C*, *E*, *F*), but as soon as a veneer of finer sediment was deposited on the sand, vegetation began to encroach on the channel and (figs. 25*D*, *E*; 30*A*, *B*) eventually completely covered it.

As discussed in the description of Arroyo Calabasas, vegetation does grow in the sandy channels when undisturbed—such as below dams that have not spilled recently—but flow in the streams of high bed movement will cause washing out of seeds and plants and prevent the development of permanent vegetation. Vegetation, therefore, will accelerate deposition but in the areas studied is not the cause of it.

CAUSES OF DEPOSITION

One of the primary purposes of this investigation is to determine, if possible, the reason for aggradation in the study areas. The major part of the sediment load is derived from different sources in the different areas. In the Bayou Gulch and Arroyo Calabasas drainage basins the sediment is produced by slope erosion and by channel erosion along the dendritic patterned tributaries and main channel. The sediment is not derived from any restricted zone within the basin, but each tributary conveys sediment to the main channel. In the Sage and Sand Creek basins, most of the sediment is derived from an escarpment forming the headwater divide.

In any event, each of the study areas is one of high sediment production. No matter what its source, high sediment yields are probably the cause of aggradation in these stream channels. The increase in sediment yields and retrenching of the Sage, Sand, and Arroyo Calabasas channels cannot be attributed to any special cause, such as climate change or overgrazing. In the absence of such evidence the channel cutting can be related only to the presence of reaches of steeper gradient in each valley, which have been built up by deposition to be inevitably trenched. This sequence of events has been proposed as the normal cycle of development of ephemeral streams (Schumm and Hadley, 1957).

Although causes for aggradation may not be completely understood, the reason for its occurrence in a particular segment of a stream channel should be considered. It seems that aggradation in these channels is associated with segments of the stream that receive only small contributions from tributaries. The loss of water into the channels of ephemeral streams (Babcock and Cushing, 1941) and its function in promoting aggradation (Schumm and Hadley, 1957) have been studied and found important. It is logical to assume that in those reaches of the channel where contributions of runoff from tributaries is minor, the concentration of sediment will increase and aggradation might occur. Other factors would undoubtedly complicate this relation, and it is know that the entrance of a steep-gradient tributary often results in deposition at and below its junction with the main channel.

Listed in the tables giving the basic data for each study area are the drainage area above each section and the stream channel length between each section (tables 2–5). The increase in drainage area per mile of channel length above and on the aggrading reaches are presented in table 8. A comparison of the ratios shows a marked difference. In each area, except that of the Arroyo de los Frijoles and Arroyo Calabasas, deposition is occurring in reaches where the increase of drainage area is much less per unit length of channel than on the stable reaches. As previously noted, most of the Arroyo Calabasas drainage basin to the west of the channel, below the junction with Arroyo de los Frijoles, is composed of volcanic rocks from which little runoff and sediment reaches the stream. If most of this area is omitted from the calculation, then the ratio on the aggrading reach drops to about one-half of its value upstream, and the ratios are comparable to those for the other study areas. This relation suggests that aggradation occurs in these small ephemeral streams on reaches of small tributary contribution, a result, perhaps, of increased sediment concentration due to water loss into the alluvium of the valley floor.

An additional important point must be the difference in general appearance between the same valley where

TABLE 8.—*Ratio of drainage area to channel length*

Study area	Non-aggrading reach	Aggrading reach	Drainage area (square miles)	Channel length (miles)	Area-length ratio
Sage Creek	1-6		12.7	5.7	2.2
		6-7	.26	1.1	.2
Sand Creek	2-6		6.4	3.6	1.8
		6-10	1.7	1.6	1.1
Arroyo de los Frijoles and Arroyo Calabasas.	C-6		19.4	3.2	6.0
		6-9	18.1	2.7	6.7
		[1] 6-9	[1] 7.2	2.7	2.7
Bayou Gulch	1-4		9.0	1.1	8.1
		4-5	.5	.2	2.5

[1] Adjusted for noncontributing area

the channel is completely filled and grassed and where trenched. In the flat-floored valley the alluvium may contain much water, thereby supporting heavy vegetation. In addition a veneer of fine sediment generally overlies the coarser sediment. In areas of predominant sand and gravel, therefore, the valley floor will be an area of much finer sediment. Upon renewed trenching, however, the coarser sediment will be exposed and a wide shallow channel will form, which will appear inconsistent with the fine surface sediment. Thus, the sampled surface of an untrenched valley floor may give an erroneous picture of the composition of the major part of the valley alluvium and its behavior during erosion.

EROSION IN EPHEMERAL STREAMS

The phase of the semiarid cycle of valley erosion that has received the most attention is channel incision or arroyo cutting. In this section, the differences between erosion and channel development in the different study areas will be discussed.

CHANNEL INCISION

Comparisons of channel erosion in the study areas and elsewhere show that after initial cutting of a grassed valley floor, the channel extends headward by headcut migration. The perpetuation of a headcut seems to require some resistant material capping the alluvium. This resistant cap may be formed by the binding action of plant roots, or a veneer of silt and clay overlying the coarser materials. If this resistant zone were lacking, the headcut would be rounded and lowered as it retreated upchannel, and it would lose its identity in a short distance. Where trenching was renewed and a headcut was not formed, Arroyo Calabasas, Bayou Gulch, and Sage Creek below the aggrading reach, a well-defined channel was already present, typified by a generally uniform resistance in vertical section. In the broad sandy channels without fine sediments and vegetation no headcut will form.

An interesting example of the removal of a nick or break in the profile of a sandy channel was found in Newlin Creek, a tributary to Cherry Creek located to the west Bayou Gulch in Douglas County, Colo. The profile of Newlin Creek, when plotted from a topographic map (Parker, Colo.) prepared in 1939, showed a prominent nick in the channel (fig. 41). The part of the Newlin Creek profile showing the nick, between the two secondary roads, in sections 17 and 20, was resurveyed in 1957. The altitude of the channel at the

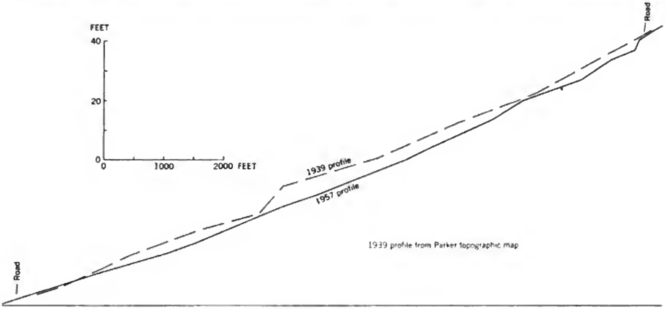

FIGURE 41.—Comparison of the longitudinal profile of Newlin Creek, Colo., in 1939 and 1957.

lower road had not changed measurably during the 18-year period, but the profile between the roads had been smoothed by removal of the nick. The small break in the 1957 longitudinal profile at its upper end is due to the road crossing at that point, which may have retarded further degradation, for the road acts as a small dam.

The changes occurring on Newlin Creek agree with those observed by Brush (1957) during flume experiments and suggest that in poorly cohesive material, not capped by a more resistant layer, the headward migration of the nick will be accompanied by a decrease in its height.

The change in channel characteristics along Newlin Creek from above the upper road to below the original position of the nick in 1939 illustrates the changes occurring during degradation of a sandy channel. Above the upper road, the channel is 130 feet wide, and sand is being deposited over another 100 feet of the valley floor. Width-depth ratio approaches 90. Below the road degradation begins; the channel narrows to 40 or 50 feet, and width-depth ratio decreases to 17. The degradation causes erosion along many interconnected water courses, forming vegetation-covered islands separated by degrading sandy channels. One channel probably will become dominant after continued erosion.

Downstream, evidence of greater erosion appears; roots of trees are exposed and cobbles and boulders appear in the channel bottom. At the site of the former nick; the gully is 10 feet deep and is 20 to 40 feet wide; width-depth ratio is about 3. Below the lower road the channel seems aggraded, shallowing and widening to its junction with Cherry Creek. Sediment samples taken in the eroding channel show only minor variation in grain size ($D_{50}=0.60$) and percent silt-clay (2.0).

BANK CAVING

Another important phenomenon that occurs during the development of a stable channel is bank caving. The relative amount of bank caving along the streams studied and its effect is markedly different in areas of cohesive and noncohesive sediment.

In poorly cohesive alluvium, or that with a small percent silt-clay, the channel widens rapidly by bank caving after initial dissection; whereas, in cohesive sediment, predominantly silt-clay, the blocks of sediment that fall into the channel are resistant and do not move or disintegrate readily, although this will depend on velocity of water movement. They may even form the nucleus for deposition along the banks and prevent further channel widening (fig. 20C). Vegetation, growing on banks before the caving, often continues to grow on the fallen block if rotation of the block was not great. The vegetation in turn promotes further aggradation in the channel.

Blocks of poorly cohesive alluvium, on the other hand, disintegrate upon impact or later under the eroding action of flood waters, and the sediment adds to the bed and suspended load of the stream. Slumping or caving of bank material into the stream channel and the function of slump blocks in sediment supply and aggradation, therefore, differ with type of bank material.

PRACTICAL CONSIDERATIONS

Because of a critical need for effective control of erosion and deposition in ephemeral streams, an attempt will be made to suggest how some of the information and conclusions stated previously might have a practical application. The differences in erosion and deposition in the study areas suggest that different types of conservation techniques may be necessary for different types of alluvium filling the valley.

Generally, in valleys where the streams are ephemeral conservation measures are not begun until improvement will require large expenditures of time and money. For example, once a gully has formed the only solution is to build either a dam or diversion structure above the headcut, to prevent its headward migration, or to plug the gully and fill it by inducing deposition in the trench (Peterson, 1950). However, if it were possible to determine at what point in the valley trenching would begin, then it might be more economical and certainly more practical to prevent the initial erosion.

Some studies in semiarid valleys suggest that a discontinuous gully will form on the steeper parts of an alluvial valley (Schumm and Hadley, 1957). If good topographic maps are available for the areas concerned, it would be possible to plot the longitudinal profile of the stream and discover the steeper reaches where trenching might begin. If maps are not available, the valley profile could be surveyed, or perhaps, the critical gradient changes could be revealed by photogrammetric methods. Once the steeper reaches have been discovered, the valley floor could be protected by restricting grazing. However, since in many areas the valley floor affords the best grazing and because the critical reach would need to be fenced, this solution may not be acceptable to the local rancher. Another possibility would be the construction of small earth diversion dikes to slow and spread the flow of water across the steeper reach. This, however, might cause deposition and further steepening on this already critical reach. This discussion of preventive conservation measures on the steeper parts of the alluvial fill emphasizes that only certain parts of a valley need be protected to conserve the entire valley.

In three of the study areas selected for this investigation, problems of erosion and deposition are acute. Conservation measures should be directed at not maintaining but restoring the valley floor to its ungullied state. This may be possible only by inducing deposition in the gully proper, thereby filling and healing the trench. Such a project can succeed best where the method used is designed to take advantage of a natural tendency to deposition. In each valley studied deposition was shown to occur naturally where tributary contribution is small, where gain of drainage area per mile of channel is less than normal (table 8). Therefore, if these limited observations are confirmed elsewhere, a structure placed in a valley to promote deposition should be located where the ratio of increase of drainage area to channel length is small.

Deposition also may be induced by using reverse delta deposition near the confluence of the channel with a trunk stream. If a dam is built on the tributary a short distance above its mouth, the retention of water will allow flood waters to enter the channel from the main stream, causing deposition below the dam and plugging of the valley. Deposition in the reservoir above the dam will also be important. The lower end of Sage Creek has been filled in this manner. Once deposition has started, care should be exercised that renewed trenching on the toe of the alluvial deposit does not occur.

If incipient aggradation could be recognized in a channel, it might be accelerated by conservation measures. As indicated by a reexamination of changes in sediment and channel character across the aggrading reaches (figs. 22, 27, 31, 35) deposition may be detected, where it is not obvious, by a decrease in gradient and an increase in percent silt-clay in the channel sediment. Perhaps width-depth ratio can be used, for width-depth ratio is increased by aggradation except for those areas of high silt-clay where initial deposition is along the channel banks for example, Sage Creek. Perhaps in similar channels if the width-depth ratio in any reach is much higher than that upstream or downstream, deposition may be expected (fig. 40).

Vegetation aids deposition only after deposition has begun. Vegetation is readily established on the fine alluvium but not in predominantly sandy material. It appears therefore if vegetation does not occur naturally in a channel, it probably cannot be induced to grow there without great expense. Planting grass and trees in a semiarid valley would be practical only as a means of stabilizing an alluvial deposit. But care should be exercised that the conservation measure may not have an eventual adverse effect on valley stability. More work is required on this and other problems related to deposition, but it becomes increasingly apparent that a careful study of each valley should be made before conservation measures of any type are initiated.

REFERENCES

Babcock, H. M. and Cushing, E. M., 1941, Recharge to ground water from floods in a typical desert wash, Pinal County, Arizona: Am. Geophys. Union Trans., v. 22, pt. 1, p. 49–56.

Blench, T., 1957, Regime behavior of canals and rivers: London, Butterworth's Publications, 138 p.

Brush, L. M., Jr., 1957, Laboratory study of knickpoint behavior in noncohesive materials [abs.]: Geol. Soc. American Bull, v. 68, p. 1704.

Burmister, D. M., 1952, Soil mechanics: New York, Columbia Univ. Press, 155 p.

Dunn, I. S., 1959, Tractive resistance of cohesive channels: Jour. Soil Mechanics and Foundations Div., Am. Soc. Civil Engineers Proc., SM 3, p. 1–24.

Hjulstrom, Filip, 1935, Studies of the morphological activity of rivers as illustrated by the River Fyris: Univ. Upsala Geol. Inst. Bull., v. 25, p. 221–527.

Leighly, J. B., 1934, Turbulence and the transportation of rock debris by streams: Geog. Rev., v. 24, p. 543–464.

Leopold, L. B. and Maddock, Thomas, Jr., 1953, The hydraulic geometry of stream channels and some physiographic implications: U.S. Geol. Survey Prof. Paper 252, 57 p.

Leopold, L. B. and Miller, J. P., 1956, Ephemeral streams—hydraulic factors and their relation to the drainage net: U.S. Geol. Survey Prof. Paper 282–A, p. 1–37.

Peterson, H. V., 1950, The problem of gullying in western valleys; *in* Trask, P. D., Applied sedimentation: New York, John Wiley & Sons, 707 p.

Schumm, S. A., 1956, The role of creep and rainwash on the retreat of badland slopes: Am. Jour. Sci., v. 254, p. 693–706.

——— 1960a, The effect of sediment type on the shape and stratification of some modern fluvial deposits: Am. Jour. Sci., v. 258, p. 177–184.

———1960b, The shape of alluvial channels in relation to sediment type: U.S. Geol. Survey Prof. Paper 352–B, p. 17–31.

Schumm, S. A. and Hadley, R. F., 1957, Arroyos and the semiarid cycle of erosion: Am. Jour. Sci., v. 255, p. 161–174.

Thornthwaite, C. W., 1941, Atlas of climatic types in the United States, 1900–1939: U.S. Dept. Agr. Misc. Pub. 421, 7 p.

Ward, Freeman, 1922, Geology of a portion of the badlands: South Dakota Geol. Survey Bull. 11, p. 1–59.

Wolman, M. G., 1955, The natural channel of Brandywine Creek, Pennsylvania: U.S. Geol. Survey Prof. Paper 271, 56 p.

Wolman, M. G. and Leopold, L. B., 1957, River flood plains—Some observations on their formation: U.S. Geol. Survey Prof. Paper 282–C, p. 87–109.

U.S. GOVERNMENT PRINTING OFFICE: 1961 O - 564835

Channel Widening and Flood-Plain Construction Along Cimarron River in Southwestern Kansas

By S. A. SCHUMM *and* R. W. LICHTY

EROSION AND SEDIMENTATION IN A SEMIARID ENVIRONMENT

GEOLOGICAL SURVEY PROFESSIONAL PAPER 352-D

Major channel changes along the Cimarron River are related to the frequency and magnitude of floods and the departure of annual precipitation from normal

---

UNITED STATES GOVERNMENT PRINTING OFFICE, WASHINGTON : 1963

UNITED STATES DEPARTMENT OF THE INTERIOR

STEWART L. UDALL, *Secretary*

GEOLOGICAL SURVEY

Thomas B. Nolan, *Director*

For sale by the Superintendent of Documents, U.S. Government Printing Office
Washington, D.C. 20402

CONTENTS

Page

- Abstract 71
- Introduction 71
- Cimarron River, southwestern Kansas, 1874–1960 71
  - Cimarron River, 1874–1913 71
  - Cimarron River, 1914–42 74
  - Cimarron River, 1943–54 76
  - Cimarron River, 1955–60 76
  - Summary 76
- Factors influencing Cimarron River channel changes 76
  - Land use 76
  - Floods 77
  - Precipitation 78
  - Vegetation 79
  - Summary 79
- Mechanics of channel widening and flood-plain construction 79
  - Channel widening 80
  - Effect of channel widening on gradient 81
  - Flood-plain construction 81
    - Island formation 81
    - Direct flood-plain construction 84
  - Flood-plain stratigraphy 84
  - Summary 85
- Comparison of Cimarron River channel changes with those of other rivers 86
  - Summary 87
- Conclusions 87
- References 88

ILLUSTRATIONS

Page

FIGURE 42. Index map of Cimarron River area 72

43–44. Photographs showing:

- 43. Channels of Cimarron River in southwestern Kansas 75
- 44. Channel changes of Cimarron River in southwestern Kansas and pre-1914 alluvium 77

45–46. Graphs showing:

- 45. Acres of plowed land and number of head of livestock 78
- 46. Average annual precipitation in southwestern Kansas 80

47. Transverse profiles of Cimarron River valley 82

48. Photographs of Cimarron River flood plain in southwestern Kansas 83

49–50. Sketches showing:

- 49. Parts of Cimarron valley covered by low, moderate, and high flows 84
- 50. Channel areas favorable for flood-plain formation 84

51. Section showing flood-plain stratification 85

52. Index map of Red River area near Burkburnett, Tex 87

TABLES

Page

TABLE 1. Channel width of the Cimarron River, Kans 73

2. Peak discharge of the Cimarron River, southwestern Kansas 79

3. Changes in channel depth between date of bridge construction and 1960 81

CHANNEL WIDENING AND FLOOD-PLAIN CONSTRUCTION ALONG CIMARRON RIVER IN SOUTHWESTERN KANSAS

By S. A. Schumm and R. W. Lichty

ABSTRACT

The channel of the Cimarron River in southwestern Kansas has changed significantly during historic times. The average width of the river was 50 feet in 1874. During and after the major floor of 1914, the river widened until an average width of 1,200 feet was reached in 1942. During the period 1943–54 flood-plain construction occurred, and the river narrowed to an average width of 550 feet in 1954. During the period 1954–60 both channel widening and narrowing occurred.

The period of channel widening was initiated by the maximum flood of record, which was followed by a long period of deficient precipitation, and was terminated by the major flood of 1942. The period of flood-plain construction was characterized by above-average annual precipitation and floods of low to moderate peak discharge. The influence of the changed climatic conditions on vegetational growth is the key to Cimarron River behavior. During the years of above-average annual precipitation, which are associated with floods of low to moderate peak discharge, vegetation became established in the wide sandy channel. The presence of vegetation in the channel in turn aided deposition and flood plain formation.

The new flood plain was constructed in a period of 12 years, predominantly by vertical accretion. It is composed of a mosaic of islands, abandoned channels, and areas of flood plain constructed adjacent to the low-water channel. Although initially a flood plain may be formed by overbank flooding and vertical accretion, lateral migration of the stream may rework the alluvium and destroy all evidence of vertical accretion.

The channel changes which have occurred along Cimarron River seem typical of sandy rivers in semiarid regions. Channel widening instead of degradation and channel narrowing instead of aggradation are characteristic.

INTRODUCTION

Flood plains are of historic interest to man. They offered fertile land, abundant water, and game to the primitive hunter and agriculturalist and became sites of early civilizations. The flood-plain dweller of today faces many of the same problems as did his ancestors. For this reason a better understanding of river and flood-plain changes may be helpful in preventing a repetition of past disasters.

Geomorphic processes proceed at rates that generally are difficult to assess, and the opportunity seldom arises to obtain data on the rates. Nevertheless, a record of modern flood-plain destruction and rebuilding is available for the Cimarron River in southwestern Kansas. This record of stream-channel and flood-plain changes, the reasons for the changes, and a description of the mechanics of the changes are presented in this report as a contribution toward a better understanding of fluvial erosion and deposition in a semiarid region.

The Cimarron River enters western Kansas about 5 miles north of the Oklahoma boundary (fig. 42) and flows northeastward through Morton, Stevens, and Grant Counties and then southeastward through Haskell, Seward, and Meade Counties before reentering Oklahoma. The Cimarron Valley in southwestern Kansas is underlain almost completely by rocks of Tertiary and Quaternary age, although small outcrops of Triassic and Cretaceous rocks occur in Morton County. The geology and ground-water resources of this area have been discussed by McLaughlin (1942, 1946), Bryne and McLaughlin (1948), and Frye (1942).

The initial widening of the Cimarron River, after the major flood of 1914, was discussed by McLaughlin (1947); his paper directed the writers' attention to the interesting series of events that have occurred along this river during the last half century.

The writers wish to acknowledge particularly the suggestions and encouragement of T. G. McLaughlin, as well as the use of his photographs (figs. 43*B*, 44*A*). Messrs. Robert Evans and Rice Davies of Liberal, Kans., very kindly gave us the benefit of their knowledge of river changes since the 1914 flood. Richard Aro instructed the writers in the techniques of tree-ring counts and made valuable suggestions with respect to the interpretation of these data.

CIMARRON RIVER, SOUTHWESTERN KANSAS, 1874–1960

CIMARRON RIVER, 1874–1913

The Cimarron River in Kansas appeared to be typical of streams in a more humid environment at the turn

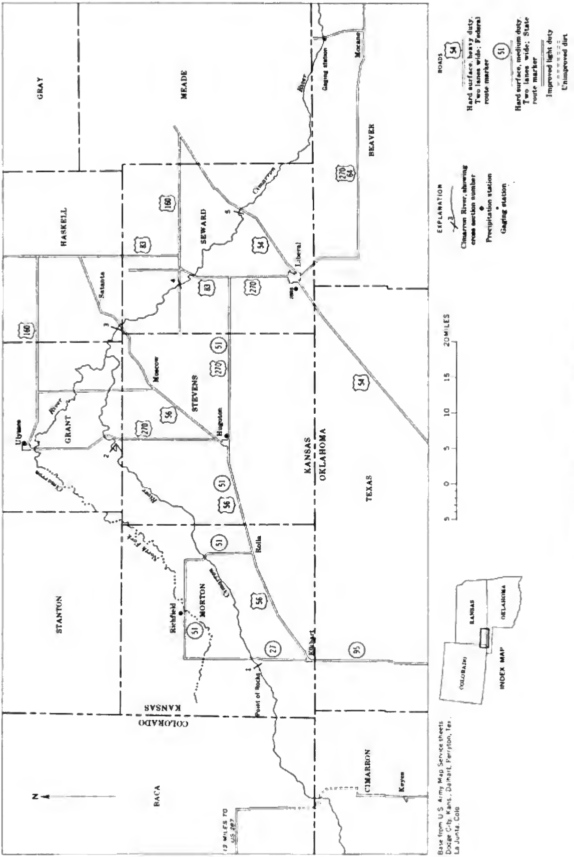

Base from U.S. Army Map Service sheets Dodge City, Kans., Dalhart, Perryton, Tex., La Junta, Colo

FIGURE 42.—Index map of Cimarron River area

of the century. Haworth (1897, p. 22) stated that "The Cimarron seems to have reached base-level and to have begun meandering across its flood plain. Beautiful ox-bow curves are frequent, and a sluggish nature is everywhere manifest during times of low water." (See fig. 43*A*.)

According to Johnson (1902, p. 664),

> Wherever within the High Plains belt the Cimarron Valley shows a living stream, it is always a meandering looping stream of uniform width, narrow, clear and deep * * *. The bottom land upon which it wanders supports a coarser and longer-stemmed grass than the uplands, the grass roots reaching to the ground water, which lies at a depth here, as a rule, of only 2 or 3 feet * * *.

The Cimarron River elsewhere, upstream to the southwest in the Oklahoma Panhandle and downstream to the southeast in Oklahoma, during historic times has always been typically a wide, shallow, sandy river. As suggested by Johnson, the great difference between the Cimarron River in Kansas and the river elsewhere may be that, in Kansas, a perennial flow was maintained by ground water. Additional testimony, confirming that the Cimarron River was a narrow, meandering perennial stream at the turn of the century, was presented by McLaughlin (1947).

Information on the width of the Cimarron River is available as a result of the survey of 1874. The data were compiled by McLaughlin (1947), and data for 120 cross sections are presented in table 1. Thirty-five of the 155 sections originally listed by McLaughlin were not remeasured; therefore, the mean values for channel widths by counties as presented in table 1 will differ slightly from those presented by McLaughlin (1947).

TABLE 1.—*Channel width, in feet, of the Cimarron River, Kans.*

[Channel width: 1874 and 1939, data from McLaughlin (1947); 1954, data from aerial photographs, scale 1:27,250; 1960, data from photomosaic sheets, scale 1:63,360; *n* equals number of sections measured]

Section	Location	Channel width			
		1874	1939	1954	1960
	Morton County				
	T. 34 S., R. 43 W.				
1	West line sec. 19	53	2,900	1,050	1,250
2	West line sec. 20	53	3,000	1,050	1,350
3	West line sec. 21	46	3,200	1,500	1,600
4	West line sec. 22	40	2,800	700	900
5	North line sec. 22	33	2,100	1,500	1,650
6	West line sec. 14	79	1,800	1,000	1,400
7	East line sec. 14	66	2,300	1,200	1,400
	T. 34 S., R. 42 W.				
8	West line sec. 7	139	1,300	800	900
9	East line sec. 7	66	2,150	1,000	1,100
10	East line sec. 5	59	1,400	650	650
11	East line sec. 4	46	2,600	400	400
12	North line sec. 3	73	1,800	1,100	1,200
	Morton County—Continued				
	T. 33 S., R. 42 W.				
13	West line sec. 35	46	3,200	950	800
14	North line sec. 35	46	800	850	850
15	East line sec. 26	46	800	650	650
	T. 33 S., R. 41 W.				
16	West line sec. 29	66	2,200	350	350
17	West line sec. 28	66	2,600	500	1,100
18	East line sec. 28	46	1,100	1,000	1,200
19	South line sec. 22	66	1,500	500	500
20	West line sec. 23	66	2,000	850	1,050
21	West line sec. 24	66	2,400	1,000	1,100
22	NE corner sec. 24	46	2,500	1,650	1,650
	T. 33 S., R. 40 W.				
23	East line sec. 18	33	300	250	250
24	South line sec. 8	33	2,100	1,000	1,000
25	West line sec. 9	66	2,900	800	900
26	SW corner sec. 3	56	2,400	450	430
27	NE corner sec. 3	43	2,600	1,000	800
	T. 32 S., R. 40 W.				
28	NE corner sec. 35	33	1,100	150	150
	T. 32 S., R. 39 W.				
29	West line sec. 30	46	2,600	550	800
30	East line sec. 30	53	1,300	400	650
31	East line sec. 29	53	1,400	250	300
	Average for Morton County (*n*=31)	56	2,050	600	900
	Stevens County				
	T. 32 S., R. 39 W.				
32	West line sec. 27	53	2,200	700	1,300
33	West line sec. 26	46	2,500	400	600
34	North line sec. 26	46	2,100	1,500	800
35	NE corner sec. 23	36	2,200	650	900
36	North line sec. 13	33	1,800	700	1,000
37	North line sec. 12	40	700	500	500
	T. 31 S., R. 38 W.				
38	SW corner sec. 29	46	1,300	850	600
39	SW corner sec. 21	40	1,700	300	400
40	North line sec. 21	46	1,000	500	800
41	West line sec. 15	40	1,100	550	800
42	NE corner sec. 15	46	800	300	800
	Average for Stevens County (*n*=11)	43	1,500	630	770
	Grant County				
	T. 30 S., R. 37 W.				
43	West line sec. 32	26	600	250	250
44	West line sec. 33	40	500	150	150
45	West line sec. 34	40	600	250	250
46	South line sec. 26	40	500	150	150
47	West line sec. 27	50	800	150	150
48	North line sec. 34	66	800	150	150
49	West line sec. 35	132	300	100	100
50	South line sec. 26	99	400	100	100
51	South line sec. 23	66	500	100	100
52	West line sec. 24	66	300	200	200
53	North line sec. 25	66	700	150	150
	T. 30 S., R. 36 W.				
54	West line sec. 21	66	200	200	200
55	West line sec. 22	66	300	400	400
56	West line sec. 23	66	500	150	150
	T. 30 S., R. 35 W.				
57	West line sec. 34	26	1,300	150	150
58	South line sec. 27	26	1,300	650	650
59	SW corner sec. 23	17	1,100	100	100
60	North line sec. 26	33	700	100	100
61	West line sec. 25	43	500	100	100
	Average for Grant County (*n*=19)	54	630	190	190

TABLE 1.—*Channel width, in feet, of the Cimarron River, Kans.*—Continued

Section	Location	Channel width			
		1874	1939	1954	1960
	Haskell County				
	T. 30 S., R. 34 W.				
62	North line sec. 30	33	800	100	100
63	East line sec. 30	33	500	200	200
64	South line sec. 29	33	500	200	200
65	East line sec. 32	26	300	450	600
66	South line sec. 33	33	300	300	200
	Average for Haskell County (n=5)	32	480	250	250
	Seward County				
	T. 31 S., R. 34 W.				
67	North line sec. 8	66	300	200	1,200
68	North line sec. 21	33	600	1,000	1,400
69	North line sec. 28	20	1,400	600	800
70	West line sec. 27	66	1,000	400	400
71	North line sec. 34	132	1,000	700	700
72	West line sec. 35	43	1,500	500	500
73	West line sec. 36	33	1,600	1,000	1,000
74	South line sec. 36	13	1,000	400	400
	T. 32 S., R. 33 W.				
75	West line sec. 6	16	1,100	250	550
76	North line sec. 7	15	1,200	600	900
77	North line sec. 18	16	300	150	150
78	West line sec. 17	16	1,000	700	700
79	North line sec. 20	18	1,000	400	400
80	West line sec. 21	18	600	300	300
81	North line sec. 28	16	1,100	150	150
82	West line sec. 27	16	900	400	400
83	North line sec. 34	13	500	400	500
84	West line sec. 35	10	1,000	500	500
85	West line sec. 36	13	1,300	500	500
86	South line sec. 36	20	500	100	100
	T. 33 S., R. 32 W.				
87	West line sec. 6	40	500	200	200
88	North line sec. 7	13	700	550	300
89	North line sec. 18	33	1,600	1,200	1,200
90	South line sec. 18	13	440	300	300
91	East line sec. 20	20	1,410	300	400
92	South line sec. 21	26	370	300	300
93	West line sec. 27	26	790	500	400
94	West line sec. 26	20	1,100	700	600
95	West line sec. 25	33	350	100	100
96	North line sec. 36	33	1,320	150	150
97	East line sec. 36	33	1,180	600	600
	T. 33 S., R. 31 W.				
98	South line sec. 31	33	880	300	900
	T. 34 S., R. 31 W.				
99	West line sec. 5	20	1,320	400	600
100	West line sec. 9	20	270	200	800
101	North line sec. 16	20	1,140	250	400
102	West line sec. 15	26	260	250	250
103	North line sec. 22	26	1,230	300	650
104	SE corner sec. 15	33	970	300	400
105	SE corner sec. 23	30	620	200	300
106	East line sec. 25	33	570	500	500
	Average for Seward County (n=40)	28	900	440	530
	Meade County				
	T. 34 S., R. 30 W.				
107	South line sec. 30	33	1,050	300	500
108	South line sec. 31	70	570	400	200
	T. 35 S., R. 30 W.				
109	East line sec. 6	40	1,320	300	300
110	South line sec. 5	43	1,410	300	300
111	South line sec. 9	53	530	350	350
112	East line sec. 16	33	1,250	300	300
113	East line sec. 15	33	800	700	700
114	East line sec. 14	66	1,000	1,400	1,400
115	East line sec. 13	132	1,000	2,000	2,000
	Meade County—Continued				
	T. 35 S., R. 29 W.				
116	East line sec. 18	100	1,100	1,300	1,300
117	East line sec. 9	98	1,600	1,200	900
118	East line sec. 10	145	1,000	950	600
119	East line sec. 11	304	1,300	750	750
120	East line sec. 13	132	800	1,650	1,650
	Average for Meade County (n=14)	92	1,050	850	800
	Average width for 120 sections	50	1,200	550	600

In 1874 the river averaged 50 feet in width through the 6 counties of southwestern Kansas; however the channel ranged in width from 10 to 304 feet (table 1). Some of the variation in width is due to the fact that measurement of channel width was made along section lines which were not normal to the channel. Nevertheless, the channel of the river in Kansas between 1874 and 1914 was narrow and probably relatively stable. The flood plain was grassed and afforded excellent grazing. Wild hay and alfalfa were cut and stacked on the flood plain during these early days (fig. 43*A*). The contrast between the river at that time and during the following 46 years is remarkable.

CIMARRON RIVER, 1914–42

Beginning in 1914 and continuing intermittently until 1942, the channel of the Cimarron River widened, until almost all the flood plain was destroyed. The channel widening began, according to the testimony of residents of the Cimarron valley, during the major flood of May 1914. This flood is the greatest of record, having an estimated gage height of 13 feet near Mocane, Okla. (fig. 42); peak discharge is estimated to have been 120,000 cfs (cubic feet per second). (See table 2.)

During the 1874 survey, the channel north of Elkhart was 66 feet wide (fig. 42). Only minor changes in width occurred between 1874 and 1914; however, in 1916 a bridge 644 feet long was required to span the channel, and in 1939 the channel at the bridge was about 1,400 feet wide (McLaughlin, 1947, p. 82). The data presented on table 1 show that the average channel widening during the period 1914–39 was 1,150 feet.

Although no aerial photographs are available to document channel changes between 1939 and 1954, other data indicate that the channel continued to widen through 1942. For example, a major flood near Liberal, Kans., occurred in 1942 with a peak discharge of 69,000 cfs. This flood originated in the headwaters

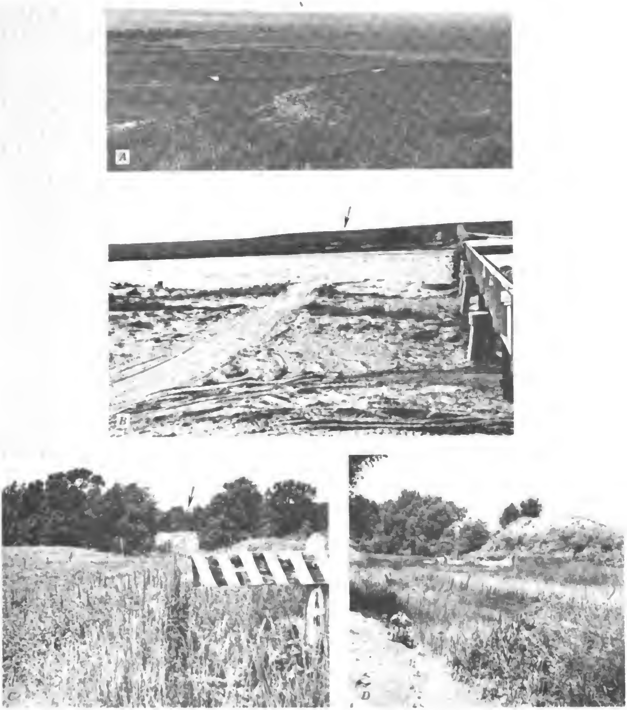

FIGURE 43.—Cimarron River in southwestern Kansas. *A*, Valley of Cimarron River in southeastern Meade County, Kans., prior to the flood of 1914. Photograph taken by W. D. Johnson in the 1890's. *B*, Cimarron River at old Highway 270 bridge north of Hugoton, Kans. (cross section 2, fig. 42), in 1943. Channel was about 700 feet wide. Arrow indicates position of windmill. Photograph taken by T. G. McLaughlin. *C*, Valley of Cimarron River at old Highway 270 bridge in 1960. Arrow indicates position of windmill shown in *B*. Trees in foreground are growing in abandoned channel shown at right end of profile *B–B′* (fig. 47). Present channel is beyond trees in background. *D*, Channel of Cimarron River at old Highway 270 bridge in 1960. Channel is 110 feet wide. Compare channel shown in this view with channel in 1943 shown in *B*.

area (peak discharge 80,000 cfs near Boise City, Okla.) and destroyed many bridges as it moved through the Cimarron River valley in Kansas. At the close of 1942 the river was at its maximum width, for the flood plain was completely destroyed at some locations. Good evidence for complete destruction of the flood plain north of Hugoton, Kans. (fig. 42), is provided by a photograph taken of the channel in 1943 (fig. 43*B*). At that time the entire valley floor was river channel. The present channel is only 110 feet wide and is located at the north edge of what was the 1942 channel (fig. 43*C*). The trees in the foreground of figure 43*C* began their growth at the south edge of the channel in 1943, as indicated by tree-ring counts. The survival of these trees is proof that the channel was never again as wide as it was after the 1942 flood.

CIMARRON RIVER, 1943–54

After the flood of 1942, a reversal of river activity occurred. Cross sections, when remeasured on aerial photographs taken in 1954, showed that the channel had become narrower (table 1). The narrowing was accomplished by flood-plain construction and, to a minor extent, by island formation. The channel width, as measured on the 1954 photographs, had decreased to an average of 550 feet (fig. 43*C*, 43*D*, 44*A*, *B*).

In 12 years the river had repaired about half the damage caused by widening during the period 1914–42. Great variability occurs among the data. At some cross sections the river narrowed to one-fifth or less of its former maximum width (table 1, sections 11, 16, 17, 31, 33, 47, 48, 51, 57, 59, 60, 61, 62, and 81), whereas at other cross sections the river width did not change (table 1, sections 54 and 66) or continued to widen (table 1, sections 14, 55, 65, 68, 114, 115, 116, and 120).

CIMARRON RIVER, 1955–60

New aerial photographs, which became available during preparation of this report, allowed measurements to be made of 1960 channel widths. The measurements were made on photoindex sheets and are less accurate than those made from contact prints of the 1954 photographs. The measurements show, however, that the period 1954–60 was not a continuation of the period 1943–54. Of 120 sections remeasured, only 10 showed continued narrowing of more than 50 feet (Table 1, sections 13, 27, 34, 38, 66, 88, 93, 108, 117, and 118); 70 sections were at about the same width; and of the remaining 40 sections, 38 showed renewed widening of more than 50 feet, whereas sections 65 and 68 have continued to widen since the first survey in 1874. The period may be characterized as one of relative stability with some tendency toward widening of the channel.

SUMMARY

The major changes in width of the Cimarron River during the 46-year period 1914–60 can be grouped into 3 distinct periods: the period 1914–42 of channel widening and flood-plain destruction (figs. 43 and 44); the period 1943–54 of channel narrowing and flood-plain construction; and the period 1955–60 of relatively minor changes (figs. 43 and 44).

The channel widening along the Cimarron River may be related to arroyo cutting, which has been prevalent throughout the Southwest since the latter part of the 19th century. However, there are two major differences between arroyo cutting and the channel changes along the Cimarron River. One is the nature of the change, widening instead of predominant deepening. The other is a trend toward rapid natural restoration of the valley to its former condition.

FACTORS INFLUENCING CIMARRON RIVER CHANNEL CHANGES

The causes of natural phenomena of the type discussed in this paper are generally complex and varied. Nevertheless, all available information will be considered in an attempt to explain the cause of destruction and rebuilding of the Cimarron River flood plain.

LAND USE

McLaughlin (1947), after an analysis of information on number of head of livestock and acres of cultivated land in southwestern Kansas, suggested that "accelerated erosion in the Cimarron valley is believed to be the result of overcultivation of land and the subsequent abandonment of thousands of farms, leaving large areas with lessened resistance to run-off." Unfortunately, there is little information on runoff for the period of channel widening. McLaughlin's data, when brought up to date (fig. 45), indicated that the period of flood-plain construction occurred during a period of major agricultural activity, 1941–50. This peak of agricultural activity probably began with the demand for more agricultural products during the war. The period 1941–50 was also a time of above average annual precipitation (fig. 46), a further stimulus to agricultural activity during these years. This coincidence of flood-plain construction and agricultural activity would seem to support McLaughlin's hypothesis; however, a shorter period of major agricultural activity also occurred between the years 1929–33 (fig. 45) during the period of channel widening. On the basis of these conflicting data, it is difficult to evaluate the effects of agricultural activity on the Cimarron River.

McLaughlin (1947) also concluded that, because there was no major change in number of head of livestock, grazing was not an important factor determining channel changes. Data on number of livestock in southwestern Kansas are presented on figure 45. Livestock density was greatest during the period of channel narrowing 1942–48. The activities of man and animals in the Cimarron River basin undoubtedly had their effects on the regime of the river, but any relation between cultivation, grazing, and channel change is obscure.

FLOODS

The period of greatest channel widening began in 1914 and ceased in 1942. Unfortunately, adequate streamflow data are not available during the period of channel widening to establish a definite trend, but the record presented in table 2 shows that large floods occurred in 1936, 1938, 1941, and 1942. Furthermore, according to C. O. Bryant (written communication),

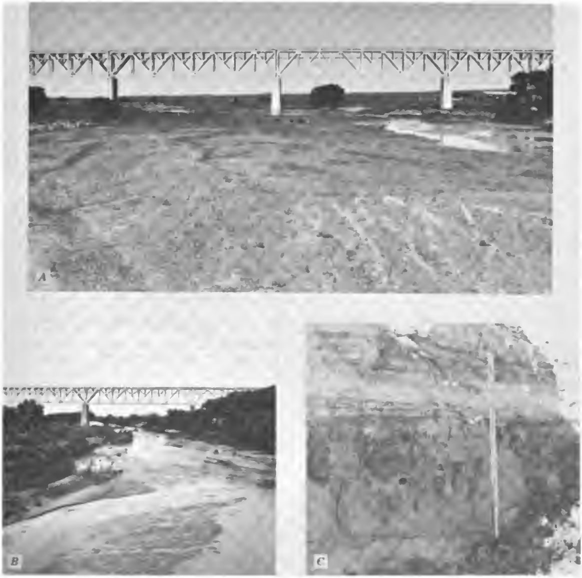

FIGURE 44.—Cimarron River in southwestern Kansas. *A*, Rock Island Railroad bridge near Arkalon in 1942. Channel was about 450 feet wide at point from which photograph was taken. Photograph taken by T. G. McLaughlin. *B*, Rock Island Railroad bridge near Arkalon in 1960. Channel is about 150 feet wide. Concrete bridge support on left of this photograph corresponds to center support shown in *A*. *C*, Pre-1914 alluvium exposed in cutbank near Highway 56 crossing. At base of cut is coarse crossbedded sand. Above sand is 2.5 feet of dark-colored homogeneous cohesive pre-1914 alluvium. Overlying the pre-1914 alluvium is 3 feet of alternate layers of sand and mud deposited from overbank floods.

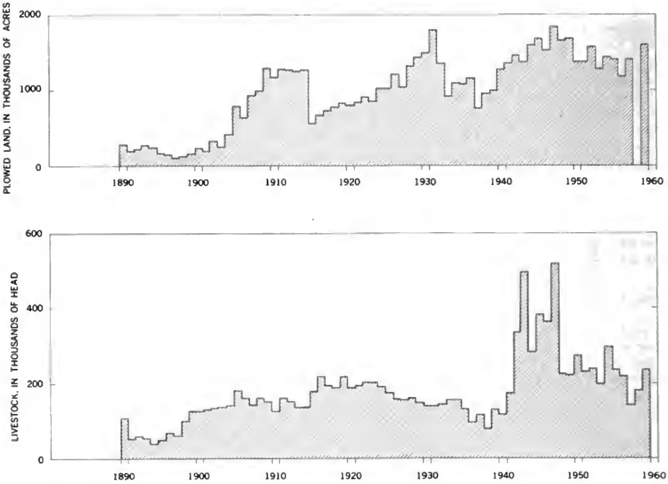

FIGURE 45.—Acres of plowed land and number of head of livestock in southwestern Kansas (Stanton, Morton, Grant, Stevens, Haskell, Meade, and Clark Counties) from 1890 to 1959. Data from annual reports of Kansas State Board of Agriculture. Information on plowed land for 1958 not available.

the Chicago, Rock Island and Pacific Railroad bridge near section 5 (fig. 42) had undergone extensive flood damage in June 1923, October 1930, and June 1937. This period, therefore, was one of destructive floods.

The period of flood-plain construction, 1943–54, was characterized by floods of low to moderate discharge. Only two large floods occurred after 1942—in May 1951 and July 1958 (table 2). The May 1951 flood approached the 1942 flood in peak discharge, but according to McLaughlin (oral communication), most of the flood waters entered the Cimarron River from North Fork Cimarron River in southeastern Grant County (fig. 42). This flood did not widen the channel appreciably because extensive channel narrowing occurred during the period 1943–54 along the Cimarron River below its confluence with the North Fork Cimarron River. The 1958 flood may have caused minor channel widening, but it obviously did not have the effect of pre-1942 floods, for the period 1955–60 was characterized by stability or only minor channel widening. Therefore, although major floods caused serious flood-plain destruction between 1914 and 1942, the post-1942 floods were not important in this respect.

PRECIPITATION

Although discharge records are incomplete, data on precipitation have been collected for long periods at several weather stations in the Cimarron River drainage basin. Precipitation data were compiled for four stations (Richfield, Hugoton, Ulysses, and Liberal, Kans.) since 1910. The records at each station show virtually the same trends during the period 1910–59, and they were combined to give an average for precipitation in the Cimarron River basin in Kansas (fig. 46).

TABLE 2.—*Peak discharge of the Cimarron River, southwestern Kansas*

[Data from U.S. Geol. Survey Water-Supply Papers. Water-year is from Oct. 1 to Sept. 30]

Water-year	Date	Momentary maximum		Station
		Gage height (feet)	Discharge (cfs)	
1896........	Apr. 12	....	90	Cimarron River near Liberal, Kans.
1914........	May 2	13 0	[1] (120,000)	Cimarron River near Mocane, Okla.
1936........	....	....	[2] (67,000)	
1938........	Sept. 5	11.0	23,000	Cimarron River near Liberal, Kans.
1939........	July 2	8.70	5,350	Do.
1940........	May 8	7.08	2,500	Do.
1941........	Sept. 24	10.5	47,000	Do.
1942........	Apr. 21	12.1	69,000	Do.
1943........	Oct. 20	3.70	625	Cimarron River near Satanta, Kans.
1944........	May 30	3.69	2,400	Do.
1945........	Aug. 23	5.12	2,560	Do.
1946........	May 29	3.96	6,360	Do.
1947........	Oct. 7	5.03	2,960	Do.
1948........	Sept. 11	4.69	5,330	Cimarron River near Mocane, Okla.
1949........	June 7	5.50	10,500	Do.
1950........	Aug. 3	4.83	6,320	Do.
1951........	May 7	9.94	53,400	Do.
1952........	Aug. 23	2.18	1,080	Do.
1953........	Aug. 20	3.60	4,650	Do.
1954........	Aug. 15	3.81	4,200	Do.
1955........	May 22	5.45	11,200	Do.
1956........	Aug. 21	3.40	2,460	Do.
1957........	May 16	5.08	9,300	Do.
1958........	July 8	6.75	21,300	Do.
1959........	May 4	3.43	3,360	Do.
1960........	June 8	3.70	4,290	Do.

[1] Maximum stage known. Estimated on basis of extension of average-stage-discharge relation (L. W. Furness, U.S. Geol. Survey, Topeka, Kans., written communication).

[2] Estimated on basis of highwater-mark elevation and subsequently defined stage-discharge relation at U.S. Highway 283, 4.3 miles south of Englewood, Kans. (L. W. Furness, U.S. Geol. Survey, Topeka, Kans., written communication).

The data show four periods of significance: (1) 1915–30, a period of great annual variability—years of precipitation in excess of the normal separated by years of drought; (2) 1931–40, a period of great precipitation deficiency; (3) 1941–51, a period of above-average precipitation; and (4) 1952–59, a period of below average precipitation. It is significant that channel widening occurred during periods 1 and 2 of variable or deficient rainfall, whereas channel narrowing occurred during period 3 of excess precipitation.

VEGETATION

The flood plain and banks of the river were vegetated prior to 1914 (fig. 43*A*). The grassed flood plain was relatively stable; however, if bank vegetation was destroyed by the 1914 flood, subsequent floods of lower peak discharge could have continued the destruction of the flood plain. Except for the 5-year period 1917–21, the great variability of precipitation during the period 1914–30 probably was unfavorable for the establishment of new vegetation in the channel or on the banks, and the period of prolonged drought 1930–40 certainly checked the growth of any new vegetation, which might have hindered the further widening of the channel. During the 9-year period of above-average precipitation after 1942, only floods of low peak discharge occurred. After 9 years of above-average precipitation, the major flood of 1951 had only minor effects on the channel, for much of the 1942 channel had been stabilized by perennial vegetation and converted to flood plain (fig. 43*C*). The establishment of perennial vegetation was a great aid to flood-plain formation. The growth of new vegetation and the resulting flood-plain construction were clearly dependent on the climatic and runoff characteristics for the period after 1942.

The period 1954–60 affords an opportunity to check the above theory of flood-plain formation, for it was a period of overall rainfall deficiency during which a large flood occurred. These conditions, according to the previous conclusions, should promote channel widening or at least prevent continued narrowing. The records (table 1) reveal that some widening did occur. The widening was not great, apparently because of the change in flood-plain vegetation since 1914—from grass to trees, grass, and weeds. The trees that border the channel offer considerable protection to the banks, and channel widening may be less easily accomplished under these conditions.

SUMMARY

The period of channel widening was characterized by below-average precipitation and by floods of high peak discharge, whereas the period of flood-plain construction was characterized by above-average precipitation and floods of low peak discharge. The influence of these conditions on vegetational growth is the key to the behavior of Cimarron River. Wet years and low water allow a vigorous growth of perennial vegetation, which stablized the existing deposits and promoted additional deposition. The stabilization of the new flood plain by vegetation was so effective that the floods of 1951 and 1958 did not cause great changes in the valley.

MECHANICS OF CHANNEL WIDENING AND FLOOD-PLAIN CONSTRUCTION

The Cimarron River affords an exceptional example of recent channel and flood-plain modification. The almost complete destruction of the flood plain makes a discussion of the manner of widening hypothetical; however, information from other sources and comparison of Cimarron River characteristics with those of other streams permit some conclusions to be drawn with regard to the manner of channel widening. A comparison of the aerial photographs taken in 1939, 1954 and 1960, information obtained by surveying five cross sections (fig. 42), and examination of flood-plain stratigraphy put a discussion of the flood-plain construction on a firmer basis.

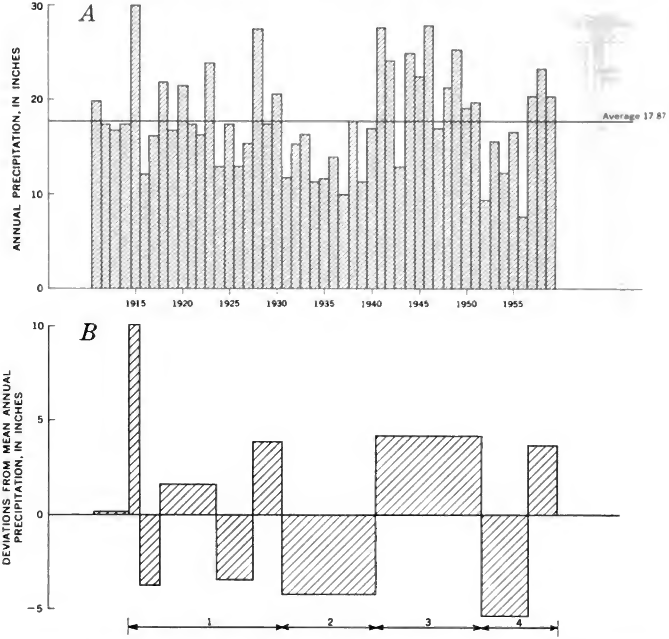

FIGURE 46.—Average annual precipitation in southwestern Kansas, 1910–59. *A*, Average annual precipitation for Liberal, Ulysses, Hugot and Richfield, Kans. *B*, Cycles of excess and deficient rainfall. The length of each cycle was determined by inspection of *A*, and the avera departure during each cycle was then computed.

CHANNEL WIDENING

The pre-1914 Cimarron River meandered across a grassed flood plain. On the basis of old photographs, the channel was determined in some localities to be as much as 7 feet deep. After the 1914 flood, the channel widened 450 to 600 feet (McLaughlin, 1947). The major flood apparently first destroyed the meander pattern; the point bars were eroded, and the valley was in effect gutted. When the meander belt was destroyed, the protective bank vegetation and finer sediments we removed; the flood-plain sediments beneath the grasse surface were then exposed. The pre-1914 flood-plai sediments are exposed at several localities along th river (fig. 44C). In a sand pit on the north bank of th river at the Highway 56 crossing (fig. 42), 40 feet alluvium is exposed. Thirty-five feet of the exposu is composed of cross-bedded gravel and coarse san Over this lies a dark-colored fine-grained (mediu grain size is 0.025 mm) zone that shows the columnar structure of a soil. The structure and dark color of this material suggest that it formed the surface of the pre-1914 flood plain. Overlying this alluvium is from 1 to 2 feet of fine sand and silt on which the present flood-plain vegetation grows. Where exposed the pre-1914 alluvium shows no stratification and appears homogeneous except for the presence of scattered pebbles. The alluvium is dense and cohesive, at least when dry, and may have offered considerable resistance to flood-plain destruction.

At present a part of the pre-1914 flood plain, which escaped destruction, is being eroded at the county road crossing north of Keyes, Okla. The bank on the north side of the river here averages 7 feet in height. The upper 1 to 1½ feet of the bank is composed of sand, which overlies 3 feet of pre-1914 alluvium. Beneath the pre-1914 alluvium, the cross-bedded channel sands are exposed at the base of the bank. The channel sands are being eroded from beneath the cohesive pre-1914 alluvium, causing slumping of the bank into the channel. Widening of the channel is occurring now, and it probably occurred in the past by bank caving that was caused by the removal of sand from beneath the cohesive pre-1914 flood-plain sediment.

EFFECT OF CHANNEL WIDENING ON GRADIENT

The gradient of the channel, as it was converted from a meandering to a straight channel, must have steepened appreciably. The gradient steepened from somewhat less than the gradient of the valley to a value probably closely approaching that of the valley itself. McLaughlin (1947) concluded that some degradation occurred during and after the 1914 flood. This conclusion is based on the formation of tributary gullies along the widened channel and on the reappearance of streamflow near the Highway 56 crossing, about 1 mile farther upstream in 1943 than prior to 1914. Gully formation, however, can be explained by the shortening of tributary stream courses by channel widening, which would induce erosion in the tributary valleys. In addition, part of the upstream migration of the head of the perennial reach near Satanta in 1943 may be explained by a rise in the water table after the floods of 1941 and 1942. Observation wells in the valley alluvium show a rise of water on the order of 3 feet after 1940. Initial channel widening and meander pattern destruction probably were associated with some degradation; but with continued bank erosion, the large amounts of bank sediments added to the channel for transport must have prevented further deepening and probably caused some aggradation of the channel.

Evidence is available to show that during the latter part of the period of channel widening and during the period of flood-plain construction the altitude of the channel floor has not changed appreciably. Data of maximum channel depth, measured from the crown of the roadbed at the time of bridge construction and again in 1960, are presented in table 3. The data show that changes in altitude of the channel are small. A change greater than 1 foot occurred at only one of the six bridges. These data support the hypothesis that degradation and aggradation may have occurred only locally after the 1914 flood; for during the period of flood-plain construction and channel narrowing there has been no consistent change in level along the Cimarron River. Similarly, Coldwell's (1957) observations on the Washita River showed that the river has widened its channel from 100 to 150 feet in 1939 to 200 to 350 feet in 1954 with no change in the altitude of the channel at the Pauls Valley gaging station.

TABLE 3.—*Changes in channel depth between date of bridge construction and 1960*

[Data for date of bridge construction and distance from crown of road to deepest part of channel at date of construction from State Highway Commission of Kansas]

Location of bridge crossing (highway)	Date of bridge construction	Distance from crown of road to deepest part of channel (feet)	
		At date of bridge construction	1960
U.S. 54	1935	20	18
U.S. 83	1948	18	18
U.S. 56	1930	23	24
U.S. 270	1949	32	32.5
Kansas 51	1938	18	17
Kansas 27	1935	12	12.5

FLOOD-PLAIN CONSTRUCTION

Favorable conditions—namely, above-average precipitation and floods of low to moderate peak discharge—permitted the Cimarron flood plain to begin to re-form after the 1942 flood. Undoubtedly, the fact that the channel was wide enough to occupy almost the entire area of the former flood plain was important.

The new flood plain was built almost entirely by a vertical accretion of sediments, which occurred in two ways as follows: (1) By island formation in the channel and subsequent attachment of the island to one bank by channel abandonment and (2) by deposition on and building up of areas not occupied by the low-water channel. Each process will be discussed in some detail.

ISLAND FORMATION

In the widening channel, sand bars and dunes formed. Bars that formed during the drought years had little chance of becoming permanent features; however, during years of average or excess precipitation, the growth of vegetation on the higher parts of the channel and on bars was the first phase of flood-plain construction. Vegetation converted the bars to permanent features of the channel.

When the channel was wide and dry, the movement of sand by wind was common. The migrating sand collected in vegetation along the perimeter of islands and built natural levees of wind-blown sand. One of these levee dunes occurs at section 1 and is shown on cross section A–A′ (fig. 47) at 950 feet. Once an island be-

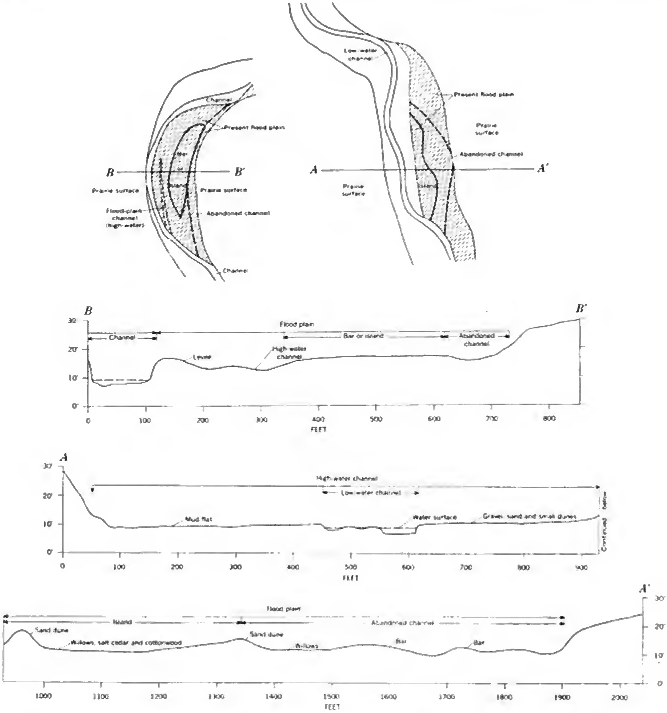

FIGURE 47.—Transverse profiles of the Cimarron River valley. *B–B′*, Cimarron valley near old Highway 270 crossing, cross section 2 (fig. 42). *A–A′*, Cimarron valley at cross section 1 (fig. 42).

came established in the channel, it would be perpetuated by deposition from subsequent floods and by the accumulation of aeolian sand deposits.

The formation of an island narrows the channel, but the presence of the island itself causes further narrowing. Depending on the orientation of the island in the channel, one or the other of the channels surrounding the island will be aggraded and abandoned (fig. 48*A*). For example, an island will rarely be situated so as to divide the water flow equally around the island. Generally, one channel will carry a larger discharge than the other. When this situation occurs, the channel carrying the lesser discharge is a branch channel. Laboratory experiments reveal that at a stream fork the channel which carries the smaller discharge has the highest concentration of bedload (Linder, 1952). In

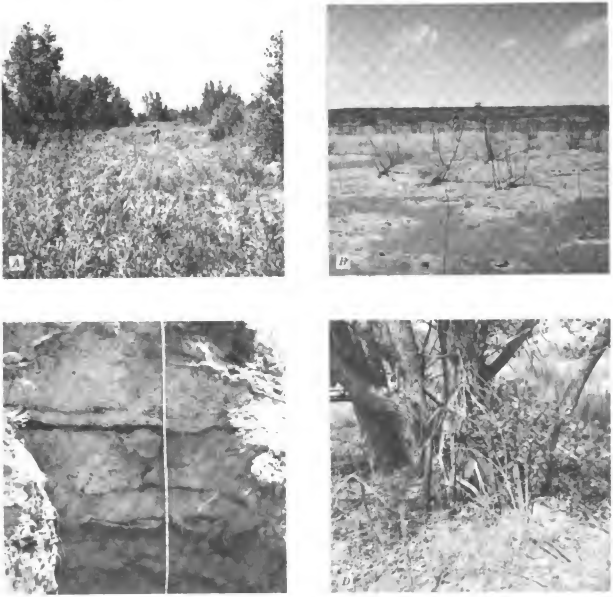

FIGURE 48.—Cimarron River in southwestern Kansas. *A*, Abandoned branch channel near State Highway 51 crossing north of Rolla, Kans., in 1960. On 1954 aerial photographs this channel contained no vegetation. *B*, One-year-old salt cedar saplings growing on mud-veneered part of channel shown at north side of profile *A*–*A'*, (fig. 47). Light-colored sediment is aeolian sand. *C*, Mud layers in flood-plain alluvium near bridge north of Moscow, Kans. Thin discontinuous mud layer just above thicker continuous layer in upper part of photograph is uppermost mud layer shown on figure 51. *D*, Partly buried automobile frame near country-road bridge north of Moscow, Kans. This frame is one of a group installed to aid bank stabilization. Trees growing to rear of frame are about 15 years old.

perennial streams this relationship may not be important, but in ephemeral streams deposition is important as the flood waters wane. The branch channel would thus be aggraded until it could carry only a minor percentage of the total discharge, and it would soon be abandoned. The cross sections in figure 47 show abandoned branch channels and islands.

The island formation and attachment method of flood-plain formation is less important than it appeared initially, for many islands that occupy the channel of Cimarron River at present were not formed in the channel but were fashioned by the detachment of portions of flood plain by channel changes. The island theory was first proposed to explain flood-plain formation and channel changes along the Red River during the Texas-Oklahoma boundary controversy (Glenn, 1925).

DIRECT FLOOD-PLAIN CONSTRUCTION

If, when the river was at its greatest width in 1943, a low-water channel meandered across the greatly widened sandy high-water channel, then a flood plain may have been already partially formed. Cross section *A–A′* of figure 47 shows the low-water channel occupying the center of a much wider sandy channel. During the survey, water filled the low-water channel. The surface to the left (north) of the low-water channel had been flooded recently and a veneer of mud had been deposited on this surface to a depth of one-half inch. This locality was revisited in the spring of 1961, and the surface was found to be supporting a new growth of salt cedar (fig. 48*B*). The presence of these plants will aid further deposition at this site. Apparently, during years of above average precipitation and low flow, the surface adjacent to a low-water channel becomes vegetated. It is then raised by deposition from flows that overtopped the low-water channel.

Figure 49 illustrates how the flows of different height affect the channel. Low flows are confined to the low-water channel and play no part in flood-plain formation, except as they afford a source of moisture for bank vegetation. Moderate flows escape the low-water channel and deposit sediment on the incipient flood plain, as on the north side of profile *A–A′* (fig. 47). High flows tend either to destroy or to build up the incipient flood plain, depending on vegetational cover.

Because the high flows tend to be destructive during the initial phase of flood-plain construction, the first patches of permanent flood-plain appear on those parts of the valley floor protected from the full force of floods. For example, aerial photographs show that initial flood-plain formation occurred in sheltered parts of the valley, at the mouth of tributaries, and in the lee of islands (fig. 50). The formation of the initial areas of flood plain naturally shielded other parts of the valley floor, which in turn became vegetated and aggraded. The coalescence of these newly formed flood-plain patches formed the existing flood plain. Each succeding flood deposited sediment on these areas, which were gradually built up to a level several feet above the present channel.

FLOOD-PLAIN STRATIGRAPHY

If the foregoing outline of flood-plain formation along the Cimarron River is correct, stratigraphic evidence in the banks of the channel should confirm it. Cross section *A–A′* of figure 47 shows the present low-water channel. The banks of the low-water channel are composed of channel sand. If these banks were built higher by overbank deposition, then each flood should have left a deposit of sand and silt as the flood waters receded from the higher surface. Depending on the sediment load carried by the water and the ability of

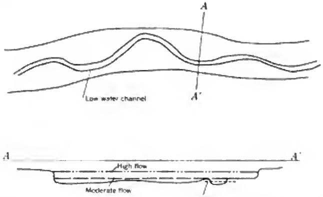

FIGURE 49.—Sketch illustrating parts of the Cimarron valley covered by low, moderate, and high flows. Enlargement of profile, ×4.

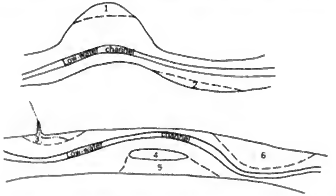

FIGURE 50.—Channel areas favorable for flood-plain formation. 1, Crest of valley meander; 2, Lee of valley bend; 3, Mouth of tributary; 4, Island; 5, Lee of island (abandoned channel); 6, Surface above low-water channel.

the higher surface to trap and hold the sediment, the rise of the flood-plain surface might be rapid or slow. Specific evidence of flood deposition would be a layer of mud left by the receding waters, as observed in 1960 on the left side of the channel. (See section *A–A′* fig. 47, and fig. 48*B*.)

At each reach of the channel visited in Kansas the recent flood-plain deposits, where exposed by excavation, show alternating thin layers of mud and sand (fig 48*C*). The mud layers are horizontal and in some places could be traced back from the channel across the flood plain to the edge of the valley. Individual mud layers were traced in existing sand pits and in holes augered or dug into the flood plain.

To examine these deposits in more detail, a vertical cut, which exposed 5 feet of the flood-plain alluvium, was made near the county road crossing north of Moscow. The base of the cut was at the level of the present channel. A diagrammatic sketch of this section is shown in figure 51. Six mud layers appear in this section (fig 48*C*).

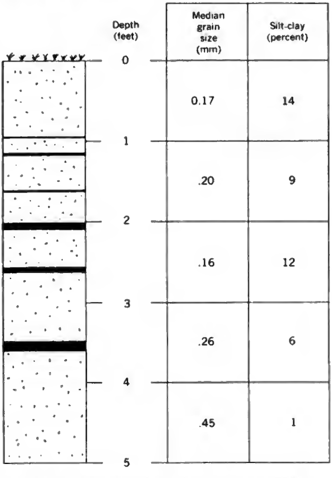

FIGURE 51.—Flood-plain stratification near county-road bridge north of Moscow, Kans. The six mud layers are shown by black lines. (See also fig. 48*C*.)

The flood plain is composed of sedimentary units deposited by overbank floods. A deposit of sand is overlain by a thin layer of fine sediment (the mud layer), which is deposited during the recession of the flood waters. A part of the sand above the uppermost mud layer (fig. 51) is composed of wind-blown sand trapped by vegetation on the flood-plain surface; undoubtedly, a part of the sand found between mud layers is aeolian, for the mud deposited in the channel in 1960 is now covered by a thin veneer of wind-blown sand (fig. 48*B*).

Other evidence of overbank deposition might be a graded deposit; that is, the alluvium exposed in the banks should show a decrease in grain size upward. In figure 51 the grading would be well defined if it were not for the occurrence of two thick mud layers between 2 and 3 feet. Except for the sample containing the mud layers, the percent silt clay also increases upward as expected. The stratigraphic evidence supports the concept of flood-plain formation by vertical accretion.

Cores were taken from several cottonwood trees growing on the newly constructed flood plain in 1961 to afford more precise information on the age of the flood plain. Trees at the south edge of the flood plain near the old Highway 270 crossing were 17 years old. Two trees were cored at the north edge of the flood plain near the bridge north of Moscow. These trees had grown around an automobile frame (fig. 48*D*), one of a group installed to aid in stabilizing the bank. The frame is now located about 250 feet from the present bank of the Cimarron River. The cored trees were found to be 14 and 15 years old. These ages support the conclusion that flood-plain construction began after the 1942 flood.

Trees on the flood plain have been partly buried by alluvium. Pits were dug at the base of three cored trees to determine the depth of burial. One small tree, located on the flood plain near Satanta, was 13 years old in 1961 and has been buried by 2 feet of alluvium. Two trees on the flood plain near the county road crossing north of Moscow and closer to the channel than those shown in figure 48*D* were excavated to the main root system at depths of 1.8 and 2.0 feet. These trees were both 11 years old. This evidence indicates that about 2 feet of flood-plain deposition has occured during the last 11 to 13 years.

SUMMARY

Once started by a major flood, the widening of the Cimarron River channel did not cease because of the ease of bank erosion and the occurrence of large floods. The widening of the channel apparently occurred by bank caving as the coarse sand was washed from beneath the relatively resistant pre-1914 flood-plain sediments.

During channel widening, degradation was probably not important. Channel gradient steepened, however, as the course of the river was shortened by destruction of the meander pattern.

The channel narrowing or flood-plain construction along the Cimarron River was the result of three factors as follows: The river had widened excessively; precipitation was above average; and the large floods were infrequent and did not erode the newly formed flood plain. The new flood plain is composed of a complex of coalesced islands, abandoned branch channels, and areas of flood plain built adjacent to the low-water channel. Large parts of the wide channel were not occupied by low-water flows, and these areas were sites of vegetational growth. The increased plant cover reduced flow velocities over these areas and promoted sediment deposition.

An examination of flood-plain stratigraphy indicates that the flood plain is composed predominantly of overbank sediment deposited during floods. An individual flood deposit consists of a layer of sand covered by a veneer of mud.

COMPARISON OF CIMARRON RIVER CHANNEL CHANGES WITH THOSE OF OTHER RIVERS

Too often in the consideration of unstable channels one is prone to think only of degradation or aggradation of the channel. Observations along Cimarron River clearly show, however, that both channel widening and narrowing may occur without a major change in the altitude of the channel floor (table 3). The rate and method of flood-plain formation noted along the Cimarron River is not unique, for similar changes have been noted along other rivers. For example, the widening of the channel of Washita River, as described by Coldwell (1957), occurred without significant changes in the altitude of the bed of the stream.

Hefley (1935) stated that the Canadian River in eastern Oklahoma has widened since the major flood of 1906 from less than half a mile to more than 2 miles in some places.

Bryan (1927) reported that the Rio Salado, a tributary to the Rio Grande near San Acacia, N. Mex., ranged from 12 to 49 feet in width in 1882, but in 1918 its width ranged from 330 to 550 feet. Bryan (1927, p. 19) stated that "Unlike many similar streams in New Mexico, which have not only widened their channels but deepended them in the same period, the Rio Salado, at least in the vicinity of Santa Rita, has even yet banks that are only 3 to 10 feet high and average 5 feet high." Leopold and Wolman (1957) reported that the channels of the Verde and Gila Rivers in Arizona were widened by large floods, but that narrowing of the channel followed establishment of vegetation. These changes may be similar to those which occurred along Cimarron River.

Smith (1940) reported on recent channel changes of several rivers in western Kansas, indicating that they have undergone Cimarron-type changes. The Smoky Hill River originally "had alternating sandy stretches and grassy stretches with series of pools. Later the former were widened, and the latter were sanded up * * *." Smith further stated that the Republican River was greatly affected by the flood of 1935.

> Formerly a narrow stream with a practically perennial flow of clear water and with well-wooded banks, the Republican now has a broad, shallow sandy channel with intermittent flow. The trees were practically all washed out and destroyed, much valuable farmland * * * was sanded over, and the channel has been filled up by several feet.

The Republican and Smoky Hill Rivers are typical of streams having sandy channels, as they have only from 2 to 5 percent silt and clay, in the sediment forming the perimeter of their channels (Schumm, 1961).

The Red River flood plain near Burkburnett, Tex. (fig. 52) was the object of intensive study as a result of the boundary dispute between Oklahoma and Texas (Glenn, 1925; Sellards, 1923). The Red River was never a narrow, meandering stream in historic times: a survey in 1874 showed the river to be about 4,000 feet wide. The channel, however, has undergone some important changes. For example, comparison of a special map prepared in 1920 (Sellards, 1923) with aerial photographs taken in 1953 showed enlargement of the flood plain. Over a 10 mile reach of the river 5.5 square miles of flood plain were added. The width of the Red River was measured at 20 sections between the confluence of the Pease and Red Rivers to the west and the confluence of Whiskey Creek and Red River to the east on aerial photographs taken in 1937, 1953, and 1957. In 1937 the river averaged three-quarters of a mile in width, close to the average for the 1874 survey. In 1953 the average width had decreased to half a mile. This channel narrowing may have been contemporaneous with that along Cimarron River. In 1957 the river averaged two-thirds of a mile wide, indicating a significant widening between 1953 and 1957. The photographs show all the types of flood-plain formation noted along the Cimarron River (fig. 50), and as suggested by Glenn (1925), the attachment of islands to the flood plain was important in the formation process.

The Red River transports large amounts of sand, red silt, and clay. The flood-plain sediments, where observed near the main highway bridges (Highways 81,

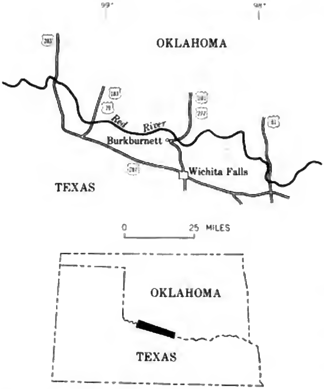

FIGURE 52.—Index map of Red River area.

281, and 183, fig. 52) show stratification characteristic of vertical accretion deposits. One section was sampled in detail near Burkburnett, Tex., where it was possible to obtain a sample of one thick mud layer not mixed with sand. The median grain size (0.002 mm) and silt and clay content (89 percent) of this layer are very similar to the median grain size (0.001 mm) and silt and clay content (85 percent) of mud recently deposited over sand at the margin of the channel. The similarity between the mud layers of the bank and the mud being deposited in the channel and the occurrence of mud layers in the banks at this location and elsewhere indicate that the Red River flood plain and islands, where observed, are built by the vertical accretion of sediment.

SUMMARY

The channel changes along the Cimarron River appear to be similar to changes which have occurred along the Washita, Canadian, Smoky Hill, Republican, and Red Rivers and Rio Salado. The changes differ from the degradation and aggradation characteristic of other unstable streams, for these rivers widen and narrow their channels as an alternative to aggradation and degradation

CONCLUSIONS

Flood-plain destruction along the Cimarron River occurred as a result of channel widening, which was initiated by the maximum flood on record. Large floods and below-average precipitation hindered a return to stability, and, in fact, were the means by which flood-plain destruction was perpetuated.

In contrast to floods observed in humid regions (Wolman and Eiler, 1958), floods in semiarid and arid environments may be tremendously destructive to the channel and flood plain. This destruction by floods may be a characteristic of erosion in a semiarid region where climatic fluctuations are common, and the streams are ephemeral or carry very low flows during long periods. Often these streams cannot adjust as readily as perennial streams to a change in stream regimen or a climatic fluctuation. Large floods may trigger an adjustment by initiating periods of severe erosion or deposition (Schumm and Hadley, 1958), and the events along Cimarron River may be of this type.

Most of the Cimarron River flood plain was constructed in only 12 years. Although rapid rates of erosion and deposition are commonly observed on other rivers, we are not aware of rates of flood-plain formation elsewhere as rapid as on the Cimarron River.

Observations in the valleys of the Cimarron and Red Rivers show that the flood plains were formed predominantly by overbank flooding and the vertical accretion of sediment. Generally, patches of flood plain in the most sheltered parts of the channel formed first. These patches coalesced and joined the islands and abandoned channels to form a composite flood plain. The flood plain, however, can be built simultaneously over large areas when an area of channel between the low-water channel and the edge of the valley is transformed as a unit to flood plain (fig. 50).

After the flood plain has been formed by vertical accretion, the stream may begin to meander. This reworking of the flood-plain alluvium by lateral migration of the stream would form a flood plain composed predominantly of lateral accretion deposits, as described by Wolman and Leopold (1957) and Adler and Lattman (1961). A flood plain may be formed by different processes, but a meandering stream migrating from one side of the valley to the other would leave a flood plain showing stratigraphic evidence only of lateral accretion. Therefore, the presence of lateral-accretion deposits forming the major part of a flood plain may not mean that the flood plain was initially formed by point-bar construction.

The type of changes occurring along the Red and Cimarron Rivers can be attributed to a large extent to the sandy alluvium forming the flood plain and channel. Channel widening instead of degradation and flood-plain construction instead of aggradation may occur commonly along sandy rivers in semiarid regions.

REFERENCES

Adler, A. A., and Lattman, L. H., 1961, Flood plain sediments of Halfmoon Creek, Pennsylvania: Mineral Industries Expt. Sta. (Pennsylvania State Univ.) Bull. 77, p. 1–11.

Bryan, Kirk, 1927, Channel erosion of the Rio Salado, Socorro County, New Mexico: U.S. Geol. Survey Bull. 790, p. 17–19.

Bryne, F. E., and McLaughlin, T. G., 1948, Geology and ground-water resources of Seward County, Kansas: Kansas Geol. Survey Bull. 69, 140 p.

Coldwell, A. E., 1957, Importance of channel erosion as a source of sediment: Am. Geophys. Union Trans., v. 38, p. 908–912.

Frye, J. C., 1942, Geology and ground-water resources of Meade County, Kansas: Kansas Geol. Survey Bull. 45, 152 p.

Glenn, L. C., 1925, Geology and physiography of Red River boundary between Texas and Oklahoma: Pan American Geologist, v. 43, no. 5, p. 365.

Haworth, Erasmus, 1897, Underground waters of southwestern Kansas: U.S. Geol. Survey Water-Supply Paper 6, 65 p.

Hefley, H. M., 1935, Ecological studies on the Canadian River flood plain in Cleveland County, Oklahoma: Ecological Mon., v. 7, p. 345–402.

Johnson, W. D., 1902, The High Plains and their utilization: U.S. Geol. Survey 22d Ann. Report, pt. 4, p. 631–669.

Leopold, L. B., and Wolman, M. G., 1957, River channel patterns: braided, meandering and straight: U.S. Geol. Survey Prof. Paper 282–B, p. 39–84.

Lindner, C. P., 1952, Diversions from alluvial streams: Am. Soc. Civil Engineers Proc., v. 78, no. 112, 25 p.

McLaughlin, T. G., 1942, Geology and ground-water resources of Morton County, Kansas: Kansas Geol. Survey Bull. 40, 126 p.

——— 1946, Geology and ground-water resources of Grant, Haskell, and Stevens Counties, Kansas: Kansas Geol. Survey Bull. 61, 221 p.

——— 1947, Accelerated channel erosion in the Cimarron Valley in southwestern Kansas: Jour. Geology, v. 55, p. 76–93.

Schumm, S. A., 1960, The shape of alluvial channels in relation to sediment type: U.S. Geol. Survey Prof. Paper 352–B, p. 17–30.

——— 1961, Effect of sediment characteristics on erosion and deposition in ephemeral stream channels: U.S. Geol. Survey Prof. Paper 352–C, p. 31–70.

Schumm, S. A., and Hadley, R. F., 1958, Arroyos and the semiarid cycle of erosion: Am. Jour. Sci., v. 255, p. 161–174.

Sellards, E. H., 1923, Geologic and soil studies on the alluvial lands of the Red River valley: Texas Univ. Bull. 2327, p. 27–87.

Smith, H. T. U., 1940, Notes on historic changes in stream courses of western Kansas, with a plea for additional data: Kansas Acad. Sci. Trans., v. 43, p. 299–300.

Wolman, M. G., and Leopold, L. B., 1957, River flood plains: Some observations on their formation: U.S. Geol. Survey Prof. Paper 282–C, p. 87–107.

Wolman, M. G., and Eller, J. P., 1958, Reconnaissance study of erosion and deposition produced by the flood of August 1955 in Connecticut: Am. Geophys. Union Trans., v. 39, p. 1–14.

Geomorphology of Segmented Alluvial Fans in Western Fresno County, California

By WILLIAM B. BULL

EROSION AND SEDIMENTATION IN SEMIARID ENVIRONMENT

GEOLOGICAL SURVEY PROFESSIONAL PAPER 352-E

Prepared in cooperation with the California
Department of Water Resources
A study of the interrelations of alluvial-fan
morphology, drainage-basin characteristics
and tectonic and climatic events

U.S. DEPARTMENT OF THE INTERIOR
March 3, 1849

UNITED STATES GOVERNMENT PRINTING OFFICE, WASHINGTON : 1964

UNITED STATES DEPARTMENT OF THE INTERIOR

STEWART L. UDALL, *Secretary*

GEOLOGICAL SURVEY

Thomas B. Nolan, *Director*

For sale by the Superintendent of Documents, U.S. Government Printing Office
Washington, D.C. 20402

CONTENTS

Page
- Glossary v
- Abstract 89
- Introduction 89
  - Purpose and scope 89
  - Acknowledgments 90
  - Geographic setting 90
    - Location and topographic features 90
    - Drainage 90
    - Climate and vegetation 91
- General geology 92
  - Regional setting 92
  - The Coast Range orogeny 93
- Geomorphology of the alluvial fans 93
  - Definitions and general features 93
  - Fan size and slope 94
  - Radial profiles of alluvial fans 94
    - Relation of stream and fan-segment gradients 100

Page
- Geomorphology of the alluvial fans—Continued
  - Possible causes of fan segmentation 103
    - Tectonic hypothesis 105
      - Fans associated with progressively gentler stream gradients 106
      - Fans associated with progressively steeper stream gradients 110
  - Cross-fan profiles 114
    - Change in shape downslope 114
  - Stream channels 114
    - Fanhead trenches 117
      - Causes of the fanhead trenching 120
- Summary and conclusions 126
- References cited 127
- Index 129

ILLUSTRATIONS

[Plates are in pocket]

PLATE 6. Topographic map of parts of Fresno, Merced, and San Benito Counties, Calif.
7. Drainage basins and alluvial fans studied in Fresno, Merced, and San Benito Counties, Calif.

Page
FIGURE 53. Map of parts of Fresno, Merced, and San Benito Counties, Calif., showing area discussed in this paper 91
54. Relations of fan area and slope to drainage-basin area and lithology 95
55. Types of radial profiles of alluvial fans in California 96
56. Radial profiles of the Tumey Gulch fan 97
57. Segments of the Tumey Gulch fan 98
58. Radial profiles of six fans whose streams head in the foothill belt 99
59. Radial profiles of fans whose streams head in the Diablo Range 100
60. Longitudinal profiles of two streams and two low terraces and the surface of the upper part of their alluvial fans 101
61. Relation of the gradients of fanhead trenches to the gradients of their adjacent lower fan segments 102
62. Terraces in the foothill belt of western Fresno County 103
63. Moisture content for core holes on the unirrigated parts of the Arroyo Hondo and Arroyo Ciervo fans 104
64. Diagrammatic sketches showing the steepening of stream gradients due to a hypothetical climatic change 105
65. Diagrammatic sketches showing two types of alluvial-fan and stream-gradient history 106
66. Relation of stream terraces to fan segments for Little Panoche Creek 107
67. Soils and fan-segment boundaries of the Little Panoche Creek fan 109
68. Diagrammatic sketch showing stages of fan-segment development 111
69. Radial profiles of the San Emigdio Creek and Santiago Creek fans, Kern County, Calif 112
70. Diagrammatic sketches showing stages of alluvial-fan development 113
71. Channel deviation from medial position on fanheads of alluvial fans in parts of Fresno and Merced Counties 114
72. Topographic map of the alluvial fans of Capita Canyon, Chaney Ranch Canyon, and Marca Canyon 115
73. Cross-fan profiles of Capita Canyon, Chaney Ranch Canyon, and Marca Canyon fans 116
74. Position of stream channels on the fanheads of the piedmont plain east of the Panoche Hills 116
75. Mudflow deposits on the natural levees of Arroyo Hondo 117
76. The fanhead trench of Tumey Gulch 117

FIGURE 77-80. Changes in the— Page
77. Depth of the Tumey Gulch fanhead trench, 1921-55 ... 118
78. Depth of the Arroyo Ciervo fanhead trench, 1921-56 ... 119
79. Width and length of the Panoche Creek fanhead trench, 1854-1959 ... 119
80. Channel configuration of Arroyo Hondo, 1855-1954 ... 121
81. Index map of central California showing the location and altitude of weather stations referred to in this report ... 122
82. Trends of annual rainfall for five stations in California, 1853-1958 ... 123
83. Trends of daily rainfall size classes, 1881-1958, Sacramento, Calif ... 124
84. Trends of daily rainfall size classes, 1901-58, Mendota Dam, Calif ... 125

TABLE

Page
TABLE 1. Basic data on drainage basins and alluvial fans of selected streams in western Fresno County, Calif ... 92

GLOSSARY

Alluvial fan, a stream deposit whose surface forms a segment of a cone that radiates downslope from the point where the stream channel emerges from a mountainous area.

Apex, the highest point on an alluvial fan, generally where the stream emerges from the mountain front (Drew, 1873, p. 447).

Braided distributary channels, secondary channels that extend downslope from the end of the main stream channel or fanhead trench and are characterized by repeated division and rejoining.

Cross-fan profile, a topographic profile of alluvial fan(s) roughly parallel to the mountain front.

Drainage basin, the area drained by a stream upstream from the fan apex.

Ephemeral stream, a stream, or part of a stream, that flows only briefly in direct response to precipitation.

Fanhead trench, a stream channel entrenched into the upper, and possibly the middle, part of the fan.

Fan segment, a part of an alluvial fan that is bounded by changes in slope.

Intermittent stream, a stream, or part of a stream, that flows only part of the time because it receives water from seasonal sources such as springs and bank storage, as well as from precipitation.

Piedmont plain, a broad sloping plain formed by the coalescence of many alluvial fans.

Radial line, a straight line on the fan surface extending from the apex to the toe.

Radial profile, a topographic profile along a radial line.

Thalweg, the line along the deepest part of the stream channel.

EROSION AND SEDIMENTATION IN A SEMIARID ENVIRONMENT

GEOMORPHOLOGY OF SEGMENTED ALLUVIAL FANS IN WESTERN FRESNO COUNTY, CALIFORNIA

By William B. Bull

ABSTRACT

The alluvial fans fringing the western border of the San Joaquin Valley in Fresno County, Calif., are derived from drainage basins that are generally similar with respect to topography, climate, and tectonic environment but that range in size from 0.2 to 206 square miles and in lithology from predominantly sandstone to predominantly mudstone or shale. Fans derived from mudstone or shale-rich basins are generally 35–75 percent steeper than fans of similar area derived from sandstone-rich basins and roughly twice as large as fans derived from sandstone basins of comparable size.

The radial profiles of the fans are not smooth curves, but, instead, comprise three or four straight-line segments. The surfaces represented by these segments form bands of approximately uniform slope that are, mainly, concentric about the fan apexes. Longitudinal profiles of terraces show that intermittent uplift has changed the stream-channel slope upstream from the fan apexes. The slope of the area of deposition and the slope of the stream channel upstream from it tend to be the same. The segmentation is a result of intermittent uplift that has changed the stream-channel slopes and the succeeding depositional slopes.

Most of the fans are associated with stream channels that have become progressively steeper. Each time the channel was steepened, the succeeding fan deposits formed a new fan-shaped segment of steeper slope that was deposited on the upper part of the pre-existing fan.

The Little Panoche Creek fan, however, has a history that is associated with progressively gentler stream-channel gradients, because the rate of downcutting by the stream has exceeded the average rate of uplift of the reach immediately upstream from the apex. The intermittent character of the uplift resulted in the cutting of a series of paired terraces which preserve a record of the deformation of the mountain front and fan-head areas. With each uplift, the end of the deepened stream channel moved farther down the fan. After each episode of trenching, the lower part of the stream channel and its adjacent area of fan deposition ultimately attained a more gentle gradient than previously.

Fan segmentation is useful for deciphering part of the tectonic history of the area because the fan profiles and the relative ages of the fan segments reflect part of the erosional and tectonic history of the drainage basins.

Two periods of fanhead trenching, apparently unrelated to tectonic activity, have been recorded since 1874 when many fans were receiving deposits near their apexes. One was from about 1875 to 1895 and the other from about 1935 to 1945. Many channels have been deepened 25–40 feet.

Rainfall data from five stations in central California show two periods of much greater than average annual rainfall, which were also periods of high frequency of large daily rainfall. They coincide with the two periods of maximum channel trenching.

INTRODUCTION

PURPOSE AND SCOPE

Alluvial fans are common in the arid and semiarid areas of the world. Ground water in many parts of the Western States is pumped from alluvial-fan deposits and recharge of many ground-water basins is through the alluvial-fan deposits that fringe the basins. Despite the importance of alluvial fans, little detailed work has been done on their sedimentary and geomorphic characteristics until recently.

This report presents data on the geomorphology of alluvial fans collected as part of an investigation of the geology of alluvial fans and their drainage basins in western Fresno County, Calif. The primary purpose of the investigation was to obtain a better understanding of the alluvial fans and their drainage basins so that the causes, magnitude, rate, and duration of near-surface subsidence could be understood better. The sedimentary features of the alluvial-fan deposits and the geomorphic and lithologic characteristics of their drainage basins are described in detail elsewhere (Bull, 1964).

The geomorphology study provided information concerning deposition and erosion of the fans. This information is reported separately in this paper because it did not reveal many criteria that could be used in appraisal of subsidence.

The relations of fan size and slope to drainage-basin area and lithology were studied. The overall shape of the alluvial fans was studied by means of radial and cross-fan profiles, and the different types of stream channels are described. Reasons for the characteristc fan shapes and the history and causes of channel trenching that occurred during the last century are discussed.

The maps used in the study include the following: General Land Office plats and survey notes of 1853–58 and 1879–81; U.S. Geological Survey 7½ minute quadrangles, 1922–31, scale 1:31,680, contour intervals 5 and 25 feet; and U.S. Geological Survey 7½ minute quadrangles, 1955–56, scale 1:24,000, contour intervals 5, 10, 20, and 40 feet.

The investigation was made under the supervision of J. F. Poland, research geologist of the Ground Water Branch, U.S. Geological Survey, in charge of land-subsidence investigations in California, and in co-
Resources.

ACKNOWLEDGMENTS

operation with the California Department of Water

S. N. Davis and G. A. Thompson of Stanford University gave advice on certain aspects of the study. Ranchers, sheepherders, farmers, and other people living in the area gave firsthand accounts of the history of channel trenching. The author also thanks his colleagues in the Geological Survey, C. S. Denny, L. A. Heindl, R. H. Meade, J. F. Poland, F. S. Riley, and W. E. Wilson, for their critical review of the manuscript.

GEOGRAPHIC SETTING

LOCATION AND TOPOGRAPHIC FEATURES

The area discussed in this paper includes about 1,400 square miles of the west side of the San Joaquin Valley and the adjacent Diablo Range in central California (fig. 53). The northern edge of the area is 10 miles south of Los Banos, and the southern boundary is the south side of the drainage basin of Domengine Creek, 12 miles north of Coalinga. The alluvial fans are in western Fresno County and in a small part of Merced County, and the drainage basins of some of the fans extend into San Benito County.

Between the flood plains of the San Joaquin River and Fresno Slough and the foothills to the southwest is a belt of coalescing alluvial fans 12–19 miles wide. The altitude at the base of this piedmont plain ranges from 130 to 175 feet, and the alluvial fans rise to altitudes of about 340–900 feet at their apexes. The slopes of the fans range from about 10 feet per mile near the base of the larger fans to about 150 feet per mile on the upper slopes of some of the smaller fans. The local relief on the fans is generally less than 5 feet, except on the upper parts where the main stream channels are incised as much as 40 feet. Erosional stream channels are not present on the fans except for minor dendritic channels on parts of some older fan surfaces bordering the Panoche Hills.

The Diablo Range in the southwestern part of the area consists of several groups of foothills fringing the San Joaquin Valley and the main range, which is generally about 10–15 miles from the western margin of the valley (pl. 6). The foothills include the Ciervo Hills, whose highest point is about 3,400 feet, and the Panoche Hills, which rise to an altitude of about 2,700 feet. The main Diablo Range has several peaks higher than 5,000 feet. Both the foothill belt and the main Diablo Range are rugged and have many steep canyons. (See pl. 6.)

Most of the geographical features mentioned in this report can be found on plate 6, and the specific drainage basins and their associated alluvial fans are outlined and identified on plate 7. The approximate boundaries of the alluvial fans were determined from aerial photographs and contour maps and by 400 gypsum content determinations. The average gypsum content of fans whose streams head in the foothill belt is five times the gypsum content of fans whose streams head in the main Diablo Range (Bull, 1964, table 12). Plate 7 also shows the section-line grid for all section references.

DRAINAGE

The drainage basins in the foothill belt are generally less than 10 miles long. The lengths of the drainage basins that head in the main Diablo Range and cross the foothill belt—Little Panoche, Panoche, and Cantua Creeks—range from 14 miles for Cantua Creek to 22 miles for Panoche Creek. Plate 7 shows how the larger basins extend around the smaller basins to drain the west side of the foothill belt. In general the streams flow toward the northeast at right angles to the trough of the San Joaquin Valley.

The streams are intermittent or ephemeral. Precipitation is too low and drainage basins are too small to support perennial streams. Little Panoche, Panoche, and Cantua Creeks are intermittent streams that receive enough ground water to flow along the entire length of their drainage basins for a few weeks after most winter rainy seasons. The channels of the ephemeral streams are always above the water table and these streams flow briefly and only in direct response to rainfall.

During the summer and autumn, reaches with flow generally alternate with dry stretches on the intermittent streams, and as the streams approach the San Joaquin Valley, they disappear. During winter floods, several hundred cubic feet per second of water may flow in these streams. Flash floods are not common on the larger streams.

The intermittent streams were described in the 1850's by the surveyors who mapped the area for the General

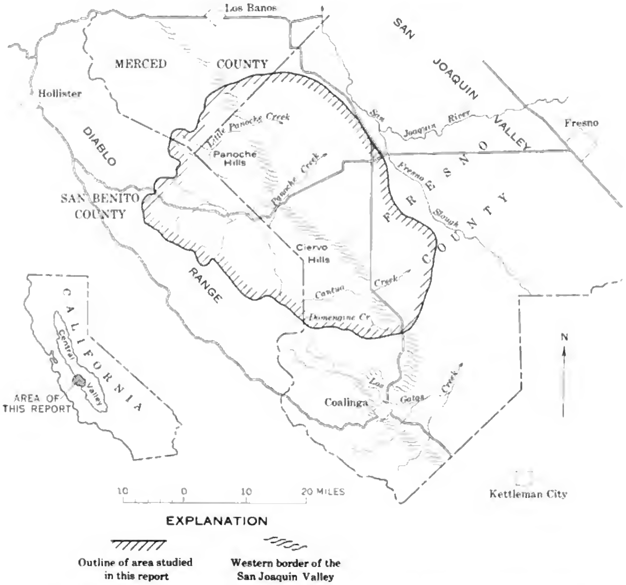

FIGURE 53.—Map of parts of Fresno, Merced, and San Benito Counties, Calif., showing area discussed in this paper.

Land Office. Panoche and Little Panoche Creeks were described in October 1854 by A. McNeill, who noted "* * * the large creek [Panoche Creek] being at this time perfectly dry and never affording any water except in the rainy season." For Little Panoche Creek he remarked that "There is however no timber or water, the creek being dry, and consequently there is little inducement for settlement." J. F. Minturn made the following notes about Cantua Creek in May 1855. "The water in this stream sinks after running about ¾ of a mile into the plains. At the edge of the hills the water runs throughout the year." These descriptions show that the streams were nearly the same 100 years ago as they are today, except that Cantua Creek rarely flows throughout the year now, and Little Panoche Creek has more water than was suggested by McNeill. These descriptions were based partly on conditions at the time of year at which the observations were recorded.

The ephemeral streams have a "flashy type" of flow which ranges from clear water to viscous mud.

CLIMATE AND VEGETATION

Nearly all the precipitation in the area occurs as rain. The average annual rainfall is 15–20 inches for most of the main Diablo Range. The main range creates a rain shadow across the foothill belt and the west side of the San Joaquin Valley. Consequently, the average annual rainfall is about 8–15 inches in the foothills and 6½–8 inches in the valley; it also decreases slightly from north to south. Most of the rainfall comes during the winter. The winter rains are carried by cyclonic storms that move inland across the Pacific coast. The spring and infrequent summer rains result generally from cyclonic storms but also occur as scattered thunderstorms.

This semiarid region is hot in the summer and mild in the winter. The daily temperature range is often 30°–40°F particularly during the summer. The prevailing winds are from the northwest. The lower slopes of the main Diablo Range are brush covered, but oak, pine, and cedar grow at the higher altitudes. The foothills and alluvial fans support shrubs such as shadscale and short grasses such as downy chess and redstem filaree.

The vegetation on the foothills and in the San Joaquin Valley is sparse, particularly during dry years. A more luxuriant growth mantles the flooded parts of alluvial fans and may continue to grow in a dry year following a wet year, if sufficient moisture is left in the ground to support the dense growth. The dryness and hot temperatures discourage the growth of many plants at the low altitudes during the summer.

GENERAL GEOLOGY

REGIONAL SETTING

The Diablo Range is mainly a broad anticline that has smaller folds trending obliquely to the course of the main range. Joaquin Ridge is one of the smaller anticlines, and Cerro Bonito and the Griswold Hills mark the trend of part of the Ciervo anticline. The Vallecitos is a conspicuous syncline to the southwest of the Ciervo anticline. Monoclinal folds are the dominant structures in much of the foothill area.

The core of the Diablo Range consists of deformed and slightly metamorphosed shale and graywacke of the Franciscan Formation of Jurassic to Late Cretaceous Age and of ultrabasic intrusive rocks. The Franciscan Formation is overlain unconformably by predominantly Cretaceous marine rocks, which dip toward the San Joaquin Valley and form the east flank of the Diablo Range. The Cretaceous marine rocks consist mainly of mudstone, sandstone, and shale which are more than 20,000 feet thick. Easily eroded Tertiary marine and unconsolidated continental sediments are exposed mainly along the foothill belt and in basins such as the Vallecitos.

Some of the basic data on selected drainage basins and alluvial fans are in table 1. The total relief of a drainage basin is the difference in altitude between the highest point of the basin and the point where the stream enters the San Joaquin Valley. The mean slope of a drainage basin is the average slope of all the land within the basin and is computed with data from contour maps. Mean slope partly controls the amount and rate of erosion in a drainage basin. The slope values in table 1 are the tangents of average slopes. The lithology and geomorphology of these drainage basins are described in detail elsewhere (Bull, 1964).

TABLE 1.—*Basic data on drainage basins and alluvial fans of selected streams in western Fresno County, Calif.*

Stream	Code letter on plate 7	Drainage basin total relief (feet)	Percentage of mudstone and shale in drainage basin	Approximate mean drainage-basin slope	Drainage-basin area (square miles)	Alluvial-fan area (square miles)	Overall alluvial-fan slope
Laguna Seca Creek	A	1,270	48	0.20	11.1	11.3	0.015
Wildcat Canyon	B	1,140	42	.16	11.4	8.3	.015
Little Panoche Creek	C	3,150	35	.24	104	53.6	.0070
Moreno Gulch	D	1,830	67	.45	11.7	20.6	.017
Gres Canyon	E	620	57	.33	.18	.36	.029
Marca Canyon	F	1,500	60	.48	1.9	4.6	.025
Chaney Ranch Canyon	G	620	40	.29	.53	.51	.026
Capita Canyon	H	1,760	67	.50	2.6	5.9	.022
Dosados Canyon	I	1,520	63	.41	.93	2.1	.023
Escarpado Canyon	J	1,130	60	.39	.56	1.4	.029
Panoche Creek	K	4,550	32	.27	296	260	.0035
Unnamed	L	770	86	.37	.49	[1] .20	.022
Tumey Gulch	M	2,590	67	.30	29.1	49.6	.012
Arroyo Ciervo	N	2,740	68	.34	8.0	10.3	.018
Unamed	O	1,600	51	.30	1.7	3.6	.022
Arroyo Hondo	P	2,550	52	.29	25.7	54.6	.0094
Cantua Creek	Q	4,610	32	.35	49.4	75.6	.0047
Salt Creek	R	3,480	41	.39	25.2	28.2	.0074
Martinez Creek	S	3,230	34	.26	8.9	7.1	.013
Domengine Creek	T	3,500	38	.33	11.2	11.4	.011

[1] Small fan area owing to removal of lower part of fan by Panoche Creek.

THE COAST RANGE OROGENY

Alluvial fans are characteristic of structurally disturbed regions (Blackwelder, 1931, p. 136–138). The area discussed in this paper has been subject to intermittent uplift that culminated in the Coast Range orogeny. This orogeny and subsequent periods of uplift determined most of the geomorphic and sedimentary characteristics of the alluvial fans in western Fresno County.

The Coast Range orogeny was preceded by several periods of uplift (Taliaferro, 1943, p. 151–158) one of which resulted in the deposition of the Tulare Formation of Pliocene and Pleistocene(?) age. In western Fresno County, parts of the Tulare consist of coarse fluvial sediments that were eroded from the ancestral Diablo Range to the west. The Tulare to the east of the Panoche Hills contains cobbles of glaucophane schist and other Franciscan rock types such as slaty shale and graywacke. The source area for these rock types was the main Diablo Range and part of Glaucophane Ridge. East of the Ciervo Hills the Tulare Formation includes red chert and serpentine detritus, rock types that are common in the main Diablo Range. Some parts of the Tulare appear similar lithologically to the present-day alluvial fans. For example, the Tulare south of the apex of the Panoche Creek fan may be part of the fan of an ancestral Panoche Creek.

> The deposition of these late Pliocene and early Pleistocene(?) beds [the Tulare Formation] was brought to a close by an even more important and widespread diastropic event [the Coast Range orogeny] than that through which they originated (Taliaferro, 1943, p. 148).

Although the age of the Coast Range orogeny is generally considered to be middle or late Pleistocene (Eaton, 1928; Reed and Hollister, 1936; Stille, 1936; Putnam, 1942; Bailey, 1943; Taliaferro, 1943), within the area studied it can be dated only as post Tulare. The Tulare generally is accepted as being of Pliocene and Pleistocene(?) age, and if this is the age of the Tulare in western Fresno County, then the foothill belt and probably the main Diablo Range were elevated during Pleistocene time.

Middle to late Pleistocene fossils have been found in tilted and folded strata in southern California, and some of these beds have been tilted by minor earth movements since the Coast Range orogeny (Bailey, 1943). Movements younger than the Coast Range orogeny also affected the Diablo Range causing changes in the development of alluvial fans as will be shown later.

Flat-lying beds of the Tulare Formation on the highest parts of the Panoche Hills suggest that during Pliocene and early Pleistocene time these beds probably covered the site of the present foothill belt, which has since been uplifted. Subsequent erosion has separated the remnants of the Tulare from their source areas in the Diablo Range.

The streams that now head in the main Diablo Range either maintained their original courses through the rising foothill belt, or took new courses around the areas of maximum uplift. Deposition of alluvial fans then took place east of the foothill belt on the older fan deposits of the Tulare Formation.

The streams that now head in the foothill belt did not exist before the Coast Range orogeny. The orogeny formed the foothills and started the deposition of new alluvial fans that are now several hundred feet thick.

The western part of the San Joaquin Valley was uplifted also. A map of the top of a widespread lacustrine clay, the Corcoran Clay Member of the Tulare Formation, shows that the western edge of the Corcoran was uplifted several hundred feet relative to its eastern edge since the end of the pluvial period associated with the clay (R. E. Miller, written communication, 1962). Alluvial-fan deposition has obscured any topographic expression of this folding in the San Joaquin Valley.

GEOMORPHOLOGY OF THE ALLUVIAL FANS

DEFINITIONS AND GENERAL FEATURES

An alluvial fan is a stream deposit whose surface forms a segment of a cone that radiates downslope from the point where the stream channel emerges from a mountainous area. The deposit may consist of water-laid sediments or mudflow deposits; the alluvial fans in western Fresno County are made up of both. A radiating surface gives a fan the distinctive shape of a segment of a cone. The channel may contain either a perennial, intermittent, or ephemeral stream. In western Fresno County the source areas range from low, rolling hills to steep, rugged mountains.

Stream channels are commonly entrenched into the fanheads, the area close to the apex, and Eckis' (1928, p. 240) term "fanhead trench" gives a good description of this feature. Downslope from the end of the fanhead trench most of the stream channels divide into several braided distributary channels which are about 1–3 feet deep and commonly change position during floods.

A piedmont plain is a broad sloping plain formed by the coalescence of many alluvial fans. The terms "compound alluvial fan" and "bajada" (Tolman, 1909, p. 142; Blackwelder, 1931, p. 136) have the same meaning. Blackwelder noted that "parallel to the mountain front the convexities of the component fans impart to the bajada an undulating surface."

FAN SIZE AND SLOPE

Alluvial fans and their drainage basins or source areas act as open systems because changes in drainage-basin conditions cause changes in fan characteristics. The area and slope of a fan are related to the size and lithology of its drainage basin. The fan slope used in computing quantitative relations is the average overall slope from the fan apex to the outer margin where the fan coalesces with another fan or with the river deposits in the trough of the San Joaquin Valley. Radial profiles drawn near the middle of a fan from apex to toe were used to help locate the lower end of the slope to be measured. The boundaries shown on plate 7 were used to determine most of the fan areas.

In general, "* * * large deep canyons have broad fans of low gradient; short ravines have small steeply sloping fans" (Blackwelder, 1931, p. 136). This general relation is true for fans in western Fresno County, as is shown by figure 54.

Statistical-fitting procedures were not used in drawing the lines, but the set of equations for each lithologic group was checked by inserting terms from the equations of figures 54*A* and 54*B* in the equations of figure 54*C*.

Overall fan size is controlled mainly by drainage-basin features, such as size, slope, rainfall, and erodibility of the exposed rocks. The fans studied range in size from 0.4 to 260 square miles. Figure 54*A* shows that all the fans derived from basins underlain mainly by mudstone and shale, and half the fans derived from basins underlain mainly by sandstone, are larger than their basins. The plotted points scatter moderately about straight lines described by the equations shown on the figure. On the logarithmic graph the slopes of the lines (0.88) are equal and show that fan area increases in about the same exponential manner as drainage-basin area increases, despite appreciable differences in lithology. The coefficients of the equations (1.3 and 2.4) show that, on the average, fans derived from drainage basins characterized mainly by mudstone and shale are roughly twice as large as the fans derived from drainage basins of comparable size characterized mainly by sandstone.

The fans studied range in overall slope from 0.0035 (0°12′) to 0.029 (1°40′). Figure 54*B* shows that the overall fan slope decreases with an increase in drainage-basin size. In drainage basins of comparable size, all but the smallest fans of mudstone and shale basins slope more steeply than fans of sandstone basins.

The relation of fan area to fan slope is shown in figure 54*C*. In general, fan slope decreases with increasing fan area. Fans derived from mudstone and shale drainage basins are larger than fans of similar slope that are derived from sandstone basins; and fans (in the size range 1–100 square miles) that are derived from mudstone and shale basins are 35–75 percent steeper than fans of similar area that are derived from sandstone basins.

The apexes of fans of mudstone and shale drainage basins are, on the average, 520 feet above the trough of the San Joaquin Valley, whereas the apexes of fans of sandstone drainage basins have an average height of 400 feet above the valley trough. The relative heights of the fan apexes, and the relations shown by figure 54, show that for drainage areas of comparable size fans derived from mudstone and shale are not only larger, but also are thicker than fans derived from sandstone. Presumably, these differences in fan volume can be attributed largely to the greater erodibility of the mudstone and shale.

In the area studied, downcutting of the stream channels in the mountains has not kept pace with uplift. The effect of uplift on stream gradients is described in the section "Tectonic hypothesis." The relations between fan slope, fan area, and drainage-basin area and lithology may be different in areas where downcutting by streams has exceeded uplift of the mountains, and erosion of part of the fan has occurred.

RADIAL PROFILES OF ALLUVIAL FANS

The radial profiles of an alluvial fan reflect its depositional history, which is controlled partly by erosional and tectonic changes in the drainage basin upstream from the fan. The radii of a fan are restricted by adjacent fans, and by stream deposits at the toe of the fan if the fan is built into a narrow valley.

The overall radial profiles of most alluvial fans are gently concave upward. Most investigators have reported that the slopes of alluvial fans decrease gradually away from the mountain front. Blissenbach (1954, p. 176) said that "from the apex of the fan the surface dips towards the base in which direction the angles of dip gradually become flatter." Trowbridge (1911, p. 714) stated that "The slope of the piedmont plain away from the mountains varies rather uniformly with distance away from the mountains." Krumbein (1937, p. 588–590), in his studies of the San Antonio Canyon fan in southern California, concluded that the slope of the profile decreases at such a constant rate that the slope can be expressed as a negative exponential function.

The slopes of the fans in western Fresno County do not decrease gradually away from the mountain front. All the fans have distinct breaks in slope, which give their radial profiles a segmented appearance. The fan segments generally have a constant slope and appear

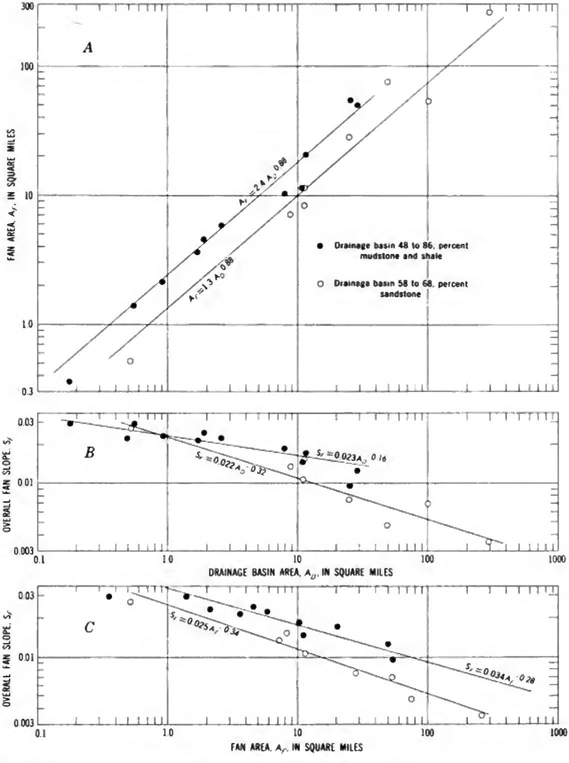

FIGURE 54.—Relations of fan area and slope to drainage-basin area and lithology. *A*, Relation of fan area to drainage-basin area. *B*, Relation of fan slope to drainage-basin area. *C*, Relation of fan slope to fan area.

as straight lines on a radial profile. The fans of Little Panoche Creek and Cantua Creek, however, each have a segment that is concave in addition to their straight-line segments (fig. 59).

The uniform slopes of straight-line segments of the radial profiles are not merely the result of interpolation between widely spaced survey control points. Maps made 30 years apart by somewhat different techniques, show consistent fan shapes, except in areas that have been affected by intense land subsidence. For example, the fan segmentation of the upper part of the Tumey Gulch fan (figs. 56, 57) was studied by using data from the Monocline Ridge quadrangle which was mapped by planetable methods in 1923 (1:31,680, 5-ft contour interval) and 1955 (1:24,000, 10-ft contour interval). According to authorities at the Pacific Area Office of the Topographic Division of the U.S. Geological Survey (oral communication), some interpolation was necessary for the 1923 map, which was based partly on surveyed profile lines spaced 1,000 feet apart. No interpolation was used on the 1955 map because the individual contour lines were surveyed in this part of the quadrangle. The radial profiles obtained from both maps are the same, and show that the fan segments have constant slopes for several miles.

A survey of topographic maps of other areas in California and in Nevada has also shown that segmented alluvial fans in western Fresno County are by no means unique. Slopes of many other California fans are segmented also as is illustrated in figure 55 which shows some common types of radial profiles. The dots represent altitudes from topographic maps. The profile of the San Antonio Canyon fan was drawn on the same radial line used by Krumbein (1937, fig. 5). Most of the profile of the fan was prepared from a topographic map with a 5-foot contour interval whereas Krumbein used a map with a 50-foot contour interval. The upper and lower segments are straight, but the middle segment is concave as is shown by the chord and the extended lines of the straight segments. The upper seg-

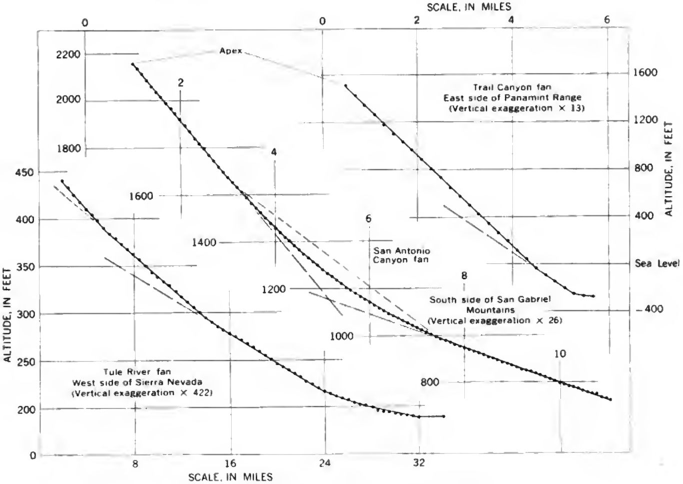

FIGURE 55.—Types of radial profiles of alluvial fans in California.

ment of the San Antonio Canyon fan has a gradient that is constant through a decrease in altitude of 500 feet in 2 miles. The base of the fan merges with other alluvial deposits near the Puente Hills. The Trail Canyon fan has a radial profile that is virtually a straight line except for a small straight-line segment of lesser slope near the toe of the fan, which merges with the old lakebed of Death Valley. The radial profile of the Tule River fan consists mainly of straight-line segments also, but the lowest part of the fan, where it merges with the deposits of Tulare Lake, has a concave profile. The angular relation between any two adjacent straight segments is indicated by extending the trace of the lower segment upslope; the curvature of the curving segment is indicated by a chord.

The profiles are subjective to the extent that different people will draw slightly different lines through the same set of control points. The author has tried to keep the profiles simple by not breaking curves into a large number of short straight segments and by averaging gently undulating slopes with straight lines rather than depicting them in detail as a series of convex and concave curves.

Vertical exaggeration is necessary to show clearly the segmented shape of the radial profiles. Steep fans such as the Trail Canyon fan require little exaggeration (13 times), but gentle fans such as the Tule River fan require much exaggeration (422 times).

A detailed study of the Tumey Gulch fan in western Fresno County shows that the angular relations and the length of the segments vary from one side of the fan to the other but that the overall profiles are very similar. Eight radial profiles of this fan are shown in figure 56 and the locations of the profiles are shown in figure 57. Each profile has three straight-line segments, and the angle between the upper and middle segments is larger than the angle between the middle and lower segments.

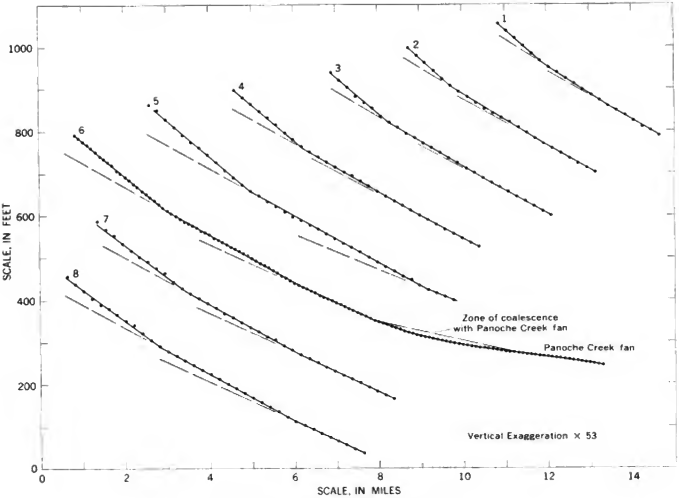

FIGURE 56.—Radial profiles of the Tumey Gulch fan.

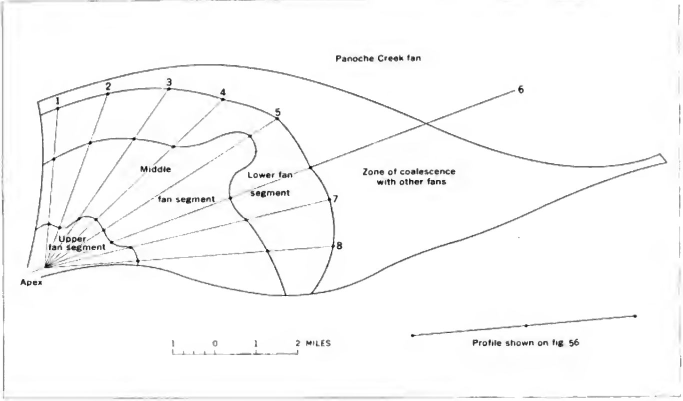

Figure 57.—Segments of the Tumey Gulch fan.

Profile 6 has been extended onto the Panoche Creek fan. The zone of coalescence between the Tumey Gulch and Panoche Creek fans for profile 6 is concave, but the profiles of the coalescence zone for half of the radial profiles (not shown in fig. 56) are straight. Most of the radial profiles in this paper show the topographic profile of a specific alluvial fan but not the profiles of zones of coalescence of two alluvial fans.

The radial profiles of figure 56 show two dimensions of the fan segments and the map of the Tumey Gulch fan in figure 57 shows the third dimension of the three fan segments. The general shape of the boundaries between the fan segments is concave toward the apex, and the upper segments have lobate tongues extending downslope.

The boundaries between the fan segments of the Capita Canyon fan (fig. 72) show that the same general features exist for this small fan. The boundaries between the fan segments cross the contour lines at a large angle, and the lobate tongue of the upper fan segment centers about the present-day stream channel.

If the upper fan segment of the Capita Canyon fan continues to spread downslope, the adjacent lower fan segment may be overlapped. Part of the lower fan segment of the Tumey Gulch fan was almost overlapped by the middle segment in the vicinity of profile 5 (figs. 56, 57).

Radial profiles near medial radial lines were drawn for 12 fans whose streams head in the foothill belt, all were found to have three straight-line segments. Radial profiles for six of these fans are shown in figure 58. (See pl. 7 for location.) Only a half or one-third of the control points are shown for most of the profiles. The average slope of the upper segments is 1°14′ (range 0°55′–1°46′); the average slope of the middle segments is 0°48′ (range 0°32′–1°14′); and the average slope of the lower segments is 0°37′ (range 0°22′–0°51′). The average angular difference between the upper and middle segments is 0°26′ (range 0°14′–0°44′); the average angular difference between the middle and lower segments is 0°11′ (range 0°4′–0°24′). The drainage-basin areas of the fans shown in figure 58 range from 2.6 square miles for Capita Canyon to 29 square miles for Tumey Gulch. Lengths of segments vary, but the lower segment of most fans is short.

The radial profile of each fan is distinct, but the fans whose drainage basins are adjacent to each other generally have roughly similar radial profiles. An example shown in figure 58 is the profiles of the Arroyo Ciervo and Arroyo Hondo fans. Other adjacent fans

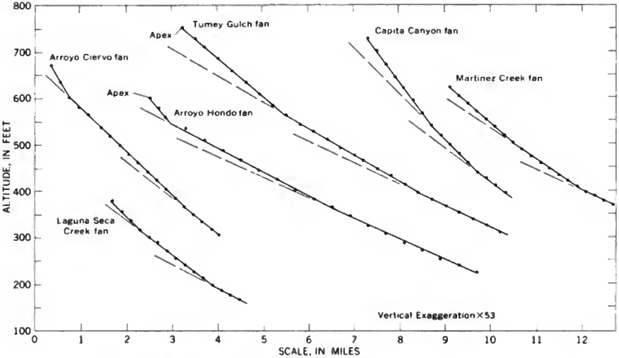

FIGURE 58.—Radial profiles of six fans whose streams head in the foothill belt.

with similar profiles, not shown in the figure, are the Martinez Creek and Domengine Creek fans, and the Capita Canyon fan and the adjacent fans to the north and south of it.

The upper segments of most of the fans are the youngest. Maps made a century ago by the General Land Office show that the stream channels were not entrenched into the upper segments of some fans. Aerial photographs show a fresh pattern of braided distributary channels on the upper fan segments as well as on the middle and lower segments, which indicates that deposition has occurred recently on most upper fan segments. The degree of soil-profile development is about the same on the upper and middle parts of most fans and cannot be used to differentiate the ages of these fan surfaces. Patches of older soils occur on the lower parts of some fans, and locally at the mountain front, where fan deposits have been warped by uplift. Charcoal from 10.5 feet below the surface of the upper fan segment of the Arroyo Hondo fan (pl. 7) gave a radiocarbon age determination of 1,040 ± 200 years before the present time (Rubin and Alexander, 1960, p. 156). The total thickness of deposits of the fan segment at this locality is estimated, by extending the slope of the adjacent fan segment, to be 24 feet. If the rate of deposition for the 24 feet is assumed to be constant, the segment has been growing for only 2,000–3,000 years.

Radial profiles of fans whose streams head in the main part of the Diablo Range have a different number of fan segments. (Compare figs. 58 and 59.) Each of the three fans has four distinct segments. The segments of the Panoche Creek fan are straight, but the uppermost segments of the Cantua Creek and Little Panoche Creek fans are slightly concave.

The Little Panoche Creek fan has two anomalous features. First, it has a steeper slope than the Cantua Creek fan, although its drainage area is twice that of Cantua Creek. Second, unlike other fans, the surface of the uppermost fan segment of the Little Panoche Creek fan is underlain by old soils that indicate that deposition has not occurred on the upper fan segment during Recent time. The history of the Little Panoche Creek fan is discussed in detail on pages 106–109.

The Panoche Creek fan, whose basin drains 296 square miles of the Coast Ranges, is the most gently sloping fan in the area studied. The slope ranges from 0°17′24″ on the uppermost fan segment to 0°8′14″ on the lowest fan segment.

Drainage-basin characteristics such as lithology and mean slope (table 1) do not seem to be related to the segmentation of a radial profile. For example, the Capita Canyon basin (67 percent mudstone, mean slope 0.50) is the source area of a fan whose radial profile (fig. 58) is similar in shape to the radial profiles (fig. 58) of the fans of the Martinez Creek basin (34 per-

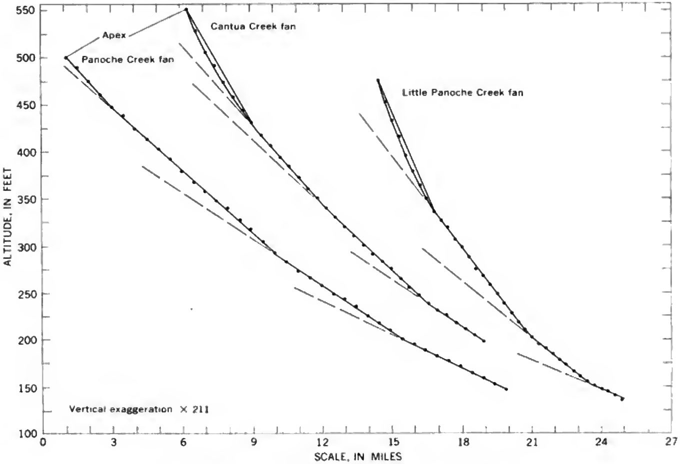

Figure 59.—Radial profiles of fans whose streams head in the Diablo Range.

cent mudstone and shale) and the Laguna Seca Creek basin (mean slope 0.20).

No consistent relation between the grain-size distribution of the fan deposits and fan segmentation has been found. Grain-size analyses of 200 surface and subsurface samples show a general decrease in maximum and median grain sizes and an increase in clay content in the downslope direction (Bull, 1964). The grain-size distribution of a particular area of a fan is influenced greatly by the periods of fanhead trenching that allow deposition to start from various points on the upper and middle parts of the fan.

RELATION OF STREAM AND FAN-SEGMENT GRADIENTS

Alluvial fans and their drainage basins are hydrologic units that function as open systems, and climatic or tectonic changes in the drainage basins affect the rate, mode, and locus of deposition on the fans. The gradient of a stream and of its fan tend to attain a steady state or equilibrium, and are sensitive to changes in the drainage basin. This tendency is important in considering the possible causes of fan segmentation.

In the area studied, steep fans form at the mouths of canyons having steep longitudinal profiles, and the gently sloping fans form at the mouths of valleys having gentle longitudinal profiles. This general relation also occurs in the White Mountains of California and Nevada where Kesseli and Beaty (1959, p. 10) have noted that "* * * the steepness of the alluvial fans is in direct relation to the steepness of the mountain canyons providing the debris out of which they are constructed."

In western Fresno County, the slope of the valley floor upstream from the apex of a fan and the upper fan segment are virtually the same. In fact, the upper fan segments and the valleys for a distance of ½–1 mile upstream from the apex have the same general slope. Of 10 valleys, 5 of them have slightly lower gradients above their apexes than their upper fan segments and 5 have slightly higher gradients than the upper fan segments. The average difference in slope is 0°10′ (range in difference, 0°3′–0°17′), which is only half the average difference in slope between the uppermost and the adjoining downslope segments of the same fans.

On most fans the slope of the upper fan segment and of the valley upstream from it are similar even where the underlying rock type is not the same (fig. 60). The stream channel of Capita Canyon is in Cretaceous and Tertiary marine rocks and slopes slightly more than the adjacent fan segment. The stream channel of Laguna Seca Creek is in Recent alluvium and slopes slightly less than the adjacent fan segment. These two stream channels were formed after the deposition of the upper fan segments. On the other hand, the terrace deposits of an unnamed stream and Arroyo Ciervo probably were deposited during the same interval as the surficial deposits of their upper fan segments, because the fans and low terraces have the same gradients. Maps made by the General Land Office show that the terrace cutting of both these streams occurred since 1858.

The previously discussed evidence shows that near the apex of most fans, deposits have accumulated that have the same general slope as the valleys upstream from the fans. Erosion predominates in the valleys before the fans have attained the same gradients as the valleys.

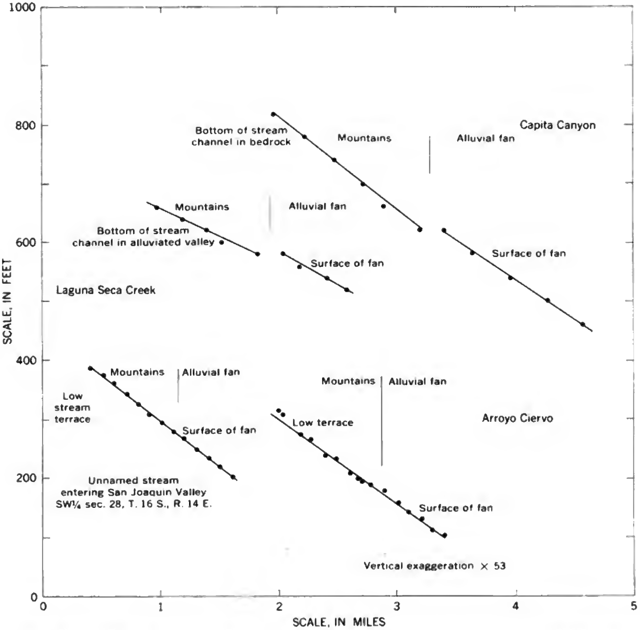

FIGURE 60.—Longitudinal profiles of two streams and two low terraces and the surface of the upper part of their alluvial fans.

After the same gradient has been attained, aggradation of the upper fan surface and stream valley maintains this common gradient—examples are the unnamed stream and Arroyo Ciervo of figure 60.

The fanhead trenches also tend to be cut down to the same gradients as adjacent lower fan segments. This adjustment of stream gradients to depositional gradients is illustrated by the gradient relations of some fanhead trenches shown in figure 61, and the same relation probably existed for the streams when the main channel ended at the top of the upper fan segment. Part of the fanhead trenches of the streams shown in figure 61 have been cut down to the same gradient as that of the adjacent lower fan segment. About a mile of the Tumey Gulch and Moreno Gulch fanhead trenches now have the same gradients as their adjacent lower fan segments, and about 5 miles of the Panoche Creek fanhead trench now has the same gradient as its adjacent lower fan segment. Most of this adjustment has occurred in the last century (fig. 77). Streams probably tend to backfill if cut to a gradient less than their adjacent lower fan segment.

The relation of the stream and fan-segment gradients is significant because it shows that the area of deposition and the stream channel upslope from it tend to maintain a uniform and common gradient. Therefore, the fan segments probably are the result of changes in stream-channel gradient that cause deposition on steeper or gentler slopes.

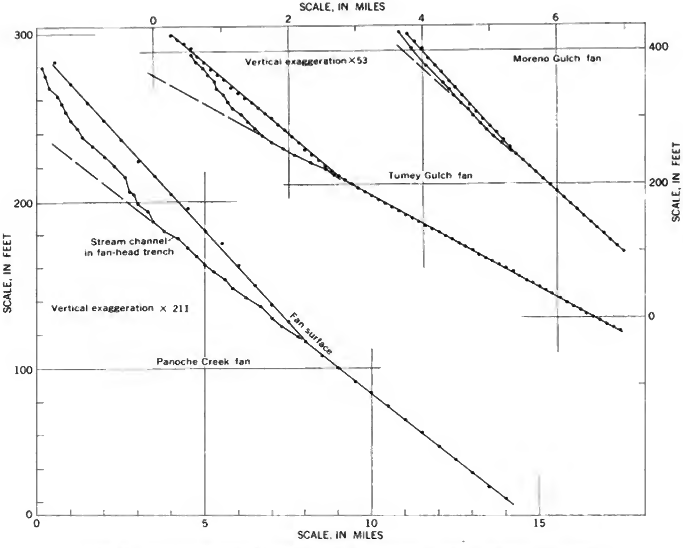

FIGURE 61.—Relation of the gradients of fanhead trenches to the gradients of their adjacent lower fan segments.

POSSIBLE CAUSES OF FAN SEGMENTATION

An explanation for the formation of segmented fans is essential to the understanding of their depositional history. Alluvial fans in western Fresno County have three to four segments which appear as straight, or rarely as slightly curving, lines on the radial profiles of the fans. The fan deposits accumulate on surfaces that have about the same gradient as the stream channel upstream from the area of deposition. Therefore, changes in the gradient of the stream channel probably have caused changes in the slope of succeeding fan segments. First, the evidence for changes in the environment of deposition will be presented, and then the possible causes of fan segmentation will be discussed.

The prominent paired, or matched, terraces of western Fresno County (Arnold and Anderson, 1910, p. 155, pl. IV–A; Anderson and Pack, 1915, p. 104–106) reflect changes in the erosional history of the drainage basins. The terraces are classified in this paper as high and low terraces. High terraces generally are more and low terraces generally less than 30 feet above the present-day stream channels. Two high terraces and one low terrace are shown in figure 62*A*. Figure 62*B* shows one pair of terraces about 100 feet above Arroyo Ciervo and a second pair of terraces, less distinct than the first, about 300 feet above the valley floor. The lower pair of terraces and the present valley floor diverge downstream. The area pictured is upstream from a zone of pronounced monoclinal folding. Paired, or matching, terraces, have a two-phase origin: first, the surface is formed by beveling or deposition; and second, the surface is entrenched by accelerated erosion. The several levels of paired terraces along the valleys indicate that the area has been rejuvenated repeatedly.

The terraces show that erosional and depositional rates have varied from time to time in western Fresno County. Changes in erosional conditions probably changed the stream gradients and the slopes of the adjacent fan deposits. The accelerated erosion that causes terracing may be due to either uplift or climatic fluctuations, or both (Bryan, 1923, p. 21–25), or to changes in base level. The entrenchment that caused the formation of many of the low terraces was caused mainly by climatic changes during the last century. (See section on "Causes of the Fanhead Trenching.") The high terraces, on the other hand, reflect tectonic changes. This is discussed on pages 106, 107.

The number of fan segments seems to be related to the number of terraces. For example, the Arroyo Ciervo fan has three segments separated by two changes in fan slope, and the drainage basin has two paired high terraces. Little Panoche Creek has four segments separated by three changes in fan slope, and the drainage basin has three paired terraces. In the following discussion, climatic, base-level, and tectonic changes will be examined as possible causes of the terracing and fan segmentation.

The alluvial fans in western Fresno County are of Quaternary age. Therefore climatic changes that affected the erosional and depositional conditions probably occurred during the formation of the fans. Extensive glaciation occurred in the Sierra Nevada during Pleistocene time, but this part of the Coast Ranges was not glaciated.

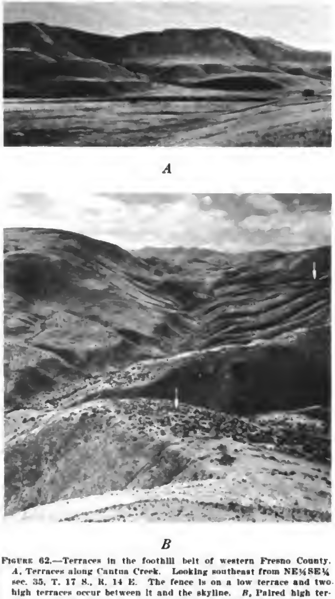

FIGURE 62.—Terraces in the foothill belt of western Fresno County. *A*, Terraces along Cantua Creek. Looking southeast from NE¼SE¼ sec. 35, T. 17 S., R. 14 E. The fence is on a low terrace and two high terraces occur between it and the skyline. *B*, Paired high terraces along Arroyo Ciervo. Looking southwest from NW¼NE¼ sec. 36, T. 16 S., R. 13 E. Arrows mark location of upper terrace.

The moisture content of some of the fan deposits, as shown by tests of core samples, provides evidence concerning possible precipitation changes in the area during fan deposition. Irrigation has produced extensive near-surface subsidence on certain fans in western Fresno County; about 125 square miles have subsided or probably would subside if irrigated. This settling of the land surface is caused by the compaction of deposits by the overburden load as the clay bond supporting the voids is weakened by water percolating through the deposits for the first time (Bull, 1964). Prior to irrigation the moisture content of these compactible deposits while in the root zone is below field capacity because plants and air remove much of the soil moisture during the hot, dry summers, reducing the moisture content to the wilting coefficient. Moisture tests (fig. 63) and the presence of near-surface subsidence indicate that these deposits continue to be moisture deficient after burial below the root zone, thus proving that water from succeeding winter rains and floods does not percolate below the root zone. The native moisture contents of these deposits represent moisture conditions that have not changed appreciably since burial below the root zone.

For example, moisture content for two 300-foot core holes in the Arroyo Hondo and Arroyo Ciervo fans are shown in figure 63. Grain-size analyses indicate that there are no major changes in lithology in the 300-foot sections. The moisture content fluctuates with depth partly because of variations in the clay content of the samples. Moisture-equivalent tests of samples from the same core holes indicate that the moisture condition of the upper 120 feet of deposits is roughly 50 percent of field capacity—about at wilting-coefficient conditions. A sharp increase in the moisture content of the Arroyo Ciervo fan deposits at about 130 feet indicates deposition under slightly wetter conditions than at present, but the deposits are still much drier than field-capacity conditions. The deficient moisture condition of these fan deposits indicates that major changes in the amount of precipitation and stream flow have not occurred during the deposition of the upper 100–200 feet of deposits, which span the time of formation of the fan segments.

An explanation of fan segmentation based on climatic change would require thick valley fills upstream from fans on which the upper segment is the youngest. In figure 64, the initial fan profile is shown (for simplicity) as a single straight line. Diagram *A* shows a fan and a stream channel upstream that have developed a common gradient. As the result of a hypothetical climatic change the stream deposits material on its bed and on the fan steepening the gradient of both surfaces (diagram *B*). In order to maintain similar fan and stream gradients, a large amount of valley filling would have to occur in conjunction with the steepened fan surface. Such a process would require more than 100 feet of valley fill less than a mile upstream from the apexes of fans such as those of Arroyo Ciervo and Tumey Gulch. The valley fill along Arroyo Ciervo is less than 20 feet thick and, along other streams that head in the foothill belt, the fill does not appear thick.

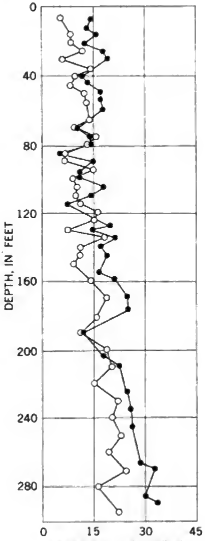

FIGURE 63.—Moisture content for core holes on the unirrigated parts of the Arroyo Hondo (○) and Arroyo Ciervo (●) fans.

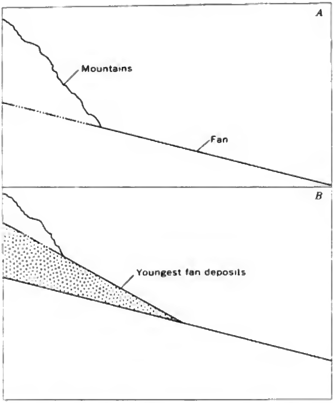

FIGURE 64.—Diagrammatic sketches showing the steepening of stream gradients due to a hypothetical climatic change.

If segmentation is caused by climatic changes, then fans with similar and adjacent drainage basins should have similar shapes. However, this is not true of fans in the area studied. The upper segment of the Tumey Gulch fan is much larger than the upper segment of the Arroyo Hondo fan. The drainage basins of the two fans have a similar size, lithology, mean slope, vegetation, and rainfall distribution. These facts indicate a similar rate of deposition and suggest that the upper segment of the Tumey Gulch fan started to form much sooner than the upper fan segment of the Arroyo Hondo fan. This, in turn, suggests that the causes of the fan segmentation did not necessarily occur over large regions at the same time.

Both regional and local base-level changes should be considered as possible causes of fan segmentation. Pleistocene lowering of sea level probably caused entrenchment of the San Joaquin River. This regional change in base level should have caused entrenchment of the streams into the fans along the west side of the San Joaquin Valley if the streams were perennial at that time. Entrenchment would steepen the stream gradients, but entrenchment also would prevent deposition on the fan. Thus, regional base-level changes apparently did not affect the development of fan segmentation.

Evidences of intermittent local base-level changes are common and are described in the next section.

TECTONIC HYPOTHESIS

The third possibility is that fan segmentation is caused mainly by tectonic changes. Parts of the mountains probably were uplifted more than 2,000 feet during and since the Coast Range orogeny. The abrupt breaks in slope between the fan segments cannot represent tectonic hinge points, however, because the segment boundaries are strongly concave toward the apexes of the fans (figs. 57, 72). This concentric distribution shows that the fan segments are depositional features instead of purely tectonic forms.

The following explanation is in accordance with the facts available from western Fresno County at the present time. In brief, terrace cutting caused by uplift of the mountains formed a steeper stream gradient, and subsequent deposition on the fan built a new fan segment at a new gradient. Repeated periods of uplift produced additional terraces and fan segments.

This explanation applies to two types of fan-segment history in western Fresno County. All the drainage basins have been uplifted, but the location of the area of maximum differential uplift (generally the mountain front) with respect to the fan apex partly determines the locus of successive stages of fan deposition. Most of the fan apexes are immediately downstream from the area of maximum differential uplift, and the stream-channel gradient upstream from the apex has become progressively steeper because downcutting has not kept pace with the uplift. Intermittent uplift associated with progressively steeper stream gradients causes fan segmentation in which the uppermost segment is the youngest, as in figure 65*A*. The second type of fan segmentation occurs where the fan apex is several miles downstream from the area of maximum differential uplift, and the stream-channel gradient upstream from the area of deposition has become progressively gentler, because the downcutting by the stream has exceeded the minor uplift in the reach immediately upstream from the apex. Intermittent uplift, or possibly climatic change, associated with progressively gentler stream gradients, causes fan segmentation in which the lowest segment is the youngest, as in figure 65*B*.

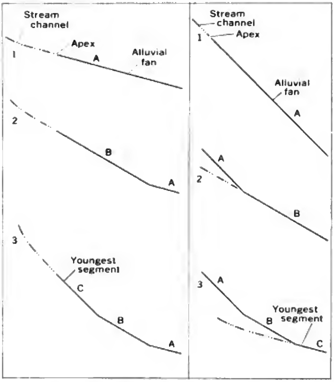

FIGURE 65.—Diagrammatic sketches showing two types of alluvial-fan and stream-gradient history. Fan associated with (*A*) has progressively steeper stream gradients and (*B*) progressively gentler stream gradients. Successive alluvial-fan surfaces A–C are shown in alphabetical order.

FANS ASSOCIATED WITH PROGRESSIVELY GENTLER STREAM GRADIENTS

Little Panoche Creek and Wildcat Canyon have fans whose uppermost segment is the oldest and whose younger segments are associated with progressively gentler stream gradients. For purposes of discussion, the Little Panoche Creek fan includes a small area near the mountain front on which some erosion has occurred. These two fans do not represent the usual occurrence in western Fresno County, because on most fans the upper segment is the youngest and because most of the fans have a history of progressively steeper gradients upstream from their apexes. Little Panoche Creek is the only stream in the area, however, that had broad terraces for which topographic maps of sufficient detail are available to allow accurate plotting of longitudinal terrace profiles. These profiles are shown in figure 66 to illustrate the relations between tectonic environment and stages of alluvial-fan deposition. A direct relation between terraces and fan segments can be shown for this type of fan.

Three prominent paired terraces occur near the mouth of Little Panoche Creek. All three are underlain by a 2- to 20-foot veneer of sand and gravel that was deposited on truncated deformed Tulare sediments. The upper terrace is dissected and much of the soil that formed in the surficial deposits has been removed by erosion. Two to four feet of caliche-cemented gravel, representing the Cca horizon (U.S. Dept. Agriculture, 1960) of a well-developed soil, commonly is found at or near the surface. The middle terrace is not extensively dissected and a moderately well developed soil has formed on the surficial deposits. The soil profile consists of 2 feet of red clayey sand and gravel that is underlain by weakly cemented calcareous material. The lower terrace is not dissected, and visible soil-profile development has not occurred. Examination of fossils[1] collected by the author from a ledge several feet beneath the Tulare dip slope (fig. 66) suggests that this part of the Tulare Formation is of Pleistocene Age. The distribution and stage of development of the terrace soils suggest that the upper and middle terraces are of late Pleistocene age and that the lower terrace is of Recent age.

Part of the tectonic history of the Little Panoche Creek drainage basin is revealed by the various surfaces shown in figure 66. Deposition of the Tulare Formation ceased in this area when the Coast Range orogeny uplifted this part of the Panoche Hills. The dip slope of the upper, or possibly the uppermost, Tulare shows a pronounced decrease in gradient near the mountain front, where gently folded Tulare beds can be seen in roadcuts.

Little Panoche Creek cut a wide valley through the hills. A period of uplift caused the stream to cut down leaving parts of the former valley floor as the upper terrace. The upper part of the fan was upwarped slightly causing it to be abandoned by Little Panoche Creek. The profile of the upper terrace (fig. 66) shows that minor anticlinal folds were superimposed on the warped surface near the mountain front where the differential uplift was greatest. Little Panoche Creek continued to cut down and then laterally during a period of little or no tectonic activity. A second period of uplift during which a narrow band of monoclinal folding occurred along the mountain front caused another stream rejuvenation, which resulted in the formation of the middle terrace. The relations of the folded and unfolded parts of the terraces indicate a differential uplift at the mountain front of 20–30 feet during each of these periods of folding.

A period of regional uplift, or possibly a climatic change, then caused the formation of the lower terrace whose smooth profile indicates that differential uplift at the mountain front did not occur. The lower terrace

---

[1] Examination made by D. W. Taylor. U.S. Geol. Survey Cenozoic fossil loc. 22692.

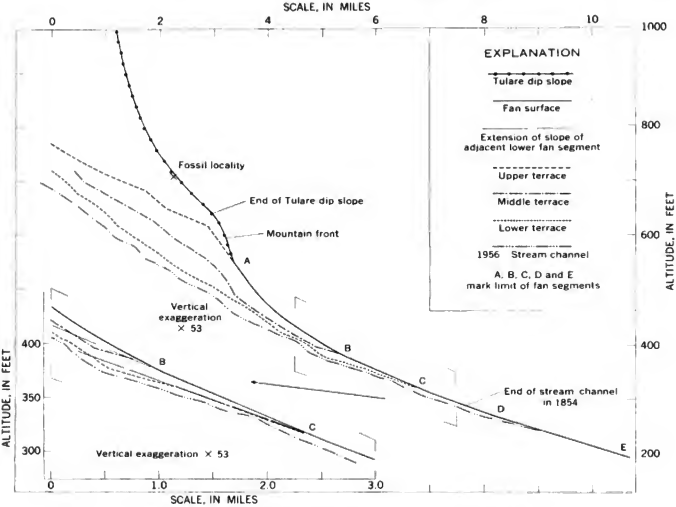

FIGURE 66.—Relation of stream terraces to fan segments for Little Panoche Creek.

converges with the stream channel downstream. Most of the convergence may be due to channel trenching caused by fluctuations in rainfall during the past century.

The longitudinal profiles in figure 66 show both divergent and convergent patterns in the downstream direction. The upper and lower terraces diverge downstream 50 feet in the first 3 miles. The divergence indicates steepening of the stream gradient by headward erosion, as the mountain front was uplifted intermittently by anticlinal and monoclinal folding.

Terrace divergence occurs upstream from the zone of maximum differential uplift, and terrace convergence occurs downstream from the zone of maximum differential uplift. Most of the terrace convergence occurs within 2 miles of the folded zone at the mountain front.

The uplifts accelerated the deepening of the stream channel, but the channel downstream from the mountain front was not uplifted appreciably. The net effect in this reach was trenching of the stream channel and extension of the end of the channel farther out on the fan. Each time this happened the area of deposition and the stream channel upstream from it developed a more gentle gradient than previously.

The slopes of the terraces are continuous with the slopes of the fan segments. The slope of the upper terrace continues onto segment A–B (fig. 66). The old mouth of Little Panoche Creek has been preserved because of an overall lateral migration to the south of this part of Little Panoche Creek. The middle terrace ends at the upslope end of fan segment B–C, and the lower terrace ends at the upslope end of the fan segment C–D. The gradient of the lower part of each terrace approximates the gradient of the adjacent lower fan segment. (See insert, fig. 66.) The soil-profile development on the fan segments and the terrace profiles both confirm that the segment nearest the mountains was formed first and that the two adjacent lower segments are younger.

The present-day stream channel ends on the upper part of the lowest fan segment (D–E), and maps made by the General Land Office show that the end of the channel in 1854 was just upslope from the upper end of this lowest segment. Thus most deposition is occurring on the lowest segment on the south side of the fan, but the stream channel is shallow and narrow enough to permit major floods to flow over the banks and deposit material on parts of the three lower segments.

Fan-segment boundaries, soil types, and selected contour lines reveal part of the history of the Little Panoche Creek fan (fig. 67). The positions of the concentric contour lines indicate that the present fan apex is 2–3 miles downslope from the mountain front (see pl. 7 for complete outline of fan) and that the old alluvial slope upstream from the apex was mainly an erosional surface. The soils data indicate a general decrease in grain size in the downslope direction. The fan-segment boundaries and the distribution of the younger alluvium (particularly the conspicuous lobes of sandy deposits) both show that most of the deposition of the younger alluvium has occurred on the north and east sides of the fan and that little deposition has occurred in the central part of the fan, where older soils and clayey younger soils predominate. The fan-segment boundaries and the areal distribution of the older and younger alluvium also indicate that the overall amount of deposition of the younger alluvium was small compared to the other fans in western Fresno County. The small amount of deposition may be due partly to the fact that the Little Panoche Creek drainage basin is the only source area studied that is underlain by a large amount of resistant Franciscan rocks.

The information shown in figures 66 and 67 can be used to reconstruct the history of the Little Panoche Creek fan. A fan-shaped alluvial slope was formed after the initial deformation of the Tulare Formation. The upper part of the slope was a small narrow erosional area, and the lower part of the slope was a large broad depositional area. The slope of the valley floor represented by the upper terrace was continuous with the upper part of the alluvial slope. Remnants of the alluvial slope are represented in figure 67 by the areas of older alluvium. The uppermost (A–B) and lowest (D–E) segments (fig. 66) were formed at this time. The uplift that caused the cutting of the upper terrace warped the uppermost segment (A–B) and determined the location of the present fan apex. The uplift also caused accelerated erosion that ultimately decreased the stream gradients in the reach upstream from the area of deposition. The fan segment B–C was deposited. Erosion that accompanied the cutting of the middle terrace caused another decrease in stream gradient in the reach upstream from the area of deposition, and the fan segment C–D was deposited at a lower gradient than that of the fan segment B–C. The segment C–D occurs on both sides of the fan which means that the stream changed position on the fan and cut through the segment B–C. Change in the position of the entrenched stream is plausible because the present-day stream channel is shallow and narrow enough at the apex to allow floods to top its banks, as it did during a flood in September, 1958, and to form natural levees such as those indicated by the 350-foot contour line of figure 67. During the deposition of the fan segments B–C and C–D, slight amounts of deposition partly covered the older alluvium on the fan segment D–E. Areas of older alluvium, however, are not exposed on the downslope part of the east side of the fan, which has been the area of principal deposition for more than a century. A new fan segment whose slope is gentler than the segment C–D and whose slope is partly controlled by the gradient of the present stream, probably is forming on this part of the fan.

The segment B–C probably had a larger areal extent formerly. Before deposition of the segment C–D, B–C would have intersected the surface of the old alluvial slope (D–E) at a point between C and D. Subsequent deposition of the fan segment C–D made an area of active deposition that probably encroached both upslope and downslope from the area where the former slopes intersected. The D fan-segment boundary line has a lobate shape that indicates downslope expansion of the fan segment. The C fan-segment boundary line, however, does not have a shape that suggests progressive overlapping by the adjacent lower fan segment.

The Little Panoche Creek fan is representative of fans whose segmentation is associated with progressively gentler stream gradients during their history. Although intermittent uplift steepened the stream gradient upstream from the mountain front, the fan apex was 2–3 miles downslope from the mountain front, and the successive areas of deposition were downstream from reaches of progressively gentler stream gradients. Each new stage of fan deposition was farther downslope and on a more gentle gradient than the previous stage.

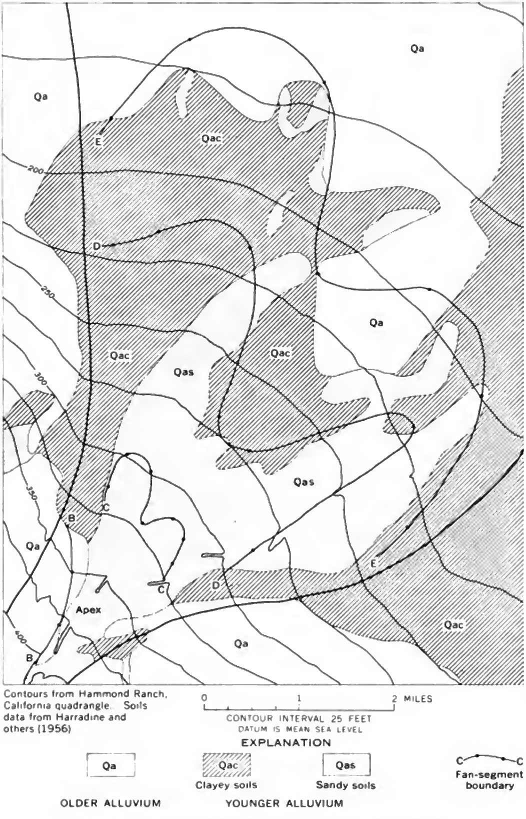

Contours from Hammond Ranch, California quadrangle. Soils data from Harradine and others (1956)

FIGURE 67.—Soils and fan-segment boundaries of the Little Panoche Creek fan.

FANS ASSOCIATED WITH PROGRESSIVELY STEEPER STREAM GRADIENTS

Most of the fans studied show a sequence of fan-segment development that is reversed from the Little Panoche Creek fan—their uppermost segments are the youngest and their lowest segments are the oldest. The youngest terrace (or stream channel of a century ago) has a slope that is continuous with the upper fan segment (fig. 60). Before the current period of fan-head trenching, the areas of most active deposition were just downstream from the mountain front. The tectonic history of most of the drainage basins is similar to that of the Little Panoche Creek basin, except that the upper parts of the fans have not been warped appreciably. The gradients of the streams above the apexes have become progressively steeper, as is shown by the downstream terrace-gradient divergence upstream from the mountain front in figure 66. In contrast, the apex of the Little Panoche Creek fan is 2–3 miles downslope from the mountain front, and the reach upstream from the area of deposition has been intermittently decreased in gradient.

Figure 68 shows diagrammatically four successive stages in the development of a single fan segment, for a fan whose upper segment is the youngest. In profile A the fan and stream channel for a short distance upstream from the apex have developed a common gradient. This equilibrium then is destroyed by rapid monoclinal folding along the mountain front, which raises the valley bottom about 40 feet, steepening the stream gradient (profile A′). The deformation induces trenching headward from the mountain front (profile B) leaving parts of the uplifted stream channel as paired terraces. The terraces probably were continuous with prior fan surfaces which have since been buried by the deposits of younger fan segments. A substantial increase in the rates of erosion and deposition results in the rapid accumulation of sediments on the fan, particularly on its upper part, where the emergent stream enters a reach characterized by a reduction in gradient. In profile C, erosion has deepened the valley and deposition raised the fan surface until a common gradient has again been attained. The fan surface now has two segments which appear as straight lines on the radial profile. Deposition continues on the fan, and the valley upstream from the apex is aggraded in order to maintain a common gradient (profile D). The upper fan segment is extended farther onto the fan, and the change in slope moves from Y to Z. Most of the deposition has occurred on the upper fan segment, but enough deposition occurs on the rest of the fan to prevent the formation of well developed soil profiles.

The above discussion postulates that a fan segment that appears as a straight line on a radial profile may be the result of rapid uplift of the drainage basin followed by a time of little or no uplift, during which the stream channel and fan attain a common slope. A fan segment that appears concave may represent the case in which a fan surface has not had sufficient time to develop a constant slope after a period of rapid uplift. (See profile B, fig. 68). A concave surface also could be the result of a period of gradual continuing uplift. During a period of continuous uplift the stream gradient would gradually steepen and the depositional slope of the fan also would become progressively steeper.

The segmented fans of western Fresno County indicate at least three or four episodes of uplift of the different parts of the Diablo Range rather than continuous uplift of the entire range. The profiles differ a little from fan to fan, indicating differences in the times and amounts of uplift and rates of erosion in their respective structural areas and drainage basins. Part of the uplift probably occurred in the last 3,000 years, as is indicated by the Arroyo Hondo radiocarbon date.

Alluvial fans whose drainage basins are in a different tectonic setting than that of western Fresno County are those along the southern border of the San Joaquin Valley, about 100 miles to the southeast of the area studied. Figure 69 shows the strikingly similar radial profiles of two large alluvial fans whose drainage basins head in the San Emigdio Mountains. These two profiles are markedly different from the radial profiles of western Fresno County fans because they have pronounced concave middle segments. The geologic environment of the two areas is similar in many respects. Both have similar climate and drainage-basin characteristics.[2] The Santiago Creek drainage basin has a total relief of 5,080 feet, and the rocks exposed in the drainage basin consist of 90 percent sedimentary rocks and 10 percent metamorphic and plutonic rocks. The San Emigdio Creek basin has a total relief of 7,330 feet, and the rocks exposed in the drainage basin consist of 40 percent sedimentary rocks and 60 percent metamorphic and plutonic rocks. Terraces that diverge downstream are common upstream from the mountain front (McGill, 1951, pl. 2).

The major difference between the San Emigdio Mountains and the Diablo Range is in their structural history and tectonic setting. The Diablo Range has been formed by anticlinal and monoclinal folding, and by minor faulting. The main part of the San Emigdio

---

[2] Drainage basin information for the fans heading in the San Emigdio Mountains from J. M. Parsons, Calif. Dept. Water Resources (oral communication, July 1961).

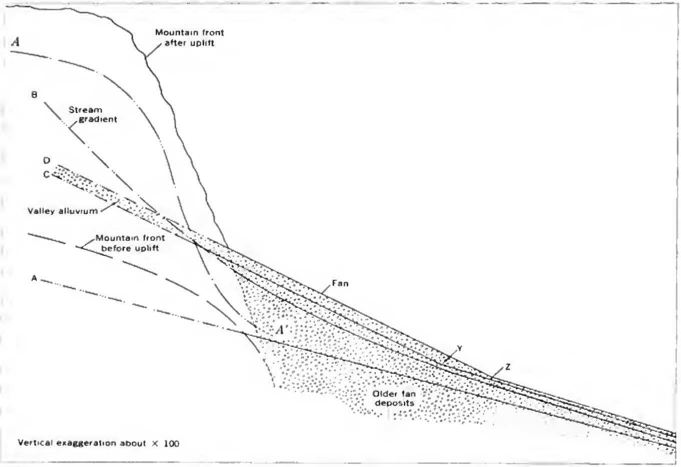
Mountain front after uplift
A
B
Stream gradient
D
C
Valley alluvium
Mountain front before uplift
A
Fan
A'
Y
Z
Older fan deposits
Vertical exaggeration about × 100

FIGURE 68.—Diagrammatic sketch showing stages of fan-segment development.

Mountains is characterized by thrust faulting and tight asymmetric folds that lean toward the San Joaquin Valley. The marked difference in radial profiles of the two fans on the northern side of the San Emigdio Mountains as compared to those for fans in western Fresno County is ascribed by the author to the different tectonic history of the two source areas.

Large changes in slope between fan segments presumably indicate greater uplift and steepening of the valley upstream from the apex than do small changes in fan slope. Uplift in western Fresno County has been mainly as monoclinal and anticlinal folding. The valley slopes could not have been made much steeper than the fan slopes if there had been a similar fault-block tilting of the mountains and fans; such fans there would have little or no segmentation. An example is the Trail Canyon fan (fig. 55) on the east side of the Panamint Range. Eastward tilting of this part of the Panamint Range and Death Valley has been described by Greene and Hunt (1960). On the west side of the Panamint Range, by contrast, some of the valley slopes have been steepened more than the fan slopes, and the segmentation of these fans is more pronounced.

Some stages of alluvial-fan development for fans whose upper segment is the youngest are summarized in figure 70. A stream channel and fan have developed a common gradient as shown in diagram 1, figure 70. Uplift steepens the stream gradient and the new fan deposits are laid down with a steeper gradient. The stream channel gradient may have been steeper after the uplift, but the slopes in diagram 2 represent equilibrium conditions near the end of the stage. Another period of uplift makes the third segment, completing a three-segment fan. Deposition continues on the fan and the stream channel upstream from the fan apex maintains the same slope as the fan by aggrading slightly (diagram 4). A temporary period of channel trenching occurs (diagram 5) and the low terrace and upper fan segment have a common slope. The downstream end of the fanhead trench has the same gradient as the adjacent lower fan segment. Valley alluviation and stream entrenchment (diagrams 4 and 5) may occur several times during the development of a fan as is

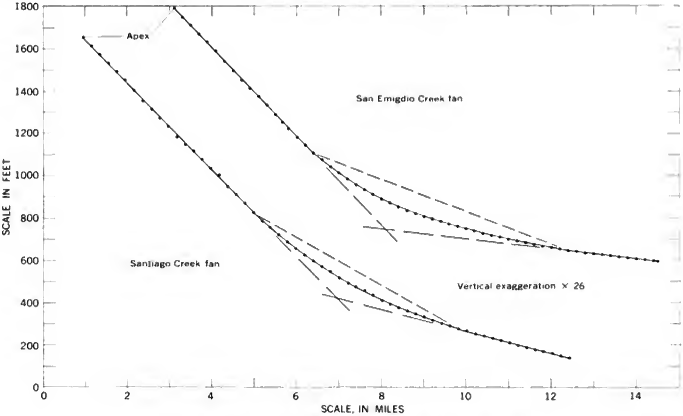

FIGURE 69.—Radial profiles of the San Emigdio Creek and Santiago Creek fans.

shown by old terrace and channel patterns on aerial photographs. Deposition probably was occurring mainly on the upper segment a century ago, but channel trenching then caused deposition to occur mainly on the middle segment as the end of the channel moved downslope (diagram 5). Present-day deposition is restricted to the area downslope from the first or second fan segment of most fans.

When an area becomes tectonically stable, permanent trenching of the fans occurs as the mountains are eroded and the streams cut below the fan apexes. Erosion gradually removes the deposits that are higher than the main channels, and the fans become alluviated slopes that are characterized by large areas of erosion as well as areas of deposition. Such slopes are common in the Basin and Range Province of California and Nevada.

Fan segmentation should be helpful in deciphering part of the tectonic and erosional history of the drainage basins of other mountain ranges. Fans are formed adjacent to a mountain front after uplift, and renewed uplift that causes progressive steepening of the stream gradients will keep the principal loci of deposition close to the mountain front. Segmentation on such fans can be attributed chiefly to tectonic causes and the youngest fan segment will be adjacent to the mountain front. If renewed uplift does not occur the stream will cut downward establishing progressively gentler gradients, and the locus of principal deposition will be progressively farther downslope from the fan apex. If it is not segmented the fan may have a smooth concave profile. Fan segmentation associated with progressively gentler stream gradients is common, however, and can be attributed to climatic as well as tectonic causes. In western Fresno County this type of fan history (Little Panoche Creek fan) can be shown to have been caused chiefly by uplift of the mountains several miles upstream from the present fan apex. However, many segmented fans in the Basin and Range Province of California and Nevada also have surficial deposits that are older near the mountains and younger near the base of the fan. Climatic changes during fan deposition should be considered as a possible dominant cause of the progressive decrease in stream gradient and associated segmentation of many of the basin and range fans.

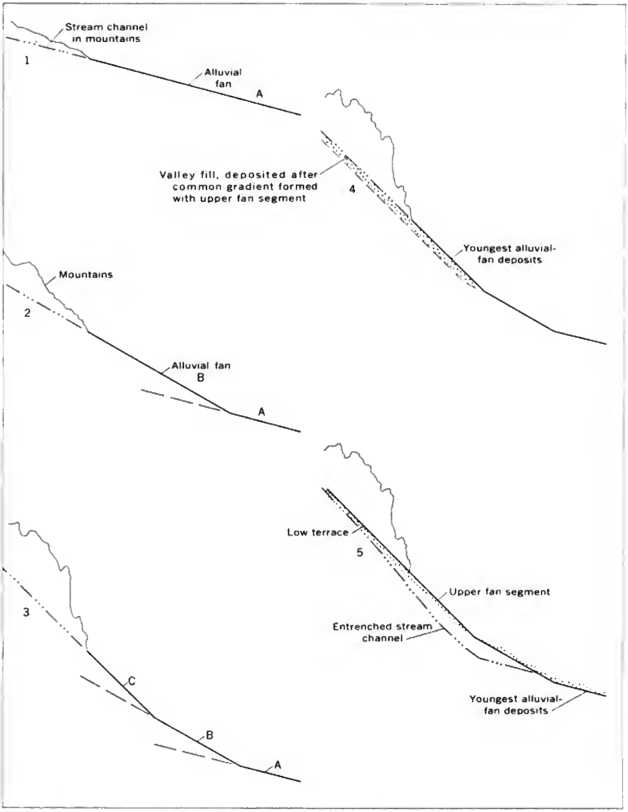
Stream channel in mountains
1
Alluvial fan
A
Valley fill, deposited after common gradient formed with upper fan segment
4
Youngest alluvial-fan deposits
Mountains
2
Alluvial fan
B
A
Low terrace
5
Upper fan segment
Entrenched stream channel
Youngest alluvial-fan deposits
3
C
B
A

FIGURE 70.—Diagrammatic sketches showing stages of alluvial-fan development. Successive alluvial-fan surfaces A–C are shown in alphabetical order.

CROSS-FAN PROFILES

Cross-fan profiles parallel to the mountain front show the convexities of the alluvial fans (figs. 73, 74). The amount of convexity depends on where the profile is drawn and on the coalescing of adjacent fans. The convex shape of a series of cross-fan profiles shows that an alluvial fan is part of a gently sloping cone. The central part of the fan generally is higher than the sides because of greater deposition on the central part.

Stream channels control the place of deposition, and the present-day channel deviation from the medial position on the fanheads of 75 fans is shown in figure 71. The distribution of channel deviation is fairly uniform from the medial position to a deviation of about 50°, but two-thirds of the channels are within 30° of the medial position. Only three channels have a deviation of more than 50°. Thirty-nine streams have an average deviation toward the northwest of 26°, and 35 streams have an average deviation toward the southeast of 23° The predominance of stream channels within 30° of the medial position implies that more deposition occurs there than in areas farther from the medial position which are not frequented as often by streams.

CHANGE IN SHAPE DOWNSLOPE

The progressive downslope decrease in the convexity of cross-fan profiles is well illustrated in the area. The fans of Capita, Chaney Ranch, and Marca Canyons are described as examples (figs. 72 and 73). The respective drainage areas for these fans are 2.6, 0.53, and 1.9 square miles. The fan of Chaney Ranch Canyon is small and coalesces with the other fans within 2 miles of the mountain front.

The Capita Canyon fan excellently displays features characteristic of many fans whose streams head in the foothill belt. The convexity of the upper part of the fan (downslope to profile *D–D'*) stands out clearly, as shown by the conspicuous curvature of the contour lines. The downslope decrease in convexity is well shown by the progressive straightening of the contour lines toward the base of the fan. The depth of the fanhead trench decreases markedly downslope from the upper fan segment and the stream channel becomes a distributary channel that is about 2 feet deep.

The six cross-fan profile lines *A–A'* through *G–G'* are spaced at half-mile intervals except for the quarter-mile spacing between *A–A'* and *B–B'* (figs. 72 and 73). The profiles across the lower parts of the fans are flat compared to the profiles across the upper parts of the fans. The decrease in the convexity of the cross-fan profiles progressively farther from the mountain front occurs much as would be expected in a series of profiles drawn progressively farther from the apex of part of a true cone.

STREAM CHANNELS

Leopold and Wolman (1957) described three characteristic channel patterns of rivers: braided, meandering and straight. A braided channel is characterized by the repeated division of the channel around islands of alluvium; a meandering stream has a series of regular looplike bends; a straight channel has little or no curvature.

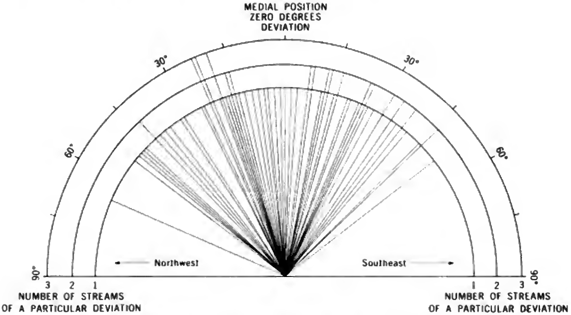

FIGURE 71.—Channel deviation from medial position on fanheads of alluvial fans in parts of Fresno and Merced Counties.

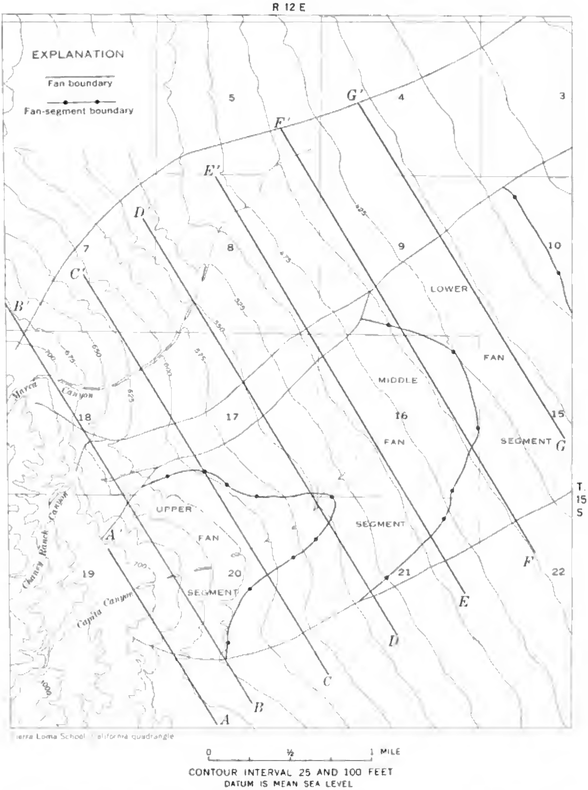

FIGURE 72.—Topographic map of the alluvial fans of Capita Canyon, Chaney Ranch Canyon, and Marca Canyon. Profiles *A–A'* to *F–F'* are shown in figure 73.

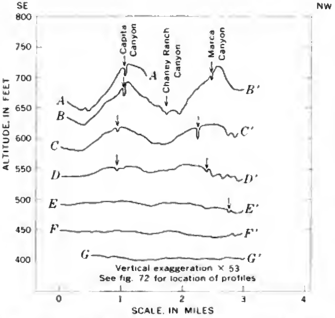

FIGURE 73.—Cross-fan profiles of Capita Canyon, Chaney Ranch Canyon, and Marca Canyon fans. Vertical exaggeration × 53. See figure 72 for location of profiles.

All three of these channel patterns are common on the fans in western Fresno County. The most common channel pattern of the fanhead trenches is the meandering type, as illustrated by Panoche Creek. (See fig. 79.) Panoche Creek also has some relatively straight sections of channel, and straight channels are common on the alluvial fans of ephemeral streams. (See Capita Canyon, fig. 72). In the straight sections, the thalweg, or the deepest part of the channel, generally weaves back and forth between the channel banks. This also occurs on straight stretches of perennial streams (Leopold and Wolman, 1957, p. 53–55). The braided channel pattern is characteristic of the distributary channels downslope from the end of the fanhead trenches but is not present in the fanhead trenches themselves.

A cross-fan profile drawn about parallel to the east edge of the Panoche Hills, and less than a mile from the hills, is show in figure 74. The stream channels are commonly on the highest parts of the fans, but they may be on any other part of a fan, as shown by the arrows in figure 74. Streams, such as the one occupying Gres Canyon, deposit so little material that they remain at the bottom of the trough formed by two adjacent large fans. The fans have a variety of cross-sectional shapes, many of which reflect the influence of the size and shape of adjacent fans. The profile between mileage markers 1–4 on the line of the section is representative of an area where several fans have coalesced.

The main channels of some of the streams do not flow at right angles to the contours of the fan. The stream channels of Marca Canyon (fig. 72, secs. 17, 18) and part of the channel of Arroyo Hondo are examples of these streams. Arroyo Hondo apparently is migrating sideways toward the downslope side of the channel; at the present time the downslope bank is 7–12 feet high in contrast to the 2- to 4-foot bank on the upslope side from which the channel has moved. These anomalous positions of stream channels may have been started by the entrenchment of a minor channel. Once such an entrenchment is started, natural levees tend to be concentrated on the lower side of the channel. The entrenchment of the channel and the formation of natural levees temporarily prevent the stream from breaking out of its channel and flowing directly down the slope. Natural levees of this type are shown by the contour lines along parts of the stream of the Marca Canyon fan (fig. 72, secs. 8, 17).

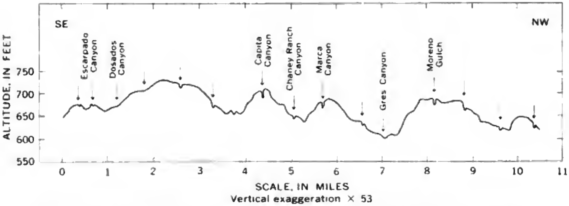

FIGURE 74.—Position of stream channels on the fanheads of the piedmont plain east of the Panoche Hills.

Natural levees are a common feature on most fans in the area. Many natural levees were formed before the recent entrenchment of the streams, and natural levees are being made along the shallow reaches of the channels at the present time. Figure 75 shows mudflow deposits on the natural levees of Arroyo Hondo. The channel was shallow enough for the mudflow to flow over the banks and spread out to add another increment to the natural levees. Bushes helped to keep the deposition within 100 feet of the channel in most places. Natural levees along the intermittent streams are made of water-laid sediments that probably were deposited as the velocity of flow decreased after the stream left the main channel. Natural levees about 3–5 feet high are shown in figure 79 along the downslope part of Panoche Creek in the NW¼ sec. 10 and the NE¼ sec. 20, T. 14 S., R. 13 E.

FANHEAD TRENCHES

The stream channel of almost every fan in the area is entrenched into the upper part of the fan. The fanhead trenches of the ephemeral streams are narrow and the fanhead trenches of the intermittent streams are wide. The sides of these incised channels in many places are nearly vertical walls. The depth of the fanhead trenches decreases away from the mountains, and eventually the channel splits into several distributary channels.

Fanhead trenches are a natural feature of alluvial fans, and traces of abandoned trenches can be found on several fans. The present cycle of arroyo cutting already had started on some fans when the first land survey was made in the early 1850's. Later surveys and the accounts of some of the first settlers show that channel trenching started on other fans in the period between 1875 and 1885. This date is about the same as the time of the channel trenching in parts of Arizona, Utah, Colorado, and New Mexico (Bryan, 1925). Cattlemen and sheepherders who have lived 30–40 years in the area agree that much of the deepening of these channels has occurred since about 1935, although the channels on most of the fans had their present areal extent by 1930.

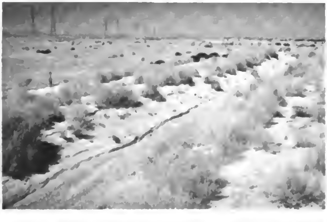

FIGURE 75.—Mudflow deposits on the natural levees of Arroyo Hondo. Arrow marks outer edge of mudflow. View northwest from the SW¼SE¼ sec. 2, T. 17 S., R. 14 E.

Many of the fanhead trenches are terraced. Tumey Gulch has scattered remnants of paired terraces 7–20 feet above the present channel, and Arroyo Hondo has 3- to 5-foot terraces, which are paired in some places. Paired terraces are excellently preserved in the fanhead trench of Arroyo Ciervo, where a narrow slot about 8–15 feet wide has been cut 5–9 feet deep into the bottom of the first-stage fanhead trench to form the terrace. The channels of the large intermittent streams are flanked by broad terraces 3–10 feet above present stream grade. Most fanhead terraces have been formed since about 1935.

The fanhead trench of Tumey Gulch a mile from the edge of the foothills is shown in figure 76. At this point the channel is 37 feet below the surface of the fan. The bushes along one side of the channel indicate the location of a narrow terrace remnant. The original land surveys show that Tumey Gulch had the same extent and position in 1854 as it does today, but in 1854 the channel was shallow enough for the surveyors to walk across as they chained the section lines.

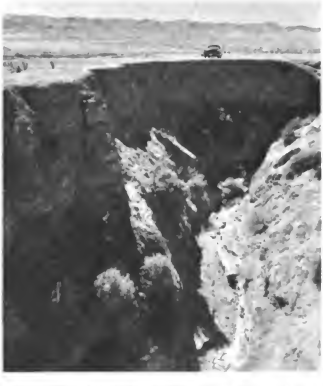

FIGURE 76.—The fanhead trench of Tumey Gulch looking upstream from SW¼SW¼ sec. 29, T. 15 S., R. 13 E.

The changes in the depth of Tumey Gulch between 1921 and 1955, based on data from topographic maps, are shown in figure 77. The fanhead trench terminates at the downslope end of the upper fan segment. The shallow channel shown in the middle fan segment is one of several distributary channels. In 1921 the fanhead trench was as much as 20 feet deep. By 1955 the upslope part of the trench was partly filled, but in places the trench was deeper than 30 feet and the deepest part was moving upstream. More than a mile of the downslope end of the 1955 trench is a continuation of the slope of the middle fan segment. Similar fanhead-trench and fan-gradient relations exist for other fans (fig. 61).

Figure 78 shows the changes in the depth of the fanhead trench of Arroyo Ciervo between 1921 and 1956. The 1858 maps do not show a gully, but the 1880 mapping reveals that a gully extended to the downslope end of the upper fan segment. Topographic maps show the 1921 channel to be 4–6 feet deep and the 1955 channel to be as much as 26 feet deep. Most of the channel deepening between 1921 and 1956 occurred within the upper fan segment and, like the channeling in Tumey Gulch, the deepening increases upstream. The channel entrenched in the Arroyo Ciervo fan differs from that in the Tumey Gulch fan because it extends downslope past the upper segment.

Unlike the channel widths of ephemeral streams, which apparently have not changed much since first reported, the channel widths of the intermittent streams have increased from about 20 to several hundred feet during the past 100 years. The pairs of numbers in figure 79 show changes in the width of Panoche Creek between 1854 and 1959. Many sections of the channel are from two to six times wider than they were in 1854. The lines of measurement along which the width was measured generally are not perpendicular to the stream channel because the surveyors in 1854 noted the channel widths between section corners; therefore the 1959 measurements also were made along section lines.

The length and depth of the channel of Panoche Creek also have changed since 1854. The fanhead trench was 5 miles long in 1854 and 10 miles long in 1959, and the channel has been deepened by erosion in some places as much as 25 feet.

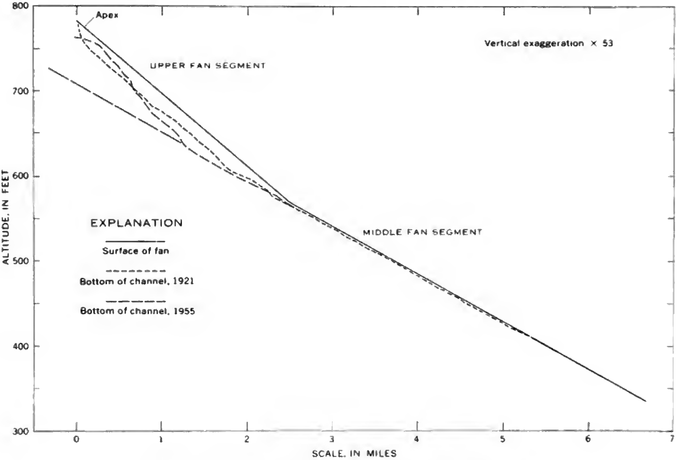

FIGURE 77.—Changes in the depth of the Tumey Gulch fanhead trench, 1921–55.

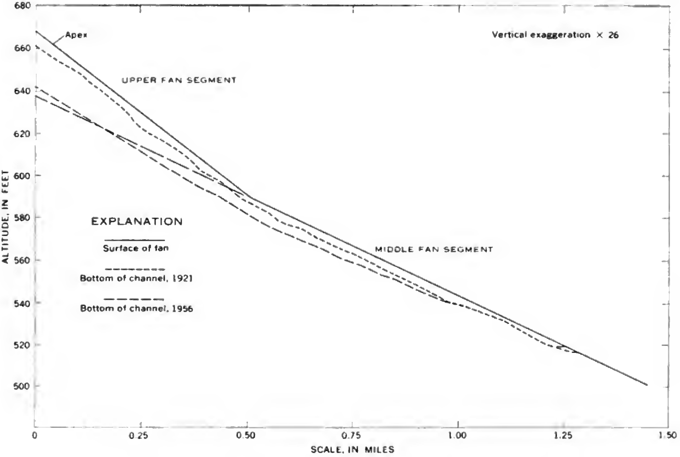

FIGURE 78.—Changes in the depth of the Arroyo Ciervo fanhead trench, 1921–56.

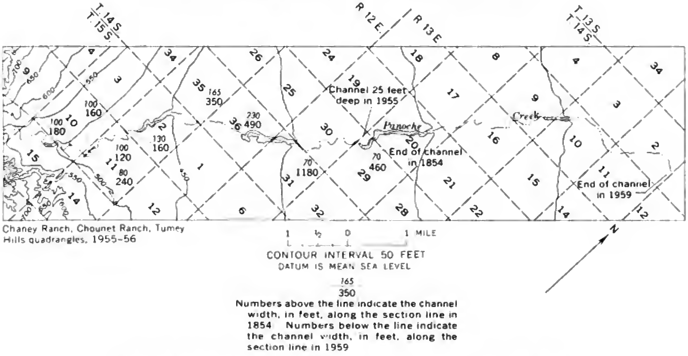
T. 14 S.
T. 15 S.
R. 12 E.
R. 13 E.
T. 13 S.
T. 14 S.
Channel 25 feet deep in 1955
Panoche
Creek
End of channel in 1854
End of channel in 1959
165
350
230
490
100
160
100
180
130
160
100
120
80
240
70
1180
70
460
Chaney Ranch, Chounet Ranch, Tumey Hills quadrangles, 1955–56
1 ½ 0 1 MILE
CONTOUR INTERVAL 50 FEET
DATUM IS MEAN SEA LEVEL
N
165
350
Numbers above the line indicate the channel width, in feet, along the section line in 1854. Numbers below the line indicate the channel width, in feet, along the section line in 1959

FIGURE 79.—Changes in the width and length of the Panoche Creek fanhead trench, 1854–1959.

The changes in the channel of Panoche Creek are less noticeable on the uppermost fan segment than on the second fan segment away from the hills. The average depth of the channel on the uppermost segment is less than on the second segment, and the width of the channel on the uppermost segment has increased

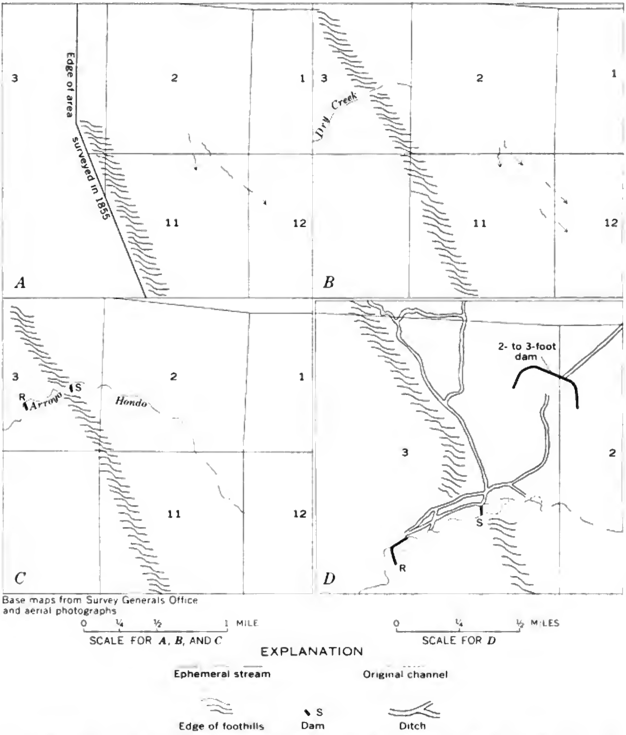

FIGURE 80.—Changes in the channel configuration of Arroyo Hondo, 1855–1954. *A*, 1855; *B*, 1881; *C*, 1924 and 1954; *D*, 1954.

from about one to three times the 1854 width, but the channel width on the second segment has increased from about 2.0 to 17 times the 1854 width.

Some of the changes in Arroyo Hondo (Dry Creek on the 1881 map) since 1855, based on maps made in 1855, 1881, 1924, and 1954, are shown in figure 80. Sometime between 1890 and 1924 the name "Dry Creek" was changed to Arroyo Hondo, which is Spanish for "deep stream," possibly because the channel had been deepened, not only on the alluvial fan but also along the valley in the foothills. In 1855 the entrenched stream either did not exist or it did not extend more than one-quarter of a mile into the valley. Figure 80*A* shows two channels on the Arroyo Hondo fan. These may have been deep parts of some braided distributary channels on the fanhead rather than principal channels. By 1881 a more noticeable channel had formed along the valley of Arroyo Hondo and this channel extended about 0.4 mile onto the fanhead. The distributary channels are still present, but now one is shown to be discontinuous and the other apparently has a new downstream extension. The stream channel had its present position in 1924 and appears to be an extension of the channel near the foothills to the distributary channels farther downslope.

The letters R and S in figure 80*C* and 80*D* mark the location of dams built in 1890 and 1907 respectively. The dams diverted the flow of the stream into ditches which were used by the early settlers to carry water out to the valley. The original channel downstream from these dams is preserved; immediately downstream from dam R it is about 9 feet deep and downstream from dam S about 16 feet deep. In 1959 the channel was 27 feet deep adjacent to dam R and 25 feet deep adjacent to dam S showing that the stream channel had deepened 18 feet adjacent to dam R since 1890 and deepened 9 feet adjacent to dam S since 1907.

Aerial photographs of the fan of Moreno Gulch taken in 1940 showed three deep discontinuous gullies, apparently similar to those on the Arroyo Hondo fan in 1881. Small fans were at the downslope end of the three gullies and at the end of the main channel of Moreno Gulch. Farming of the land prevented the discontinuous gullies from becoming a continuous channel. Entrenched streams apparently have formed from discontinuous gullies in other semiarid regions (Bryan, 1928, p. 279–281; Leopold and Miller, 1956, p. 29–33; Schumm and Hadley, 1957).

CAUSES OF THE FANHEAD TRENCHING

Channel trenching has been ascribed by most authors to periods of increased runoff during which floods deepened stream channels. The increased runoff has been attributed to the removal of vegetation by overgrazing and to climatic fluctuations.

Accelerated erosion in the southwestern States was ascribed to overgrazing by Rich (1911), Bailey (1935), and Thornthwaite, Sharpe, and Dosch (1942). On the other hand, Gregory (1917, p. 132) said that some parts of Arizona not used for grazing present the same features as the areas that were overgrazed. Leopold (1951a) studied the vegetation of several areas in the southwest that had been photographed between 1895 and 1903 and again between 1937 and 1946. He concluded that better quality forage might have been available in some spots at the turn of the century, but his general impression was that there has been little change in the volume of growth during the 50-year interval and therefore that grazing was not a primary cause of arroyo cutting.

It is unlikely that overgrazing was the dominant factor in starting the channel trenching in western Fresno County, because traces of older gullies on some fans indicate that fanhead trenches existed before sheep were brought into California in 1853 and before large-scale cattle ranching was introduced in western Fresno County. Adolph Domengine (oral communication, August 1959), a rancher, said that there are more stock now than in the 19th century because feed and water can be brought in now to support the herds during dry years.

Severe reduction in vegetation might increase the runoff to the streams and perhaps Bryan (1928, p. 281) was close to the truth when he said that "* * * the introduction of livestock and the ensuing overgrazing should be regarded as a mere trigger pull which timed a change about to take place."

Variation in the intensity and amount of rainfall is the most likely regional cause for the fanhead trenches. Richardson (1945, p. 17) and Antevs (1952, p. 382) stated that vegetation is the immediate factor controlling erosion which in turn is controlled by precipitation.

The precipitation records of five U.S. Weather Bureau stations were examined to determine if trends in the amount of rainfall coincided with the times of fanhead trenching. These weather stations are: New Idria in the Diablo Range; Coalinga in a sheltered valley adjacent to the San Joaquin Valley; Mendota Dam station in the trough of the San Joaquin Valley; Fresno on the east side of the San Joaquin Valley; and Sacramento in the southern Sacramento Valley. Their locations and altitudes are shown in figure 81.

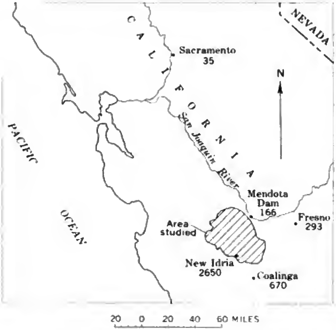

FIGURE 81.—Index map of central California showing location and altitude, in feet, of weather stations referred to in this report.

The trends of the annual rainfall (Weather Bureau climatic year July 1–June 30) at the five stations are shown in figure 82; second order moving averages were used to remove minor irregularities in the curves. The patterns of rainfall at the stations are similar despite the variety of physiographic settings and the distances between stations. This similarity suggests that cyclonic storms that move southeastward across the Pacific coast are a common source of rainfall for all the stations. Annual rainfall decreases generally from north to south and increases with an increase in altitude. The New Idria station, at an altitude of 2,650 feet, receives only slightly less rain than the Sacramento station 150 miles to the north at an altitude of 35 feet.

The period of highest rainfall, well defined at all the stations, was between 1935 and 1945. Although several peaks of excessive rainfall between 1850 and 1910 are shown on the Sacramento record, the broadest highest peak occurred in the general period 1875–95. The Fresno record shows highs during the same time interval. The 1875–95 and 1935–45 intervals coincide with the two periods of fanhead trenching reported since 1854. This conclusion contrasts with the work of Thornthwaite, Sharpe, and Dosch (1942) and Leopold (1951b) who, in their discussions of accelerated erosion in the southwest, suggested that there is no significant relation between annual precipitation and periods of arroyo cutting.

Leopold (1951b) pointed out that the New Mexico records show significant trends in the number of rains of a given size group. He showed that between 1850 and 1870 there was a decrease in the annual number of rains of 0.01–0.49 inch in a day, and he pointed out that this decrease would weaken protective vegetation such as summer grasses. This, combined with a high frequency of large rains at some stations, apparently contributed to the accelerated erosion. The trends of the daily rainfall size classes of California stations were analyzed in about the same way as Leopold treated the New Mexico data.

Figure 83 shows the trends of some daily rainfall size classes at Sacramento. Rainfall of 0.01–0.24 inch per day would promote the growth of grasses but would provide little runoff. The number of rains in this size class was at its lowest level for the years between 1881 and 1900 and about average between 1935 and 1945. Between 1875–95 and 1935–45 the number of days of rainfall of more than 0.50 inch were among the highest on record. These heavy rains would produce above-normal runoff to erode the stream channels. Again, the years that had a high frequency of large daily rainfall coincide with the times of known arroyo cutting in western Fresno County. A comparison of figures 82 and 83 shows that periods of large annual rainfall were also periods of more than the usual number of large daily rainfalls. This suggests that in this region years of high annual rainfall coincide with years of abnormally large numbers of large daily rainfalls.

Mendota Dam is the only station in western Fresno County for which daily rainfall records are available as far back as 1900. The trend in the amounts of daily rainfall are shown in figure 84. Daily rainfalls greater than 0.50 inch are not as common at Mendota Dam as at Sacramento. The period between 1930 and 1945 shows the same general characteristics as the Sacramento record except that there was a high frequency of daily rainfalls in the 0.01–0.24-inch-size class as well as a marked increase in the 0.50–0.99-size class. The pronounced peak in the 0.50–0.99-size class coincides with the period of high annual rainfall and with the time at which channel deepening was known to have occurred.

The rainfall analyses offer a reason for the arroyo cutting that began on some streams about 1880. The periods of most of the arroyo cutting (1875–95, 1935–45) also were periods of above-normal daily and annual rainfall. A combination of a high frequency of the large rainfalls and a low frequency of the small rainfalls coincided to produce above-normal runoff and less vegetation, thus allowing the above-normal runoff to erode the stream channels. Once started, channels probably became semipermanent although they may

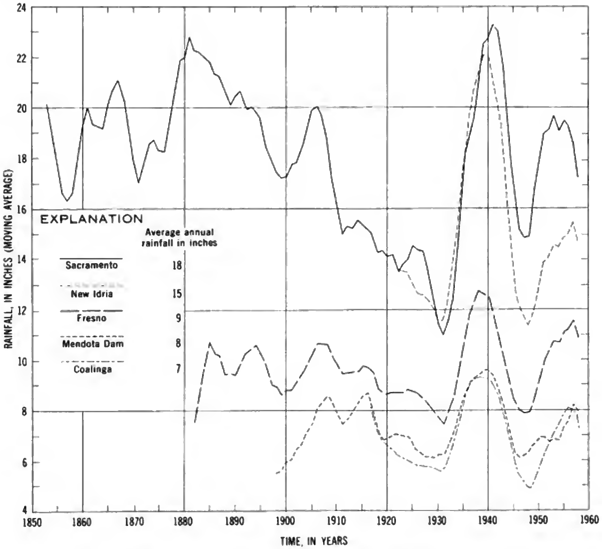

FIGURE 82.—Trends of annual rainfall for five stations in California, 1853–1958.

have been partly filled with deposits during dry periods such as 1920–35 and 1945–52. Figures 83 and 84 show a low frequency of large rainfalls during dry-year periods and therefore few large runoffs to keep the channels scoured of the material deposited in them by small amounts of runoff. About 1935 the channels began to be deepened again, coincident with another period of high frequency of large daily rainfalls. Renewal of channel entrenchment resulted in the terraces within the fanhead trenches.

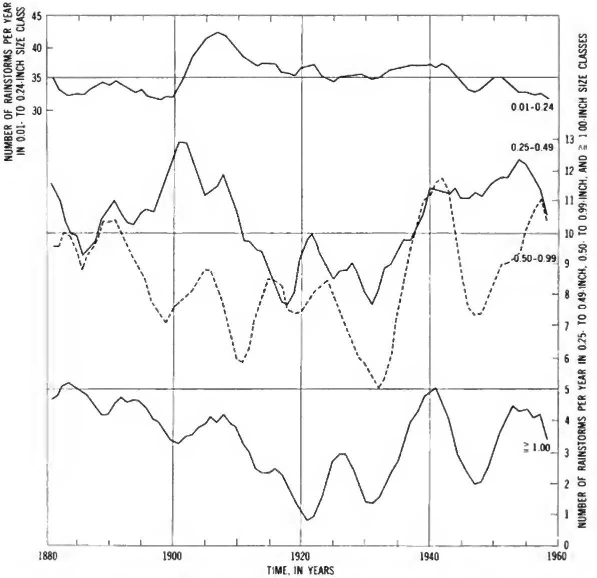

FIGURE 83.—Trends of daily rainfall size classes, 1881–1958, Sacramento, Calif.

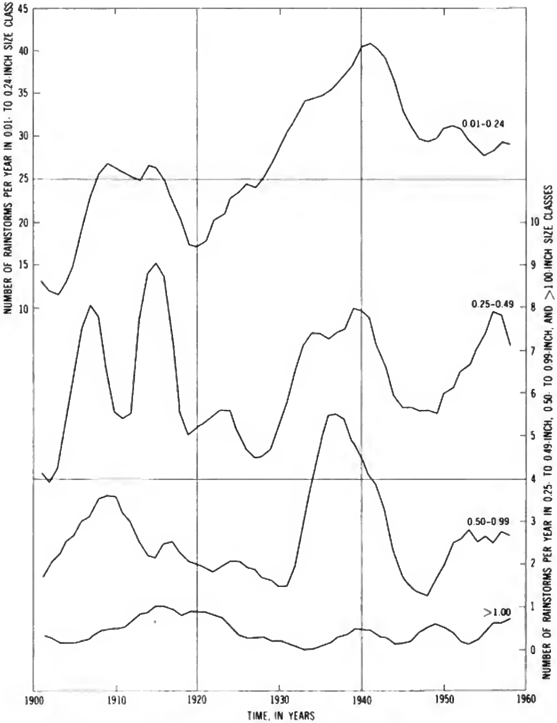

FIGURE 84.—Trends of daily rainfall size classes, 1901–58, Mendota Dam, Calif.

SUMMARY AND CONCLUSIONS

Between the trough of the San Joaquin Valley and the Diablo Range in western Fresno County is a belt of coalescing alluvial fans 12–19 miles wide. The shapes, areas, slopes, and histories of deposition of the individual fans reflect a tendency toward a state of equilibrium, or balance, among a complex set of controlling factors, which include the area, lithology, mean slope, and vegetative cover of the drainage basin; slope of the stream channel; climatic and tectonic environment; and the geometry of the adjacent fans and the depositional basin itself. Changes in one or more of these factors will tend to cause a readjustment of the fan morphology.

The fans are derived from drainage basins that are generally similar with respect to topography, climate, and tectonic environment but that range in size from 0.2 to 296 square miles and in lithology from predominantly sandstone to predominantly mudstone or shale. The fan slopes range from 10 feet per mile near the base of the larger fans to 150 feet per mile near the apexes of some small fans. Fans derived from mudstone or shale-rich basins are generally 35–75 percent steeper than fans of similar area derived from sandstone-rich basins, and roughly twice as large as fans derived from sandstone basins of comparable size. These facts indicate that the volume of fan deposits derived from the two rock types differs; presumably the difference can be attributed mainly to the greater erodibility of the mudstone and shale.

The equations expressing these relations between fan area, A_f, drainage-basin area, A_d, and fan slope, S_f, are as follows. Drainage basins underlain by 48–86 percent mudstone and shale:

$$A_f = 2.4A_d^{0.88}$$
$$S_f = 0.023A_d^{-0.16}$$
$$S_f = 0.034A_f^{-0.28}$$

Drainage basins underlain by 58–68 percent sandstone:

$$A_f = 1.3A_d^{0.98}$$
$$S_f = 0.022A_d^{-0.32}$$
$$S_f = 0.025A_f^{-0.34}$$

The overall radial profiles of the alluvial fans are gently concave, but the slopes do not decrease at a uniform rate downslope from the apexes. Instead, the radial profiles of most of the fans consist of several straight-line segments. The surfaces represented by these segments form bands of approximately uniform slope that are, in most cases, concentric about the fan apexes. The fans whose streams head in the foothill belt have three segments, each of which has a constant slope. The fans of streams that head in the main Diablo Range have four segments. The three lower segments have constant slopes, but two fans have uppermost segments that are concave.

The changes in fan slope are associated with changes that have occurred in the slope of the stream channel upstream from the fan apex. Longitudinal profiles of terraces show that intermittent uplift has changed the slope of the stream channels upstream for most fan apexes. The slope of the area of deposition and the slope of the stream channel upstream from it tend to be the same. Therefore, changes in the stream-channel slope caused by intermittent uplift have caused changes in the slope of the succeeding depositional surfaces and thus have produced the fan segmentation.

Most of the fans are associated with stream channels that have become steeper as a result of the intermittent uplift. Each time the channel was steepened the succeeding fan deposits formed a new fan segment of steeper slope that was deposited on the upper part of the preexisting fan.

The Little Panoche Creek fan, however, has a history that is associated with progressively gentler stream-channel gradients, because the rate of downcutting by the stream has exceeded the average rate of uplift of the reach immediately upstream from the apex. The intermittent character of the uplift resulted in the cutting of a series of paired terraces which preserve a record of the deformation of the mountain front and fanhead areas. With each uplift, the end of the deepened stream channel moved farther down the fan. After each episode of trenching, the lower part of the stream channel and its adjacent area of fan deposition ultimately attained a more gentle gradient than previously.

Progressive trenching and extension of the downslope end of stream channels would occur also in tectonically stable areas. In such cases the overall fan profile—including upper reaches long since abandoned as areas of deposition—might be expected to show a smooth curvature, as the result of a gradual and continuous flattening of gradients and downslope migration of the locus of deposition. Under these circumstances all but the uppermost edge of any given constant-slope fan segment would be covered and obliterated by subsequent downslope deposition at progressively flatter gradients. In the case of the Little Panoche Creek fan, however, intermittent uplift and accompanying channel trenching repeatedly caused rapid downstream displacement of the locus of deposition. In this manner the intervening part of the preexisting fan slope was preserved, together with a set of paired terraces which terminates at the upslope end of the fan segment that was receiving deposits when the terrace cutting started.

Fan segmentation is useful for deciphering part of the tectonic history of some mountain ranges, and in certain cases, segmentation may be an indicator of climatic change, because the fan profile and the relative age of the fan segments reflect part of the erosional and tectonic history of the drainage basin.

The stream channels of the alluvial fans may be braided, straight, or meandering. Some of the channels are not perpendicular to the contours of the fan. Natural levees are a typical feature along intermittent and ephemeral stream channels, where streams have flowed over their banks occasionally to deposit sediment as the flows spread out and decreased in velocity.

Reports of early settlers, old maps, and field evidence indicate that two periods of fanhead trenching, apparently unrelated to tectonic activity, have occurred since 1854, when many fans were receiving deposits near their apexes.

The trenches generally have a maximum depth of 20–40 feet, and commonly terminate at the downslope ends of fan segments. The downslope part of many of the trenches tends to be eroded down to the same slope as the adjacent lower fan segment.

The fanhead trenching occurred principally during two periods of exceptionally high annual rainfall; one from about 1875 to 1895 and the other from about 1935 to 1945. These periods of high annual rainfall were also periods of high frequency of large daily rainfalls and about average frequency of the small daily rainfalls. Most of the small daily rainfalls would be absorbed by the soil to support vegetation that would tend to check erosion, but the larger rains would furnish the large runoff required to erode the stream channels.

Relict fanhead trenches, nearly obliterated by filling and bank slumping, may be seen on several fans, indicating that relatively short-term cycles of trenching and backfilling of the main stream channel may be a typical morphogenetic response to short-term climatic oscillations.

REFERENCES CITED

Anderson, Robert, and Pack, R. W., 1915, Geology and oil resources of the west border of the San Joaquin Valley north of Coalinga, California: U.S. Geol. Survey Bull. 603, 220 p.

Antevs, E., 1952, Arroyo-cutting and filling: Jour. Geol., v. 60, p. 375–386.

Arnold, Ralph, and Anderson, Robert, 1910, Geology and oil resources of the Coalinga district, California: U.S. Geol. Survey Bull. 398, 354 p.

Bailey, R. W., 1935, Epicycles of erosion in the valleys of the Colorado Plateau Province: Jour. Geol. v. 43, p. 337–355.

Bailey, T. L., 1943, Late Pleistocene Coast Range orogenesis in southern California: Geol. Soc. America Bull., v. 54, p. 1549–1568.

Blackwelder, Eliot, 1931, Desert plains: Jour. Geology, v. 39, p. 133–140.

Blissenbach, Erich, 1954, Geology of alluvial fans in semiarid regions: Geol. Soc. America Bull., v. 65, p. 175–189.

Bryan, Kirk, 1923, Geology and ground-water resources of the Sacramento Valley, California: U.S. Geol. Survey Water-Supply Paper 495, 285 p.

——— 1925, Date of channel trenching in the arid Southwest: Science, v. 62, p. 338–344.

——— 1928, Historic evidence on changes in the channel of Rio Puerco, a tributary of the Rio Grande in New Mexico: Jour. Geology, v. 36, p. 265–282.

Bull, W. B., 1964, Alluvial fans and near-surface subsidence in western Fresno County, California: U.S. Geol. Survey Prof. Paper 437–A (in press).

Drew, Frederick, 1873, Alluvial and lacustrine deposits and glacial records of the upper Indus basin: Geol. Soc. London Quart. Jour., v. 29, p. 441–471.

Eaton, J. E., 1928, Divisions and duration of the Pleistocene in southern California: Am. Assoc. Petroleum Geologists Bull., v. 12, p. 111–141.

Eckis, Rollin, 1928, Alluvial fans in the Cucamonga district, southern California: Jour. Geology, v. 36, p. 224–247.

Greene, G. W., and Hunt, C. B., Observations of current tilting of the earth's surface in the Death Valley, California, area: Art. 124 *in* U.S. Geol. Survey Prof. Paper 400–B, p. B275–B276.

Gregory, H. E., 1917, Geology of the Navajo country, Arizona: U.S. Geol. Survey Prof. Paper 93.

Harradine, F. F., and others, 1956, Soil Survey of the Mendota Area, California: U.S. Dept. Agriculture, ser. 1940, no. 18, 96 p., soil map 1:63, 360.

Kesseli, J. E., and Beaty, C. B., 1959, Desert flood conditions in the White Mountains of California and Nevada: U.S. Army Quartermaster Research and Engineering Command, Tech. Rept. EP–108, 107 p.

Krumbein, W. C., 1937, Sediments and exponential curves: Jour. Geology, v. 45, p. 577–601.

Leopold, L. B., 1951a, Vegetation of the southwestern watersheds in the nineteenth century: Geol. Rev., v. 41, p. 295–316.

Leopold, L. B., 1951b, Rainfall frequency: An aspect of climatic variation: Am. Geophys. Union Trans., v. 32, p. 347–357.

Leopold, L. B., and Miller, J. P., 1956, Ephermeral streams—hydraulic factors and their relation to the drainage net: U.S. Geol. Survey Prof. Paper 282–A, 37 p.

Leopold, L. B., and Wolman, M. G., 1957, River channel patterns: braided, meandering and straight: U.S. Geol. Survey Prof. Paper 282–B, p. 39–84.

McGill, J. T., 1951, Quaternary geology of the north-central San Emigdio Mountains, California: California Univ. at Los Angeles, unpub. thesis.

Putnam, W. C., 1942, Geomorphology of the Ventura region, California: Geol. Soc. America Bull., v. 53, p. 691–754.

Reed, R. D., and Hollister, J. S., 1936, Structural evolution of southern California: Tulsa, Oklahoma, Am. Assoc. Petroleum Geologists, 157 p.

Rich, J. L., 1911, Recent stream trenching in the semiarid portion of southwestern New Mexico, a result of removal of vegetation cover: Am. Jour. Sci., v. 32, p. 237–245.

Richardson, H. L., 1945, The significance of terraces due to climatic oscillation: Discussion: Geol. Mag., v. 82, p. 16–18.

Rubin, Meyer, and Alexander, Corrinne, 1960, U.S. Geol. Survey radiocarbon dates V: Am. Jour. Sci. Radiocarbon Supp., v. 2, p. 129–185.

Schumm, S. A., and Hadley, R. F., 1957, Arroyos and the semiarid cycle of erosion: Am. Jour. Sci., v. 255, p. 161–174.

Stille, Hans, 1936, Present tectonic state of the earth: Am. Assoc. Petroleum Geologists Bull., v. 20, p. 849–880.

Taliaferro, N. L., 1943, Geologic history and structure of the central Coast Ranges of California: California Div. Mines Bull. 118, p. 119–163.

Thornthwaite, C. W., Sharpe, C. F. S., and Dosch, E. F., 1942, Climate and accelerated erosion in the arid and semiarid southwest, with special reference to the Polacca Wash drainage basin, Arizona: U.S. Dept. Agr. Tech. Bull. 808, 134 p.

Tolman, C. F., 1909, Erosion and deposition in the southern Arizona bolson region: Jour. Geology, v. 17, p. 136–163.

Trowbridge, A. C., 1911, The terrestrial deposits of Owens Valley, California: Jour. Geology, v. 19, p. 706–747.

U.S. Dept. Agriculture, 1960, Soil classification, a comprehensive system, 7th approximation: Soil Survey Staff, Soil Conserv. Service, 265 p., 44 figs., 6 tables.

INDEX

[Italic page numbers indicate major references]

Page

- Alluvial fans 89, 99
  - area 92
    - relation to drainage-basin area, lithology *94*
  - boundaries 90, 94
  - cross-fan profiles *114*
  - definition v
  - deposits 89
    - lithology 100, 104
    - moisture content 104
  - radial profiles *94*
    - definition v
    - of streams heading in foothill belt *97*
  - segmentation. *See* fan segments.
  - slope 92
    - concepts of previous investigators 94
    - relation to drainage-basin area, lithology *94*
  - zone of coalescence 98, 116
- Alluvial slopes 108, 112
- Apex, definition v
- Arroyo Ciervo, drainage basin and fan characteristics 92, 99
  - fanhead trenching *118*
  - moisture content of deposits 104
  - terraces 101, 103
  - valley fill, amount of 104
- Arroyo Hondo, drainage basin and fan characteristics 92, 99, 105
  - fanhead trenching *120*
  - moisture content of fan deposits 104
  - natural levees 117

- Braided distributary channels, definition v

- Cantua Creek 90
  - drainage basin and fan characteristics 92, 100
  - terraces 103
- Capita Canyon, cross-fan profiles *111*
  - drainage basin and fan characteristics 92, 99
  - terraces 103
- Capita Canyon, cross-fan profiles *111*
  - drainage basin and fan characteristics 92, 99
  - fan segmentation *98*
- Chaney Ranch Canyon, drainage basin and fan characteristics 92
- Ciervo Hills 90
- Climatic changes 91, 122
  - effect on erosion of stream channels *122*
  - effect on fan segmentation *108*
- Coast Range orogeny 93
- Cross-fan profiles *114*
  - change in shape downslope 114
  - definition v

- Death Valley region fans *96*, 111
- Diablo Range *90*, 110

- Domengine Creek, drainage basin and fan characteristics 92, 99
- Dosados Canyon, drainage basin and fan characteristics 92
- Drainage basin 90
  - area 92
    - relation to fan area, slope *94*
  - definition v
  - mean slope 92, 99
  - percentage mudstone and shale 92
    - relation to fan area, slope *94*, 99
  - total relief 92
  - vegetation 92

- Ephemeral stream 90
  - definition v
- Escarpado Canyon, drainage basin and fan characteristics 92

- Fan segments, as indicators of tectonic history *105*
  - causes of fan segmentation *108*
  - concentric distribution 98, 105
  - decreasing slope *94*, 99, 110
  - definition v
  - relation of stream and fan-segment gradients *100*
  - relative age 99, *105*
  - uniform slope *94*, 110
- Fanhead trenches *117*
  - causes of trenching *120*
  - definition v
  - history of trenching *118*

- General Land Office surveys 90, *117*
- Glossary v
- Gres Canyon, drainage basin and fan characteristics 92

- Intermittent stream *90*
  - definition v

- Laguna Seca Creek, drainage basin and fan characteristics 92, 99
- Little Panoche Creek 91
  - alluvial-fan history *108*
  - drainage basin and fan characteristics 92, 100
  - fan segmentation *99*
  - lithology of fan *108*
  - terraces *102*
    - relation to fan segments *107*

- Marca Canyon, cross-fan profiles *114*
  - drainage basin and fan characteristics 92
- Martinez Creek, drainage basin and fan characteristics 92, 99
- Moreno Gulch, drainage basin and fan characteristics 92

- Natural levees *116*
- Near-surface subsidence 104

- Panoche Creek 90
  - drainage basin and fan characteristics 92, 100
  - fanhead trenching *118*
- Panoche Hills 90, 93
- Piedmont plain, definition v

- Radial line, definition v
- Radiocarbon date of fan deposits 99
- Rainfall *91*
  - annual trends *120*
  - daily trends *122*

- Salt Creek, drainage basin and fan characteristics 2 92
- San Antonio Canyon fan *96*
- San Emigdio Creek fan *110*
- Santiago Creek fan *110*
- Soils, profile development 99, 105
  - relative ages 99, *108*
- Stratigraphy 92
- Stream channels 116
  - deviation from medial position 114
  - gradients, relation to fan segments *100*, *105*
    - relation to tectonic activity *105*
  - patterns 114, 116

- Tectonic activity 93
  - amount of 93, *105*
  - effect on stream gradients and fan morphology *105*
  - variation of *110*
- Terraces, Arroyo Ciervo 103
  - Cantua Creek 103
  - high, mode of formation 103, 106
  - Little Panoche Creek 106
  - longitudinal profiles, diverging and converging 107
  - low 101, 117
    - mode of formation *122*
  - relation of terraces to fan segments *106*
- Thalweg, definition v
- Trail Canyon fan *96*, 111
- Tulare Formation 93
  - deformation of 93, 106
  - fossil locality 106
- Tule River fan *96*
- Tumey Gulch, drainage basin and fan characteristics 92, 105
  - fan segmentation *97*
  - fanhead trenching *117*

- Wildcat Canyon, drainage basin and fan characteristics 92

Clastic Sedimentation in Deep Springs Valley California

By LAWRENCE K. LUSTIG

EROSION AND SEDIMENTATION IN A SEMIARID ENVIRONMENT

GEOLOGICAL SURVEY PROFESSIONAL PAPER 352-F

A study of the bolson environment and the
formation of alluvial fans

U.S. DEPARTMENT OF THE INTERIOR
March 3 1849

UNITED STATES DEPARTMENT OF THE INTERIOR

STEWART L. UDALL, *Secretary*

GEOLOGICAL SURVEY

Thomas B. Nolan, *Director*

For sale by the Superintendent of Documents, U.S. Government Printing Office
Washington, D.C. 20402

CONTENTS

Page
Abstract 131
Introduction 132
Acknowledgments 133
Physical Setting 133
  Geography 133
    Location and topography 133
    Drainage 133
    Alluvial fans 134
    Vegetation 134
    Climate 135
      Precipitation 135
      Temperature 137
      Winds 137
  Summary of Geology 137
    Aspects of Pleistocene Geology 140
Basic Data 141
  Clastic sediments 145
  Largest particles 145
  The pebble fraction 145
  The granule-to-clay fraction 149
    Granules 149
    Silt and clay 154
    Parameters of the size distribution 156
      Mean size 156
      Standard deviation 158

Page
Basic Data—Continued
  The granule-to-clay fraction—Continued
    Parameters of the size distribution—Continued

      Skewness 158
      Kurtosis 160
      Summary of size-distribution parameters 162
    Clay mineralogy 162
Sediment Transport 165
  Competence considerations 165
  Distribution of estimated tractive force 167
  Directions of sediment transport 167
Channels on alluvial fans 170
Cause of trenching 174
  Tectonic explanation 175
  Tractive-force explanation 175
Contrast between the modern and former processes 176
  Mudflows 176
  The former process 177
  Frequency of precipitation 179
Process rates 180
Formation of the alluvial fans 182
  The evolutionary hypothesis 182
  The equilibrium hypothesis 182
  The climatic hypothesis 183
References 190

ILLUSTRATIONS

PLATE 8. Generalized geologic map of Deep Springs Valley, Calif ..... In pocket
9. Map and profile of the active channel on the Antelope Springs fan ..... In pocket

FIGURE 85–89. Aerial photographs:

Page
  85. Antelope Springs fan 135
  86. Southeastern part of Deep Springs Valley 136
  87. Wyman-Crooked Creeks fan 137
  88. Paiute Chute 138
  89. Crystal Peak reentrant 139
90. Map showing sampling stations in the north end of Deep Springs Valley 142
91. Map showing sampling stations on the Antelope Springs fan 143
92. Graph showing the relation of maximum particle size to slope at stations in the north end of Deep Springs Valley 146
93. Graph showing the relation of maximum particle size to slope at stations on the Antelope Springs fan 147
94. Map showing mean pebble size in the north end of Deep Springs Valley 148
95. View of a shallow wash in the Crystal Peak area 149
96. Map showing mean pebble roundness in the north end of Deep Springs Valley 150
97. Map showing pebble lithology in the north end of Deep Springs Valley 151
98. View of the basalt mass and small fan at the base of Piper Mountain 152
99. Map showing the distribution of granules in the north end of Deep Springs Valley 153
100. Map showing silt:clay ratios and the inferred wind track in the north end of Deep Springs Valley 155
101. Map showing the mean size of the granule-to-clay fraction in the north end of Deep Springs Valley 157
102. Graph showing the relation of the mean size of the granule-to-clay fraction to distance from the fan apex in the Antelope Springs channel 158

Page
FIGURE 103. Map showing the standard deviation of the granule-to-clay size fraction in the north end of Deep Springs Valley ... 159
104. Graph showing the relation of the standard deviation of the granule-to-clay size fraction to distance from the fan apex in the Antelope Springs channel ... 160
105. Map showing the skewness of the granule-to-clay size fraction in the north end of Deep Springs Valley ... 161
106. Graph showing the relation of the skewness of the granule-to-clay size fraction to distance from the fan apex in the Antelope Springs channel ... 162
107. Map showing the kurtosis of the granule-to-clay size fraction in the north end of Deep Springs Valley ... 163
108. Graph showing the relation of the kurtosis of the granule-to-clay size fraction to distance from the fan apex in the Antelope Springs channel ... 164
109. Three-component diagram showing montmorillonite : illite : kaolinite and (or) chlorite ratios for 43 clay samples ... 164
110. Lateral view of the upper reach of the Owens Valley mudflow ... 166
111. View downstream in the upper reach of the Owens Valley mudflow ... 166
112. Map showing estimated tractive force and inferred sediment transport paths in the north end of Deep Springs Valley ... 168
113. Map showing estimated tractive force and inferred sediment transport paths on the Antelope Springs fan ... 169
114. Map showing the distribution of estimated tractive force on Paiute Chute ... 170
115. Map showing the distribution of estimated tractive force in the channel of a miniature fan in Westgard Pass ... 170
116. Map showing the distribution of estimated tractive force in a second miniature fan in Westgard Pass ... 171
117–127. Photographs:
    117. Antelope Springs channel, 1.5 miles above the mountain front ... 171
    118. Low terrace in the Antelope Springs channel, 1 mile above the mountain front ... 171
    119. Apex region of the Antelope Springs fan ... 172
    120. Hanging fan above the Antelope Springs channel ... 173
    121. Low Terrace at station 9 in the Antelope Springs channel ... 173
    122. Wyman-Crooked Creeks fan ... 173
    123. Downfan at the bankfull deposition zone above station 126 on the Antelope Springs fan ... 173
    124. Channel heading in the bankfull deposition zone at station 126 ... 174
    125. Gravels, winnowed of fine sediment, on the Antelope Springs fan ... 174
    126. Small plunge pool at the contact between a dissecting channel and the bankfull deposition zone above the highway ... 174
    127. Bankfull deposition zone near station 318 in the Antelope Springs channel ... 174
128. View of a channel cut by a mudflow in the Guil Basin, France ... 177
129. View of the aftermath of a mudflow in the Grand Tetons, Wyo ... 178
130–136. Photographs:
    130. Lower reach of the Owens Valley mudflow showing clear-water dissection ... 179
    131. Lower reach of the Owens Valley mudflow showing floating debris on the thin deposit ... 179
    132. Apex region of the active channel in Paiute Chute ... 179
    133. Fine matrix in the levee wall along the active channel of Paiute Chute ... 179
    134. Antelope Springs channel at station 400 ... 180
    135. Fire-hearth site in the Antelope Springs channel ... 181
    136. Painted gravel bar at section *A–A'* in the Antelope Springs channel ... 181
137. Diagram showing the formation of alluvial fans during one cycle, according to the climatic hypothesis ... 185

TABLES

Page
TABLE 1. Slope and maximum particle-size measurements in Deep Springs Valley ... 186
2. Mean size, mean roundness, and lithology of pebbles in Deep Springs Valley ... 187
3. Basic data on the tails of the granule-to-clay size distribution ... 189
4. Sedimentary parameters of the granule-to-clay size fraction ... 189
5. Sample modes and their weight percentage of the granule-to-clay size fraction ... 190
6. Clay-mineral ratios of selected samples ... 190

EROSION AND SEDIMENTATION IN A SEMIARID ENVIRONMENT

CLASTIC SEDIMENTATION IN DEEP SPRINGS VALLEY, CALIFORNIA

By Lawrence K. Lustig

ABSTRACT

This report treats the size distribution of sedimentary deposits in Deep Spring Valley, Calif., and the formation of alluvial fans.

The distribution of clastic sediments and the parameters of the size distribution have been mapped when possible. Maps of the mean size, mean roundness, and lithology of pebbles, and the weight percentage of granules and silt: clay ratios of the granule-to-clay size fraction are presented. Maps of the mean size, standard deviation, skewness, and kurtosis of the granule-to-clay size fraction are also included. The largest particles exhibit fluctuation in size in a downfan direction and cannot be mapped on a reasonable contour interval; the relation of maximum particle size to local slope is shown on scatter diagrams. These data indicate that size fluctuation and poor sorting of sediments are characteristic of the environment.

Granules range in abundance from about 3 to 5 percent in the basin center to about 15 to 20 percent near bedrock outcrops. Because the abundance of granules is greatest in coarse polymodal sediments—whereas their abundance decreases with decreasing grain size and the tendency toward unimodality—it is suggested that granules consist of aggregates of sand-sized particles that are rapidly reduced to these components by mechanical weathering rather than by the action of water. The general absence of granules in ancient sediments is thought to be related to the scarcity of discrete constituents in source rocks in the 2- to 4-mm size range.

Clay is scarce in both the surface sediments and modern mudflows. The weight percentage of clay in the granule-to-clay fraction ranges from about 0 to 6 percent and averages about 2 percent in the 90 samples studied. Silt is much more abundant than clay and is the primary mode in most of the polymodal samples. The mapped distribution of silt-clay ratios shows that these ratios are probably governed in part by wind transport and deposition. The path of infinite silt: clay ratios is interpreted as a reflection of the present wind track in the basin.

The maps of mean size, standard deviation, skewness, and kurtosis of the granule-to-clay size fraction are interrelated, and proper interpretation of both the distribution and mixing of sediments within the basin is greatly aided by considering this interrelation. The tails of the distribution, namely granules and silt-clay, are shown to be of primary importance because they exert a marked effect upon the several parameters. Skewness and kurtosis are shown to be mappable and useful parameters in such studies. The field zero skewness, for example, defines a zone of sediment mixing in the basin because it reflects a balance between the tails of the size distribution. Kurtosis isopleths, however, show a high that trends across the zero skewness field, indicating that, although balance of the tails is attained, the magnitude of the spread of the tails increases. It is thought that skewness and kurtosis, which are commonly neglected in basin studies, provide information of a nature not attainable by other means. Moreover, absolute values of kurtosis may be of importance in sediment transport problems because these values probably reflect the competence of flow to some extent.

A semiquantitative method, based upon measurement of the integrated intensity of the (001) reflection, was used to determine clay-mineral ratios. The data show that a considerable range of montmorillonite: illite values occurs despite the rather uniform climatic conditions that prevail, thus suggesting a relation between clay minerals and source-rock composition. Kaolinite and (or) chlorite comprise about 20 percent of the average sample and are relatively constant in abundance.

The competence of transport is approximated by using field data to estimate tractive force in the expression $\tau = \gamma\, dS$. Maximum particle size and local slope values are substituted for d, the depth of flow, and S, the slope of the energy gradient, respectively; the specific weight γ is omitted. The dS products, which are directly proportional to tractive force, are given for about 500 sampling stations, and the distribution of values is shown by maps.

A set of orthogonals, drawn through isopleth trends, is thought to represent paths of sediment transport. The predictive possibilities of the method are tested, and the results show that this particular set of orthogonals does represent sediment transport paths because the orthogonals coincide with active channels on alluvial fans. The results also show that tractive force within the channels is generally greater than that associated with surface sediments. It is suggested that this implies a change in process and that the greater tractive force associated with the modern process results from an increase in the average density of flow.

The data and observations of alluvial fans acquired during this investigation suggest that the following characteristics of fans are common to those in the western part of the Great Basin and perhaps to other fans as well; any hypothesis of the formation of the fans must therefore account for these features:

1. The loci of deposition on alluvial fans have shifted from areas well within their catchment areas to the middle reaches of fans, far below the mountain front.

2. Trenches in the apex regions of fans are misfit relative to present flow conditions by reason of their excessive depth, which ranges to about 200 feet.
3. Paired terraces that are continuous with fan surfaces occur within catchment areas and may extend to the divide.
4. Abandoned braided channels occur on fan surfaces at higher elevations than the floors of the modern active channels.
5. Fan surfaces and abandoned channels exhibit desert varnish and (or) weathering stain, whereas in the active channels and on modern deposits these are absent.
6. Hanging fans occur in tributary canyons within the catchment areas, and their surfaces are continuous with both terraces and fan surfaces below the mountain front.
7. The estimated tractive force is greater within the active channels than on fan surfaces.
8. The percentages of clay and organic material in both surface sediments and modern mudflows are extremely small.

The applicability of three general hypotheses of the formation of alluvial fans, namely the evolutionary or Davisian, dynamic equilibrium, and climatic, is discussed. It is concluded that although certain elements of truth are contained within each of these three hypotheses, the climatic explanation can best account for the characteristics cited above. It is thought that the conditions and consequences of one climatic cycle, of the several that have occurred during the formation of the fans, are as follows.

During a period of fan building, aggradation occurred within catchment areas and on fan surfaces, below the mountain front, at correlative levels. Precipitation was more frequent and more widespread than today. In response to this climatic regime, the abundance of both clay and vegetation was greater, and the fan surfaces were more resistant to erosion. Water: sediment ratios were higher, and the medium of transport had a lesser tractive force. Floods of more frequent occurrence spilled over numerous shallow channels onto the fan surfaces, spreading laterally as they emerged from the mountain front. Sediment was deposited over wide areas of the fans as a consequence of these conditions.

Climatic change was manifested by a change from widespread to local precipitation and by a lesser frequency of precipitation. This resulted in a reduction of vegetation and a decrease in the abundance of clay. Both catchment slopes and previous deposits became more easily erodible, thus contributing toward a reduction in the water: sediment ratio of a given flood and the more frequent occurrence of mudflows. These flows of greater density, viscosity, and tractive force deepened the trunk channels in catchment areas and trenched the upper reaches of the fans. Terraces in catchment areas and hanging fans in tributary canyons were thus produced, and the sediment removed in the process was deposited far downfan.

The shift of the loci of deposition downfan, in response to climatic conditions, produces growth of fans at their lower boundaries and a general decrease of slope in the upper reaches. The sediment added in these lower reaches is redistributed and incorporated into the basin fill during the subsequent climatic episode. At this time, lake levels will rise, the trenches will gradually fill with sediment, and aggradation in catchment areas and on fan surfaces will again occur.

The morphology of fans thus tends toward equilibrium with successive climatic fluctuations. The attainment of such equilibrium, however, is a function of the duration and intensity of each climatic episode, and it may or may not occur during these periods. Fan growth is both upward and outward, during alternate intervals, and will continue for some finite period, at the end of which time a given basin will be completely filled with sediment.

INTRODUCTION

Two of the most common generalizations that emerge from the literature on alluvial fans are (1) local floods in arid regions transport sediment to the mountain front and deposit it in a fanlike form as a consequence of a decrease in gradient and the absence of lateral restriction, and (2) alluvial fans are the product of a balance between erosion of the mountains and deposition in adjacent basins.

Although each of the foregoing statements appears to be quite logical, their widespread acceptance tends to obscure the fact that the formation of alluvial fans is poorly understood. The problem can best be considered in terms of its component parts, namely: (1) What is the distribution of sediments on alluvial fans? (2) What is the competence of the transporting medium? (3) What is the dominant mechanism of sediment transport today? (4) Has this or another transport mechanism been dominant in the past? (5) What is the nature and significance of channels on alluvial fans? (6) Is the modern process one of fan building or of degradation? (7) Does this process differ from that of the past? and (8) What is the rate of the modern process?

This study was undertaken to answer these questions and thereby enlarge our understanding of the formation of alluvial fans. A considerable part of the paper is devoted to question (1) above, the distribution of sediments, and to such component questions as: (1) What is the size distribution of sediments on alluvial fans and on the valley floor? (2) Are all the sedimentary parameters mappable? and (3) Which parameters would best serve to characterize the clastic sediments of a bolson environment?

The field investigation covered by this report comprised 8 months during the summers of 1960 and 1961 in eastern California and western Nevada. Quantitative data were obtained in Deep Springs Valley, Calif., and observations of a qualitative nature, particularly of channels on alluvial fans, were made in Fish Lake, Eureka, Saline, Panamint, Death and Owens Valleys. All are in the general vicinity of Deep Springs Valley.

In considering the question of the distribution of sediments within the environment, the first four moments of the size-frequency distribution were studied. If conclusions are based upon study of but a single parameter, such as the mean size or median size, then it must be assumed that this parameter is the most significant. The writer would hesitate to make this assumption, because the significance of other variables, such as kurtosis, is not well understood. For this reason the mean size, standard deviation, skewness, and kurtosis of the size distribution were mapped, thus providing a sound basis for a discussion of sediment mixing and the geologic significance of these parameters.

It was thought that the best approach to the question of possible differences between the modern and former processes lay in consideration of the competence of the transporting medium. Accordingly, a field approximation for this variable was sought and the results mapped. The conclusions that are presented, regarding differences between past and present processes, stem largely from a consideration of these maps and their implications and are supported by other data and field observations.

ACKNOWLEDGMENTS

The project reported on in this paper served as the basis for a doctoral thesis submitted to Harvard University in 1962. The project was conducted largely under the guidance of the late John P. Miller. The many stimulating discussions of the problems involved and the technical assistance which he provided, in both Cambridge and the field, more than satisfied the requirements of an adviser. Of still greater importance, however, was his interest in the study and evident enthusiasm; these provided a source of encouragement that cannot be too strongly emphasized.

The writer is indebted to Raymond Siever for several valuable suggestions during discussions of many aspects of the problem and to Alan V. Jopling, who read an initial draft of this manuscript. This paper has benefited from the constructive criticism of both Gordon M. Wolman and Lucien M. Brush, Jr., to whom the writer is grateful for their fine reviews.

Field assistance was capably provided by Donald Newberg in 1960 and Stephen Eittreim in 1961.

Blair Jones, of the U.S. Geological Survey, and Clem Nelson, of the University of California, provided valuable insight into the problems of their respective work on the basin hydrology and geology during discussions in the field.

Lorenzo Aristarain simplified the task of clay-mineral determinations for the writer by supplying several key references as well as valuable discussions of techniques.

F. M. Fryxell, of Augustana College, Rock Island, Ill., and J. Tricart, of the Institut de Geographie, Strasbourg, France, kindly granted permission for the reproduction of their previously published photographs in this report.

Meyer Rubin, of the U.S. Geological Survey laboratory, furnished the radiocarbon-age determination of the fire hearth (sample W-185).

These acknowledgments would be incomplete without mention of the information, hospitality, and assistance generously given by several residents of the Deep Springs area. Among these are Mr. Rudehouse, former manager of the Deep Springs Junior College; Alma Rossi, of Big Pine; and Bill Jenkins, former foreman of the Deep Springs highway maintenance station.

PHYSICAL SETTING

GEOGRAPHY

LOCATION AND TOPOGRAPHY

Deep Springs Valley is located in the western part of the Great Basin, one mountain range east of Owens Valley, Calif., and approximately midway between Mono Lake to the northwest and Death Valley to the southeast. Considering the Great Basin in its entirety, Deep Springs Valley is an atypical basin only by reason of its small size and perfect closure (pl. 8).

The White Mountains border the valley on the west, as far south as Westgard Pass. South of the pass, as well as on the east side of the valley, the name Inyo Mountains is applied. The maximum relief is about 3,100 feet in the vicinity of Deep Springs playa and about 5,600 feet in the north end of the valley. From the northwest corner of the drainage basin (pl. 8) to a point about 10 miles south along the divide, elevations generally range from 10,000 to 11,000 feet. Elevations decrease gradually to 7,300 feet at Westgard Pass, then rise again and average about 8,500 feet around the south rim of the basin. Elevations elsewhere are generally 6,000–7,000 feet at the divide, excepting breaks at Soldier Pass and Piper Mountain which are at 5,400 and 7,700 feet, respectively.

DRAINAGE

The interior drainage of Deep Springs Valley is typical of closed basins. About 40 ephemeral streams enter the valley proper, an area of about 47 square miles. Total drainage area of the basin (pl. 8) is about 144 square miles, exclusive of the valley proper.

The relation between fan area and catchment area noted by Denny (1965) in Death Valley does not hold in Deep Springs Valley. The Wyman-Crooked Creeks drainage area, for example, is nearly equal to the entire area of the valley (pl. 8) and is about three times as large as the Westgard Pass catchment area. Planimetric measurement of the respective fans from either topographic sheets or aerial photographs, however, would show that they are roughly equal in area.

Several reasons exist for this discrepancy between fan area and catchment area. A relation between the drainage area of a watershed and discharge has been demonstrated by many workers, but correlation of fan area with drainage area implies that the planimetric measurements reflect volumes. Clearly, the basic relation involved is that the volume of sediment removed from a given drainage basin should equal that which is deposited below the mountain front. Because differences in relief can occur despite equality of watershed areas, the planimetric measurement of drainage areas may not accurately reflect the volumes of sediment that have been removed. Likewise, such measurements may also fail to reflect the volumes of sediment in alluvial fans, because planimetric areas are a function of the surface slopes, which will vary.

A second consideration involves basin tectonics. It is not reasonable to assume that the downfaulted basin floors are horizontal in the light of much seismic evidence to the contrary. The volumes of sediment in alluvial fans may therefore differ because of basement tilting and subsequent burial of sediment, despite present equivalent surface expression.

ALLUVIAL FANS

Each of the ephemeral streams in Deep Springs Valley traverses an alluvial fan. The fans are larger on the west and northwest sides of the basin than on the southeast. The larger fans generally extend 2–3 miles from their apexes into the valley, whereas fans in the vicinity of Paiute Chute (pl. 8) can be as small as a few hundred feet in extent. The depth of alluvium is unknown, but it exceeds 700 feet in the vicinity of the bench mark in the north end of the valley (pl. 8), where a waterwell of this depth did not reach bedrock.

The general aspect of alluvial fans in Deep Springs Valley is similar to that of fans elsewhere in the Basin and Range province and need not be considered in detail. The most important features of fans, the active and abandoned channels, will be treated below. The approximate limits of the two fans discussed extensively in this report, Antelope Springs and Wyman-Crooked, are shown on plate 8.

Although some fans are clearly defined, merging of adjacent fans is not uncommon. These produce a continuous apron of alluvium and render difficult the task of drawing individual fan boundaries on maps. The merger of the Antelope Springs fan (pl. 8) with those adjacent to it can be seen in figure 85, and the apron of debris that occurs southeast of the playa is shown in figure 86. The darker areas visible owe their color partly to a preponderance of dark quartzite, in contrast to much white marble on the Antelope Springs fan, and partly to the presence of varnish and desert pavement.

An occurrence of color contrast on a single fan that does not result from the presence of a desert pavement is found on the Wyman-Crooked Creeks fan (fig. 87) in the north end of the valley. Although the dark area seen in the background contains a greater abundance of basalt than other parts of the fan surface, much of the color contrast results from the presence of weathering stain or varnish. No closely packed mosaic of stones occurs, however. Both the spacing of particles and range in size is comparable to that which occurs elsewhere on the fan. The presence of varnish in Deep Springs Valley is therefore independent of desert pavements, although both may occur together.

The alluvial fans considered in detail in this report are too few in number to provide valid correlations among such variables as slope, drainage area, and lithology. The data obtained suggest, however, that fans containing coarse debris are generally of steeper slope than, for example, the Antelope Springs fan. The slope of the latter ranges from 3 to 8 percent over much of its surface, and the largest particles present do not exceed 4 feet in intermediate diameter. Slopes on the Wyman-Crooked Creeks fan (fig. 87) range from about 2 to 11 percent and boulders 6–8 feet in diameter are not uncommon. Still greater slopes and larger particles occur on the fans rimming the south end of the basin (fig. 86) and on Paiute Chute (fig. 88), just north of the playa. On the other hand, the reentrant (fig. 89) just north of Crystal Peak (pl. 8) is as much as 16 percent in slope and consists mainly of granitic sand with few large particles. Particle size is, of course, largely a function of the lithology of the source area and the presence or absence of joints, cleavage, and other structural features. Given a source rock that produces no particles larger than cobbles, for example, neither discharge, slope, nor any other factor can enlarge the resulting particle size. Fans consisting of the finer debris contributed by such a source rock, however, are usually of gentle slope.

VEGETATION

The vegetation in the Deep Springs Valley drainage basin reflects orographic control. Sage and other shrubs floor the valley, attaining a maximum height of about 3–4 feet. The active channels on alluvial fans are generally bare of vegetation, but scattered-to-dense sage occurs on the bordering low terraces. In the active channel of the Wyman-Crooked Creeks fan (fig. 87), however, phreatophytes are abundant. This may reflect subsurface seepage beneath the channel, which is derived from the perennial flow in Wyman Canyon.

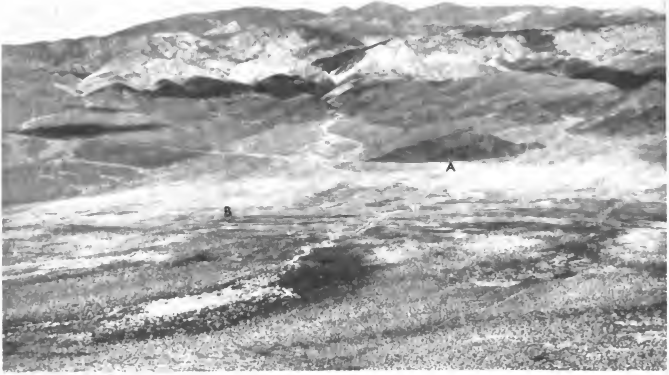

FIGURE 85.—Aerial view of the Antelope Springs fan showing its merger with adjacent fans. Note the contrast between the color of the sediments within the channels and that of the fan surface, which is darker. The transition from a relatively straight to a braided channel pattern on the fan coincides with the first depositional zone below the mountain front. The former lake level at about 5,200 feet and the linear ridges that mark the most recent expansion of Deep Springs Lake are designated as *A* and *B*, respectively.

Piñon and juniper occur between elevations of about 6,000 and 9,000 feet, together with sage that becomes less abundant with increasing altitude. Above 9,000 feet, the famous bristlecone pine is dominant in the White Mountains. These trees are restricted to some extent by lithology as well as altitude. They are most prevalent in areas where the white Reed Dolomite of Precambrian(?) age crops out; this can readily be seen either in the field or on aerial photographs. The writer noticed that the rather gnarled bristlecones all appeared to twist in the same direction along their axes. This was true whether they occurred on north- or south-facing slopes. From a chance encounter with a botanist in the mountains, who was engaged in a study of the trees, the writer learned that "as everyone knows, the twisting is in response to the Coriolis Force."

CLIMATE

PRECIPITATION

Climate is also a function of elevation, as attested to by records from the two weather stations in the area. One of these stations is in the White Mountains at an elevation of 10,150 feet, in the northwest corner of the drainage basin (pl. 8). The other station is in the valley at an elevation of 5,225 feet. The average annual precipitation in the mountains is about 13 inches, whereas it ranges from 3 to 5 inches in the valley. The maximum 24-hour precipitation for these two stations was 3.10 and 1.50 inches, respectively. It should be pointeed out, however, that one cannot state with certainty that the latter values were maxima in the area; they are maxima only for their respective locations and for the period of record.

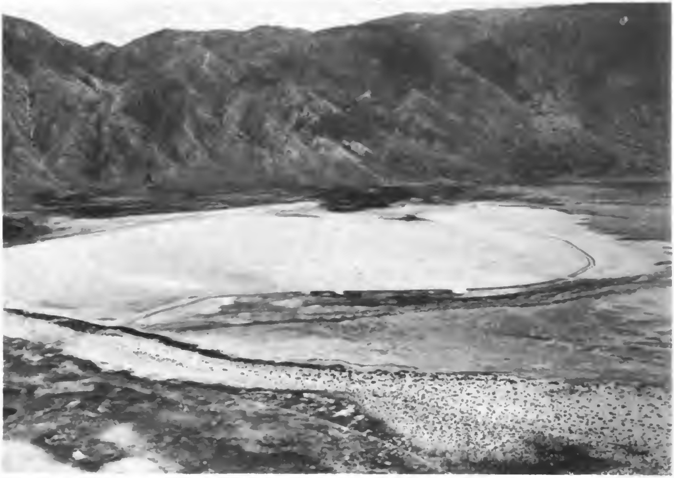

FIGURE 86.—Aerial view of the southeastern part of Deep Springs Valley. Note the apron of alluvium, produced by the merger of fans, beyond the playa and to the right. The channel at *A* is entrenched, and lighter colored sediment, indicative of modern transport, can be seen along its course and at the lower boundary of the fan.

During the winter months precipitation in the White Mountains is derived mainly from the residue of cyclonic storms that migrate across the Sierra Nevada and Owens Valley from west to east. The sporadic occurrence and distribution of thunderstorms and cloudbursts in desert areas in summer, however, is well known and Deep Springs Valley is no exception. Although the period of observation in the area was short, comprising only two summers, the writer gained the impression that certain tracks of thunderstorms across the valley were followed with greater frequency than others. The track of six thunderstorms in 1961 was from the southeast, over the playa, and directly across the Antelope Springs fan to the mountains (pl. 8). A second group of storms also arrived from the southeast, but these entered the valley between Paiute Chute and the general vicinity of Soldier Pass. These storms produced some minor precipitation at the valley weather station and proceeded to the Wyman-Crooked Creeks canyon area.

Storms arriving from the north or northeast produced rainfall on Piper Mountain (7,700 ft) and continued in a southerly direction, again passing over the valley weather station.

The remaining storms entered the valley from the southwest, west, or northwest. In these instances, precipitation usually ceased somewhere within the drainage area of the White Mountains and little, if any, rain fell in the valley proper.

Despite the paucity of data on the frequency of track of these storms, two facts are indicated. First, the frequency of precipitation is not everywhere equal within the basin. It will later be shown that this accords with the occurrence of certain hanging fans in tributary valleys. Second, frequency of precipitation in the valley proper is also not everywhere the same, and the total amount of precipitation on basin floors is not great. This may account for the preservation of scattered lake terraces in desert basins; in

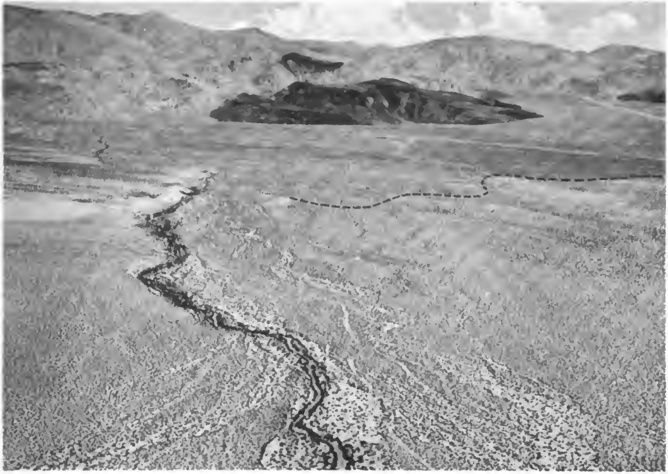

FIGURE 87.—Aerial view of the Wyman-Crooked Creeks fan. The darker color of the fan surface, above the dashed line, results from numerous basalt boulders and varnished or stained boulders. The basalt boulders are derived from basalt outcrops within the catchment area and from the dark mass in the background. Note the vegetation in the active channel, which is entrenched to a depth of about 40 feet, and the abandoned distributary channels at higher elevations than the active channel.

addition, it suggests that local runoff on alluvial fans is small compared with that in the mountains.

TEMPERATURE

The difference between the average annual temperature at the White Mountain weather station (pl. 8) and that in the valley is 18°F. Maximum temperatures greater than 105° have not been officially recorded in the valley, but in the absence of an official shade tree, temperatures from 115° to 120° were common. During two rather warm periods sun temperatures of 130° were recorded; ground temperatures are probably even greater.

WINDS

Information on wind intensities and dominant tracks in the valley is not available. The usual diurnal fluctuation of track, up and down canyons, was observed. It is unknown, however, whether any net transport of fine sediment results from this process.

Only three major duststorms occurred during the period of observation. The direction of sediment transport during each storm was from south to north, again prompting the question of frequency of track. Data on silt: clay ratios, to be discussed below in the section entitled "Silt and clay," suggest that the observed track may in fact be preferred in the valley.

SUMMARY OF GEOLOGY

The geology in the Deep Springs Valley area has been treated by Knopf (1918), Miller (1928), Nelson (1962, 1963), and others. Nelson conducted a detailed stratigraphic study and mapped the geology of the area. Much of the information to follow stems from his work complemented by personal observations. An outline of the geology, pertinent to this report, is shown on plate 8.

In the White Mountains the stratigraphic section consists of 21,000 feet of Precambrian(?) and Lower

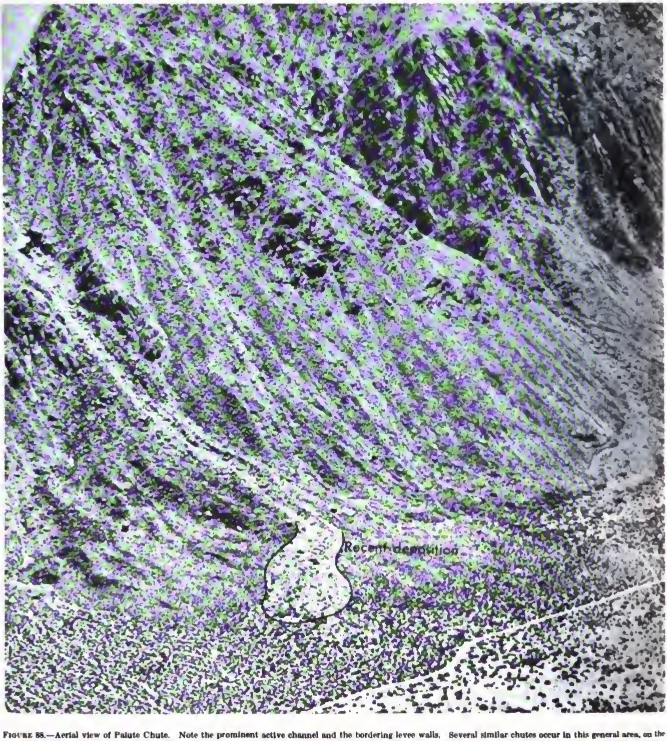

FIGURE 88.—Aerial view of Paiute Chute. Note the prominent active channel and the bordering levee walls. Several similar chutes occur in this general area, on the east side of the valley. The area of recent deposition on this young fan is below the termination of the active channel and at the lower margin of the fan, bounded as shown in the photograph.

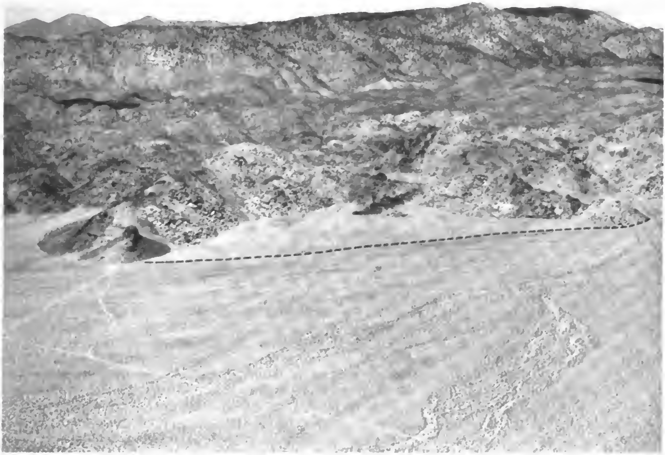

FIGURE 89.—Aerial view of the Crystal Peak reentrant. Crystal Peak is the small plug to the left of the dashed line that delineates the steeply sloping reentrant. Surface slopes are as much as 16 percent.

Cambrian strata and about 1,600 feet of Middle Cambrian sedimentary rocks; the latter are relatively restricted in outcrop area. Of the 10 formations described by Nelson (1962), only those pertinent to a discussion of the distribution of clastic sediments in the valley are mentioned here.

The sedimentary sequence has been folded, intruded by a granitic batholith and one or more stocks, and faulted. Structurally, the White Mountains are a southerly plunging anticline within the drainage basin considered. Because the fold axis trends nearly due south, whereas the topographic trend is southeast, the adjacent syncline to the east is exposed farther south in the Inyo Mountains. Erosion of the fold in the White Mountains has therefore revealed the oldest rocks in the section. The structural relationships become apparent in Wyman Canyon (pl. 8) where, despite considerable local complexity, repetition of strata to either side of the Precambrian(?) heart of the fold can be seen.

The formations of Precambrian(?) age encountered in Wyman Canyon, which cuts across the fold axis, are the Wyman, Reed, and Deep Spring. The Wyman Formation is greater than 9,000 feet thick (base unexposed), and the Reed Dolomite and Deep Spring Formation are 2,000 and 1,500 feet thick, respectively. These units crop out over a distance of about 6 miles along the canyon. The Wyman Formation consists of crumpled and contorted schists, phyllites, shales, and quartzites which are mottled gray, brown, or black and are generally banded. The overlying Reed Dolomite is a white to light-bluish-gray dolomite, and the younger Deep Spring Formation consists mainly of reddish-brown or yellowish-brown sandstones. South of Wyman Canyon the Wyman Formation gradually pinches out because the fold plunges in this direction. It comprises only a minor percentage of the rock types within the Antelope Springs catchment area, whereas the Reed Dolomite and Deep Spring Formation crop out in abundance.

A Cretaceous(?) granitic intrusive, of roughly 5 square miles in outcrop area, has pierced the sedimentary rocks between Antelope Springs and Wyman canyons and a contact metamorphic sequence occurs. South of the Antelope Springs drainage area the younger, Lower Cambrian sedimentary rocks, crop out. Dark sandstones and shales with varying amounts of limestone predominate; this assemblage, in varying proportions, continues around the south end of the basin. The contact between the sedimentary rocks and the granite occurs east of the playa, and the Inyo Range on the east side of the valley is granitic from this point northward.

Scattered remnants of Tertiary basalt and an underlying white friable tuff crop out along Crooked Creek, to the north of the Wyman-Crooked Creeks fan (fig. 87), and in the northeast corner of the basin.

The foregoing summary of the geology of the area indicates that certain rock types are sufficiently distinctive and restricted in area to serve as indices of probable source area at sampling stations in the valley. An abundance of sedimentary rocks derived from the Wyman Formation, for example, unquestionably indicates transport from the Wyman-Crooked Creeks system (pl. 8) in the northwestern part of the basin even if it occurs near the playa. Knowledge of the distribution of basalt remnants and color and other distinctions among specific basalt sources also proved useful during this study, particularly in treating the problem of sediment mixing within the basin and attendant effects upon the sedimentary parameters. Although several fine distinctions were drawn during the study, for convenience the lithologic data on the valley sediments have been summarized under the gross headings of granitic rocks, sedimentary rocks and basalt (table 2).

ASPECTS OF PLEISTOCENE GEOLOGY

No evidence of extensive glaciation in the White Mountains, within the drainage basin considered, was noted by the writer. This may not be true for the part of the range farther north, however. During the Pleistocene the snowline was undoubtedly much lower than it is today, but even at the headwaters of Wyman and Crooked Creeks (pl. 8) at elevations of 10,000–11,000 feet, evidence of cirques or moraines is lacking. A buried soil occurs in the headwaters of Crooked Creek, and signs of frost action were noted at several localities; these features represent the only evidence of Pleistocene climates in the mountains. An extensive snow cover and local ice caps probably existed in the higher parts of the range, however. If so, then combined with greater precipitation and lower temperatures, these local caps and the snow cover must have contributed to a much greater runoff and discharge than obtain today.

Miller (1928) was the first to discuss the Pleistocene lake in the valley and its probable extent. He estimated that its maximum depth was on the order of 400–500 feet. Given present elevations, a lake 500 feet deep would nearly cover the entire valley floor. The highest known stand of the lake was at about 5,200 feet, which accords with gravel deposits around the south end of the valley. The 5,200-foot contour follows the base of the low bedrock hill to the right of the Antelope Springs fan (fig. 85). Color contrasts also suggest a former high stand at this level. If the lake did not rise above this level, however, then according to present elevations, it could not have reached the northern end of the valley. The bench mark at 5,220 feet (pl. 8) would represent the northern limit of the former lake. A 5,200 foot-level would appear to insure that the lake did not overflow the basin; but present topography is not sufficient proof of this, and a former connection should be sought.

The former connection of many lakes in the Mohave region with the Pleistocene Owens Lake, as a result of overflow from one basin to another, is well known; the subject has been reviewed by Blackwelder (1954), among others. Westgard Pass, however, is at an elevation of 7,300 feet (pl. 8), sufficient to ensure that Deep Springs Lake was not part of this chain by way of Owens Lake. If a former connection in some other direction is sought, then the "new map" showing the distribution of pluvial lakes by Feth (1961) is of no greater assistance than the original compilation by Flint (1957, p. 227). It is probable that every basin in this region contained a lake, although not all overflowed their basin. A field reconnaissance of the Great Basin could provide much of the missing data.

Deep Springs Valley is adjacent to Eureka Valley, to the east, and Fish Lake Valley, to the northeast. A direct connection between Fish Lake Valley and Deep Springs Valley is possible, but field evidence suggests that the two may also have been connected by way of Eureka Valley. Horse Thief Canyon, which connects Fish Lake and Eureka Valleys, was traversed, and many solution pockets were noted by the writer along the base of the canyon walls. The divide between these two valleys is within Fish Lake Valley at an elevation of about 5,280 feet, and Horse Thief Canyon runs downgrade over its entire length into Eureka Valley.

Soldier Pass (pl. 8), which joins Deep Springs and Eureka Valleys, was also traversed. A carbonate-cemented pebble conglomerate probably formed in Pleistocene time and now largely stripped away, crops out along the floor and walls of the pass. The gravel fraction consists entirely of angular granitic fragments. The beds dip to the west, suggesting postlake uplift and tilting. Other evidence of uplift during Recent time can be seen at several localities on the east side of Deep Springs Valley. In the vicinity of the present playa another carbonate-cemented conglomerate crops out above the valley floor; scarps trend abruptly across alluvial deposits, and springs and bogs occur in this zone. Nelson (oral commun., 1961) has suggested that a major fault follows the zone east of the playa to the north and then turns east through Soldier Pass. Differences in elevation within the Inyo Mountains on either side of the pass are in accord with this suggestion.

Uplift of about 200 feet in the vicinity of Soldier Pass appears reasonable. If this is true, then the pluvial Deep Springs Lake overflowed through the pass into Eureka Valley. A small isolated playa occurs in a reentrant of the Inyo Mountains, on the Eureka Valley side of the divide, at the same latitude as the Deep Springs playa. Overflow from the pluvial Deep Springs Lake may have spilled into this sink, which has subsequently been uplifted.

Another conglomerate locality in the north end of Deep Springs Valley also indicates postlake uplift and tilting. These carbonate-cemented conglomerates occur near the most southern of the group of small drainage systems just southwest of Piper Mountain (pl. 8). The beds dip to the west, and in a few places they are as much as 200 feet above the present valley floor. They represent an absolute criterion for uplift, because the gravels are of lithologic types derived solely from the Wyman-Crooked Creeks drainage area across the valley. The gravels are well rounded and range in size from pebbles to large cobbles. This occurrence suggests that sediment from the Wyman-Crooked Creeks system must formerly have been transported directly across the valley floor in a more easterly direction than today. Former channels on the Wyman-Crooked Creeks fan also trend in this direction. Uplift and tilting, following withdrawal of the lake, produced the present southerly trend leading to the playa.

In summary, it is considered probably that Deep Springs Lake did extend over the entire valley floor, but the absolute depth or extent of this lake cannot be judged from present topography. This example of postlake uplift probably holds true for many of the western basins. Traverses of likely interbasin canyons provide a better field test of possible former connections between lakes than does examination of present elevations of accordant levels.

BASIC DATA

The quantitative data obtained in Deep Springs Valley are listed in tables 1 through 6 and were used to construct the various maps presented in this report. Sampling stations in the north end of the valley and on the Antelope Springs fan are shown in figures 90 and 91, respectively. The data include (1) measurements of local slope and maximum particle size at 496 stations; (2) 12,400 determinations of pebble size, roundness, and lithology; (3) sedimentary parameters of 90 samples of the granule-to-clay size fraction; and (4) approximate clay-mineral ratios for 43 samples. A planetable map of the active channel on the Antelope Springs fan (pl. 9) was constructed from data from about 600 stations on a scale of 1 inch = 100 feet.

Sampling stations in the north end of the valley are 1,000 feet apart, based upon an arbitrary grid system. The bench mark at 5,220 feet (pl. 8) was used as point 0.0 (fig. 90). Stations were located by means of pace and compass, or by odometer and compass if the point could be reached by jeep. Although the odometer was checked over measured miles for accuracy and tire pressures were not overlooked, some lack of precision must inevitably result because of the roughness of terrain. The same is true of paced distances in the area. The resultant inaccuracies of the maps, however, do not detract from the general trends shown.

Sampling stations on the Antelope Springs fan are located along contours that differ in elevation by 50 feet, determined by altimeter, and are 200 feet apart on each contour line.

Stations on Paiute Chute (fig. 88) and on the miniature fans in Westgard Pass, treated below, are 100 and 5 feet apart, respectively. Bearings taken from each station to the fan apex permitted the plotting of sampling points. This procedure was also followed at each station on the Antelope Springs fan (fig. 91).

The largest particle within a 50-foot radius of the sampling stations was located by observation, and the length of the intermediate axis was measured to the nearest tenth of a foot. Both the search for the largest particle and its measurement required some digging in many places. Slopes were measured to the nearest one-half percent with an Abney level over a 100-foot reach between the particle and the apex region of the fan. Because paths of sediment transport do not necessarily coincide with a straight line from the fan apex to a given particle, the 100-foot reach chosen was that which appeared to be the most probable transport path from field observation. If a particle occurred within a channel or boulder train, for example, then slope was measured along these trends regardless of deviation in direction from the apex. The rock types of the largest

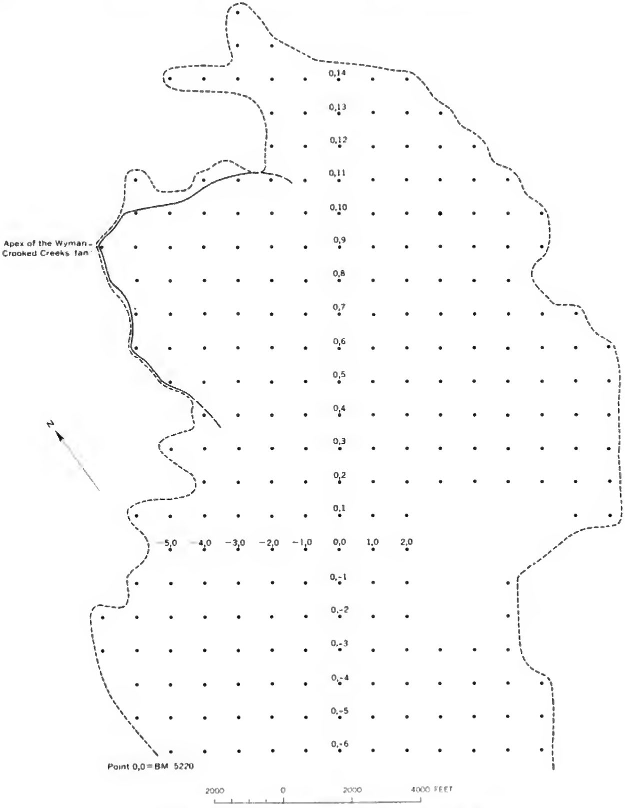

FIGURE 90.—Map showing sampling stations in the north end of Deep Springs Valley.

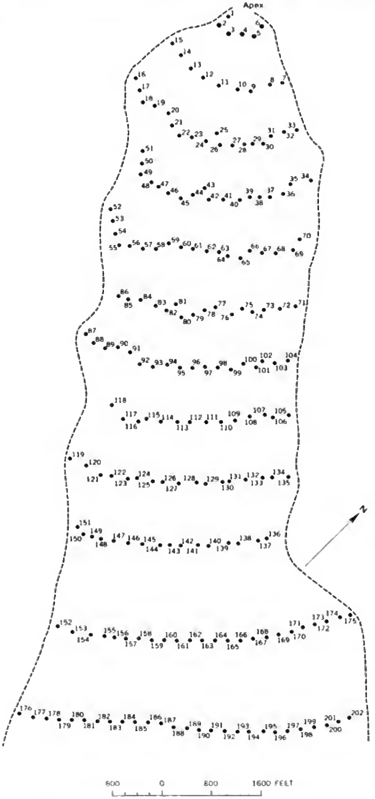

FIGURE 91.—Map showing sampling stations on the Antelope Springs fan.

particles were also obtained, but they are not included in the tables.

Data on pebbles were obtained only in the north end of the valley. At each sampling station (fig. 90) 50 pebbles were selected. These were obtained by pacing off a rough square, of about 12 paces to a side, and picking up the pebble nearest to the toe of the boot with each pace. Unlike the method described by Miller (1958) for sampling the Sangre de Cristo streams, the pebbles were not selected with eyes averted because of possible objection to the entire procedure by reptiles and other desert denizens.

For each pebble, the smallest, intermediate, and largest axis was measured with a vernier caliper to the nearest tenth of a millimeter, and the lithology was determined with a hand lens. The roundness of each pebble was determined by visual means and recorded as angular, subangular, subrounded, rounded, or well rounded. These categories were later assigned values of 0, 1, 2, 3, and 4, respectively, and the mean roundness for each rock type and for the entire sample was calculated.

In order that these procedures not appear to be open to the influence of preconceptions, it might be well to point out that the time requirements and other factors insured objectivity. The number of stations sampled per day was understandably small, because of the amount of data gathered. This prevented consecutive sampling from the valley floor to the mountain front along sampling lines. Also, as a matter of convenience, sampling lines were often left uncompleted and were returned to several days later when sampling along perpendicular lines. These factors alone would be sufficient to insure that one would not select larger or smaller particles of a given degree of roundness according to some concept of what the data "should be" at a given point. In addition, no mean value was computed until all stations in the north end had been sampled. The maps of the several variables presented indicate that the arbitrary sampling grid cuts across most trends at odd angles; this would not result from subjective sampling.

Samples of the granule-to-clay fraction were obtained from a total of 290 stations. Excepting grab samples from two mudflows, the upper 4 inches of sediment within a 5-foot radius of each point was obtained with a can or small shovel and successively quartered until the remainder would fill a 4- by 6-inch sample bag. Much care was expended to insure that the finer fraction not be lost during this procedure. Ultimately, 90 samples were chosen for analysis. These include 66 from the north end of the valley, 19 from the active channel on the Antelope Springs fan (fig. 9), 2 from Paiute Chute, 2 from a mudflow in Owens Valley, and 1 from a thin mudflow in Wyman Canyon.

These samples were split in order to obtain about 50 grams of each and then wet sieved through a 62-micron mesh. After oven drying, the granules were separated from the sands, and the latter were sieved with U.S. Standard Sieves; this provided a separation at half phi intervals. The less than 62-micron fraction was washed into settling tubes, and any additional sediment of this size that was obtained as a pan fraction during sieving of the sands was added. Silt and clay were separated at the 4-micron boundary by successive decantations. Time intervals for decantation were determined by settling velocities at the temperatures that prevailed. Because of the height of fall, which was 25 cm, the average time interval was about 4.25 hours. Most samples required about 10 decantations, but this varied, of course, with the amount and proportions of the sediment. The <4-micron fraction was drawn off, and after a few days were allowed for settling, a concentrated slurry was obtained and clay-mineral mounts were made by sedimentation on glass slides. The silt fraction was oven dried and weighed, and the weight of clay was determined by difference.

The mudflow samples were boiled in chlorox several times before separation of the size fractions, and the weight of organic matter was later determined by difference.

The weight percent of each class interval, from granules to clay, was calculated and the results cumulated. The cumulative percents were then plotted on arithmetic probability paper against phi diameter, and the values necessary for determination of the statistics used were read from each curve. The statistical measures used in this report to characterize the size distribution of the granule-to-clay fraction are those suggested by Folk and Ward (1957). They are as follows:

$$\text{Mean size } (Mz)=\frac{\phi_{16}+\phi_{50}+\phi_{84}}{3},$$

$$\text{Inclusive graphic standard deviation } (\sigma_I)=\frac{\phi_{84}-\phi_{16}}{4}+\frac{\phi_{95}-\phi_5}{6.6},$$

$$\text{Inclusive graphic skewness } (Sk_I)=\frac{\phi_{16}+\phi_{84}-2(\phi_{50})}{2(\phi_{84}-\phi_{16})}+\frac{\phi_5+\phi_{95}-2(\phi_{50})}{2(\phi_{95}-\phi_5)},$$

and

$$\text{Graphic kurtosis } (Kg)=\frac{\phi_{95}-\phi_5}{2.44(\phi_{75}-\phi_{25})}.$$

These measures represent a reasonable compromise between including a sufficiently large percentage of the size distribution to obtain the information desired and attempting to minimize the effort expended in attaining it. McCammon (1962) has recently reviewed the efficiency of various statistics of mean size and sorting. He shows that the measure of mean size (*Mz*) used in this report has an efficiency of 88 percent, whereas $\frac{\phi_{16}+\phi_{84}}{2}$, for example, has an efficiency of 74 percent. The respective efficiencies of inclusive graphic standard deviation (σ_I) and $\frac{(\phi_{75}-\phi_{25})}{1.35}$ are 79 and 37 percent. To further increase the efficiencies of the statistics chosen, it would be necessary either to include additional percentiles within the range considered or to increase the range, or both.

CLASTIC SEDIMENTS

The clastic sediments of Deep Springs Valley range in size from boulders to clay. At a given point, therefore, a volume sufficient to fill a small truck might be required in order to investigate the size distribution of a single sample. For this reason, and also because the implications of the size distribution are the primary concern, it was thought best to treat three discrete fractions of the total sediment. These are the largest particles, the pebble fraction, and the granule-to-clay fraction. Although this treatment is not entirely satisfactory, several considerations show it to be useful. First, separate treatment of the largest particles permits a discussion of competence; second, the weight percentages determined for such significant size classes as silt and clay are maxima; finally, the alternatives are in some respects still less satisfactory. If particles that occur at a given tape interval are measured, for example, there is an inherent tendency to skew the distribution toward the larger particles because pebbles will invariably be selected in preference to granules when both are present.

LARGEST PARTICLES

The 496 particles that represent the maximum size present at each station are listed in table 1 together with the slopes on which they occurred. Although large particles occur more frequently near apex regions of fans, they are not restricted to these areas. Figure 92 shows the relation between maximum size and slope for stations in the north end of the valley (fig. 90). The only station omitted from figure 90 is −7, 9 where a 16.5-foot particle occurred on a slope of 11 percent. The next largest size present at these stations was slightly <8 feet in intermediate diameter, and for reasons of convenience the ordinate was not extended beyond 10 feet.

The scatter of points on figure 92 is apparent. This can partly be explained by considering that several fans are represented and that variations of lithology, and especially joint spacings, will produce blocks of unequal size at the source. A plot of slope and maximum particle size for 202 stations on the Antelope Springs fan (fig. 93) shows a rather good trend, except for the particles on gentle slopes.

Blissenbach (1952, 1954) claimed that the relation between maximum particle size and slope was arithmetic for fans in Arizona and that the decrease in size downfan was uniform. His data were scanty, however; even the data for Antelope Springs (fig. 93), consisting of a limited size range, would not plot well on an arithmetic scale. In this report, the scatter of points is thought to be of greater significance than the general trend because understanding of process is the goal.

Particles larger than 1 foot in diameter occur in areas of zero slope, and particles larger than 5 feet in diameter occur on slopes of 2 percent in the north end of the valley (fig. 92). On the other hand, particles as small as 0.2 foot in diameter are the maximum size present on slopes as steep as 14 percent. For the Antelope Springs fan, where the range of both size and slope is more restricted (fig. 93), particles half the size of the largest present occur on slopes as gentle as 2 percent. Conversely, particles as small as 0.1 foot in diameter can represent the maximum size on slopes as great as 5 percent, although this fan exhibits maximum slopes of only 8 percent. It might be argued that the examples cited are the extremes of the distribution and therefore of little consequence. Regardless of the trend of the means, however, the extreme values require explanation.

The fact that boulders have been reported on playas (McAllister and Agnew, 1948; Kirk, 1952; Clements, 1952; and others) clearly indicates that the phenomenon of large particles in areas of zero slope is not restricted to Deep Springs Valley. Guilcher and Cailleux (1950) observed pebbles moving along an icy road in Denmark under the impetus of the wind. This observation led to a wind tunnel experiment by Grove and Sparks (1952) who duplicated the phenomenon. Extrapolation of their data by Schumm (1956) indicated that a velocity of 122 miles per hour would be required to move a rock weighing 1 pound across ice. Although the movement of boulders on playas is usually considered apart from any question of transport on fans, it is obvious that any boulder must first have been moved down a fan if it occurs on a playa. An explanation for the fluctuation of maximum particle size in a downfan direction will be offered below (p. 167).

THE PEBBLE FRACTION

The distribution of the mean pebble size in the north end of Deep Springs Valley is shown on figure 94. Although several trends are apparent, the most striking feature of the map is fluctuation in size, which is represented by closures around high and low values.

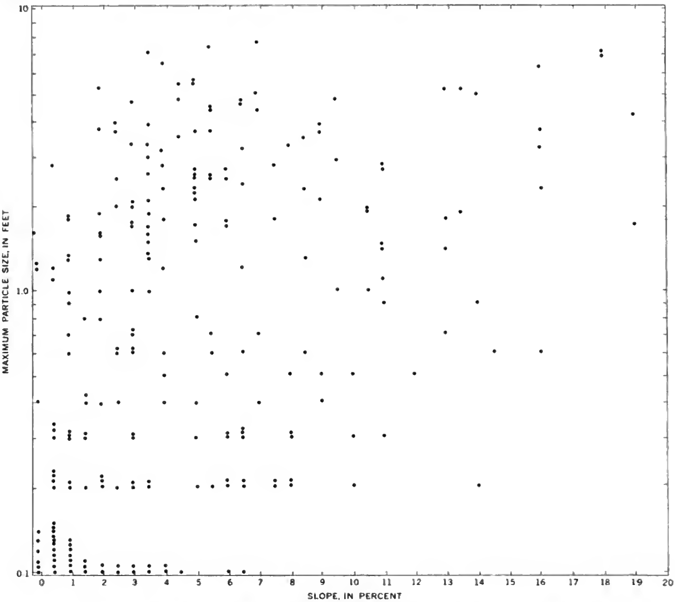

FIGURE 92.—Graph showing the relation of maximum particle size to slope at stations in the north end of Deep Springs Valley.

Some closures around high values are the result of sampling in a wash. This is true, for example, of the 34-mm high in the southwest corner of the map and the 28-mm high farther north. This 28-mm high defines the shallow wash shown in figure 95. Other high and low values result from extremes at only one or two points; this deserves further consideration.

First, it should be acknowledged that two individuals will seldom, if ever, produce identical isopleth maps from the same data. Nevertheless, there are limits that will restrict the possible differences. If the pebble data (table 2) were in accord with a uniform decrease in size downfan, then isopleths would be forced to conform with the basin boundary to some extent, or trends on individual fans would at least emerge more clearly. Neither is true of the map under consideration. Second, the question can be raised whether the mean or the extremes of the distribution is to be emphasized. If stress is to be placed upon average or mean trends, then the variations can be reduced by constructing a moving average map. Choice of a larger isopleth interval would also achieve this end. As with the largest particles, however, the fluctuations in size probably are significant and for this reason no attempt should be made to obscure the fact that they occur by smoothing the data. Each point on the map represents the average of 50 measurements; the map is therefore thought to depict accurately the distribution of pebble size.

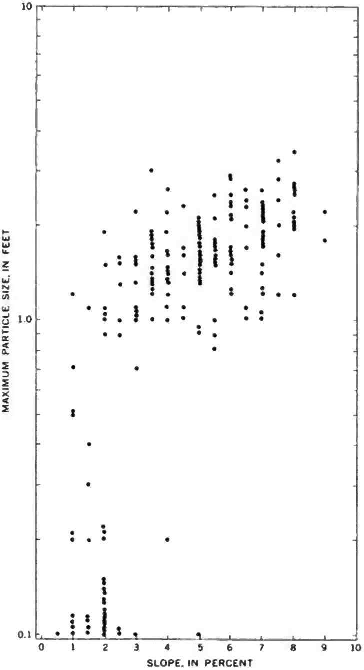

FIGURE 93.—Graph showing the relation of maximum particle size to slope at stations on the Antelope Springs fan.

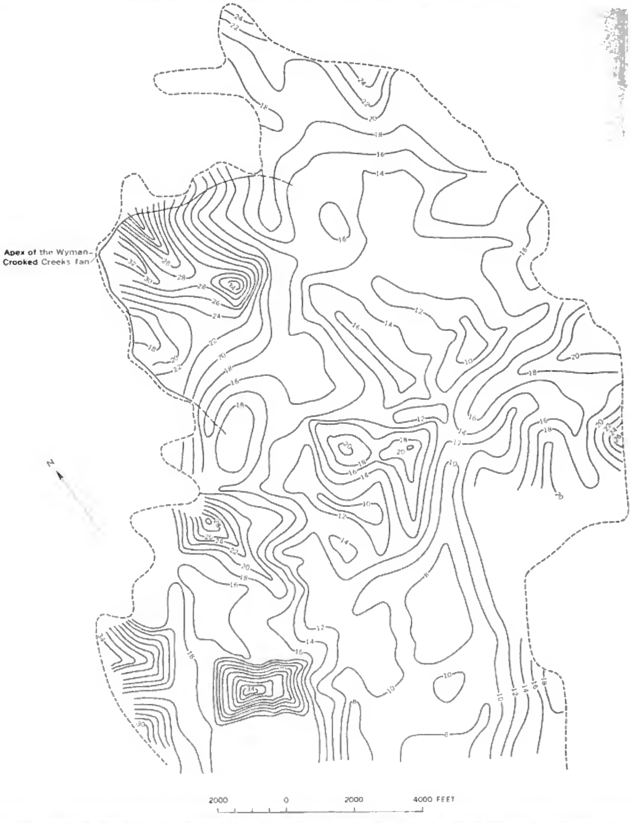

FIGURE 94.—Map showing mean pebble size (in millimeters) in the north end of Deep Springs Valley. Dashed line represents approximate bedrock basin boundary.

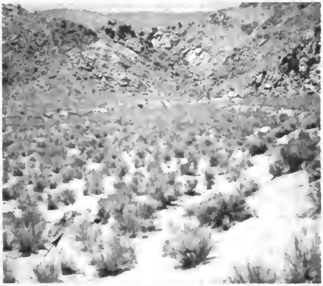

FIGURE 95.—View of a shallow wash in the Crystal Peak area. The wash at this point is approximately 193 feet wide and 2 feet deep. The sediments are predominantly of sand size, consisting of granitic weathering products. The boulder in the foreground (arrow), however, is about 4 feet in diameter.

The roundness (fig. 96) and the lithology (fig. 97) of pebbles in the north end of Deep Springs Valley are correlative. Fields of high mean roundness outline two main lithologic groups. These are the metamorphic and sedimentary types that issue from the Wyman-Crooked Creeks canyons (pl. 8) and the basalts derived from the cap on Piper Mountain and the low tilted masses at its base. The latter can be seen in figure 98. The color contrast at the base of the slope roughly coincides with the 50-percent contour in this area on figure 97 and with the roundness field of 1 on figure 96. Quartz and feldspar pebbles, derived from coarse grained granites and a few pegmatites, and scattered pebbles from aplite dikes are included in the plutonic rock percentage. These pebbles, in addition to the angular granite pebbles that occur close to their source areas, are more angular than the sedimentary, metamorphic, and volcanic rock types. For this reason the mean roundness reflects the lithologic distribution. The occurrence of closures on both the roundness and lithology maps is worthy of note. These reflect fluctuations in the distribution similiar to those found for mean size (fig. 94).

It is apparent from the roundness and lithology maps that a zone of mixing of sediments occurs along the central and east-central parts of the basin. Sediments from the Wyman-Crooked Creeks system, the northern and northeastern parts of the basin, and from the granitic Inyo Mountains on the east all merge in this area. The sedimentary parameters of the granule-to-clay fraction, to be discussed below, also reflect this mixing of sediments.

THE GRANULE-TO-CLAY FRACTION

GRANULES

In a review of the various size grades, Pettijohn (1957, p. 47) notes that the results of many studies indicate that granules (2–4 mm) are less abundant in nature than are other size groups. He also states that there appears to be a deficiency of very coarse sand as well. The basis for these statements is the fact that a sedimentary deposit consisting of both gravel and sand generally exhibits a distinct mode for each of these two fractions. The break in the frequency curve, between these 2 modes, falls within the 1- to 4-mm size range.

Several attempts have been made to explain the frequency minimum. Sundborg (1956, p. 191–194), for example, argues on hydraulic grounds that particles between 1 and 6 mm are those most readily moved when bed transport commences and are the last to come to rest when it ceases. According to this argument, granules are scarce in nature because they are in nearly constant motion, relative to other size classes, and therefore simply wear out. Kagani (1961) also advances a hydraulic explanation and, in addition, advocates placing size-class boundaries at all conspicuous frequency minima. This would, in effect, tend to remove granules entirely from consideration as a distinct size class.

An investigation of the clastic sediments in Deep Springs Valley, Calif., provided a good opportunity to consider the problem of the scarcity of granules. Because sediment transport is typically both brief and intermittent in a bolson environment, the conditions postulated by Sundborg (1956) do not pertain. A simple test of the hydraulic theory can therefore be applied; granules should occur in no lesser abundance than other size classes if the theory is correct. The basic data for the following discussion are listed in table 5; the weight percentages of granules are listed in table 3.

The weight percentage of granules in the granule-to-clay size fraction was determined for 90 samples. In addition to 19 samples from the Antelope Springs active channel (pl. 9), 71 samples were studied. These include 66 from the north end of the valley, 2 from Paiute Chute, and 3 from mudflows. Of these samples, 24 were unimodal and 47 were bimodal. In the unimodal group no mode coincided with the granule, very coarse sand, fine-sand, and clay sizes. Granules, however, occurred as the primary mode of 4 and the secondary mode of 5 of the bimodal samples. Among the

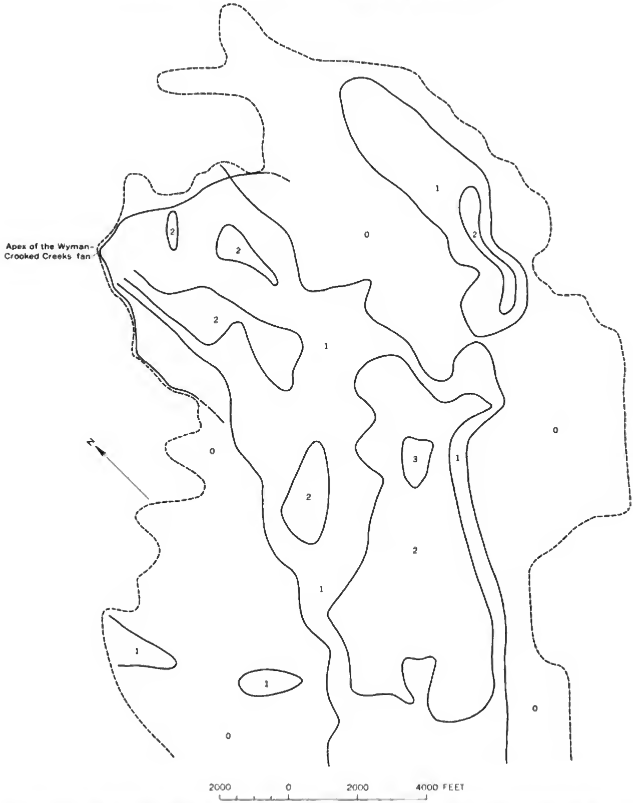

FIGURE 96.—Map showing mean pebble roundness in the north end of Deep Springs Valley. Dashed line represents approximate bedrock basin boundary. Isopleth values: 0 = angular; 1 = subangular; 2 = subrounded; 3 = rounded; 4 = well rounded.

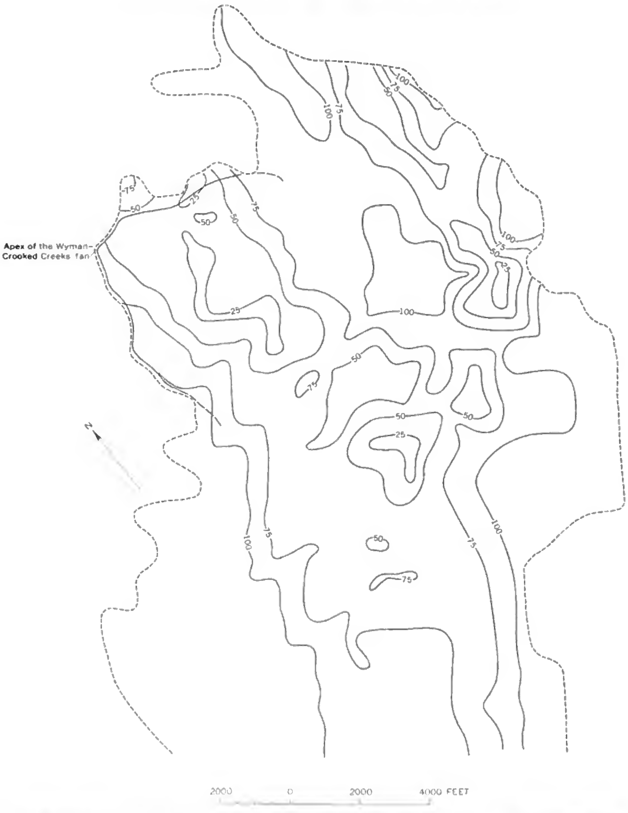

FIGURE 97.—Map showing pebble lithology in the north end of Deep Springs Valley. Dashed line represents approximate bedrock basin boundary. Values represent the percentage of plutonic rocks, including quartz and feldspar. Isopleth interval 25 percent.

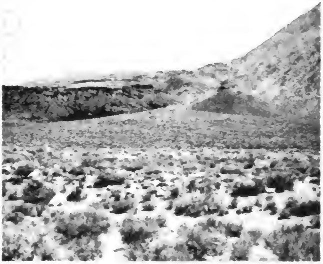

FIGURE 98.—View of the basalt mass and small fan at the base of Piper Mountain. The roundness and lithology of pebbles in the north end of the valley are greatly affected by the basalt particles derived from this area. The lighter colored debris in the foreground is mainly granitic and is derived from the northernmost point in the basin, to the left of the photograph.

19 Antelope Springs channel samples, 13 were unimodal and 6 were bimodal. Granules again failed to occur as the modal class in the unimodal sediments. The secondary mode of 5 of the 6 bimodal samples, however, did coincide with the granule size class. If the frequency of occurrence of the 8 size classes as both primary and secondary modes is calculated, then one finds that granules occur more frequently than 3 and less frequently than 4 of the size classes. On this basis, therefore, granules are very nearly the median mode of the bolson sediments.

The basis for this calculation is arbitrary and results in an exaggeration of the frequency of modal occurrence of granules. Although the fact is frequently overlooked, modality is also arbitrary, however. Only a single sample among the 90 studied was unimodal when class intervals were chosen at half phi units; the remaining 89 samples were polymodal. Upon grouping weights to produce intervals in accord with the full phi units of the Wentworth size classification, however, the 37 unimodal samples discussed previously were produced. Because any classification of size must be considered arbitrary rather than natural, the obvious conclusion to be drawn is that the unimodal samples result from averaging of the data. Many of the bimodal samples could be transformed into unimodal distributions by setting the class intervals equal to 2 phi units. In the limit, of course, any sediment could be shown to be not only unimodal but of the same size class as any other.

A more pertinent factor than frequency of occurrence as a modal class, however, is the absolute abundance of granules. Their abundance in the granule-to-clay size fraction (fig. 99) ranges from 15 to 20 percent near the basin margin to the north and east and is slightly less on the western side, in the Wyman-Crooked Creeks fan area. This fact may reflect greater absolute transport distances for these sediments. At least 3–5 percent of this fraction consists of granules at any point in the center of the basin. Although this percentage is a maximum for the total sediment, because gravel has been omitted, it is pertinent to the observations of Yatsu (1959), who argued that the break in slope along the intersection of an alluvial fan with the valley floor coincides with the modal frequency break in the gravel-to-sand distribution referred to above. Granules should, therefore, be absent below this break in slope or in the central part of the basin. The evidence from Deep Springs Valley, however, suggests a decrease in abundance of granules toward the basin center but not their disappearance.

The granule high in the southwestern part of the area shown is difficult to account for, except as an actual "island" of granules. It will be shown below that the area between this high and the 25-percent granule high to the east is, in effect, a crossroad of sediment mixing in the basin. The seemingly anomalous high may therefore represent the sum of granule contributions from the northeast and eastern trends which has subsequently been isolated by a flood of finer sediments from the Wyman-Crooked Creeks system.

The decrease in abundance of granules within relatively short distances from source areas not only requires explanation but serves to refute the hydraulic answer provided by Sundborg (1956). Because transport of the surface sediments considered here is relatively infrequent, constant motion of the granule size class cannot be appealed to in the search for the cause. Selective sorting in a downfan direction might appear to be a likely alternative. The studies referred to by Pettijohn (1957, p. 47), however, treated ancient as well as recent sediments. If selective sorting of sediment is the general explanation for the reported scarcity of granules, then it is difficult to understand why granule concentrations are absent in ancient sediments; lag deposits would necessarily have to accumulate in some areas but, to the writer's knowledge, none have been reported in the literature. A mechanical theory, suggested by the data from Deep Springs Valley, is thought to be the most reasonable explanation.

About 80 percent of the granules examined was found to consist of polymineralic rock fragments; quartz and feldspar grains constituted the remainder.

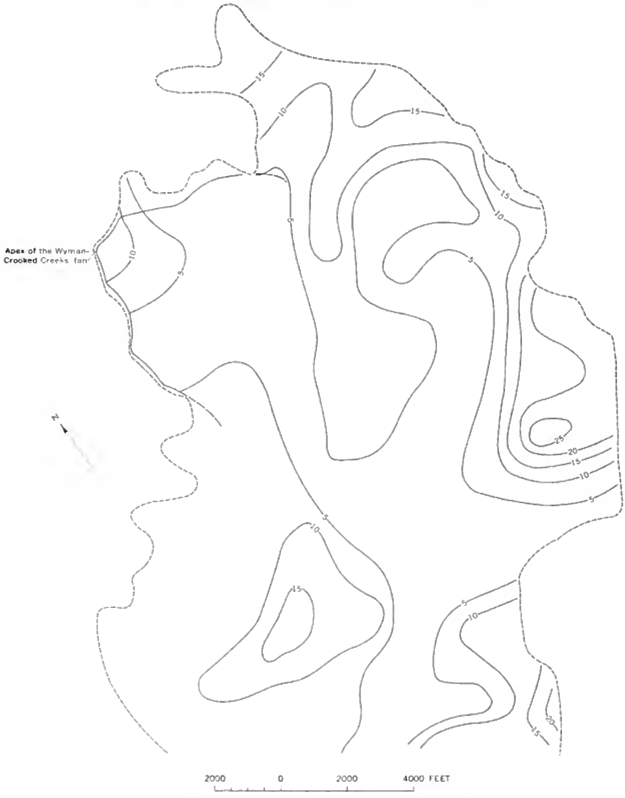

FIGURE 99.—Map showing the distribution of granules in the north end of Deep Springs Valley. Isopleth interval 5 percent by weight of the granule-to-clay size fraction

This implies that the plutonic rocks, which are the primary source of the clastic sediments considered, must consist of mineral grains that are predominantly less than 2 mm in size. The results of Dake (1921), who found that less than 10 percent of the quartz grains in plutonic rocks exceeded 1 mm in size, tend to confirm this implication. The fact that medium or coarse sand is the dominant size class in all of the unimodal samples studied, whereas granules are more abundant in the bimodal samples, suggests that the polymineralic granules are unstable aggregates of sand-size grains. These aggregates tend to disappear in nature by reason of rapid reduction to their components. The reduction is achieved by mechanical disintegration through weathering and is aided by periods of transport, however brief. The transition from polymineralic granules to sand-size components is accompanied by a consequent change from predominantly bimodal to unimodal frequency distributions. The deficiency of discrete mineral grains in the 2- to 4-mm size range in plutonic source rocks should be regarded as the fundamental cause of the relative scarcity of granules in nature.

SILT AND CLAY

The most striking single feature shared by all but 2 of the 90 samples studied is the scarcity of clay. The 2 exceptions will be explained below. The weight percentage of clay (table 3) in samples from the north end of the valley ranged from 0 to 6.37 and averaged about 2.0 percent. Samples from the Antelope Springs channel (pl. 9) range from 0 to 2.76 percent. Samples from Paiute Chute and the Owens Valley mudflow averaged about 2.5 and 3.0 percent, respectively. Although much care was taken in both collection and analysis of the samples, it is probable that some clay was lost. Because these weight percentages apply to the granule-to-clay fraction alone, however, the percentage of clay would be still lower if the total sediment provided the basis for calculation.

In contrast to the scarcity of clay, silt is very abundant. Silt occurred as either the primary or secondary mode in 31 of the 47 bimodal samples, referred to previously, and had the greatest modal frequency on this basis. The relative abundance of silt to clay is given in table 3. Noteworthy is the fact that even the thin atypical Wyman mudflow, which contained 17.38 percent clay, had a silt:clay ratio of more than 4 to 1. This ratio is in accord with those of the more typical samples from the Owens Valley mudflow (BP-1, BP-2) and Paiute Chute.

Because silt:clay ratios appeared to be consistent in the mudflow samples despite dissimilarity of the flows, it was thought that this variable might prove to be significant. Accordingly, the ratios for samples in the north end of the valley were plotted (fig. 100). Isopleths were not drawn for two reasons. First, it was apparent that four general areas occurred in which silt:clay ratios were markedly low in comparison to a relatively uniform and higher value elsewhere in the basin. Second, samples that contained no clay had, of course, infinite ratios. The path along which these infinite values occurred was recognized as that of the most frequent wind track observed in the field (p. 137). For these reasons the four areas of low ratio were outlined, and an average value was obtained for the samples that occur within each area. The same procedure was used to separate the remainder of the basin area into fields of average silt:clay values, as shown, and the inferred wind track was drawn along the path of 0 clay percent.

Several features of figure 100 are worthy of discussion. If the inferred wind track is followed as drawn, from the southeast corner northward, then the field of lowest silt:clay values in the basin (1.37) can be seen to lie in a reentrant to the right that is a natural depositional area. One of the samples within this field is 5, —1 which is one of the two exceptional samples noted above. The high clay content (26.58 percent) of this sample can best be explained by recourse to the wind deposition postulated.

The loop drawn in the inferred wind track to the northeast of the 1.37 field could not have been constructed exactly as shown from the data alone; the latter indicate only that the path must turn sharply to the left. A small incipient playa occurs precisely in this area, however. On several occasions, while in the field, gusts of wind approached this playa and circled it for a considerable length of time. The resulting windblown cloud of dust could be readily observed. The silt:clay ratios reflect this fact; high values encircle the playa and attest to the winnowing of clay, whereas much clay is present on the playa proper. The great bulk of Piper Mountain (pl. 8) apparently deflects the wind track to the west of the playa as shown (fig. 100); the remainder of the track is problematical. The field with average ratios of 4.44 may reflect both deposition of windblown clay along the elongate tongue pointing west and some contribution of clay from the northeast corner of the basin by runoff. The clays derived from the basalts in the northeast corner are well delineated by the 6.50 field.

The infinite value that occurs in the extreme north end of the basin is also interpreted as part of the wind track. Wind directions in this area were not noted in the field, however, and the track is arbitrarily shown leaving rather than entering the basin. Upon

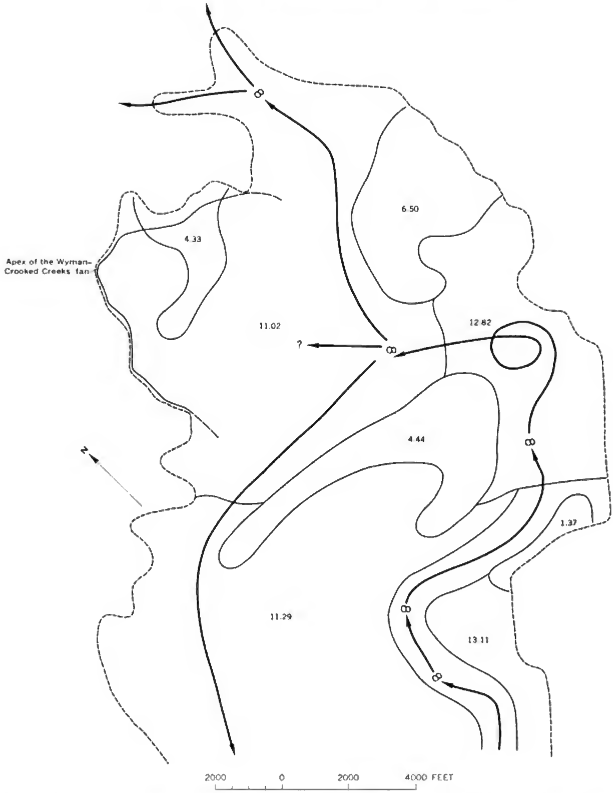

FIGURE 100.—Map showing silt : clay ratios and the inferred wind track in the north end of Deep Springs Valley. Values are means of sample ratios within areas shown. Infinite values occur along track.

occasion, the winds might equally well enter the basin along this route.

The remaining field of low silt:clay ratios (4.33) in the northwestern part of the basin is not thought to result from wind action. The basalt mass in this area (fig. 87) has probably contributed to the relatively high clay content represented by the field.

Samples from the Antelope Springs channel contain less clay, on the average, than do those from the north end of the valley or elsewhere (table 3). This may be attributed to the fact that much runoff occurs within the channel or that the rock types present do not weather as readily as basalt and granite. No consistent downchannel changes in clay abundance or in silt: clay ratios occur. This probably results from the fact that each zone of bankful deposition (pl. 9), to be discussed below, acts as a separate source area at various points in the channel system.

In summary, the study of silt and clay indicate that (1) clay is relatively scarce, whereas silt is abundant today; this is true not only for fan surface and channel samples but for mudflows as well; (2) silt: clay ratios reflect, in part, the effect of wind action, and in Deep Springs Valley the dominant wind track can be inferred from these ratios; and (3) wind action can affect the size distribution of basin sediments by reapportionment of the finer fractions.

PARAMETERS OF THE SIZE DISTRIBUTION

It should be apparent from the foregoing discussion of granules and silt: clay ratios that any attempt to characterize the granule-to-clay fraction in a bolson environment that ignores the tails of the frequency distribution is apt to be useless. The statistical measures used in this report were chosen, as noted above, because they encompass a reasonably large percentage of the total distribution of any given fraction and therefore reflect the variations in abundance of granules and silt and clay in the basin sediments.

Previous studies of the size distribution of sediments have treated beach, dune, and river sands in various combinations (Mason and Folk, 1958; Friedman, 1961). These studies have mainly sought to establish criteria for distinction between the environments cited, and they have met with varying degrees of success. The approach consisted of the determination of mean size, standard deviation, skewness, and kurtosis, followed by plotting of these variables against each other in one or more of the six possible combinations. In the present report the approach employed was to contour the areal distribution of each of the parameters. Certain of these maps have no parallel in the literature, to the writer's knowledge, and therefore cannot be compared with previous work. In addition, the granule-to-clay fraction has been treated as a distinct sedimentary unit, whereas the usual practice is to consider only the <2-mm fraction or else to treat the entire sediment if gravel and sand occur together. For this reason the absolute values (table 4) of the size-distribution parameters also cannot be compared with previous results. The treatment in this report, however, lends itself particularly well to both visual interpretation of the distribution of sediments and the geologic interpretation of skewness and kurtosis.

MEAN SIZE

The distribution of mean size of the granule-to-clay fraction in the north end of Deep Springs Valley is shown on figure 101. Because the contour interval is in phi units, the values are inversely proportional to mean size in terms of millimeters. It is instructive to compare this map with those of mean pebble size (fig. 94) and others and to note the approximate correspondence of closures or fluctuations. In figure 101, the large 2.0-phi closure on the Wyman-Crooked Creeks fan, the contour gap near the apex, and the size reversal along the northern edge of the fan all have their equivalents on the pebble map. This distribution probably reflects the fine sediment that is contributed from the basalt mass (fig. 87) at the basin margin. The silt: clay field of 4.33 (fig. 100) in this region and the location of the 5-percent granule contour (fig. 99) around the fan apex indicate that this is true.

Size fluctuation in the center of the pebble map (fig. 94), which bears resemblance to a pair of "sunny-side" eggs, is represented on figure 101 by the 1.5-phi reversal belt in the same location.

The flood of fine sediments contributed from the weathering of basalts in the northeast corner of the basin is roughly outlined by the linear 2.0-phi field on the right side of figure 101. This contribution was noted in discussion of silt: clay ratios and is shown on figure 100. There is also a general deficiency of granules within the area (fig. 99).

The zones of sediment mixing in the north end of the valley apparently result not only from the intersection of sediment transport paths, but they also reflect additional complications produced by wind action and the differing size contributions of individual rock types. The mean-size distribution (fig. 101) suggests that mixing occurs, but the map cannot reveal how or why without recourse to the additional data discussed.

Fluctuation of mean size in the Antelope Springs channel (pl. 9) is shown on figure 102. As noted above, each zone of bankfull deposition probably represents

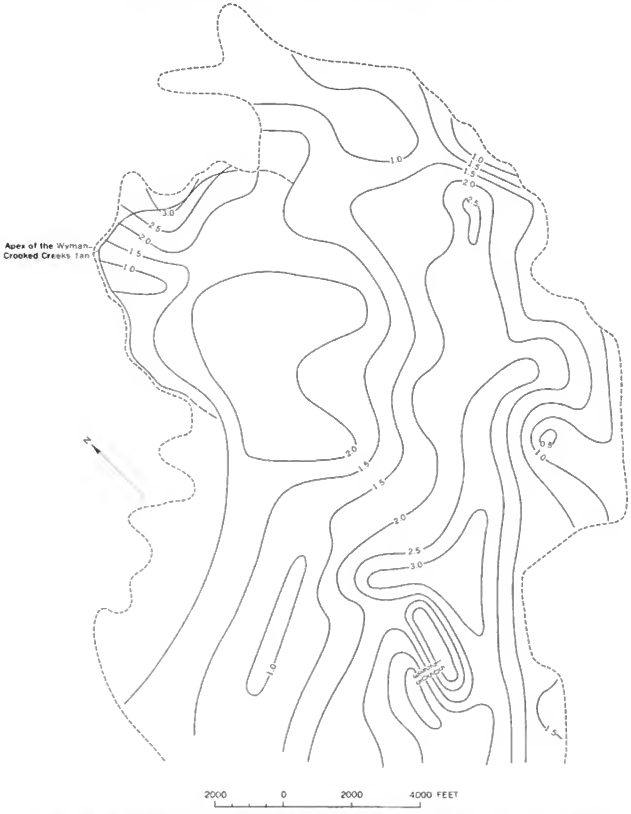

FIGURE 101.—Map showing the mean size of the granule-to-clay fraction in the north end of Deep Springs Valley. Isopleth interval 0.5 ϕ. $\phi = -\log_2 D$ (mm).

an individual source area for the respective reach below, and variation in mean size in a down-channel direction can be expected.

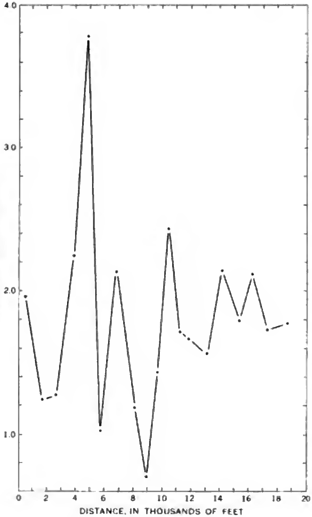

FIGURE 102.—Graph showing the relation of the mean size of the granule-to-clay fraction to distance from the fan apex in the Antelope Springs channel.

STANDARD DEVIATION

The inclusive graphic standard deviation (σ_I) of the granule-to-clay fraction in the north end of Deep Springs Valley is shown on figure 103. The degree of sorting increases down the Wyman-Crooked Creeks fan toward the basin center, from the northeastern rim of the basin. The map suggests that the more highly sorted material in the lower right corner, enclosed by the $1.9\sigma\phi$ isopleth, may be derived from the Wyman-Crooked Creeks fan because of the accordance of trends. This was not implied by the mean-size map (fig. 101); the origin of the sediments in this area was indeterminate.

Sorting decreases to either side of the best sorted sediments, culminating in 2 belts of $2.7\sigma\phi$, labeled *A* and *B*, but the reason is not evident from the map. If silt : clay ratios and the inferred wind track (fig. 100) are considered, however, then one explanation can be offered. The area of windblown clay deposition in the basin reentrant (1.37 field) is adjacent to one of these isopleths (A_1) on figure 103. The surface samples in the 1.37 field contain abundant fine material and are well sorted ($1.5\sigma\phi$). The belt of $2.7\sigma\phi$ values to the left at A_2, however, lies just to the north of the inferred wind track, and the poorly sorted material in this zone might be expected because of the $3.1\sigma\phi$ high that heads into this area from the northeast.

The other $2.7\sigma\phi$ belt to the west (*B*) and the large adjacent $2.3\sigma\phi$ field probably result from influx of clay (fig. 100) combined with the granule concentration (fig. 99) in this area. The distribution of mean size of both pebbles (fig. 94) and the granule-to-clay fraction (fig. 101) also shows high values in this part of the basin.

The data on granules and silt:clay ratios, which represent the tails of the granule-to-clay-size frequency distribution, show that standard deviation also reflects the complex mixing of sediments in the north end of the valley. Standard deviation, like mean size, cannot alone describe the distribution of sediment.

Standard deviation is plotted against distance from the fan apex in the Antelope Springs channel on figure 104. The data suggest a general downstream trend; standard deviation decreases from about 2.0 to $1.0\sigma\phi$. This decrease accords with a disappearance of granules, the low abundance of clay, and the fact that most of the channel samples are unimodal. These factors may indicate that the sediments have been subjected to more frequent runoff than have those in the north end of the valley and therefore tend to become better sorted.

SKEWNESS

Inclusive graphic skewness (Sk_I) of the granule-to-clay fraction in the north end of Deep Springs Valley is shown in figure 105. The general appearance of this map, in contrast to those showing mean size (fig. 101) and standard deviation (fig. 103), is striking. The writer must confess that if he were confronted with such a map in the literature, the urge to test the validity of the contouring would be irresistible. The reader is provided with the opportunity to satisfy his own urge through access to the basic data in table 4.

The most important single feature of the distribution is the field of zero skewness. This defines more clearly than before the zone of sediment mixing in the basin because it reflects a balance between the tails of the frequency distribution. With recourse again to the granule (fig. 99) and silt : clay ratio (fig. 100) distribu-

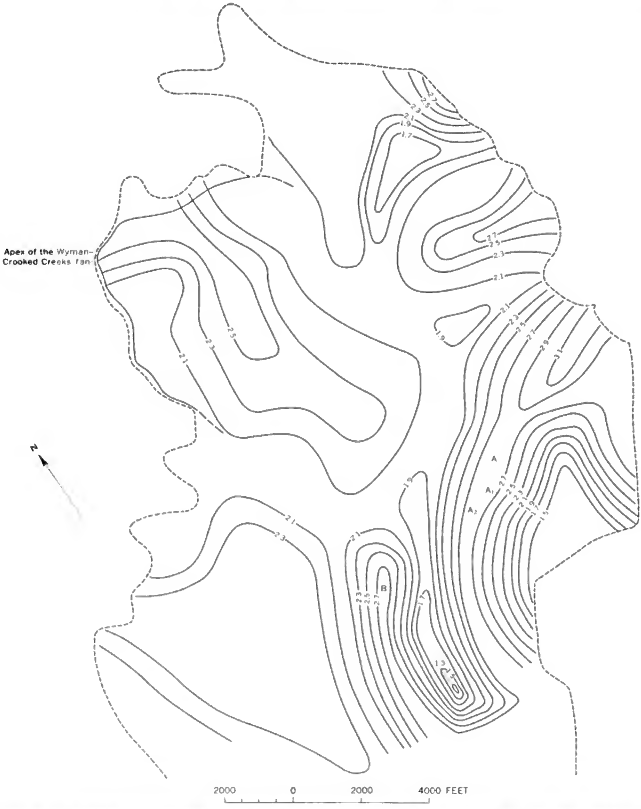

FIGURE 108.—Map showing the standard deviation of the granule-to-clay size fraction in the north end of Deep Springs Valley. The sorting of sediments in the regions labeled *A* and *B* is discussed in the text. Isopleth interval 0.2 $\sigma\phi$.

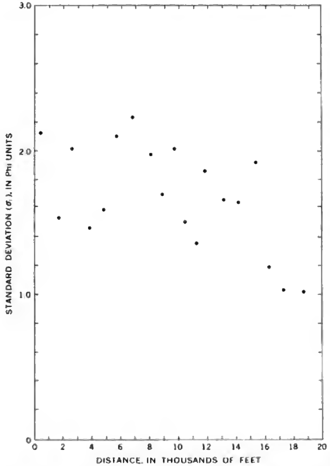

FIGURE 104.—Graph showing the relation of the standard deviation of the granule-to-clay size fraction to distance from the fan apex in the Antelope Spring channel.

tions, the skewness map can be seen to depict accurately the effects of mixing of sediments within the basin. High skewness values occur in areas where granules are abundant and decrease to zero where this size class either disappears or is balanced by an influx of fine-grained sediment.

Skewness of the granule-to-clay fraction in the samples from the Antelope Springs channel is shown on figure 106. Skewness ranges from +0.62 to −0.30. The channel samples are, on the average, only slightly positively skewed, and values fluctuate around +0.15, approximately. This might be expected in light of data previously provided; two-thirds of the samples are unimodal, and all have a high concentration of sediment in the medium-sand size class.

KURTOSIS

As defined in the discussion of basic data (p. 144), graphic kurtosis is the ratio of the spread of the tails of the distribution to that of the central portion. It is a measure of considerable sensitivity, and it was anticipated that kurtosis might prove useful in a treatment of bolson sediments, because the tails of the distribution are of primary concern. One would expect that the kurtosis distribution would complement that of skewness, because the latter reflects the relative balance of the tails whereas kurtosis reflects their relative abundance. This expectation has largely been satisfied; it will be shown by comparison of skewness (fig. 105) with kurtosis (fig. 107) distributions in the north end of Deep Springs Valley.

Kurtosis values are shown (fig. 107) in terms of departure from normality ($Kg = 1.00$) times 100. This means that the largest map value (85), for example, represents samples for which the spread from ϕ_5 to ϕ_{95} is 1.85 times as large as it would be for samples with normal kurtosis. It is evident that the belt of greatest departures on figure 107 cuts across the upper portion of the zero skewness field (fig. 105) in an east-west direction. This shows that although the tails of the distribution become balanced, the magnitude of the spread of the tails remains high and actually increases to the west. Consideration of the granule distribution (fig. 99) and silt:clay ratios (fig. 100) provides good reason for the location of the high kurtosis closure in the basin center; an abundance of both clay and granules occurs there.

The adjacent high kurtosis closure to the south, with a map value of 30, reflects the complexities of sediment mixing referred to above. These complexities include windblown clay deposition, the occurrence of granules and coarse sands contributed by the eastern reentrant, products of the weathered basalt from the northeast, and sediments derived from the Wyman-Crooked Creeks system. Kurtosis is sufficiently sensitive to the presence or absence of fine sediment in the basin samples to suggest that the inferred wind track (fig. 100) may be slightly mislocated as drawn. If the track were shifted slightly to the north along its reach between the 1.37 and 4.44 silt:clay ratio fields, then it would better coincide with the break between the two adjacent kurtosis highs of 85 and 30 (fig. 107).

The remainder of the inferred wind track need not be altered. It is interesting to note the support that each variable lends to the other. This would, of course, be predicted from theoretical considerations. The kurtosis low (−20) to the east of the two highs discussed above, roughly accords with the loop in the wind track (fig. 100) at the incipient playa. As the wind track is followed from the playa to the west and then south it coincides with a well-defined area of nearly normal kurtosis values that border the dominant (85) high. Another belt of high kurtosis values that extends from the northeast corner of the basin to its center is prob-

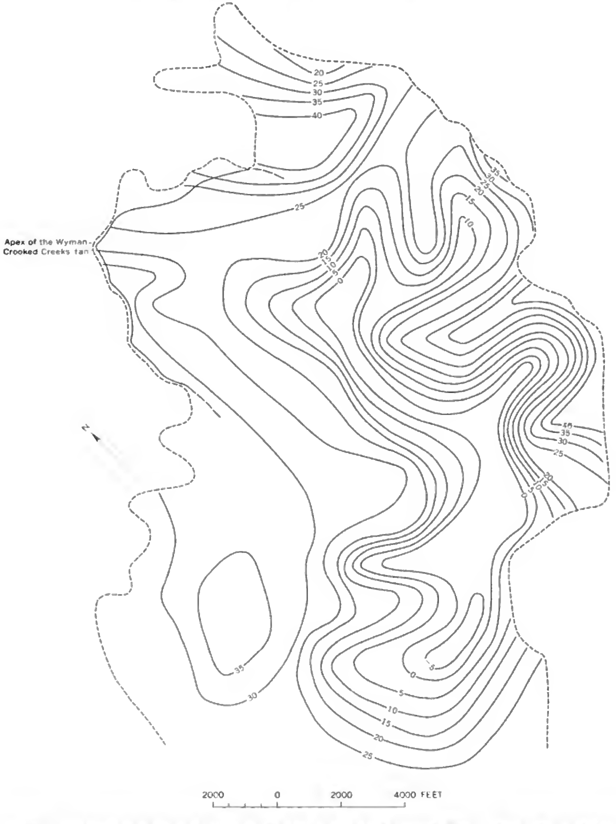

FIGURE 105.—Map showing the skewness of the granule-to-clay size fraction in the north end of Deep Springs Valley. Isopleth values = 100 × departure from $Sk_I = 0.0$.

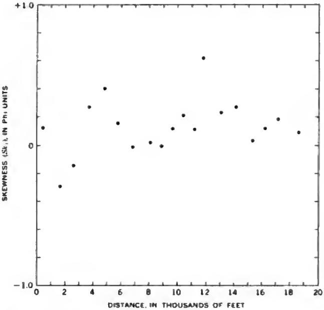

FIGURE 106.—Graph showing the relation of the skewness of the granule-to-clay size fraction to distance from the fan apex in the Antelope Springs channel.

ably a reflection of the merger between the granule tongue (fig. 99) in the upper part of the basin and the 6.50 silt: clay ratio field (fig. 100).

Finally, kurtosis values on the Wyman-Crooked Creeks fan are worthy of note. Despite the fact that the basalt on the north side of the fan (fig. 87) contributes fine sediment, as shown by both the mean size (fig. 101) and silt: clay (fig. 100) distributions, granules are relatively scarce (fig. 99) and this has produced low kurtosis values. The zero field ($Kg = 1.00$) accords with the fan limits in this region (fig. 107). In addition, kurtosis is the only parameter discussed thus far to suggest that the sedimentary trend of the fan is toward the east as well as toward the south. The probability that sediments from the Wyman-Crooked Creeks area were formerly transported to the east was mentioned earlier in connection with Pleistocene history. Sediment transport paths inferred from the tractive force data, to be discussed below, also support this contention. These facts also attest to the usefulness and sensitivity of kurtosis in the interpretation of clastic sediments in such an environment.

A scatter plot of kurtosis against distance downfan in the Antelope Springs channel (fig. 108) shows that within a wide scatter kurtosis decreases slightly, approaching normality near the end of the channel.

SUMMARY OF SIZE-DISTRIBUTION PARAMETERS

It has been shown that each of the parameters of the granule-to-clay fraction is a mappable variable and that useful information can be derived from such maps. The tails of the size distribution are of fundamental importance in the interpretation of bolson sediments because they have a marked effect upon the parameters. It is probable that significant quantities of granules and deposition or winnowing of fine sediment are common to all bolsons. The parameter maps and their implications should, therefore, have application to basins other than Deep Springs Valley and possibly to ancient sedimentary deposits as well.

The map of each of the four parameters of the size distribution required some knowledge of the distribution of the tails for satisfactory interpretation and, of course, all the maps are indeed interrelated. For this reason it is not possible to claim that certain of the parameter maps are of greater significance than others, but the reader of this report will probably agree at this point that the two orphans of basin studies, namely skewness and kurtosis, have been much neglected in the past. In addition to the merits of these two variables in investigations of sediment mixing, their absolute values may someday prove to be of significance. If competence is affected by the range of size of the sediment present (Fahnestock, 1961), then absolute kurtosis values are the best means of comparing range of size. Hence, the kurtosis of sediments should be considered in sediment-transport problems.

CLAY MINERALOGY

To determine the kinds of clay minerals present in the basin sediments and their relative abundance, 43 samples were studied. These include 18 from the Antelope Springs channel, 20 from the northern end of Deep Springs Valley, 2 from Paiute Chute, and 3 samples from mudflows. Two of the last were obtained from a mudflow that occurred in Owens Valley, west of Big Pine, Calif., on August 22, 1961. These samples are listed in table 6 together with their respective clay-mineral ratios that are discussed below.

Oriented clay aggregates were prepared on glass slides by sedimentation, and diffraction data were obtained from a Norelco X-ray diffractometer with automatic recording unit. The samples were initially run untreated; after saturation with distilled water a second pattern was obtained for each. All untreated samples exhibited one peak intensity corresponding to an interlayer spacing ranging from 14.21 A to 15.80 A. Saturation with water shifted this peak to smaller 2 θ values, indicating expansion. The expanded interlayer spacings ranged from 17 A to 20 A.

Because this paper is not devoted to an intensive quantitative study of clay mineralogy and because of the marked expansion with water noted above, glycolation was not deemed necessary. The mineral

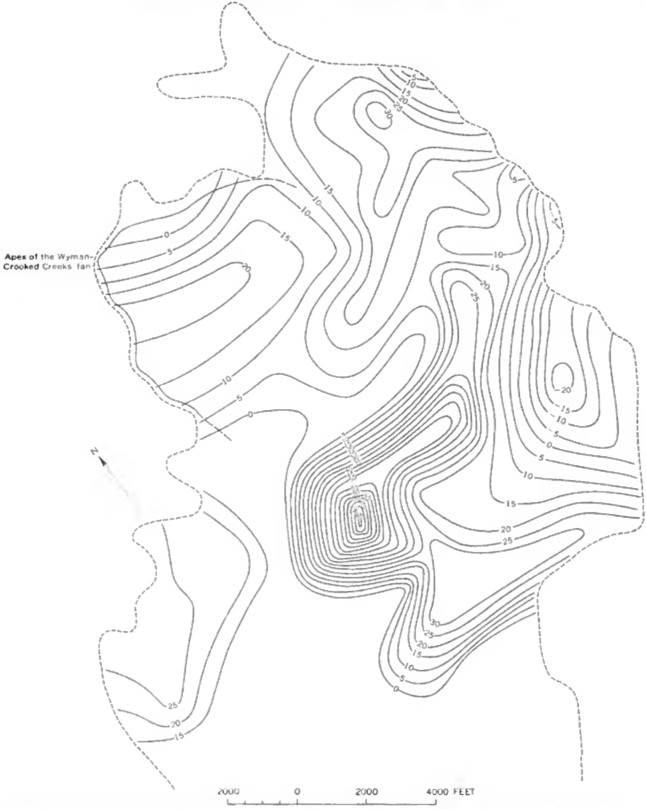

FIGURE 107.—Map showing the kurtosis of the granule-to-clay size fraction in the north end of Deep Springs Valley. Isopleth values=100×departure from $K_G=1.00$

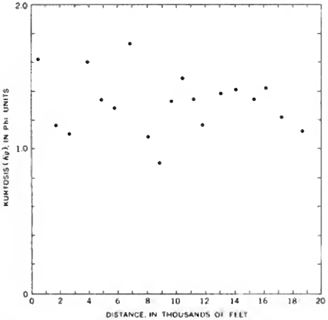

FIGURE 108.—Graph showing the relation of the kurtosis of the granule-to-clay size fraction to distance from the fan apex in the Antelope Springs channel.

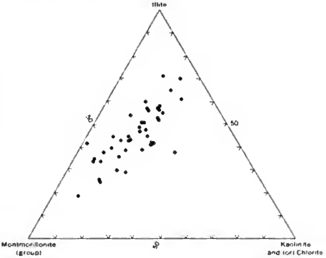

FIGURE 109.—Three-component diagram showing montmorillonite : illite : kaolinite and (or) chlorite ratios for 43 clay samples.

group that expands from 2 A to 4 A in the presence of water is designated as montmorillonite in the ratios presented. It should be stressed, however, that this designation undoubtedly includes various mixed-layer clay minerals. This is attested to by the lack of sharpness of many of the peaks and not uncommon base distance of about 4° 2 θ.

A nonexpanding clay mineral with an interlayer spacing of 10 A has been designated as illite and a second mineral, with a peak corresponding to a spacing of 7 A, as kaolinite and (or) chlorite. The separation of the (002) reflection of chlorite from the (001) reflection of kaolinite by heating or other methods was not attempted. It was noted, however, that no recognizable peak corresponding to 14 A was present after water saturation of the samples. This would suggest that chlorite is not very abundant in the samples studied; the fact that chlorite and (or) kaolinite is not abundant can be seen from the data (fig. 109).

To determine the ratio of montmorillonite: illite: kaolinite and (or) chlorite, as they are defined above, the integrated areas of the (001) reflections were determined by planimeter. These areas are linear functions of the weight percent of each mineral (Talvenheimo and White, 1952). Many factors will, of course, affect the reflection intensities. Among these are the polarization, Lorentz, and temperature factors, the degree of crystallinity, chemical composition, and others (Cullity, 1956). Because these factors have been ignored and because montmorillonite is defined on the sole criterion of expandability, the results presented must be regarded as approximations.

Weaver (1958) stated that a sample with equal amounts of montmorillonite and illite will yield an integrated intensity ratio of 3:1 in favor of montmorillonite. This result holds for 14 A montmorillonite; other ratios, varying with the montmorillonite interlayer spacing, have been published. As previously indicated, a montmorillonite group rather than pure 14 A montmorillonite is treated in this report. Because some value must be chosen, however, a factor of 3.0 was assigned for montmorillonite group spacings as wide as 14.9 A and 3.5 for spacings of 15.0 A and greater. Accordingly, planimeter measurements of the integrated intensity values for the (001) reflection of illite have been multiplied by 3.0, as appropriate, in order to arrive at the montmorillonite: illite ratios given.

Johns, Grim, and Bradley (1954) state that equal amounts of kaolinite, sedimentary chlorite, and illite will yield equal integrated intensities. The illite: kaolinite and (or) chlorite ratios can therefore be determined directly from planimeter measurements of the integrated intensities of the respective (001) reflections.

The montmorillonite (group): illite: kaolinite and (or) chlorite ratios, determined as described above, were recalculated to a base of 10 and used to plot the three-component diagram shown on figure 109. Despite the qualitative to semiquantitative approach employed, which renders the data valid only as a first approximation, two conclusions may be drawn from the diagram. First, a considerable range of montmorillonite: illite values exist despite the fact that all samples occur in a relatively uniform climatic environment. This suggests a relationship between clay-mineral type and source-rock composition, which is to some extent borne out by the data. Samples exhibiting high montmorillonite: illite values occurred mainly in basalt-rich areas, whereas all samples but one from the Antelope Springs channel contained more illite than montmorillonite. The source rocks of the Antelope Springs sediments are complex, but they include no basalt. The suggestion that a correlation exists is supported by previous work.

Droste (1961) studied the clay-mineral assemblages in several California basins that are in the neighborhood of Deep Springs Valley. He found that the clay suites strongly reflect parent rock types; samples rich in montmorillonite often contained volcanic glass. Eardley and Gvosdetsky (1960) also reported the occurrence of abundant montmorillonite in association with an ash layer in their study of a core from the Great Salt Lake.

The approximate constancy and relative scarcity of kaolinite and (or) chlorite suggested by the data on figure 109 also agrees with Droste's (1961) results. In Deep Springs Valley the sum of illite plus montmorillonite in the average sample is about 80 percent.

Because of these facts, the writer was tempted to treat clay mineralogy in the same manner as other variables already discussed and map the distribution in the basin. The data obtained, however, are both too few and too approximate. In addition, recourse to mixing of clays by means of wind action in order to explain exceptions proved necessary in an initial attempt. For these reasons it was considered best not to proceed beyond the presentation on figure 109. Clay mineralogy might well prove to be a mappable parameter in many western basins, however, if detailed studies were undertaken.

SEDIMENT TRANSPORT

An important aspect of the transport of sediments on alluvial fans is the competence of the transporting medium. Although the occurrence of large particles on alluvial fans implies a high degree of competence, it should be borne in mind during the discussion that follows that the nature of the source rock is a factor of importance. The competence of the transporting medium may have been sufficient to move still larger particles than those seen on fans, had they been available at the source. It cannot be assumed, therefore, that the competence of transport was necessarily greater on fans that exhibit the largest particles.

COMPETENCE CONSIDERATIONS

Competence is usually equated with the velocity of flow, and the relationship is stated in terms of particle diameter. Leliavsky (1955, p. 24) states that the earliest formula was provided in 1753 by Brahms who employed particle weight rather than diameter; but the report of Suchier (1883), listing velocities required to transport particles of "pea," "hazelnut," and "pigeon egg" dimensions, is typical of several early treatments. Gilbert (1914) considered the transport of particles as large as 6 mm in diameter, as did Nevin (1946) who reviewed the competence problem. The basic competence curves of Hjulström (1935, p. 298) have been extended and modified to include the transport of cobbles (Menard, 1950) and boulders (Fahnestock, 1961). Menard's work provides some information on the velocities necessary to keep a moving cobble in motion, but these are not comparable to the velocities required to initiate movement. The study by Fahnestock has produced the most pertinent data; the particles considered were as large as 1.8 feet in diameter. It was found that these particles moved more readily than would have been predicted; this was attributed to the presence of a mixture of sediment sizes. Even the data of Fahnestock (1961), however, cannot be safely extrapolated to include particles from several to many times as large, that occur on alluvial fans. The use of any velocity power law is, therefore, best avoided.

As an alternative measure of competence, tractive force can be employed. This is expressed as $\tau = \gamma dS$, where γ is the specific weight of the transporting medium, d is the depth of flow, and S is the slope of the energy gradient. The tractive force thus defined pertains to the shear exerted on the upper layer of the bed material. The formula, or some variant thereof, is widely used in engineering studies and provides one of the few available means of obtaining an approximation of the competence of transport. It is used in this report because S and d can more readily be estimated than the velocity of flow.

It should be emphasized that, at best, only an approximation to the true competence of transport can be sought in the field. For this reason several slightly more sophisticated formulae have not been considered. The shear exerted upon a boulder in a channel bed, for example, might be determined from the relationship $\frac{F/A}{\rho v^2/2} = C_D$ (Rouse, 1950, p. 122), where A is the area of the projecting surface, normal to the direction of flow, ρ is the density and v the velocity of flow, C_D is a drag coefficient, and F is the force or shear exerted. Any attempt to substitute values for the density, velocity, and drag coefficient required, however, would be a guess at best; such variables cannot be derived from field data.

Having chosen the simple expression $\tau = \gamma d S$, the main problem lies in equating field data with the required variables so that tractive force, or competence, can be determined. The key to a field approximation of tractive force is thought to lie in consideration of the largest particles. Several boulders contained pockets of pebbles, sand, silt, and clay on their uppermost side, several feet above fan surfaces. Because the finer sediment in these pockets is diverse in both lithology and size, it may represent a part of the sediment load that was transported together with the boulder and trapped upon cessation of the flow. Although later floods might have emplaced some of this sediment, this possibility seems more remote. The fan surfaces show no sign of subsequent floods; weathering stain or varnish extend down the sides of boulders to precisely the level of the fan surface on which they rest.

These observations suggest that either the depth of flow exceeded the diameter of the largest particle during transport or the finer sediment was acquired by the rolling of boulders through a shallower flow. Leopold and Miller (1956) state that cobbles moved in flash floods in arroyos even when the water was no deeper than half the diameter of the rolling object. On the other hand, the upper reaches of the Owens Valley mudflow (figs. 110, 111) clearly exceeded in depth the diameter of the largest particle. Depth of flow can therefore range from a lower limit of half the diameter of the largest particle to several times this value. Because a relationship exists, maximum particle size has been substituted for *d*, the depth of flow, in the tractive force expression. This value may be too low for the upper reaches of fans and too high for the lower reaches. It should be noted that this substitution cannot be made in areas that contain desert pavements, because in such areas the largest particles break down to smaller fragments and the original dimensions are therefore unknown.

The required slope in the tractive-force expression is that of the energy gradient, whereas the slopes measured in the field, by methods previously described (p. 141), are equivalent to bed gradients. Many measurements indicate that the bed slope is often a good approximation of the energy gradient, however. Moreover, efforts were made to measure a reach that corresponded with the most probable paths of sediment transport. Although local runoff may produce modification of slopes on fan surfaces, this modification might well consist of uniform lowering over a given reach. For these reasons the local slopes at each sampling point have been substituted for *S*, the slope of the energy gradient, in the tractive force expression. Field values are believed to be better approximations of the slopes that prevailed during true flow conditions than values obtained from topographic maps.

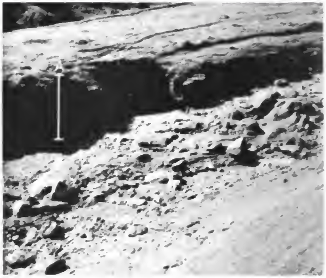

FIGURE 110.—Lateral view of the upper reach of the Owens Valley mudflow. The depth of flow at *A* was about 12 feet and exceeded the diameter of the largest particle that was transported. The mudflow has been dissected by a subsequent high-water stage; flowing water is visible below *A* and to the left of center. Note the dark color and viscous character of the mudflow deposit.

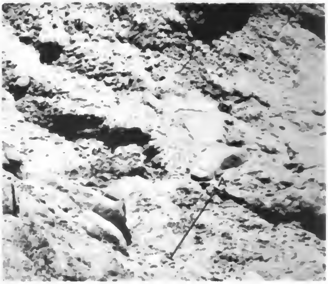

FIGURE 111.—View downstream in the upper reach of the Owens Valley mudflow. Much of the mudflow has been flushed from the channel by the turbulent water; the width of flow at *A* is about 5 feet. Openwork gravels may result from this process when subsequent high-water stages flush material in bankfull deposition zones.

The remaining variable is specific weight, or density times the acceleration of gravity. Because no single value for the density of a flow down an alluvial fan can reasonably be substituted in the tractive-force expression, this variable has been omitted. The tractive-force approximation in this report consists, therefore, of computing dS products, which are directly proportional to tractive force. These products were computed for each sampling station, their distribution mapped, and the maps interpreted as reflections of the competence of the transporting medium. The actual tractive-force values can only be determined if one assumes an arbitrary value for the specific weight of the transporting medium.

DISTRIBUTION OF ESTIMATED TRACTIVE FORCE

The distribution of slope-maximum particle-size products, or estimated tractive force, in the north end of Deep Springs Valley is shown on figure 112, and the distribution on the Antelope Springs fan is shown on figure 113. The basic data are listed in table 1, and the location of sampling stations is shown on figures 90 and 91.

The spacing of isopleths of estimated tractive force on the Antelope Springs fan (fig. 113) is rather uniform and is only slightly less so in the north end of the valley (fig. 112). The size distribution of pebbles (fig. 94) does not accord with a uniform decrease toward the basin center, however, and the relation of maximum particle size to slope (figs. 92, 93) exhibits considerable scatter. Large particles occur more frequently in apex regions (p. 145), but they are by no means restricted to these areas, as attested to by the occurrence of boulders on playas. Unless an exceedingly gross contour interval is chosen, the distribution of the largest particles cannot be mapped. If the isopleths shown on figures 112 and 113 reflect the distribution of competence, then one is confronted with the fact that, although the decrease in competence downfan is fairly uniform, maximum particle size exhibits considerable fluctuation.

This anomaly requires explanation. If one stresses the fact that a decrease in the average maximum particle size occurs on fans in order to obviate the problem, then the question of why the average size should decrease, will arise. This could be answered by recourse to selective sorting, but the bolson environment is notorious for the poor sorting that occurs therein. The floods described by Krumbein (1940) and Sharp and Nobles (1953), for example, both produced poor sorting and an irregular decrease of size. Moreover, floods of sufficient competence to transport the largest particles present probably lie in the mass transport region of the sediment transport spectrum, for which a high degree of selective sorting is not characteristic.

It is possible that floods of variable discharge could transport sediment over correspondingly varied distances downfan, but this would still fail to explain the transport of large particles across regions of gentle or zero slope. It is thought that transport by density flows, attended by buoyancy and momentum effects, provides the most reasonable answer to the observed anomaly.

DIRECTIONS OF SEDIMENT TRANSPORT

If slope-maximum particle-size isopleths are accepted as an approximation of competence isopleths, then orthogonals to these contours should represent directions of sediment transport. This assumes only that competence should decrease in the direction of flow. Although an infinite set of orthogonals can be drawn through any isopleths, those orthogonals shown (figs. 112, 113) represent a logical choice because they were drawn through contour trends. After drawing these orthogonals, it became apparent that their paths correspond closely to the location of channels on the fans. Field notes confirmed this correspondence, but to test the predictability of the method, two additional areas were studied. Paiute Chute (fig. 88) is a small fan that contains a very obvious active channel. Traverses were made up the active channel to the fan apex and down the fan surface, following boulder trains and other features suggestive of a former flow path, north of the channel. Slope and maximum particle size were determined as before at 100-foot intervals along these 2 routes. Slope-maximum particle-size products and sample locations are shown on figure 114 and the basic data are listed in table 1.

Figure 114 shows that competence, approximated as before, decreases in a relatively uniform manner downfan. The data (table 1) show that the largest particle in the active channel occurred approximately at midfan in this instance. Estimated tractive force isopleths drawn for Paiute Chute would show a trend in the contours along the path of the active channel, because the values within the channel are greater than on the fan surface.

Two miniature deposits in Westgard Pass (pl. 8) were treated in a similar manner. Despite their small size, each contains a pronounced active channel, and estimated tractive-force data were obtained. Values along the active channels of these small fans are shown on figures 115 and 116, respectively, and the basic data are listed in table 1. Sampling stations were 5 feet apart, and slopes were measured by placing a Brunton compass on a board 1 foot long on the channel floors. One of the fans (fig. 116) was too small to allow a surface traverse, and the opportunity to chase a possible flood in another area interfered with completion of a surface traverse on the other (fig. 115).

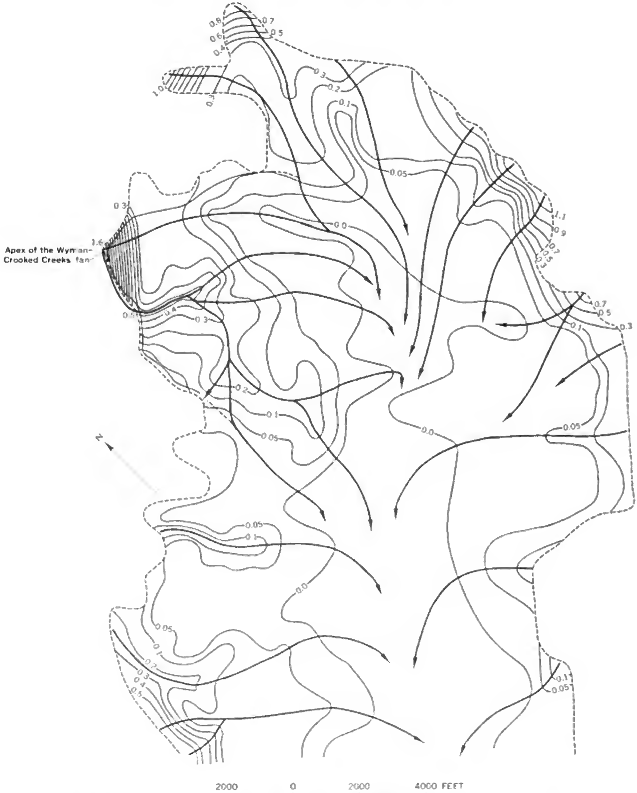

FIGURE 112.—Map showing estimated tractive force and inferred sediment transport paths in the north end of Deep Springs Valley. Isopleth values are slope-maximum particle-size products. Arrows indicate inferred paths of sediment transport. Dashed line represents approximate bedrock basin boundary.

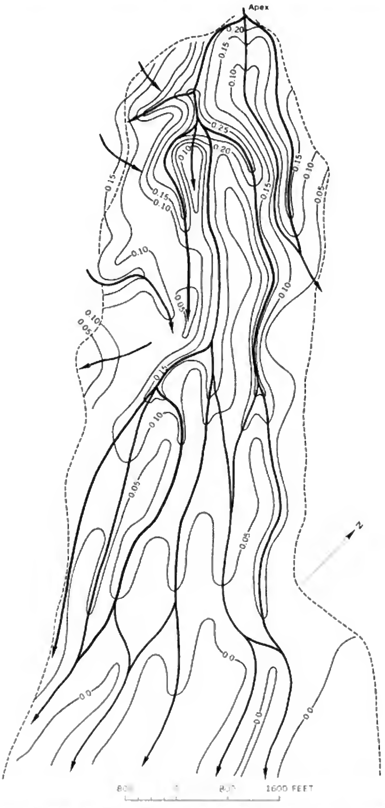

FIGURE 113.—Map showing estimated tractive force and inferred sediment transport paths on the Antelope Springs fan. Isopleth values are slope-maximum particle-size products. Arrows indicate inferred paths of sediment transport. Dashed line represents approximate fan boundary.

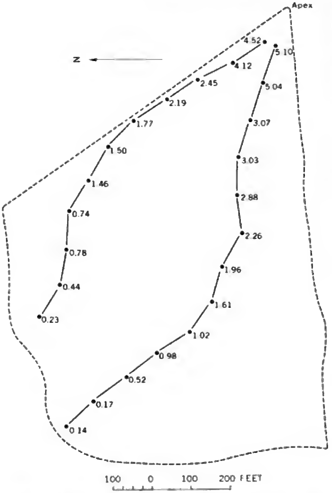

FIGURE 114.—Map showing the distribution of estimated tractive force on Paiute Chute. Values at the left were obtained from the fan surface at the indicated sampling stations; values at the right were obtained within the active channel. It is apparent that values in the channel are greater than on the surface. If estimated tractive-force isopleths were drawn, they would be convex downfan over the active channel.

The results show, however, that the values approximating competence again decrease downfan with greater regularity than does maximum particle size.

The evidence cited suggests that orthogonals drawn through estimated tractive-force isopleths delineate paths of sediment transport. Those orthogonals drawn through dominant trends in the contours coincide with active channels on alluvial fans, which are the most recent paths of sediment transport.

CHANNELS ON ALLUVIAL FANS

All the fans observed, both in Deep Springs Valley and in the neighboring basins noted above, contain channels that extend from trunk canyons far above their apex region to the middle or lower reaches of the fans. Channels are invariably entrenched and depths in the apex regions of the fans range from 20 to 200 feet below the surface. The sediment transported by modern floods is confined within these channels and can be readily distinguished in the field because of the color contrast with surface material. Regardless of actual color, the recent sediment is of lighter hue because weathering stain is absent; not only the more obvious channel on the Antelope Springs fan but parts of channels on adjacent fans can be distinguished by color contrast. (See fig. 85.)

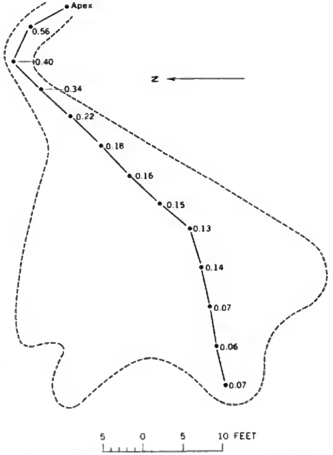

FIGURE 115.—Map showing the distribution of estimated tractive force in the channel of a miniature fan in Westgard Pass. Although the values fluctuate slightly, they decrease downfan far more consistently than maximum particle size.

Because recent sediment transport has occurred along entrenched channels, no material has been added to the fan surfaces "at the mountain front" on any fan. From a purely qualitative viewpoint it is impossible to observe this and conceive that this state of affairs has always obtained; the modern process must differ in kind from that of the past. Further visual evidence is provided by the terraces that occur within the trunk canyons above fan apexes. These extend back into the mountains over distances on the order of miles and in some instances to the divide areas. The low terraces shown on figures 117 and 118 are about 1 mile above the apex region of the Antelope Springs fan. In the general vicinity of the mountain front, the highest terrace level present is continuous with the fan surface below; this is true for all fans. The aerial view of the Antelope Springs apex region (fig. 119) illustrates this continuity. The higher of the two terrace levels that occur on the right side of the channel in the photograph is clearly identical with the level of the fan surface. The hanging fan seen at this point will be discussed below. The two levels on the right side of the channel are more evident in a ground view (fig. 120). The terrace relationships within the Antelope Springs drainage system are similar to those observed elsewhere in the Basin and Range province by the writer, and these relations suggest that at some former time aggradation took place within catchment areas as well as on the fan surfaces. Degradation has occurred since that time, however, and the loci of deposition have shifted far downfan.

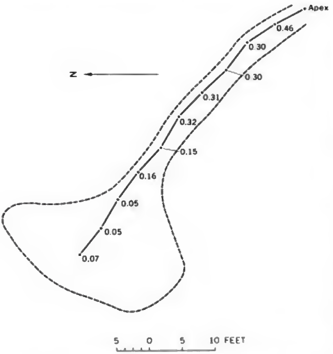

FIGURE 116.—Distribution of estimated tractive force in the channel of a second miniature fan in Westgard Pass. Although the values fluctuate slightly, they decrease downfan far more consistently than maximum particle size.

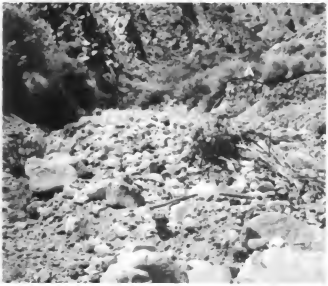

FIGURE 117.—View of the Antelope Springs channel, 1.5 miles above the mountain front. Note the terrace at *A*, about 8 feet above the bed along the right bank of the channel. This represents the former level of aggradation within the catchment area; it is continuous with the fan surface, below the mountain front. The heterogeneous character of the channel sediments and the occurrence of uprooted trees and shrubs are typical of the active channel.

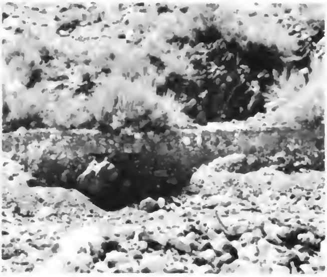

FIGURE 118.—View of a low terrace in the Antelope Springs channel, 1 mile above the mountain front. Note that bedrock has been exhumed by channel cutting and that the part of the dipping strata below the terrace level is lighter in color than that above, which is weathered. The height of the low terrace is about 2.5 feet.

The active channel on the Antelope Springs fan (pl. 9) was mapped in its entirety and may be used as an example to substantiate this conclusion. The areas designated as zones of bankfull deposition represent the only parts of the fan where recent sediment has actually attained the level of the fan surface. At all points above the first bankfull zone, sediment has clearly been removed and not added. The low terrace

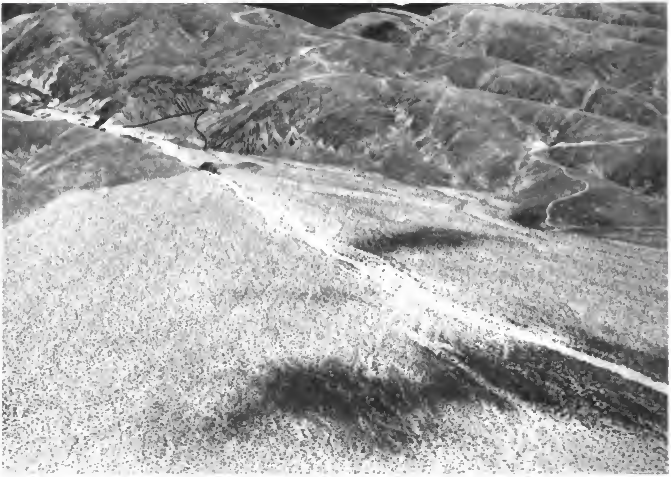

FIGURE 119.—Aerial view of the apex region of the Antelope Springs fan. Note the hanging fan (outlined) that is formed by the fill in the small tributary canyon to the right. Its surface is continuous with that of the Antelope Springs fan and with terraces farther upstream. The abandoned braided channels, visible on the fan surface in the foreground, are at a higher elevation than the floor of the active channel.

near the fan apex has a cover of sage and other vegetation, and the surface sediment exhibits a weathering stain. A view of this terrace in section near station 9 is shown in figure 121. A few hundred feet below station 9 and on the opposite side of the channel, this low terrace has been removed by erosion within the active channel. The fact that the active channel has indeed been deepened in the apex region is suggested by the abandoned channels (pl. 9) with floors at the level of the low terrace. Other abandoned channels, farther downfan, are visible in the aerial view of figure 119. It is apparent that the floors of all the abandoned channels, although below the fan surface, are at a higher elevation than is the floor of the active channel. This can also be seen on the Wyman-Crooked Creeks fan. The aerial view (fig. 87) shows several meandering and braided channels that are abandoned; the active channel is incised to a depth of about 40 feet below their floors. The ground view (fig. 122) indicates that the area occupied by the abandoned channels may again represent the level of a low terrace, as on the Antelope Springs fan, because there is a higher accordant level that was not apparent from the air.

The deposition that occurs today on the Antelope Springs fan is restricted predominantly to those areas at and below the first zone of bankfull deposition (pl. 9). It does not occur in widespread sheets over this entire area, but in various transitory locations that depend upon the migration of braided channels. The aerial view of the fan (fig. 85) clearly shows the point at which extensive braiding begins; this point corresponds to the location of station 126 on plate 9. The various channels that head in the bankfull depositional zones may result from the high-water stages that follow

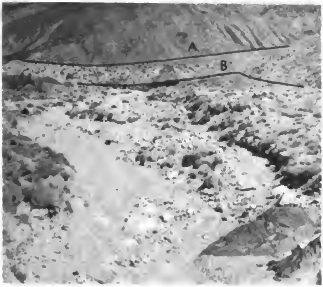

FIGURE 120.—View of the hanging fan above the Antelope Springs channel. The surface level of the hanging fan (*A*) is continuous with the higher of the 2 terraces that are present and is about 25 feet above the floor of the active channel, which terminates the fan. The low terrace is labeled *B*. The bedrock in the lower right corner of the photograph has been exhumed.

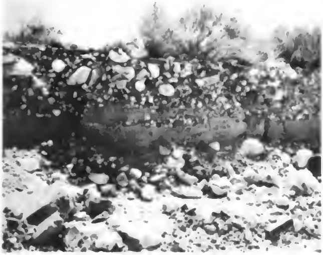

FIGURE 121.—View of the low terrace at station 9 in the Antelope Springs channel. Note the alternation of beds of coarse and fine sediment in the terrace, which is about 5 feet high. The largest particles on the floor of the active channel generally exceed the size of those present in the banks and on the fan surface in this area.

on the heels of mudflows (figs. 110, 111) and may be enlarged by seasonal runoff. Valley precipitation, as previously discussed, is probably insufficient to produce these features. The view downfan at station 126 (figs. 123, 124) shows the abrupt occurrence and rapid enlargement of one such channel. Two other channels, heading in the bankfull deposition zone just above the highway (pl. 9), are shown at the point of contact with the gravels in figures 125 and 126. The gravels are commonly openwork to considerable depth. Relatively clear water, flowing across and through these depositional sites, can account for both the winnowing of finer sediment and the fluctuation in mean size of the granule-to-clay fraction (fig. 102) noted above.

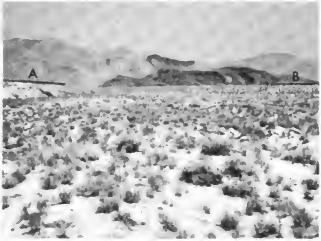

FIGURE 122.—Ground view of the Wyman-Crooked Creeks fan. The accordance of the surface of the ridge at *A* and the top of the low hill at *B* suggests that these may be remnants of a former continuous level. The active channel follows the base of the ridge at *A* and is incised to a depth of about 40 feet, below the general level seen in the foreground.

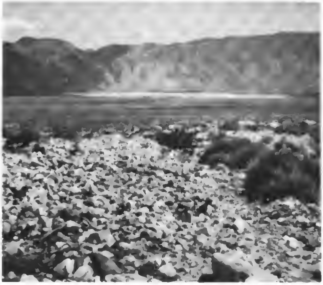

FIGURE 123.—View downfan at the bankfull deposition zone above station 126 on the Antelope Springs fan. There is a tendency toward convexity of profile in this region. The dissecting channel in the center of the photograph heads abruptly in the gravels, which are at, or slightly above, the elevation of the fan surface.

The last zone of bankfull deposition (fig. 127) is opposite station 318 (pl. 9) and clearly indicates that coarse debris has been transported far downfan in recent time. It is probable that deposition in the mid-

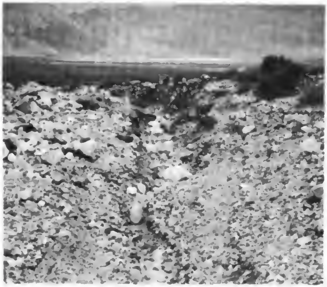

FIGURE 124.—Closeup view of the channel heading in the bankfull deposition zone at station 126. Note the rapid enlargement of the channel over a short distance and the convexity of profile.

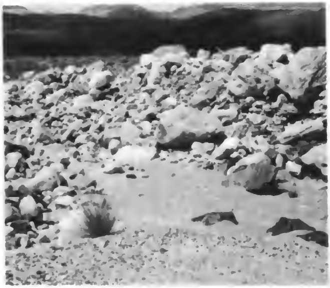

FIGURE 125.—View of gravels, winnowed of fine sediment, on the Antelope Springs fan. The largest particle visible is about 4 feet in intermediate diameter. Note the poor sorting of the gravels and the abundance of finer sediment in the foreground, suggesting winnowing.

dle and lower reaches of the Antelope Springs fan and degradation elsewhere is typical of most fans in the region today. This fan is entrenched only to a small extent in comparison with larger fans that contain channels as deep as 200 feet; and yet, abandoned channels and terrace levels occur as described. If the catchment and apex region has been subjected to degradation and if deposition occurs predominantly below midfan today then this fan is not being built up

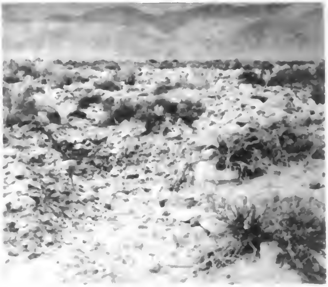

FIGURE 126.—View of a small plunge pool at the contact between a dissecting channel and the bankfull deposition zone above the highway. An abrupt break in profile at the contact is typical; here the plunge pool is about 2 feet deep. The fresh light-colored debris in the right background is slightly above the level of the fan surface.

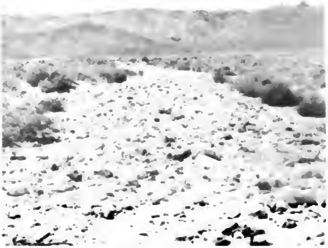

FIGURE 127.—View of the bankfull deposition zone near station 318 in the Antelope Springs channel. This fresh deposit is slightly above the general surface level. It represents sedimentation at the lower limits of the fan that tends to build it outward, into the valley proper.

by modern processes in a manner suggested by the usual view of fan building. The question to be answered is "Why has trenching of fans occurred between the divide areas and midfan?"

CAUSE OF TRENCHING

The occurrence of trenches in alluvial fans is a fact noted by many authors, certain of whom have discussed the results produced by trenching rather than its cause. Eckis (1928), for example, thought that a geomorphic cycle was involved and that the onset of trenching signaled the beginning of the end for the fans. Buwalda (1951) considered the more effective transport of sediment to be expected, arguing that the trenches would act like flumes and funnel material downfan. Many authors have offered the view that deposition will occur where the trenches end and the width: depth ratio increases. This truth has little bearing upon the cause of trenching of alluvial fans, however. Two possible causes will be considered here, tectonic movements and variation in tractive force.

TECTONIC EXPLANATION

Tectonic explanations for a variety of phenomena have been invoked in local studies within the Basin and Range province and elsewhere. The trenching of fans referred to in this report, however, is extremely widespread and requires a regional rather than local explanation. If uplift induces downcutting, then approximately synchronous movements of most of the ranges in the Basin and Range province must be invoked to explain the trenching of fans. Even where uplift can be demonstrated for an individual range, however, several difficulties emerge from direct cause-and-effect correlation of uplift and the trenching of fans.

The tectonic hypothesis is predicated on the concept that uplift will increase channel slopes and the velocity of flow, thereby inducing erosion or degradation. The actual increase in slope that can occur from a given uplift is seldom cited, however. If the White Mountains (pl 8.) are used as an example, the calculation is instructive.

The range is about 20 miles wide, and the relief is roughly 5,000 feet. An approximation to the overall slope, from the divide to a fan apex, is therefore 0.094 foot per foot. The actual channel slope will exceed this value near the divide but will be less than this value near the mountain front. If an absolute uplift of 1,000 feet occurred instantaneously, this value would become 0.113, an increase of 0.019 foot per foot. This is a rather small increase in view of the extreme uplift conditions postulated. Epply (1961) has shown that even the most severe earthquakes with high Mercalli intensities are usually associated with throws along faults of no more than about 30 feet. The effect of the average uplift upon slope will therefore be extremely small.

Moreover, velocity and slope are related by the Manning equation, namely, $v=\frac{1.49}{n} R^{2/3}S^{1/2}$, where v is velocity, R is the hydraulic radius, and S is the slope. The exponents in this equation show that changes in the hydraulic radius, which is a function of discharge, have a greater effect upon velocity than changes in slope. In addition, it has been pointed out by many authors that velocities are not necessarily high in the mountains, where steep slopes occur. The mean velocity of rivers, in fact, tends to either increase or remain constant in a downstream direction (Leopold, 1962). This would be expected because drainage area and, consequently, discharge, both increase downstream.

It is true that local fault scarps can produce a nickpoint that will retreat through time, but aside from other considerations, this explanation for trenching would again require simultaneity of tectonic activity on a regional scale. It is probable, therefore, that the main role to be ascribed to tectonism in regard to trenching is the change induced in the pattern of precipitation and vegetation, both of which vary orographically and can affect the processes under discussion. Magnitudes of uplift cannot be directly equated with sedimentation or erosion. The cause of trenching will be further pursued by considering the implications of the tractive-force distribution.

TRACTIVE-FORCE EXPLANATION

The sediment transport orthogonals (figs. 112, 113), which coincide with fan channels, generally intersect estimated tractive-force isopleths where they are convex downfan. Because the estimated tractive-force values decrease downfan, this means that tractive force within the channels is greater than at adjacent points on the fan surfaces. This was shown to be true for Paiute Chute (fig. 114), for example. Because modern floods are confined within the channels, the tractive force associated with the modern process must be greater than that which accompanied transport in the past. If this is true, then one or more of the three component variables that comprise tractive force must be greater today than in the past.

Of the three component variables, it might appear that deviation of past and present slope would be simplest to ascertain. If an active channel is traced downfan, then a point will eventually be reached at which the slope of the channel intersects the fan surface; this is a zone of bankfull deposition (pl. 9). It would not, however, be correct to conclude that the slope today must be less than in the past, because the slope in question is that which obtained before deposition in these zones. The deposit is itself an indication of change in process. The information desired is whether change in slope altered tractive force and therefore initiated the trenching indirectly. In this sense the answer is indeterminate but field observations suggest that the slopes of the channels do not markedly differ from those of fan surfaces, except in the vicinity of zones of bankfull deposition.

The depth of flow may be greater today than in the past, if the depth of the confining channels or trenches is accepted as a criterion. This would imply greater discharge and a correspondingly greater tractive force in the channels. The fact that former lakes throughout the region are today playas, however, suggests that the discharge of modern floods is probably less than floods of the past. The modern floods, in fact, may be misfit (Dury, 1958) in relation to their confining trenches in the upper reaches of fans; evidence of overbank flooding in the vicinity of the mountain fronts is generally lacking. Moreover, if an increase in tractive force initiated trenching, then selection of depth of flow as the responsible variable would be equivalent to attributing both cause and effect to this factor.

The remaining component, specific weight of the medium, can be considered in terms of density. If the density of the average flow is greater today than in the past, then mudflows should be a more frequent mechanism of transport. Observations suggest that this may be true. It remains to be proved that sound reasons exist for postulating that a contrast in density characterizes the difference between the modern and former processes. The tractive-force hypothesis, however, can be summarized at this point. The implication of the maps of estimated tractive force is that the modern process is attended by a greater tractive force than that of the past. Greater tractive force provides a logical explanation for the cause of trenching; simply stated, the explanation is that the shearing stress on fan surfaces increased at some time in the past. The stress was produced during sediment transport, and each effective flood deepened the channels until the designation "trench" could more fittingly be applied; this is still true today. Although a combination of factors may have brought about the increase in tractive force, an increase in the density of flow, including buoyancy effects, is thought to be an important cause. The evidence for this suggestion will be considered in the following discussion.

CONTRAST BETWEEN THE MODERN AND FORMER PROCESSES

MUDFLOWS

Descriptions of mudflows, the magnitudes of the particles transported, and descriptions of attendant features such as levees, have been provided by Rickmers (1913), Pack (1923), Blackwelder (1928), Sharp (1942), Wooley (1946), Kesseli and Beaty (1959), and several others cited in this report. Such information is common knowledge today, but the important question is whether mudflows actually cut channels by reason of their high density and consequent high tractive force. Most reports convey the impression that mudflows serve only to build fans, but some information to the contrary does exist in the literature. This is worthy of stress because it is germane to any discussion of past and present processes.

A statement by Wooley (1946, p. 78) is revealing:

> The mudflow of 1938 scarred the surface of the fan in a course 60 to 125 feet wide from the apex down the crest of the slope. The courses of a number of earlier mudflows are marked by windrows or small ridges of alluvium, which remain along the edge of the flow as the channel is cut deeper.

And on page 80 of the same report he states:

> Although degradation by mudflows is not an uncommon natural process in the deserts and semiarid areas of the west, there is little information available as to the mechanics of mudflow operation.

In a recent paper treating erosion of the Wasatch Mountain front, Croft (1962) provides numerous examples and much pertinent data attesting to the fact that mudflows in recent time have caused much channel erosion. Two photographs taken from the literature and reproduced here serve to illustrate the point. Figure 128 shows one of the many trenches produced by the catastrophic flood of June 1957 in the basin of the Guil River, France; figure 129 shows the results of 1 of 100 mudflows that occurred in Grand Teton National Park, Wyo., in August 1941. These particular examples were chosen because neither area is semiarid. They therefore illustrate the fact that degradation in the upper reaches of the path of flow is a characteristic feature of mudflows. When they occur, erosion results whether the climate is humid or arid. If these two examples are compared with the view of Painte Chute (fig. 88), it can be seen that the features of all three are identical.

The views suggest that debris is stripped from the upper reaches of each area and is transported to and deposited on the lower slopes. This is precisely the relationship observed on most alluvial fans in the Basin and Range province today. The catchment areas up to the divides, and the apex regions of the fans, are source areas for mudflows; deposition occurs below midfan.

The actual mechanics of mudflows is poorly understood, and the hypothesis set forth in this report, namely, that mudflows produce degradation primarily by reason of their greater tractive force, is based largely upon inference and deduction. As pointed out in the American Society of Civil Engineers, Task Force

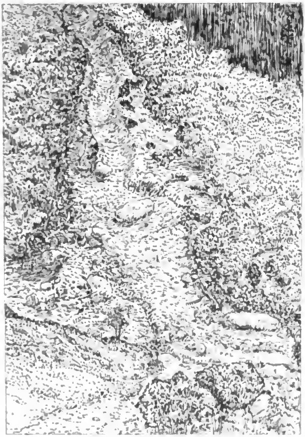

FIGURE 128.—View of a channel cut by a mudflow in the Guil Basin, France (after Tricart, 1961, fig. 2). The region is fairly humid, but the results of the mudflow are comparable with the features of Paiute Chute (fig. 88); addition of sediment largely occurs in the lower reaches of the path of flow.

Committee on Hydromechanics report (1963), however, there can be no question that the effect of dispersions of sediment is to increase viscosity, which in turn, alters the bed form because of a reduction in fall velocity of the bed material. The report cites Le Conte (1896) on page 125 as follows:

> The results show conclusively the powerful influence of viscosity due to sediment in suspension. A channel lined with cobblestones will stand a clear water velocity of 6 to 8 feet per second, but when it is followed by a more viscous stream heavily charged with material in suspension, although at a reduced velocity of only 4 to 6 feet per second, the cobblestones will be at once picked up and transported with the flow.

Although the flows discussed by Le Conte are not the equivalent of modern mudflows, it is suggested that density flows can erode the floors of channels by the removal of bed material that is too large to be transported by clear water. The fact that there is no evidence to the contrary, coupled with the several observations previously cited, implies that greater tractive force is associated with the modern process as a result of an increase in the average density of flow.

THE FORMER PROCESS

If the onset of trenching was initiated by density flows of higher tractive force, such as the relatively infrequent modern mudflows, then the inference to be drawn from the tractive-force hypothesis is that sediment transport was formerly achieved by a medium of lesser density. Given flows of lesser density than a mudflow but of necessarily greater density than clear water, and the absence of the deep confining channels of today, it appears probable that the flows of the former process must have spread laterally below the mountain front and aggraded the apex regions that are being eroded today. It is suggested, therefore, that the former process was more nearly akin to sheet floods than to the channelized density flows of today. Discharge was probably greater in the past; but because of lesser density and shallow depth of flow, the resultant tractive force was less.

If the former flows were of lesser density, then the water:sediment ratios must have been greater. This accords with the concept that greater precipitation prevailed in the area during several former time intervals. From this point of view the relative scarcity of clay and abundance of silt in nearly all the samples studied is worthy of note.

One might argue that the surface samples have been winnowed of clays by local runoff, but clearly, the basin surface today represents a time plane. If these samples have been winnowed, then samples obtained from fan cross sections should also contain little clay. Bull (1960) has examined such sections in the attempt to find criteria that will aid in distinguishing among mudflow deposits, water-laid deposits, and intermediate types. Although clay content is probably not a diagnostic feature of deposits in other areas, it is instructive to note that the main criterion used by Bull to distinguish ancient mudflow deposits in Fresno County, Calif., is a high clay content. He gives a value of about 30 percent for the samples studied. The Owens Valley mudflow, however, is by no means an atypical example of mudflows of today. The nature of the flow can be seen from the photographs of the upper reach (figs. 110, 111) as well as of the lower reach (figs. 130, 131). Samples from this mudflow contained 2.41 and 4.22 percent clay; these values pertain to the granule-to-clay fraction alone and therefore are maxima for the flow.

Sample locations in the active channel of Paiute Chute are shown in figures 132 and 133. The matrix of a recent flow is still present in the channel banks or levees; data on clay content are therefore pertinent. The percentage of clay, again in the granule to clay fraction, is 2.10 at the apex and 3.00 at midfan.

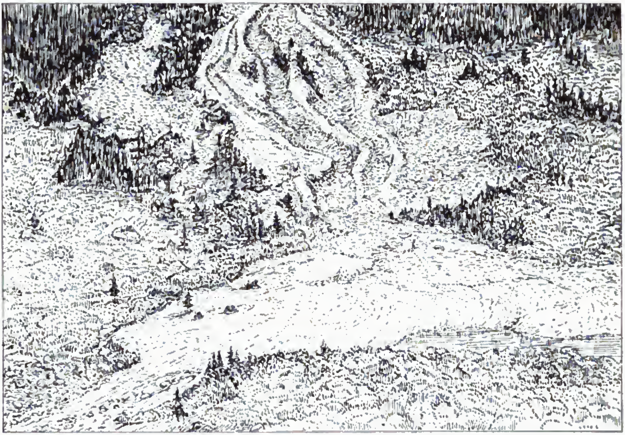

FIGURE 129.—View of the aftermath of a mudflow in the Grand Tetons, Wyo. (after Fryxell and Horberg, 1943, pl. 2, fig. 1). Note the similarity of the chutes that occur here and those shown in figures 88 and 128. The large deposit in the foreground is derived from preexisting talus deposits that were trenched by the mudflow.

Similar low values were obtained from the mudflow of Wrightwood, Calif. (Sharp and Nobles, 1953); little clay was present.

These data suggest that former transport conditions may have differed from those of today by reason of greater clay content. One might argue that a greater clay content in former flows implies still greater density of flow, but it should be recognized that the rate of production of clays is, in good part, a function of precipitation. Little clay will be produced if precipitation is deficient; from this point of view, if more clay was associated with the former process, then this supports the inference that water: sediment ratios were formerly greater. It should also be noted that given a greater abundance of clay in the surface sediments of fans, cohesion and resistance to trenching will be increased.

A second factor suggesting that fluctuation in regime may have occurred is the contrast between the organic content of mudflows today and that of older deposits. Despite the typical dark-brown to deep black color of the Owens Valley mudflow (figs. 110, 111, 130, 131), the organic content was quite low. Weight percentages are 1.89 and 2.80 in the granule to clay fraction for the 2 samples obtained. Wyman Canyon is choked with vegetation and contains a perennial stream. Predictably, the thin atypical Wyman mudflow contained a much higher percentage (14.05) of organic matter. Eardley and Gvosdetsky (1960) reported evidence of about six thin mudflow deposits in core samples from the Great Salt Lake. They state that a high humus content is present in these old flows but do not give percentages; such data are extremely rare. Croft (1962) reported the organic content of soils developed on old and recent mudflow deposits, but these values are not comparable to the content of mudflows. The paucity of data permits only the conclusion that the organic content of modern flows is not great. This results, of course, from the fact that vegetation is not abundant today. It is probable that both clay and vegetation were formerly more abundant, because both require the same type of climatic regime. Higher precipitation is not the only characteristic of the former regime, however; the frequency of precipitation must also be considered.

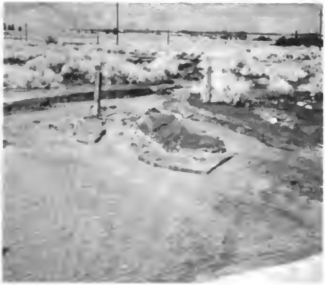

FIGURE 130.—View of the lower reach of the Owens Valley mudflow showing clear-water dissection. Although the deposit is undergoing dissection, it is apparent that sedimentation has occurred across a wide flat area at the lower boundary of the fan. The fenceposts shown parallel the main highway through the valley, which is about 8 miles below the mountain front of the Sierra Nevada at this point. Note the dark color of the deposit.

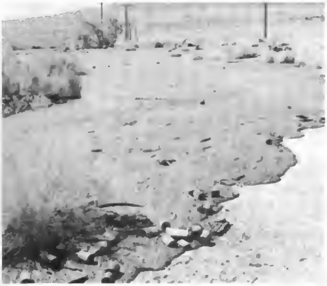

FIGURE 131.—View of the lower reach of the Owens Valley mudflow showing floating debris on the thin deposit. The flow was quite dense and viscous in this area (approx. 0.25 mile south of the clear-water flow shown in fig. 130), and in addition to the cans seen in the foreground, many cobble-size particles were also rolled and carried across a wide area of low slope.

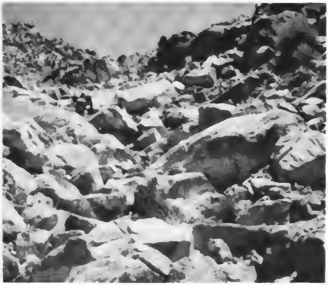

FIGURE 132.—View of the apex region of the active channel in Paiute Chute. The intermediate axis of the large boulder to the right of center is 10.4 feet in length. The divide of the small catchment area extends along the ridge summit shown. Fine sediment is rather scarce.

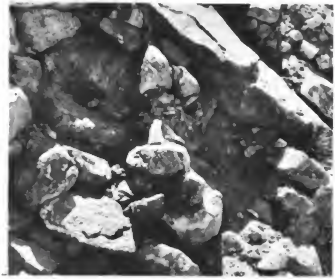

FIGURE 133.—View of the fine matrix in the levee wall along the active channel of Paiute Chute. The occurrence of the fine matrix surrounding the tightly wedged granitic boulders indicates that a mudflow produced the deposit and that Paiute Chute is not of rockslide or similar origin. The sample bag in the center of the photograph is 4 by 6 inches.

FREQUENCY OF PRECIPITATION

In semiarid or arid regions much of the annual precipitation today falls in few and infrequent storms. The slopes are largely bare of vegetation, little clay is present, and resistance to erosion is low. This combination of conditions favors the occurrence of mudflows. Given a more equitable distribution, as well as an absolute increase of annual precipitation, this situation will be reversed, and mudflows will become less frequent. The precipitation that accompanied the mudflows in the Grand Tetons (Fryxell and Horberg, 1943) represented a great departure from the norm for that area. Rainfall throughout the summer of 1941 was above average and was higher in each succeeding month; it was five times the average during the month of August, when the flows occurred. During June, July, and August no more than 3 successive days passed without recorded precipitation. The mudflows in the Guil Basin (Tricart, 1961) were also brought on by uncommonly high precipitation. Heavy rainfall over a period of 48 hours, entirely without precedent in the region, produced the flows. It cannot be claimed, therefore, that mudflows can only occur where the frequency of precipitation is low, but observations suggest that they are much more common in such areas. Variations in the frequency of precipitation are known to have occurred in semiarid areas (Leopold, 1951) and, by implication, in arid areas as well. It is thought that such changes in the frequency of precipitation can account for the prevalence of a former flow regime that was characterized by higher clay content, organic content, and water: sediment ratios.

Although the requirement of greater frequency of precipitation is often stated during discussions of former processes, it is difficult to prove on the basis of field evidence. One can, of course, easily argue in the case at hand that if the frequency of precipitation remained at its present value in the Great Basin while annual precipitation increased, then the only result would be more intense cloudbursts and still greater degradation by mudflows. It is thought, however, that the hanging fan shown in figures 119 and 120 does constitute field evidence that a greater frequency of precipitation must formerly have prevailed.

The fill in the small tributary canyon to the right of the main channel represents the level of aggradation that was attained throughout the Antelope Springs catchment area and by the fan proper. This is the high terrace level. The fill has been truncated by erosion within the main channel, and it may best be designated a hanging fan. This same phenomenon was observed in several small canyons that are tributary to the lower reaches of Wyman Canyon and in basins other than Deep Springs Valley. The occurrence of these hanging fans suggests that precipitation and sediment transport no longer occur in every canyon within the catchment areas. The infrequent cloudbursts of today may follow preferred tracks, as noted previously, and most of the precipitation will occur in the divide areas. The mudflows and the resultant trenches occur primarily in the trunk canyons and in the larger tributary canyons that head near divide areas. The precipitation pattern that accompanied uniform aggradation in the catchment areas must have differed from that which pertains today. Precipitation was certainly widespread rather than localized and, hence, was probably more frequent in occurrence.

The relationship discussed above may well be relevant to the problem posed by many hanging valleys that have been interpreted in terms of tectonism. Uplift of a range may result in more frequent precipitation in the divide areas and a decreased probability of precipitation in certain tributary valleys. A contrast in both discharge and frequency of floods could account for greater erosion within the main valleys and the bypassing of tributary valleys. For reasons cited previously, this explanation for hanging valleys would appear much more reasonable than any assumed linear relationship between uplift and downcutting.

PROCESS RATES

A charcoal pod was found at station 400 in the Antelope Springs channel (pl. 9). A general view of the channel in this area is shown in figure 134. The pod occurred 6 feet above the channel floor in the right bank, which is 12 feet high at this point (fig. 135). The presence of fire-blackened stones directly above the charcoal indicated that the pod was a fire hearth. A radiocarbon date of 1,380 ±250 years B.P. was obtained for a sample from this hearth. The field relationship therefore indicates that 6 feet of deposition and 12 feet of erosion have occurred since this date.

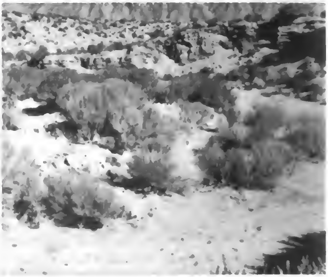

FIGURE 134.—View of the Antelope Springs channel at station 400. The view is downchannel from the fire-hearth site. Note the fresh character of the cobbles to the left of the meandering channel, indicating that modern transport has extended far out into the valley. The sage ranges from about 1 to 3 feet in height.

Any estimate of the process rates involved will depend upon the establishment of some arbitrary ratio between the rate of deposition and the rate of erosion. If it is assumed that the rate of erosion is equal to the rate of deposition, then 18 feet of either process has occurred in the last 1,130–1,630 years. This yields respective rates of 0.016 and 0.011 foot per year. If it is assumed that the rate of deposition was only half as great as the rate of erosion, which may be more reasonable at this location, then the equivalent of 24 feet of process has occurred during the same period. The respective rates in this case would be 0.021 and 0.015 foot per year.

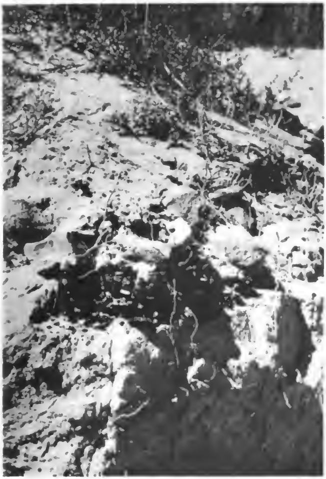

FIGURE 135.—View of the fire-hearth site in the Antelope Springs channel. The channel bank is 12 feet high at this point, and the bottom of the hearth is 6 feet below the top of the bank. Note the fire-blackened stone resting directly upon the charcoal pod, thus indicating that it is in fact a fire hearth.

These rates, ranging from about 1 to 2 feet per hundred years, should properly be applied only to events in the vicinity of the sample. Some estimate of the time of the last expansion of Deep Springs Lake can therefore be made, because the linear ridges that indicate this expansion (fig. 85) are in this general area. If it is assumed that the 6 feet of deposition in this area coincided with the expansion of the lake, then the linear ridges on the basin surface are 300–600 years younger than the fire hearth, depending upon the rate of deposition chosen. The high stand represented by the ridges occurred, therefore, between 700 and 1000 B.P., if the radiocarbon date is correct. Langbein (1961) has estimated the date of the last expansion of several lakes based upon the time represented by the total dissolved salt content. The value obtained for Owens Lake was 1,700 years, and a few other lakes expanded still more recently. The estimated date of the last expansion of Deep Springs Lake is therefore not unreasonable.

If the relatively minor climatic changes of Recent time could bring about the expansion and contraction of lakes and trenching to a depth of 12 feet at the fire-hearth location discussed above, then the much greater changes that marked the Pleistocene Epoch in this area may have coincided with the initiation of trenching in catchment and upper fan areas. It is worthy of note that an erosion rate of about 3 feet per hundred years would suffice to produce even the deepest trenches that occur in the region.

To obtain some future data on process rates in Deep Springs Valley, chains were installed in the channel bed at five locations in the Antelope Springs channel (pl. 9). At each section, particles in the channel were painted in order that some information on sediment transport might also be obtained in the course of the monitoring program. At sections *A–A′*, *B–B′*, and *C–C′*, entire gravel bars were painted; the first mentioned is shown in figure 136. Section *C–C′* is in the vicinity of the fire hearth. At sections *D–D′* and *E–E′* no gravel bars were present, and particles that occurred on the channel floor were alined perpendicular to the

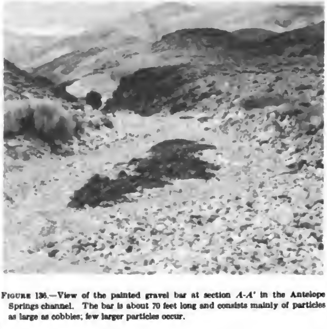

FIGURE 136.—View of the painted gravel bar at section *A-A′* in the Antelope Springs channel. The bar is about 70 feet long and consists mainly of particles as large as cobbles; few larger particles occur.

direction of flow. The information gained from this program over a period of years will not only provide data on modern process rates, but it should also serve to confirm the contention that trenching is the dominant long-term process in the upper fan reaches today.

FORMATION OF THE ALLUVIAL FANS

The formation of alluvial fans has been discussed ever since these striking sedimentary deposits were first noted during the early western exploratory surveys. The opinions expressed to explain the formation of fans may be conveniently grouped into three general categories, namely (1) evolutionary, (2) equilibrium, and (3) climatic hypotheses. Although the writer favors the climatic hypothesis, each holds some measure of truth, and because the truth often occupies middle ground in such problems, each hypothesis is treated here.

THE EVOLUTIONARY HYPOTHESIS

The concept that all landforms result from a geographic cycle that proceeds through the successive stages of youth, maturity, and old age is today commonly termed "Davisian philosophy." The specific choice of anthropomorphic stage names was probably influenced by the publication of the doctrine of evolution in the 19th century; the concept can therefore be appropriately designated an evolutionary hypothesis. Davis (1905) applied this concept to alluvial fans by emphasizing the importance of stage and thereby denigrating process. He suggested that alluvial fans would form in basins adjacent to uplifted mountain ranges in desert regions. The stage of youth was thought to be indicated by V-shaped canyons in the mountains and by small but rapidly growing fans. As the mountains wore down, Davis reasoned, the fans would continue to enlarge, and thus would fill the basin with sediment, and in the final stage—old age—the mountain remnants would be buried beneath a continuous cover of alluvium.

The inevitable reaction to one of the several failings of the concept of cycles, namely to treat processes and thereby gain some insight into the mode of formation of any given landform, set in with the advent of quantitative geomorphology. The modern view of the geographic cycle has, to a large degree, been summarized by Chorley (1962), who equates Davisian philosophy to closed-system thinking or the single-cause school of thought. Davis was quite correct in two important particulars, however.

First, despite the writer's disenchantment with tectonic explanations for magnitudes of sedimentation and erosion, as previously explained, it cannot be denied that slope and discharge are both intimately related to the production of sediment. An infinite discharge over a zero slope will have little more effect than zero discharge down a vertical rock wall. From this point of view, there can be no question that some uplift must first occur to provide the requisite differential relief for the formation of an alluvial fan at some initial time t_o.

Second, unless an infinite duration of uplift is postulated, then a given basin must completely fill with sediment at some finite time t_f. It is therefore reasonable to assume that at time t_f some mountain remnants will indeed be buried beneath an alluvial cover. The extent of this cover will depend upon coincidence, or its absence, of time t_f in each of many basins. The peneplain conceived by Davis (1889) will probably not result, but it is undeniable that old age, as Davis defined it, must ultimately be attained by any given basin.

The evolutionary hypothesis, admittedly based upon deduction, provides a reasonable description of alluvial fans in their formative and ultimate stages of development or morphology. Largely omitted, however, is consideration of the time between t_o and t_f and of the processes involved in fan formation.

THE EQUILIBRIUM HYPOTHESIS

The equilibrium hypothesis relates the morphology of a landform, or Davisian stage, with the processes acting upon it in terms of dynamic systems in which mass and energy are considered as functions of time. The two general systems defined by Von Bertalanffy (1950) are closed systems, in which materials and energy cannot be exchanged beyond the confines of a well-defined boundary, and open systems, in which materials, energy, or both can be exchanged with outside environments. As pointed out by Strahler (1952), most landforms represent open dynamic systems that tend toward equilibrium or a steady state. This view is widely accepted today (Leopold and Langbein, 1962; Chorley, 1962).

Although the equilibrium hypothesis is basically valid, certain difficulties of both application and interpretation arise when considering alluvial fans. An assumption must be made that a balance exists between erosion of the mountains and deposition in an adjacent basin. This is obviously reasonable, but if alluvial fans are in dynamic equilibrium, then a second, more particular assumption must be made, namely that the rates of sedimentation and erosion on a given fan are equal. Unless these rates are equal, then a fan will either grow or diminish in size as a function of the difference between the two rates. Denny (1965) contends that these rates are equal, or nearly so, and that alluvial fans are therefore in dynamic equilibrium with the processes acting upon them. Aside from correlations between planimetric measurements of source areas and their respective fans, which are somewhat suspect for reasons cited above (p. 133), little evidence exists to substantiate this contention. Rates of sedimentation and erosion on alluvial fans are not known. The amount of local runoff required to remove sediment from fans in order to balance the sediment added is also not known. Local runoff, however, can only be produced by either flows from the mountains or precipitation in the valley proper. It is not obvious that either of these sources will suffice to achieve the required balance; mountain floods must overcome seepage into the permeable alluvium, and local precipitation is not great. Because of orographic effects, the precipitation on most basin floors, and presumably on the fans as well, is very low, ranging from less than 2 inches per year in Death Valley to about 5 inches per year in basins at higher elevations. Moreover, the fact that highly erodible sediments, which represent former lake levels, have existed for thousands of years on the lower reaches of many fans does not support the view that a balance has been achieved or dynamic equilibrium attained.

The primary problem involved in the application of the equilibrium hypothesis, therefore, is to demonstrate conclusively that dynamic equilibrium has indeed been attained, rather than to merely assume that this is true. Even if one grants that alluvial fans have attained a steady state, however, a second problem will arise, namely the proper interpretation of this information.

Possible misinterpretation can be illustrated by consideration of the formation of playas. If their widespread occurrence, time contemporaneity, and the existence of strand lines at higher elevations are ignored, then it may be erroneously concluded that climatic change or other cyclic phenomena are not pertinent and that the interrelationship of their morphology with present processes is sufficient for an understanding of their formation.

Morphology and processes may be clearly interrelated, but the demonstration of dynamic equilibrium at any instant in time, even if conclusively proven, does not preclude the possibility that changes in both the intensities and types of processes may have occurred through time. Moreover, unlike water bodies, many landforms adjust to such changes very slowly, and although they tend toward equilibrium with modern processes, they may in fact be far removed from a steady state today. Leopold and Langbein (1962) state that it is improbable that time periods as long as geologic epochs could elapse before the attainment of equilibrium by fluvial processes in adjustable channels. Although the absolute duration of an epoch depends upon the geologic period considered, their meaning is clarified by a declaration of agreement with Hack (1960), who thought that no important time period is necessary. These statements do not, however, refute the fact that Pleistocene relicts that are thousands of years old exist today in all parts of the world. Hanging valleys, raised beaches, river terraces, dry waterfalls, the strand lines cited previously, and many other features attest to a lack of equilibrium with modern processes; in the absence of proof to the contrary, it is not unreasonable to suppose that some trenches in alluvial fans may be akin to the misfit river channels discussed by Dury (1958). Why, then, in the absence of any substantial proof should alluvial fans be thought to have attained dynamic equilibrium?

The concept of dynamic equilibrium of landforms represents a major advance beyond the application of Davisian principles. As previously stated, however, this does not mean that certain truths should be ignored merely because they are founded upon deduction. The equilibrium hypothesis requires blending with caution, lest a new generation of workers seek everywhere to demonstrate equilibrium as those before them sought cycles and peneplains. Dynamic equilibrium for any given landform must be conclusively proved, rather than simply claimed because the concept is in vogue, and if demonstrated to exist, then equilibrium conditions should not be cited as proof that the modern processes are necessarily identical with those of the past.

THE CLIMATIC HYPOTHESIS

The evidence suggesting that present climatic conditions are not identical with those of the past is legion. In response to changes in temperature, precipitation, evaporation rates, and the location of cyclonic storm tracks, changes in the regimen of rivers and lakes and in the distribution of plants and animals occurred. Jamieson (1863) recognized more than a century ago that climatic change regulated the expansion and contraction of saline lakes in arid regions. In the Great Basin, the existing lakes are largely confined to the area north of the 39th parallel. Hubbs and Miller (1948) have suggested that this comparatively wet region is representative of the former pluvial conditions that prevailed in those parts of the province that are driest today. Studies of pluvial lakes in New Mexico, such as Lake Estancia (Leopold, 1951), for example, indicate that this is true.

The occurrence of alternating climatic episodes, based upon various kinds of evidence, has been suggested by Bryan (1941), Judson (1953), and Miller and Wendorf (1958) in New Mexico, by Hack (1942) in Arizona, by Richmond (1962) in Utah, by Hunt (1954) in Death Valley, and by many others. Morrison (1961) is one of several workers that has suggested that climatic changes have been virtually synchronous throughout the Great Basin. Most of the reports cited treat climatic fluctuation within Recent time. Although less drastic than the Pleistocene fluctuations, changes during Recent time have been sufficient to produce recognizable imprints upon the sedimentary record, and four or five distinct climatic episodes are thought to have occurred within this time interval.

Data on the age of the alluvial fans in the Basin and Range province are generally unavailable. Although all the fans are not necessarily of equal age, it seems most probable that climatic changes have occurred during their formation. Because climatic change induces changes in the regimen of streams and alters the abundance of vegetation and edaphic characteristics, the climatic hypothesis requires that features thought to attest to such changes be widespread and common to most fans in the region. The features and characteristics of the fan environment that are thought to be indicative of climatic change have been previously discussed in this report. They include the following:

1. The loci of deposition on alluvial fans have shifted from areas well within catchment basins to the middle or lower reaches of the fans, far below the mountain front.
2. Trenches in the apex regions of the fans are misfit relative to present flow conditions by reason of their excessive depth, which is as much as 200 feet.
3. Paired terraces that are continuous with fan surfaces occur within catchment areas and in some places extend to the divide.
4. Abandoned channels occur on fan surfaces at higher elevations than the floors of the active channels.
5. The fan surfaces and the abandoned channels exhibit weathering stain and (or) desert varnish, whereas in the active channels and on modern deposits these are absent.
6. Hanging fans occur in tributary canyons within the catchment areas, and their surfaces are continuous with terraces and fan surfaces below the mountain front.
7. The estimated tractive force is greater within the active channels than on the fan surfaces.
8. The percentages of clay and organic material in both surface sediments and modern mudflows are extremely low.

The formation of the type of alluvial fan discussed in this report according to the climatic hypothesis is shown on figure 137. The observations and data that have been presented suggest the occurrence of the following events during one climatic cycle.

During a period of fan building (fig. 137*A*) aggradation occurred within catchment areas and on fan surfaces at continuous levels. Precipitation was both more abundant and more frequent than it is today. In response to this climatic regime, the abundance of both clay and vegetation was greater, and the fan surfaces were more resistant to erosion. Although discharge was greater, water:sediment ratios were higher, and the medium of transport had a lesser tractive force. Frequent floods spilled over numerous shallow channels onto the fan surfaces, spreading laterally below the mountain front. Sediment was deposited over wide areas of the fans as a consequence of these conditions.

Climatic change, manifested by a change from widespread to local or concentrated precipitation and by a lesser frequency of precipitation, produced a reduction of vegetation and a decrease in the abundance of clay. Catchment slopes and surface deposits became more easily erodible, thus contributing toward a reduction in water:sediment ratios and a greater frequency of mudflows. These flows of greater density, and correspondingly greater tractive force, deepened the trunk channels in catchment areas and trenched the upper reaches of the fans (fig. 137*B*). Terraces and hanging fans in the catchment areas were produced by these processes, and the sediment removed was deposited farther downfan, far below the mountain front.

The trenching of fans does not signal their demise within a geographic cycle, as suggested by Eckis (1928). During an episode of trenching, in response to the climatic conditions outlined above, the shift in the loci of deposition results in the addition of material at the lower limits of the fans. During any part of a climatic cycle, the fans are therefore constantly growing; they grow upward during intervals of general aggradation within the catchment areas and below the mountain front, and are built outward into the basin during periods of trenching in the upper reaches.

The sediment added at the lower margins of the fans may be redistributed and obscured by a subsequent rise in lake level within a given basin. This will produce an alternating alluvial fan-lacustrine facies, such as those commonly reported from core studies. At this time the conditions postulated in figure 137*A* will again occur; the trenches will fill with sediment, and deposition on fan surfaces will again build them upward, provided that the magnitude of the climatic shift is sufficient to accomplish this result before conditions change once again.

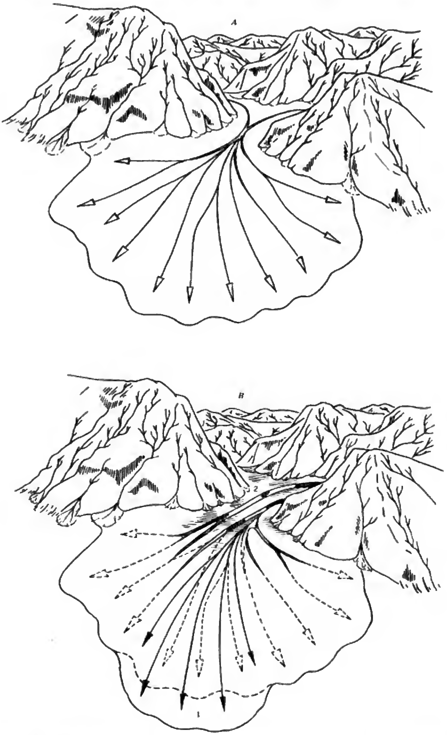

FIGURE 137.—Diagram showing the formation of alluvial fans during one cycle, according to the climatic hypothesis. *A*, During more humid or pluvial periods aggradation occurs within the catchment area and below the mountain front at continuous levels. Frequent floods with high water: sediment ratios spill over the shallow braided channels below the mountain front and deposit sediment over wide areas, building the fans upward. *B*, During a subsequent drier climatic period trenching occurs along main channels within the catchment area and on the upper reaches of the fan. Mudflows and other infrequent density flows transport the sediment they erode to the lower reaches of the fan, building it outward, into the valley (1). The terraces within the catchment area and the abandoned channels on the fan surface are produced as a consequence of this change in process. The small tributary canyon (2) receives little of the infrequent and localised precipitation. Because of trenching in the main channel, the previously deposited sediment is left as a hanging fan at the level of the high terrace as shown.

Both the Davisian and equilibrium theories therefore contain elements of truth. An understanding of the formation of alluvial fans, however, requires recognition of changes of processes through time that are accompanied by consequent changes in fan morphology. Because the most likely cause of such changes is climatic fluctuation, known to have occurred throughout the region, the climatic hypothesis is thought to provide the most reasonable explanation of the formation of fans. It should not be concluded that the equilibrium and climatic hypotheses are mutually exclusive from the foregoing treatment. As summarized so well by Braithwaite (1955, p. 339)—

> The world is not made up of empirical facts with the addition of the laws of nature: what we call the laws of nature are conceptual devices by which we organize our empirical knowledge and predict the future. From this point of view any general hypothesis whose consequences are confirmed by experience is a valuable intellectual device; and the profitable use of such a hypothesis does not presuppose that it will not at some future time be subsumed under some more general hypothesis in a more widely applicable deductive system, nor that the facts that it explains will not some time be explicable by a quite different hypothesis in another deductive system.

TABLE 1.—*Slope and maximum particle-size measurements in Deep Springs Valley, Calif.*

Sample	Slope (feet per foot)	Maximum particle size (feet)	Sample	Slope (feet per foot)	Maximum particle size (feet)
North end of Deep Springs Valley (fig. 90)					
−5, −6	0.160	3.2	−2, 1	0.010	0.3
−4, −6	.075	.2	−1, 1	.020	.1
−3, −6	.035	3.0	−4, 2	.130	.7
−2, −6	.035	2.1	−3, 2	.060	.2
−1, −6	.010	.2	−2, 2	.020	1.6
−6, −5	.160	3.7	−1, 2	.020	.1
−5, −5	.100	.2	−5, 3	.105	1.0
−4, −5	.035	1.6	−4, 3	.145	.6
−3, −5	.040	2.3	−3, 3	.030	.6
−2, −5	.035	1.3	−2, 3	.020	1.9
−1, −5	.030	2.0	−1, 3	.020	3.6
−6, −4	.110	2.7	−4, 4	.050	.2
−5, −4	.065	3.2	−3, 4	.020	5.3
−4, −4	.040	1.8	−2, 4	.025	4.0
−3, −4	.025	3.7	−1, 4	.030	4.7
−2, −4	.030	1.7	−5, 5	.075	.2
−1, −4	.025	.6	−4, 5	.085	2.3
−7, −3	.035	7.0	−3, 5	.055	3.7
−6, −3	.060	1.7	−2, 5	.035	1.7
−5, −3	.040	.1	−1, 5	.035	3.9
−4, −3	.060	2.1	−6, 6	.080	.5
−3, −3	.030	1.7	−5, 6	.040	3.2
−2, −3	.085	1.5	−4, 6	.060	2.3
−1, −3	.015	.1	−3, 6	.065	2.5
−7, −2	.105	1.9	−2, 6	.035	1.9
−6, −2	.070	.4	−1, 6	.025	2.5
−5, −2	.060	.3	−6, 7	.070	7.7
−4, −2	.030	.2	−5, 7	.040	6.4
−3, −2	.035	.2	−4, 7	.065	4.6
−2, −2	.020	.2	−3, 7	.045	5.4
−1, −2	.005	.1	−2, 7	.040	2.8
−6, −1	.120	.5	−1, 7	.030	.3
−5, −1	.060	.1	−6, 8	.060	3.5
−4, −1	.065	.1	−5, 8	.070	5.1
−3, −1	.035	.2	−4, 8	.095	4.8
−2, −1	.030	.6	−3, 8	.035	3.3
−1, −1	.000	.1	−2, 8	.025	2.0
−5, 0	.080	.2	−1, 8	.025	.6
−4, 0	.060	1.7	−7, 9	.110	16.5
−3, 0	.110	1.4	−6, 9	.050	2.2
−2, 0	.005	2.8	−5, 9	.095	2.9
−1, 0	.010	.9	−4, 9	.075	2.8
−6, 1	.100	.5	−3, 9	.040	.6
−5, 1	.090	.4	−2, 9	.030	3.3
−4, 1	.080	.2	−1, 9	.030	.7
−3, 1	.065	.2	−6, 10	.090	2.7

TABLE 1.—*Slope and maximum particle-size measurements in Deep Springs Valley, Calif.*—Continued

Sample	Slope (feet per foot)	Maximum particle size (feet)	Sample	Slope (feet per foot)	Maximum particle size (feet)
North end of Deep Springs Valley (fig. 90)—Continued					
−5, 10	0.085	3.5	4, 3	0.025	0.2
−4, 10	.050	.8	5, 3	.060	.5
−3, 10	.040	.4	6, 3	.085	.6
−2, 10	.040	.1	7, 3	.090	.5
−1, 10	.020	.4	8, 3	.130	1.8
−6, 11	.090	.3	0, 4	.010	.3
−4, 11	.130	1.4	1, 4	.010	.3
−3, 11	.050	1.5	2, 4	.015	.4
−2, 11	.050	1.7	3, 4	.010	1.3
−1, 11	.045	3.5	4, 4	.010	1.0
−2, 12	.055	4.4	5, 4	.065	.3
−1, 12	.050	5.6	6, 4	.065	.2
−2, 13	.045	4.8	7, 4	.080	.3
−1, 13	.055	4.5	8, 4	.140	.9
−5, 14	.160	6.2	0, 5	.015	.4
−4, 14	.055	7.4	1, 5	.020	.8
−3, 14	.050	3.7	2, 5	.015	.2
−2, 14	.100	2.5	3, 5	.030	.2
−1, 14	.080	3.3	4, 5	.010	.7
−3, 15	.070	4.4	5, 5	.030	.7
−2, 15	.065	4.7	6, 5	.050	.4
−3, 16	.190	4.2	7, 5	.065	.3
0, −6	.005	.1	8, 5	.110	1.4
1, −6	.000	.1	0, 6	.000	1.2
2, −6	.010	.0	1, 6	.015	.3
3, −6	.000	.1	2, 6	.015	.1
4, −6	.010	.3	3, 6	.010	.1
5, −6	.030	.2	4, 6	.005	1.2
6, −6	.065	.2	5, 6	.035	.1
0, −5	.005	.2	6, 6	.055	.6
1, −5	.010	.1	7, 6	.070	.7
2, −5	.010	.2	8, 6	.135	1.9
3, −5	.005	.0	0, 7	.020	1.3
4, −5	.005	.0	1, 7	.020	.1
5, −5	.030	.1	2, 7	.010	.1
6, −5	.060	.2	3, 7	.010	.1
0, −4	.000	.1	4, 7	.000	1.6
1, −4	.000	.0	5, 7	.030	.1
2, −4	.005	.1	6, 7	.095	1.0
3, −4	.010	.1	7, 7	.140	5.0
4, −4	.005	.0	0, 8	.010	.1
5, −4	.045	.1	1, 8	.025	.1
6, −4	.050	3.0	2, 8	.025	.1
0, −3	.005	.1	3, 8	.010	1.3
1, −3	.005	.1	4, 8	.010	1.8
2, −3	.000	.1	5, 8	.010	.9
3, −3	.005	.1	0, 9	.020	.2
4, −3	.005	.0	1, 9	.035	.1
5, −3	.065	.3	2, 9	.020	1.0
0, −2	.005	.3	3, 9	.015	.8
1, −2	.005	.1	4, 9	.010	.6
2, −2	.010	.1	5, 9	.065	.7
5, −2	.065	.6	6, 9	.135	5.2
0, −1	.005	.3	0, 10	.000	1.0
1, −1	.000	.1	1, 10	.040	.5
2, −1	.005	.0	2, 10	.025	.4
5, −1	.110	1.1	3, 10	.030	.3
0, 0	.000	1.2	4, 10	.015	.4
1, 0	.005	.1	5, 10	.065	1.3
2, 0	.005	.1	6, 10	.180	7.0
0, 1	.005	1.1	0, 11	.050	2.8
1, 1	.005	.2	1, 11	.035	1.3
2, 1	.000	.4	2, 11	.030	2.0
7, 1	.110	.3	3, 11	.035	1.0
8, 1	.160	.6	4, 11	.065	1.2
0, 2	.010	1.8	5, 11	.180	6.7
1, 2	.005	.2	0, 12	.035	2.6
2, 2	.005	.1	1, 12	.055	2.5
3, 2	.005	.3	2, 12	.050	2.7
4, 2	.060	.3	3, 12	.110	2.8
5, 2	.060	.3	4, 12	.130	5.2
6, 2	.140	.2	0, 13	.040	1.2
7, 2	.100	.3	1, 13	.075	1.8
8, 2	.110	.9	2, 13	.065	2.4
0, 3	.015	.1	3, 13	.205	1.7
1, 3	.010	.1	0, 14	.100	2.3
2, 3	.005	.2	1, 14	.090	3.9
3, 3	.005	.1	2, 14	.105	1.9
Palute Chute; on fan surface (fig. 114)					
1[1]	0.080	2.9	7	0.290	6.1
2	.130	3.4	8	.465	4.7
3	.135	5.8	9	.090	3.6
4	.245	3.0	10	.490	8.4
5	.235	6.2	11[2]	.435	10.4
6	.230	6.5			

See footnotes at end of table.

TABLE 1.—*Slope and maximum particle-size measurements in Deep Springs Valley, Calif.*—Continued

Sample	Slope (feet per foot)	Maximum particle size (feet)	Sample	Slope (feet per foot)	Maximum particle size (feet)
Paiute Chute; in recent channel (fig. 114)					
1 [1]	0.035	4.1	8	0.370	6.1
2	.065	3.0	9	.400	7.2
3	.100	5.2	10	.505	6.0
4	.140	7.0	11	.530	5.6
5	.175	5.8	12	.630	8.0
6	.215	7.5	13 [2]	.680	7.2
7	.300	9.8			
Westgard Pass (fig. 115)					
1 [1]	0.170	0.4	7	0.270	0.6
2	.160	.4	8	.230	.6
3	.230	.3	9	.430	.5
4	.280	.5	10	.380	.9
5	.320	.4	11	.500	.8
6	.230	.6	12 [2]	.800	.7
Westgard Pass (fig. 116)					
1 [1]	0.220	0.6	6	0.400	0.8
2	.240	.2	7	.440	.7
3	.230	.2	8	.500	.6
4	.400	.4	9	.590	.5
5	.390	.4	10	.660	.7
Antelope Springs fan (fig. 91)					
1	0.075	2.8	36	0.060	2.5
2	.080	2.2	37	.060	1.5
3	.070	1.7	38	.070	1.9
4	.070	2.1	39	.080	2.0
5	.080	2.0	40	.060	1.4
6	.080	1.3	41	.060	1.6
7	.065	2.4	42	.070	2.6
8	.050	3.7	43	.080	2.1
9	.040	2.6	44	.050	1.8
10	.055	1.5	45	.080	2.7
11	.070	1.8	46	.050	2.0
12	.090	2.2	47	.075	1.6
13	.080	2.7	48	.070	1.7
14	.065	1.7	49	.060	1.7
15	.075	1.2	50	.070	2.1
16	.070	2.5	51	.040	1.9
17	.070	1.0	52	.060	2.1
18	.090	1.8	53	.075	2.0
19	.070	1.4	54	.060	2.1
20	.070	1.7	55	.055	1.7
21	.075	3.2	56	.055	2.1
22	.070	1.8	57	.080	2.3
23	.065	1.1	58	.090	1.6
24	.080	2.0	59	.065	1.0
25	.080	2.5	60	.050	1.3
26	.050	2.6	61	.060	1.3
27	.075	2.4	62	.050	2.4
28	.080	6.4	63	.055	2.3
29	.080	2.6	64	.050	2.6
30	.070	1.5	65	.050	2.5
31	.055	1.6	66	.070	1.2
32	.065	2.6	67	.050	3.0
33	.070	2.3	68	.055	2.5
34	.070	1.0	69	.055	1.5
35	.060	2.1	70	.050	1.6

TABLE 1.—*Slope and maximum particle-size measurements in Deep Springs Valley, Calif.*—Continued

Sample	Slope (feet per foot)	Maximum particle size (feet)	Sample	Slope (feet per foot)	Maximum particle size (feet)
Antelope Springs fan (fig. 91)—Continued					
71	0.055	0.6	137	0.035	1.6
72	.045	1.0	138	.030	1.6
73	.055	.9	139	.035	1.3
74	.070	2.1	140	.030	1.5
75	.060	1.2	141	.040	.2
76	.070	1.2	142	.035	1.3
77	.060	2.9	143	.040	1.4
78	.070	2.3	144	.030	1.0
79	.060	1.5	145	.035	1.2
80	.040	1.0	146	.030	2.2
81	.050	1.7	147	.035	1.3
82	.060	1.8	148	.040	1.4
83	.050	1.7	149	.020	1.9
84	.035	1.7	150	.030	1.0
85	.060	1.8	151	.035	1.7
86	.050	1.3	152	.035	1.8
87	.050	1.5	153	.025	.9
88	.055	1.0	154	.025	1.5
89	.040	1.3	155	.020	.9
90	.050	2.0	156	.030	.1
91	.055	1.5	157	.030	1.1
92	.045	1.7	158	.025	.1
93	.070	2.1	159	.030	.1
94	.065	2.0	160	.020	.1
95	.060	1.9	161	.010	.5
96	.050	.9	162	.020	.1
97	.080	2.6	163	.020	.1
98	.050	2.5	164	.030	.1
99	.045	2.6	165	.020	.1
100	.055	1.7	166	.015	.1
101	.050	3.2	167	.030	1.0
102	.040	2.2	168	.020	.1
103	.060	1.2	169	.025	1.6
104	.035	1.4	170	.020	1.5
105	.040	1.1	171	.025	1.3
106	.035	1.0	172	.030	1.1
107	.050	1.7	173	.030	.1
108	.060	.9	174	.025	.1
109	.065	1.6	175	.020	.2
110	.050	1.5	176	.030	.7
111	.060	1.5	177	.015	.6
112	.060	1.4	178	.020	.1
113	.060	1.9	179	.015	.1
114	.045	1.1	180	.010	1.2
115	.060	1.6	181	.015	1.1
116	.050	2.4	182	.010	.2
117	.035	6.0	183	.015	.2
118	.055	1.6	184	.030	.1
119	.030	1.5	185	.020	.1
120	.030	1.6	186	.020	.1
121	.035	1.7	187	.010	.1
122	.040	1.6	188	.015	.1
123	.040	1.2	189	.020	.2
124	.020	1.0	190	.010	.1
125	.035	1.6	191	.010	.5
126	.045	1.4	192	.015	.4
127	.045	1.4	193	.020	.1
128	.040	1.3	194	.010	.7
129	.040	1.6	195	.005	.1
130	.050	1.5	196	.015	.1
131	.060	1.3	197	.010	.1
132	.040	1.4	198	.010	.1
133	.035	1.2	199	.020	.2
134	.045	1.6	200	.020	.1
135	.025	1.0	201	.005	.1
136	.020	1.0	202	.010	.1

[1] At toe of fan.

[2] At fan apex.

TABLE 2.—*Mean size, mean roundness, and lithology of pebbles in Deep Springs Valley, Calif.*

Sample	Mean size (mm)	Mean roundness	Lithology (per 50 pebbles)			Sample	Mean size (mm)	Mean roundness	Lithology (per 50 pebbles)		
			Granitic rocks	Sedimentary rocks	Basalt				Granitic rocks	Sedimentary rocks	Basalt
−5, −6	22.9	0.3	50	0	0	−3, −4	36.2	1.4	50	0	0
−4, −6	17.4	.2	50	0	0	−2, −4	25.3	1.3	49	1	0
−3, −6	15.1	.4	50	0	0	−1, −4	13.0	.7	50	0	0
−2, −6	13.6	.4	50	0	0	−7, −3	36.0	1.6	50	0	0
−1, −6	16.9	.9	50	0	0	−6, −3	31.0	1.8	49	1	0
−6, −5	31.5	.0	50	0	0	−5, −3	18.6	.3	50	0	0
−5, −5	19.3	.4	49	1	0	−4, −3	15.7	.5	50	0	0
−4, −5	17.9	.1	50	0	0	−3, −3	15.9	.1	50	0	0
−3, −5	14.2	.2	50	0	0	−2, −3	17.3	.2	50	0	0
−2, −5	13.1	.2	50	0	0	−1, −3	15.8	.5	49	1	0
−1, −5	15.9	.4	50	0	0	−7, −2	31.6	1.0	50	0	0
−6, −4	18.4	.1	50	0	0	−6, −2	16.1	.1	50	0	0
−5, −4	17.3	.4	50	0	0	−5, −2	18.7	.1	50	0	0
−4, −4	17.3	.2	50	0	0	−4, −2	14.2	.1	50	0	0

TABLE 2.—*Mean size, mean roundness, and lithology of pebbles in Deep Springs Valley, Calif.*—Continued

Sample	Mean size (mm)	Mean roundness	Lithology (per 50 pebbles)			Sample	Mean size (mm)	Mean roundness	Lithology (per 50 pebbles)		
			Granitic rocks	Sedimentary rocks	Basalt				Granitic rocks	Sedimentary rocks	Basalt
−3, −2	17.4	0.4	50	0	0	5, −5	12.6	0.3	50	0	0
−2, −2	15.2	.3	50	0	0	6, −5	17.6	.0	50	0	0
−1, −2	10.9	1.9	33	16	1	0, −4	8.9	2.2	41	6	3
−6, −1	17.6	.0	50	0	0	1, −4	10.9	2.2	38	12	0
−5, −1	18.5	.1	50	0	0	2, −4	9.1	1.8	47	1	2
−4, −1	15.9	.1	50	0	0	3, −4	11.1	2.4	38	7	5
−3, −1	15.6	.1	50	0	0	4, −4	8.3	2.6	32	9	9
−2, −1	19.3	.3	50	0	0	5, −4	12.9	.1	50	0	0
−1, −1	11.8	1.8	34	13	3	6, −4	23.2	.0	50	0	0
−5, 0	16.8	.0	50	0	0	0, −3	10.5	2.4	36	12	2
−4, 0	17.6	.1	50	0	0	1, −3	11.7	2.0	41	9	0
−3, 0	22.4	.1	50	0	0	2, −3	7.7	2.3	40	6	4
−2, 0	12.4	1.5	32	16	2	3, −3	7.4	2.1	39	8	3
−1, 0	9.5	2.0	38	7	5	4, −3	8.3	2.4	29	10	11
−6, 1	16.2	.1	50	0	0	5, −3	13.6	.0	50	0	0
−5, 1	16.6	.1	50	0	0	0, −2	10.2	2.3	37	12	1
−4, 1	20.4	.2	50	0	0	1, −2	10.9	2.6	33	10	7
−3, 1	20.6	.2	50	0	0	2, −2	7.7	2.8	42	5	3
−2, 1	19.6	2.1	28	15	7	5, −2	22.8	.0	50	0	0
−1, 1	13.3	2.2	29	17	4	0, −1	11.8	2.0	35	12	3
−4, 2	18.2	.0	50	0	0	1, −1	9.0	2.3	38	11	1
−3, 2	15.5	.1	50	0	0	2, −1	8.0	2.1	39	11	0
−2, 2	12.4	1.8	34	12	4	5, −1	21.3	.0	50	0	0
−1, 2	10.3	2.3	35	12	3	0, 0	15.3	1.8	27	21	2
−5, 3	23.9	.0	50	0	0	1, 0	11.8	2.2	25	23	2
−4, 3	17.3	.0	50	0	0	2, 0	11.9	2.2	29	17	4
−3, 3	20.6	1.4	39	11	0	0, 1	11.9	1.5	34	12	4
−2, 3	13.0	1.6	32	15	3	1, 1	10.0	2.1	34	12	4
−1, 3	11.6	2.0	24	19	7	2, 1	16.8	2.2	29	16	5
−4, 4	18.1	.0	50	0	0	7, 1	18.9	.0	50	0	0
−3, 4	19.9	1.9	33	14	3	8, 1	22.4	.0	50	0	0
−2, 4	14.5	1.8	34	9	7	0, 2	14.1	1.7	35	14	1
−1, 4	14.6	1.6	31	18	1	1, 2	11.9	1.9	30	13	7
−5, 5	24.1	.1	50	0	0	2, 2	18.2	3.3	9	40	1
−4, 5	18.7	.5	50	0	0	3, 2	9.2	2.4	37	10	3
−3, 5	15.9	1.5	34	13	3	4, 2	14.6	.1	50	0	0
−2, 5	15.4	2.0	31	16	3	5, 2	14.3	.2	50	0	0
−1, 5	17.3	.9	38	10	2	6, 2	20.2	.0	50	0	0
−6, 6	19.2	.0	50	0	0	7, 2	17.8	.0	50	0	0
−5, 6	19.2	.2	47	2	1	8, 2	18.3	.0	50	0	0
−4, 6	21.8	2.0	29	19	2	0, 3	21.1	1.8	23	22	4
−3, 6	19.1	1.7	32	14	4	1, 3	17.3	2.7	8	42	0
−2, 6	17.5	2.4	9	40	1	2, 3	20.5	3.1	7	42	1
−1, 6	17.3	1.9	19	27	4	3, 3	11.9	2.1	27	18	5
−6, 7	16.1	.3	47	3	0	4, 3	12.1	.2	46	4	0
−5, 7	20.7	2.3	27	17	6	5, 3	12.4	.2	50	0	0
−4, 7	23.7	2.3	10	37	3	6, 3	20.1	.1	50	0	0
−3, 7	23.9	2.1	11	34	5	7, 3	16.4	.0	50	0	0
−2, 7	18.5	1.8	9	40	1	8, 3	26.6	.0	50	0	0
−1, 7	13.9	1.6	21	26	3	0, 4	14.8	1.5	21	25	4
−6, 8	26.9	2.1	28	17	5	1, 4	14.1	2.1	32	18	0
−5, 8	29.6	1.8	20	25	5	2, 4	10.6	2.0	29	16	5
−4, 8	28.0	1.9	11	29	10	3, 4	12.2	2.2	29	19	2
−3, 8	35.5	1.2	24	17	9	4, 4	17.3	2.1	13	2	35
−2, 8	18.2	2.1	15	35	0	5, 4	11.6	.6	43	6	1
−1, 8	13.7	.7	45	1	4	6, 4	14.4	.9	41	9	0
−7, 9	43.3	3.0	31	15	4	7, 4	15.5	.0	50	0	0
−6, 9	32.1	1.1	19	27	4	8, 4	18.6	.0	50	0	0
−5, 9	34.8	2.0	15	32	3	0, 5	15.6	1.8	22	26	2
−4, 9	25.8	1.8	11	34	5	1, 5	13.4	2.4	14	32	4
−3, 9	30.2	2.3	14	34	2	2, 5	17.3	2.4	9	39	2
−2, 9	16.6	1.4	26	24	0	3, 5	11.1	.7	46	3	1
−1, 9	15.7	.7	48	1	1	4, 5	14.4	1.8	20	1	29
−6, 10	16.6	1.3	18	24	8	5, 5	17.9	.2	50	0	0
−5, 10	28.0	2.1	14	30	6	6, 5	16.2	.1	49	1	0
−4, 10	19.2	1.3	27	20	3	7, 5	17.5	.1	49	1	0
−3, 10	14.8	1.3	23	25	2	8, 5	17.9	.2	48	2	0
−2, 10	19.4	.9	43	4	3	0, 6	14.3	1.7	34	14	2
−1, 10	15.2	.7	47	1	2	1, 6	16.2	1.7	28	21	1
−6, 11	17.0	.6	39	7	4	2, 6	13.8	1.0	42	7	1
−4, 11	23.1	1.8	8	16	26	3, 6	13.1	.9	45	0	5
−3, 11	16.4	.9	31	13	6	4, 6	8.2	.9	46	1	3
−2, 11	18.2	.5	49	1	0	5, 6	14.6	.4	49	0	1
−1, 11	14.9	.3	43	0	7	6, 6	15.7	.1	50	0	0
−2, 12	18.6	.7	46	2	2	7, 6	21.6	.0	50	0	0
−1, 12	18.1	.2	48	1	1	8, 6	23.0	.0	50	0	0
−2, 13	17.2	.2	45	3	2	0, 7	16.4	1.7	30	19	1
−1, 13	15.6	.0	50	0	0	1, 7	13.6	.7	50	0	0
−5, 14	20.2	.1	44	0	6	2, 7	12.6	.7	50	0	0
−4, 14	17.9	.6	42	3	5	3, 7	11.0	.4	50	0	0
−3, 14	17.3	.5	43	2	5	4, 7	11.5	1.7	19	0	31
−2, 14	20.5	.2	50	0	0	5, 7	14.7	2.1	8	0	42
−1, 14	18.6	.2	49	0	1	6, 7	14.0	.0	50	0	0
−3, 15	18.9	.1	50	0	0	7, 7	17.7	.0	50	0	0
−2, 15	21.1	.0	49	0	1	0, 8	13.2	.8	47	2	1
−3, 16	24.5	.0	50	0	0	1, 8	15.1	1.0	48	1	1
0, −6	6.9	1.5	45	4	1	2, 8	13.5	.7	50	0	0
1, −6	8.8	2.0	40	8	2	3, 8	13.2	.9	50	0	0
2, −6	7.5	1.7	39	10	1	4, 8	13.5	.7	50	0	0
3, −6	7.1	1.7	43	6	1	5, 8	15.8	2.3	8	0	42
4, −6	9.0	2.0	27	16	7	0, 9	14.9	.5	49	0	1
5, −6	15.9	.1	50	0	0	1, 9	13.6	.8	50	0	0
6, −6	16.9	.0	50	0	0	2, 9	12.8	.8	50	0	0
0, −5	7.8	1.6	47	2	1	3, 9	13.1	.6	50	0	0
1, −5	8.4	1.8	40	6	4	4, 9	13.1	2.2	15	0	35
2, −5	8.5	2.0	39	9	2	5, 9	13.7	.1	50	0	0
3, −5	9.0	2.3	37	9	4	6, 9	17.3	.0	50	0	0
4, −5	7.7	2.0	39	6	5	0, 10	15.9	.4	47	2	1

TABLE 2.—*Mean size, mean roundness, and lithology of pebbles in Deep Springs Valley, Calif.*—Continued

Sample	Mean size (mm)	Mean roundness	Lithology (per 50 pebbles)			Sample	Mean size (mm)	Mean roundness	Lithology (per 50 pebbles)		
			Granitic rocks	Sedimentary rocks	Basalt				Granitic rocks	Sedimentary rocks	Basalt
1, 10	12.7	0.6	50	0	0	0, 12	16.6	0.4	50	0	0
2, 10	12.7	.7	49	0	1	1, 12	16.9	1.6	36	1	13
3, 10	16.8	1.5	33	0	17	2, 12	16.6	1.8	23	0	27
4, 10	18.5	2.2	16	1	33	3, 12	15.6	1.2	50	0	0
5, 10	15.3	.2	50	0	0	4, 12	27.1	1.7	33	4	13
6, 10	15.9	.0	50	0	0	0, 13	19.0	.7	50	0	0
0, 11	14.4	.4	46	4	0	1, 13	21.6	2.3	18	0	32
1, 11	13.2	.9	46	1	3	2, 13	19.6	1.2	24	0	26
2, 11	13.8	1.3	39	0	11	3, 13	18.2	.0	50	0	0
3, 11	15.0	1.9	25	0	25	0, 14	20.4	.8	40	0	10
4, 11	15.1	1.6	32	9	9	1, 14	25.2	1.0	13	0	37
5, 11	17.0	.1	50	0	0	2, 14	18.5	.2	50	0	0

TABLE 3. *Basic data on the tails of the granule-to-clay size distribution*

Sample	Granules (weight percentage)	Clay (weight percentage)	Silt/Clay	Sample	Granules (weight percentage)	Clay (weight percentage)	Silt/Clay
Antelope Springs active channel (pl. 9)							
9	4.21	1.55	6.44:1	291	9.44	2.76	2.26:1
62	9.39	.57	5.61:1	301	2.88	.00	∞
85	15.69	.83	6.44:1	318	2.92	1.24	3.67:1
126	.25	1.52	5.21:1	353	3.92	2.12	3.11:1
149	.14	1.17	21.59:1	400	2.24	1.41	4.94:1
199	14.21	1.42	4.97:1	437	1.28	.91	10.84:1
214	8.28	1.72	5.54:1	463	7.29	1.51	3.62:1
241	13.35	.54	9.75:1	480	.80	1.50	2.94:1
279	17.71	.20	14.83:1	512	.13	.77	4.80:1
				553	.99	1.74	1.66:1
Paiute Chute							
P-1[1]	10.60	2.10	4.32:1	P-2[2]	12.90	3.00	4.92:1
Mudflows							
BP-1[3]	17.12	2.41	4.30:1	Wy-1[5]	0.00	17.38	4.28:1
BP-2[4]	8.42	4.22	3.57:1				
North end of Deep Springs Valley (fig. 90)							
−5, −4	6.06	1.43	8.30:1	0, 1	2.81	0.99	11.82:1
−4, −4	10.29	.49	26.58:1	7, 1	4.94	2.17	1.68:1
−7, −3	9.04	.96	7.23:1	2, 2	2.60	.75	11.47:1
−2, −3	16.76	1.71	6.30:1	4, 2	6.01	3.62	6.11:1
−5, 0	7.51	1.10	7.48:1	0, 3	5.27	3.79	3.06:1
−3, 0	8.49	4.12	2.96:1	6, 3	28.80	.00	∞
−1, 0	13.21	.34	32.95:1	8, 3	20.00	2.01	6.80:1
−1, 3	2.16	1.24	11.52:1	3, 4	3.14	2.46	4.92:1
−3, 5	6.85	.96	17.60:1	0, 5	8.30	.97	13.30:1
−5, 6	1.85	1.15	8.46:1	4, 5	3.27	3.11	5.05:1
−5, 7	4.76	2.15	4.76:1	6, 5	17.82	1.61	16.64:1
−4, 7	4.02	2.70	5.76:1	8, 5	21.19	1.72	8.00:1
−5, 8	5.69	.92	5.63:1	2, 6	7.95	.00	∞
−7, 9	13.32	1.67	8.90:1	0, 7	5.34	1.11	11.80:1
−5, 9	6.08	2.14	7.10:1	4, 7	.34	1.48	10.15:1
−5, 10	1.79	6.37	3.91:1	6, 7	23.60	.64	27.28:1
−3, 10	3.04	1.83	5.76:1	2, 8	5.75	1.45	7.67:1
−1, 12	8.76	1.31	8.46:1	3, 8	2.84	2.34	6.48:1
−2, 14	14.99	.00	∞	0, 9	10.91	.78	15.30:1
0, −6	5.02	2.35	7.04:1	3, 9	8.60	1.36	11.19:1
3, −6	1.90	2.89	11.05:1	5, 9	8.02	1.37	10.78:1
4, −5	2.62	3.93	5.81:1	1, 10	3.52	1.07	5.95:1
6, −5	20.40	.70	12.00:1	4, 10	3.94	2.18	7.91:1
0, −4	5.70	1.65	8.00:1	6, 10	15.19	1.74	10.06:1
2, −4	1.74	3.91	11.12:1	0, 11	11.39	.84	11.23:1
3, −4	5.61	.00	∞	3, 11	4.16	1.68	7.16:1
5, −4	11.88	1.04	19.18:1	5, 11	22.65	1.68	6.26:1
4, −3	12.58	3.53	8.16:1	2, 12	9.99	.67	7.30:1
1, −2	11.19	2.48	6.78:1	4, 12	9.99	1.28	4.16:1
2, −2	3.68	.00	∞	1, 13	16.58	.88	10.44:1
1, −1	5.59	3.22	10.87:1	3, 13	15.04	2.50	6.70:1
5, −1	3.79	26.58	1.06:1	0, 14	10.21	.89	9.96:1
2, 0	3.28	1.29	7.81:1	2, 14	16.05	1.26	9.44:1

---

[1] At fan apex.
[2] At midfan.
[3] 2 miles below mountain front.
[4] 8 miles below mountain front.
[5] At BM 5220.

TABLE 4.—*Sedimentary parameters of the granule-to-clay size fraction, in phi units*

Sample	Median	M_z	σ_I	Sk_I	K_G	Sample	Median	M_z	σ_I	Sk_I	K_G
Antelope Springs active channel (pl. 9)											
9	1.95	1.96	2.12	0.12	1.62	301	2.40	2.43	1.35	0.21	1.49
62	1.28	1.22	1.53	−.30	1.16	318	1.67	1.71	1.25	.11	1.34
85	1.65	1.27	2.01	−.15	1.10	353	1.60	1.66	1.86	.62	1.16
126	2.14	2.24	1.46	.27	1.60	400	1.73	1.56	1.65	.23	1.39
149	3.32	3.78	1.59	.40	1.34	437	1.99	2.14	1.63	.27	1.41
199	1.02	1.02	2.10	.15	1.28	463	1.71	1.59	1.92	.03	1.34
214	2.26	2.12	2.23	−.03	1.73	480	2.07	2.11	1.19	.12	1.42
241	1.30	1.18	1.97	.02	1.06	512	1.65	1.72	1.03	.19	1.22
279	.80	.70	1.69	−.01	.90	553	1.73	1.77	1.02	.08	1.12
291	1.40	1.43	2.01	.12	1.33						
Paiute Chute											
P-1[1]	1.64	1.53	2.17	0.07	1.59	P-2[2]	1.30	1.67	2.67	0.27	1.04
Mudflows											
BP-1[3]	0.96	1.13	3.47	0.25	1.15	Wy-1[5]	6.30	6.29	1.67	0.02	0.83
BP-2[4]	1.53	2.01	3.75	.31	1.19						
North end of Deep Springs Valley (fig. 90)											
−5, −4	1.70	1.80	2.20	0.18	1.24	7, 1	1.12	1.27	1.56	.19	1.28
−4, −4	.74	1.25	3.34	.30	1.13	2, 2	1.51	1.71	1.83	.27	1.17
−7, −3	1.01	1.20	2.03	.27	1.22	4, 2	2.90	2.89	2.77	.04	1.14
−2, −3	.40	1.03	2.45	.41	1.11	0, 3	1.93	2.03	2.24	.20	1.31
−5, 0	1.00	1.27	2.03	.29	1.24	6, 3	−.18	.06	1.71	.33	1.01
−3, 0	1.49	1.72	2.50	.37	1.20	8, 3	.55	1.11	2.65	.40	.96
−1, 0	.70	1.07	2.29	.34	1.19	3, 4	2.51	2.39	1.96	.04	1.49
−1, 3	1.78	2.02	2.04	.28	1.17	0, 5	1.61	1.70	2.30	.17	1.09
−3, 5	1.70	2.35	2.44	.25	1.05	4, 5	2.00	2.29	2.46	.25	1.15
−5, 6	1.56	1.73	1.95	.28	1.17	6, 5	3.73	2.49	3.13	−.03	.77
−5, 7	1.50	1.61	2.12	.24	1.30	8, 5	.49	1.06	2.62	.41	.97
−4, 7	1.98	2.26	2.36	.24	1.19	2, 6	1.23	1.44	2.09	.22	1.44
−5, 8	.81	1.34	1.64	.29	1.22	0, 7	2.31	2.14	2.09	.00	1.22
−7, 9	1.35	1.54	2.55	.22	1.02	4, 7	2.37	2.44	1.90	.22	1.22
−5, 9	1.68	1.97	2.42	.25	1.08	6, 7	.60	1.25	3.77	.40	.83
−5, 10	2.89	3.30	2.60	.28	.97	2, 8	1.72	1.78	2.15	.16	1.14
−3, 10	1.65	1.83	2.06	.31	1.12	3, 8	2.21	2.34	2.16	.20	1.25
−1, 12	1.51	1.61	2.24	.18	1.18	0, 9	1.30	1.49	2.27	.22	1.11
−2, 14	.71	1.02	2.22	.30	1.00	3, 9	1.40	1.73	2.67	.28	1.06
0, −6	2.10	2.30	2.38	.24	1.16	5, 9	1.92	1.88	2.35	.15	1.09
3, −6	3.13	3.35	2.65	.12	.87	1, 10	1.80	1.82	1.71	.10	1.28
4, −5	3.10	3.23	2.91	.10	1.20	4, 10	2.46	2.51	2.59	.11	1.17
6, −5	.57	.79	2.23	.27	1.24	6, 10	1.20	1.67	2.78	.30	.95
0, −4	2.11	2.01	2.21	.07	1.14	0, 11	.71	1.12	2.23	.36	1.18
2, −4	3.80	3.83	2.74	.00	1.01	3, 11	1.65	1.84	2.14	.27	1.16
3, −4	1.31	1.27	1.28	−.06	1.09	5, 11	.42	.86	2.48	.38	1.04
5, −4	1.95	2.11	2.72	.15	.93	2, 12	.51	.67	1.61	.24	1.26
4, −3	3.20	2.98	3.13	−.06	.84	4, 12	.70	.87	1.86	.25	1.25
1, −2	1.80	2.04	2.67	.16	1.04	1, 13	.35	.81	2.22	.41	1.33
2, −2	1.52	1.61	1.59	.15	1.28	3, 13	1.52	1.61	2.80	.23	1.14
1, −1	3.30	3.38	2.93	.03	.82	0, 14	1.20	1.35	2.13	.20	1.19
2, 0	1.99	2.10	1.83	.21	1.33	2, 14	.94	1.33	2.46	.26	1.02
0, 1	1.62	1.84	1.97	.28	1.85						

---

[1] At fan apex.
[2] At midfan.
[3] 2 miles below mountain front.
[4] 8 miles below mountain front.
[5] BM 5220.

TABLE 5.—*Sample modes and their weight percentage of the granule-to-clay size fraction*

Sample	Primary mode	Weight percent	Secondary mode	Weight percent
Antelope Springs active channel (pl. 9)				
9	Medium sand	26.31	None	
62	do	29.38	do	
85	do	25.55	Granules	15.69
126	do	31.84	None	
149	Very fine sand	33.79	do	
199	Medium sand	22.75	Silt	7.03
214	Fine sand	26.36	Granules	8.28
241	Medium sand	22.49	do	15.35
279	do	23.68	do	17.71
291	do	24.92	None	
301	Fine sand	30.21	Granules	2.88
318	Medium sand	38.26	None	
353	do	21.95	do	
400	do	31.49	do	
437	do	33.06	do	
463	do	26.50	do	
480	do	33.52	do	
512	do	46.93	do	
553	do	43.43	do	
Paiute Chute				
P-1 [1]	Medium sand	28.41	Granules	10.60
P-2 [2]	Coarse sand	16.91	Silt	14.70
Mudflows				
BP-1 [3]	Medium sand	17.46	Granules	17.12
BP-2 [4]	do	18.80	Silt	15.07
Wy-1 [5]	Silt	77.25	None	
North end of Deep Springs Valley (fig. 90)				
−5, −4	Medium sand	21.88	None	
−4, −4	Coarse sand	22.90	Silt	13.00
−7, −3	do	22.24	None	
−2, −3	Very coarse sand	23.07	Silt	10.78
−5, 0	Coarse sand	25.15	None	
−3, 0	Very coarse sand	19.81	Silt	12.20
−1, 0	do	22.71	do	11.20
−1, 3	Medium sand	24.15	do	14.31
−3, 5	Coarse sand	19.12	do	17.29
−5, 5	do	25.40	None	
−5, 7	do	22.09	do	
−4, 7	Medium sand	21.28	Very fine sand	16.17
−5, 8	Coarse sand	29.63	None	
−7, 9	Very coarse sand	17.34	Silt	14.87
−5, 9	Coarse sand	19.86	do	15.21
−5, 10	Silt	24.81	Medium sand	19.43
−3, 10	Coarse sand	23.27	Very fine sand	15.44
−1, 12	Medium sand	20.04	None	
−2, 14	Coarse sand	20.64	Silt	9.65
0, −5	Medium sand	18.67	Very fine sand	17.39
3, −6	Silt	31.96	Medium sand	14.25
4, −5	Very fine sand	24.87	None	
6, −5	Coarse sand	22.50	Granules	20.40
0, −4	Very fine sand	18.96	None	
2, −4	Silt	40.35	Very coarse sand	7.45
3, −4	Medium sand	32.30	None	
5, −4	Silt	19.95	Medium sand	13.47
4, −3	do	28.80	Granules	12.58
1, −2	Very fine sand	17.17	Coarse sand	15.68
2, −2	Medium sand	31.97	None	
1, −1	Silt	35.10	Medium sand	12.37
5, −1	do	28.06	Coarse sand	15.39
2, 0	Medium sand	26.60	None	
0, 1	do	25.04	do	
7, 1	Coarse sand	28.51	do	
2, 2	do	25.18	do	
4, 2	Very fine sand	22.33	Medium sand	12.94
0, 3	Medium sand	20.71	Very fine sand	16.99
6, 3	Granules	28.50	Silt	4.02
8, 3	Very coarse sand	20.49	do	13.72
3, 4	Very fine sand	22.90	None	
0, 5	Coarse sand	18.24	Very fine sand	15.84
4, 5	Medium sand	18.76	do	17.09
6, 5	Silt	26.80	Granules	17.82
8, 5	Granules	21.19	Silt	13.75
2, 6	Coarse sand	21.06	Very fine sand	13.79
0, 7	Very fine sand	21.69	None	
4, 7	Medium sand	24.30	Very fine sand	21.00
6, 7	Granules	23.60	Silt	13.45
2, 8	Medium sand	19.71	None	
3, 8	do	21.15	do	
0, 9	Coarse sand	20.15	Silt	11.91
3, 9	do	20.60	do	15.29
5, 9	Very fine sand	17.37	Medium sand	16.68
1, 10	Medium sand	28.28	None	
4, 10	Very fine sand	21.12	Medium sand	17.14
6, 10	Silt	17.48	Very coarse sand	17.26
0, 11	Coarse sand	22.99	Silt	9.45
3, 11	do	21.76	Very fine sand	15.21
5, 11	Granules	22.65	Silt	10.46
2, 12	Coarse sand	30.39	None	
4, 12	do	24.99	do	
1, 13	Very coarse sand	24.92	Silt	9.20
3, 13	Silt	16.80	Very coarse sand	15.75
0, 14	Medium sand	21.32	None	
2, 14	Coarse sand	18.02	Silt	11.89

[1] At fan apex.
[2] At midfan.
[3] 2 miles below mountain front.
[4] 8 miles below mountain front.
[5] BM 5220

TABLE 6.—*Clay-mineral ratios of related samples, in parts per ten*

Sample	Mont-morillonite group	Illite	Kaolinite and (or) chlorite	Sample	Mont-morillonite group	Illite	Kaolinite and (or) chlorite
Antelope Springs active channel (pl. 9)							
9	5.2	3.8	1.0	301	2.1	5.8	2.1
85	1.3	6.5	2.2	318	2.2	5.7	2.1
126	2.6	5.6	1.8	353	3.3	4.9	1.8
149	3.1	4.8	2.1	400	2.1	5.5	2.4
199	.7	7.0	2.3	437	3.1	4.2	2.7
214	2.4	5.3	2.3	463	3.2	4.2	2.6
241	4.0	4.3	1.7	480	3.4	4.7	1.9
279	2.5	6.0	1.5	512	1.3	7.1	1.6
291	3.7	3.9	2.4	553	2.2	5.6	2.2
Paiute Chute							
P-1	7.1	1.9	1.0	P-2	5.5	3.4	1.1
Mudflows							
BP-1 [1]	2.4	5.2	2.4	Wy-1 [2]	5.7	3.5	0.8
BP-2 [1]	4.6	2.9	2.3				
North end of Deep Springs Valley (fig. 90)							
2, 14	3.3	4.1	2.6	−5, 8	1.1	6.8	2.1
3, 13	5.8	3.4	.8	3, 6	4.2	4.5	1.3
4, 12	6.0	2.5	1.5	−5, 7	4.3	3.9	1.8
5, 11	5.1	3.0	1.9	−4, 7	3.4	5.4	1.2
6, 10	6.0	2.6	1.4	−5, 5	3.9	4.5	1.6
−5, 10	5.6	4.2	.2	−3, 5	4.3	4.3	1.4
4, 10	4.8	4.0	1.2	−1, 3	2.6	5.7	1.7
−5, 9	3.1	5.1	1.8	1, −1	4.0	4.3	1.7
5, 9	4.7	3.6	1.7	0, 1	4.5	4.5	1.0
3, 9	3.0	5.1	1.9	4, 7	3.4	5.2	1.4

[1] At Big Pine.
[2] BM 5220

REFERENCES

American Society of Civil Engineers, Task Force Committee on Hydromechanics, 1963, Friction factors in open channels: Am. Soc. Civil Engineers Proc., Jour. Hydraulics Div., v. 89, no. HY 2, p. 97-143.

Antevs, E. V., 1948, The Great Basin, with emphasis on glacial and post-glacial times. 3, Climatic changes and pre-white man: Univ. Utah Bull., v. 38, no. 20, p. 168-191.

———1952, Cenozoic climates of the Great Basin: Geol. Rundschau, v. 40, p. 94-108.

Blackwelder, Elliot, 1928, Mudflows as a geologic agent in semi-arid mountains: Geol. Soc. America Bull., v. 39, p. 465-484.

Blackwelder, Elliot, 1954, Pleistocene lakes and drainage in the Mohave region, southern California: California Div. Mines Bull. 170, Chap. 5, p. 35–40.

Blissenbach, Erich, 1952, Surface angle and particle size distribution on alluvial fans: Jour. Sed. Petrology, v. 22, p. 25–28.

———1954, Geology of alluvial fans in semi-arid regions: Geol. Soc. America Bull., v. 65, p. 175–190.

Braithwaite, R. B., 1955, Scientific explanation: A study of the function of theory, probability, and law in science: London, Cambridge Univ. Press, 376 p.

Bryan, Kirk, 1941, Correlation of the deposits of Sandia Cave, New Mexico, with the glacial chronology: Smithsonian Misc. Colln., v. 99, no. 23, p. 45–64.

Bull, W. B., 1960, Type of deposition on alluvial fans in western Fresno Co., California [abs.]: Geol. Soc. America Bull., v. 71, p. 2052.

Buwalda, J. P., 1951, Transportation of coarse material on alluvial fans [abs.]: Geol. Soc. America Bull., v. 62, p. 1497.

Chorley, R. J., 1962, Geomorphology and general systems theory: U.S. Geol. Survey Prof. Paper 500–B, p. B1–B10.

Clements, T., 1952, Wind-blown rocks and trails on Little Bonnie Claire Playa, Nye Co., Nevada: Jour. Sed. Petrology, v. 22, p. 182–186.

Croft, A. R., 1962, Some sedimentation phenomena along the Wasatch mountain front: Jour. Geophys. Research, v. 67, p. 1511–1524.

Cullity, B. D., 1956, Elements of X-ray diffraction: Reading, Mass., Addison-Wesley, 514 p.

Dake, C. L., 1921, The problem of the St. Peter sandstone: Missouri School Mines and Metall. Bull., v. 6, p. 158–163.

Davis, W. M., 1889, The rivers and valleys of Pennsylvania: Natl. Geog. Mag., v. 1, p. 183–253.

———1905, The geographical cycle in an arid climate: Jour. Geology, v. 13, p. 381–407.

Denny, C. S., 1965, Alluvial fans in the Death Valley region, California and Nevada: U.S. Geol. Survey Prof. Paper 466, 62 p.

Droste, J. B., 1961, Clay minerals in sediments of Owens, China, Searles, Panamint, Bristol, Cadiz, and Danby Lake basins, California: Geol. Soc. America Bull., v. 72, p. 1713–1722.

Dury, G. H., 1958, Tests of a general theory of misfit streams: British Geog. Inst. Trans. and Papers Pub. 25, p. 105–118.

Eardley, A. J., and Gvosdetsky, V., 1960, Analysis of a Pleistocene core from Great Salt Lake, Utah: Geol. Soc. America Bull., v. 71, p. 1323–1344.

Eckis, Rollin, 1928, Alluvial fans of the Cucamonga district, southern California: Jour. Geology, v. 36, p. 224–247.

Eppley, R. A., 1961, Earthquake history of the United States; Part II, Stronger earthquakes of California and western Nevada: U.S. Dept. Commerce Pub. 41–1, rev. ed. (1960), 55 p.

Fahnestock, R. K., 1961, Competence of a glacial stream: U.S. Geol. Survey Prof. Paper 424–B, p. 211–213.

Feth, J. H., 1961, A new map of the western coterminous United States showing the maximum known or inferred extent of Pleistocene lakes: U.S. Geol. Survey Prof. Paper 424–B, p. 110–112.

Flint, R. F., 1957, Glacial and Pleistocene geology: New York, John Wiley & Sons, 553 p.

Folk, R. L., and Ward, W. C., 1957, Brazos River bar; a study in the significance of grain size parameters: Jour. Sed. Petrology, v. 27, p. 3–26.

Freidman, G. M., 1961, Distinction between dune, beach, and river sands from their textural characteristics: Jour. Sed. Petrology, v. 31, p. 514–529.

Fryxell, F. M., and Horberg, C. L., 1943, Alpine mud flows in Grand Teton National Park, Wyoming: Geol. Soc. America Bull., v. 54, p. 457–472.

Gilbert, G. K., 1914, Transportation of debris by running water: U.S. Geol. Survey Prof. Paper 86, 263 p.

Grove, A., and Sparks, P. W., 1952, Le deplacement des galets par le vent sur la glace: Rev. Géomorphologie Dynamique, v. 3, p. 37–39.

Gulicher, A., and Cailleux, A., 1950, Relief et formations quarternaires du centre-est des Pays-Bas: Rev. Géomorphologie Dynamique, v. 1, p. 128–143.

Hack, J. T., 1942, The changing environment of the Hopi Indians of Arizona: Harvard Univ., Peabody Mus. Archeol. and Ethnol. Papers, v. 35, no. 1, 85 p.

———1960, Interpretation of erosional topography in humid temperate regions: Am. Jour. Sci., Bradley Volume, v. 258A, p. 80–97.

Hjulström, Filip, 1935, Studies of the morphological activity of rivers as illustrated by the River Fyris: Upsala, Univ., Geol. Inst. Bull., v. 25, p. 221–527.

Hubbs, C. L., and Miller, R. R., 1948, The zoological evidence: correlation between fish distribution and hydrographic history of western United States. Part II, The Great Basin: Univ. Utah Bull., v. 38, no. 20, 166 p.

Hunt, Alice, 1960, Archeology of the Death Valley salt pan, California: Univ. Utah Anthropol. Papers, 47, 313 p.

Hunt, C. B., 1954, Pleistocene and recent deposits of the Denver area, Colorado: U.S. Geol. Survey Bull. 996–C, p. 91–139.

Jamieson, T. F., 1863, On the parallel roads of Glen Roy, and their place in the history of the glacial period: Geol. Soc. London Quart. Jour., v. 19, p. 235–259.

Johns, W. D., Grim, R. E., and Bradley, W. F., 1954, Quantitative estimates of clay minerals by diffraction methods: Jour. Sed. Petrology, v. 24, p. 242–251.

Judson, Sheldon, 1953, Geology of the San Jon site, eastern New Mexico: Smithsonian Misc. Colln., v. 21, 70 p.

Kagani, H., 1961, Modal analysis of marine sediments in the southern part of Tokyo Bay: Japanese Jour. Geology and Geography, v. 32, p. 523–532.

Kessell, J. E., and Beaty, C. B., 1959, Desert flood conditions in the White Mountains of California and Nevada: U.S. Army Quartermaster Research and Eng. Tech. Rept. EP–108, 107 p.

Kirk, L., 1952, Trails and rocks observed on a playa in Death Valley National Monument: Jour. Sed. Petrology, v. 22, p. 173–181.

Knopf, Adolph, 1918, A geologic reconnaissance of the Inyo Range and the eastern slope of the Sierra Nevada, California: U.S. Geol. Survey Prof. Paper 110, 130 p.

Krumbein, W. C., 1940, Flood gravel of San Gabriel Canyon, California: Geol. Soc. America Bull., v. 51, p. 639–676.

Langbein, W. B., 1961, Salinity and hydrology of closed lakes: U.S. Geol. Survey Prof. Paper 412, 20 p.

Le Conte, L. J., 1896, Discussion of "The Suspension of Solids in Flowing Water," by E. H. Hooker: Am. Soc. Civil Engineers Trans., v. 36, p. 338–340.

Leliavsky, Serge, 1955, An intrdouction to fluvial hydraulics: London, Constable & Son, 257 p.

Leopold, L. B., 1951, Pleistocene climates in New Mexico: Am. Jour. Sci., v. 249, p. 152–167.

———1951, Rainfall frequency—an aspect of climatic variation: Am. Geophys. Union Trans., v. 32, p. 347–357.

———1962, Rivers: Am. Scientist, v. 50, p. 511–537.

Leopold, L. B., and Langbein, W. B., 1962, The concept of entropy in landscape evolution: U.S. Geol. Survey Prof. Paper 500–A, 20 p.

Leopold, L. B., and Miller, J. P., 1956, Ephemeral streams—Hydraulic factors and their relation to the drainage net: U.S. Geol. Survey Prof. Paper 282–A, 37 p.

McAllister, J. F., and Agnew, A. F., 1948, Playa scrapers and furrows on Racetrack Playa, Inyo Co., California [abs.]: Geol. Soc. America Bull., v. 59, p. 1377.

McCammon, R. B., 1962, Efficiencies of percentile measures for describing mean size and sorting of sedimentary particles: Jour. Geology, v. 70, p. 453–465.

Mason, C. C., and Folk, R. L., 1958, Differentiation of beach, dune, and aeolian flat environments by size analysis, Mustang Island, Texas: Jour. Sed. Petrology, v. 28, p. 211–226.

Menard, H. W., 1950, Sediment movement in relation to current velocity: Jour. Sed. Petrology, v. 20, p. 148–160.

Miller, J. P., 1958, High mountain streams—effects of geology on channel characteristics and bed material: New Mexico Inst. Mining and Technology Mem. 4, 53 p.

Miller, J. P., and Wendorf, Fred, 1958, Alluvial chronology of the Tesuque Valley, New Mexico: Jour. Geology, v. 66, p. 177–194.

Miller, W. J., 1928, Geology of Deep Springs Valley, California: Jour. Geology, v. 36, p. 510–525.

Morrison, R. B., 1961, Correlation of the deposits of Lakes Lahonton and Bonneville and the glacial sequences of the Sierra Nevada and Wasatch Mountains, California, Nevada, and Utah: U.S. Geol. Survey Prof. Paper 424–D, p. D122–D124.

Nelson, C. A., 1962, Lower Cambrian-Precambrian succession, White-Inyo Mountains, California: Geol. Soc. America Bull., v. 73, p. 139–144.

———1963, Preliminary geologic map of the Blanco Mountain quadrangle, Inyo and Mono Counties, California: U.S. Geol. Survey Mineral Inv. Map MF–256.

Nevin, C., 1946, Competency of moving water to transport debris: Geol. Soc. America Bull., v. 57, p. 651–674.

Pack, J. F., 1923, Torrential potential of desert waters: Pan Am. Geol., v. 40, p. 349–356.

Pettijohn, F. J., 1957, Sedimentary rocks: 2d ed., New York, Harper & Bros., 718 p.

Richmond, G. M., 1962, Quaternary stratigraphy of the La Sal Mountains, Utah: U.S. Geol. Survey Prof. Paper 324, 135 p.

Rickmers, W. R., 1913, The Duab of Turkestan; a physiographic sketch and an account of some travels: London, Cambridge Univ. Press, 564 p.

Rouse, Hunter, 1950, Engineering hydraulics: New York, John Wiley & Sons, 1039 p.

Schumm, S. A., 1956, The movement of rocks by wind: Jour. Sed. Petrology, v. 26, p. 284–286.

Sharp, R. P., 1942, Mudflow levees: Jour. Geomorphology, v. 5, p. 222–227.

Sharp, R. P., and Nobles, L. H., 1953, Mudflows of 1941 at Wrightwood, southern California: Geol. Soc. America Bull., v. 64, p. 547–560.

Strahler, A. N., 1952, Dynamic basis of geomorphology: Geol. Soc. America Bull., v. 63, p. 923–938.

Suchier, A., 1883, Die Bewegung der Geschiebe des Oberrhein: Deutsche Bauzeitung, no. 56, p. 331.

Sundborg, Åke, 1956, The River Klaralven; a study of fluvial process: Geografiska Annaler, v. 38, p. 127–316.

Talvenheimo, G., and White, J. L., 1952, Quantitative analysis of clay minerals with the X-ray spectrometer: Analytical Chemistry, v. 24, p. 1784–1789.

Tricart, J., and others, 1961, Mécanismes normaux et phénomènes catastrophiques dans l'évolution des versants du bassin du Guil (Hautes-Alpes, France): Zeitschr. Geomorphologie, v. 5, p. 277–301.

Von Bertalanffy, Ludwig, 1950, The theory of open systems in physics and biology: Science, v. 111, p. 23–29.

Weaver, C. E., 1958, Geological interpretation of argillaceous sediments: Am. Assoc. Petroleum Geologists Bull., v. 42, p. 254–271.

Wooley, R. R., 1946, Cloudburst floods in Utah, 1850–1938: U.S. Geol. Survey Water-Supply Paper 994, 127 p.

Yatsu, E., 1959, On the discontinuity of grainsize frequency distributions of fluvial deposits and its geomorphological significance: Internat. Geog. Union, Regional Conf. Japan, Toyko 1957, Proc., p. 224–242.

U S GOVERNMENT PRINTING OFFICE : 1965 O—766-876

Beryl Resources of New Hampshire

By JAMES J. PAGE and DAVID M. LARRABEE

GEOLOGICAL SURVEY PROFESSIONAL PAPER 353

Prepared on behalf of the U.S. Atomic Energy Commission, and in part in cooperation with the New Hampshire State Planning and Development Commission

U.S. DEPARTMENT OF THE INTERIOR
March 3, 1849

UNITED STATES GOVERNMENT PRINTING OFFICE, WASHINGTON : 1962

UNITED STATES DEPARTMENT OF THE INTERIOR

STEWART L. UDALL, *Secretary*

GEOLOGICAL SURVEY

Thomas B. Nolan, *Director*

The U.S. Geological Survey Library has cataloged this publication as follows:

Page, James Jeffers, 1920–
Beryl resources of New Hampshire, by James J. Page and David M. Larrabee. Washington, U.S. Govt. Print. Off., 1961.

iii, 49 p. maps (part col., part in pocket) tables. 31 cm. (U.S. Geological Survey. Professional paper 353)
Prepared on behalf of the U.S. Atomic Energy Commission, and in part in cooperation with the New Hampshire State Planning and Development Commission.
Bibliography: p. 48–49.

(Continued on next card)

Page, James Jeffers, 1920– Beryl resources of New Hampshire. 1961. (Card 2)

1. Beryl. 2. Pegmatites. 3. Mines and mineral resources—New Hampshire. I. Larrabee, David Marcel, 1909– joint author. II. New Hampshire. State Planning and Development Commission. III. Title. (Series)

For sale by the Superintendent of Documents, U.S. Government Printing Office
Washington 25, D.C.

CONTENTS

Page
Abstract 1
Introduction 1
Beryl mining, production, and uses 2
Internal structure and mineralogy of pegmatites 3
Methods used in estimating resources 3
Beryl resources 3
Description of pegmatites 10
  Grafton district 10
    Palermo No. 1 mine 10
  Keene district 13
    Beryl Mountain mine 13
    Chickering mine 14
  Raymond region 16
    Corson mine 16
    McGall mine 17
    McMullen prospect 18
    Vatcher prospect 18
Description of pegmatites—Continued
  Raymond district 19
    General geology 21
  Minor districts 43
    Millard Chandler mine 43
    Parker Mountain mine 44
  Reconnaissance of other areas 45
    Alton quadrangle 45
    Gorham quadrangle 45
    Mount Pawtuckaway quadrangle 46
    Mount Washington quadrangle 47
    Plymouth quadrangle 48
Literature cited 48

ILLUSTRATIONS

[Plates are in pocket]

PLATE 1. Geologic map and sections of the Palermo No. 1 mine, Groton, Grafton County, N.H.
2. Geologic map and sections of the Beryl Mountain mine, Acworth, Sullivan County, N.H.
3. Geologic map and section of the Chickering mine, Walpole, Cheshire County, N.H.
4. Geologic map of the Corson mine, Nottingham, Rockingham County, N.H.
5. Geologic map of the McGall mine, Raymond, Rockingham County, N.H.
6. Geologic map and section of the Vatcher prospect, Raymond, Rockingham County, N.H.
7. Geologic map and sections of the Chandler mine (pegmatite 7), Raymond, Rockingham County, N.H.
8. Geologic map and section of the Smith No. 1 mine (pegmatites 9 and 10), Raymond, Rockingham County, N.H.
9. Geologic map of pegmatite 37, Raymond, Rockingham County, N.H.
10. Geologic map of the Smith No. 3 prospect (pegmatite 49), Raymond, Rockingham County, N.H.
11. Geologic map of the Blake mine (Mafera mine or pegmatite 56), Raymond, Rockingham County, N.H.
12. Geologic map and sections of the Welch mine (pegmatite 62), Raymond, Rockingham County, N.H.
13. Geologic map of pegmatites 69, 70, 71, 72, and 73, Raymond, Rockingham County, N.H.
14. Geologic map and section of the Hurley prospect (pegmatites 84, 85, and 86), Raymond, Rockingham County, N.H.
15. Geologic map and section of the Millard Chandler mine, Chatham, Carroll County, N.H.
16. Geologic map and generalized section of the Parker Mountain mine, Strafford, Strafford County, N.H.

Page
FIGURE 1. Index map showing locations of principal pegmatites described in this report 1
2. Sketch map of workings at the Palermo mine, Groton, Grafton County, N.H 10
3. Geologic map of the Raymond district, Rockingham County, N.H., showing locations of pegmatite exposures studied 20

TABLES

Page

TABLE 1. Beryl in New Hampshire pegmatites 4

2. Size of pegmatites, and distribution of minerals therein, Raymond district, N.H 22

3. Mineral assemblages in zoned pegmatites of the Raymond district, Rockingham County, N.H 24

BERYL RESOURCES OF NEW HAMPSHIRE

By James J. Page and David M. Larrabee

ABSTRACT

In the course of this study, more than 200 pegmatites were examined either in reconnaissance fashion or in detail, and the most important actual or potential sources of beryl were carefully studied. These included the Palermo No. 1, Beryl Mountain, Blake, Chickering, Smith No. 1, Corson, McGall, Chandler, Millard Chandler, Welch, and Parker Mountain mines, and the Vatcher, Hurley, and Smith No. 3 prospects.

The pegmatites of the Raymond district received special attention, for these previously have received little study and there was a need for knowledge of any beryl resources present. These resources are of no great magnitude, but resources of milling-grade feldspar are of interest. The Palermo No. 1 and Beryl Mountain pegmatites were restudied following development after World War II; these pegmatites are of special interest as both have been known for many years as important sources of beryl.

The relation of beryl to other minerals of the zones, the BeO content of the beryl, where determined, and the grade of the ore are indicated in the report and in tables 1 to 3. Some of these data were obtained by the U.S. Geological Survey during World War II, but much new and more detailed information has resulted from this study.

The total estimated resources of beryl in New Hampshire are 1,780 tons, of which about 1,200 tons are probably in crystals at least 1 inch in diameter, and therefore hand-cobbable at 1957 prices. Most of this beryl is so scattered throughout the pegmatites that it represents less than 0.10 percent of the containing rock, and it is recoverable only as a byproduct from feldspar and mica mining activities. Large deposits containing fine-grained, nearly indistinguishable white beryl are unknown in the State, but there has been little if any attempt to search for them. In 1957, any such resources would be classed as "potential ore," but could be of great significance in the future. Search for such ore, and research on beneficiation methods, are recommended.

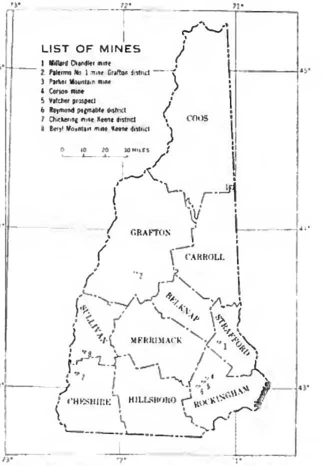

FIGURE 1.—Index map showing locations of principal pegmatites described in this report.

INTRODUCTION

Beryl occurs sparingly in many pegmatites scattered throughout the southern two-thirds of New Hampshire. The deposits of most economic importance are in the Grafton and Keene districts (fig. 1) in the west-central and southwestern parts of the State, respectively. The Raymond district (figs. 1 and 3) in the southeastern part of the State may be the third most important, although it has yielded little beryl to 1957.

Although the pegmatites occur in schists, gneisses, quartz monzonites, and granites, most of the economically important pegmatites are in schist of the Littleton formation of Devonian age. This formation consists chiefly of mica-quartz or quartz-mica schist, in places containing appreciable amounts of sillimanite, actinolite, or andalusite. Some parts are quartzitic, conglomeratic, or include lime-silicate rocks. Relations of the pegmatites to wallrocks and to major structures have been described by Cameron (Cameron and others, 1954, p. 15–19, 22–24).

The pegmatite deposits of New Hampshire have been investigated by members of the U.S. Geological Survey intermittently since 1914. A comprehensive account of the detailed work completed during 1942–45 is given by

Cameron and others (1954), and their report also contains a summary of studies before World War II. Field studies in 1947 led to a report by Olson (1950) on the feldspar in the pegmatites. This phase of the investigations was conducted in behalf of the New Hampshire State Planning and Development Commission.

The purpose of this report is to summarize and bring up to date the information on beryl gained in the pegmatite investigations of 1942–45, to examine in detail certain beryl-bearing pegmatites discovered in recent years, and to study other pegmatites known or suspected to contain beryl. Fieldwork was started by J. C. Olson and J. W. Adams in 1947, and was continued by J. J. Page in 1948–50. This work was done on behalf of the Division of Raw Materials of the U.S. Atomic Energy Commission and in cooperation with the New Hampshire State Planning and Development Commission. Field assistance in 1948 and 1949 was provided by L. F. Delwig, and in 1949 by P. K. Brown, Jr., and for 1 week by Frederick Stugard, Jr. L. R. Page and D. M. Larrabee briefly restudied the Beryl Mountain mine in 1955. Mapping was done by planetable and telescopic alidade, except where otherwise stated. The descriptions of individual pegmatite deposits (except the Beryl Mountain pegmatites) and tables 2 and 3 were prepared in draft form by J. J. Page. Larrabee revised this draft and tables, wrote the rest of the report, and completed preparation of the maps and tables. The writers are indebted to mine owners and operators for their cooperation and to members of the U.S. Geological Survey who furnished active field assistance and other valuable service.

The two most important beryl-bearing pegmatites are the Palermo No. 1, in Groton, and Beryl Mountain, in Acworth, both of which were mined extensively after World War II. The small area southwest of Raymond village, referred to as the Raymond district, contains 87 pegmatites that were studied in detail. Other pegmatites that have been mined or prospected and mapped in detail are: the Corson mine, Nottingham; the Chickering mine, Walpole; the Millard Chandler mine, Chatham; the Parker Mountain mine, Strafford; and the Vatcher prospect, Raymond. Reconnaissance studies were made elsewhere in the State, notably in the vicinity of Raymond outside the Raymond district, in Strafford, in the general vicinity of Gorham and the Presidential Range of the White Mountains, and east of the productive Grafton district.

BERYL MINING, PRODUCTION, AND USES

Only rarely in New Hampshire has it been economically feasible to mine a pegmatite over an extended period solely for one mineral, and this probably will be so in the future. The economics of pegmatite mining have been described by Bannerman (1943), and Bannerman and Cameron (1946). During World War II, under subsidy prices for strategic mica and beryl, some deposits were operated profitably for mica, but not for long periods. Mines were operated for mica and for beryl during the Korean emergency, again under Government-sponsored subsidy programs that were continued in 1957.

According to data in the Minerals Yearbooks of the U.S. Bureau of Mines, beryl production in New Hampshire since 1939 was as follows:

Year	*Tons*	*Year*	*Tons*
1939	(1)	1948	(1)
1940	---	1949	(1)
1941	(1)	1950	106
1942	16	1951	50
1943	42	1952	(1)
1944	(1)	1953	57
1945	1	1954	12
1946	5	1955	20
1947	(1)		

[1] Not listed separately. However, production generally was very small.

Beryl has an ideal composition of $Be_3 Al_2 Si_6 O_{18}$. This formula indicates a content of 14.0 percent BeO or 5 percent Be (Fleischer and Cameron, 1946). Commercial beryl concentrates have a lower BeO content partly because other elements substitute for Be in the mineral structure and also because the concentrates contain other minerals. These minerals may be small inclusions or alteration products in the beryl. More commonly, however, the contaminants are minerals from the matrix surrounding the beryl, chiefly quartz, feldspar, and mica. Many beryl crystals are euhedral, and where surrounded by quartz they break clean on crystal faces; thus a clean product can be produced by hand-cobbing. Other beryl crystals are intergrown with the minerals of the matrix, especially feldspar, and the cobbed concentrate is therefore impure.

Mining has been by small-scale methods, mostly in open pits from which the beryl was concentrated by hand-cobbing. Recently some beryl has been sold to the General Services Administration and some to private companies. In 1957 the Government paid a flat rate of $0.20 per pound or $400 per ton for beryl accepted on visual inspection. The price of analyzed beryl is based on the content of BeO. Beryl containing 8.0 to 8.9 percent BeO is bought at $40 per unit, 9.0 to 9.9 percent BeO at $45 per unit, 10.0 to 11.9 percent BeO at $50 per unit, and 12 percent or more at $55 per unit. As an example, beryl having 12 percent BeO is worth $660 per ton. For comparison, in the late 1920's and early 1930's, beryl sold for $35 per ton.

Beryl is the only known economic source of beryllium, which has been used primarily in beryllium-copper alloys for special types of springs and bushings; it has many other uses. New applications of beryllium of great importance are in the atomic-energy field as a moderator and reflector of neutrons. The uses and technology of beryllium have been discussed by Reno (1956) *in* "Mineral Facts and Problems," published by the U.S. Bureau of Mines. A more complete compendium on beryllium is contained in "Materials Survey, Beryllium," compiled by the U.S. Bureau of Mines (1953) with the cooperation of the U.S. Geological Survey in behalf of the National Security Resources Board.

INTERNAL STRUCTURE AND MINERALOGY OF PEGMATITES

The internal structure and mineralogy of granitic pegmatites have been described many times in recent years (Bannerman, 1943; Cameron and others, 1949, 1954; Jahns, 1955; Page and others, 1953), and the details are outlined only briefly here.

Pegmatites that can be mined economically ordinarily show some degree of systematic arrangement of the constituent minerals into two or more lithologic units or zones, and the mineral to be extracted is more abundant in some units than in others. Boundaries between units are marked by changes in mineralogy, proportions of minerals, or texture. In many pegmatites these boundaries are gradational, in others they are sharp and easily distinguished. The names of the units are formed by hyphenating the names of the chief mineral constituents, the names of the minerals appearing in order of abundance.

Zones are defined as continuous or discontinuous shells or units that in many pegmatites have the same shape as the entire body. Zones are classified as follows, in order from the outside; border zone, wall zone, intermediate zones, and core.

Border zones are commonly less than 6 inches thick, and are made up chiefly of quartz, muscovite, and plagioclase. Wall zones are much thicker; they also consist of quartz, muscovite, and plagioclase, but some contain perthite. Intermediate zones have more perthite and less plagioclase than outer units. The cores are commonly quartz and perthite, or quartz alone.

Fracture fillings are commonly tabular bodies that fill fractures in previously consolidated pegmatite. Replacement bodies are formed along boundaries between pegmatite units, along fractures, at the contact of pegmatite and wallrock, or along other structural features within the pegmatite. Many replacement bodies are controlled by fractures.

In a general way, grain sizes referred to in the text may be described as follows:

Fine	Less than 1 inch
Medium	1 to 4 inches
Coarse	4 to 12 inches
Very coarse	Greater than 12 inches

METHODS USED IN ESTIMATING RESOURCES

To eliminate the confusion arising from the common use of the terms "reserves" and "resources" interchangeably in past work, the definitions of Blondel and Lasky (1956) are used in this report. Reserves refer to minerals exploitable under present economic and technologic conditions; potential ores are those awaiting more favorable conditions; resources are the sum of the reserves and potential ores.

The percentage of beryl in a pegmatite may be determined by several methods: (a) by measuring the area of all beryl crystals on representative exposures of each unit; (b) measuring the length of crystals along equally spaced traverses, as in the Rosiwal petrographic method; (c) measurement of crystals intersected in core drilling; or (d) by analyses of representative samples of the beryl-bearing pegmatite. Visual estimates, although used at times, are much less accurate and commonly misleading. The tendency is to greatly over estimate the amount of beryl present.

The volume of the beryl-bearing unit is determined by projection along strike, dip, and plunge. Where more than one structural interpretation of the beryl-bearing unit can be made on the basis of available data, it is necessary to acquire more information by field exploration. The determination of grade and reserves of pegmatite minerals is treated by Norton and Page (1956).

The BeO content of the beryl is determined by measuring the omega index of refraction of the crystal, as this index varies with the BeO content. This method was developed by W. T. Schaller and R. E. Stevens (Norton and others, 1958).

BERYL RESOURCES

The resources of beryl in known pegmatites of New Hampshire may be 1,634 tons in the indicated and inferred category. In the Raymond district an additional 146 tons of potential ore may be present, making a total of 1,780 tons. Of this quantity about 1,200 tons are in crystals at least 1 inch in diameter and therefore recoverable by hand-cobbing. Most of the beryl in New Hampshire is so scattered throughout any given zone or zones in a pegmatite that it can be recovered only as a byproduct from mining for other minerals, such as feldspar or mica. The beryl content of the different zones ranges from a trace to an average of 9.6 percent in one pegmatite, but in most it is less than 0.10 percent. Only a very minute part of the beryl listed in table 1 is suitable for gems.

TABLE 1.—*Beryl in*

[Many data are from Cameron and others (1954) whose fieldwork was done in 1942-45;

Property	Type of deposit (includes zones, units, and mine dumps)	Size of beryl-bearing deposits (feet)				Shape of deposit	Beryl in rock (percent)
		Thickness		Length	Depth		
		Range	Average				
							Carroll
Millard Chandler	Core-margin zone					Cylindrical	0.10
Weeks	Wall zone					do	.50
							Cheshire
Allen	(?)						
Beauregard:							
Main pegmatite	Wall zone and core					Cylindrical	0.30
	Dumps						.09
Other pegmatites	Core margin (wall zone); wall (east).					Cylindrical	.06
Big	Mainly in core (northeast)		150	600	200	Lenticular	.05
Blister	Core and biotite unit		40	150	100	do	.02
Britton:							
North Pegmatite	Core		20	40	>35	do	1.7
Burroughs	Border and wall zones		50	550	>30	Cylindrical	.016
Chickering	Core-margin zone		10	200	>40	do	.11
	Dumps						.11
Colony	Core margin?		50	450	>150	Cylindrical?	.41
Cory	do					do	
	Dumps						
Fames	(?)						
French	Wall zone					Cylindrical	.125
Howe Ledge:							
North pegmatite	Pegmatite with beryl-bearing and fracture-controlled bodies.		70	500	25	Tabular	.09
South pegmatite	do		80	400	20	do	.007
Isham	Core margin?					Cylindrical?	Tr.
Island	Wall zone (hanging wall)		30	30	20	Tabular	.83
Kidder	Disseminated						Tr.
Kirk No. 1	Core					Lenticular	
Nichols	Wall and intermediate zones			450	100	Cylindrical	
Nina	Core		8	40	>10	Lenticular	.5
Porter, George	Wall zone		5	100	>10	Cylindrical?	.35
Price	Core-margin zone		15	40	>10	do	.025
Surry Dam	Core?					Lenticular	
White, High	Pegmatite with core margin?		25	100	>20	do	.2
White, Jehial	Disseminated	2-8	5	100	>20	Very irregular	Tr.

See footnotes at end of table.

New Hampshire pegmatites

the rest are from fieldwork done in 1948–50, except for that on Beryl Mountain, done in 1955]

Basis	Size of crystals		Percent[1] hand-cobbable beryl	Percent BeO in beryl	Associated industrial minerals (not in order of abundance)
	Average (square inches)	Maximum (inches)			
County					
Mineral measurements	7.37		80	13.5–13.7	Potassic and sodic feldspar, scrap mica.
Production data		6 by 23	85		Potassic and sodic feldspar, scrap mica, columbite.
County					
					Potassic and sodic feldspar, scrap mica.
Mineral measurements	2.34		50		Potassic and sodic feldspar, scrap and sheet mica.
do.	2.46		50		
Estimate		8 by 36[3]	50		
Estimate of local area	23.5		90		Do.
Mineral measurements of local area	1		15		Do.
Mineral measurements		13 by 26	80		Potassic and sodic feldspar, scrap mica.
Mineral measurements of entire pegmatite	1.54		25		Do.
Mineral measurements	10.6		75	12.4–13.1	Do.
Estimate					Lithium minerals (minor).
Mineral measurements of local area		12 by 36	90		Potassic and sodic feldspar, scrap mica.
Estimate		6 by 6			Potassic and sodic feldspar, scrap and sheet mica.
do.					
					Potassic and sodic feldspar, scrap mica.
Mineral measurements of local area					Potassic and sodic feldspar, scrap and sheet mica.
Mineral measurements	3.6		50		Potassic and sodic feldspar, scrap mica.
do.	3.6		50		
Estimate		12 by 15	90		Potassic and sodic feldspar, scrap and sheet mica.
Mineral measurements	14.1		90		Sodic feldspar, scrap and sheet mica.
					Potassic and sodic feldspar, scrap mica.
Estimate		12 by 30			Potassic and sodic feldsdar, scrap and sheet mica.
do.	.75		20		Do.
Estimate of local area		1 by 1.5	10		Potassic and sodic feldspar, scrap mica.
Mineral measurements	1.9		30		Sodic feldspar, scrap and sheet mica, tantalite reported.
Estimate		1 by 1.5	10		Potassic and sodic feldspar, scrap and meet mica.
		4 by 12	90		Sodic feldspar, scrap and meet mica.
Mineral measurements	10		80		Potassic and sodic feldspar, scrap mica.
Estimate					Potassic and sodic feldspar, scrap and sheet mica.

TABLE 1.—*Beryl in*

[Many data are from Cameron and others (1954) whose fieldwork was done in 1942-45;

Property	Type of deposit (includes zones, units, and mine dumps)	Size of beryl-bearing deposits (feet)				Shape of deposit	Beryl in rock (percent)
		Thickness		Length	Depth		
		Range	Average				
Grafton							
African	Disseminated					Very irregular	Tr.
Alger No. 1	Core or core margin?		20	40	>20	Cylindrical	0.25
Atwood	Intermediate zone					do	Tr.
Bennett	do					do	Tr.
Braley Hill	Core margin (pods)					Lenticular	
Burgess	Fracture-controlled bodies		4.5	28		Tabular	
Carpenter	Disseminated?						Tr.
Clement (South)	do		3	85	>10	Tabular	.07
Davis, Charles	Core					Lenticular	Tr.
DeMott	Core-margin and wall zones					Cylindrical	
Diamond Ledge	Core	3-4				Lenticular	
Eight-ball	Core-margin zone	1.5-2		120	>20	Cylindrical	
Evans:							
Main pegmatite	Dumps						
East pegmatite	Core		4	100	>20	Lenticular	.22
Fellows	Core (quartz-rich parts)	2-6				Lenticular?	Tr.
Fletcher	Core-margin					Cylindrical	
Ford, Harry	Intermediate zone					do	Tr.
Hobart Hill	Core-margin zone		5	10	10	do	Tr.
Hutchins Hill	Intermediate zone	4-60	30	560	>20	Lenticular	.01
Keniston	Disseminated				>20	Very irregular	.01
Keyes No. 1	Wall zone	3-4		240	>20	Cylindrical	.01
	Intermediate zone	1-2		240	>20	do	.01
	Dumps						.01
Keyes No. 2	Core-margin zone					Cylindrical	
Kilton	Intermediate zone					Cylindrical?	
McGinnis	Core-margin zone		1	20	>20	Cyclindrical	
Marston	Core? (west)					Lenticular?	
Mud	Wall zones		2	>450	>170	Cylindrical?	.01
			5	>450	>170	do	.01
New Gove	Core (pods)					Lenticular	Tr.
Palermo No. 1	Core-margin zone	10-20		300	40	Cylindrical	1.5
	Dumps						.02
Palermo No. 2	Intermediate zone					Cylindrical	
Palermo No. 3	Wall zone					Cylindrical?	
Rice-Palermo Pegmatite No. 29	Core (pods)	0.5-4		2-12		Lenticular	
Pattuck	Core		15	450	>20	do	.3
Rogers	Core-margin zone	Core almost entirely removed				Cylindrical	.05
Ruggles	do					do	
Saunders							
Smith, E. E.:							
Upper	Core-margin zone		1	>40	>60	Cylindrical	.6
Middle	Pegmatite with beryl-bearing intermediate zone.		30	100	>20		.034
Standard	Wall zone	200-350		950	>20	Cylindrical	
Valencia	do		70	200	>10	do	.01
Wadhams-Tucker	Core	6-10				Lenticular	
West Branch pegmatite	Core-margin zone					Cylindrical?	.30
Williams	Disseminated	10-90		250	>20	Lenticular?	.05
Merrimack							
Bog Mountain							Tr.
Currier	Core-margin zone	2-3		30	>20	Cylindrical	
Danbury	do					do	Tr.
Elkins	do					do	Tr.
Mica Queen (East)	do					do	Tr.
Pickwick	Beryl-bearing wall zone and core		80	300	>20	Lenticular	0.005
Stewart Hill	Core-margin zone					Cylindrical	Tr.
Wild Meadows	Core-margin and core					Lenticular	Tr.
Wilmot No. 2	Wall and core-margin?					Cylindrical	

See footnotes at end of table.

New Hampshire pegmatites—Continued

the rest are from fieldwork done in 1948–50, except for that on Beryl Mountain, done in 1955]

Basis	Size of crystals		Percent[1] hand-cobbable beryl	Percent BeO in beryl	Associated industrial minerals (not in order of abundance)
	Average (square inches)	Maximum (inches)			
County					
Estimate					Scrap and sheet mica.
do			75		Potassic and sodic feldspar, scrap and sheet mica.
do		1-2 by 4-6			Do.
do		2 by 4.5 [3]			Do.
do	11.5		70		Do.
do		9 by 3	40		Potassic and sodic feldspar, scrap mica.
do					Potassic and sodic feldspar, scrap and sheet mica.
Production data		3 by 8	40		Potassic feldspar, scrap and sheet mica.
Estimate					Potassic and sodic feldspar, scrap and sheet mica.
do					Do.
do		12 [4]			Potassic and sodic feldspar, scrap mica.
do		5 by 4-6			Potassic and sodic feldspar, scrap and sheet mica.
do			80		Sodic feldspar, scrap mica.
Mineral measurements		10 by 11	90		Do.
Estimate		2 by 2 by 8			Sodic feldspar, scrap and sheet mica.
do			80		Potassic and sodic feldspar, scrap and sheet mica
do					Potassic and sodic feldspar, scrap mica, spodumene (minor).
do					Potassic and sodic feldspar, scrap and sheet mica.
do					Do.
do					Do.
do					Do.
do		5 by 12			
do					Potassic and sodic feldspar, scrap mica.
		8 by 20			Sodic feldspar, scrap mica.
		2 by 5			Sodic feldspar, scrap and sheet mica.
		3 by 12			Potassic and sodic feldspar, scrap and sheet mica.
					Do.
Estimate					Do.
do					Do.
do		1.5 by 3			Scrap mica.
Mineral measurements	7.5	24 by 30	95	13.3–13.5	Potassic and sodic feldspar, scrap and sheet mica, phosphates.
Estimate					
do					Potassic feldspar, scrap and sheet mica.
					Potassic and sodic feldspar, scrap and sheet mica.
Estimate					Do.
Production data		24 by 60			Potassic and sodic feldspar, sheet and scrap mica, columbite.
Estimate					Potassic and sodic feldspar, scrap mica.
		24 by 60	90		Potassic and sodic feldspar, sheet and scrap mica.
					Do.
Mineral measurements		4 by 4 by 12	90		Potassic and sodic feldspar, scrap and sheet mica, columbite.
do		4 by 14	50		Potassic and sodic feldspar, scrap mica.
					Potassic and sodic feldspar, scrap and sheet mica.
Estimate		6 by 6	25		Do.
		3 [4]			Do.
Mineral measurements of local area	1.6		30		Potassic and sodic feldspar, scrap mica.
Production data		2 by 8	35		Sodic feldspar, scrap and sheet mica.
County					
Estimate		0.5 by 1.25			Scrap mica.
		0.75 by 3			Potassic and sodic feldspar, scrap mica.
Estimate		4 by 4 by 8			Potassic and sodic feldspar, scrap and sheet mica.
do		2 by 5			Do.
do	2.7		40		Do.
Mineral measurements					Do.
Estimate		1 by 2 by 2			Potassic and sodic feldspar, scrap mica.
do		0.5 by 3 [3]	10		Potassic and sodic feldspar, scrap and sheet mica.
do		5 by 8			Do.

TABLE 1.—*Beryl in*

[Many data are from Cameron and others (1954) whose fieldwork was done in 1942-45;

Property	Type of deposit (includes zones, units, and mine dumps)	Size of beryl-bearing deposits (feet)				Shape of deposit	Beryl in rock (percent)
		Thickness		Length	Depth		
		Range	Average				
							Rockingham
Corson	Core-margin zone					Cylindrical	0.15
McGall	Core		2	60	20	Lenticular	.74
	Wall zone		2	60	20	Cylindrical	.74
McMullen	3 pegmatites					Lenticular	.08
Vatcher	Beryl-bearing core and fracture-controlled bodies.		75	400	>40	Lenticular and tabular	.38
	Wall and border zones					Cylindrical	.01
No. 4	do	3-20		100	>20	do	.08
No. 7, Chandler	Wall zone					do	.85
	Intermediate zones					do	.02
	Core		20	40	30	Lenticular	9.60
No. 9, Smith-West	Disseminated	10-50		110	>20	do	.01
No. 10, Smith:							
Main	Core-margin and wall zone		40	120	>50	Cylindrical	.002
No. 18	Disseminated		8	15	20	Lenticular	.14
No. 19	Beryl-bearing fracture-controlled body?.		15	190	>20	do	.015
No. 23	Core					Cylindrical	.6
No. 25	Entire pegmatite	10-50		130	>20	Lenticular	.008
No. 26	do		25	140		do	.06
No. 37	Intermediate zone and core		10	140	>20	Cylindrical	.04
No. 39	Entire pegmatite		50	160	>20	Lenticular	.0035
No. 40	do		50	850	>20	do	.0006
No. 42	Intermediate zone		15	50	>8	Tabular	.06
No. 46	Wall zone					Cylindrical	.038
No. 49	do					do	.0036
No. 51	Entire pegmatite (blocks)		4	80	>20	Lenticular	.02
No. 54	Wall zone and fracture-controlled body.					Cylindrical and tabular	.02
No. 55	Entire pegmatite		8	100	>20	Lenticular	.125
No. 56, Blake	First intermediate zone	3-10		100	>20	Cylindrical	.12
	Dumps						.37
No. 57, Lane							.03
Southeast	Entire pegmatite		50	750		Lenticular	.03
Northwest	do					do	.014
No. 58	do		15	130	>20	do	.01
No. 62, Welch:							
Southeast	do		80	200		do	.04
	Dumps						.03
No. 64	Entire pegmatite	10-50		500	>20	Lenticular	.003
No. 65, Mills	Wall zone					Cylindrical	.04
No. 69	Entire pegmatite	5-200	30	850	>20	Lenticular	.03
No. 73	do		15	200		do	.0065
No. 74	do		30	370	>40	do	.0125
No. 77	do		10	170	>40	do	.019
No. 78	do		4	105	>40	do	.015
No. 82	do	10-15	12	280	>40	do	.127
No. 83, Gillingham	do		15	60	>20	do	.066
							Strafford
Felker, John	Wall zone	3-11		>30		Cylindrical	Tr.
Parker Mountain	Core		10	135	>20	Lenticular	0.22
	Wall zone		2	30	>40	Tabular	.89
	Dumps						.10
							Sullivan
Balla, John (potassic feldspar)	Core and core-margin zone		5	10	10	Lenticular	3.8
Beryl Mountain	Intermediate zone	2-7	6	300	25	Cylindrical	[6] 5.0 [8] 32.75
Chandler Mills	Pods in intermediate unit		5	10	5	Lenticular	.12
Columbian Gem	Core-margin (pods)					Cylindrical	Tr.
Globe (East)	Core-margin zone					do	
Ledge Pond	do					do	Tr.
Melvin Hill Nos. 1, 2	Core; wall zone						Tr.
Nichols, Justin	Core					Lenticular	Tr.
Playter	Wall zone					do	Tr.
Smith, G. F	Core					do	

[1] Crystals larger than 1 inch in diameter.
[2] West.
[3] One crystal.
[4] In length.
[5] In core.
[6] Average.
[7] Approximately.
[8] Maximum.
[9] Maximum average.

New Hampshire pegmatites—Continued

the rest are from fieldwork done in 1948–50, except for that on Beryl Mountain, done in 1955]

Basis	Size of crystals		Percent [1] hand-cobbable beryl	Percent BeO in beryl	Associated industrial minerals (not in order of abundance)
	Average (square inches)	Maximum (inches)			
County					
Mineral measurements	1.25		25		Potassic and sodic feldspar, scrap mica.
do	19.3		90		Potassic and sodic feldspar, scrap mica, spodumene, columbite
do	19.3		90		
do	.14		5		Potassic and sodic feldspar, scrap mica.
do	20.8		75		Potassic and sodic feldspar, scrap mica, columbite.
do	.9		10		
do	.33		10	13.2–13.4 13.0	Potassic feldspar, scrap mica.
do	9		60	12.6–13.0	Potassic and sodic feldspar, scrap mica, columbite, spodumene, lepidolite, phosphates.
do	9		60	12.5–12.6	
do	9		60	12.3–12.5	
do	.38		10		Potassic and sodic feldspar, scrap mica, columbite.
Production data		10 by 10	75		Potassic and sodic feldspar, scrap mica.
Mineral measurements	3		50	13.1	Potassic feldspar.
do	1.65		25	13.1	Potassic feldspar, scrap mica.
do	1.36		25	13.0	Scrap and sheet mica, columbite.
do	.72		15	13.0–13.1	Potassic feldspar, scrap mica, columbite.
do	.9		20	12.8	Potassic feldspar, scrap and sheet mica.
do	.65		15		Potassic feldspar, scrap mica.
do	.16		5	12.8–13.2	Do.
do	.15		5	12.9–13.2	Do.
do	3.25		80	12.9–13.1	Potassic feldspar, scrap and sheet mica.
do	.42		10	13.0	Potassic feldspar, scrap mica.
Mineral measurements of entire pegmatite	.16		5		Do.
do	.07		5	13.4	
Mineral measurements	.1		6	13.1–13.2	Potassic feldspar, scrap mica.
do	.6		15	13.0	Do.
Production data		2 by 4	75		Potassic feldspar, scrap and sheet mica, columbite.
Mineral measurements			15		
do	7.34		80	12.5–12.8	Potassic feldspar, scrap mica.
do	.9		20	12.8–13.2	Do.
do	.23		10	12.9–13.0	Do.
do	3.3		80		Potassic feldspar, scrap mica, columbite.
do			15		
do	.6		15	12.8–13.1	Potassic feldspar, scrap mica.
do	1.13		25	12.9–13.0	Do.
do	.8		20		Do.
do	.05		0		Do.
do	.22		10	12.8–13.0	Do.
do	.14		5	12.9	Potassic feldspar.
do	.4		10	13.0	
do	.3		10	12.7–13.1	Potassic feldspar, scrap mica, columbite.
Production data	31.3		100	13.0–13.1	Potassic feldspar, scrap mica.
County					
Estimate		**0.5 by 3.5**	**20**		**Scrap and sheet mica.**
Mineral measurements	**7.2**		**90**		**Potassic and sodic feldspar, scrap and sheet mica, columbite.**
do	**.036**		**10**		
Estimate					
County					
Mineral measurements	**45.8**		**90**		**Potassic and sodic feldspar, scrap mica.**
do	**[3] 144**		**90**	**13.8–14.0**	**Potassic and sodic feldspar, scrap mica, quartz.**
Mineral measurements of local area		**8 by 8 by 12**	**75**		**Potassic and sodic feldspar, scrap and sheet mica.**
Estimate		**.75 by 2**			**Do.**
		18 [4]			**Do.**
Estimate					**Do.**
do					**Do.**
do					**Do.**
do					**Potassic and sodic feldspar, scrap mica.**
do		**4 by 8 [5]**	**60**		**Sodic feldspar, scrap and sheet mica.**

Some pegmatites may contain additional beryl that has not been recognized in the field because it is extremely fine grained and white. During World War II, such beryl was not looked for, generally, as it was not recoverable. Such beryl can be recovered only by milling, and suitable methods have not yet been developed. Although the estimated tonnage of hand-cobbable beryl in New Hampshire is small there are few areas in the United States that contain more. If a domestic supply of beryllium is urgently needed, more sound research in milling and beneficiation of fine-grained beryl is needed.

DESCRIPTION OF PEGMATITES

GRAFTON DISTRICT

PALERMO NO. 1 MINE

Although many pegmatites have been mined in the Grafton district, the Palermo No. 1 mine not only has been the sole significant source of beryl but also has yielded the largest production of beryl in New Hampshire during World War II. Production since 1945 has greatly exceeded that of former years as a result of much higher selling prices. This mine (pl. 1) is 1 mile S. 61° W. of the village of North Groton, Grafton County, and about 2 miles by State, town, and mine-access roads from that village. The Palermo mine is one of the best known localities for collecting pegmatite minerals in New Hampshire (Sterrett, 1915, 1923; Berman, 1927; Verrow, 1940, 1941; Frondel, 1941; Frondel and Lindberg, 1948).

The mine was opened for sheet mica in 1863 and most of the underground work was done before 1900. In 1914, the mine was purchased by the General Electric Co., Schenectady, N.Y. In 1914–15, General Electric operated the mine for mica, mostly above the level of the lower opencut, and sometime after 1920 the small opencuts on top of the outcrop were made for feldspar. In 1942–43 this company again mined for mica and beryl near the top of the pegmatite, but some of their mica production during this period was from the dumps. Following these operations, H. A. Ashley (later as the Ashley Mining Corp.) mined mica, feldspar, scrap mica, and beryl until late 1949.

Sterrett (1923, p. 131–132) visited the mine in October 1914, and described the underground workings shown in figure 2 in the following fashion (numbers refer to features shown on fig. 2):

> At the (north) end of the lower, or southern, open cut [1] there is a large tunnel or room [2] 50 feet long with deep inclined stopes [7] extending from it to the northeast and east and a drift with stopes extending upward to the north; an upraise [3] connects with workings from the outcrop about 50 feet higher and to the west, where an open cut [4] 30 feet long had been made with drifts and stopes carried underground from it. Another open cut [5] 40 feet long and 35 feet deep had been made northeast of the main lower open cut and about 40 feet higher. From this open cut [5] an inclined shaft [6] was sunk that connected with the main stopes [7] at a depth of 4 feet below the bottom of the main open cut [1].

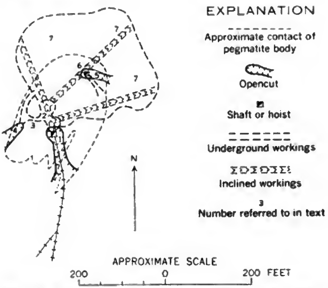

Figure 2.—Sketch map of workings at the Palermo mine, Groton, Grafton County, N.H. (after Sterrett, 1923).

In 1948–49 the accessible workings consisted of the lower open cut (1), that part of the tunnel or room (2) still accessible above water level, the raise (3), the opencut (4) and some of the drifts and stopes from it, and possibly part of the opencut (5) and inclined shaft (6). The large stopes (7) are filled with water. Small opencuts were made on top of the outcrop north of the older workings before 1944, and by November 1949 an opencut 140 feet long, 110 feet wide, and 40 feet deep had been developed.

The mine has been mapped and studied by the following members of the U.S. Geological Survey from 1944 to 1949: J. B. Hadley, F. H. Main, and A. H. McNair in 1944–45 (Cameron and others, 1954, p. 215–217); J. C. Olson and J. W. Adams in 1947 (Olson, 1950); and J. J. Page, L. F. Dellwig, Frederick Stugard, Jr., and P. K. Brown, Jr. in 1948–49 (pl. 1).

The pegmatite is roughly tadpole shaped with a blunt northeast end that thins rapidly south of the main opencut (pl. 1). It is at least 280 feet long and as much as 140 feet wide. The average strike seems to be nearly N. 45° E. and the dip is variable to the southeast. The hanging wall dips from 40° SE. to vertical. The footwall dips steeply southeast near the surface, flattens slightly a short distance below the surface, and apparently steepens again to include the older water-filled stopes reached from the old lower opencut. The average dip of the footwall is about 50° SE. The pegmatite appears to plunge 20° northeastward under the overlying schist. It is mostly concordant with the wallrock which is quartz-mica-sillimanite schist. Sillimanite needles and larger crystals as much as one-half by 2 inches are commonly altered to sericite. The wallrock on the footwall side of the pegmatite south of the opencut has been injected by pegmatitic material.

There are six pegmatite units at the Palermo mine: a quartz-muscovite-plagioclase border zone; a plagioclase-quartz-muscovite wall zone containing sheet mica; a plagioclase-quartz-perthite intermediate zone containing sheet mica; a quartz-plagioclase-perthite intermediate zone; plagioclase-quartz-muscovite-perthite intermediate (core-margin) zone containing beryl, phosphates, and uranium minerals; and a quartz-perthite core. Five of these are shown on plate 1; the border zone is too thin to be shown at the scale used.

The border zone is very fine grained quartz-muscovite-plagioclase pegmatite. It is exposed at the north and east (hanging-wall) contacts of the pegmatite and schist, and is ordinarily less than 4 inches thick. At the footwall contact, the schist has been injected by pegmatitic material, and the contact between wallrock and the wall zone of the pegmatite is too gradational to permit separation of a border-zone unit. The unit consist of 40–50 percent quartz, 30–40 percent muscovite, and 10–20 percent plagioclase (An_{12}). Biotite, probably from the wallrock, is a minor accessory mineral.

The medium-grained plagioclase-quartz-muscovite wall zone was the source of most of the sheet mica produced at the Palermo mine. This unit is most continuous and probably thickest near the north and east contacts of the pegmatite, where it is exposed along the hanging wall. Where exposed, the unit does not exceed 5 feet in thickness. It seems to be the unit mined in the old underground workings described by Sterrett (1923, p. 131–132). The average composition of the unit is 50 percent plagioclase (An_{4-7}), 35 percent quartz, and 15 percent muscovite. Biotite and black tourmaline are minor accessory minerals.

The first intermediate zone is medium- to coarse-grained plagioclase-quartz-perthite pegmatite containing sheet muscovite. This zone is exposed in and near the old workings at the south and southwest sides of the pegmatite. It is as much as 25 feet thick and part of it was the unit mined for sheet mica in these workings. This unit, and the second intermediate zone, exposed in and around the main opencut to the north, are so similar in position, texture, and location in relation to the other units that they could be considered the same unit, but they are sufficiently different in composition to show them on the map as separate units. The average composition is 45 percent plagioclase (An_{4-7}), 25 percent quartz, 25 percent perthite, and 5 percent muscovite. The proportions of these minerals vary greatly in the zone. Black tourmaline and biotite are the most common accessory minerals, biotite commonly occurring in strips intergrown with muscovite. Other minerals are apatite, lazulite, pyrite, and chalcopyrite.

The second intermediate zone is medium- to coarse-grained quartz-plagioclase-perthite pegmatite. It is as much as 40 feet thick on the east side of the pegmatite but thins at depth on the west side. The unit is absent in some of the accessible underground workings. Its shape suggests that it may have originally formed a hood over the top of the pegmatite that extended farther downdip on the hanging-wall side than on the footwall. The average composition is 35 percent quartz, 35 percent plagioclase (An_{4-7}), and 30 percent perthite. This zone is variable in composition, and any 1 of the 3 major constituents locally may comprise as much as 75 percent of the unit. Perthite was mined from this unit before 1942.

The third intermediate (core-margin) zone is fine- to coarse-grained pegmatite consisting of plagioclase, quartz, muscovite, and perthite, with accessory beryl and phosphate minerals. This unit is thickest, possibly 30 feet thick, on the footwall side of the core; only discontinuous lenses of the unit are found on the hanging-wall side. Mapping in 1944 (Cameron and others, 1954) showed a small exposure of beryl-bearing pegmatite on top of the outcrop near the present center of the opencut, suggesting that the core-margin zone completely surrounded the core.

The composition of the unit is variable; the average is 30 percent plagioclase (An_{2-4}), 25 percent quartz, 25 percent muscovite, and 20 percent perthite. The plagioclase is cleavelandite that occurs in oval aggregates as much as 10 feet long and 5 feet wide bordered by rims of greenish-yellow muscovite. Equally large aggregates of medium-grained muscovite and quartz separate the cleavelandite aggregates. Quartz is commonly massive and similar to that of the core. Large crystals of beryl are most abundant near the inner edge of the unit adjacent to massive quartz of the core, but smaller crystals are found in the muscovite aggregates. Lenses of phosphate-rich minerals are present near the core. Uranium minerals are in the muscovite masses.

This unit contains most of the rare minerals reported at the Palermo mine. A list of some of the minerals found at the mine by Frondel (1941, p. 145), Verrow (1941, p. 208–211), and Frondel and Lindberg (1948, p. 135–141) is given below:

Amblygonite
Apatite
Autunite
Brazilianite
Cyrtolite
Dufrenite
Eosphorite-childrenite
Fairfieldite
Ferri-sicklerite
Graftonite
Gummite
Heterosite
Lazulite
Limonite
Löllingite
Ludlamite
Manganite
Melanterite
Messelite (?)
Psilomelane
Pyrite
Rhodochrosite
Siderite
Triphylite
Triploidite
Uranophane
Vivianite
Whitlockite
Zeolite

The core-margin zone includes the minerals and features attributed to replacement bodies in and adjacent to the core during earlier studies of the Palermo pegmatite (Cameron and others, 1954). During the 1948–49 investigations, further study of the relation of this unit to the adjacent units indicated that it could be described best as a true zone and that the replacement features could be explained without requiring a separate replacement body of later age. The best evidence of the zonal characteristics of this unit is its spatial relation to other units of the pegmatite. It has a definite and predictable location in the sequence of units, and although it is discontinuous on the hanging-wall side of the core, so also are many zones, whereas replacement units commonly show crosscutting relation to surrounding units. Similar units have been mapped as zones in other pegmatites such as the Hyatt Beryl pegmatite, Larimer County, Colo., and the Bob Ingersol Dike No. 2 pegmatite, Keystone, S. Dak. (Page, 1950, p. 28). Replacement textures, such as those produced by the corrosion of earlier formed crystals, have been used to indicate that this unit was a "replacement body," but these textures are as easily explained by the action of the residual pegmatite liquid on earlier formed crystals during the normal sequence of pegmatite crystallization.

The core consists of very coarse grained quartz-perthite pegmatite occurring in the thickest part of the body. Massive quartz (60 percent) surrounds large subhedra of perthite (40 percent); some perthite crystals are as much as 30 feet long and 10 to 15 feet in cross section. Plagioclase is a minor accessory mineral, commonly occurring as thin rims of sugary-textured albite (An_4) between perthite and quartz.

The Palermo pegmatite has yielded large quantities of sheet and scrap mica, potassic feldspar, and beryl. Reserves of these minerals are unknown, but probably are much less than the past production. Large parts of the core and core-margin zones have been mined out, and the great extent of underground workings indicate that sheet-mica-bearing units have been largely removed.

Beryl is concentrated near the inner edge of the core-margin zone. The discontinuous lenses of this zone on the hanging-wall side of the core contained the largest crystals of beryl. The largest seen measured 2 feet in diameter and 6 feet in length but larger ones were recovered according to operators and mineral collectors. Blue-green beryl is on the hanging-wall side of the core, where it is ordinarily associated with quartz. In places it approaches aquamarine in quality, and some gem stock was recovered in 1942–45. The BeO content ranges from 13.3 to 13.5 percent. Most beryl on the footwall side of the core is dull blue or green and is associated with plagioclase and quartz. Small glassy green beryl crystals occur in the scrap-mica masses, and orange to golden crystals are found near uranium minerals. The BeO content of beryl in the scrap-mica masses is 13.1 to 13.4 percent. Beryl adjacent to lenses of phosphate minerals is gray to brown and, except for its crystal form, difficult to distinguish from alteration products of the phosphate minerals. The BeO content, however, is similar to other beryl in the unit, about 13.4 percent.

The beryl content of the core-margin zone on the footwall side of the core was determined by mineral measurements to be 1.5 percent. On the hanging-wall side of the core, the crystals are larger and, because they have been almost completely removed during mining operations, mineral measurements in these discontinuous lenses are of little value. During operations by the Ashley Mining Corp., most visible chips of beryl were saved, and an estimated 95-percent recovery was made by hand-cobbing.

Potassic feldspar has been mined from the core and the second intermediate zone. The best feldspar was from the large perthite subhedra in the core. Some of these probably contained as much as 350 tons of high-quality potassic feldspar free of waste. In November 1949, that part of the core of the pegmatite still unmined was thickest in the central part of the main open-cut, and was thinner to the northeast and south. Additional potassic feldspar has been recovered from the second intermediate zone. Commercial grade potassic feldspar in this unit must be separated from quartz and plagioclase by hand-cobbing.

Sheet mica has been recovered in large quantities, but the most promising and easily accessible areas have been worked out and even the dumps have been reworked. The percentage of sheet mica originally in the wall zone is unknown; all rock exposed in 1949 was not mined in earlier operations because the sheet-mica content was too low, and therefore the exposures were not representative of that part of the zone formerly mined. The sheet-mica content of the first intermediate zone is variable, but about 1 percent of the muscovite present seems to be of sheet quality. The sheet mica is hard, rum to ruby, and free splitting. Books seen in the wall zone and first intermediate zone are no larger than 3 inches long by 2 inches wide by 1 inch thick, but all outcrops observed are low-grade areas left during mining operations. Sterrett (1923, p. 133) reported one book of mica 4 feet 2 inches long and 28 inches wide and another 2 feet in diameter and 2 feet thick. Scrap mica can be recovered from the core-margin zone by hand-cobbing from aggregates having a very high muscovite content. Muscovite of scrap quality is a constituent of all units in the pegmatite except the core, but it could be recovered from most of these units only by milling methods.

A small tonnage of phosphate minerals, mostly triphylite from lenses in the core-margin zone, may have been used for experimental work on a process to recover lithium. There is no published record of the result of these investigations.

Secondary uranium minerals are present in extremely small quantities at places in the core-margin zone. These are in scrap-mica masses and commonly are associated with golden beryl and dark-gray quartz.

KEENE DISTRICT

Many pegmatites of the Keene district have long been of economic importance. They have been an intermittent but important source of sheet mica and feldspar since about 1810 when the Big mine was first opened. Some beryl has been recovered as a byproduct of feldspar and mica mining since the late 1930's, but before that time there was little demand for it. Most mines in this district were studied in detail in 1942–45; for the purpose of this report, the Chickering mine and the Beryl Mountain mine were examined.

BERYL MOUNTAIN MINE

Beryl Mountain (pl. 2) is in the town of Acworth, 0.8 mile S. 32° W. of South Acworth village, Sullivan County. One of the two pegmatites present is a well-known mineral collecting ground, and many descriptions of the minerals have been reported (Shepard, 1830, p. 353–360; Teschemacher, 1844, p. 191–192; 1847, p. 87–89; Holden, 1918, p. 199–200). The beryl-bearing pegmatite was first mined by a Mr. Bowers before 1844 (Jackson, 1844, p. 59, 182) and has been operated intermittently since that time. It was not operated during World War II, despite the increased demand for beryl at that time. In May 1949, H. A. Ashley bought the mine from Miss Sadie A. Cohen, long-time owner, and began operations that resulted in the production of a large but unrecorded tonnage of easily hand-cobbed beryl. Although the date he ceased mining is not known, it probably was about 1953.

The pegmatites were studied by H. M. Bannerman in 1942 (Cameron and others, 1954, p. 276), when much of the beryl-bearing pegmatite was mapped by him and J. B. Headley, Jr. In 1943, the Bureau of Mines cleared the floor of the largest opencut and drove a 50-foot exploratory adit beneath the floor. S. B. Levin, who was in charge of the project, mapped and studied part of the pegmatite (Levin, 1948).

The two large pegmatites were mapped in 1948 by J. J. Page and L. F. Dellwig. Details of the rich beryl deposit exposed at that time are shown on plate 2. After the mine was reopened in 1949 by H. A. Ashley, the mine was remapped by Page and P. K. Brown, Jr. (pl. 2). In June 1955, probably about 2 years after Ashley ceased operations, the map of the mine was brought up to date during a 2-day field study by L. R. Page and D. M. Larrabee (pl. 2).

The mine is an opencut about 140 feet long, from 20 to 40 feet wide, and as much as 40 feet deep. Small underground workings extend westward from the opencut. The pegmatite also has been exposed in two shallow trenches near the northeast end, and in several shallow pits near the hilltop south of the main working.

The pegmatites on Beryl Mountain are discordant to the enclosing biotite gneiss and amphibolite. Amphibolite has been altered to a granulitic rock extending as much as 3 feet from the contact. The attitude of foliation varies greatly, as shown on plate 2. The average strike is northeast, and the dip is commonly to the east or southeast. The plunge of minor folds generally is 10° to 15° NE.

The pegmatite west of the mine is about 700 feet long, and its outcrop width is about 50 feet. It strikes northeast and dips steeply southeastward. A small shallow opencut has been made in the northeastern part of this pegmatite. This body consists of a thin border zone, a wall zone of plagioclase-quartz-perthite pegmatite, and an apparent core of perthite-quartz-plagioclase pegmatite.

The main beryl-bearing pegmatite spanning the summit of Beryl Mountain trends northeast, dips steeply southeast, probably has a length of more than 1,100 feet, and is exposed over a maximum width of about 180 feet.

The pegmatite probably plunges 10° to 15° N. 30° E., parallel to rolls in the pegmatite contact and to the arches in the bottom of the quartz core as shown in sections *C–C′* to *G–G′* (pl. 2). The estimated maximum depth of the bottom of the pegmatite is about 100 feet.

A very narrow border zone, absent in places, surrounds a thick wall zone of plagioclase-quartz-perthite pegmatite. This latter zone consists of about 60 percent plagioclase, 30 percent quartz, 10 percent perthite, and minute quantities of muscovite books less than 2 inches in diameter and black tourmaline crystals less than 4 inches long.

Plagioclase-muscovite-quartz-perthite-beryl pegmatite comprises the intermediate zone, which has an average thickness of about 2 feet but is as much as 7 feet thick near the hilltop south of the mine face. The most distinctive characteristic of this zone is the large quantity of muscovite in wedge-shaped crystals. The composition of the zone is about 35 percent plagioclase, 30 percent muscovite, 25 percent quartz, 5 percent perthite, and 5 percent beryl (13.8 to 14.0 percent BeO). Locally the zone may be much richer in any single constituent, as for example: 90 percent plagioclase, 80 percent muscovite, 90 percent quartz, 20 percent perthite, or 30 percent beryl. Grain sizes vary greatly; the largest sizes observed are: plagioclase aggregates, 2 by 6 feet; muscovite books, 1.5 feet in diameter; quartz aggregates, 5 feet in diameter; perthite crystals, 5 feet in diameter; and beryl crystals, 1.5 by 6 feet.

The core consists of white granular quartz containing irregular streaks of pale-rose quartz. The quartz grains are less than one-eighth inch in diameter. The outer part of the core in places contains perthite crystals as much as 20 feet long. Locally, fracture fillings of quartz from the core invade the intermediate zone. Where the perthite-rich parts of the core are absent and the mica-rich intermediate zone is in contact with the core, beryl crystals extend into the core as much as 7 feet. The core has a length of 500 feet and a maximum thickness of about 60 feet; the average thickness is about 25 feet.

A unit of perthite-quartz-plagioclase lithologically similar to the apparent core of the western pegmatite occurs south of the main opencut and along the east side of the pegmatite. In some places this is within the wall zone but in others it is between the wall zone and eastern, hanging-wall contact.

In the south face of the opencut, the quartz core arches over the wall zone, the axis of the arch plunging 10° to 15° N. 30° E. This is a remnant of the quartz saddle so well exposed in earlier operations. Here the wall zone on the southeast side of the cut pinches out to the northeast, the end plunging 15° N. 30° E., as shown by rolls in the quartz and wall-zone surfaces. To the southeast this sliver of quartz core and intermediate zone pinches out.

Most beryl of the intermediate zone is blue green, but some is olive to brown and some nearly golden (pl. 2). The beryl is coarse grained, euhedral, and although in places rimmed with plagioclase, nearly all of it can be broken free by hand-cobbing. Crystal measurements made in 1955, after the most accessible beryl had been removed by mining, indicated the following beryl content in the intermediate zone and outer part of the core:

Location	Percent	Area of rock measured (square feet)
West side of high point	4.5	196
North end of main cut	4.6	216
Roof of underground working on main floor of cut	6.5	162

Thus the average beryl content is about 5 percent.

The intermediate zone is about 300 feet long; it has an average thickness of 2 feet, and probably has an average depth of 25 feet where unmined. In most places this zone is in contact with the quartz core. Thus, the total thickness of the beryl-bearing pegmatite is about 6 feet. Recovery of most of this beryl will require underground mining methods; the present opencut cannot be expanded economically.

Most of the potassic feldspar of the outer part of the core has been removed during past operations but some hand-cobbable material remains southwest of the large opencut. Scrap mica could be recovered by hand-cobbing as a coproduct with beryl of the intermediate zone. Much clean quartz remains east of the exploration adit and south of the opencut; samples of especially pure material analyzed for the New Hampshire State Planning and Development Commission (Meyers, 1941) had a content of 99.38 percent SiO_2, 0.30 percent Al_2O_3, and 0.016 percent Fe_2O_3.

CHICKERING MINE

The Chickering feldspar mine is 2.3 miles N. 83° E. of Walpole village, in the town of Walpole, Cheshire County. The mine was last worked for potassic feldspar in about 1925 by the Whitehall Co., Inc. The irregular opencut is 80 feet long and as much as 70 feet wide. The highest point on the rim of the cut is about 40 feet above the floor. The cut is now used to store water for fire protection, and the water ranges from 5 to 20 feet in depth depending on the rainfall. A prospect pit 20 feet long, 10 feet wide, and as much as 15 feet deep is 50 feet south-southeast of the main cut.

The size of the Chickering pegmatite can only be estimated because the eastern (hanging-wall) contact and the northern and southern ends are not exposed (pl. 3). The pegmatite can be traced for 350 feet

N. 20° W., which probably is the average strike of the body. It is at least 80 feet thick and dips eastward about 50°. The plunge of linear elements in quartz-mica-staurolite schist of the wallrock is 10° to 12° SE., but small rolls on the footwall contact of the pegmatite plunge 5° to 10° N. 20° W. The south end of a smaller pegmatite crops out 75 feet west of the opencut. It trends N. 20° W. and is at least 130 feet long and 18 feet wide. Its dip is unknown.

Five units have been mapped in the Chickering pegmatite. One of these contains spodumene, lepidolite, and beryl. This is the only pegmatite in the Keene district where these minerals are known to be constituents of a single unit. The border zone consists of very fine grained quartz-muscovite-plagioclase pegmatite. The zone is commonly only a few inches thick, and can be shown on the map (pl. 3) only on a dip slope at the west side of section *A–A′*. The plagioclase is An_{2-4}.

The wall zone is fine- to medium-grained plagioclase-quartz-perthite pegmatite. Plagioclase (An_{3-5}), including cleavelandite, is about equal in abundance to quartz, and each is nearly twice as abundant as perthite. Muscovite is an accessory mineral. The smaller pegmatite body consists entirely of material similar to the border and wall zones of the main pegmatite.

The first intermediate zone is medium- to coarse-grained quartz-cleavelandite-perthite pegmatite. The average composition is 45 percent quartz, 30 percent cleavelandite (An_{1-3}), and 20 percent perthite. Muscovite is the chief accessory mineral, and black, blue, and green tourmaline and apatite are minor accessory minerals. Cleavelandite occurs as veinlets cutting the coarser grained perthite and also forms rims around perthite. Quartz and muscovite comprise the finer grained matrix between the perthite-cleavelandite masses.

The second intermediate zone consists of the same essential minerals as the first intermediate zone but with the addition of accessory spodumene, lepidolite, beryl, columbite, and several phosphate minerals; the texture is also similar. This zone is discontinuous and on the footwall side of the pegmatite, its average thickness is 2 feet; on the hanging-wall side, it is as much as 10 feet thick, but its average thickness is much less. The small isolated patches of the unit shown on plate 3 are either at the margin of the core or in a position that could have been marginal to the core before its removal by erosion or mining.

Crystals of spodumene are more abundant than crystals of other accessory minerals, but nearly all the spodumene has been completely altered to a very fine grained aggregate of muscovite and quartz. Locally 15 to 20 percent of the pegmatite of this zone consists of spodumene crystals as much as 2 feet long, 6 inches wide, and 4 inches thick. Lepidolite is much less abundant than altered spodumene. It is commonly gray and occurs in small, very fine grained irregular aggregates. Beryl (12.4 to 13.1 percent BeO) is white, and difficult to distinguish from some of the feldspar, quartz, and amblygonite. A few small plates of columbite are present. Spodumene and lepidolite are most abundant in the inner half of the zone, whereas beryl is most abundant in the outer half; in a few places, these minerals occur together.

Phosphate minerals, commonly triphylite but also less abundant amblygonite and apatite, occur in isolated exposures of quartz-cleavelandite-perthite pegmatite. Sulfides and carbonates, probably mostly siderite, are commonly associated with the phosphates. The approximate outline of the phosphate- and carbonate-bearing parts of the zone are commonly indicated by brown- to black-stained areas colored by iron and manganese oxides derived from the weathering of these minerals.

The core is medium- to coarse-grained perthite-quartz-plagioclase pegmatite in which the perthite content exceeds 50 percent. Quartz is almost twice as abundant as plagioclase.

Beryl occurs only in the second intermediate zone, where it is most abundant in the outer half. The beryl is white and very difficult to distinguish. The size of the crystals is such that a recovery of 75 percent might be obtained by hand-cobbing if the workers were skillful in recognizing the beryl. Mineral measurements indicate that the average beryl content of the zone is 0.11 percent. The beryl contains 12.4 to 13.1 percent BeO.

The largest potassic feldspar resources are in the core, where the crystals are sufficiently large to permit recovery by hand-cobbing. The perthite in other units could be recovered only by milling. Much of the perthite in the opencut is heavily stained by iron and manganese oxides from the phosphate-carbonate-sulfide aggregates of the second intermediate zone; this staining may disappear a few feet below the surface, but the iron- and manganese-bearing minerals are sufficiently abundant in this unit to require their separation in concentrating potassic feldspar.

Sodic feldspar is present in all units, but the grain size is too small to permit an economic recovery by hand-cobbing. By the use of milling methods, sodic feldspar could be recovered with potassic feldspar.

No sheet mica was seen at the Chickering mine. Scrap mica could be recovered from all units except the core by milling. Most of the muscovite occurs in books and flakes too small to be recovered by hand-cobbing.

RAYMOND REGION

Many pegmatites are in the general vicinity of Raymond village, and four of the most important ones are described in this section. These are all northeast of the smaller Raymond district (p. 19). Several have been prospected or mined for feldspar and associated minerals. Nearly all such activity was by the Whitehall Co., Inc., after World War II.

CORSON MINE

The Corson feldspar mine is in one of the most important pegmatites in the Raymond region. It is in the town of Nottingham, Rockingham County, 3.9 miles N. 45° E. of Raymond village. The mine was operated by the Whitehall Co., Inc., during their postwar activity in the Raymond region, and until operations ceased in 1948, the mine supplied feed for the mill at the Chandler mine, 3 miles southwest of Raymond. Workings consist of an opencut 70 feet long, 25 to 40 feet wide, and 10 feet deep, and two small prospect pits.

Two pegmatite bodies, perhaps connected below the surface, crop out at the mine (pl. 4). The northeastern body, containing the main opencut, is the larger and better exposed. The main part of this pegmatite is 100 feet long and 65 feet wide, but an offshoot as much as 30 feet thick extends 80 feet farther to the south. Contacts of this irregularly shaped pegmatite are generally discordant to bedding in the interbedded mica-quartz schist and lime-silicate country rocks. The dip is probably nearly vertical, but there are many variations in the attitudes of the contact. The plunge is unknown, but the pegmatite may parallel a minor fold in schist that plunges 60° S. 25° W. The second pegmatite, 50 feet southwest of the opencut, is nearly circular, with a diameter of about 50 feet. The attitude of this body is unknown.

Four pegmatite units have been mapped at the Corson mine, and two others, a thin border zone and a late fracture filling, are not shown on plate 4. The second intermediate zone, consisting of quartz-cleavelandite-muscovite pegmatite, crops out only in and near the opencut, but the other zones are present in both pegmatites.

The border zone consists of very fine grained quartz-muscovite pegmatite with accessory plagioclase. The unit is from one-quarter to 2 inches thick.

The wall zone is fine- to medium-grained plagioclase-quartz-perthite pegmatite with accessory muscovite and minor accessory biotite and garnet. The average composition is 55 percent plagioclase, 30 percent quartz, 10 percent perthite, and 5 percent accessory minerals. About one-fourth of the plagioclase is cleavelandite. Muscovite constitutes as much as 5 percent of the unit, but the average content is 1 percent. Very thin radiating strips of biotite 2 to 3 inches long and 1 inch wide are exposed in small areas within the unit. The thickness ranges from 6 inches to 30 feet in the offshoot from the main pegmatite.

The first intermediate zone is medium- to coarse-grained plagioclase-perthite-quartz pegmatite with accessory muscovite. The average composition is 55 percent plagioclase, 30 percent perthite (including some graphic granite), 10 percent quartz, and 5 percent accessory minerals. About one-fourth of the plagioclase is cleavelandite.

The second intermediate zone is medium-grained quartz-cleavelandite-muscovite pegmatite forming a discontinuous unit between the first intermediate zone and the core. Its average composition is 75 percent quartz, 10 percent cleavelandite, 10 percent muscovite, and 5 percent accessory minerals including perthite and beryl. This is the only zone containing beryl.

A 2-inch fracture filling of quartz-beryl pegmatite cuts the second intermediate zone. It contains many small yellow beryl crystals arranged normal to its walls; one crystal extends almost completely across the unit.

The core consists of coarse-grained quartz-perthite pegmatite with accessory muscovite and plagioclase. The average composition is 75 percent quartz, 20 percent perthite, and 5 percent accessory minerals. Perthite is in euhedral to subhedral blocks in the gray quartz. In the southwest pegmatite, a small exposure of similar rock is surrounded by the wall zone rather than being within the first intermediate zone.

The beryl content of the second intermediate zone is 0.15 percent, and most of it could be recovered only by milling. Most beryl crystals are less than 1 inch long, but a few are as much as 8 inches long. They are yellow, yellow-green, or golden. Columbite plates as much as 1 inch long, 1 inch wide, and one-half inch thick are rare in the second intermediate zone.

Potassic feldspar can be recovered from the core by hand cobbing, and a small amount of the perthite in the first intermediate zone can be recovered. These units would not support mining operations under the economic conditions of 1950, and the resources of both potassic and sodic feldspar could be more efficiently recovered by milling methods. The pegmatite is too small to support a mill that is not also supplied by other nearby pegmatites. No sheet mica was seen at the mine, and the scrap mica could be recovered only by milling.

McGALL MINE

The McGall feldspar mine is in the town of Raymond, Rockingham County, 1.0 mile S. 5° E. of Raymond village. The mine was opened by the Whitehall Co., Inc. in September 1948 and was worked until March 1949 when all mining activity ceased. Workings consist of an opencut 100 feet long, 35 to 80 feet wide, and as much as 25 feet deep, and three small prospect pits.

Two large and three small pegmatites crop out at the mine (pl. 5). The opencut was developed in an ovaloid pegmatite, 110 feet long and as much as 70 feet wide, that strikes about N. 20° W. The contacts dip outward at angles ranging from 55° to 75° except on the east side where the dip is 70° inward. The pegmatite is generally discordant to the bedding in the quartz-mica schist wallrocks, but in places it is parallel to an induced foliation present in the wallrock within a few feet of the contact. The plunge of minor folds and lineation in the wallrock adjacent to the pegmatite ranges from 15° to 40° SW.

The largest pegmatite is a lenticular body 320 feet long and as much as 60 feet wide. It is generally discordant, trends due east, and dips 55° to 65° S. at the east end, and 65° to 75° N. at the west end. A roll in the north contact 100 feet east of the west end of the pegmatite plunges 40° NE. This is the only feature indicating a possible plunge of the body.

A smaller pegmatite southwest of the larger opencut, having no exposed contacts with wallrock, is known only from outcrops. A pegmatite 1 foot thick and at least 10 feet long is exposed in the east wall of the opencut, 7 feet south of the probable contact of the main pegmatite. It strikes about east and dips 50° S. Another small pegmatite crops out 30 feet north of the east end of the largest pegmatite. No contacts are exposed, but the two small outcrops trend S. 70° W.

Five pegmatite zones have been distinguished at the McGall mine, and all except the border zone are shown on plate 5. Fracture fillings also have been recognized.

The border zone consists of very fine grained quartz-muscovite-plagioclase pegmatite. Although commonly less than one-half inch thick, in places it is as much as 6 inches thick.

The wall zone is fine-grained plagioclase-quartz-muscovite pegmatite with accessory perthite and minor accessory garnet, apatite, beryl, and columbite. The average composition of the zone is 60 percent plagioclase, 20 percent quartz, 10 percent muscovite, and 10 percent accessory minerals. In exposures near the entrance to the main opencut, most of the plagioclase is clevelandite, but elsewhere in the unit cleavelandite is only in isolated patches. This zone is 2 to 3 feet thick along the outer margins of the larger pegmatites, and is the sole constituent of the smaller pegmatites.

The first intermediate zone is medium- to coarse-grained perthite-plagioclase-quartz pegmatite with accessory muscovite and minor accessory beryl, garnet sphalerite, and pyrite. The average composition is 45 percent perthite, 35 percent plagioclase, 15 percent quartz, and 5 percent accessory minerals. Perthite is commonly coarse grained, and set in a matrix of plagioclase, quartz, and muscovite. Part of the perthite is in graphic granite. Cleavelandite and normal plagioclase are about equally abundant. The first intermediate zone is the largest unit exposed in the two main pegmatites.

The second intermediate zone is medium-grained quartz - muscovite - perthite - spodumene - cleavelandite pegmatite. The average composition is 40 percent quartz, 20 percent muscovite, 15 percent perthite, 15 percent spodumene, and 10 percent cleavelandite. This zone is exposed only in the opencut where it surrounds the northwestern exposure of the core of the pegmatite. It is 2 feet thick.

The core is medium- to coarse-grained quartz-spodumene pegmatite. Grain measurements in the core give an average composition of 86 percent quartz, 13 percent spodumene, and 0.74 percent beryl. Columbite and triphylite are minor accessory minerals. Two segments of the core are in the opencut, one on the northwest wall of the cut and the other on the south and southeast walls. These segments are not now connected although they are reported by the operator to have formed a continuous unit across the cut at one stage of mining operations. The core has an average thickness of 2 feet.

The large pegmatite has a central unit of quartz pegmatite, 25 feet long and 2 feet thick, near its east end. Although spodumene is a minor accessory mineral, this unit is otherwise similar to the core of the pegmatite in the opencut. Quartz pegmatite also occurs as pods or fracture fillings in the prospect pit near the north contact.

A few tabular fracture-controlled units of quartz-rich pegmatite cut the first intermediate zone in the opencut. Beryl and muscovite are minor accessory minerals. Small vugs at the ends of these units are lined with crystals of plagioclase and quartz.

Beryl is most abundant in the core, and possibly extends into the second intermediate zone. It is also present as a minor accessory mineral in the wall and first intermediate zones, and in fracture fillings. In the core, beryl is yellow to yellow-green. The average surface area of individual crystals is about 20 square inches, and most crystals could be recovered by hand-cobbing. Grain measurements indicate that the grade is 0.74 percent. Crystals of light-green beryl as large as 7 by 7 inches occur in the wall zone, but most crystals are less than 1 inch in diameter and are widely scattered throughout the unit. This fine-grained beryl could be recovered only by milling methods. The major resources of beryl depend on the size of the cores of the two main pegmatites at depth; reports from miners indicate that the core segments in the opencut decreased in size with depth. There is no evidence of a possible increase in size of the core of the larger pegmatite.

Potassic feldspar resources at the McGall mine are in the first intermediate zone. The coarsest grained perthite is in the walls of the opencut, but it is neither sufficiently abundant nor large enough to warrant its recovery by hand-cobbing under economic conditions of 1949. Most of the feldspar was trucked to the mill at the Chandler mine, crushed, and separated from waste rock on picking belts. Potassic and sodic feldspar, with scrap muscovite as a byproduct, might be recovered by milling.

Sodic feldspar, present in all units of the pegmatites, is most abundant in the wall zone. The grain size of plagioclase in the pegmatites is too small to permit hand-cobbing, and recovery would be possible only by milling.

No sheet mica was seen at the mine. The wall zone contains a greater percentage of scrap mica than other units, but the largest resources are in pegmatite of the first intermediate zone, because of its greater size.

Spodumene is present in the core and second intermediate zones, and resources, like those of beryl, depend on an increase in the size of the two inner units at depth. Spodumene in the core is hard and fresh where enclosed by quartz but is soft and altered to muscovite where enclosed by feldspar. The spodumene content of the core is 13 percent.

Columbite is a very minor accessory mineral of the core and wall zones. The grains are very small and could not be recovered by hand-cobbing.

McMULLEN PROSPECT

The McMullen feldspar prospect consists of three pegmatites 1.0 mile S. 12° W. of Raymond village, and about 0.3 mile west of the McGall mine. The prospect was worked by the Whitehall Co., Inc., for a few weeks in September and October 1948. A shallow opencut is 100 feet long, 10 to 75 feet wide, and has a maximum depth of about 10 feet. The northeast ends of the northern and central pegmatites were mined.

The three pegmatites are parallel, but arranged en echelon so that the southern pegmatite extends farther east than the others. The bodies are lenticular, concordant, 220 to 260 feet long, and 2 to 40 feet thick. They strike N. 70° E., dip vertically or steeply southward, and probably plunge 1° to 15° SW. The wallrock is quartz-mica schist. A concordant mafic dike 10 feet thick is between the central and southern pegmatites.

Most of the mining has been in the central pegmatite, which consists of two poorly defined zones. An irregular core of quartz-perthite pegmatite in the center is surrounded by fine- to medium-grained plagioclase-quartz-perthite pegmatite containing accessory muscovite and minor accessory beryl. The average composition is 45 percent plagioclase, 40 percent quartz, and 15 percent perthite. On the south wall of the cut, small irregular areas of very fine grained aplitic material occur in the matrix between perthite blocks. This matrix consists of plagioclase (An_8), quartz, and garnet, and is separated from perthite by a thin layer of cleavelandite (An_2). About two-thirds of the plagioclase in this unit is cleavelandite. Measurements of beryl grains across the west wall of the opencut indicate a grade of 0.08 percent. Most of the beryl is in crystals less than 1 inch in diameter although 1 crystal, possibly from the core, may have been 1 foot in diameter.

Production of pegmatite minerals from the McMullen prospect will depend on the use of milling methods. Perthite is not sufficiently abundant for hand-cobbing, and plagioclase, scrap mica, and beryl are too fine grained to be recovered economically by hand methods.

VATCHER PROSPECT

The Vatcher feldspar prospect is 2.5 miles N. 50° E. of Raymond village. In 1947, the Whitehall Co., Inc., removed the overburden from much of the pegmatite and opened two small prospect pits in search of potassic feldspar (pl. 6).

The pegmatite is at least 400 feet long and 90 feet in outcrop width. The strike of the hanging-wall contact, the only one visible, is about N. 60° E., and the dip is 30° to 60° SE. The pegmatite is concordant with bedding in the mica-quartz schist. The plunge of the pegmatite appears to be about 20° in an easterly direction. The footwall contact is not exposed nor is the extension of the pegmatite southwestward from the area mapped. A very fine grained, highly altered mafic dike 7 inches thick strikes N. 45° W. across the pegmatite and dips 30° SW.

A thin border zone of very fine grained quartz-muscovite-plagioclase pegmatite is present along the hanging-wall contact. It is less than 6 inches thick, and locally is less than 1 inch thick. The exposures shown on the map (pl. 6) have been exaggerated in order to be shown. The average composition is 55 percent quartz, 20 percent muscovite, 20 percent plagioclase, and 5 percent accessory minerals including cleavelandite, beryl, and garnet.

The wall zone consists of fine- to medium-grained plagioclase-quartz-perthite pegmatite with accessory muscovite, biotite, and cleavelandite, and minor accessory black tourmaline, garnet, beryl, columbite, and sulfides. The average composition is 40 percent plagioclase, 30 percent quartz, 25 percent perthite, and 5 percent accessory minerals. The relative abundance of the essential minerals in the zone varies widely. The thickness of the zone is unknown, but in many exposures it seems to be a thin cap over the core.

The core is medium- to coarse-grained perthite-quartz-cleavelandite pegmatite. It also contains muscovite, blocky plagioclase, and minor accessory beryl, columbite, and garnet. The average composition is 45 percent perthite, 40 percent quartz, and 10 percent cleavelandite. The quartz is gray, pink, and white. Perthite in massive quartz is euhedral, but elsewhere it is in subhedral blocks with a matrix of finer grained quartz and cleavelandite.

The core has been exposed only locally by erosion of the wall-zone cap. The core probably extends the entire length of the pegmatite (pl. 6, section *A–A′*). Pegmatitic material with a composition similar to that of the core is exposed in roughly tabular fracture-filled bodies extending from the central part of the pegmatite across the wall and border zones to the hanging-wall schist. At one place the contact is offset slightly at its junction with the fracture filling.

An irregularly shaped unit of cleavelandite-perthite-muscovite pegmatite near the center of the northeastern part of the pegmatite probably was formed by the replacement of earlier pegmatite, and its composition varies greatly. The pegmatite is fine grained to medium grained, and contains an average of 45 percent cleavelandite, 40 percent perthite, and 10 percent fine-grained greenish muscovite. Other minerals include quartz, blocky plagioclase, and minor quantities of garnet and sulfides. The perthite is corroded and veined by cleavelandite. The most noticeable difference in composition between pegmatite of this unit and of the zones is the markedly lower quartz content of the replacement unit.

Southwest of the road, this unit is very irregular, and seems to be later than the pegmatite of the adjacent fracture filling. A few perthite crystals in the fracture filling have been completely replaced by cleavelandite; others are rimmed by cleavelandite. The composition here is about 60 percent cleavelandite, 20 percent perthite, and 15 percent fine-grained greenish muscovite.

Economic possibilities at the Vatcher prospect depend on the size of the core, which contains most of the economically important minerals. If it extends most of the length of the pegmatite, as shown on plate 6, section *A–A′*, the resources of these minerals would be sufficiently great to warrant future operations.

Beryl forms 0.38 percent of the core, as determined by mineral measurements. The beryl content of the wall and border zones is 0.01 percent. About 75 percent of the beryl in the core could be recovered by hand cobbing. Virtually no beryl could be recovered from the wall and border zones. The beryl is light green in the outer units and very pale green to white in the core.

The average perthite content of the core is 45 percent, although the fracture fillings may contain only 20 to 30 percent. Although recovery of potassic feldspar by hand-cobbing might be a marginal operation, milling of the entire pegmatite to yield a combined product of perthite and plagioclase might be an economically promising method of recovery. Biotite and garnet, although most abundant in the wall zone, are also present in other pegmatite units, and would be the major contaminants of a feldspar product. The average feldspar content of the entire pegmatite, including both perthite and albite, is about 60 percent.

No sheet mica was seen in the Vatcher pegmatite, but muscovite of scrap quality could be recovered by milling, especially from the replacement unit. A few masses of columbite as much as 2 inches across occur in the core, but the estimated content is less than 0.001 percent of the richest exposure of this unit.

RAYMOND DISTRICT

The group of pegmatites, called the Raymond pegmatite district in this report (fig. 3) are in the southwest corner of the Raymond region, Rockingham County. The district is about 1.25 miles long and 1 mile wide. All but one of the pegmatites investigated are in the town of Raymond although the area mapped extends southward into the town of Chester. Three-quarters of the district is in the southwest corner of the Mount Pawtuckaway quadrangle, and one-quarter is in the northwest corner of the Hampstead quadrangle. The Raymond Road, mostly graveled but partly paved, is near the north edge of the area mapped; a graveled road parallel to the Raymond Road but about 1 mile south of it forms the southern boundary. Two abandoned dirt roads are the approximate east and west boundaries; the one on the west is passable in dry weather, but nearly half the length of the one on the east side is overgrown and impassable. Mine-access

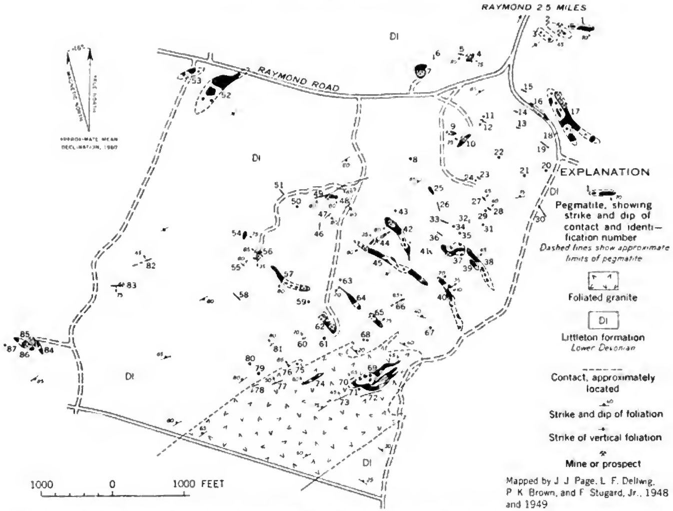
RAYMOND 2.5 MILES
RAYMOND ROAD
Dl
EXPLANATION
Pegmatite, showing strike and dip of contact and identification number
Dashed lines show approximate limits of pegmatite
Foliated granite
Dl
Littleton formation
Lower Devonian
Contact, approximately located
Strike and dip of foliation
Strike of vertical foliation
Mine or prospect
1000 0 1000 FEET
Mapped by J. J. Page, L. F. Dellwig, P. K. Brown, and F. Stugard, Jr., 1948 and 1949

FIGURE 3.—Geologic map of the Raymond district, Rockingham County, N.H., showing locations of pegmatite exposures studied.

roads extend southward from the Raymond Road to mines and prospects that have been operated recently.

The pegmatites of the Raymond district have been known for many years, and a few small prospect pits had been opened before 1942. When further fruitless prospecting was done in search of sheet mica-bearing pegmatites during World War II, the possibility of producing feldspar from these pegmatites was recognized. The Whitehall Co., Inc., through its office in Keene, N. H., began operations in the area during the war, and an extensive prospecting program was carried out after the war in search of commercial deposits of potassic feldspar. Overburden was stripped from several pegmatites, and small prospect pits were opened. Most of the work was done at 4 mines (Chandler, Smith No. 1, Welch, and Blake mines) and at 2 prospects (Smith No. 3, and Hurley prospects). A small mill was established at the Chandler mine, and the coarsely crushed feldspar was separated from waste rock on picking belts. Mining activity in the Raymond district ended in September 1948, but the mill continued to operate until early 1949 using ore from the McGall mine, about 2 miles northeast of the Chandler.

Detailed mapping was done in June July, and August 1948 by the senior author with the assistance of L. F. Dellwig. The larger mines and pegmatites were studied at different times between September 1948 and July 1949. Frederick Stugard, Jr., assisted in the work for 1 week in September 1948, and L. F. Dellwig and P. K. Brown, Jr., assisted in 1949. Mapping was done by pace and compass, and almost every outcrop within the Raymond district was visited. The southwestern part shown on the topographic map of the Mount Pawtuckaway quadrangle was enlarged to a scale of 1 : 12,000 for use as a base map. Selected pegmatites were mapped by planetable and alidade.

GENERAL GEOLOGY

The geology of the Mount Pawtuckaway quadrangle has been mapped and studied by Jacob Freedman (1950), who kindly permitted the use of his geologic map before publication. The following brief summary of the general geology of the Mount Pawtuckaway quadrangle in the vicinity of the Raymond district is modified from his work. The district is underlain by metamorphic rocks of the Littleton formation (Lower Devonian). These are metamorphosed sedimentary rocks, consisting largely of mica-quartz schists containing some sillimanite, with interbedded impure quartzite and lime-silicate rocks. The quartzite and lime-silicate rocks probably constitute less than 10 percent of the formation and are commonly in beds less than 1 foot thick. Foliation and bedding in the schists are about parallel. The average strike is N. 55° E., parallel to the regional trend of the formation, and the dip is commonly almost vertical.

The south-central part of the district, in the Hampstead quadrangle, is underlain by a fine- to medium-grained, strongly foliated granitic rock unlike any seen in the Mount Pawtuckaway quadrangle. This gneissic granite consists of feldspar, quartz, and muscovite. Potassic feldspar is almost twice as abundant as plagioclase (An_{11}), and together they constitute about 50 percent of the rock. About 30 percent of the rock is quartz, 20 percent is muscovite, and biotite is a minor accessory mineral. Quartz commonly occurs as flat plates, and these, together with flakes of muscovite and biotite, give the rock its foliation.

The schists seem to wrap around the northeast end of the granite body. The strike of bedding in the schists ranges from the regional trend, N. 55° E., through north to almost west parallel to the contact between the granite and the schist. In detail, this contact is not concordant to bedding, and apophyses of the granite extend into the schists. Foliation in the granite is parallel to the regional strike, but the dip is consistently 50° to 80° NW., in contrast to the steeper dip of the schist.

The location of 87 pegmatite exposures or groups of exposures in the Raymond district are shown in figure 3, where they are identified by number. Most are in the east half of the area, where outcrops are most abundant.

The pegmatites are exposed along their strike from 2 to 1,200 feet, and are from a few inches to as much as 250 feet thick (table 2). Many of the larger pegmatites are discordant to bedding in the wallrock, although a few are concordant or nearly so.

Most of the pegmatites are lenticular, tabular, or pipelike, but several are so irregular that they cannot be classified under any of these terms. The lenticular and tabular bodies are both concordant and discordant to the structure of the wallrock. Many of the lenticular bodies are so long and thin that they approach a tabular form. The only pegmatite consisting of a series of interconnected lenses is the one at the Smith No. 3 prospect (pl. 10). Apophyses of this pegmatite are good examples of the tabular shape; one apophysis extends more than 500 feet northeastward parallel to bedding, and has a nearly constant thickness for this entire distance. The Chandler pegmatite (pl. 7) is the best example of a pipelike body.

Nearly half of the pegmatites in the Raymond district are concordant to foliation of the enclosing wallrock. All the pegmatites in the gneissic granite are concordant; the average strike is N. 65° E., and the dip 50° NW. The average strike of concordant pegmatites in schist is N. 55° E., and the average dip steeply northwestward. The discordant pegmatites commonly strike N. 40° to 60° W., and dip steeply northeastward. In the east-central part of the area, pegmatites of similar strike are generally concordant to bedding that wraps around the northeast end of the gneissic granite body. Pegmatite Nos. 37, 38, 39, and 40 are concordant, northwestward-striking bodies. They dip at angles ranging from 10° to 70° NE.

The pegmatites contain varying proportions of plagioclase, perthite, quartz, muscovite, and accessory minerals such as biotite, black tourmaline, garnet, beryl, columbite, spodumene, lepidolite, löllingite, sulfides, and phosphates. Differences in the proportions of the major constituent minerals and differences in texture permit zones to be distinguished in 38 of the pegmatites. Table 3 gives the sequence of mineral assemblages inward from the contact in each of the zoned pegmatites.

Forty-nine pegmatites are not known to be zoned. In most of these the exposures are inadequate for recognition of zones. About half of these pegmatites consist of varying proportions of plagioclase, quartz, and perthite, and in most, plagioclase is more abundant than perthite. Fracture-controlled units were noted in eight pegmatites. These generally consisted of quartz, muscovite, perthite, and plagioclase (commonly cleavelandite). In three pegmatites, these units are zoned.

Beryl from pegmatites in the Raymond district could be a major byproduct of feldspar milling if special equipment were installed to permit its recovery. Most of the crystals are too small for hand-cobbing, although a few tons of beryl could be recovered in this way from the core of the Chandler and a few other pegmatites. Very fine grained beryl was observed in pegmatite 74, and other pegmatites may contain crystals of equal or even smaller size that have been overlooked. This very

TABLE 2.—*Size of pegmatites, and distribution of minerals therein, Raymond district, New Hampshire*

[Abbreviations used are as follows: Status of operation: No=no operation, P=prospect only, St=overburden stripped, only, Oc=opencut. Relation to foliation: P=parallel, X=crosscutting. Essential minerals: apl=aplite, b=beryl, cl=cleavelandite, gg=graphic granite, m=muscovite, p=perthite, pl=plagioclase, q=quartz, s=spodumene. Distribution of major useful minerals: A=throughout pegmatite, C=core, FC=fracture-controlled body, FW=footwall, I=intermediate zone, W=wall zone]

Pegmatite	Status of operation	Exposed size of pegmatite (feet)		Relation to foliation	Pegmatite zoned	Essential Minerals (in order of abundance)				Distribution of major useful minerals					
		Length	Thickness			Wall zone	Intermediate zone	Core	Other units or unzoned pegmatite	Beryl	Sheet muscovite	Scrap muscovite	Perthite	Columbite-tantalite	Other
1	No	400	75	±P	No				pl-q-p	A		A	A		
2	P	400?	125?	X	Yes?	pl-q-m		p-q-pl	p-q-pl cl-m-q	A	?	A	A		
3	No	200	?	X?	No				pl-q-p			A	A		
4	No	80	20-60	±X	Yes	pl-q-p	p-q-pl	p-q-pl		W		W	I		
5	No	115	5	X	Yes?	q-pl-m		p-q-pl		W					
6	St	35	2	±X	No?				p-m-q						
[1] 7	Oc	150	70-170	X	Yes	p-pl-q	m-cl-q q-cl-m	q-b-s		A		I	W	C	Spodumene, lepidolite.
8	No	5	1	X	No				q-m-b	A					
[2] 9	P	110	10-50	±X	No				p-q-pl	A	A?	A	A	A?	
[3] 10	Oc	270	10-50	P	Yes	pl-q-p-m pl-q-p	p-q-pl pl-q-p	q-p	q-p-b-m	W C, W	W, I	W, I A	C, I	I I, C	Lithium minerals. Lepidolite.
11	St	25	6	P	No				q						
12	St	100	8	±X	Yes	q-p-pl		p-q	pl-p-q						
13	No	60	15	X	No				p-pl				A		
14	P	40	±20	X	Yes?	pl-q-p		p-q					C		
15	No	125	25	X	No				q-p-pl			A	A		
16	No	350	50	X	No				pl-q-p			A	A		
[4] 17	P	1,100	200	X	No				p-q-pl			A	A	A	
18	No	15?	8	P	Yes	pl-p-q	p-q	q	pl-p-q	A			A		
19	No	150	±15	X	Yes?	pl-p-q		q-p-pl	q-m	FC?, C			C		
20	No			X	No				pl-q-p						
21	No	15	3	P	Yes	pl-q		p-q-pl							
22	No	20	1.5	P	Yes			q-p		W?					
23	No	65	20	X	Yes	q-pl		q-pl-m		C	?	W	C, W		
24	No	10	3	X	No				pl-q-apl						
25	P	125	10-50	X?	Yes?	p-q		p-q-pl		A		A	C	C	
26	No	120	25	X	Yes?	q-p-pl		q-p-m		C	?	A	A		
27	No	±50	±3	P?	No				q-p						
28	P	±50	4-20	P	No				pl-p-q	A?					
29	No	25	10	P?	No				pl-p-q						
30	No	200	±10	X	No				pl-q-p			A	A		
31	St	20	±5	±P	Yes?	p-q-m		p-q		W			C		
32	St	45	8	X	Yes?	q-pl-m		q-p		A			C		
33	No	125	25	X	No				q-p-pl			A	A		
34	No	2	.5	±P	No				p						
35	St	>20	25	X	Yes?	gg-q		q-p-m							
36	No	100	±10	±X	No				q-p-pl			A	A		
37	St	350	170	±P	Yes	pl-q-p	q-p-pl	p-q-pl-gg		I		A	A		
38	No	730	60	P	No				q-p-pl			A	A		
39	No	150	50	±P	No				q-p-pl	A		A	A		
40	P	800	±30	±X	No				q-pl-p	A		A	A		
41	No	35	4	X	No				pl-q-m						
42	P	700	10-100	X	Yes	pl-q-p	pl-p-q-m	p-q-pl		I	I?	I, A	A		
43	No	8	.5	P	No				q-pl-m	A					
[5] 44	P	375	25	P	Yes?	q-p-pl		q-p-pl		W		A	A		
45	P	1,200	±80	X	Yes?	q-pl-p-m		p-cl-m		W		A	A		
46	No	130	5-25	X	Yes?	q-pl-p		p-q		W		W	C		
47	No	125	4	P	Yes	q-m-pl		p-pl-q		W		W			
48	No	25	3	P	Yes	q-pl-m		pl-q		W					
[6] 49	P	200	20-50	X	Yes	pl-q-p		p-q-pl		A		A	A		
50	St	20	4	X	Yes	pl-q-m		q-p		A		A			
51	No	±90	±4	X	No?				q-pl-m	A		A			
52	No	1,000	200	P	Yes?	q-pl-p		p-q				A	A	C	
53	No	400?	100?	P	No				q-pl-p			A	A		
54	St	60	20	X	Yes	pl-q-p		p-q	q-m-b	W, FC		A	A		
55	No	100	5	X	No				q-pl-p	A		A	A		
[7] 56	Oc	130	70	P	Yes	q-m-pl	p-q-pl	q-p		W, I	W	I, W	I, C	I, C	
[8] 57	P	750	50	X	Yes	pl-q-p-m	p-q-m	q		A		W, I	I		
58	No	140	30	X	No				q-pl-p	A		A	A		
59	No	10	1	±P	No				q-pl						
60	No	40	2	P	Yes	m-q-pl	pl-q-p	q		W, I					
61	No	10	2	±X	No				q-pl-p	A					
[9] 62	Oc	820	85	X	Yes	pl-q-p	apl-p-pl-q	p-q-m-cl		A		A	A	I?	

							p-pl.								
							p-q-pl.								
63	No	8	3.5	±P	No.				q-p-pl-m.			A.			
64	No	800	10-50	X	Yes?	q-m-pl.		q-pl-p.		A.		A.	C.		
[9] 65	P	250	20-60	X	Yes.	q-p-pl-m.	p-q.	q.		W, C.		W.	W, I.	W.	
66	No	200	15-20	P	Yes?	q-pl-p.		q.			?	W.	W.		
67	No	20?	3	X	No.				q-pl.						
68	No	10	?	X	No.				pl-q.						
69	No	850	250	P?	Yes.	pl-q-p.		p-q-pl.		A.		A.	A.	A.	Lepidolite.
73	No	250	15	P	No.				pl-q-p.	A.		A.	A.		
74	No	300	25	P	No.				p-q-pl.	PC.					
75	No	10	3	X	No.				q-pl-p.	A.					
76	No	50	3	P	No.				p-pl-q.	A.					
77	No	170	3-15	P	No.				p-pl-q.	A.		A.	A.		
78	No	105	4	P	Yes?	q-m-pl.		p-pl-q.		C.					
79	No	2.5	1	P	No.				q-m-pl.						
80	No	20	1	P	No.				q-pl.						
81	No	60	1	P	No.				q-pl.						
82	No	280	12	P	Yes?	pl-q-p.		q-pl-p.		A.		A.	A.	W?	
[10] 83	P	60	15	X	No.				p-q-pl-m.	A.	A.	A.	A.	A.	
[11] 84	P	120	45	X	No.	pl-q-p.	pl-q-p-m.	p-q.							
[11] 85	P	120	45	X	Yes.	pl-q-p.	pl-q-p-m.	p-q.				I.	A.		
[11] 86	P	250	80	X	Yes.	pl-q-p.	pl-q-p-m.	p-q.				I.	A.		
87	No	40	20	X	No.				p-pl-q.			A.	A.		

---

[1] Chandler pegmatite.
[2] Smith No. 1 pegmatite.
[3] Guinea pegmatite.
[4] Smith No. 2 pegmatite.
[5] Smith No. 3 pegmatite
[6] Blake pegmatite.
[7] Lane pegmatite.
[8] Welch pegmatite.
[9] Mills pegmatite.
[10] Gillingham pegmatite.
[11] Hurley pegmatite.

TABLE 3.—*Mineral assemblages in zoned pegmatites*

[Sequence inward

	Mineral assemblage	Pegmatite number														
		4	5	7	10	12	14	18	19	21	22	23	25	26	31	32
	Wall zone															
1	Plagioclase-quartz-muscovite															
2	Plagioclase-quartz-perthite	×			×		×									
3	Quartz-plagioclase-muscovite		×													×
4	Perthite-plagioclase-quartz			×												
5	Plagioclase-quartz-perthite-muscovite				×											
6	Quartz-perthite-plagioclase					×								×		
7	Plagioclase-perthite-quartz							×	×							
8	Plagioclase-quartz									×						
9	Quartz-plagioclase											×				
10	Perthite-quartz-plagioclase-aplite												×			
11	Perthite-quartz-muscovite														×	
12	Quartz [1]															
13	Quartz-plagioclase-perthite-muscovite															
14	Quartz-plagioclase-perthite															
15	Quartz-muscovite-plagioclase															
16	Muscovite-quartz-plagioclase															
17	Quartz-perthite-plagioclase-muscovite															
	Intermediate zone(s)															
18	Perthite-quartz-plagioclase	×			×											
19	Muscovite-cleavelandite-quartz			×												
20	Quartz-cleavelandite-muscovite			×												
21	Perthite-quartz							×								
22	Quartz-perthite-plagioclase															
23	Plagioclase-perthite-quartz-muscovite															
24	Perthite-quartz-muscovite															
25	Plagioclase-quartz-perthite				×											
26	Perthite-plagioclase-quartz [2]															
27	Quartz-plagioclase															
28	Plagioclase-quartz-perthite-muscovite															
	Core															
29	Perthite-quartz-plagioclase	×	×							×						
30	Quartz-beryl-spodumene			×												
31	Perthite-quartz					×	×								×	
32	Quartz							×								
33	Quartz-perthite-plagioclase								×							
34	Quartz-perthite				×						×					×
35	Quartz-plagioclase-muscovite											×				
36	Quartz-perthite-muscovite													×		
37	Perthite-quartz-plagioclase [1]															
38	Perthite-cleavelandite-muscovite															
39	Perthite-plagioclase-quartz															
40	Plagioclase-quartz															
41	Perthite-quartz-muscovite-cleavelandite															
42	Quartz-plagioclase-perthite															
43	Perthite-quartz-plagioclase												×			

[1] In graphic granite. [2] In aplite.

fine grained beryl would be recoverable only if a milling method was developed. The composition of the beryl ranges from about 11.6 to 13.5 percent BeO and averages about 13.0 percent. In 50 pegmatites in the Raymond district, beryl was noted in a total of 56 zones and in some it was present throughout the entire pegmatite. The distribution of beryl-containing units as follows: Wall zone, 15; intermediate zone, 4; core, 6; fracture-controlled bodies, 3; entire pegmatite, 28.

Potassic feldspar was the major product recovered during recent mining activity in the Raymond district and it would be the major product of any future operations under the 1947–50 demand for pegmatite minerals. Perthite is an essential mineral of every large pegmatite in the area. Its grain size, however, is ordinarily too small to permit recovery by hand-cobbing methods. A few pegmatites scattered throughout the area contain coarse-grained, perthite-rich units, but most of these units are so small that they could be mined only by removing large tonnages of finer grained pegmatite in the adjacent units. Resources in any one of these units are at most only a few hundred tons of potassic feldspar.

Beneficiation methods in which potassic and sodic feldspar are recovered by flotation or other means seem to be the only solution for future production. The district is at an economic disadvantage compared with others in New Hampshire because of the small average size of the individual pegmatites and the lack of a resident supply of labor with a knowledge of mining. It is favored, however, by the fairly uniform average composition of the pegmatites, the high feldspar content, and the small and uniform content of iron-bearing accessory minerals which are especially harmful in any feldspar product. The establishment of a mill that is easily accessible from all parts of the area, the use *of the Raymond District, Rockingham County, N.H.*

from the contact]

Pegmatite number—Continued																								
35	37	42	44	45	46	47	48	49	50	52	54	56	57	60	62	64	65	66	69	78	82	83	86	
Wall zone—Continued																								
									×															1
	×	×						×			×				×				×		×	×	×	2
							×																	3
																								4
													×											5
			×																					6
																								7
																								8
																								9
																								10
																								11
×																								12
				×																				13
					×					×								×						14
						×						×				×				×				15
														×										16
																	×							17
Intermediate zone(s)—Continued																								
												×			×									18
																								19
																								20
																	×							21
	×																							22
		×																						23
													×											24
														×										25
															×									26
															×									27
																						×	×	28
Core—Continued																								
		×						×																29
																								30
					×					×	×											×		31
													×	×			×	×						32
			×																					33
									×			×												34
																								35
×																								36
	×																							37
				×																				38
						×														×				39
							×																	40
															×									41
																×					×		×	42
																								43

of mining equipment that could be moved easily from one location to another as individual deposits were mined out, and the use of equipment and methods that would permit low-cost mining of large tonnages of rock all would be necessary to insure economic recovery of feldspar.

Sodic feldspar could be recovered only through milling methods, which would yield a product combined with potassic feldspar. The grain size of the plagioclase is too small to permit its recovery by hand-cobbing, and only a small recovery could be obtained by the use of crushing plants and picking belts.

The possibility of recovering muscovite of sheet quality from pegmatites of the Raymond district is very poor. No pegmatite units were seen that would support mining operations solely for sheet mica under prices similar to those in 1942–45. Crude mica books yielding small sheets are present at a few places, but in only one pegmatite (the Blake, pegmatite 56) is there a sufficient concentration to permit economic recovery. Scrap mica can be recovered at 1 or 2 places by hand-cobbing, but most of the muscovite in the pegmatites is too small to be recovered except through milling methods. Muscovite occurs in almost every pegmatite, and the average content probably ranges from 2 to 5 percent. Its recovery as a byproduct of feldspar milling offers the best possibility for future production.

Columbite is most abundant in the core of the Chandler pegmatite where most of it can be recovered by hand-cobbing. In other pegmatites, it is a minor accessory mineral and only a few small plates can be seen. Recovery during feldspar milling could be made by simple gravity methods.

The Chandler pegmatite also contains spodumene and lepidolite in the core, and spodumene in what is probably an inner intermediate zone. Much of the spodumene has been altered to muscovite, and present exposures do not indicate sufficient resources to warrant its recovery. Lepidolite resources in the core are also very small. Other pegmatites in the area may contain lithium minerals, but none have been observed.

PEGMATITE 1

Pegmatite 1 is poorly exposed and crops out in an area 75 feet wide and 400 feet long. This body strikes east and dips 70° S. at the one place where a contact is exposed, and it is generally concordant. It is unzoned fine- to medium-grained plagioclase-quartz-perthite pegmatite. Beryl (12.8 percent BeO) is a minor accessory mineral. Possible products are milling-grade feldspar and scrap mica.

PEGMATITE 2

Pegmatite 2, also poorly exposed, crops out in an area 125 by 400 feet. Two small prospect pits were opened for feldspar near the contacts by the Whitehall Company, Inc. The pegmatite strikes N. 65° W., dips 65° SW., and is discordant. It has at least two zones: a wall zone of plagioclase (An_{12})-quartz-muscovite pegmatite and a core of medium-grained perthite-quartz-plagioclase pegmatite. A small unit in the north pit, apparently not a zone, consists of medium-grained cleavelandite (An_1), muscovite, and quartz; it contains as much as 30 percent muscovite of scrap quality. Green tourmaline is associated with cleavelandite; "watermelon" tourmaline also has been reported from this pegmatite. Possible products are milling-grade feldspar and scrap mica.

PEGMATITE 3

Pegmatite 3 is represented by several small exposures in an area that extends N. 50° W. for 200 feet; some may be boulders. The rock is unzoned fine- to medium-grained plagioclase-quartz-perthite pegmatite. Possible products are milling-grade feldspar and scrap mica.

PEGMATITE 4

Pegmatite 4 is a poorly exposed, very irregular, discordant pegmatite that crops out in an area 50 by 80 feet. The strike is variable, averaging north, and the dip is 55° E. to vertical. The zoning consists of a thin border zone of very fine grained plagioclase (An_{10})-quartz pegmatite, a wall zone from 3 to 25 feet thick of fine- to medium-grained plagioclase (An_4)-quartz-perthite pegmatite, and a core of medium- to coarse-grained perthite-quartz-plagioclase pegmatite. The beryl in the border zone, seen only under a microscope, contains 12.95 percent BeO; beryl in the wall zone contains 13.2 to 13.4 percent BeO. Mineral measurements indicate that the wall zone contains 0.06 percent beryl. Possible products are hand-cobbed perthite from the core, and feldspar and scrap mica of milling grade.

PEGMATITE 5

Pegmatite 5 is discordant, poorly exposed, and from 1½ to 5 feet thick; it is at least 115 feet long, and strikes N. 70° W. and dips 85° SW. It consists of a wall zone of medium-grained quartz-plagioclase-muscovite pegmatite and a core of medium-grained perthite-quartz-plagioclase pegmatite; the plagioclase of the wall zone is of slightly different composition on the hanging-wall (An_4) and footwall (An_{7-8}) sides of the pegmatite. Beryl is a minor accessory mineral in the wall zone.

PEGMATITE 6

Pegmatite 6, an irregular body, is exposed in an area 2 by 35 feet. It is a discordant intrusive mass that trends N. 20° W. and dips 70° W. It consists of fine- to medium-grained perthite-muscovite-quartz pegmatite that contains small masses of very fine grained plagioclase (An_7) and quartz.

PEGMATITE 7, CHANDLER MINE

The Chandler feldspar mine is 2.9 miles S. 52° W. of the village of Raymond, near the north edge of the Raymond pegmatite district. It was opened in 1946 by the Whitehall Co., Inc., and was operated by them until September 1948. A small crushing plant was built northwest of the mine workings, and the crushed product was passed over picking belts on which feldspar and waste rock were separated. After the closing of the Chandler mine, the plant was operated on material from the McMullen prospect and the McGall mine until the company suspended operations in the Raymond region in early 1949.

The mine was studied by J. C. Olson and J. W. Adams (written communication, 1948) of the Geological Survey in October 1947 and May 1948, respectively, and part of the following description is based on their investigation.

The workings consist of an irregular opencut. The earliest development was a cut 100 feet long, 70 feet wide, and as much as 30 feet deep, which was driven northeastward into a steep hillside. Later work extended this cut southeastward for about 120 feet from the southwest end of the earlier working. It is about 50 feet wide and 20 feet deep and is nearly filled with water.

The pegmatite is irregularly fan shaped (pl. 7) causing the width of exposure to range from 50 feet at the south end to 180 feet at the north end; the north-south dimension is about 180 feet. The pegmatite is an irregular pipelike body that probably plunges 55°

to 60° W. The contact with mica-quartz schist is commonly discordant, and wide variations in strike and dip were recorded. Several thin schist septa between pegmatite lobes were partly responsible for discontinuing northeastward development of the earlier cut into the hillside.

A dike of fine-grained mafic rock cutting the pegmatite is exposed in the floor and walls of the pit. It strikes N. 60° W., dips 35° NE., and is as much as 12 feet thick. This rock weathers much more rapidly than the pegmatite or schist, and a depression has been formed along the strike of the dike. During excavation of the lower pit, 10 to 15 feet of sand and gravel were removed from this depression.

Seven internal structural units have been distinguished in the Chandler pegmatite, but only four are shown in plate 7. The border zone is too thin to map, and two intermediate zones have been mined out. The border zone is very fine grained quartz-muscovite-plagioclase pegmatite. It is a discontinuous zone, rarely more than 1 inch thick.

The wall zone consists of medium- to coarse-grained perthite-plagioclase-quartz pegmatite with accessory cleavelandite and muscovite and small quantites of black tourmaline, beryl, apatite, garnet, and columbite. The composition varies but the average is 45 percent perthite, 30 percent plagioclase, 20 percent quartz, and 5 percent accessory minerals. Plagioclase is most abundant within a few feet of the wallrock. Blocky plagioclase is predominant near the outer contact and cleavelandite predominates in the inner part of the zone. Irregular bodies of coarse-grained quartz and graphic granite form much of this zone. Small masses of altered spodumene, altered black tourmaline, and lepidolite may have been introduced after consolidation of the wall zone. The roughly tabular shape of some of the lepidolite aggregates and their crosscutting relations to sporadic large perthite crystals indicate that they formed along fractures. The wall zone, at least 30 feet thick, forms most of the exposures at the mine.

The first intermediate zone is a discontinuous unit of medium-grained muscovite-cleavelandite-quartz pegmatite that is exposed only in the southwestern part of the lower opencut. The chief accessory minerals are plagioclase and beryl, but there also are minor black tourmaline and apatite. The average composition is 45 percent muscovite, 30 percent cleavelandite, 15 percent quartz, and 10 percent accessory minerals. The zone is about 5 feet thick.

The second intermediate zone consists of fine- to medium-grained quartz-cleavelandite-muscovite pegmatite with minor accessory beryl, plagioclase, and black tourmaline. The average composition is probably 60 percent quartz, 25 percent cleavelandite, and 15 percent muscovite. Cleavelandite is interstitial to the coarser grained quartz. Muscovite occurs as flakes, small flat books, and as small hemispherical books. The zone is a discontinuous unit with a maximum exposed thickness of 30 feet.

J. W. Adams (written communication, 1947) noted a coarse-grained microcline-rich unit on the northwest and southeast sides of the core in the lower opencut. This unit, the third(?) intermediate zone, was mined out by July 1948. It reportedly consisted mainly of blocky cream-colored microcline. The extent of this unit and its exact position in the zonal sequence are unknown.

The fourth(?) intermediate zone, also mined out, is medium-grained quartz-spodumene-muscovite pegmatite recognizable only from blocks on the dump. In composition it seems to be a transitional unit between the second intermediate zone and the core. The average composition of blocks is 45 percent quartz, 35 percent spodumene and its alteration products, and 20 percent muscovite. About half of the spodumene has been altered to a silvery muscovite, and crystals in all stages of alteration have been found. The extent and position of this unit in the zonal sequence are unknown.

The core is coarse-grained, quartz-beryl-spodumene pegmatite. Its average composition, as determined from mineral measurements, is 80 percent quartz, 10 percent anhedral pink beryl, 5 percent altered spodumene, 3 percent lepidolite, 1.5 percent phosphates, and 0.5 percent columbite. The core is exposed for 50 feet along the southwest wall of the lower opencut. Beryl is most abundant in the central and higher parts of the core, and altered spodumene is mostly in the outer and lower parts. Lepidolite is most common at the edge of the beryl-rich part of the core.

Beryl is present in each of the pegmatite units shown on plate 7. Mineral measurements indicate that the grade of the wall zone is 0.85 percent. The composition of this beryl ranges from 12.6 to 13.0 percent BeO, and most of the specimens are near the higher end of the range. It is light green to white and is too small to be recovered by hand-cobbing.

Beryl occurs in large crystals in the first and second intermediate zones. Much of the beryl is in skeletal crystals with roughly concentric layers of light-yellow-green beryl, quartz, and cleavelandite parallel to the crystal outlines. Although about 50 percent of the beryl could be recovered by hand cobbing, the BeO content of the concentrate would be reduced by the impurities in the shells. The average content of beryl in these zones is 0.62 percent, but the grade ranges from

10 percent in certain areas of the first intermediate zone to 0.5 percent in the second intermediate zone. The average BeO content is about 12.5 percent, somewhat lower than that of beryl from the wall zone.

The richest beryl reserves are in the core. Mineral measurements show that the grade is 9.6 percent, nearly all of which could be recovered by hand-cobbing. Pink anhedral masses of beryl, as much as 11 by 18 inches in size, are surrounded by quartz. The BeO content of this beryl is lower than that in the wall or intermediate zones, ranging from 12.3 to 12.5 percent, thus indicating an increase in the alkali content from zone to zone toward the center of the pegmatite.

Reserves of potassic feldspar at the Chandler mine are only in the wall zone. Although most of the production of hand-cobbed feldspar was from the microcline-rich intermediate unit, this unit was completely mined out, and there are no indications that similar material is at depth. Perthite was recovered from the wall zone by the use of crushers and picking belts for several months prior to September 1948 when the mine was closed. The average perthite content of the wall-zone pegmatite is 45 percent, but a satisfactory recovery could be made only by milling and beneficiation.

Sodic feldspar resources are largest in the wall zone, but smaller tonnages could be recovered from pegmatite of the first and second intermediate zones which contain 30 percent and 25 percent cleavelandite, respectively. The grain size of the sodic feldspar in these units is so small (seldom greater than 2 inches in diameter) that these resources could be recovered only by milling in conjunction with the recovery of potassic feldspar.

Muscovite of scrap quality is most abundant in the first intermediate zone, where the average content is 45 percent. About 75 percent of this could be recovered by hand-cobbing. An occasional book might yield a small quantity of sheet mica, but recovery would be limited to a few pounds from each ton of crude mica. The greenish-rum muscovite in this unit is soft, badly cracked, and contains many mineral inclusions. The second intermediate zone contains 15 percent muscovite, and the wall zone contains about 2 percent; scrap mica could be recovered from these only by milling.

Columbite occurs in the core, where mineral measurements indicate the average content is 0.65 percent. The irregular masses are as much as 3 by 5 inches, and most could be recovered by hand-cobbing. Small plates of columbite occur with beryl in the wall zone but could be recovered only by milling; the grade is estimated to be less than 0.001 percent.

Spodumene occurred in the fourth intermediate zone, which is now mined out; the only spodumene remaining is in the greatly altered crystals forming about 5 percent of the core. These are as much as 2 feet long, 8 inches wide, and 3 inches thick. Color ranges from white to lilac to olive green.

Lepidolite occurs in very fine grained irregular aggregates that are purple, gray, or green. It constitutes 3 percent of the core, about half of which could be recovered by hand-cobbing.

PEGMATITE 8

Pegmatite 8 is a discordant, 8- to 12-inch-thick body that is exposed for only 5 feet. It strikes N. 60° W. and dips 80° NE. It is a quartz-muscovite-beryl pegmatite containing accessory plagioclase. The beryl contains 13.2 percent BeO.

PEGMATITES 9 AND 10, SMITH NO. 1 MINE

The Smith No. 1 feldspar mine (pl. 8) is 2.95 miles S. 47° W. of the village of Raymond. The pegmatite was prospected by Cyrus G. Smith of Raymond in 1942, but the major operations for feldspar were begun by the Whitehall Co., Inc., in 1946 and continued into 1947.

The main opencut in pegmatite 10 is 120 feet long, as much as 40 feet wide, and probably about 40 feet deep. A small prospect pit 50 feet southwest of the main opencut is 20 feet long, 10 feet wide, and 5 feet deep. At the southwest end of the pegmatite, an opencut has been driven 50 feet northeastward; it is 20 feet wide and as much as 10 feet deep. This was to have been developed into an incline extending to the bottom of the main cut, but was not completed. An opencut 20 feet wide, 25 feet long, and 10 feet deep, and a small prospect pit were opened in pegmatite 9,200 feet west of the main cut.

Pegmatite 9 is at least 100 feet long and from 10 to at least 50 feet wide. The contact is exposed at only two places, where the strike is N. 5° W. and N. 40° E. However, the general trend of the exposures is almost east, discordant to the wallrock. The dip is 55° to 60° W. and the plunge of a roll on the contact is 40° N. 30° W. This pegmatite has no known connection with pegmatite 10.

Pegmatite 10, the main pegmatite, is 270 feet long and as much as 50 feet thick. It pinches out in the southwest opencut and apparently also pinches out a few feet beyond the northeasternmost exposure. It is concordant and strikes N. 40° E. The dip was measured as 55° SE. at the southwest end, and 75° NW. along the northwest wall of the opencut, and it continues to steepen to the north. The average dip is probably about 75° NW. The plunge of the pegmatite probably is to the northeast, parallel to a roll in the contact that plunges 65° N. 25° E. The bottom, or keel, of the pegmatite lens is exposed in the southwest opencut. The outcrop northeast of the main cut has one large schist septum that extends nearly across the pegmatite; this may be a roof pendant near the crest of the lens.

A fault of small but unknown displacement is exposed along the southeast wall of the main opencut and continues as far as the southwest end of the pegmatite. It strikes N. 40° E., dips 75° SE.

Six zones have been mapped, and there may be additional unexposed units. The sequence of the exposed units in the pegmatite is obscure because the relations were not distinguishable when they were mapped. The only evidence of fracture-controlled replacement units is the presence on the dump of specimens showing very fine grained lepidolite aggregates similar to those at the Chandler mine. The border zone consists of very fine grained quartz-muscovite-plagioclase pegmatite. It is commonly less than one-half inch thick, therefore it is not shown on plate 8.

The wall zone is fine- to medium-grained plagioclase-quartz-perthite-muscovite pegmatite. The average composition is 45 percent plagioclase, 35 percent quartz, 10 percent perthite, and 10 percent muscovite. Black tourmaline, garnet, apatite, and beryl are minor accessory minerals. It is a discontinuous unit exposed only along the southeast contact of the main pegmatite, where it is as much as 4 feet thick.

The first intermediate zone consists of medium- to coarse-grained perthite-quartz-plagioclase pegmatite. The average composition is 50 percent perthite, 25 percent quartz, and 25 percent plagioclase. Black tourmaline, garnet, apatite, and muscovite are accessory minerals. Perthite crystals as large as 1 by 2 feet are separated by a medium-grained matrix of quartz and plagioclase. This unit is exposed only at the ends of pegmatite 10, and it is the only mappable unit in pegmatite 9.

A medium-grained unit of plagioclase-quartz-perthite pegmatite, probably the second intermediate zone, is exposed along the northwest wall of the large opencut and extends for a short distance southwest of the cut. The average composition is 40 percent plagioclase, 35 percent quartz, and 25 percent perthite. Muscovite is an accessory mineral, and garnet and apatite are minor accessory minerals. In most exposures, the unit is in contact with the wallrock.

Medium-grained plagioclase-quartz-muscovite pegmatite, probably the third intermediate zone, is exposed in the northwest wall of the opencut, where it is 2 to 4 feet thick. The average composition is 60 percent plagioclase, 35 percent quartz, and 5 percent muscovite. Garnet and apatite are minor accessory minerals.

A unit that seems to be the fourth intermediate zone in the sequence consists of medium- to coarse-grained quartz-perthite-biotite-muscovite pegmatite. The average composition is 50 percent quartz, 30 percent perthite, 10 percent biotite, and 10 percent muscovite. Black tourmaline is an accessory mineral and garnet and columbite are minor accessory minerals. This unit is exposed only at the ends and southeast side of the main opencut, although it is reported by the operator to have formed a hood over the perthite-quartz pegmatite of the core. The hood extended somewhat farther downdip on the southeast side than on the northwest side of the core. On the southeast wall it is between the core and the wall zone, but its relative position to other units on the northwest wall is unknown.

The core is coarse-grained quartz-perthite pegmatite. Most exposures were inaccessible, but the average composition seemed to be about 65 percent perthite and 35 percent quartz. Muscovite, plagioclase, and tiny flakes of autunite and torbernite are accessory minerals. Columbite and beryl may have been recovered from this unit.

The only visible beryl is in the wall and border zones; the grade of the entire pegmatite is probably less than 0.002 percent. Most of the production was probably from the core, where the percentage recovered by hand-cobbing must have been high, as indicated by the absence of fragments or small crystals on the dumps.

The major source of potassic feldspar at the Smith No. 1 mine has been perthite from the core, where recovery was by hand-cobbing. Most exposures of this unit are no longer accessible, but men who worked at the mine stated that potassic feldspar was abundant in the floor of the opencut. Perthite in the vicinity of the fault is stained by iron oxides, but, as plate 8, section *A–A′* shows, the fault dips southward out of the core. Small resources of perthite are present in all other units except the third intermediate zone, but recovery could be only by milling. The common impurities are the iron-bearing minerals that are most abundant in the fourth intermediate zone, which probably does not extend below the level of the present workings.

Sodic feldspar would be recovered with the potassic feldspar in any milling operation using present methods of recovery. The intermediate and wall zones of pegmatites 9 and 10 have the largest resources, but none of these units contains hand-cobbable sodic feldspar.

Muscovite, although present in all units, is abundant only in the wall zone and the third and fourth intermediate zones. About one-half of the mica might be recovered by hand-cobbing, but the remainder could be obtained only by milling. The muscovite is almost entirely of scrap quality.

Small crystals of columbite are scattered throughout quartz-rich portions of the biotite-bearing hood, and larger crystals may have been recovered from the core. The grade of the entire pegmatite is only a fraction of a pound per ton.

PEGMATITE 11

Pegmatite 11, a concordant quartz-rich pegmatite 6 feet thick, is exposed for 25 feet N. 80° E. along its strike. It dips 80° N. to vertical. It contains schist inclusions and scattered small biotite flakes where schist has been reworked. Perthite is a minor accessory mineral.

PEGMATITE 12

Pegmatite 12 is an irregular, generally discordant pegmatite 100 feet long and from 5 to 10 feet thick. It strikes from west to northwest and dips 75° to 80° S. to SW. The deposit consists of a poorly developed wall zone of fine- to medium-grained quartz-perthite-plagioclase pegmatite surrounding a core of medium-grained perthite-quartz pegmatite containing some graphic granite.

PEGMATITE 13

Pegmatite 13 is exposed over an area of 15 by 60 feet, and trends N. 70° W. It is a discordant body consisting of medium- to coarse-grained pegmatite containing virtually no exposed quartz and less than 1 percent muscovite. Perthite is the predominant mineral. Garnet is a minor accessory mineral. Potassic feldspar could be recovered by hand-cobbing. Further exploration should be done to determine the size of this pegmatite and the extent of the feldspar-rich unit.

PEGMATITE 14

Pegmatite 14 is a small body that crops out in an area 20 by 40 feet. No contacts were visible, but the outcrop trends N. 50° W. and seems to be discordant. A small prospect pit for feldspar is 5 by 15 feet. The pegmatite has a wall zone of fine- to medium-grained plagioclase-quartz-perthite pegmatite and a core of medium- to coarse-grained perthite-quartz pegmatite. Possible products are milling-grade feldspar and a small quantity of potassic feldspar recoverable by hand-cobbing.

PEGMATITE 15

Pegmatite 15 is exposed in an outcrop as much as 20 feet wide and 125 feet long, and trends N. 65° W. No contacts are visible, but it seems to be discordant. It is an unzoned fine- to medium-grained quartz-perthite-plagioclase pegmatite with accessory muscovite. Possible products are milling-grade feldspar and scrap mica.

PEGMATITE 16

Pegmatite 16 is poorly exposed in an area 50 by 350 feet. It appears to strike approximately northwest, but the dip is unknown. It is a discordant unzoned body consisting of fine- to medium-grained plagioclase-quartz-perthite pegmatite containing accessory muscovite, garnet, and black tourmaline. Possible products are milling-grade feldspar and scrap mica.

PEGMATITE 17, GUINEA PROSPECTS

The Guinea prospects are three small pits near the northwest end of a large discordant unzoned pegmatite. Its maximum exposed length is about 1,100 feet, and its width is as much as 200 feet. It forks at the southeast end. The average strike is N. 30° W., but the dip is unknown. The body consists of fine- to medium-grained perthite-quartz-plagioclase pegmatite with muscovite and minor quantities of black tourmaline, garnet, biotite, beryl, and columbite. Two small beryl crystals each contain 12.7 percent BeO. Most columbite plates are less than 1 inch across. Possible products are milling-grade feldspar and scrap mica.

PEGMATITE 18

Pegmatite 18 is exposed in the road bounding the east edge of the district. The length is unknown and the width is 5 to 8 feet. It is probably concordant, striking about N. 40° E. and dipping almost vertically. Zones are poorly developed. They include a wall zone of fine- to medium-grained plagioclase-perthite-quartz pegmatite, a thin intermediate zone of perthite-quartz pegmatite, and quartz pods representing segments of the core. A beryl crystal from the core contains 13.1 percent BeO. The beryl content of the entire pegmatite is 0.14 percent.

PEGMATITE 19

Pegmatite 19 is a poorly exposed discordant pegmatite, probably less than 20 feet thick, that trends N. 55° W. for at least 190 feet. The dip is unknown. Although poorly zoned, it contains a wall zone of fine- to medium-grained plagioclase-perthite-quartz pegmatite and a core of quartz-perthite-plagioclase pegmatite. A fracture-controlled unit about 1 foot thick, striking N. 70° W., contains quartz and accessory muscovite. Beryl (13.1 percent BeO) is a minor accessory mineral in the core and in the fracture-controlled body. The beryl content of the entire pegmatite is 0.015 percent. Possible products are milling-grade feldspar and scrap mica.

PEGMATITE 20

Pegmatite 20 consists of three poorly exposed stringers ranging from 6 inches to 4 feet in thickness that crop out for less than 5 feet along their strikes. Two strike N. 60° W. and the other strikes N. 60° E.; the dips are vertical. The bodies consist of unzoned fine-grained plagioclase-quartz-perthite pegmatite.

PEGMATITE 21

Pegmatite 21, a concordant pegmatite 2 to 3 feet thick, is exposed for 15 feet along its strike, N. 70° E. It contains a wall zone of fine-grained plagioclase-quartz pegmatite and a core of fine- to medium-grained perthite-quartz-plagioclase pegmatite.

PEGMATITE 22

Pegmatite 22 is a concordant pegmatite 1½ feet thick and 20 feet long that strikes N. 60° E. It consists of a thin border zone of very fine grained quartz-muscovite-plagioclase pegmatite and a core of fine- to medium-grained quartz-perthite pegmatite.

PEGMATITE 23

Pegmatite 23 is a curved, discordant pegmatite 65 feet long and 20 feet wide. It strikes about N. 70° W.; but the dip is unknown. The pegmatite consists of a wall zone of fine- to medium-grained quartz-plagioclase pegmatite and a core of medium-grained quartz-plagioclase (An_{1-8})-muscovite pegmatite. Perthite is an accessory mineral in both zones, and muscovite is an accessory mineral in the wall zone. Beryl (13.0 percent BeO) and columbite are minor accessory minerals in the core. The beryl content of the core is 0.6 percent. Possible products are milling-grade feldspar and scrap mica.

PEGMATITE 24

Pegmatite 24, a small, unzoned, discordant body, is 10 feet long and 3 feet thick. It strikes N. 80° E., and the dip is vertical. It consists of plagioclase-quartz pegmatite, but also contains 15 percent of aplitic quartz-plagioclase (An_{9-10}) aggregates scattered irregularly throughout the exposure.

PEGMATITE 25

Pegmatite 25 is represented by blocks and outcrops in an area 125 feet long and as much as 50 feet on the crest and sides of a low ridge. No contacts were seen, but the trend of the exposures is N. 60° W., and the pegmatite probably is discordant. Two units are present: medium- to coarse-grained perthite-quartz pegmatite and fine- to medium-grained perthite-quartz-plagioclase pegmatite containing small irregular masses of very fine grained aplitic material. Muscovite, beryl (13.1 percent BeO), and columbite are minor accessory minerals in the coarser grained unit. Muscovite, biotite, and beryl (13.0 percent BeO) are accessory minerals in the finer grained unit. Plagioclase (An_{2-8}) is an accessory mineral in the coarser unit. The beryl content of the entire pegmatite is 0.008 percent. Possible products are milling-grade feldspar and scrap mica.

PEGMATITE 26

Pegmatite 26 is discordant, 25 feet thick, and at least 130 feet long; it strikes N. 40° W. and dips 60° SW. It consists of a wall zone of fine- to medium-grained quartz-perthite-plagioclase pegmatite and segments of a discontinuous core of quartz-perthite-muscovite pegmatite containing accessory beryl (12.8 percent BeO). The beryl content of the entire pegmatite is 0.05 percent. Possible products are feldspar, scrap mica, and beryl of milling grade. A small quantity of sheet mica could be recovered from the core.

PEGMATITE 27

Pegmatite 27 is an irregular body exposed on the face of a cliff. It is about 50 feet long and 2 to 4 feet thick and is concordant with bedding that strikes N. 45° W. and dips 45° NE. It is near the crest of a small anticline that plunges eastward at about 40°. It is an unzoned body that consists of irregular masses of quartz and medium-grained intergrowths of quartz and perthite. A few radiating groups of elongate black crystals of allanite(?) are in the quartz-perthite aggregates.

PEGMATITE 28

Pegmatite 28, also an irregular body, is exposed on a steep hillside. It strikes about N. 65° W., dips 40° NE., and has a maximum exposed thickness of 20 feet. It is concordant to the structure of the contorted wallrock. It is an unzoned body of fine- to medium-grained plagioclase-perthite-quartz pegmatite. Irregular patches of very fine grained aplitic material are exposed near the base of the hill. Garnet and white beryl (13.0 percent BeO) are minor accessory minerals in and adjacent to the aplitic aggregates.

PEGMATITE 29

Pegmatite 29 is an outcrop or large boulder 10 by 25 feet in size that is in the floor of the stream valley below pegmatites 27 and 28. No contacts are exposed. It consists chiefly of plagioclase-perthite-quartz pegmatite with accessory muscovite. A fracture-controlled quartz body 6 to 8 inches thick strikes N. 35° W. and dips 40° NE. Beryl (13.0 percent BeO) is a minor accessory mineral of this unit.

PEGMATITE 30

Pegmatite 30 is 5 to 15 feet wide and crops out almost continuously for 200 feet N. 35° W. No contacts are exposed, but the trend is discordant to foliation in the nearest wallrock exposures. Several schist inclusions are present. It is an unzoned body of fine- to medium-grained plagioclase-quartz-perthite pegmatite containing minor accessory muscovite. Possible products are milling-grade feldspar and scrap mica.

PEGMATITE 31

Pegmatite 31 is a concordant body at least 20 feet long and as much as 8 feet wide. It strikes N. 45° E. and dips steeply northwestward. The pegmatite consists of a thin border zone of very fine grained perthite-quartz-muscovite pegmatite, a wall zone of the same composition but fine to medium grained, and a core of coarse-grained perthite-quartz pegmatite. Beryl (13.1 percent BeO) is a minor accessory mineral in the wall zone.

PEGMATITE 32

Pegmatite 32 has been stripped for a length of at least 45 feet, and a width of 8 feet. It is discordant; no contacts were seen, but the trend of exposures is N. 5° E. Poorly developed units include a wall zone of fine-grained quartz-plagioclase-muscovite pegmatite and a core of medium-grained quartz-perthite pegmatite. Beryl (13.1 to 13.5 percent BeO) is a minor accessory mineral in the core and wall zone.

PEGMATITE 33

Pegmatite 33 is discordant, unzoned, at least 125 feet long, and as much at 25 feet thick. It strikes N. 65° W. and dips steeply southwestward. The rock is medium- to coarse-grained quartz-perthite-plagioclase pegmatite containing muscovite and minor quantities of beryl. Possible products are milling-grade feldspar and scrap mica.

PEGMATITE 34

Pegmatite 34, a very small irregular discordant body, is 2 feet long and 6 inches thick. It strikes east, dips 70° N., and consists principally of white perthite.

PEGMATITE 35

Pegmatite 35 is a discordant body 25 feet thick, exposed for 20 feet N. 45° W. along its strike. It dips steeply northeastward. There is no apparent zoning although graphic granite is abundant for 8 feet inward from the footwall; otherwise the body is quartz-perthite-muscovite pegmatite. Beryl and garnet are minor accessory minerals.

PEGMATITE 36

Pegmatite 36 is represented by boulders and small outcrops trending N. 65° W. for 100 feet. No contacts were seen, but the pegmatite probably is discordant. It is an unzoned fine- to medium-grained quartz-perthite-plagioclase pegmatite with accessory muscovite. Possible products are milling-grade feldspar and scrap mica.

PEGMATITE 37

Pegmatite 37 is 3.15 miles S. 44° W. of Raymond village. Although it never has been mined, the Whitehall Co., Inc., stripped part of the overburden in 1947 while prospecting for feldspar in the Raymond district.

As mapped, the pegmatite is roughly rectangular (pl. 9). It is about 350 feet long and has an average width of 170 feet. Contacts with quartz-mica schist are very poorly exposed at two places. Near the northwest corner of the pegmatite, the strike is north, and the dip ranges from 25° to 60° E. The pegmatite seems to be concordant on the northwest and southeast sides and discordant elsewhere. Although pegmatite 38 is only 25 feet from the southeast corner of pegmatite 37, there is no evidence that the two are connected. A plunge of 15° to 20° NE. is suggested by the structure of the intermediate zone around the core and by the direction and angle of plunge of minor folds in the wallrock.

The pegmatite is poorly exposed except in those places where the overburden has recently been removed during prospecting. Four units, of which three have been mapped (pl. 9) can be distinguished in these exposures. Possibly the present land surface truncates only the upper part of outer units of the pegmatite, and more zones are present at depth. The border zone is very fine grained quartz-muscovite-plagioclase pegmatite present at the few places where the contact is exposed. It is about one-half inch thick, and thus cannot be shown on plate 9.

The wall zone consists of fine- to medium-grained plagioclase-quartz-perthite pegmatite with accessory muscovite, garnet, and minor accessory apatite and biotite. The average composition is 40 percent plagioclase, 30 percent quartz, 25 percent perthite, and 5 percent accessory minerals. Plagioclase and quartz-muscovite intergrowths form a matrix for the coarser grained perthite crystals. The average thickness of the zone is unknown. The broad areas of wall zone shown on plate 9 may be a thin cover above inner zones.

The intermediate zone is a discontinuous unit of fine- to medium-grained quartz-perthite-plagioclase pegmatite exposed around the northeast end of the core. This unit is less than 10 feet thick and pinches out southwestward. The average composition is 40 percent quartz, 30 percent perthite, 25 percent plagioclase, and 5 percent accessory minerals. It contains the same accessory minerals as the wall zone, and in addition, beryl. Mineral measurements indicate a beryl content of 0.04 percent, but beryl is more abundant immediately adjacent to the core.

The core is medium- to coarse-grained perthite-quartz-plagioclase pegmatite in which graphic granite is abundant, especially in the exposure near the northwest corner of the pegmatite. The average composition is 55 percent perthite, 30 percent quartz, 10 percent plagioclase, and 5 percent accessory minerals. The accessory minerals are muscovite, garnet, cleavelandite, and beryl. The beryl consisted of one crystal, found near the intermediate zone. The exposures of the core shown on plate 9 are probably parts of a single unit that has been only partly uncovered by erosion. The core may be nearer the footwall than the hanging wall.

Beryl occurs as small crystals in the intermediate zone, and is most abundant adjacent to the core. Mineral measurements show that the grade of this zone is 0.04 percent, but these crystals are too small to recover by hand-cobbing. One crystal 5 by 7 inches is in the core adjacent to the intermediate zone.

Pegmatite 37 is one of the few in the Raymond district that offers possibilities for the recovery of potassic feldspar by hand-cobbing. Coarse-grained perthite in the core is associated with only minor amounts of garnet and graphic quartz. The entire pegmatite has a composition and size that would make it a logical source of millfeed if a mill were established in the area.

Plagioclase is most abundant in the wall zone, and would be recoverable only with perthite through milling that would separate feldspar from the other minerals.

Muscovite is most abundant in the wall and intermediate zones, although it is also an accessory mineral in the core. Almost all books are less than 1 inch in diameter, and could be recovered only by milling methods. All the mica is of scrap quality.

PEGMATITE 38

Pegmatite 38 is represented by outcrops and blocks extending N. 30° W. for 750 feet. The pegmatite is at least 60 feet thick, and dips 45° NE.; it is generally concordant. The rock is fine- to medium-grained quartz-perthite-plagioclase pegmatite containing accessory muscovite. Possible products are milling-grade feldspar and scrap mica.

PEGMATITE 39

Pegmatite 39 is a generally concordant unzoned body 50 feet thick and 150 feet long that strikes N. 40° W. and probably dips northeastward. It has fine- to medium-grained quartz-perthite-plagioclase pegmatite with accessory muscovite, as well as minor amounts of beryl and garnet. The beryl content of the entire pegmatite is 0.0035 percent. Crystals associated with irregular quartz bodies contain 12.8 to 12.85 percent BeO; other crystals contain 13.0 to 13.2 percent BeO. Possible products are milling-grade feldspar and scrap mica.

PEGMATITE 40

Pegmatite 40 is marked by outcrops and blocks, extending N. 20° W. for 800 feet, that are probably parts of a single discordant body. The maximum width is less than 100 feet. The dip ranges from 70° NE. near the northwest end to 10° E. near the center of the pegmatite. The rock is fine- to medium-grained quartz-plagioclase-perthite pegmatite containing accessory muscovite. Green (12.9 percent BeO) and white (13.1 to 13.2 percent BeO) beryl are minor accessory minerals. The beryl content of the entire pegmatite is approximately 0.0006 percent. Possible products are milling-grade feldspar and scrap mica.

PEGMATITE 41

Pegmatite 41 is represented by boulders and small outcrops extending 35 feet N. 35° W. The pegmatite probably is discordant, and dips northeastward at a low angle. It has fine- to medium-grained plagioclase-quartz-muscovite pegmatite that is cut by fracture-controlled quartz bodies 2 inches thick.

PEGMATITE 42

Pegmatite 42 is a discordant pegmatite 700 feet long and as much as 100 feet thick; it has a strike ranging from almost north at the southeast end to northwest at the northwest end. The average dip is 80° SW. Two small feldspar prospect pits were opened by the Whitehall Co., Inc., in the bulbous northwest end. The zones, observed only near the pits, include a wall zone, 5 to 15 feet thick, of fine- to medium-grained plagioclase-quartz-perthite pegmatite that thickens to the southeast until it is the only unit present; an intermediate zone, 6 to 25 feet thick, of medium-grained plagioclase-perthite-quartz-muscovite and biotite pegmatite present only along the footwall side; a core-margin zone, 2 to 3 feet thick, of medium-grained plagioclase-quartz-perthite-muscovite pegmatite intermittently exposed between the first intermediate zone and the core; and a core of perthite-quartz-plagioclase pegmatite. Small parts of the core contain graphic granite. Muscovite occurs in all units. Beryl is a minor accessory mineral in the first intermediate zone, which has a beryl content of 0.06 percent. A specimen of stained beryl from this unit contains 12.9 percent BeO, and another of fresh green beryl contains 13.1

percent BeO. Near the prospect pits, possible products are hand-cobbed perthite and mica of milling grade.

PEGMATITE 43

Pegmatite 43 is at a locality that contains two concordant pegmatites 5 to 6 inches thick exposed for 8 to 12 feet N. 65° E. along their strike. Both are fine grained. One is an unzoned quartz-plagioclase-muscovite pegmatite with accessory beryl (13.9 percent BeO); the other has a 2-inch zone of perthite and quartz along the footwall, a 2-inch core of quartz-muscovite pegmatite, and a 2-inch zone of quartz-muscovite-plagioclase pegmatite along the hanging wall.

PEGMATITE 44

Pegmatite 44 is concordant, 375 feet long, and is exposed over a width of 25 feet. The pegmatite strikes N. 60° E. and dips 35° NW. It consists of a wall zone of fine- to medium-grained quartz-perthite-plagioclase pegmatite and a core of medium-grained material of similar composition. Muscovite is an accessory mineral in both units, and beryl (11.6 percent BeO) is a minor accessory mineral in the wall zone. A small prospect pit was opened by the Whitehall Co., Inc. Possible products are milling-grade feldspar and scrap mica.

PEGMATITE 45, SMITH NO. 2 PROSPECT

Pegmatite 45 is a discordant body that crops out intermittently for 1,200 feet along a trend of N. 60° W. Although the contacts are poorly exposed, the maximum thickness probably is about 75 feet. The dip is 80° SW. Two small prospect pits were opened for feldspar near the northwest end by the Whitehall Co., Inc. In these pits the pegmatite consists of a wall zone of fine- to medium-grained quartz-plagioclase-perthite-muscovite pegmatite with minor accessory beryl (11.6 percent BeO), and a core of perthite-cleavelandite-muscovite pegmatite with accessory garnet and pyrite. The core locally extends to the wall of the pegmatite. Zoning is not distinguishable southeast of the pits, where the pegmatite consists of quartz, perthite, and plagioclase. Possible products are hand-cobbed perthite containing pyrite and garnet impurities, and feldspar and scrap mica of milling grade.

PEGMATITE 46

Pegmatite 46 is marked by scattered pegmatite blocks and outcrops extending 130 feet N. 5° W. The exposure ranges from 5 to 25 feet in width, and the dip is unknown. This is a discordant pegmatite consisting of 2 units of about equal size; 1 contains fine- to medium-grained quartz-plagioclase-perthite pegmatite and the other contains medium-grained perthite-quartz pegmatite. Either of the two units may be adjacent to wallrock. Accessory minerals include muscovite, minor amounts of beryl (13.0 percent BeO), and black tourmaline. Albite (An_{8-10}) is an accessory mineral in perthite-quartz pegmatite. The beryl content of the quartz-plagioclase-perthite pegmatite is 0.038 percent. Possible products are milling-grade feldspar and scrap mica.

PEGMATITE 47

Pegmatite 47 is represented by scattered blocks and outcrops extending 125 feet N. 40° E. The maximum exposed width is 4 feet. No contacts were seen, but the pegmatite seems to be concordant. It contains a wall zone, 1 foot thick, of fine-grained quartz-muscovite-plagioclase pegmatite and an inner unit of perthite-plagioclase (An_{2-4})-quartz pegmatite. White beryl (13.2 percent BeO) is a minor accessory mineral in the wall zone.

PEGMATITE 48

Pegmatite 48 crops out in the road, strikes N. 65° E., dips 80° SE., and is concordant. It is 3 feet thick and at least 25 feet long. It contains a 2-inch border zone of very fine grained plagioclase-quartz-muscovite pegmatite, a wall zone of fine-grained quartz-plagioclase-muscovite pegmatite, and a core of very fine grained sugary-textured plagioclase (An_8)-quartz pegmatite. There are streaks of very fine grained garnet in the sugary-textured rock. Beryl (13.4 percent BeO) is a minor accessory mineral in the wall zone.

PEGMATITE 49, SMITH NO. 3 PROSPECT

The Smith No. 3 feldspar prospect is 3.3 miles S. 50° W. of Raymond village. In 1947, the Whitehall Co., Inc. removed the overburden from the pegmatite and opened a small prospect pit to test for feldspar.

The pegmatite consists of three connected podlike bodies (pl. 10) that trend eastward for 200 feet. These irregular bodies range in size from about 20 by 50 to 50 by 50 feet. At the northwest corner, tabular apophyses extend northeastward and southwestward. The southwest apophysis, ranging from 1½ to 5 feet in thickness, can be traced for at least 120 feet S. 70° W. The northeast apophysis shown on plate 10 extends for 170 feet N. 55° E. and can be traced for an additional 350 feet N. 70° E. There is no evidence that these tabular bodies are of different age than the main pegmatite, and they seem to have been injected along bedding planes of the wallrock at the same time that the generally discordant main pegmatite was injected. The apophyses dip steeply southeastward; the contacts of the main pegmatite dip either vertically or steeply away from the center, indicating enlargement of the pegmatite at depth.

A thin border zone, a wall zone, and a discontinuous core can be distinguished in this pegmatite. The border zone consists of very fine grained quartz-muscovite-plagioclase pegmatite. The maximum thickness is 12 inches, but it commonly is less than 1 inch thick, and thus is too thin to be shown on plate 10.

The wall zone is fine-grained plagioclase-quartz-perthite pegmatite. The average composition of this unit is 55 percent plagioclase, 30 percent quartz, 10 percent perthite, and 5 percent accessory minerals including muscovite, garnet, biotite, and beryl.

The core is medium- to coarse-grained perthite-quartz-plagioclase pegmatite. Cleavelandite and muscovite are accessory minerals; garnet and beryl are minor accessory minerals. Small masses of cleavelandite-quartz-muscovite-perthite pegmatite occurs in the unit, but these are probably local variations in the composition of the core rather than a separate unit. Fine-grained graphic granite is particularly abundant in the eastern part of the main body of pegmatite.

Mineral measurements indicate that the beryl content of the entire pegmatite is about 0.0036 percent. Most of the crystals are too small to be recovered by hand-cobbing.

Perhaps 30 percent of the perthite in the core could be recovered by hand-cobbing, but the only economically important production would come through milling the entire pegmatite. Plagioclase, because of its small grain size, could be recovered only by mechanical means, and in most present-day processes would be recovered with the perthite. The small size of the pegmatite does not favor its use as millfeed except in combination with other pegmatites in the area.

No muscovite of sheet quality was observed. Scrap mica forms only about 2 percent of the entire pegmatite.

PEGMATITE 50

Pegmatite 50 is discordant, 4 feet thick, and exposed for 20 feet along its strike of N. 40° W.; it dips 80° SW. It consists of a hanging-wall unit of fine-grained plagioclase-quartz-muscovite pegmatite, a core of coarse-grained quartz-perthite pegmatite, and a footwall unit of fine-grained plagioclase-quartz-perthite pegmatite. Muscovite is an accessory mineral, and beryl is a minor accessory mineral in all units. Beryl from the hanging-wall unit contains 13.4 percent BeO.

PEGMATITE 51

Pegmatite 51 is represented by scattered pegmatite blocks extending 80 feet N. 50° W.; there are no definite outcrops. The thickness and dip are unknown, but the pegmatite is probably discordant. Possible zones consist of a thin border unit of very fine grained muscovite-quartz-plagioclase pegmatite and a core of fine-grained quartz-plagioclase pegmatite containing accessory muscovite and perthite. Beryl (13.4 percent BeO) is a minor accessory mineral in both units; the beryl content of the entire pegmatite is 0.02 percent.

PEGMATITE 52

Pegmatite 52 is a large poorly exposed concordant pegmatite 1,000 feet long and possibly 200 feet thick. The average strike is about N. 60° E., but the dip is unknown. The pegmatite is poorly zoned, and consists mostly of fine- to medium-grained quartz, plagioclase, and perthite, although there are small masses of coarse-grained perthite and quartz. Muscovite is an accessory mineral in the finer grained unit, and columbite is a minor accessory mineral of the coarser grained unit. Possible products are hand-cobbable perthite, and feldspar and scrap mica of milling grade.

PEGMATITE 53

Pegmatite 53 crops out along a trend of N. 70° E. No contacts were exposed, but its dimensions may be as much as 400 feet by 100 feet. The dip is unknown, and the trend of the pegmatite suggests that it is probably concordant. It consists of quartz-plagioclase-perthite pegmatite with accessory muscovite. The plagioclase is partly cleavelandite (An_{0-2}).

PEGMATITE 54

Pegmatite 54, a discordant pegmatite at least 60 feet long and 20 feet thick, strikes N. 15° E. and dips 75° E. It consists of a wall zone of fine- to medium-grained plagioclase-quartz-perthite pegmatite and a thin core, 3 to 7 feet thick, of medium- to coarse-grained perthite-quartz pegmatite. Muscovite and beryl are accessory minerals. A fracture-controlled body 4 inches thick cuts the wall zone. This body contains quartz, muscovite, beryl, and minor amounts of plagioclase (An_{1-2}). The beryl content of the entire pegmatite is 0.02 percent. The beryl in the wall zone has 13.2 percent BeO; that in the fracture-controlled body contains 13.1 percent BeO. Possible products are milling-grade feldspar and scrap mica.

PEGMATITE 55

The trend of pegmatite 55 is indicated by outcrops and blocks extending N. 40° W. for 100 feet. The pegmatite is discordant and unzoned. The width of exposure ranges from 2 to 20 feet, and the dip of the pegmatite is 80° NE. The rock is fine- to medium-grained quartz-plagioclase (An_{5-6})-perthite pegmatite with accessory muscovite and beryl. Beryl (13.0 percent BeO) content of the entire pegmatite is 0.135 percent. Possible products are milling-grade feldspar and scrap mica.

PEGMATITE 68, BLAKE (MAFERA) MINE

The Blake feldspar mine (pl. 11) is 3.6 miles S. 49° W. of Raymond village. It was opened in 1945 and was operated by the Whitehall Co., Inc., until 1947 when it was closed reportedly because of litigation concerning ownership. It was worked from an opencut 100 feet long, 15 to 60 feet wide, and as much as 35 feet deep at the north end. The cut is filled with water to an average depth of 15 feet.

The pegmatite is about 130 feet long and as much as 70 feet thick. The average strike is N. 30° E., which is roughly concordant with the bedding of the enclosing mica-quartz schist, and the dip is steep to the northwest. The plunge of the pegmatite might be about 45° SW., but no accurate measurements of the angle and direction of plunge could be made. At the southwest corner of the opencut, an offshoot from the main body can be traced for 50 feet N. 70° W. It is as much as 15 feet thick.

The border zone is very fine grained quartz-muscovite pegmatite with accessory plagioclase, garnet, and beryl. This unit is not everywhere present at the contact and is nowhere more than 1 inch thick.

The wall zone is fine- to medium-grained quartz-muscovite-plagioclase pegmatite, and is exposed only at the south end of the opencut. The average composition is 40 percent quartz, 30 percent muscovite, 25 percent plagioclase, and 5 percent accessory minerals. It is 2 feet thick where exposed.

The first intermediate zone consists of fine- to medium-grained quartz-plagioclase pegmatite. In some places it is adjacent to the schist contact, and the outer two zones are absent. The average composition is 65 percent quartz, 30 percent plagioclase, and 5 percent accessory perthite and muscovite and minor accessory garnet, beryl, and apatite. The pegmatite offshoot at the southwest corner of the opencut is composed of a variety of this zone in which plagioclase is nearly as abundant as quartz, and perthite forms more than 5 percent of the rock.

The largest unit is medium- to coarse-grained perthite-quartz-plagioclase pegmatite, from which most of the perthite was mined. The average composition is 55 percent perthite, 30 percent quartz, 10 percent plagioclase, and 5 percent accessory minerals. The accessory minerals are chiefly muscovite and cleavelandite, but also include garnet and apatite. Columbite and beryl are reported to have been recovered from this unit.

The core-margin unit, or third intermediate zone, consists of medium-grained plagioclase-muscovite-quartz-perthite pegmatite. It is exposed only on the east side of a small segment of the quartz-perthite pegmatite of the core, where it is less than 2 feet thick. The average composition is 40 percent plagioclase, 30 percent muscovite, 15 percent quartz, 10 percent perthite, and 5 percent accessory minerals. About one-half the plagioclase is cleavelandite.

Small discontinuous segments of the coarse-grained quartz-perthite core are exposed. Larger segments may be in the floor of the water-filled opencut. The average composition of the core is 70 percent quartz and 30 percent perthite. Minor accessory minerals include sphalerite, chalcopyrite, covellite, and löllingite. Columbite has been reported from this unit.

Beryl is present in the first intermediate and border zones. Mineral measurements made on the east wall of the opencut indicate a beryl content of 0.148 percent in the first intermediate zone, and this is in close accord with recovery data. Four mineral measurements, however, randomly selected on the surface of the dump, indicated a beryl content of 0.37 percent. This increase was partly caused by the residual concentration of beryl in the dump material from which large tonnages of feldspar were removed, and perhaps partly by carelessness in cobbing. The largest crystal reported by the operator was 2 by 4 feet, but the average size of the crystals measured was 2 by 4 inches. With careful hand-cobbing, 75 percent of the beryl might be recovered.

The largest reserves of potassic feldspar are in the second intermediate zone and core, the same units that produced this mineral in the past. The size of perthite crystals in these units is large enough to permit the recovery of at least 60 percent by hand-cobbing.

The Blake pegmatite is one of the few in the Raymond district that could yield small amounts of sheet mica. The wall zone at the south end of the opencut contains an estimated 30 percent muscovite of which perhaps 1 percent is of sheet size and quality. The extent of this unit downdip is unknown, and it is exposed along its strike for only 15 feet. The muscovite is greenish-rum colored and clear, but most of the books are badly fractured. The largest sheets that could be trimmed from books observed in this unit were about 1½ by 2 inches. A few muscovite books from the core-margin zone also may contain small sheets of flat mica. Scrap mica could be recovered by hand-cobbing only from the wall and core-margin zones. More than a third of the total muscovite in these units could be recovered by this method. Milling of the entire pegmatite, which has an estimated muscovite content of 2 percent, would permit a much larger recovery.

Columbite was reported by workmen to have occurred throughout the pegmatite and it is probable that most was recovered from the inner units. The average size of the plates seen was 1 inch long, one-half inch wide, and one-fourth inch thick, but larger crystals have been reported by the former operator. The pegmatite is estimated to contain about one-third of a pound of columbite per ton of rock.

PEGMATITE 57, LANE PROSPECT

The Lane prospect contains two small pits opened by the Whitehall Co., Inc., for feldspar near the southeast end of a discordant pegmatite 750 feet long and as much as 50 feet thick. The average strike is N. 55° W., and the dip is 80° SW. The thicker southeast end consists of a wall zone of fine- to medium-grained plagioclase-quartz-perthite-muscovite pegmatite, a core-margin zone of medium- to coarse-grained perthite-quartz-muscovite pegmatite, and a core of quartz pegmatite. Minor accessory minerals are biotite, beryl, garnet, black tourmaline, and apatite. Northwestward from the prospect pits, the pegmatite thins and has only a wall zone of quartz-plagioclase (An_{4-5})-perthite-muscovite pegmatite ranging from 4 to 5 feet in thickness and a core of quartz-perthite pegmatite. The beryl content is 0.03 percent in the southeastern part of the pegmatite; the mineral is commonly stained and has a BeO content of 12.5 to 12.8 percent. In the northwestern part, beryl is less abundant (0.014 percent) and has a BeO content ranging from 12.8 percent in a specimen from midway between the ends of the pegmatite, to 13.2 percent in a specimen from the northwest end. Possible products are hand-cobbed perthite and milling-grade feldspar, scrap mica, and beryl.

PEGMATITE 58

Pegmatite 58, a poorly exposed body, is at least 140 feet long and 20 feet thick. It strikes N. 55° W., dips 75° SW., and is discordant. It constits of fine- to medium-grained quartz-plagioclase (An_{8-9})-perthite pegmatite. Muscovite and cleavelandite (An_{2-3}) are the chief accessory minerals; biotite, beryl (12.9–13.0 percent BeO), and garnet are minor accessory minerals. The beryl content of the entire pegmatite is 0.01 percent. Possible products are milling-grade feldspar and scrap mica.

PEGMATITE 59

Pegmatite 59, from 6 to 12 inches thick and 10 feet long, strikes N. 60° E. parallel to foliation of the wallrock. It dips steeply northwestward across the dip of the foliation. It is an unzoned quartz-plagioclase pegmatite with accessory muscovite.

PEGMATITE 60

Pegmatite 60, a concordant pegmatite from 2 to 3½ feet thick, is exposed intermittently for 40 feet along a strike of N. 65° E.; it dips 70° NW. It contains a wall zone of fine-grained muscovite-quartz-plagioclase (An_{15}) pegmatite, a core-margin zone of medium-grained plagioclase-quartz-perthite pegmatite, and a core of massive quartz. Beryl is a minor accessory mineral in the wall zone (13.1 percent BeO) and in the core-margin zone.

PEGMATITE 61

Pegmatite 61 is unzoned and small, not more than 2 feet thick. It is very irregular and both concordant and locally discordant to the foliation of the enclosing wallrock. The dip is probably vertical. It is quartz-plagioclase-perthite pegmatite with accessory muscovite and beryl.

PEGMATITE 62, WELCH MINE

The Welch feldspar mine is 3.6 miles S. 45° W. of Raymond village. It was operated intermittently from 1943 until 1947; the most recent work was done by the Whitehall Co., Inc. The overburden has been stripped from much of the pegmatite. The larger working is an opencut 100 feet long, as much as 40 feet wide and 20 feet deep, that was driven northeastward into the pegmatite. A smaller opencut was started near the northwest corner of the pegmatite.

The contact between pegmatite and wallrock is nowhere exposed, although the enclosing rocks are probably no more than a few feet beyond the pegmatite outcrops (pl. 12). The pegmatite is exposed for 320 feet N. 35° W. and has a maximum exposed width of 85 feet. The strike is probably nearly the same as the trend of the outcrops, and the dip appears to be 60° SW. The plunge of the pegmatite is unknown, but the alinement of quartz masses, probably discontinuous segments of the core, indicates a plunge of 50° S.

The southeastern half of the Welch pegmatite consists of well-developed zones; the northwestern half, however, contains only units that seem to be of replacement origin, and well-arranged zones are not present. The change between the two halves of the pegmatite is at or near the fault exposed in the opencut. The fault plane strikes N. 60° E. and dips 50° SE., and although its displacement is not known, it is not necessarily large. The fault gouge may have acted as an impermeable barrier that permitted alteration of pre-existing pegmatite northwest of the fault by later sodic-rich pegmatite solutions. If this were true, the fault must be later than the consolidation of the zoned pegmatite but earlier than the last stage of pegmatitic activity in the whole body.

In the southeast half of the pegmatite the outer unit, probably the wall zone although no contacts with wallrock were seen, is fine- to medium-grained plagioclase-quartz-perthite pegmatite. The average composition is 35 percent plagioclase, 30 percent quartz, 30 percent perthite, and 5 percent accessory minerals. Muscovite is a common accessory mineral, and garnet and beryl are minor accessory minerals. Plagioclase and quartz are finer grained than the perthite, and are interstitial to it. The unit thickens at the southeast end of the pegmatite exposure but thins northwestward.

The first intermediate zone is characterized by aggregates of very fine grained granitic material. The average composition is 30 percent perthite, 20 percent plagioclase, 15 percent quartz, 30 percent granitic material, and 5 percent accessory minerals. Muscovite and cleavelandite are the chief accessory minerals, and garnet, apatite, and beryl are minor accessory minerals. Graphic granite is more abundant in this unit than elsewhere in the pegmatite.

Pods of granitic materials, consisting of plagioclase, quartz, perthite, and minor muscovite and garnet, are scattered at random throughout the zone. Grains are commonly less than one-quarter inch in diameter, but some of the perthite is 1 inch long. The very fine grained areas grade into the coarser grained perthite-plagioclase-quartz pegmatite. The granitic material has corroded large perthite crystals, and single cleavage faces of perthite can be traced into the finer grained material. The gradation in texture between fine- and coarse-grained parts of the zone, its regular occurrence in the zonal sequence, and its similarity in extent to other zones indicate that the very fine grained material is virtually contemporaneous with other material of the zone. Therefore it has corroded only those crystals that had developed in the earliest consolidation stages of the unit.

The second intermediate zone is a medium- to coarse-grained perthite-quartz-plagioclase pegmatite that has been the major source of potassic feldspar recovered at the mine. The average composition is 50 percent perthite, 30 percent quartz, 15 percent plagioclase, and 5 percent accessory minerals. Muscovite and cleavelandite are the most abundant accessory minerals, and garnet, beryl, columbite, and apatite are minor accessory minerals.

The third intermediate zone consists of fine- to medium-grained quartz-plagioclase pegmatite. The average composition is 65 percent quartz, 30 percent plagioclase, and about 5 percent accessory minerals. Muscovite and beryl are the major and minor accessory minerals, respectively. About half of the plagioclase is cleavelandite. This unit crops out near the center of the pegmatite southeast of the fault and in the main opencut.

The core is fine- to coarse-grained perthite-quartz-muscovite-cleavelandite pegmatite. The average composition is 40 percent perthite, 35 percent quartz, 15 percent muscovite, and 10 percent cleavelandite, but in any single exposure of the unit, one or more of these minerals may be absent. The muscovite is fine grained, yellowish green, and is the typical "burr" mica often associated with cleavelandite. The core is discontinuous, consisting of several segments near the center of the pegmatite.

The replaced northwest part of the pegmatite consists mostly of medium- to coarse-grained perthite-plagioclase-muscovite pegmatite with accessory garnet and pyrite, chalcopyrite, sphalerite, and other sulfides. The average composition is 45 percent perthite, 40 percent plagioclase, 10 percent muscovite, and 5 percent accessory minerals. Locally the muscovite content increases to 40 percent of the unit. Although in most places the fault acts as a sharply defined contact with zoned pegmatite, a few small muscovite-rich pods occur southeast of the fault. These appear to have been superimposed on the normal pegmatite of the zones and may be at places where solutions passed through the generally impermeable barrier along the fault. The muscovite books and flakes northwest of the fault are commonly less than one-half inch in maximum dimension and are green, yellowish-green, or greenish-rum. In the pegmatite especially rich in muscovite, the books are larger and mostly greenish-rum. The small pods southeast of the fault contain fine-grained yellowish-green flakes and very small books of muscovite. The feldspars of the unit are commonly stained by iron oxide, and the plagioclase characteristically is vuggy.

The unit northwest of the fault is characterized by an extremely low percentage of quartz, probably less than 1 percent of the rock. Most quartz occurs as small crystals lining vugs surrounded by feldspar, and only rarely does it occur in irregular intergrowths with plagioclase typical of the zones. Many of the vugs in the plagioclase appear to have the characteristic shape and size of quartz in the pegmatite of the second intermediate zone southeast of the fault. In one place, quartz in vugs in perthite has the same arrangement and size as the quartz in typical graphic granite. These features suggest that quartz has been removed by solutions acting on perthite-quartz-plagioclase pegmatite of the second intermediate zone.

The second unit distinguished northwest of the fault is similar in texture and composition to the one described above except that muscovite forms less than 5 percent of the unit.

Thus the textures and the different mineralogy suggest that the northwest part of this pegmatite consists of material formed by replacement of previously solidified zones. The subdivision into two units may reflect differences in the composition of zones before the replacement stage. It is not clear whether the fault is prereplacement, and thus was a barrier to the fluids, or postreplacement, and caused juxtaposition of unlike rocks.

Beryl is present only in the zoned pegmatite southeast of the fault, where it has been found in all zones. Mineral measurements indicate the beryl content of this part of the pegmatite to be about 0.04 percent. The third intermediate zone contains the largest beryl concentrations. Measurements made at random on the surface of the dumps indicate a grade of 0.03 percent. The average crystals have an exposed surface area of 3.3 square inches, and 50 percent probably could be recovered by hand cobbing.

Potassic feldspar resources are in all zones southeast of the fault, except the third intermediate zone. The average perthite content of this part of the pegmatite is about 40 percent, and recovery by hand-cobbing is possible in both the second intermediate zone and the core. Northwest of the fault, the average perthite content is about 50 percent, and three-fourths of it could be recovered by hand-cobbing. Much of this feldspar is stained by iron oxides.

Sodic feldspar comprises 20 percent of the pegmatite southeast of the fault and 45 percent northwest of it. Southeast of the fault the grain size is too small to permit recovery by hand-cobbing, and only an estimated 25 percent of the total sodic feldspar northwest of the fault could be recovered by this method. This feldspar is stained by iron oxides. Recovery of sodic feldspar by milling would be much greater than by hand methods, but the product would be combined with potassic feldspar.

Muscovite in the Welch deposit could be used for scrap purposes, but only a very few small books contain material of sheet quality. About 75 percent of the muscovite in the richest areas northwest of the fault could be recovered by hand-cobbing, but in other places recovery by this method would be very low. The average grade of the entire pegmatite northwest of the fault is estimated to be 5 percent; southeast of the fault it is 3 percent.

A few plates of columbite occur in the zoned pegmatite. The largest specimen seen on the dump was 3 inches long, 1 inch wide, and one-half inch thick.

PEGMATITE 63

Pegmatite 63, 3½ feet thick, is exposed for 8 feet along its strike of N. 45° E. It dips 80° SE. and is nearly concordant. It is quartz-perthite-plagioclase (An_6)-muscovite pegmatite with accessory garnet.

PEGMATITE 64

Pegmatite 64, a discordant body, is at least 500 feet long and 10 to 50 feet thick; it strikes N. 45° W., and dips 70° SW. Zoning consists of a 6-inch wall zone of fine-grained quartz-muscovite-plagioclase pegmatite and a fine- to medium-grained core of quartz, plagioclase (locally An_1), and perthite. White beryl is a minor accessory mineral in both units; in the wall zone it contains 13.1 percent BeO, in the core 12.8 to 13.0 percent BeO. The beryl content of the entire pegmatite is 0.003 percent. Possible products are milling-grade feldspar and scrap mica.

PEGMATITE 65, MILLS PROSPECT

Pegmatite 65 is at least 250 feet long and as much as 60 feet thick. It is discordant, strikes N. 45° W., and probably dips 75° NE. Three small prospect pits have been opened for feldspar. The body consists of a wall zone of fine- to medium-grained quartz-perthite-plagioclase (An_{4-6})-muscovite pegmatite, a core-margin zone of medium- to coarse-grained perthite-quartz pegmatite, and segments of a discontinuous core of quartz. Beryl (12.9 to 13.0 percent BeO) is a minor accessory mineral in the wall zone and in the core. The beryl content of the wall zone is 0.04 percent. Possible products are hand-cobbed perthite and milling-grade feldspar, scrap mica, and beryl.

PEGMATITE 66

Pegmatite 66 is intermittently exposed for 200 feet along its strike of N. 65° E., and it dips 65° NW. It is 15 to 20 feet thick and concordant. The poor exposures show a border zone of fine-grained quartz-muscovite-plagioclase pegmatite less than 1 inch thick, a wall zone of fine- to medium-grained quartz-plagioclase-perthite pegmatite, and segments of a discontinuous quartz-pegmatite core. Muscovite is an accessory mineral in the wall zone and in the core. Possible products are milling-grade feldspar and scrap mica.

PEGMATITE 67

Pegmatite 67, a discordant, irregular pegmatite, is about 3 feet thick and is exposed for 20 feet downdip. It probably strikes N. 20° W. and dips 20° E. It is unzoned, and consists of fine- to medium-grained quartz-plagioclase (An_{21}) pegmatite with accessory perthite, muscovite, and biotite.

PEGMATITE 68

Pegmatite 68 is at a locality that contains two small irregular pegmatites that are discordant to the foliation of the wallrock. The larger is exposed for about 10 feet on the face of a cliff, where it strikes N. 40° W. and dips 80° NE. The smaller body strikes N. 10° E. and dips 65° E. Both are unzoned, and consist of plagioclase-quartz pegmatite with accessory muscovite and biotite.

PEGMATITES 69 TO 73

Pegmatites 69 to 73 are 3.6 miles S. 43° W. of Raymond village, and have not been prospected. Plate 13 shows the very irregular shape of the pegmatites, and the characteristically poor bedrock exposures in this area.

Pegmatite 69, the largest, probably is 850 feet long and as much as 250 feet wide. It is thickest near the southwest end, and four narrow fingerlike bodies extend northeastward from it. The average strike is N. 65° E. parallel to the foliation of the gneissic granite wallrock. The average dip is 50° NW., at a lower angle than the dip of foliation, which averages 70° NW. The direction or angle of plunge could not be determined, but the shape of the pegmatite and its relation to topography suggest a westward plunge. Under this interpretation, the fingers are roots extending downward from the bulbous part of the body, and the small patch of wallrock near the southwest end is a remnant of the cap over the top of the body.

The largest pegmatite (No. 69) consists of perthite, plagioclase, and quartz with accessory muscovite, biotite, garnet, beryl, and columbite. The pegmatite is poorly zoned, and the exposures are so scattered and small that no attempt was made to map the units. At least two zones are present, a wall zone of fine- to medium-grained plagioclase-quartz-perthite pegmatite, and a medium- to coarse-grained core of perthite-quartz-plagioclase pegmatite. The average composition of the wall zone is 50 percent plagioclase, 35 percent quartz, 10 percent perthite, and 5 percent accessory minerals such as muscovite, biotite, garnet, and beryl. The average composition of the core is 45 percent perthite, 30 percent quartz, 20 percent plagioclase, and 5 percent accessory minerals such as muscovite, garnet, and some beryl. The wall zone may be 10 to 20 feet thick; it is the only unit present in some of the fingers that extend northeastward. The core is exposed in the thicker parts of the pegmatite; podlike masses of coarse-grained quartz, perthite, and muscovite are in the perthite-rich core.

A few thin, fracture-controlled units cut the wall zone along the hanging-wall side of the pegmatite, and one extends into wallrock. These are commonly from 5 to 10 feet long, as much as 3 feet thick, and are about normal to the contact. Most of these units consist of quartz pegmatite, and have sharply defined contacts. Two of them, however, are of medium-grained quartz-perthite pegmatite with accessory muscovite and beryl, and have gradational contacts with the earlier formed pegmatite.

Pegmatites 70, 71, and 72 are smaller lenticular or tabular bodies exposed near pegmatite 69. Pegmatite 73, a tabular body at least 200 feet long and 15 feet thick, strikes N. 70° E. and dips 40° NW. A small outcrop of pegmatite in the hanging-wall granite about 25 feet north of the most northeastern pegmatite exposure of pegmatite 73 may be a fracture-controlled extension of this pegmatite that strikes N. 55° W., but its junction with the main pegmatite is not exposed.

Pegmatites 70, 71, and 72 consist of plagioclase-quartz-perthite pegmatite with accessory muscovite and garnet. The rock is mostly fine grained. Pegmatite 73 has a similar composition but contains very fine grained beryl as a minor accessory mineral. Mineral measurements in one outcrop indicated that 155 beryl crystals had a total exposed area of 7.4 square inches; of this total, 2.4 square inches were in one crystal and most of the others were 0.1 by 0.1 inch. Beryl may be more abundant than the 0.0085 percent indicated by the mineral measurements, because the crystals are so extremely small that they could be seen only in fresh exposures, and there may be other crystals that were not observed.

Products of possible economic value from pegmatites 69 and 73 are milling-grade feldspar, scrap mica, and beryl. Although perthite crystals as much as 1 foot in diameter occur most are less than 4 inches across, and are so surrounded by finer grained quartz, plagioclase, and muscovite that they would be very difficult to recover by hand-cobbing. Muscovite commonly occurs in books or flakes less than 1 inch in diameter. The beryl content of pegmatite 69, except for the two central fingers that contain no distinguishable beryl, is about 0.03 percent. The crystals are small, the average area exposed is 0.8 square inch, and they could be recovered only by milling. The beryl content of pegmatite 73 is 0.0085 percent, and the crystals are extremely fine grained.

PEGMATITE 74

Exposures of pegmatite 74 extent intermittently for at least 360 feet N. 65° E. The average exposure width is about 25 feet. The dip at the southwest end is 60° NW., and the body is concordant. The pegmatite contains 4 fracture-filled units, 3 of which extend into wallrock; the first strikes N. 15° W., is 15 feet long, and 3 feet thick; the second strikes N. 35° W., is 50 feet long, and 12 feet thick; the third strikes north, is 35 feet long, and 11 feet thick; and the fourth is wholly in pegmatite, strikes N. 45° W., is 5 feet long, and 1 foot thick. All dip vertically. Junctions of the first three with the main pegmatite are not exposed. The main pegmatite is chiefly unzoned, containing fine- to medium-grained perthite, quartz, and plagioclase (An_3), and muscovite and beryl (12.8 to 12.9 percent BeO) as minor accessory minerals. The beryl content of the entire pegmatite, including the fracture-controlled bodies, is 0.0125 percent. The fracture-controlled bodies are zoned, especially the one to the southwest, where a wall zone of fine-grained plagioclase-perthite-quartz pegmatite contains minor accessory beryl (13.0 percent BeO), and the core consists of fine- to medium-grained quartz-perthite pegmatite. Possible products of this pegmatite are milling-grade feldspar, scrap mica, and beryl.

PEGMATITE 75

Pegmatite 75 is unzoned, discordant, and 3 feet thick, and exposed for 10 feet along its strike of N. 10° W.; it dips 80° W. It consists of fine- to medium-grained quartz-plagioclase (An_8)-perthite pegmatite with muscovite and beryl (13.0 percent BeO) as minor accessory minerals.

PEGMATITE 76

Pegmatite 76 is at a locality that contains a group of concordant pegmatite lenses and tabular bodies exposed near the contact of foliated granite with mica-quartz schist. Many quartz bodies are associated with the pegmatitic material; some of them plunge 20° N. 55°E. The largest pegmatite is an unzoned body 50 feet long and 3 feet thick; it is perthite-plagioclase-quartz pegmatite with minor accessory beryl (13.1 percent BeO) and muscovite.

PEGMATITE 77

Pegmatite 77 is concordant, and is at least 170 feet long and from 3 to 15 feet thick. It strikes N. 60° E. and dips 50° NW. It is an unzoned fine- to medium-grained perthite-plagioclase-quartz pegmatite with minor accessory muscovite and beryl (12.9 percent BeO). The beryl content of the entire pegmatite is 0.019 percent. Possible products are milling-grade feldspar and scrap mica.

PEGMATITE 78

Pegmatite 78 is exposed intermittently for 105 feet along its strike of N. 65° E. The average exposed thickness is 4 feet, and the dip is unknown. It probably is concordant. Although poorly zoned, it has a fine-grained wall zone of quartz-muscovite-plagioclase pegmatite and a core of fine- to medium-grained perthite-plagioclase-quartz pegmatite containing accessory muscovite and minor accessory beryl (13.0 percent BeO). The beryl content of the entire pegmatite is 0.015 percent.

PEGMATITE 79

Pegmatite 79 is 10 inches thick and is exposed for only 2½ feet along its strike of N. 55° E.; it dips 80° NW., concordant with the schist. It is fine-grained quartz-muscovite-plagioclase (An_{14}) pegmatite.

PEGMATITE 80

Pegmatite 80 is 1 foot thick and is exposed intermittently for 20 feet along its strike of N. 60° E.; it dips 85° NW. It is concordant, unzoned, and consists of fine-grained quartz-plagioclase (An_{3-4}) pegmatite with accessory muscovite.

PEGMATITE 81

Pegmatite 81 is 1 foot thick, is exposed intermittently for 60 feet along its strike of N. 60° E., and dips 80° NW. It is concordant, unzoned, and contains fine-grained quartz-plagioclase pegmatite with accessory muscovite.

PEGMATITE 82

Pegmatite 82, a concordant body at least 280 feet long and from 10 to 15 feet thick, strikes N. 65° E. and dips 65° NW. It contains a wall zone of fine- to medium-grained plagioclase-quartz-perthite pegmatite and segments of a discontinuous core of medium-grained quartz-plagioclase-perthite pegmatite. Plagioclase in the wall zone ranges in composition from An_1, where associated with quartz near the core, through An_{3-4}, also near the core, to An_{6-7} near the hanging wall, and to An_{12} where associated with minor accessory columbite near the hanging wall. Beryl is a minor accessory mineral of both the core and the wall zone, and ranges in composition from 12.7 to 12.9 percent BeO in the core, to 12.9 to 13.1 percent BeO in the wall zone. The beryl content of the entire pegmatite is 0.127 percent. Muscovite is an accessory mineral of both units. Possible products are milling-grade feldspar, scrap mica, and beryl.

PEGMATITE 83, GILLINGHAM PROSPECT

The Gillingham prospect is an unzoned pegmatite opened for feldspar by the Whitehall Co., Inc. The pegmatite is 15 feet thick and at least 60 feet long. It strikes eastward, dips 75° S., and the east end terminates in a blunt nose. It is medium- to coarse-grained perthite-quartz-plagioclase-muscovite pegmatite. Black tourmaline and apatite are accessory minerals, and beryl (13.0 to 13.1 percent BeO) is a minor accessory mineral. Plagioclase (An_{1-3}) veinlets from the finer grained matrix cut perthite. The beryl content of the entire pegmatite is 0.088 percent. Possible products are hand-cobbed perthite and feldspar, and scrap mica of milling grade.

PEGMATITES 84 TO 86, HURLEY PROSPECT

The three pegmatites at the Hurley prospect are 4.2 miles S. 52° W. of Raymond village. In 1947 the overburden was removed from most of the central and western pegmatites and two small cuts were opened by the Whitehall Co., Inc.

The easternmost pegmatite, No. 84 (pl. 14), is at least 120 feet long and as much as 45 feet thick. It strikes about N. 40° W. and dips 80° NE. The central pegmatite, No. 85, is also at least 120 feet long and as much as 45 feet thick; it strikes about N. 35° W. and probably dips steeply northeastward. A roll on the footwall contact plunges 60° S. 55° E. The westernmost and largest pegmatite, No. 86, strikes about N. 60° W., and where the contact is exposed, dips 65° NE.

Pegmatites 84 and 85 are separated by a northwestward-trending band of schist probably ranging from 8 to 10 feet in thickness; the schist separating pegmatites 85 and 86 is 2 to 18 feet thick. Schist is exposed in the southeast corner of the main opencut, and its probable relation to pegmatite 86 is shown in plate 14, section *A–A′*. The attitude of bedding in the narrow schist bands between the pegmatite bodies is similar to that in schist some distance from the contact. The outcrop pattern indicates that the pegmatite exposures may be parts of a single body, only partly exposed by erosion, which strikes about N. 80° W. and dips northward. The diagonal bands of wallrock are most likely uneroded remnants of the original cap of this body. Furthermore, the three pegmatites are similar in composition.

The border zone consists of very fine grained quartz-muscovite pegmatite that is not everywhere exposed along the contact. It is rarely more than one-half inch thick.

The wall zone is medium-grained plagioclase-quartz-perthite pegmatite with accessory muscovite, biotite, black tourmaline, garnet, and sulfides. The average composition is about 45 percent plagioclase, 25 percent quartz, 25 percent perthite, and 5 percent accessory minerals. Locally, the perthite content may increase to 50 percent, and some is in graphic intergrowth with quartz. Plagioclase near the inner edge of the unit is partly cleavelandite. Much of the feldspar is stained by iron oxides along cleavages and fractures. The wall zone is the largest unit exposed, and is the only unit exposed in the easternmost pegmatite.

The intermediate zone contains the same minerals as the wall zone plus strips of intergrown biotite and muscovite. The average composition is 45 percent plagioclase, 30 percent quartz, 10 percent perthite, 10 percent intergrown biotite and muscovite, and 5 percent accessory minerals. The biotite is partly chloritized. The biotite-muscovite intergrowths occur as strips as much as 1½ feet long, 3 inches wide, and one-half inch thick. Cleavelandite is more abundant in pegmatite of this zone than in the wall zone, and comprises about 25 percent of the plagioclase. The intermediate zone completely encloses 1 of the 3 exposures of the core, partly surrounds the second, but is not exposed in the vicinity of the third.

The core is coarse-grained perthite-quartz pegmatite. Some of the exposures of this unit shown on the map (pl. 14) are very quartz rich, and others are perthite rich, but all are probably parts of a single central unit of the pegmatite. Accessory minerals are plagioclase (commonly cleavelandite), muscovite, minor biotite, black tourmaline, beryl, columbite, and löllingite. The composition ranges from about 85 percent perthite and 15 percent quartz on the east wall of the larger opencut to 65 percent quartz, 20 percent perthite, 10 percent plagioclase, and 5 percent accessory minerals in the exposure east of the north end of the larger opencut. At the exposure south of the larger cut, the composition is 75 percent quartz and 25 percent perthite with minor amounts of accessory minerals. In the perthite-rich areas, the feldspar is slightly stained by iron oxides. In the quartz-rich areas, perthite occurs as large euhedral crystals in the quartz. The quartz of the unit ranges from gray to pink to white, and there are small areas of clear, highly fractured, colorless quartz.

Resources of potassic feldspar recoverable by hand-cobbing occur only in the core. Present exposures of this unit are small, but if the three pegmatites are connected at depth, the size of the core would be increased with a proportional increase in resources of hand-cobbable perthite.

Sodic feldspar is too fine grained to be recovered by hand-cobbing. The use of the entire pegmatite for millfeed would permit the recovery of much of the plagioclase as well as much of the perthite. The presence of biotite, garnet, and black tourmaline in the different units would require additional equipment for removing iron-bearing minerals.

Some small sheets of hard flat clear ruby mica as much as 2 by 2 inches in diameter could be obtained from muscovite-biotite intergrowths of the intermediate zone, but economically important quantities of sheet mica could not be produced. Scrap mica could be recovered by milling methods because muscovite is a constituent of each unit of the pegmatite, although the size of most of the books is too small for hand-cobbing. Biotite is a contaminant that might have to be removed.

PEGMATITE 87

Pegmatite 87 is a poorly exposed unzoned body that extends for 40 feet N. 50° W. Its maximum thickness probably is less than 20 feet. It is perthite-plagioclase-quartz pegmatite with minor accessory muscovite. Possible products are milling-grade feldspar and scrap mica.

MINOR DISTRICTS

Although many pegmatites occur in scattered areas remote from the well-known pegmatite mining districts of Grafton and Keene, few of economic interest have not been studied. Of the two pegmatites selected for careful study, one was developed after World War II, and the other has been prospected since last described in 1943.

MILLARD CHANDLER MINE

The Millard Chandler (North Star) feldspar mine is in the town of Chatham, Carroll County, and is 1.15 miles N. 7° E. of the village of North Chatham. It is on a steep hillside about one-quarter mile west of the Evans Notch Road at a point about one-half mile west of the New Hampshire-Maine boundary. The mine was worked for feldspar before World War II by the Whitehall Co., Inc. An opencut 70 feet long, 50 feet wide, and as much as 45 feet deep has been driven westward into the pegmatite (pl. 15).

The pegmatite is exposed for 360 feet along its strike. Near the opencut it is about 60 feet thick, but it thins southward and thickens northward. It strikes about north and dips from 10° to 35° W. The steeper dips are on the footwall contact, but these may represent only a local steepening of a generally low dip to the west. The pegmatite is slightly discordant to the structure of the wallrock, which strikes from N. 5° to 40° E., averaging N. 20° E., and dips from 10° to 35° W., averaging about 15° W. The wallrock is a medium-grained granite gneiss formed by the introduction of granitic, and locally pegmatitic, material into biotite schist. Four mafic dikes, ranging from 6 inches to 2 feet in thickness, cut pegmatite and wallrock in and north of the opencut. Most of these strike N. 30° E. and dip 70° to 75° SE. Two additional mafic dikes south of the opencut are from 4 to 6 feet thick, strike more eastward than the others, and dip from 65° to 75° S. These dikes have sharp but irregular contacts with pegmatite and wallrock, and in detail are seen to have many small apophyses extending into the surrounding rock. Five units have been distinguished at the mine. Contacts between the units are gradational and very irregular, and the contacts shown on plate 15 are generalized.

The narrow border zone is fine-grained quartz, plagioclase (An_{10}), perthite, and muscovite with accessory biotite and garnet. It is similar to the gneissic bands of the granitic and pegmatitic material in the wallrock, and for this reason the actual contact of the pegmatite is difficult to distinguish. The accessory biotite and garnet may contain material derived from the wallrock.

The wall zone is fine- to medium-grained plagioclase-quartz pegmatite. About 50 percent of the unit is plagioclase (An_6), 30 to 45 percent is quartz, and 5 to 15 percent is perthite. Muscovite is commonly present, and biotite, garnet, and apatite are minor accessory minerals. The wall zone is thickest on the footwall side of the pegmatite.

The core-margin or intermediate zone is the most irregular. The average composition is 40 percent perthite and graphic granite, 35 percent plagiocase, and 25 percent quartz. The coarse-grained perthite and graphic-granite masses are surrounded by fine- to medium-grained plagioclase-quartz pegmatite of a composition similar to the wall zone and to small areas surrounding perthite in the core. Perthite occurs mostly as graphic granite in which the quartz intergrowths are less angular and less regular in spacing than in typical graphic granite. Potassic feldspar increases in abundance toward the core. Beryl and scrap muscovite are present adjacent to the core, particularly in areas of plagioclase and quartz between the graphic granite masses. Locally, there are many small vugs in the plagioclase (An_6). Some beryl crystals are rimmed and cut by veinlets of cleavelandite; one of these veinlets contains plagioclase of higher sodic content (An_3) than the normal type in the zone. A few books of scrap muscovite as large as 4 by 3 by 1 inches occur adjacent to the core.

The core consists of coarse-grained quartz and perthite with small areas of medium-grained plagioclase-quartz-muscovite pegmatite. Perthite crystals are as large as 3½ by 6 by 2 feet, and aggregates of crystals are even larger. Locally, the unit may consist entirely of either quartz or perthite, but the average content ranges from 55 to 60 percent quartz, and 40 to 45 percent perthite. The core is discontinuous in surface exposures, but appears to thin southward and thicken northward, as does the pegmatite. Löllingite and sulfides are minor accessory minerals in this unit.

A very fine grained sugary-textured plagioclase-rich unit is south of the opencut. It is exposed for a length of 35 feet and a width of 5 feet, and its location in the sequence of pegmatite units suggests that a section of the core of the body has been replaced by plagioclase-rich material. This unit consists of 80 to 90 percent plagioclase (An_4) with minor quartz and greenish muscovite. Garnet is a rare accessory mineral.

Beryl occurs in the intermediate zone adjacent to the core. It is in blue-green to light-green crystals as large as 6 by 15 inches. Some crystals contain veinlets of, and are rimmed with, cleavelandite. Mineral measurements indicate a beryl content of about 0.10 percent, of which 80 percent could be recovered by hand-cobbing. The beryl contains from 13.5 to 13.7 percent BeO.

Potassic feldspar is economically the most important mineral in the pegmatite. The largest reserves are in the core and intermediate zone. Most of the perthite in the core and perhaps one-half of it in the intermediate zone could be recovered by hand-cobbing. In the intermediate zone, however, the product would be quartz rich because of the high proportion of graphic granite. There are no iron-bearing minerals in the pegmatite to contaminate a mill product, but the mafic dikes would cause contamination in any large-scale operation.

No sheet mica was seen at the mine. Scrap mica could be recovered from all units by milling, but the mica content of this pegmatite is small. Some books of scrap mica in the intermediate zone adjacent to the core could be recovered by hand-cobbing.

PARKER MOUNTAIN MINE

The Parker Mountain (Foss, Foss Ledge) mine is in the town of Strafford, 2.4 miles N. 46° W. of Center Strafford village, Strafford County. The pegmatite has been described by Sterrett (1923, p. 156–158), Switzer (1938), and most recently by Stewart (*in* Cameron and others, 1954, p. 270–271). In 1947, the Whitehall Co., Inc., removed the overburden from pegmatite at the southeast end of the opencut while prospecting for feldspar. This permitted a more extensive study of the internal structure of the pegmatite than was possible in 1943 when Stewart did his work. Although his map is used as a base for plate 16, minor changes were necessary to bring it up to date and to show the slightly different interpretation of the internal structure.

The old working at the Parker Mountain mine is an opencut 100 feet long, from 10 to 75 feet wide, and as much as 40 wide deep. Narrow inclined stopes extend for an undetermined distance below the present floor of the cut along the hanging wall of the pegmatite. These stopes are now filled with waste rock and water. The mine was last operated in 1936–38 by A. E. Buzzo of Center Strafford, who worked it for feldspar (Cameron and others, 1954, p. 270–271). Although the mine was prospected by the Whitehall Co., Inc., in 1947, no production was reported.

The wallrock of the pegmatite is fine-grained massive aplite consisting of quartz, microcline, albite (An$_6$), muscovite, and minor amounts of tourmaline, biotite, and apatite (Cameron and others, 1954, p. 270–271). The aplite body trends N. 25° E., is at least 130 feet wide, and is in quartz-mica schist that strikes about north and dips 40° to 60° W.

The pegmatite apparently was emplaced along a fracture in the massive aplite body. The pegmatite strikes N. 40° W., dips 70° to 80° NE., and extends diagonally across the entire width of the aplite body. It is lenticular and has a maximum thickness of 40 feet.

Four internal structural units have been mapped in the Parker Mountain pegmatite. These are similar to the ones described by Stewart (in Cameron and others, 1954, p. 270–271) but differ slightly because of the relations and compositions shown in new exposures southeast of the opencut.

The border zone consists of fine-grained perthite and quartz in graphic granite. The thickness ranges from 1 inch to 3 feet, and is commonly too thin to show on the map and section. This unit is most prominent along the hanging-wall contact, but is absent in many places elsewhere.

The wall zone is medium-grained perthite-cleavelandite-quartz-muscovite pegmatite with minor accessory beryl, black tourmaline, and apatite. It is a discontinuous unit as much as 5 feet thick on the hanging-wall side; most exposures are remnants left on the hanging-wall and footwall sides of the opencut.

The first intermediate zone is medium-grained perthite-cleavelandite-quartz pegmatite of a texture and composition similar to the wall zone except that muscovite is only an accessory mineral. The unit is discontinuous; it is most conspicuous on the footwall side of the pegmatite, and extends entirely across the pegmatite southeast of the opencut where it seems to form a cap over the core.

The core consists of coarse-grained quartz-perthite pegmatite with accessory cleavelandite and muscovite and minor quantities of accessory beryl, garnet, apatite, triphylite, spodumene, and other minerals. The average composition is 50 percent quartz, 40 percent perthite, and 10 percent accessory minerals. Quartz is intergrown with perthite and also occurs as individual bodies as much as 5 feet wide and 25 feet long. Most of the quartz is gray, but colorless and dark smoky quartz also are present. The core is as much as 20 feet thick.

A pipelike body of medium-grained muscovite-perthite-quartz-cleavelandite pegmatite is centrally located in the core near the northwest end of the opencut. It is as much as 6 feet across but its length is unknown.

Beryl occurs in the wall and first intermediate zones and in the core. The beryl content of the core in the outcrop southeast of the opencut is 0.22 percent. The average crystal has an exposed area of 7 square inches, and most of the beryl could be recovered by hand-cobbing. The wall zone on the southwest side of the opencut contains 0.89 percent beryl; the average crystal has an area of 5 square inches, and much of this beryl also could be recovered by hand-cobbing. No beryl was seen in the hanging-wall part of the wall zone. The beryl of the core is blue green and is associated chiefly with the larger quartz bodies. Beryl from the wall zone is light green and is associated with muscovite.

Most of the resources of potassic feldspar are in the core below the level of present exposures and below the waste rock in the floor of the opencut. Most perthite in the core could be recovered by hand-cobbing. Perthite also is in the other units of the pegmatite but could be recovered from them only by milling.

Sodic feldspar, mostly cleavelandite, is in every unit, but the grains are too small to permit economic recovery by hand-cobbing. The use of the entire pegmatite for millfeed would result in the recovery of the plagioclase in addition to the potassic feldspar.

Sheet mica has been recovered from the wall zone of the pegmatite, particularly on the hanging-wall side, and reserves of sheet mica probably are in this unit below the old workings. Scrap-mica reserves are most abundant in the pipelike unit of muscovite-rich pegmatite. About 80 percent of the unit is muscovite, most of which is recoverable by hand cobbing. Muscovite is also in the other units but except in the sheet-mica-bearing wall zone, would be recoverable only by milling.

The pegmatite also contains columbite, spodumene, and triphylite, and according to Switzer (1938, p. 811–820), it contains amblygonite, cassiterite, and autunite. The quantities of these minerals available at the Parker Mountain mine are too small to be of value under present economic conditions (1957).

RECONNAISSANCE OF OTHER AREAS

ALTON QUADRANGLE

Three pegmatites have been worked or prospected in the Alton quadrangle, all of them in the town of Strafford. The largest working is at the Parker Mountain (Foss, Foss Ledge) mine previously described. The John Felker mica prospect, the Ashton Rollins prospect, and from 20 to 25 other pegmatites on the Rollins property also have been described by Stewart (*in* Cameron and others, 1954, p. 270–274). With the exception of the Parker Mountain pegmatite, none of these seems to offer economic possibilities for future production of sheet or scrap mica, feldspar, or beryl.

Five other small pegmatites, also in Strafford, were studied in 1949 during the short time spent on reconnaissance in this quadrangle. The largest one is about one-fourth of a mile north of the road intersection east of the Blue Hills School. This pegmatite is exposed for nearly 100 feet in the bed of a stream, strikes N. 45° E., dips 60° SE., and is 20 feet thick. An 8-inch border zone of fine-grained, quartz-muscovite pegmatite and a core of perthite-quartz pegmatite are the only internal units exposed. Lath-shaped perthite crystals in quartz of the core commonly have their long axes oriented normal to the contact. Accessory black tourmaline crystals have a similar orientation. The other pegmatites visited are very small and are unzoned.

GORHAM QUADRANGLE

Two pegmatites have been worked or prospected in the Gorham quadrangle. The Millard Chandler (North Star) mine is in the town of Chatham. It was operated for feldspar by the Whitehall Co., Inc. in 1940. A study of this mine was undertaken in August 1949, and the results are discussed on pages 43–44. The deposit has small reserves of feldspar, scrap mica, and beryl. The Fischer mica prospect is in the town of Shelburne and has been described by Larrabee (*in* Cameron and others, 1954, p. 139). This property has never been worked and does not seem to offer any possibilities for the production of economic pegmatite minerals.

The results of a brief reconnaissance in 1949 indicate that this quandrangle is unfavorable for the production of pegmatite minerals. Large parts of the quadrangle are comparatively inaccessible, and the transportation difficulties in these areas would be great. For this reason, the reconnaissance was confined to a few of the more accessible areas adjacent to the Wild River in Beans Purchase, the Androscoggin River in Shelburne, and the Peabody River in Pinkham Notch. The pegmatites examined represent only a very small fraction of the actual number in the area. The pegmatites are small, rarely more than 5 feet thick or 50 feet long, and most are tabular or lenticular. They are commonly concordant to the foliation of the enclosing quartz-mica schist and gneiss. Locally, the pegmatites seem to have filled openings between blocks of a coarse breccia and are very irregular and variable in size. They are principally unzoned bodies of fine- to medium-grained perthite-plagioclase-quartz pegmatite. Accessory minerals are muscovite, biotite, black tourmaline, and garnet. No beryl was seen. Commercial quantities of feldspar are lacking, and only a few small books of sheet mica were seen.

MOUNT PAWTUCKAWAY QUADRANGLE

Reconnaissance in the Mount Pawtuckaway quadrangle was a logical outgrowth of detailed mapping in the Raymond pegmatite district. The results of the Raymond district study were sufficiently favorable to warrant an investigation of adjoining areas in search of pegmatites of possible economic interest. A reconnaissance was made in the Mount Pawtuckaway quadrangle northeastward from the Raymond pegmatite district to near the village of Nottingham Square. A smaller pegmatite district was studied in the towns of Deerfield and Northwood, mainly between Deerfield Center and Coffeetown School, and scattered pegmatite outcrops were seen elsewhere in the quadrangle. In addition, areas were examined south, southwest, and west of the Mount Pawtuckaway quadrangle in the Hampstead, Manchester, and Suncook quadrangles, respectively, but only a few pegmatites were seen.

Bedrock exposures are sparse in large parts of the Mount Pawtuckaway quadrangle, and pegmatites occur in only a few of these exposures. Except in the Raymond district, where nearly every pegmatite outcrop was examined, the reconnaissance nature of the work resulted in the study of only those pegmatites that were seen along traverse lines and in road cuts.

The geology of the Mount Pawtuckaway quadrangle has been mapped and described by Freedman (1950, p. 449–491). The petrology of the igneous complex in the Pawtuckaway Mountains has been described by Roy and Freedman (1944, p. 905–919).

Freedman (1950, p. 449–491) shows that metamorphosed sedimentary rocks trend northeastward across the southeast half of the quadrangle. They form the steeply dipping southeast limb of a syncline that probably plunges northeastward and includes the Eliot formation (probably Ordovician and Silurian) consisting of phyllite, quartz-mica schist, quartzite, and lime-silicate rock; the Berwick formation (probably Ordovician and Silurian) also consisting of phyllite, quartzite, quartz-mica schist, and lime-silicate rock; and the Littleton formation (Lower Devonian) consisting of quartzite, mica-schist, mica-garnet schist, mica-staurolite schist, and mica-sillimanite schist. Rocks of the New Hampshire plutonic series (Upper Devonian?) are widespread in the northwest half of the quadrangle, where they consist of quartz diorite, quartz monzonite, binary granite, and microcline granite. Quartz monzonite is the most abundant rock unit of the series and is discordant to the Littleton formation that adjoins it on the southeast; offshoots of the quartz monzonite locally extend across the Littleton into the Berwick formation. Rocks of the White Mountain plutonic-volcanic series (Mississippian?), ranging in composition from monzonite to gabbro, are best exposed in the Pawtuckaway Mountains, where they were emplaced in quartz monzonite of the New Hampshire plutonic series by forceful injection and cauldron subsidence. Metamorphism decreases southeastward and northwestward from the granitic rocks of the New Hampshire plutonic series. The pegmatites of the quadrangle are associated with rocks of the New Hampshire plutonic series and are not found with younger rocks.

In addition to the 87 pegmatites of the Raymond district described elsewhere in this report, 4, the Corson, McMullen, McGall, and Vatcher pegmatites are described in the section on detailed studies of individual mines in the Raymond region. In the Mount Pawtuckaway quadrangle 85 other pegmatites or groups of pegmatites were investigated. Of these, 61 are in the metamorphic rocks and in small associated bodies of igneous rocks between the Raymond district and the village of Nottingham Square. In the towns of Deerfield and Northwood 24 were visited; most of these are between the village of Deerfield Center and the Coffeetown School.

Mica schist is the wallrock of most of the pegmatites in the towns of Raymond, Nottingham, and Epping. A few pegmatites are in small bodies of schist surrounded by granitic rocks; others are in small granite bodies in metamorphic rocks. In the Raymond district, the pegmatites are in the Littleton formation, 1½ to 2 miles southeast of its contact with granitic rocks. The McGall, Vatcher, and Corson pegmatites and the pegmatite area near Nottingham Square are at or near the contact of the Littleton and Berwick formations. With the exception of the McGall pegmatite, these are about 1½ miles from the main granitic rocks. The pegmatites in the towns of Deerfield and Northwood are in igneous rocks or in metamorphic rocks included in, or adjacent to, the igneous rocks.

Most of the pegmatites are thin tabular or lenticular bodies that range from 5 to 1,000 feet in length and from a few inches to 300 feet in thickness; the average body is exposed for about 50 feet along its strike and is about 10 feet thick. The attitudes of many pegmatites are difficult or impossible to determine because of the absence of exposures showing contacts with wallrock. Nearly half of those in the Raymond district are concordant to the bedding of the enclosing wallrock, as are about two-thirds of those between the Raymond district and Nottingham Square. In the Deerfield area, more than half are concordant.

Internal structural units were not distinguishable in many pegmatites because of the poor exposures. The best examples of zoning are at mines or prospects where small opencuts have been developed or where the overburden has been removed. Many other pegmatites would show internal structural units if better exposures were available.

The upper surfaces of many of the pegmatites seem to have been uncovered by erosion recently during the geologic history of the district. Small patches of schist and border-zone material occur on the upper surfaces of several outcrops. The dips of contacts indicate that some pegmatites thicken at depth, suggesting that only their tops have been uncovered. At several of the mines and prospects, a greater variety of zones is found in the walls and floors of the opencuts than is exposed at the surface, and wall zones can be seen to form a capping over other zones. Although many of the other pegmatites seem to consist of only two units—a thin border zone and an apparent core that has the composition and texture of typical wall zones—if erosion had extended to slightly greater depths additional zones might have been exposed. When further prospecting is done in the district, it should be confined to the thicker bulbous parts of the pegmatites in which unexposed inner zones are most likely to be found.

No zoned pegmatites were seen in the Deerfield area, but elsewhere 2 to 5 zones were recognized in pegmatites observed during the reconnaissance study. A border zone is commonly adjacent to the wallrock, and consists of very fine grained quartz-muscovite pegmatite with or without plagioclase; it is rarely more than 1 inch thick, and in many places less than one-quarter inch thick. The wall zone, the unit next inside the border zone, may be the only other unit exposed, and thus is an apparent core. It normally has a fine- to medium-grained texture and consists of plagioclase, quartz, and perthite with accessory muscovite. The first intermediate zone, where present, consists of perthite, quartz, and plagioclase. It is coarser grained and contains more perthite and less plagioclase than the wall zone. The second intermediate zone, or core-margin zone, is 1 to 2 feet thick and consists of perthite, quartz, and muscovite. This zone surrounds a quartz core or small quartz bodies that are segments of a discontinuous core. These quartz bodies, however, should not be confused with quartz pods that are randomly distributed throughout many unzoned pegmatites.

The only other internal structural units are fracture-controlled bodies that are either crosscutting or parallel with the zones. These commonly are a few inches thick, less than 10 feet long, and consist chiefly of quartz. One pegmatite in the Nottingham Square area contains fracture-controlled bodies ranging from 5 to 10 feet in length and as much as 3 feet in width; these consist of quartz-perthite-muscovite pegmatite with accessory beryl in crystals as large as 3 by 6 inches.

Fifteen pegmatites, excluding those previously described, contain visually distinguishable beryl, but none has a grade or tonnage sufficiently high to warrant commercial operations. The richest pegmatite has a beryl content of 0.124 percent and inferred beryl reserves of about 3 tons. The pegmatite area near Nottingham Square has a higher proportion of beryl-bearing pegmatites than any other area except the Raymond district.

Muscovite is a characteristic mineral of every pegmatite, but it is rarely of sufficient size or quality to be used for sheet mica. Three pegmatites contain minor quantities of sheet mica, and in each the mica is in a different unit. One has sheet mica in a wall zone of cleavelandite-quartz pegmatite, another in a core-margin zone of perthite-quartz pegmatite, and the third in a fracture-controlled unit of quartz-perthite-muscovite pegmatite. Many of the pegmatites contain an estimated 2 to 5 percent muscovite suitable for scrap mica, but the books are so small that milling would be required for economical recovery.

Reserves of potassic feldspar recoverable by hand-cobbing are small. One characteristic that might favor the use of these pegmatites for milling is the comparative absence of iron-bearing minerals such as biotite, black tourmaline, or garnet.

Production of economically important quantities of pegmatite minerals in the Mount Pawtuckaway quadrangle and adjacent areas will probably be slight; the most favorable deposits are confined almost exclusively to the Raymond district itself. The writers found no new pegmatite deposits of value under present (1957) economic conditions in their reconnaissance of selected pegmatite districts. Further work does not seem to be justified in the Raymond region until other districts in New Hampshire have been more thoroughly examined and their resources have been evaluated. If interest in the pegmatites of this region develops in the future, the most favorable location for further work is between the Raymond district and Nottingham Square.

MOUNT WASHINGTON QUADRANGLE

In 1949, a brief reconnaissance was made of the pegmatites on the north flank of Mount Adams, in the town of Randolph, and in Low and Burbanks Grant. The locations of several pegmatites are shown on a geologic map of the quadrangle prepared by M. P. Billings and others (1946).

Three pegmatites in this area were examined, and two others represented only by loose blocks were observed. The pegmatites are poorly exposed but seem to be discordant bodies of plagioclase, quartz, and perthite in feldspathic quartz-mica gneiss. They are fine- to medium-grained and are chiefly unzoned. The best exposures are of a pegmatite in Spur Brook, Low and Burbanks Grant. The average grain size of this pegmatite is less than 1 inch in greatest dimension but locally perthite crystals are as much as 10 inches long and quartz pods are as much as 4 feet long and 1 foot wide. Small books of greenish muscovite ranging from one-half to 2 inches in diameter are most abundant near the gray quartz pods. None of these pegmatites has reserves of sheet mica or visually distinguishable beryl, and the small resources of milling-grade perthite are not of commercial value.

Pegmatites are present on Mount Washington and Mount Madison, but the comparative inaccessability of all except one located on the Carriage Road on Mount Washington would limit future development to small-scale operations. The pegmatite on the Carriage Road is not suitable for economic development.

PLYMOUTH QUADRANGLE

The Plymouth quadrangle was selected for reconnaissance in 1949 because of its location east of the northern limit of the productive Grafton district and because of the similarity of rock types. The locations of many of the pegmatites are shown on the geologic map prepared by C. B. Moke (1946). Three mica mines were operated in this quadrangle during 1942–44: the two Crystal mines in Campton, and the White Mountain Mica Co. (Thornton Hill) mine in Thornton (Cameron and others, 1954, p. 160–162, 259–261). Although the White Mountain Mica Co. mine and one of the pegmatites at the Crystal mines do not contain economically important quantities of sheet mica, the "Upper" Crystal mine has possibilities for future production of this mineral.

During reconnaissance, 30 pegmatites or groups of pegmatites along the valley walls of the Pemigewasset River and its tributaries were examined. Sixteen pegmatites are in quartz-mica schists of the Littleton formation, 13 in Kinsman quartz monzonite, and 1 in Concord granite. The attitude of 28 of the bodies could be determined, and 15 of these are discordant to the structure of the enclosing rock.

Most of the pegmatites are small. Few are exposed for more than 20 feet along their strike, and they range from a few inches to a maximum of 35 feet in thickness, averaging about 5 feet. Eleven pegmatites show a crude zoning; most of them consist of a very thin border zone of quartz-muscovite-plagioclase pegmatite, a wall zone of plagioclase-quartz-perthite pegmatite, and a thin intermediate (core-margin) zone of muscovite pegmatite around small quartz pods that form a discontinuous core. Zoned pegmatites are almost twice as abundant in the quartz-mica schists as in the quartz monzonite. There is no apparent relation between the size of the pegmatite and the presence of zoning.

The pegmatites are fine- to medium-grained, with an average grain diameter of less than 2 inches. Perthite crystals as large as 8 by 12 inches are present in a beryl-bearing pegmatite that crops out in West Branch Brook, on the Campton-Thornton town line. Muscovite books range from one-half to 2 inches in diameter. Strips of intergrown biotite and muscovite as much as 2 by 4 inches and less than one-fourth inch thick were seen in one exposure. Minor accessory garnet, beryl, and black tourmaline occur as small euhedral crystals.

None of the pegmatites seem to contain any mineral or group of minerals in sufficient quantity to warrant their commercial development under present (1957) economic conditions or under those during 1942–45. None is large enough to support the operation of a flotation mill for the recovery of feldspar, and no single area has a reserve tonnage sufficient for such an operation.

The best feldspar and beryl prospect is in West Branch Brook, 3.05 miles N. 39° W. of West Campton village, on the Campton-Thornton town line. This pegmatite is at least 100 feet long and as much as 25 feet wide. Although very irregular, it is generally concordant to the foliation of the wallrock. Poor exposures and indistinct zoning make any estimation of resources questionable. Perthite crystals as large as 8 by 12 inches form about 30 percent of the plagioclase-perthite-quartz pegmatite of the wall zone. About 25 percent could be recovered by hand-cobbing. Forty-one beryl crystals measured in quartz-muscovite pegmatite of the core-margin zone indicate that the eastern half of the exposure contains about 0.3 percent beryl.

LITERATURE CITED

Bannerman, H. M., 1943, Structural and economic features of some New Hampshire pegmatites: New Hampshire Plan. and Devel. Comm., Mineral Resources Survey, pt. 7, 22 p.

Bannerman, H. M., and Cameron, E. N., 1946, The New England mica industry: Am. Inst. Mining Metall. Engineers Tech. Pub. 2024, 8 p.

Berman, Harry, 1927, Graftonite from a new locality in New Hampshire: Am. Mineralogist, v. 12, no. 4, p. 170–172.

Billings, M. P., Fowler-Billings, Katherine, Chapman, C. A., and Goldthwait, R. P., 1946, The geology of the Mount Washington quadrangle, New Hampshire: New Hampshire Plan. and Devel. Comm., 56 p.; Geol. Soc. America Bull., v. 57, no. 3, p. 261–273.

Blondel, F., and Lasky, S. G., 1956, Mineral reserves and mineral resources: Econ. Geology, v. 51, no. 7, p. 686-697.

Cameron, E. N., Jahns, R. H., McNair, A. H., and Page, L. R., 1949, Internal structure of granitic pegmatites: Econ. Geology, Mon. 2, p. 61, 65.

Cameron, E. N., Larrabee, D. M., McNair, A. H., and others, 1954, Pegmatite investigations, 1942–45, New England: U.S. Geol. Survey Prof. Paper 255, 352 p.

Fleischer, Michael, and Cameron, E. N., 1946, Geochemistry of beryllium [report to Manhattan Project 1945, revised as MDDC–643, 1946]; 1955, p. 80–92, *in* Quill, L. L., ed., The chemistry and metallurgy of miscellaneous materials: U.S. Atomic Energy Comm. TID–5212, U.S. Atomic Energy Comm. Tech. Inf. Service, Oak Ridge, Tenn.

Freedman, Jacob, 1950, Stratigraphy and structure of the Mt. Pawtuckaway quadrangle, southeastern New Hampshire: Geol. Soc. America Bull., v. 61, no. 5, p. 449–492.

Frondel, Clifford, 1941, Whitlockite; a new calcium phosphate, $Ca_3(PO_4)_2$: Am. Mineralogist, v. 26, no. 3, p. 145–152.

Frondel, Clifford, and Lindberg, M. L., 1948, Second occurrence of brazilianite: Am. Mineralogist, v. 33, no. 3–4, p. 135–141.

Holden, E. F., 1918, Famous mineral localities; Beryl Mountain, Acworth, New Hampshire: Am. Mineralogist, v. 3, p. 199–200.

Jackson, C. T., 1844, Final report on the geology and mineralogy of the State of New Hampshire: Concord, 376 p.

Jahns, R. H., 1955, The study of pegmatites: Econ. Geology, 50th Anniversary Volume, p. 1025–1130.

Levin, S. B., 1948, Beryl Mountain, Sullivan County, N. H.: U.S. Bur. Mines Rept. Inv. 4216, 3 p.

Meyers, T. R., 1941, New Hampshire minerals and mines: New Hampshire Plan. and Devel. Comm., Mineral Resources Rept., 49 p.

Moke, C. B., 1946, The geology of the Plymouth quadrangle, New Hampshire: New Hampshire Plan. and Devel. Comm., 21 p.

Norton, J. J., Griffitts, W. R., and Wilmarth, V. R., 1958, Geology and resources of beryllium in the United States: Internat. Conf. on the Peaceful Uses of Atomic Energy, 2d, Geneva, Proc., v. 2, p. 21–34.

Norton, J.J., and Page, L. R., 1956, Methods used to determine grade and reserves of pegmatites: Mining Eng., v. 8, no. 4, p. 401–414; Am. Inst. Mining and Metall. Engineers Trans., v. 205, p. 401–414.

Olson, J. C., 1950, Feldspar and associated pegmatite minerals in New Hampshire: New Hampshire Plan. and Devel. Comm., Mineral Resources Survey, pt. 14, 50 p.

Page, L. R., 1950, Uranium in pegmatites: Econ. Geology, v. 45, no. 1, p. 28.

Page, L. R., and others, 1953, Pegmatite investigations 1942–1945, Black Hills, South Dakota: U.S. Geol. Survey Prof. Paper 247, 228 p.

Reno, Horace T., 1956, Beryllium, *in* U.S. Bureau of Mines, Mineral facts and problems: U.S. Bur. Mines Bull. 556, p. 95–101.

Roy, C. J., and Freedman, Jacob, 1944, Petrology of the Pawtuckaway Mountains, New Hampshire: Geol. Soc. America Bull., v. 55, no. 7, p. 905–919.

Shepard, C. U., 1830, Mineralogical journey in the northern parts of New England: Am. Jour. Sci., 1st ser., v. 17, p. 353–360; v. 18, p. 289–303.

Sterrett, D. B., 1915, Some deposits of mica in the United States: U.S. Geol. Survey Bull. 580, p. 72–74.

——— 1923, Mica deposits of the United States: U.S. Geol. Survey Bull. 740, p. 130–133.

Switzer, George, 1938, The paragenesis of the Center Strafford, New Hampshire, pegmatite: Am. Mineralogist, v. 23, no. 11, p. 811–820.

Teschemacher, J. E., 1844, On the beryl from Acworth, New Hampshire: Boston Soc. Nat. History, Proc. v. 1, p. 191–192.

——— 1847, On the occurrence of uranium in the beryl locality at Acworth, New Hampshire: Boston Jour. Nat. History, v. 5, p. 87–89.

U.S. Bureau of Mines, 1939–55, Beryllium, *in* Minerals Yearbook.

——— 1953, Materials survey, beryllium: Rept. compiled for Natl. Security Resources Board by U.S. Bur. Mines with the cooperation of the U.S. Geol. Survey.

Verrow, H. J., 1940, New Hampshire pegmatites productive: Mineralogist, v. 8, no. 8, p. 329–330.

——— 1941, Pegmatite minerals of the Palermo quarry, North Groton, N.H.: Rocks and Minerals, v. 16, no. 6, p. 208–211.

RECEIVED
JUN 3 0 1997
S.I.O. LIBRARY

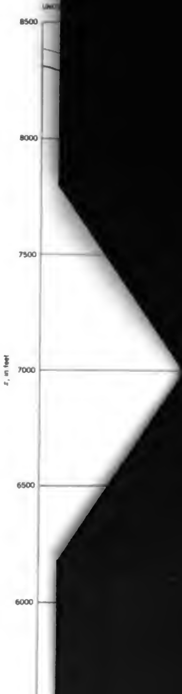
8500
8000
7500
7000
6500
6000
5500
z, in feet